VALUE-ADDED PRODUCTS FROM AGRO-INDUSTRIAL RESIDUES BY BIOLOGICAL APPROACHES

EDITED BY: Xiaoyan Liu, Zhipeng Wang, Myeong-Sok Lee, Jun Xia and Shangyong Li

PUBLISHED IN: Frontiers in Bioengineering and Biotechnology

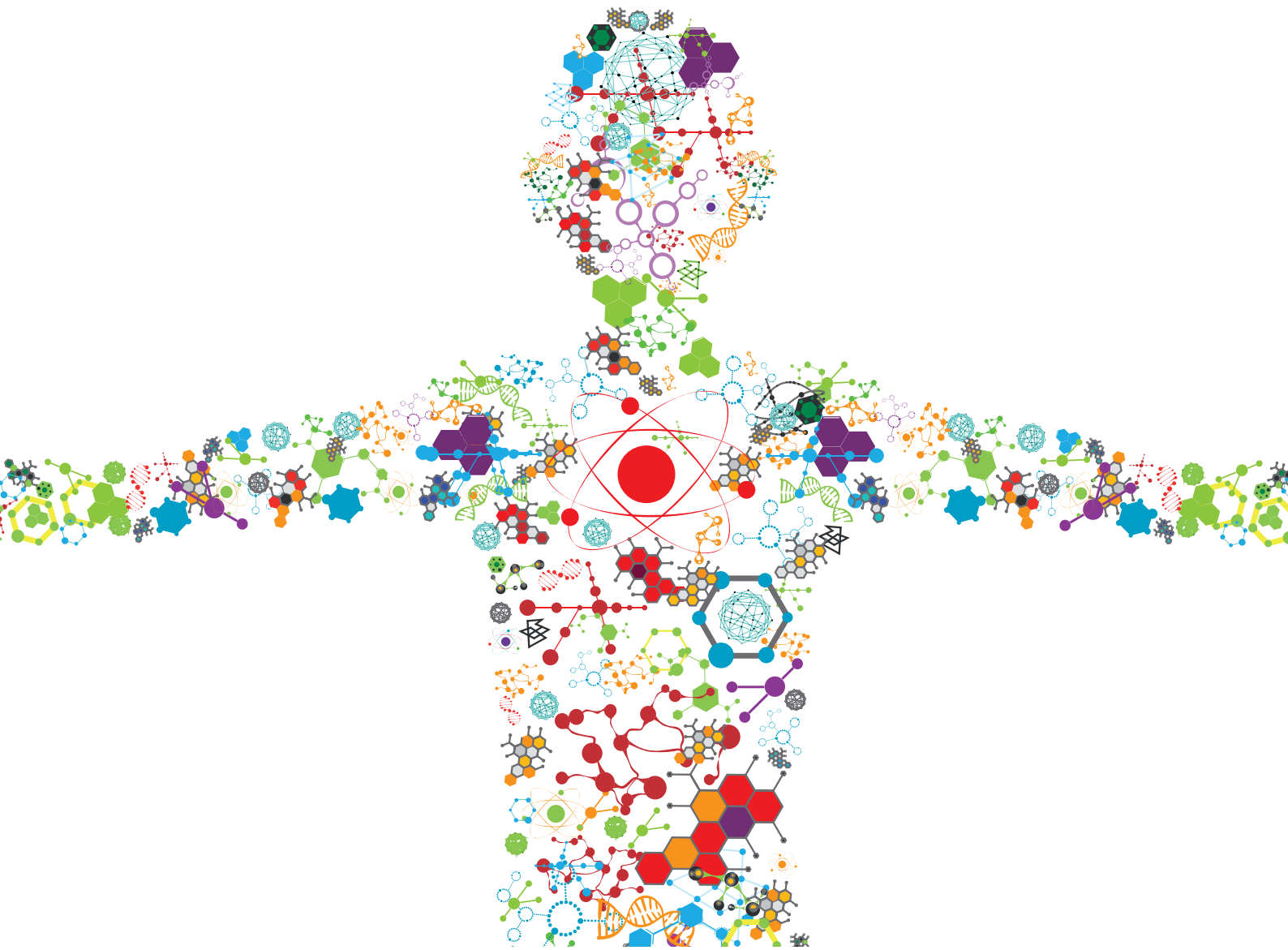

frontiers Research Topics

ISSN 1664-8714
ISBN 978-2-88976-690-1
DOI 10.3389/978-2-88976-690-1

About Frontiers

Frontiers is more than just an open-access publisher of scholarly articles: it is a pioneering approach to the world of academia, radically improving the way scholarly research is managed. The grand vision of Frontiers is a world where all people have an equal opportunity to seek, share and generate knowledge. Frontiers provides immediate and permanent online open access to all its publications, but this alone is not enough to realize our grand goals.

Frontiers Journal Series

The Frontiers Journal Series is a multi-tier and interdisciplinary set of open-access, online journals, promising a paradigm shift from the current review, selection and dissemination processes in academic publishing. All Frontiers journals are driven by researchers for researchers; therefore, they constitute a service to the scholarly community. At the same time, the Frontiers Journal Series operates on a revolutionary invention, the tiered publishing system, initially addressing specific communities of scholars, and gradually climbing up to broader public understanding, thus serving the interests of the lay society, too.

Dedication to Quality

Each Frontiers article is a landmark of the highest quality, thanks to genuinely collaborative interactions between authors and review editors, who include some of the world's best academicians. Research must be certified by peers before entering a stream of knowledge that may eventually reach the public - and shape society; therefore, Frontiers only applies the most rigorous and unbiased reviews.
Frontiers revolutionizes research publishing by freely delivering the most outstanding research, evaluated with no bias from both the academic and social point of view. By applying the most advanced information technologies, Frontiers is catapulting scholarly publishing into a new generation.

What are Frontiers Research Topics?

Frontiers Research Topics are very popular trademarks of the Frontiers Journals Series: they are collections of at least ten articles, all centered on a particular subject. With their unique mix of varied contributions from Original Research to Review Articles, Frontiers Research Topics unify the most influential researchers, the latest key findings and historical advances in a hot research area! Find out more on how to host your own Frontiers Research Topic or contribute to one as an author by contacting the Frontiers Editorial Office: frontiersin.org/about/contact

VALUE-ADDED PRODUCTS FROM AGRO-INDUSTRIAL RESIDUES BY BIOLOGICAL APPROACHES

Topic Editors:
Xiaoyan Liu, Huaiyin Normal University, China
Zhipeng Wang, Qingdao Agricultural University, China
Myeong-Sok Lee, Sookmyung Women's University, South Korea
Jun Xia, Huaiyin Normal University, China
Shangyong Li, Qingdao University, China

Citation: Liu, X., Wang, Z., Lee, M.-S., Xia, J., Li, S., eds. (2022). Value-Added Products from Agro-Industrial Residues by Biological Approaches. Lausanne: Frontiers Media SA. doi: 10.3389/978-2-88976-690-1

Table of Contents

frontiers | Frontiers in Bioengineering and Biotechnology

TYPE Editorial
PUBLISHED 21 October 2022
DOI 10.3389/fbioe.2022.990004

OPEN ACCESS

EDITED AND REVIEWED BY
Helen Treichel,
Universidade Federal da Fronteira Sul, Brazil

*CORRESPONDENCE
Zhi-Peng Wang,
wangzpmbio@163.com
Shang-Yong Li,
lisy@qau.edu.cn
Xiao-Yan Liu,
lxy@hytc.edu.cn
Jun Xia,
xiajun050219@126.com

SPECIALTY SECTION
This article was submitted to Bioprocess Engineering, a section of the journal Frontiers in Bioengineering and Biotechnology

RECEIVED 09 July 2022
ACCEPTED 11 October 2022
PUBLISHED 21 October 2022

CITATION
Wang Z-P, Li S-Y, Liu X-Y and Xia J (2022), Editorial: Value-added products from agro-industrial residues by biological approaches.
Front. Bioeng. Biotechnol. 10:990004.
doi: 10.3389/fbioe.2022.990004

Editorial: Value-added products from agro-industrial residues by biological approaches

Zhi-Peng Wang[1]*, Shang-Yong Li[2]*, Xiao-Yan Liu[3]* and Jun Xia[3]*

[1]School of Marine Science and Engineering, Qingdao Agricultural University, Qingdao, China, [2]School of Basic Medicine, Qingdao University, Qingdao, China, [3]Jiangsu Collaborative Innovation Center of Regional Modern Agriculture & Environmental Protection, Huaiyin Normal University, Huaian, China

KEYWORDS

value-added products, agro-industrial residues, biological approaches, fermentation, enzyme

Editorial on the Research Topic
Value-added products from agro-industrial residues by biological approaches

Agro-industrial residues at low costs are generated in a considerable amount along the whole chain from harvesting to deep processing. Developing high value-added products with these residues instead of costly food materials has been recommended recently and is supposed to be of increasing economic importance. However, few processes based on biological means are proved feasible economically at present. Optimizing the methods of pretreating different residues or integrating their pretreatment and the subsequent bioprocess is capable of making the value-added production more efficient. From another perspective, creating strategies for the recovery of bioactive molecules from agro-industrial residues is critical to the sustainable development of a bio-based economy.

This Research Topic encompasses ten original research articles and two review articles focusing on this field. Each article shares a remarkable insight into agro-industrial residues, construction of bioprocess, and/or potential applications. The Research Topic centers on the advance of enabling biological approaches and the discovery of functional components (Figure 1). It is expected to see that some descriptions in the Research Topic can present numerous integrated strategies and demonstrate their practical applications to yield value-added products.

Generally, fermentation is the first choice for residue processing. Value-added bioactive compounds can be produced by fermentation using various microorganisms. The fermentation product becomes a participant in microbial cell metabolism or is extracted under the microorganism's action. Scholars have designed different fermentation routes to maximize the conversion efficiency of the residues. *Aspergillus ibericus* has been used in the solid-state fermentation (SSF) of brewers' spent grain, which is a fungus without mycotoxin production and has good performance in hydrolyzing the lignocellulosic matrix of agro-industrial residues. Being rich in xylanase and cellulase, the

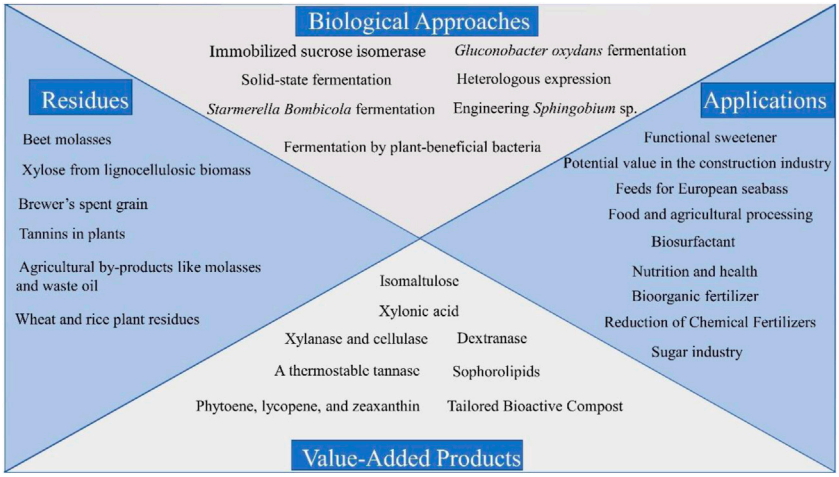

FIGURE 1
A general categorization of the keywords of the ten research articles.

crude extract can serve as an enzyme supplement to aquafeed given to European seabass (*Dicentrarchus labrax*) juveniles, thereby playing a promoting role in feed and protein utilization (Fernandes et al.). Imran et al. proposed a feasible strategy to produce composted organic fertilizer with wheat and rice crop residues and enriched the compost with plant-beneficial bacteria. They found tomato and chili pepper had better growth and a higher yield in the presence of bioactive compost. Thus, an effective way to manage rapidly increasing farm waste is to convert it into compost.

Submerged fermentation based on engineered strains derived from residues has been reported feasible for the bioproduction of chemicals. Liu et al. engineered *Sphingobium* sp. to enrich various carotenoids from common agro-industrial residues, such as soybean meal, soy pulp, and corn steep liquor. Astaxanthin, a member of the carotenoid family, has been biosynthesized at high titer with *Sphingobium* sp., which highlights the potential of microorganisms as resources of industrial importance. Another study indicates that transforming the *Vitreoscilla hemoglobin* gene into *S. bombicola* is conducive to alleviating oxygen limitation (Li et al.). The findings provide evidence to enhance the efficiency of oxygen utilization by *S. bombicola* in the production of SLs on an industrial scale with agro-industrial residues (e.g., molasses and waste oil) as fermentation feedstock.

Notably, agro-industrial residues with unique composition in two articles contribute to efficient bioproduction (He et al.; Wang et al.). With high sucrose content, beet molasses acted as the substrate for isomaltulose production. Immobilized SIase showed good reusability in repeated batch reactions of converting beet molasses pretreated under optimal conditions into isomaltulose. The sucrose conversion reached 97.5% in the first batch and was still higher than 94% after 11 batches (Wang et al.). The process is effective and promising for the industrial production of the functional sweetener isomaltulose. Xylose in a large amount fails to be metabolized and fermented efficiently because lignocellulosic biorefinery is subjected to strain limitations. Therefore, xylonic acid with great value in the construction industry is selected as a substitute for xylose in biorefinery. However, low productivity poses a challenge to xylonic acid fermentation. For this reason, response surface methodology was employed to optimize the specific productivity of xylonic acid. The study made clear the effects of three reaction parameters (biomass concentration, agitation, and aeration) on the production of xylonic acid by *Gluconobacter oxydans* and optimized key process parameters (Wang et al.). These results can provide reference for the efficiency improvement of biotransforming xylose into xylonic acid.

Lemes et al. overviewed the main bioactive components of agro-industrial residues and their biological extraction strategies. The researches provide information to broaden the applications of these bioactive components, especially in the pharmaceutical and food industries. Ma et al. reviewed the production of gluconic acid (GA) and its derivatives through microbial fermentation. They introduced the substitution of agro-industrial residues for carbon sources and integrated routes involving cascade hydrolysis, genetically modified strains, and/or micro- and nanofiltration with a membrane. The review outlines recent state-of-the-art progress, points out existing challenges, and puts forward the development direction of GA production.

Some reports reveal that tannins are partially responsible for the low food intake, growth rate, fodder utilization rate, and protein breakdown of laboratory animals. A study characterized a thermostable tannase sourced from *Aureobasidium melanogenum* T9 and probed into its secretory expression,

which was found to be a potential candidate for agricultural and food processing (Liu et al.). Dextran has received increasing attention as a primary pollutant found in sucrose production and storage. Since the hydrolysates of dextranase feature excellent thermal stability and simplicity, it has become a promising enzyme to remove dextran and yield isomaltotriose in the sugar industry (Liu et al.). Besides, both the microbial responses and fungal inhibition of agricultural soil pathogen to the reduction of chemical fertilizers were studied (Shen et al.; Shen et al.).

In conclusion, the valorization of agro-industrial residues helps build a bright future for a bio-based economy. The articles in this Research Topic are believed able to provide much contemporary and valuable information advantageous to the advancement of industrial biotechnology.

Author contributions

Z-PW, S-YL, X-YL, and JX drafted the Editorial. All authors listed have made a substantial, direct, and intellectual contribution to the work and approved it for publication.

Acknowledgments

The authors are thankful to the contributors to this Research Topic as well as the Editorial support of the Journal.

Conflict of interest

The authors declare that the research was conducted in the absence of any commercial or financial relationships that could be construed as a potential conflict of interest.

Publisher's note

frontiers in Bioengineering and Biotechnology

ORIGINAL RESEARCH
published: 16 July 2021
doi: 10.3389/fbioe.2021.691547

Direct Isomaltulose Synthesis From Beet Molasses by Immobilized Sucrose Isomerase

Qin-Qing Wang[1,2], Ming Yang[3], Jian-Hua Hao[4,5] and Zai-Chao Ma[1]**

[1] National Glycoengineering Research Center, State Key Laboratory of Microbial Technology, Shandong University, Qingdao, China, [2] School of Marine Sciences, Sun Yat-sen University, Guangzhou, China, [3] Helmholtz International Lab for Anti-Infectives, Shandong University-Helmholtz Institute of Biotechnology, State Key Laboratory of Microbial Technology, Shandong University, Qingdao, China, [4] Key Laboratory of Sustainable Development of Polar Fishery, Ministry of Agriculture and Rural Affairs, Yellow Sea Fisheries Research Institute, Chinese Academy of Fishery Sciences, Qingdao, China, [5] Laboratory for Marine Drugs and Bioproducts, Qingdao National Laboratory for Marine Science and Technology, Qingdao, China*

OPEN ACCESS

Edited by:
Helen Treichel, Universidade Federal da Fronteira Sul, Brazil

Reviewed by:
Vesna Milorad Vučurović, University of Novi Sad, Serbia
Małgorzata Krzywonos, Wrocław University of Economics, Poland

***Correspondence:**
Jian-Hua Hao
haojh@ysfri.ac.cn
Zai-Chao Ma
mazc@sdu.edu.cn

Specialty section:
This article was submitted to Bioprocess Engineering, a section of the journal Frontiers in Bioengineering and Biotechnology

Received: *06 April 2021*
Accepted: *23 June 2021*
Published: *16 July 2021*

Citation:
Wang Q-Q, Yang M, Hao J-H and Ma Z-C (2021) Direct Isomaltulose Synthesis From Beet Molasses by Immobilized Sucrose Isomerase. Front. Bioeng. Biotechnol. 9:691547. doi: 10.3389/fbioe.2021.691547

Isomaltulose is becoming a focus as a functional sweetener for sucrose substitutes; however, isomaltulose production using sucrose as the substrate is not economical. Low-cost feedstocks are needed for their production. In this study, beet molasses (BM) was introduced as the substrate to produce isomaltulose for the first time. Immobilized sucrose isomerase (Slase) was proved as the most efficient biocatalyst for isomaltulose synthesis from sulfuric acid (H_2SO_4) pretreated BM followed by centrifugation for the removal of insoluble matters and reducing viscosity. The effect of different factors on isomaltulose production is investigated. The isomaltulose still achieved a high concentration of 446.4 ± 5.5 g/L (purity of 85.8%) with a yield of 0.94 ± 0.02 g/g under the best conditions (800 g/L pretreated BM, 15 U immobilized Slase/g dosage, 40°C, pH of 5.5, and 10 h) in the eighth batch. Immobilized Slase used in repeated batch reaction showed good reusability to convert pretreated BM into isomaltulose since the sucrose conversion rate remained 97.5% in the same batch and even above 94% after 11 batches. Significant cost reduction of feedstock costs was also confirmed by economic analysis. The findings indicated that this two-step process to produce isomaltulose using low-cost BM and immobilized Slase is feasible. This process has the potential to be effective and promising for industrial production and application of isomaltulose as a functional sweetener for sucrose substitute.

Keywords: beet molasses, isomaltulose, sucrose isomerase, immobilization, economic analysis

INTRODUCTION

Molasses is a viscous by-product of sugar refineries with a sweet taste and color ranging from brown to dark-brown, which mainly includes cane molasses (CM), soy molasses (SM), and beet molasses (BM). The molasses is rich in sucrose and is also composed of a minimum amount of carbohydrates (like glucose) and other components (e.g., proteins, vitamins, and heavy metals) (Wang et al., 2019a; Palmonari et al., 2020). Particularly, large amounts of BM, annually, (more than 300,000 tons) were

discharged in China in the past years, and only a little amount was used as grinding aid, feed, and carbon source (Gao et al., 2011; Yan et al., 2011), aggravating BM waste and causing serious environmental concerns. In other countries, BM has been utilized as sucrose-containing feedstock for microbes to produce value-added products, such as bioethanol (Razmovski and Vučurović, 2012; Vučurović et al., 2019), lipids (Taskin et al., 2016), hydrogen (Emrah et al., 2018), baker's yeast (Ferrari et al., 2001), and inulinase (Germe and Turhan, 2020). Therefore, BM is a very valuable raw material. Recently, BM has attracted increasing attention for different industrial applications worldwide, including China, due to its higher sucrose content (about 50%) than those (about 30–50%) of other molasses (Álvarez-Cao et al., 2019; Ozdal and Başaran Kurbanoglu, 2019; Wang et al., 2019a; Zheng et al., 2019; Palmonari et al., 2020; Zhan et al., 2020).

Sucrose is of importance as a widely used sweetener in the daily diet; however, high sucrose diet could trigger health problems, such as obesity, dental caries, type 2 diabetes, and Alzheimer's disease, due to the rapid increase in blood glucose and high sweet content of sucrose (Tian et al., 2019; Du et al., 2020; Yeh et al., 2020). Therefore, safe sweeteners with suitable sweetness were required for sucrose alternatives. Isomaltulose shows a similar appearance and taste to sucrose (Zhang et al., 2020) and has approximately 50% sweetening power of sucrose (Shyam et al., 2018). In addition, isomaltulose has been authorized as "generally recognized as safe" by the United States Food and Drug Administration (Mu et al., 2014), sharing advantageous health benefits including lower glycemic index, lower calorie content, body-weight reduction, higher stability, more tooth-friendly, and promoting probiotics as well as prebiotics activities (Shyam et al., 2018; Lightowler et al., 2019; Wang et al., 2019a; Lee et al., 2020). Hence, isomaltulose is a promising functional sweetener and can be utilized as an available sucrose substitute.

As a structural isomer of sucrose, isomaltulose is a natural disaccharide consisting of glucose and fructose connected by α-1,6-glycosidic bond. It can be converted from sucrose through isomerization catalyzed by sucrose isomerase (SIase), which is primarily derived from microbial processes and also produces small amounts of trehalulose, glucose, and fructose (Liu et al., 2020; Zhang et al., 2020). SIase-producing microbes for isomaltulose biosynthesis have been mainly found in bacteria including *Pantoea dispersa* (Wu and Birch, 2004), *Enterobacter* spp. (Park et al., 2010), *Protaminobacter rubrum* (de Oliva-Neto and Menão, 2009), *Serratia plymuthica* (Duan et al., 2016), *Klebsiella* spp. (Li et al., 2003), and *Erwinia* spp. (Li et al., 2011). Recently, to improve isomaltulose production *via* a safe and efficient enzymatic method, various measures on heterologous expression of SIase gene, such as optimizing the promoter and/or signal peptide (Park et al., 2010; Zhang et al., 2018), site-directed mutagenesis for high thermostability (Duan et al., 2016), and displaying it on the cell surface of bacteria and fungi (Lee et al., 2011; Li et al., 2013, 2017; Wu et al., 2017; Zheng et al., 2019; Zhan et al., 2020), are explored. Among the targeted expression systems above, an ascomycetous yeast, *Yarrowia lipolytica*, seems to be the most attractive one based on relatively high isomaltulose yield (0.96 g/g) production (Li et al., 2017; Zhang et al., 2018). Noteworthily, sucrose substrate is indeed responsible for cell growth as a carbon source and isomerization of SIase during bioconversion processes, leading to the decrease of isomaltulose yield and unexpected products formation (Li et al., 2017; Zhang et al., 2018; Tian et al., 2019). The inner consumption of sucrose and non-target products formation are still inevitable, including using free or immobilized cells for isomaltulose production, suggesting that using free or immobilized SIase to produce isomaltulose directly will be expected to reduce the formation of non-target products (Li et al., 2003, 2011; Tian et al., 2019).

The cost of sucrose for isomaltulose production accounts for more than half of the total cost (Wang et al., 2019b). To reduce the cost of isomaltulose production for wide industrial applications, using cost-effective feedstocks as substrate apart from efforts in improving SIase expression is also needed. BM is a low-cost and readily available raw material, which has been employed as a carbon source for microbial growth; however, a strategy to use BM as a simple substrate for isomaltulose production has not been reported yet.

Several engineered *Y. lipolytica* strains with food grade can be used to produce isomaltulose from sucrose, CM, and SM (Zhang et al., 2018; Wang et al., 2019a,b). Pretreated SM was exactly used as a favorable substrate to produce isomaltulose by microbial fermentation (Wang et al., 2019b), and immobilized SIase could elevate the conversion rate of sucrose and isomaltulose concentration (Zhang et al., 2019). This study aims to explore the pretreatment and the effect of different factors on the potential of low-cost BM as the sole substrate for isomaltulose production using immobilized SIase. The final goal of this investigation is to reduce enzyme demand and explore the feasibility of this process for the industrial production of isomaltulose by economic analysis.

MATERIALS AND METHODS

Strain and Media

The yeast *Y. lipolytica* JD is a transformant carrying the strong promoter (TEFin) and SIase gene from *P. dispersa* UQ68J, which was cultivated in the medium containing glucose (30 g/L) and corn steep powder (20 g/L) with an initial pH of 6.0 for 72 h under the conditions of 30°C and 180 rpm to achieve extracellular SIase (49.3 U/mL) (Zhang et al., 2019). The strain JD was used for SIase production in this study. Another strain, *Y. lipolytica* G82, expressing the α-galactosidase gene was used to produce extracellular α-galactosidase (121.6 U/mL) when cultivated in the GPPB medium [containing 30 g/L glucose, 1.0 g/L $(NH_4)_2SO_4$, 6.0 g/L yeast extract, 2.0 g/L KH_2PO4, 3.0 g/L K_2HPO_4, and 0.1 g/L $MgSO_4.7H_2O$, pH 6.0] at 30°C for 3 days (Wang et al., 2019b).

Determination of Sugar Concentration of Molasses

Raw CM was obtained from a sugar refinery in Guangxi. Raw SM was provided from a local soybean oil factory, and raw

BM was supplied from Xinjiang. Different sugars contents of these raw molasses were detected by high-performance liquid chromatography (HPLC) using an Agilent 1200 system (Agilent Technologies, United States) and NH_2 column (Thermo Fisher Scientific, United States). The carbohydrates (e.g., sucrose, glucose, fructose, stachyose, xylose, galactose, isomaltulose, and trehalulose) were all calculated according to peak areas and retention time.

Pretreatment of BM

Beet molasses was treated as the described method (Cheng et al., 2017). Briefly, BM was acidified to the pH of 3 by 3 M sulfuric acid (H_2SO_4) and boiled for 5 min. The mixture would be centrifuged at 8,000 rpm for 30 min after keeping it at 4°C for about 12 h. $Ca(OH)_2$ was added to the supernatant obtained to adjust pH to 6. Then, it was centrifuged at the same condition to remove insoluble matters and evaporated to obtain the dry matter as 78.0%. Then, the pretreated BM was diluted with distilled water to the targeted content. The clarified molasses solution was stored at 4°C until further use.

SM Pretreated by α-Galactosidase

The pretreatment of SM was carried out by adding α-galactosidase with the activity of 121.6 U/mL from the crude fermentation broth of G82 strain, which was cultivated at 45°C and pH of 4.5 for 4 h, and the usage of α-galactosidase was 15 U/g of SM as described by Wang et al. (2019b). For sugar content determination, the obtained hydrolysate was analyzed by HPLC.

Isomaltulose Production Using Free and Immobilized SIase

Isomaltulose production was conducted by free SIase and immobilized SIase from the crude fermentation broth of *Y. lipolytica* strain JD using sucrose as substrate, BM, and pretreated BM. Crude-free SIase was obtained by centrifugation (10,000 × *g*, 20 min, 4°C). In addition, SIase immobilization was carried out according to the previous study (Zhang et al., 2019). Briefly, polyvinyl alcohol (PVA, 10%) and sodium alginate (1%) were mixed with distilled water to obtain the final concentration of 1 g/100 ml and autoclaved at 115°C for 20 min. Then, SIase solution (40 U/g) was dropped to the PVA-alginate mixture after cooling it to room temperature. The SIase-PVA-alginate suspension (2 ml) was added through syringe needle dropwise into the crosslink boric acid solution (pH 8.0) under continuous steering, and the beads of PVA-borate SIase were immersed in it for 2 h at 4°C to ensure sufficient gelation reaction. Subsequently, the beads were washed with distilled water to remove the excess borate ions from the surface. The enzyme recovery rate was defined as the ratio of immobilized SIase activity to total SIase activity. Free or immobilized SIase was added to 300 g/L sucrose or 500 g/L BM, with the SIase dosage of 15 U/g at 40°C and pH 6 in the isomerization process. The sucrose concentrations in 500 g/L raw BM and pretreated BM were 256 g/L and 304.5 g/L, respectively, making the sucrose contents similar to 300 g/L. The produced isomaltulose content was also analyzed by using HPLC.

Investigation of the Effect of Main Process Parameters on the Conversion of Pretreated BM to Isomaltulose

The catalysis condition of immobilized SIase was determined for the best of isomaltulose production using one-way ANOVA. The reaction factors pH (5.5–7.5), pretreated BM of different concentrations (400–900 g/L), and SIase adding dosages (5–25 U/g) were implemented for isomaltulose production. Corresponding sucrose concentrations in pretreated BM were 243.6 g/L, 304.5 g/L, 365.4 g/L, 426.3 g/L, 487.2 g/L, and 548.1 g/L, respectively. The reusability of immobilized SIase was evaluated under the best conditions for 16 cycles based on the conversion rate of the substrate at 40°C and pH 6.0. When the optimal duration of 12 h of each cycle was finished, the beads were filtrated with a 1 μm filter membrane and washed with distilled water, and then reused in the next cycle (Zhang et al., 2019). The contents of isomaltulose and others in the mixture in each cycle were determined by HPLC.

Process Parameters

Related parameters in this study were all calculated. Isomaltulose proportion (%) was calculated with the content of produced isomaltulose divided by total sugars containing other produced sugars and residual sugars. Sucrose proportion (%) was presented with the sucrose content divided by the content of molasses. The yield of isomaltulose using immobilized or free SIase (g/g) represents the isomaltulose content divided by the sucrose content in molasses. Sucrose conversion rate (%) was described as the consumed sucrose for isomaltulose production divided by the total sucrose content in molasses. The dosage of SIase (U/g) was calculated with enzyme activity (U) divided by sucrose content (g). The dosage of α-galactosidase (U/g) meant that enzyme activity (U) was divided by SM content (g).

Statistical Analysis

All tests were performed three times. The obtained data in experiments were analyzed through one-way ANOVA using SPSS 22.0 software (SPSS Inc., Chicago, MI, United States), and showed as mean ± SD. *p*-values were calculated by Student's *t*-test ($n = 3$), and considered statistically significant when $P < 0.05$.

RESULTS AND DISCUSSION

Difference of Sugar Content in Three Kinds of Molasses

Molasses as low-cost feedstock plays an important role in microbial production due to high sugar content (Zhan et al., 2020). The sucrose content is responsible for the performance to be the substrate for producing isomaltulose. The sucrose content (51.2%) and dry matter (78.3%) in BM were shown in **Figure 1A**, the sucrose proportion reached 97.2% in all the carbohydrates of BM, which is the highest among the molasses, including α-galactosidase treated SM. In addition to the major constituent sucrose, SM and CM had a higher content of other sugars. For instance, approximately 30% of monosaccharides

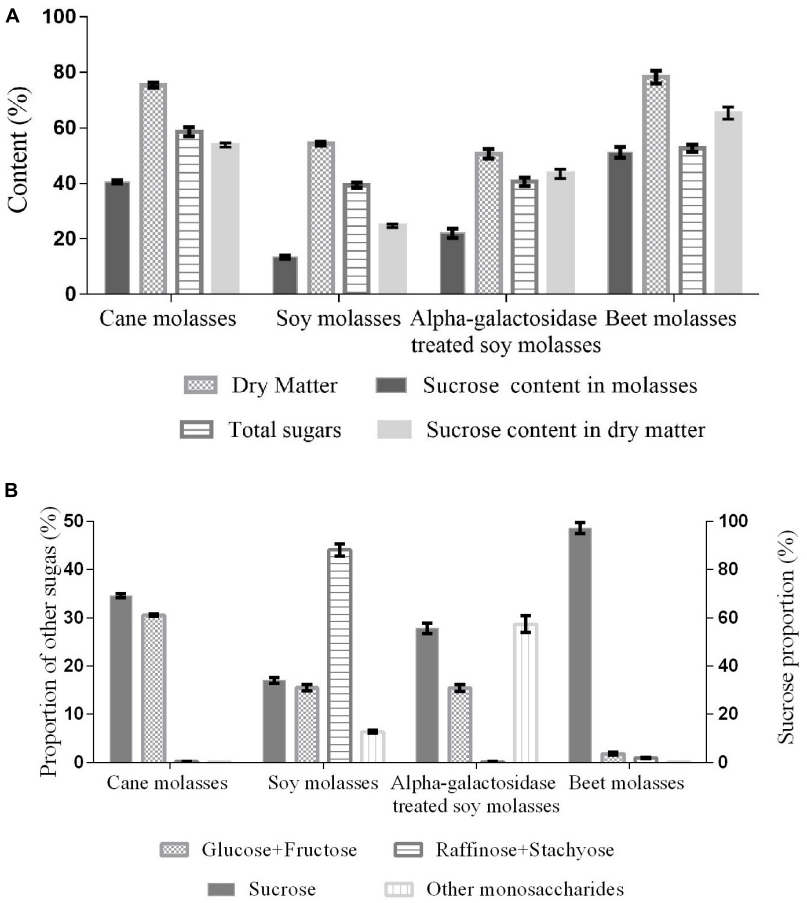

FIGURE 1 | Sugar content **(A)** and proportion **(B)** in different molasses.

(glucose and fructose) in CM and 44% of raffinose family oligosaccharides in SM were also exhibited (**Figures 1A,B**). This phenomenon possibly results from the differences in raw materials and processing technology of sugar manufacturing (Álvarez-Cao et al., 2019; Palmonari et al., 2020).

Feeding livestock with molasses is likely to bring metabolic diseases (urea toxicity, molasses toxicity, and bloat) (Senthilkumar et al., 2016). Microorganisms can use the sugars of molasses both as a carbon source and substrate through fermentation of food-grade strains to generate diverse high value-added products, such as bioethanol, α-galactosidase, and isomaltulose (Álvarez-Cao et al., 2019; Roukas and Kotzekidou, 2020; Zhan et al., 2020). For example, CM (350 g/L) could be used to produce 161.2 g/L isomaltulose by *Y. lipolytica* S47 strain (Wang et al., 2019a). By contrast, BM richer in sucrose than CM would show a higher capacity to serve as a suitable cost-effective substrate for isomaltulose production.

Comparison of Isomaltulose Production Using Free and Immobilized SIase

To avoid sucrose consumption and non-target products formation, specific enzyme catalysis application instead of free or immobilized microbial cells has been approved, which could improve substrate concentration and product purity (Zhang et al., 2019). As shown in **Figure 2**, the productions (287.8 ± 8.3 g/L) of isomaltulose synthesized by free SIase and immobilized SIase from sucrose were of the same highest values, and so did the yields (0.96 ± 0.03 g/g), among all the substrates. The results obtained keep the highest level from engineered *Y. lipolytica* strains using sucrose or CM to date (Zhang et al., 2018; Wang et al., 2019a).

Using immobilized SIase, the substrate pretreated BM achieved a higher isomaltulose production (240.8 g/L) and a higher yield (0.86 g/g) compared with free SIase, which were all significantly higher than those (198.8 g/L, 0.78 g/g) from raw BM using free or immobilized SIases (**Figure 2**). In contrast, the results obtained from raw BM decreased possibly due to the existence of metal ions restraining SIase activity. Most isomerases, including SIase, have been proved to be inhibited by metal ions, such as Ca^{2+}, Ba^{2+}, Cu^{2+}, Zn^{2+}, which are relatively rich in BM (Palmonari et al., 2020; Zhang et al., 2020). Pretreatment can reduce the content of those metal ions in BM, thus increasing the isomaltulose yield.

However, the production and yield of isomaltulose obtained from pretreated BM using immobilized SIase still hold distinctly

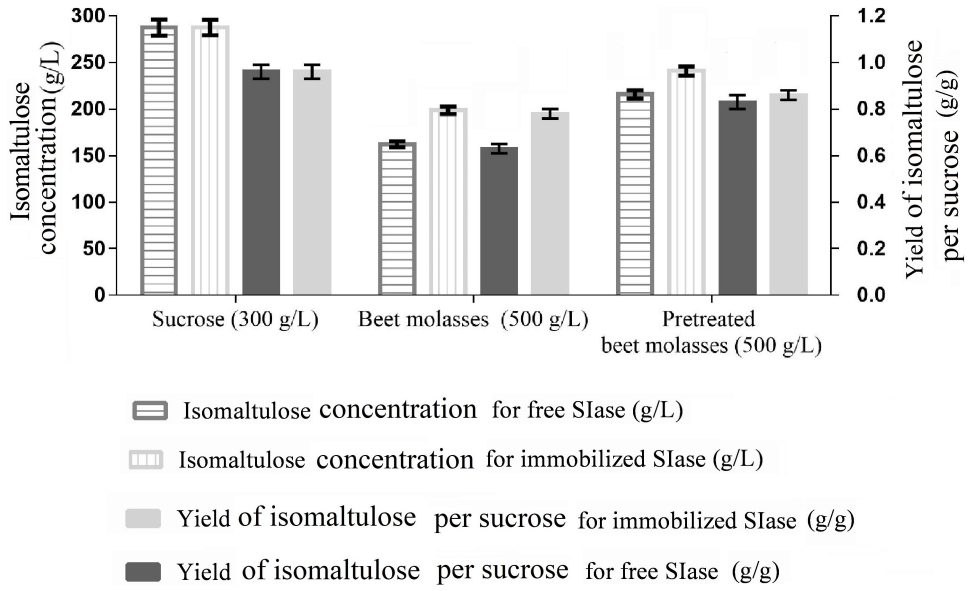

FIGURE 2 | Isomaltulose production from different substrates by free and immobilized sucrose isomerase (Slase) under the conditions of Slase dosage of 15 U/g, pH of 6, and temperature of 40°C.

higher levels than those catalyzed by different immobilized cells (such as *Erwinia* sp. D12, *Klebsiella* sp. K18, and *S. plymuthica* ATCC15928) (Mu et al., 2014) and many recombinant strains like *Escherichia coli* BL21(DE3) and *Y. lipolytica* (Li et al., 2017; Zheng et al., 2019; Zhang et al., 2020). The results confirmed that the pretreatment of BM is essential for efficient isomaltulose production. Simultaneously, immobilization of SIase benefits for production and yield of isomaltulose from pretreated BM.

The Effect of Main Process Parameters on Isomaltulose Production by Immobilized SIase

To further enhance the catalysis of immobilized SIase for isomaltulose synthesis, the catalysis conditions were examined. As exhibited in **Figure 3A**, isomaltulose was produced efficiently in a wide range of pH (5–7.5), especially ranging from 5 to 6, and the pH 5.5 was most suitable for isomaltulose synthesis, showing that the process is pH-dependent and agrees with the activity of immobilized SIase (Zhang et al., 2019). In general, high substrate concentration facilitates catalysis using the immobilized enzyme. It was observed that the production of isomaltulose was continually rising as pretreated BM concentration increased, while the yield showed no significant changes before 800 g/L pretreated BM but reduced remarkably beyond it (**Figure 3B**), achieving the best pretreated BM concentration of 800 g/L, containing 487.2 g/L of sucrose. The high concentration of pretreated BM could be used for isomaltulose production due to the good tolerance of the immobilized SIase to high sucrose concentration (700 g/L) (Zhang et al., 2019), and the H_2SO_4-based pretreatment removing insoluble matters and reducing the viscosity of BM (Cheng et al., 2017); however, the concentration of 900 g/L pretreated BM, equivalently with 668.7 g/L whole dry matter, was not dissolved very well, indeed, which would be the main point responsible for lowering the yield of isomaltulose. This finding is higher than 350 g/L CM but is similar to the reported 800 g/L SM used to produce isomaltulose (Wang et al., 2019a,b). Besides, the results in **Figure 3C** implied that 15 U/g of SIase was the best dosage from a series of dosages examined for isomaltulose production.

The reusability of immobilized SIase also needed to be evaluated in terms of industrial application. Under examined conversion conditions, the conversion rate of sucrose in pretreated BM remained at a high level exceeding 97.5% within the first eight cycles of repeated batches to produce isomaltulose (**Figure 3D**). Obviously, after which it decreased slightly from 9 to 11 cycles (>94%) and decreased rapidly beyond 11 cycles (**Figure 3D**). To avoid disturbing crystal separation of isomaltulose by other sugars and obtain high-purity isomaltulose, the eighth batch was terminated when the conversion rate of sucrose was about 97.5%. The finding was close to that (>90%) by using sucrose substrate isomerized to isomaltulose using the targeted SIase for the first 13 batches (Zhang et al., 2019). Meanwhile, Wu et al. (2016) found that bacterial SIase immobilized onto ε-PL-gelatin remained about 80% conversion rate of sucrose from pure sucrose for the first 156 h. The results stated that immobilized SIase has outstanding operational stability and good reusability using pretreated BM for industrial production of isomaltulose.

Analysis of Sugar Composition in the Final Reaction Liquid for Isomaltulose Production

Given the immobilized SIase of the eighth repeated batch still showed a high sucrose conversion rate (97.5%), we conducted the

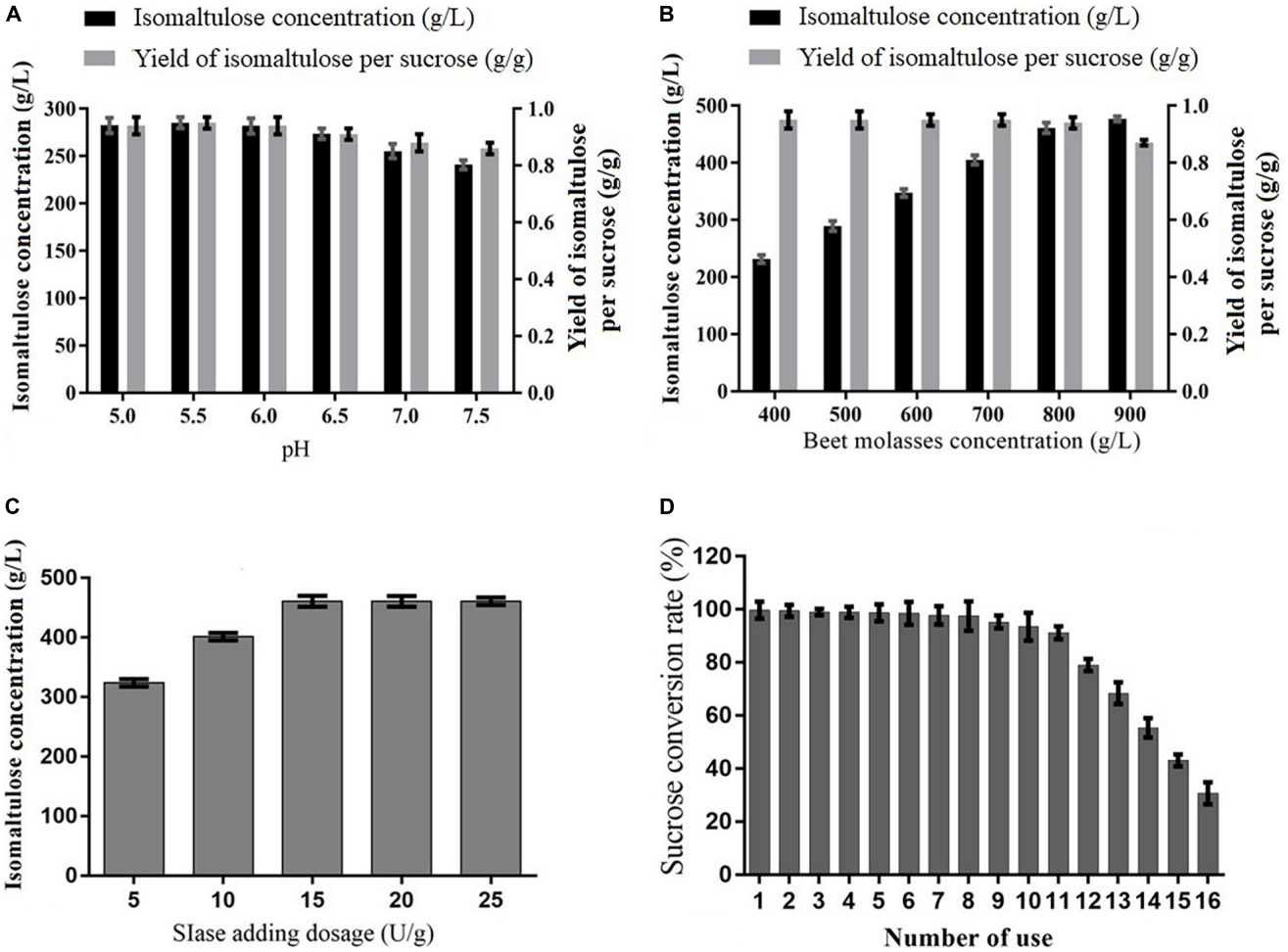

FIGURE 3 | Effects of different factors on isomaltulose production from pretreated beet molasses (BM) by immobilized SIase. **(A)** pH, **(B)** pretreated BM concentration, **(C)** SIase adding dosage, and **(D)** the effect of recycling number of immobilized SIase on sucrose conversion rate.

time course of the catalytic reaction. Under the best conditions (800 g/L pretreated BM, 40°C, 15 U SIase/g, pH 5.5) examined above, sucrose along with fast catalytic velocity was reduced to 12.18 g/L at 10 h (**Figure 4**). Meanwhile, isomaltulose was increasingly accumulated to 446.4 ± 5.5 g/L with the yield of 0.94 ± 0.02 g/g, yet small amounts of glucose and fructose (37.51 g/L), and trehalulose (24.1 g/L) were all slightly elevated due to hydrolysis and isomerization of SIase (**Figures 4**, **5**). The isomaltulose production was improved dramatically than that of an initial condition (**Figure 2**), which is much higher than those (184.8 g/L, 209.4 g/L, 212.6 g/L) produced by engineered *Y. lipolytica* strains and *Bacillus subtilis* from CM or SM (Wu et al., 2017; Wang et al., 2019b; Zheng et al., 2019). In contrast, the high yield (0.94 ± 0.02 g/g) observed is close to that (0.96 g/g) produced from pure sucrose (Zhang et al., 2018, 2019). These results demonstrated that most of the sucrose in pretreated BM is converted to isomaltulose within 10 h in the eighth batch.

As shown by HPLC analysis in **Figure 5**, the purity of produced isomaltulose in the final reaction liquid was further identified to be 85.8%, which is lower than (95.5%) pure sucrose (Zhang et al., 2019), but distinctly overs the purity of isomaltulose (64%) derived from SM by *Y. lipolytica* before using other strains to eliminate non-target sugars (Wang et al., 2019b). Interestingly, trehalulose only accounted for 4.6% of the total sugars, similar to the reported result (4%) (Wu and Birch, 2004). It may be attributed to little flux of sucrose to trehalulose supported by SIase and heavy metals, such as Ca^{2+}, Ba^{2+}, Cu^{2+}, Zn^{2+}, in BM inhibiting SIase activity (Palmonari et al., 2020; Zhang et al., 2020). Furthermore, dried isomaltulose syrup (content ≥80%), approved as GRAS (No. 681) in 2017 by FDA, can replace sucrose at the same level as sweeteners in foods and beverages (Tian et al., 2019).

Calculated with the conversion rate of the eighth batch, the total yield of isomaltulose per initial mass of pretreated BM was 0.558 g/g, while the total yield of isomaltulose per pure sucrose was 0.96 g/g. Considering the low cost of BM, the yield was desirable. In addition, by repeated enzymatic conversion, immobilized SIase (1 U) could catalyze the synthesis of 0.51 g of isomaltulose. Using fermented SIase

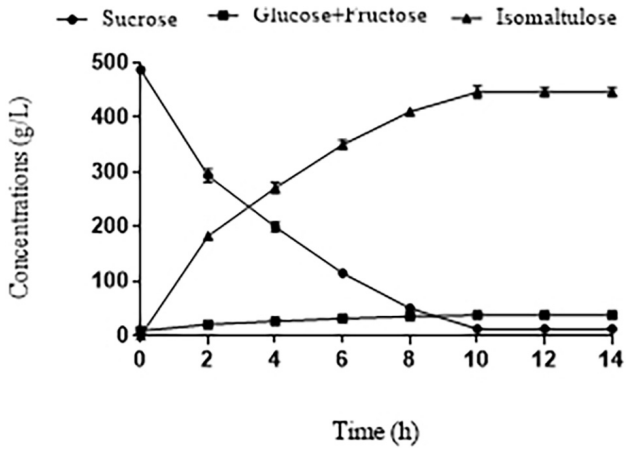

FIGURE 4 | Time course of sucrose conversion in pretreated BM under the best conditions (800 g/L pretreated BM, 40°C, 15 U/g of Slase, pH 5.5) by immobilized Slase in the eighth cycle.

TABLE 1 | Comparison of the costs from different substrates for isomaltulose production by different engineered food-grade strains and the purity of isomaltulose.

Strains	Substrate cost (yuan/ton isomaltulose)	Isomaltulose production (g/L)	Isomaltulose proportion (%)	References
Lactococcus lactis	Sucrose, 9000	36	<90	Park et al., 2010
Saccharomyces cerevisiae	Sucrose, 9000	<4	<10	Lee et al., 2011
Y. lipolytica	Sucrose, 8300	572.1	97.8	Zhang et al., 2018
Bacillus subtilis	CM, 3800	212.6	<92.4	Wu et al., 2017
Y. lipolytica	CM, 3600	161.2	97.4	Wang et al., 2019a
Y. lipolytica	SM, 3800	209.4	97.8	Wang et al., 2019b
Y. lipolytica	BM, 2700	446.4	85.8	This study

with an activity of 49.3 U/mL, SIase of 1 ml taken from the fermentation broth could catalyze the synthesis of 25 g of isomaltulose. Pretreatment can reduce the content of those metal ions in BM, thus increasing the isomaltulose yield and the immobilization of enzyme notably reduced the enzyme demand. These results indicated that the bioprocess using pretreated BM and immobilized SIase is a feasible alternative approach for isomaltulose production.

Comparison of the Cost for Isomaltulose Production

The cost of sucrose accounts for a substantial part of the total cost of producing isomaltulose based on the sole substitute sucrose or for microbial conversion needing sucrose and other nutrients (Zhang et al., 2019, 2020). The estimation of alternative feedstock cost is indispensable for sustainable industrial production of isomaltulose. The costs of feedstocks were based on the current market prices. As shown in **Table 1**, high substrate costs for isomaltulose production were evaluated by engineered strains cultivated from sucrose-containing substrates; however, the cost of single BM in this study was observed at 2700 yuan (RMB) per ton isomaltulose based on the whole yield (isomaltulose obtained from the substrate) (**Table 1**). This reduces the feedstock costs by 25–28.9% and by more than 70%, compared with the cost of other molasses and sucrose as the substrate (**Table 1**), respectively. More important, the immobilized SIase with high reusability could remarkably reduce the enzyme demand and production cost. The cost of the enzyme can

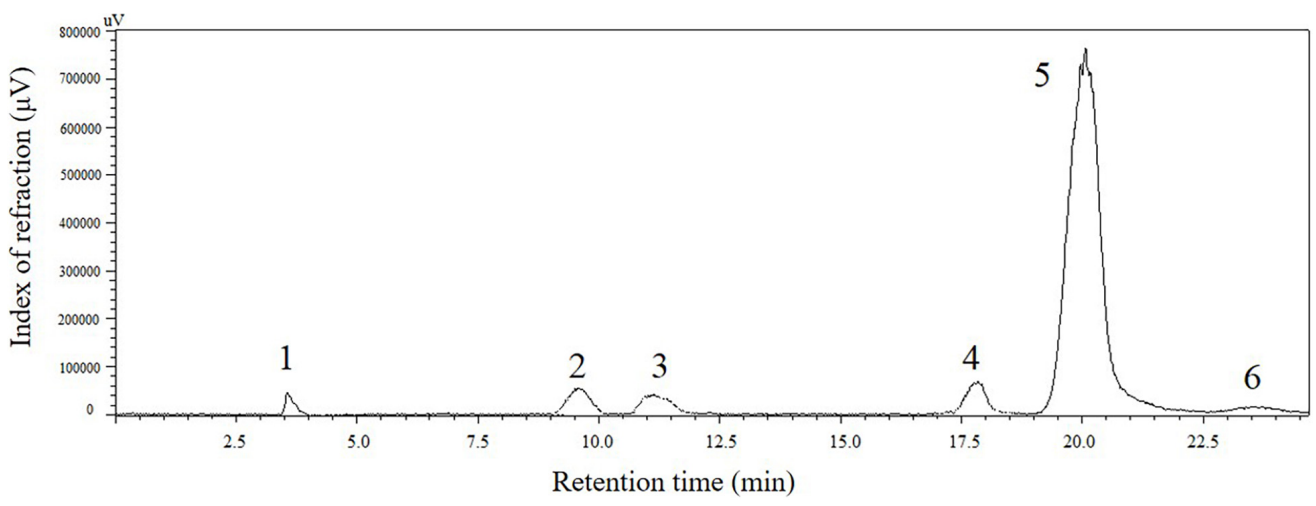

FIGURE 5 | High-performance liquid chromatography (HPLC) profile of products in catalytic liquid of pretreated BM using immobilized Slase in the eighth cycle at 10 h. The numbers from 1 to 6 represent solvent, glucose, fructose, sucrose, isomaltulose, and trehalulose, respectively.

be negligible, in general. Economic analysis revealed that significant cost reduction of isomaltulose production from low-cost BM in this study is reliable for industrial application.

CONCLUSION

A two-step process for isomaltulose production from cost-effective BM instead of sucrose was introduced. The H_2SO_4 pretreated BM confirmed a more efficient substrate to synthesize isomaltulose than untreated BM, and the immobilized SIase using pretreated BM as a substrate was verified to be the best for isomaltulose production. This process could produce a high concentration level of isomaltulose of 446.4 ± 5.5 g/L with a yield of 0.94 g/g and a purity of 85.8% under the best conditions in the eighth batch, and also remain 97.5% of the sucrose conversion rate. Immobilized SIase used in repeated batch reaction showed good reusability to convert pretreated BM into isomaltulose. It is also economically feasible as shown by economic analysis. This study provides an economical, effective, and promising approach for potential industrial isomaltulose production.

DATA AVAILABILITY STATEMENT

The original contributions presented in the study are included in the article/supplementary material, further inquiries can be directed to the corresponding authors.

AUTHOR CONTRIBUTIONS

Q-QW performed the experiment and wrote the manuscript. J-HH implemented fermentation and revised the manuscript. Z-CM designed the experiment and published the manuscript. All authors contributed to the article and approved the submitted version.

FUNDING

This research was funded by the Central Public-interest Scientific Institution Basal Research Fund, CAFS (No. 2020TD67) and Shandong Provincial Natural Science Foundation (ZR2016BQ42).

REFERENCES

Álvarez-Cao, M. E., Cerdán, M. E., González-Siso, M. I., and Becerra, M. (2019). Bioconversion of beet molasses to alpha-galactosidase and ethanol. *Front. Microbiol.* 10:405. doi: 10.3389/fmicb.2019.00405

Cheng, C., Zhou, Y., Lin, M., Wei, P., and Yang, S. T. (2017). Polymalic acid fermentation by *Aureobasidium pullulans* for malic acid production from soybean hull and soy molasses: fermentation kinetics and economic analysis. *Bioresour. Technol.* 223, 166–174. doi: 10.1016/j.biortech.2016.10.042

de Oliva-Neto, P., and Menão, P. T. P. (2009). Isomaltulose production from sucrose by *Protaminobacter rubrum* immobilized in calcium alginate. *Bioresour. Technol.* 100, 4252–4256. doi: 10.1016/j.biortech.2009.03.060

Du, Q., Fu, M., Zhou, Y., Cao, Y. P., Guo, T. W., Zhou, Z., et al. (2020). Sucrose promotes caries progression by disrupting the microecological balance in oral biofilms: an in vitro study. *Sci. Rep.* 10, 1–12.

Duan, X., Cheng, S., Ai, Y. X., and Wu, J. (2016). Enhancing the thermostability of *Serratia plymuthica* sucrose isomerase using B-factor-directed mutagenesis. *PLoS One* 11:e0149208. doi: 10.1371/journal.pone.0149208

Emrah, S., Siamak, A., Kamal, E., Harun, K., Ufuk, G., Inci, E., et al. (2018). Biological hydrogen production from sugar beet molasses by agar immobilized *R. capsulatus* in a panel photobioreactor. *Int. J. Hydrogen Energ.* 43, 14987–14995. doi: 10.1016/j.ijhydene.2018.06.052

Ferrari, M. D., Bianco, R., Froche, C., and Loperena, M. L. (2001). Baker's yeast production from molasses/cheese whey mixtures. *Biotechnol. Lett.* 23, 1–4.

Gao, X., Yang, Y., and Deng, H. (2011). Utilization of beet molasses as a grinding aid in blended cements. *Constr. Build. Mater.* 25, 3782–3789. doi: 10.1016/j.conbuildmat.2011.04.041

Germe, M., and Turhan, I. (2020). Thermostability of *Aspergillus niger* inulinase from sugar-beet molasses in the submerged fermentation and determination of its kinetic and thermodynamic parameters. *Biomass Convers. Bior.* doi: 10.1007/s13399-020-00809-8

Lee, E. J., Moon, Y., and Kweon, M. (2020). Processing suitability of healthful carbohydrates for potential sucrose replacement to produce muffins with staling retardation. *LWT* 131:109565. doi: 10.1016/j.lwt.2020.109565

Lee, G. Y., Jung, J. H., Seo, D. H., Hansin, J., Ha, S. J., Cha, J., et al. (2011). Isomaltulose production via yeast surface display of sucrose isomerase from *Enterobacter* sp. FMB-1 on *Saccharomyces cerevisiae*. *Bioresour. Technol.* 102, 9179–9184. doi: 10.1016/j.biortech.2011.06.081

Li, L. J., Wang, H. W., Cheng, H. R., and Deng, Z. X. (2017). Isomaltulose production by yeast surface display of sucrose isomerase from *Pantoea dispersa* on *Yarrowia lipolytica*. *J. Func. Foods* 32, 208–217. doi: 10.1016/j.jff.2017.02.036

Li, S., Cai, H., Qing, Y. J., Ren, B., Xu, H., Zhu, H. Y., et al. (2011). Cloning and characterization of a sucrose isomerase from *Erwinia rhapontici* NX-5 for isomaltulose hyperproduction. *Appl. Biochem. Biotech.* 163, 52–63. doi: 10.1007/s12010-010-9015-z

Li, S., Xu, H., Yu, J., Wang, Y., Feng, X., and Ouyang, P. (2013). Enhancing isomaltulose production by recombinant *Escherichia coli* producing sucrose isomerase: culture medium optimization containing agricultural wastes and cell immobilization. *Bioproc. Biosyst. Eng.* 36, 1395–1405. doi: 10.1007/s00449-012-0877-z

Li, X., Zhao, C., An, Q., and Zhang, D. (2003). Substrate induction of isomaltulose synthase in a newly isolated *Klebsiella* sp. LX3. *J. Appl. Microbiol.* 95, 521–527. doi: 10.1046/j.1365-2672.2003.02006.x

Lightowler, H., Schweitzer, L., Theis, S., and Henry, C. J. (2019). Changes in weight and substrate oxidation in overweight adults following isomaltulose intake during a 12-week weight loss intervention: a randomized, double-blind, controlled trial. *Nutrients* 11:2367. doi: 10.3390/nu11102367

Liu, L., Bilal, M., Luo, H. Z., Zhao, Y. P., and Duan, X. G. (2020). Studies on biological production of isomaltulose using sucrose isomerase: current status and future perspectives. *Catal. Lett.* 151, 1868–1881. doi: 10.1007/s10562-020-03439-x

Mu, W., Li, W., Wang, X., Zhang, T., and Jiang, B. (2014). Current studies on sucrose isomerase and biological isomaltulose production using sucrose isomerase. *Appl. Microbiol. Biot.* 98, 6569–6582. doi: 10.1007/s00253-014-5816-2

Ozdal, M., and Başaran Kurbanoglu, E. (2019). Use of chicken feather peptone and sugar beet molasses as low cost substrates for xanthan production by *Xanthomonas campestris* MO-03. *Fermentation* 5:9. doi: 10.3390/fermentation5010009

Palmonari, A., Cavallini, D., Sniffen, C. J., Fernandes, L., Holder, P., Fagioli, L., et al. (2020). Short communication: characterization of molasses chemical composition. *J. Dairy Sci.* 103, 6244–6249. doi: 10.3168/jds.2019-17644

Park, J. Y., Jung, J. H., Seo, D. H., Ha, S. J., Yoon, J. W., Kim, Y. C., et al. (2010). Microbial production of palatinose through extracellular expression of a sucrose isomerase from *Enterobacter* sp. FMB-1 in *Lactococcus lactis* MG1363. *Bioresour. Technol.* 101, 8828–8833. doi: 10.1016/j.biortech.2010.06.068

Razmovski, R., and Vučurović, V. (2012). Bioethanol production from sugar beet molasses and thick juice using *Saccharomyces cerevisiae* immobilized on maize stem ground tissue. *Fuel* 92, 1–8. doi: 10.1016/j.fuel.2011.07.046

Roukas, T., and Kotzekidou, P. (2020). Rotary biofilm reactor: a new tool for long-term bioethanol production from non-sterilized beet molasses by *Saccharomyces cerevisiae* in repeated-batch fermentation. *J. Clean. Prod.* 257:120519. doi: 10.1016/j.jclepro.2020.120519

Senthilkumar, S., Suganya, T., Deepa, K., Muralidharan, J., and Sasikala, K. (2016). Supplementation of molasses in livestock feed. *Int. J. Sci. Environ. Technol.* 5, 1243–1250.

Shyam, S., Ramadas, A., and Chang, S. K. (2018). Isomaltulose: recent evidence for health benefits. *J. Funct. Foods* 48, 173–178. doi: 10.1016/j.jff.2018.07.002

Taskin, M., Ortucu, S., Aydogan, M. N., and Arslan, N. P. (2016). Lipid production from sugar beet molasses under non-aseptic culture conditions using the oleaginous yeast *Rhodotorula glutinis* TR29. *Renewable Energy* 99, 198–204. doi: 10.1016/j.renene.2016.06.060

Tian, Y. Q., Deng, Y., and Zhang, W. M. (2019). Sucrose isomers as alternative sweeteners: properties, production, and applications. *Appl. Microbiol. Biot.* 103, 8677–8687.

Vučurović, V. M., Puskas, V. S., and Miljic, U. D. (2019). Bioethanol production from sugar beet molasses and thick juice by free and immobilised *Saccharomyces cerevisiae*. *J. I. Brewing* 125, 134–142. doi: 10.1002/jib.536

Wang, Z. P., Wang, Q. Q., Liu, S., Liu, X. F., Yu, X. J., and Jiang, Y. L. (2019a). Efficient conversion of cane molasses towards high-purity isomaltulose and cellular lipid using an engineered *Yarrowia lipolytica* strain in fed-batch fermentation. *Molecules* 24:1228. doi: 10.3390/molecules24071228

Wang, Z. P., Zhang, L. L., Liu, S., Liu, X. Y., Liu, X. Y., and Yu, X. J. (2019b). Whole conversion of soybean molasses into isomaltulose and ethanol by combining enzymatic hydrolysis and successive selective fermentations. *Biomolecules* 9:353. doi: 10.3390/biom9080353

Wu, L., and Birch, R. G. (2004). Characterization of *Pantoea dispersa* UQ68J: producer of a highly efficient sucrose isomerase for isomaltulose biosynthesis. *J. Appl. Microbiol.* 97, 93–103. doi: 10.1111/j.1365-2672.2004.02274.x

Wu, L., Qiu, J., Wu, S., Liu, X., Liu, C., Xu, Z., et al. (2016). Bioinspired production of antibacterial sucrose isomerase-sponge for the synthesis of isomaltulose. *Adv. Synth. Catal.* 358, 4030–4040. doi: 10.1002/adsc.201600705

Wu, L. T., Wu, S. S., Qiu, J. J., Xu, C. X., Li, S., and Xu, H. (2017). Green synthesis of isomaltulose from cane molasses by *Bacillus subtilis* WB800-pHA01-palI in a biologic membrane reactor. *Food Chem.* 229, 761–768. doi: 10.1016/j.foodchem.2017.03.001

Yan, D., Lu, Y., Chen, Y. F., and Wu, Q. (2011). Waste molasses alone displaces glucose-based medium for microalgal fermentation towards cost-saving biodiesel production. *Bioresour. Technol.* 102, 6487–6493. doi: 10.1016/j.biortech.2011.03.036

Yeh, S. H. H., Shie, F. S., Liu, H. K., Yao, H. H., Kao, P. C., Lee, Y. H., et al. (2020). A high-sucrose diet aggravates Alzheimer's disease pathology, attenuates hypothalamic leptin signaling, and impairs food-anticipatory activity in APPswe/PS1dE9 mice. *Neurobiol. Aging* 90, 60–74. doi: 10.1016/j.neurobiolaging.2019.11.018

Zhan, Y. J., Zhu, P., Liang, J. F., Xu, Z., Feng, X. H., Liu, Y., et al. (2020). Economical production of isomaltulose from agricultural residues in a system with sucrose isomerase displayed on *Bacillus subtilis* spores. *Bioproc. Biosyst. Eng.* 43, 75–84. doi: 10.1007/s00449-019-02206-6

Zhang, F., Cheng, F., Jia, D. X., Gu, Y. H., Liu, Z. Q., and Zheng, Y. G. (2020). Characterization of a recombinant sucrose isomerase and its application to enzymatic production of isomaltulose. *Biotechnol. Lett.* 43, 261–269. doi: 10.1007/s10529-020-02999-7

Zhang, P., Wang, Z. P., Liu, S., Wang, Y. L., Zhang, Z. F., Liu, X. M., et al. (2019). Overexpression of secreted sucrose isomerase in *Yarrowia lipolytica* and its application in isomaltulose production after immobilization. *Int. J. Biol. Macromol.* 121, 97–103. doi: 10.1016/j.ijbiomac.2018.10.010

Zhang, P., Wang, Z. P., Sheng, J., Zheng, Y., Ji, X. F., Zhou, H. X., et al. (2018). High and efficient isomaltulose production using an engineered *Yarrowia lipolytica* strain. *Bioresource Technol.* 265, 577–580. doi: 10.1016/j.biortech.2018.06.081

Zheng, Y., Wang, Z. P., Ji, X. F., and Sheng, J. (2019). Display of a sucrose isomerase on the cell surface of *Yarrowia lipolytica* for synthesis of isomaltulose from sugar cane by-products. *3 Biotech* 9:179.

Conflict of Interest: The authors declare that the research was conducted in the absence of any commercial or financial relationships that could be construed as a potential conflict of interest.

frontiers in Bioengineering and Biotechnology

ORIGINAL RESEARCH
published: 13 August 2021
doi: 10.3389/fbioe.2021.729988

Optimization of Specific Productivity for Xylonic Acid Production by *Gluconobacter oxydans* Using Response Surface Methodology

Tao He[1,2†], *Chaozhong Xu*[1,2†*], *Chenrong Ding*[1,2], *Xu Liu*[1,2] *and Xiaoli Gu*[1,2*]

[1]Jiangsu Co-Innovation Center of Efficient Processing and Utilization of Forest Resources, College of Chemical Engineering, Nanjing Forestry University, Nanjing, China, [2]Jiangsu Key Lab of Biomass-based Green Fuels and Chemicals, Nanjing, China

OPEN ACCESS

Edited by:
Zhipeng Wang,
Qingdao Agricultural University, China

Reviewed by:
Kris Niño Gomez Valdehuesa,
University of Manchester, United Kingdom
Jakub Zdarta,
Poznań University of Technology, Poland

***Correspondence:**
Chaozhong Xu
xucz@njfu.edu.cn
Xiaoli Gu
guxiaoli@njfu.edu.cn

†*These authors have contributed equally to this work and share first authorship*

Specialty section:
This article was submitted to Bioprocess Engineering, a section of the journal Frontiers in Bioengineering and Biotechnology

Received: *24 June 2021*
Accepted: *30 July 2021*
Published: *13 August 2021*

Citation:
He T, Xu C, Ding C, Liu X and Gu X (2021) Optimization of Specific Productivity for Xylonic Acid Production by Gluconobacter oxydans *Using Response Surface Methodology. Front. Bioeng. Biotechnol. 9:729988. doi: 10.3389/fbioe.2021.729988*

Large amounts of xylose cannot be efficiently metabolized and fermented due to strain limitations in lignocellulosic biorefinery. The conversion of xylose into high value chemicals can help to reduce the cost of commercialization. Therefore, xylonic acid with potential value in the construction industry offers a valuable alternative for xylose biorefinery. However, low productivity is the main challenge for xylonic acid fermentation. This study investigated the effect of three reaction parameters (agitation, aeration, and biomass concentration) on xylose acid production and optimized the key process parameters using response surface methodology The second order polynomial model was able to fit the experimental data by using multiple regression analysis. The maximum specific productivity was achieved with a value of 6.64 ± 0.20 g g_x^{-1} h^{-1} at the optimal process parameters (agitation speed 728 rpm, aeration rate 7 L min^{-1}, and biomass concentration 1.11 g L^{-1}). These results may help to improve the production efficiency during xylose acid biotransformation from xylose.

Keywords: xylonic acid, specific productivity, oxygen transfer, oxygen uptake, response surface methodology

INTRODUCTION

Xylose, which constitutes about 25% of the total biomass components, is unable to be converted in the lignocellulosic biorefinery process due to the limitation of microorganisms (Zaldivar et al., 2001). Therefore, the utilization of xylose is one of the key factors affecting the commercial production of lignocellulose (Nogue and Karhumaa, 2015). Currently, the bioconversion of xylose to xylonic acid is considered as a promising pathway and has gained much attention (Zhou et al., 2015, Zhou et al., 2017). Xylonic acid (XA), a bio-based chemical of great interest in recent years, is a non-toxic, non-volatile, non-corrosive, water-soluble organic acid. This aldonic acid compound has a similar structure and properties to gluconic acid, and shows a wide variety of applications in various fields. XA can be used as a dispersant to improve the dispersibility of concrete, which can effectively reduce the amount of concrete. In addition, XA has been also used as a raw material for chelating agent, antibiotic, polyamide, hydrogel modifier and 1,2,4-butanetriol precursor (Gupta et al., 2001; Deppenmeier et al., 2002; Chun et al., 2006).

Compared to other bacteria such as *Saccharomyces cerevisiae* and *Escherichia coli, Gluconobacter oxydans* has been the most productive in producing XA (Toivari et al., 2012a). *G. oxydans* is known for its rapid but incomplete oxidation of sugars and sugar alcohols as an obligate aerobic bacterium with a wide range of industrial applications (Toivari et al., 2012b; Zhang et al., 2016a). XA is derived

primarily from the further oxidation of xylose, relying on xylose dehydrogenase on the cell membrane of *G. oxydans* (Mientus et al., 2017). Then, XA is recovered from the culture broth by ion exchange or precipitation methods for downstream processing (Liu et al., 2012; Cao and Xu, 2019). Although *G. oxydans* shows great potential for XA fermentation, low production efficiency is the main challenge. For bioengineering, an important goal is to achieve high productivity in order to ensure an adequate supply of valued product and to reduce manufacturing costs (Handlogten et al., 2018). Therefore, improving the production efficiency of *G. oxydans* oxidized xylose would provide new options for large-scale production of XA.

For aerobic bacteria, the inability to utilize sufficient oxygen is the main cause of low productivity. Biochemically speaking, the xylose biocatalysis by *G. oxydans* is a closely coupled bio-oxidation reaction of cellular respiration and dehydrogenation that relies heavily on oxygen supply (Hoelscher et al., 2009). However, the solubility of oxygen in the broth is less than 0.21 mmol L^{-1}, and the metabolism of bacterial cells is significantly constrained (Hua et al., 2020), leading to a decrease in the catalytic performance of the biological process (Garcia-Ochoa and Gomez, 2009). Therefore, the level of oxygen utilization is a key factor in the final production efficiency.

Often, oxygen utilization is related to the interaction between the oxygen transfer and the oxygen uptake. During aerobic biological reactions, oxygen transfer is the process by which oxygen is transferred from the gas into the liquid phase to come into contact with the cells, while oxygen uptake is the process by which oxygen is utilized by the cells (Garcia-Ochoa et al., 2010). Theoretically, increasing the biomass concentration would enhance the level of oxygen uptake for aerobic biological reactions, but it would break the relationship between oxygen uptake and oxygen transfer. This leads to a decrease in the dissolved oxygen concentration in the broth and thus reduces the catalytic performance of the bacteria, which ultimately leads to a decrease in productivity. Therefore, it is necessary to adjust the appropriate level of oxygen transfer (by changing the agitation and aeration) and oxygen uptake (by changing the biomass concentration) to increase productivity.

To address these issues, this study attempts to use a response surface approach to improve the productivity of xylonic acid fermentation. Response surfaces were used to understand the interactions of aeration, agitation, and biomass concentration on the productivity of xylonic acid production from whole-cell catalytic xylose by *G. oxydans* using a statistical model. Optimized fermentation conditions were designed to address the low productivity limitations that exist in xylonic acid fermentation. These optimized conditions will provide guidance for the design of xylonic acid production process.

MATERIALS AND METHODS

Microorganism

G.oxydans NL71 purchased from Nanjing Forestry University of China, was stored on sorbitol agar (sorbitol 50 g L^{-1}, yeast extract 5 g L^{-1}, agar 15 g L^{-1}) at 4°C. The inoculum of *G. oxydans* NL71 was prepared in 250 ml shake flasks containing 50 ml of medium (sorbitol 50 g L^{-1}, yeast extract 5 g L^{-1}) and incubated at 220 rpm and 30°C for 24 h. The proliferation medium was centrifuged at 6,000 *g* for 5–10 min to collect cells, and the centrifuged cells were transferred to the fermentation medium on an ultra-clean bench (Zhou et al., 2015).

Whole-Cell Catalysis

The fermentation equipment consists of a stirred tank bioreactor, motor, and control system. Whole-cell catalysis is performed in a 5 L stirred tank reactor containing 3 L of production medium. The biotransformation medium: 5.0 g L^{-1} yeast extract, 0.5 g L^{-1} MgSO4, 1.0 g L^{-1} KH_2PO_4, 2.0 g L^{-1} K_2HPO_4 and 5.0 g L^{-1} $(NH_4)_2SO_4$ (Zhou et al., 2017). The temperature was maintained at 30°C throughout the fermentation process. The pH of the medium was monitored online by means of electrodes connected to the pH meter. The peristaltic pump was controlled to add 10% NaOH to maintain the pH at 5.5 automatically (Zhou et al., 2015; Zhang et al., 2017; Zhou et al., 2017).

Experimental Design and Statistical Optimization

A three-factor, three-level Box-Behnken experiment design was used, with specific productivity values (*Px*) as response values to understand the combined effect of agitation (A), aeration (B) and biomass concentration (C). **Table 1** shows the range of agitation, aeration, and biomass concentration of the RSM.

Fifteen experiments (**Table 2**) were designed using Design-Expert 12, and the fermentation results were finally subjected to multiple regression analysis to obtain the optimal fermentation conditions. A second-order polynomial equation was designed to express the predicted response (*Y*) as a polynomial equation in the independent variable (*A*-*C*), expressed as **Eq. 1**:

$$Y = x_0 + x_1A + x_2B + x_3C + x_{11}A^2 + x_{22}B^2 + x_{33}C^2 + x_{12}\mathrm{AB} + x_{13}\mathrm{AC} + x_{23}\mathrm{BC} \quad (1)$$

where *Y* is the response, $x_0$is the intercept coefficient,x_1,x_2, $x_3$are the linear coefficients andx_{11},x_{22},x_{33} are the squared coefficients; andx_{12}, x_{13}, andx_{23} are the interaction coefficients.

Biomass Measurement

The optical density (OD) of the cells was measured at 600 nm using a UV-Vis spectrophotometer (Ultrospec 2100, Amersham Biosciences Corp., United States). Samples were diluted with deionized water and a blank control was also used for the measurements.

Determination of Xylose and Xylonic Acid Content

The simultaneous determination of xylose and XA was performed using high performance anion exchange chromatography combined with pulsed amperometric detection (Thermo ICS-5000) using a CarboPac™ PA10 column (Wang et al., 2014). The samples were filtered (0.22 μm membrane) and injected (10 μL)

TABLE 1 | Experimental range of variables studied during designing of experiments.

Factors	Symbols and units	Coded levels		
		Low (-1)	Mid (0)	High (+1)
Agitation	A (rpm)	200	500	800
Aeration	B (L min^{-1})	1	4	7
Biomass concentration	C (g L^{-1})	1	1.5	2

TABLE 2 | Experimental matrix design.

Run	Factor A	Factor B	Factor C	Response: P_X
	Agitation (rpm)	Aeration (L min^{-1})	Biomass concentration (g L^{-1})	(g g_x^{-1} h^{-1})
1	200	1	1	0.32
2	200	7	1	1.28
3	500	4	1	5.75
4	800	1	1	6.00
5	800	7	1	6.33
6	200	4	1.5	0.94
7	500	1	1.5	4.67
8	500	4	1.5	5.50
9	500	7	1.5	5.76
10	800	4	1.5	6.01
11	200	1	2	0.33
12	200	7	2	0.93
13	500	4	2	3.18
14	800	1	2	4.07
15	800	7	2	4.45

on a CarboPac PA-10 guard column (2 mm × 50 mm) attached to a CarboPac PA-10 anion-exchange analytical column (2 mm × 250 mm). The column temperature was maintained at 30°C. 100 mM NaOH was used as mobile phase at a flow rate of 0.3 ml min^{-1}. Before each injection, the column was re-equilibrated by running for 15 min with 6 mM NaOH to achieve good repeatability.

Specific Productivity and Volumetric Productivity

XA specific productivity (P_X) was calculated for each experiment employing **Eq. 2**:

$$P_X = \frac{C_{XA}^{\max}}{C_X \cdot t^{\max}} \tag{2}$$

Volumetric productivity (Q_P) was calculated by **Eq. 3**:

$$Q_P = \frac{C_{XA}^{\max}}{t^{\max}} \tag{3}$$

where $C_{XA}^{\max}$ (g L^{-1}) is the maximum XA concentration for each experiment, C_X is the biomass concentration (g L^{-1}) and t^{max} (h) is the time in which the maximum XA concentration is reached.

Determination of k_La

The dissolved oxygen concentration was monitored using a fast dissolved oxygen electrode (605-ISM, Mettler Toledo, United States), and the k_La values were determined by the dynamic method. First, aeration was stopped, and dissolved oxygen levels were decreased to measure oxygen uptake rate. Then, the broth was reaerated with air until the steady state was reached, and k_La value was calculated by the dissolved oxygen mass balance equation (Garcia-Ochoa and Gomez, 2009).

RESULTS AND DISCUSSION

Statistical Analysis

In comparison to univariate experiments, RSM takes into account the interaction of all factors on response variables, and also obtains appropriate optimization conditions. In this study, the RSM examined the effect of three variables: agitation (A), aeration (B) and biomass concentration (C) on P_X. The evaluation results show that the model has 9 degrees of freedom (df) and the 'lack of fit' has 5 df, indicating that the design is suitable for model development. The model with second-order polynomial was defined according to the coding factor as follows:

$$Y = 5.21 + 2.31A + 0.3366B - 0.6698C - 0.1057\text{AB} - 0.4338\text{AC} - 0.0386\text{BC} - 1.67A^2 + 0.0725B^2 - 0.6721C^2 \tag{4}$$

The results in **Table 3** were verified by Fisher's test for analysis of variance (ANOVA), which showed that the experimental data fitted well with the second-order polynomial function. The Model

TABLE 3 | Analysis of variance (ANOVA) for all model terms.

Source	Sum of squares	df	Mean square	F-value	*p*-value
Model	77.82	9	8.65	44.44	<0.0001
A-Agitation	53.27	1	53.27	273.77	<0.0001
B-Aeration	1.13	1	1.13	5.80	0.0469
C-Biomass concentration	4.49	1	4.49	23.06	0.0020
AB	0.0894	1	0.0894	0.4597	0.5196
AC	1.50	1	1.50	7.71	0.0274
BC	0.0114	1	0.0114	0.0588	0.8154
A^2	7.44	1	7.44	38.21	0.0005
B^2	0.0141	1	0.0141	0.0723	0.7957
C^2	1.21	1	1.21	6.22	0.0413
Residual	1.36	7	0.1946	—	—
Lack of Fit	1.29	5	0.2580	7.14	0.1273
Pure Error	0.0722	2	0.0361	—	—
Cor Total	79.18	16	—	—	—

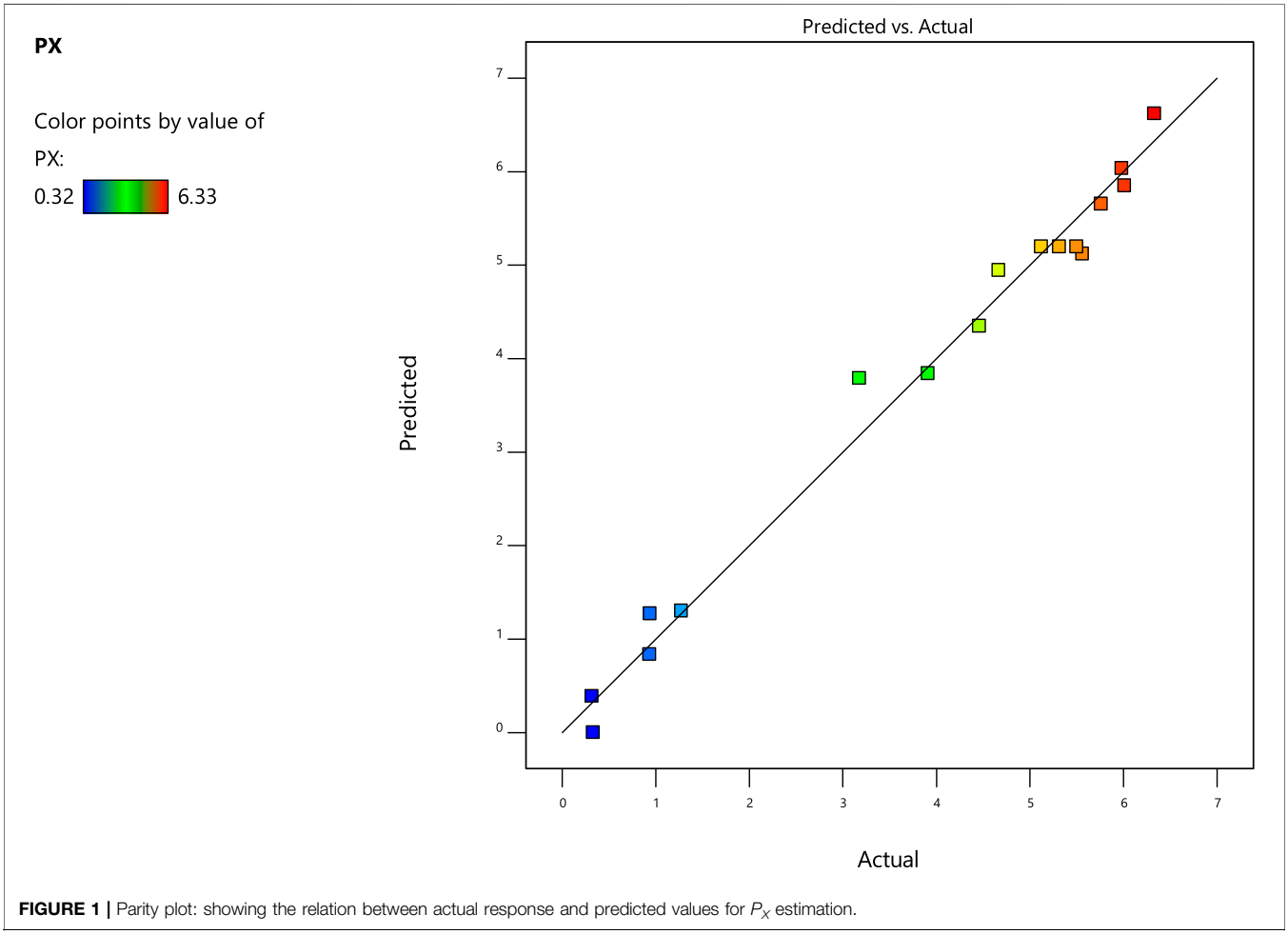

FIGURE 1 | Parity plot: showing the relation between actual response and predicted values for P_X estimation.

F-value of 44.44 implied the model was significant. The probability of not getting the results predicted by the regression model is only 0.01%. The large *p*-value for 'lack of fit' (0.1273 > 0.05) indicated that the "lack of fit" is not significant relative to the pure error. The R^2 value of 98.28% indicated that the response model explains 98.28% of the total variation. Usually, regression models with R^2 values above 0.9 are considered to have a robust correlation (Ávila-Lara et al., 2015). The value of the adjusted coefficient of determination (R^2_{Adj} = 96.07%) was also high enough to indicate the significance

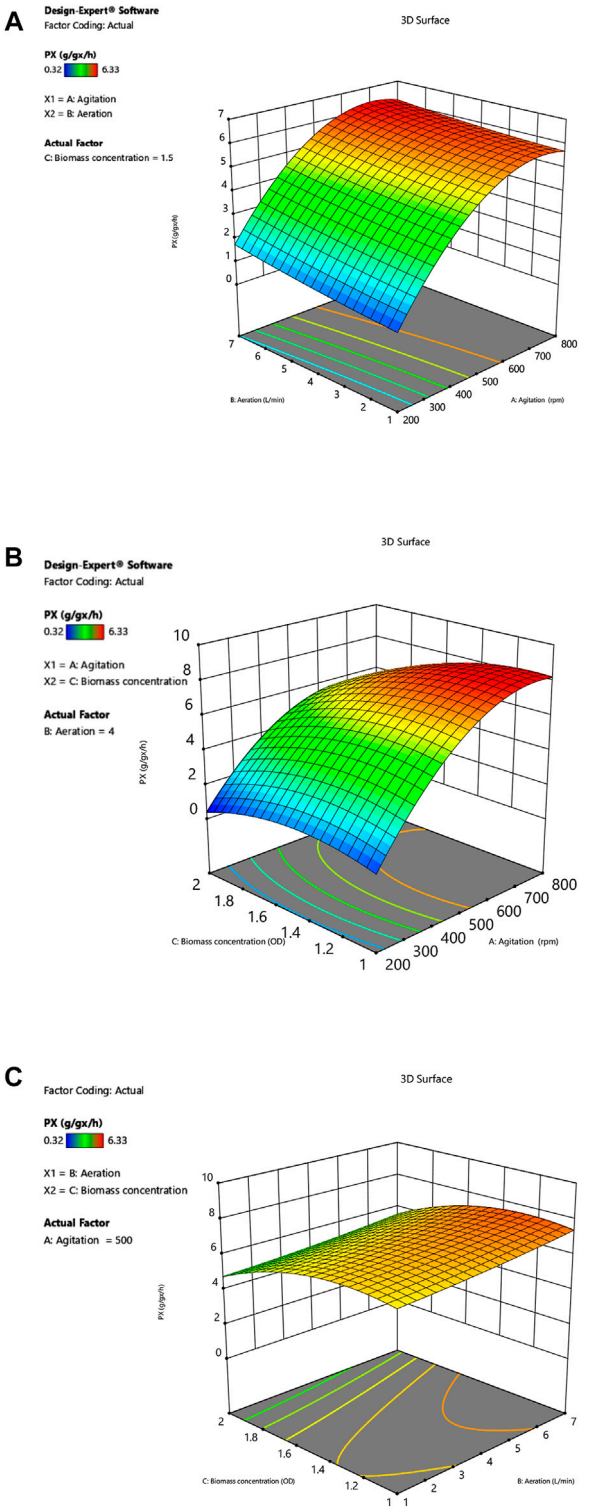

FIGURE 2 | (A) Interactive effect of agitation and aeration on P_X. **(B)** Interactive effect of agitation and biomass concentration on P_X. **(C)** Interactive effect of aeration and biomass concentration on P_X.

TABLE 4 | Mass transfer coefficients (k_La) in fermenters under different operating conditions.

Run	Agitation (rpm)	Aeration (L min^{-1})	k_La (s^{-1})
1	200	1	0.0018
6	200	4	0.0035
2	200	7	0.005
7	500	1	0.0143
3	500	4	0.029
9	500	7	0.037
4	800	1	0.04
10	800	4	0.08
5	800	7	0.11

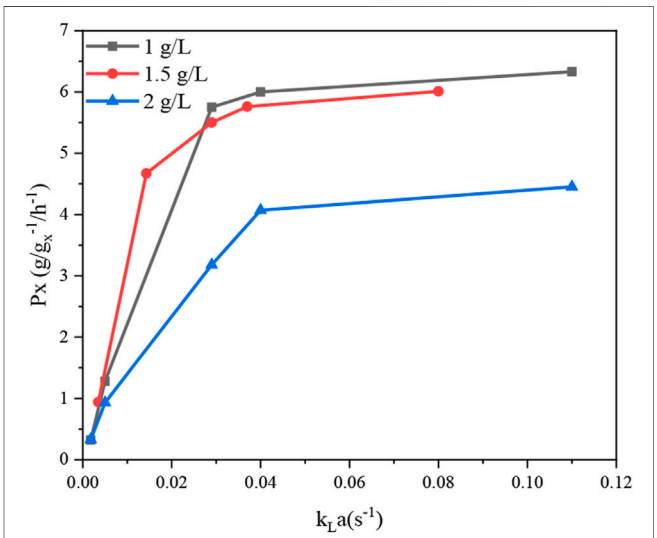

FIGURE 3 | Specific productivity of XA production using different concentrations of *G. oxydans* NL71 at different k_La conditions.

of the model. These results all suggest that the model can appropriately account for the cumulative as well as univariate effects of all selected variables on productivity in this biotransformation system.

Figure 1 shows the good correlation between the predicted values and the actual values. The predicted values of the model can match well with the actual values, indicating the good applicability of the model. The model gave the optimized levels of agitation speed (728 rpm), aeration rate (7 L min^{-1}), and biomass concentration (1.11 g L^{-1}), and experiments were conducted in the fermenter. The final P_X reached 6.64 ± 0.20 g g$_x^{-1}$ h^{-1}, which is slightly lower than the model value of 6.74 g g$_x^{-1}$ h^{-1}.

Interactive Effect of the Selected Variables on P_X

Three different response surface plots (**Figures 2A–C**) were used to determine the interaction effect between the selected variables

on P_X. In **Figure 2A**, the response surface plot shows that the P_X value was small at lower agitation speed and aeration rates; as the value of agitation and aeration increase, P_X was also enhanced. Theoretically, both agitation speed and aeration affect the oxygen transfer in the fermenter, and an increase in the agitation speed and aeration rates can effectively increase the oxygen transfer coefficient (k_La) in the fermenter (**Table 4**). Meanwhile, **Figure 3** shows that P_X was significantly improved as k_La was increased from 0.0018 s^{-1} to 0.04 s^{-1}, while the increase in P_X flattened out as k_La continued to increase. In addition, similar productivity was achieved when k_La was increased from 0.04 s^{-1} to 0.08 s^{-1} at a biomass concentration of 1 g L^{-1} and 1.5 g L^{-1}, respectively. From these results, it can be concluded that the production efficiency of *G.oxydans* can be effectively increased with an appropriate value of k_La. However, the production efficiency could not be further improved by increasing k_La to a higher level. It can be considered that the overall rate of the biological process is controlled by oxygen transfer when k_La is less than 0.04 s^{-1}. When increasing the oxygen transfer coefficient to more than 0.04 s^{-1}, the reaction efficiency cannot be further improved effectively. At this stage, the overall rate of the biological process is controlled by oxygen uptake. In addition, it can be observed that the curve of aeration is slightly curved on the surface. This observation suggests that the dominant factor in the interaction is agitation, which has been confirmed by previous studies (Dixit et al., 2015; Li et al., 2019). This is in agreement with the report of Pooja Dixit et al. (2015), who also found that agitation has the most decisive effect on k_La. The reason is that agitation reduces the bubble size and increases the gas-liquid contact area.

However, it can be observed that the P_X value tends to a plateau in the high agitation region (**Figure 2A**). In addition, an examination of the data (**Table 2**) showed that the increase in agitation value from 200 to 500 rpm (run no. 6 and 8) caused an increase in P_X value from 0.94 g g_x^{-1} h^{-1}–5.50 g g_x^{-1} h^{-1}, whereas an increase in agitation from 500 to 800 rpm (run no. 8 and 10) increased the P_X value from 5.50 g g_x^{-1} h^{-1}–6.01 g g_x^{-1} h^{-1}, which was not so significant as compared to previous experiments (run no. 6 and 8). It can be concluded that the improved oxygen transfer conditions brought about by the agitation speed of 800 rpm provide an adequate oxygen supply for oxygen uptake, thus enabling the maximum catalytic performance of the strain.

Figure 2B shows the dependence of P_X on biomass concentration C_X and agitation at a specific aeration rate. In the low agitation region, the value of P_X is small; as the agitation speed is enhanced, P_X is also increased. The P_X increase tends to level off when the agitation speed exceeds 500 rpm. The maximum *Px* of 6.33 g g_x^{-1} h^{-1} was reached at an agitation speed of 800 rpm, which indicates that the catalytic capacity of the bacteria is close to the maximum value at this operating condition. When the capacity of oxygen uptake was enhanced, the results showed that P_X instead decreased. It can be confirmed by comparing the data of run 3 and 13 (**Table 2**), where P_X decreased from 5.75 g g_x^{-1} h^{-1}–3.18 g g_x^{-1} h^{-1} by increasing the biomass concentration from 1 g L^{-1}–2 g L^{-1}. Previously, Yuan et al. (2016) reported similar observations and suggested that the oxygen limitation brought about by the growth of the bacterium at the beginning of fermentation could affect the expression of transhydrogenase on the *G. oxydans* membrane, which might reduce the catalytic performance of the bacteria. Theoretically, an increase in biomass concentration could improve the level of oxygen uptake, but the imbalance between oxygen uptake and oxygen transfer leads to lower dissolved oxygen levels in the medium. Lack of oxygen may affect the activity of enzymes on the cell membrane.

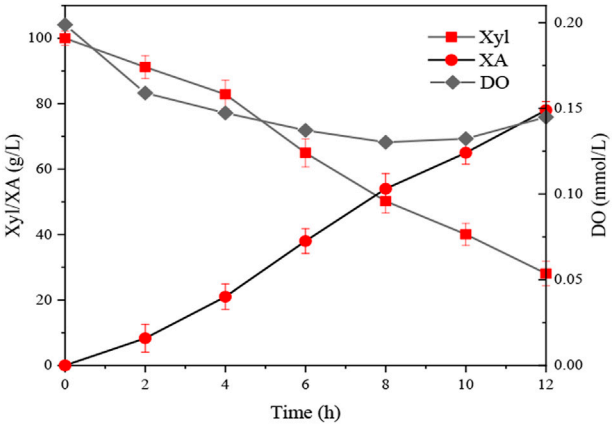

FIGURE 4 | XA production under the optimized conditions. Xyl = xylose; XA = xylonic acid; DO = dissolved oxygen.

Figure 2C depicts the effect of biomass concentration and agitation on P_X at a specific agitation rate. The response surface plots show that the interaction between aeration rate and biomass concentration on P_X is not significant. Although *Px* is appropriately enhanced by increasing aeration rate, simultaneous increase of in aeration and biomass concentration cause a decrease in P_X. The reason is that the increase in biomass concentration leads to an increase in oxygen demand by the cells, while the increase in aeration rate does not bring about optimal oxygen transfer conditions, resulting in oxygen transfer limitation.

Optimization of Specific Productivity for Xylonic Acid Fermentation

By solving **Eq. 4**, the optimal operating conditions were estimated to be agitation speed 728 rpm, aeration rate 7 L min^{-1}, and biomass concentration 1.11 g L^{-1} by response surface analysis. Triplicate fermentation experiments were conducted using the predicted optimal conditions to verify the applicability of **Eq. 4**. After 12 h of whole-cell catalysis, the DO, xylose, and XA content of the fermentation broth decreased from 0.200 mmol L^{-1} to 0.140 mmol L^{-1}, 100 g L^{-1} to 21.04 ± 2.6 g L^{-1}, and 0 g L^{-1} increased to 88.44 ± 2.7 g L^{-1}, respectively (**Figure 4**).The experimental value of P_X was 6.64 ± 0.20 g g_x^{-1} h^{-1}, which is in excellent agreement with the predicted value (6.74 g g_x^{-1} h^{-1}).

A Comparison of Specific Productivity for Xylonic Acid Fermentation in the Literature

It can be said that the commercialization of any fermentation technology is impossible without the economic cost considerations.

TABLE 5 | Comparative literature report on the production of XA under various process conditions.

References	Operating conditions	Strain	C_X (g L^{-1})	Xylose (g L^{-1})	Qp (g L^{-1} h^{-1})	P_X (g gx^{-1} h^{-1})
Present study	Agitation-728 rpm, aeration-7 L min^{-1}	*G. oxydans* NL71	1.11	100	7.37	6.64
Zhang et al. (2017)	Agitation-500 rpm, aeration-2.5 L min^{-1}	*G. oxydans* DSM 2003	2.50	63	5.42	2.17
Zhou et al. (2015)	Agitation-500 rpm, aeration-3 L min^{-1}	*G. oxydans* NL71	2	450	3.67	2.35
Zhou et al. (2017)	Agitation-500 rpm, aeration-3 L min^{-1}	*G. oxydans* NL71	6	300	32.5	5.26
Dai et al. (2020)	Agitation-300 rpm, aeration not mentioned	*G. oxydans* NL71	4	141	4.48	1.12
Zhou et al. (2019)	Agitation-300 rpm, aeration- L min^{-1}	*G. oxydans* NL71	10	200	7.10	0.71
Zhang et al. (2016b)	Agitation-500 rpm, aeration-2.5 L min^{-1}	*G. oxydans* DSM 2003	1.5	40	1.43	-
Hou et al. (2018)	Agitation-500 rpm, aeration-1 vvm	*G. oxydans* DSM 2003	5%	54	0.82	-
Hou et al. (2019)	Agitation-500 rpm, aeration-1 vvm	*G. oxydans* DSM 2003	5%	60	0.96	-
Yim et al. (2017)	Shaking at 200 rpm	*Corynebacterium glutamicum*	2%	20	1.02	-
Liu et al. (2012)	Agitation-650 rpm, aeration-0.5 vvm	*E. coli*	3.2	40	1.09	0.34
Toivari et al. (2010a)	Agitation-500 rpm, aeration-01 vvm	*S. cerevisiae Xyd1*	4.6	20	0.03	0.0065
Toivari et al. (2010b)	Agitation-500 rpm, aeration-01 vvm	*S. cerevisiae B67002 xylB*	7	49	0.44	0.06

Therefore, it is important to produce xylonic acid economically with a high volumetric productivity. In the literature, many strategies have been conducted to obtain high product titer of xylonic acid. For example, Toivari et al. (2012a) reported that *S. cerevisiae* was engineered to increase xylonic acid production by genetic engineering. 43 g L^{-1} of xylonic acid was produced in *S. cerevisiae B67002 xylB* with a specific productivity of 0.06 g g_x^{-1} h^{-1}. However, the much lower productivity compared to *G. oxydans* is still a serious weakness. Hahn et al. (2020) reported the effect of different nitrogen sources on the growth and subsequent xylonic acid production. With the addition of 0.32 g L^{-1} glutamate and 0.15 g L^{-1} ammonium sulfate as inexpensive nitrogen sources, a xylonic acid volumetric productivity of 2.92 g L^{-1} h^{-1} is obtained. The increase in the volumetric productivity was due to the higher cell content obtained by changing the medium conditions. However, the volumetric productivity of 2.92 g L^{-1} h^{-1} is still lower when compared to other literature. In shake flask fermentation, oxygen utilization is not the main issue. However, oxygen transfer limitations should be considered when the fermentation system changes from a shake flask to a fermenter. **Table 5** shows a comparison of the experimental results for xylonic acid production by other authors. Dai et al. (2020) reported an attempt to use powdered activated carbon treatment to reduce the viscosity of concentrated pre-hydrolysis products and other non-sugar compounds, and 143.6 g L^{-1} XA and *Qp* of 4.48 g L^{-1} h^{-1} were achieved at 300 rpm. Reducing the viscosity of the medium can change the physicochemical properties and improve the oxygen transfer coefficient, but the final *Px* of the biotransformation process was only 1.12 g g_x^{-1} h^{-1}.The result indicating that this mass transfer conditions was not sufficient to maximize the catalytic capacity of the strain. Zhang et al. (2017) reported the production of XA using xylose from cellulosic ethanol distillation distillate with a Qp of 5.42 g L^{-1} h^{-1} at 500 rpm and 2.5 L min^{-1}. This study provided a practical process option for the production of XA from lignocellulosic feedstock, but the Px was only 2.18 g g_x^{-1} h^{-1}. The agitation rate at 500 rpm and aeration rate at 2.5 L min^{-1} still does not take advantage of the maximum catalytic capacity of this strain when compared to other reports in the literature. Zhou et al. (2017) reported the improvement of oxygen transfer by increasing the fermenter pressure and introducing pure oxygen, and obtain a total *Qp* of 32.5 g L^{-1} h^{-1} and a P_X of 5.26 g g_x^{-1} h^{-1} at a biomass concentration of 6.08 g L^{-1}, which is the maximum volumetric yield and specific productivity achieved so far. The elevated pressure changes the solubility of oxygen in the medium and the supply of pure oxygen increases the dissolved oxygen concentration, resulting in a significant improvement in oxygen delivery. The high level of oxygen supply makes it feasible to provide the large amounts of oxygen required for high biomass concentration, thus achieving high productivity. However, the costs associated with the supply of pure oxygen and the potential operational difficulties under elevated pressure conditions cannot be ignored. Moreover, Zhou et al. (2019) reported the use of PVA-alginate immobilized *G. oxydans* NL71 as a biocatalyst for whole-cell catalysis of xylose. Although the immobilized cells could improve the catalytic performance, with a volumetric yield of 7.10 g L^{-1} h^{-1} at a biomass concentration up to 10 g L^{-1}, the P_X was only 0.71 g g_x^{-1} h^{-1}, which severely wasted the catalytic performance of *G. oxydans* NL71. The reason may be the oxygen transfer limitation imposed by immobilized cells, which limits the level of oxygen uptake.

To solve the problem of low productivity caused by the mismatch between oxygen transfer and oxygen uptake, the fermentation conditions (agitation, aeration, biomass concentration) were optimized by Box-Behnken response surfaces. A final P_X of 6.64 ± 0.20 g gx^{-1} h^{-1} is achieved, which is significantly higher than that was reported in the literature. The above results indicate that the developed model can be used to improve the production efficiency of xylonic acid.

CONCLUSION

The efficient bioconversion of xylonic acid using *G. oxydans* NL71 as a biocatalyst has been investigated using response surface methodology. Also, the maximum P_X for xylonic acid production

was successfully obtained by multivariate optimization such as agitation, aeration and biomass concentration. A maximum specific productivity of 6.64 ± 0.20 g g_x^{-1} h^{-1} for xylonic acid was obtained under optimized conditions (728 rpm, 7 L min^{-1}, 1.11 g L^{-1}). The optimized variables not only proved the validity of the models, but also effectively improved the production efficiency of *G. oxydans* NL71 in the whole-cell catalytic xylose process. Therefore, this study presents the potential application in improving the efficiency of xylonic acid production.

DATA AVAILABILITY STATEMENT

The original contributions presented in the study are included in the article/supplementary material, further inquiries can be directed to the corresponding authors.

AUTHOR CONTRIBUTIONS

TH and CX conceived and designed the experiments, TH, CD and XL performed the experiments, TH wrote the original draft, CX helped write, review and edit the manuscript. XG acquired the funding. All co-authors performed proofreading of the manuscript.

FUNDING

This work was financially supported by the National Natural Science Foundation of China (21774059), the Priority Academic Program Development (PAPD) of Jiangsu Higher Education Institutions, and the opening funding of Jiangsu Key Lab of Biomass-based Green Fuels and Chemicals.

REFERENCES

Ávila-Lara, A. I., Camberos-Flores, J. N., Mendoza-Pérez, J. A., Messina-Fernández, S. R., Saldaña-Duran, C. E., Jimenez-Ruiz, E. I., et al. (2015). Optimization of Alkaline and Dilute Acid Pretreatment of Agave Bagasse by Response Surface Methodology. *Front. Bioeng. Biotechnol.* 3, 146. doi:10.3389/fbioe.2015.00146

Cao, R., and Xu, Y. (2019). Efficient Preparation of Xylonic Acid from Xylonate Fermentation Broth by Bipolar Membrane Electrodialysis. *Appl. Biochem. Biotechnol.* 187, 396–406. doi:10.1007/s12010-018-2827-y

Chun, B. W., Dair, B., Macuch, P. J., Wiebe, D., Porteneuve, C., and Jeknavorian, A. (2006). The Development of Cement and concrete Additive: Based on Xylonic Acid Derived via Bioconversion of Xylose. *Appl. Biochem. Biotechnol.* 129-132, 645–658. doi:10.1385/ABAB:131:1:645

Dai, L., Jiang, W., Zhou, X., and Xu, Y. (2020). Enhancement in Xylonate Production from Hemicellulose Pre-hydrolysate by Powdered Activated Carbon Treatment. *Bioresour. Techn.* 316, 123944. doi:10.1016/j.biortech.2020.123944

Deppenmeier, U., Hoffmeister, M., and Prust, C. (2002). Biochemistry and Biotechnological Applications of Gluconobacter Strains. *Appl. Microbiol. Biotechnol.* 60, 233–242. doi:10.1007/s00253-002-1114-5

Dixit, P., Mehta, A., Gahlawat, G., Prasad, G. S., and Choudhury, A. R. (2015). Understanding the Effect of Interaction Among Aeration, Agitation and Impeller Positions on Mass Transfer during Pullulan Fermentation by *Aureobasidium Pullulans*. *RSC Adv.* 5, 38984–38994. doi:10.1039/c5ra03715h

Garcia-Ochoa, F., and Gomez, E. (2009). Bioreactor Scale-Up and Oxygen Transfer Rate in Microbial Processes: an Overview. *Biotechnol. Adv.* 27, 153–176. doi:10.1016/j.biotechadv.2008.10.006

Garcia-Ochoa, F., Gomez, E., Santos, V. E., and Merchuk, J. C. (2010). Oxygen Uptake Rate in Microbial Processes: An Overview. *Biochem. Eng. J.* 49, 289–307. doi:10.1016/j.bej.2010.01.011

Gupta, A., Singh, V. K., Qazi, G. N., and Kumar, A. (2001). *Gluconobacter oxydans*: Its biotechnological applications. *Microbiol. Biotechnol.* 3, 445–456. doi:10.1016/S0167-7012(01)00251-2

Hahn, T., Torkler, S., van Der Bolt, R., Gammel, N., Hesse, M., Möller, A., et al. (2020). Determining Different Impact Factors on the Xylonic Acid Production Using *Gluconobacter Oxydans* DSM 2343. *Process Biochem.* 94, 172–179. doi:10.1016/j.procbio.2020.04.011

Handlogten, M. W., Lee-O'Brien, A., Roy, G., Levitskaya, S. V., Venkat, R., Singh, S., et al. (2018). Intracellular Response to Process Optimization and Impact on Productivity and Product Aggregates for a High-Titer CHO Cell Process. *Biotechnol. Bioeng.* 115, 126–138. doi:10.1002/bit.26460

Hölscher, T., Schleyer, U., Merfort, M., Bringer-Meyer, S., Görisch, H., and Sahm, H. (2009). Glucose Oxidation and PQQ-dependent Dehydrogenases in *Gluconobacter Oxydans*. *J. Mol. Microbiol. Biotechnol.* 16, 6–13. doi:10.1159/000142890

Hou, W., Kan, J., and Bao, J. (2019). Rheology Evolution of High Solids Content and Highly Viscous Lignocellulose System in Biorefinery Fermentations for Production of Biofuels and Biochemicals. *Fuel* 253, 1565–1569. doi:10.1016/j.fuel.2019.05.136

Hou, W., Zhang, M., and Bao, J. (2018). Cascade Hydrolysis and Fermentation of Corn stover for Production of High Titer Gluconic and Xylonic Acids. *Bioresour. Techn.* 264, 395–399. doi:10.1016/j.biortech.2018.06.025

Hua, X., Zhou, X., Du, G., and Xu, Y. (2020). Resolving the Formidable Barrier of Oxygen Transferring Rate (OTR) in Ultrahigh-Titer Bioconversion/biocatalysis by a Sealed-Oxygen Supply Biotechnology (SOS). *Biotechnol. Biofuels.* 13, 1. doi:10.1186/s13068-019-1642-1

Li, C., Tian, J., Wang, W., Peng, H., Zhang, M., Hang, H., et al. (2019). Numerical and Experimental Assessment of a Miniature Bioreactor Equipped with a Mechanical Agitator and Non-invasive Biosensors. *J. Chem. Technol. Biotechnol.* 94, 2671–2683. doi:10.1002/jctb.6076

Liu, H., Valdehuesa, K. N. G., Nisola, G. M., Ramos, K. R. M., and Chung, W.-J. (2012). High Yield Production of D-Xylonic Acid from D-Xylose Using Engineered *Escherichia coli*. *Bioresour. Techn.* 115, 244–248. doi:10.1016/j.biortech.2011.08.065

Mientus, M., Kostner, D., Peters, B., Liebl, W., and Ehrenreich, A. (2017). Characterization of Membrane-Bound Dehydrogenases of *Gluconobacter Oxydans* 621H Using a New System for Their Functional Expression. *Appl. Microbiol. Biotechnol.* 101, 3189–3200. doi:10.1007/s00253-016-8069-4

Nogue, V. S., and Karhumaa, K. (2015). Xylose Fermentation as a challenge for Commercialization of Lignocellulosic Fuels and Chemicals. *Biotechnol. Lett.* 37 (4), 761–772. doi:10.1007/s10529-014-1756-2

Toivari, M. H., Nygård, Y., Penttilä, M., Ruohonen, L., and Wiebe, M. G. (2012b). Microbial D-Xylonate Production. *Appl. Microbiol. Biotechnol.* 96, 1–8. doi:10.1007/s00253-012-4288-5

Toivari, M. H., Ruohonen, L., Richard, P., Penttilä, M., and Wiebe, M. G. (2010a). *Saccharomyces cerevisiae* Engineered to Produce D-Xylonate. *Appl. Microbiol. Biotechnol.* 88 (3), 751–760. doi:10.1007/s00253-010-2787-9

Toivari, M., Nygård, Y., Kumpula, E.-P., Vehkomäki, M.-L., Benčina, M., Valkonen, M., et al. (2012a). Metabolic Engineering of *Saccharomyces cerevisiae* for Bioconversion of D-Xylose to D-Xylonate. *Metab. Eng.* 14 (4), 427–436. doi:10.1016/j.ymben.2012.03.002

Wang, X., Xu, Y., Lian, Z., Yong, Q., and Yu, S. (2014). A One-step Method for the Simultaneous Determination of Five wood Monosaccharides and the Corresponding Aldonic Acids in Fermentation Broth Using High-Performance Anion-Exchange Chromatography Coupled with a Pulsed Amperometric Detector. *J. Wood Chem. Techn.* 34, 67–76. doi:10.1080/02773813.2013.838268

Yim, S. S., Choi, J. W., Lee, S. H., Jeon, E. J., Chung, W.-J., and Jeong, K. J. (2017). Engineering ofCorynebacterium Glutamicumfor Consolidated Conversion of Hemicellulosic Biomass into Xylonic Acid. *Biotechnol. J.* 12, 1700040. doi:10.1002/biot.201700040

Yuan, J., Wu, M., Lin, J., and Yang, L. (2016). Enhancement of 5-Keto-D-Gluconate Production by a Recombinant *Gluconobacter Oxydans* Using a Dissolved Oxygen Control Strategy. *J. Biosci. Bioeng.* 122, 10–16. doi:10.1016/j.jbiosc.2015.12.006

Zaldivar, J., Nielsen, J., and Olsson, L. (2001). Fuel Ethanol Production from Lignocellulose: a challenge for Metabolic Engineering and Process Integration. *Appl. Microbiol. Biotechnol.* 56 (1-2), 17–34. doi:10.1007/s002530100624

Zhang, H., Han, X., Wei, C., and Bao, J. (2017). Oxidative Production of Xylonic Acid Using Xylose in Distillation Stillage of Cellulosic Ethanol Fermentation Broth by *Gluconobacter Oxydans*. *Bioresour. Techn.* 224, 573–580. doi:10.1016/j.biortech.2016.11.039

Zhang, H., Liu, G., Zhang, J., and Bao, J. (2016a). Fermentative Production of High Titer Gluconic and Xylonic Acids from Corn stover Feedstock by *Gluconobacter Oxydans* and Techno-Economic Analysis. *Bioresour. Techn.* 219, 123–131. doi:10.1016/j.biortech.2016.07.068

Zhang, H., Shi, L., Mao, X., Lin, J., and Wei, D. (2016b). Enhancement of Cell Growth and Glycolic Acid Production by Overexpression of Membrane-Bound Alcohol Dehydrogenase in *Gluconobacter Oxydans* DSM 2003. *J. Biotechnol.* 237, 18–24. doi:10.1016/j.jbiotec.2016.09.003

Zhou, X., Han, J., and Xu, Y. (2019). Electrodialytic Bioproduction of Xylonic Acid in a Bioreactor of Supplied-Oxygen Intensification by Using Immobilized Whole-Cell *Gluconobacter Oxydans* as Biocatalyst. *Bioresour. Techn.* 282, 378–383. doi:10.1016/j.biortech.2019.03.042

Zhou, X., Lü, S., Xu, Y., Mo, Y., and Yu, S. (2015). Improving the Performance of Cell Biocatalysis and the Productivity of Xylonic Acid Using a Compressed Oxygen Supply. *Biochem. Eng. J.* 93, 196–199. doi:10.1016/j.bej.2014.10.014

Zhou, X., Zhou, X., and Xu, Y. (2017). Improvement of Fermentation Performance of *Gluconobacter Oxydans* by Combination of Enhanced Oxygen Mass Transfer in Compressed-Oxygen-Supplied Sealed System and Cell-Recycle Technique. *Bioresour. Techn.* 244, 1137–1141. doi:10.1016/j.biortech.2017.08.107

Conflict of Interest: The authors declare that the research was conducted in the absence of any commercial or financial relationships that could be construed as a potential conflict of interest.

Publisher's Note: All claims expressed in this article are solely those of the authors and do not necessarily represent those of their affiliated organizations, or those of the publisher, the editors and the reviewers. Any product that may be evaluated in this article, or claim that may be made by its manufacturer, is not guaranteed or endorsed by the publisher.

frontiers in Bioengineering and Biotechnology

ORIGINAL RESEARCH
published: 26 October 2021
doi: 10.3389/fbioe.2021.773104

Vitreoscilla Hemoglobin Improves Sophorolipid Production in *Starmerella Bombicola* O-13–1 Under Oxygen Limited Conditions

Jun-feng Li[1], Hong-fang Li[1], Shu-min Yao[2], Meng-juan Zhao[1], Wen-xun Dong[1], Sheng-kang Liang[3] and Xing-yong Xu[4]*

[1]Shandong Provincial Key Laboratory of Biochemical Engineering, Qingdao Nucleic Acid Rapid Detection Engineering Research Center, College of Marine Science and Biological Engineering, Qingdao University of Science and Technology, Qingdao, China, [2]College of Life Science, Qufu Normal University, Qufu, China, [3]Key Laboratory of Marine Chemistry Theory and Technology, Ministry of Education, Ocean University of China, Qingdao, China, [4]Fourth Institute of Oceanography, Ministry of Natural Resources, Beihai, China

OPEN ACCESS

Edited by:
Zhipeng Wang,
Qingdao Agricultural University, China

Reviewed by:
Jingdan Liang,
Shanghai Jiao Tong University, China
Xiaojing Ma,
Hefei University of Technology, China

***Correspondence:**
Sheng-kang Liang
liangsk@ouc.edu.cn

Specialty section:
This article was submitted to Bioprocess Engineering, a section of the journal Frontiers in Bioengineering and Biotechnology

Received: *09 September 2021*
Accepted: *12 October 2021*
Published: *26 October 2021*

Citation:
Li J-f, Li H-f, Yao S-m, Zhao M-j, Dong W-x, Liang S-k and Xu X-y (2021) Vitreoscilla Hemoglobin Improves Sophorolipid Production in Starmerella Bombicola O-13–1 Under Oxygen Limited Conditions. Front. Bioeng. Biotechnol. 9:773104. doi: 10.3389/fbioe.2021.773104

Sophorolipids (SLs) are homologous microbial secondary metabolites produced by *Starmerella bombicola* and have been widely applied in many industrial fields. The biosynthesis of SLs is a highly aerobic process and is often limited by low dissolved oxygen (DO) levels. In this study, the *Vitreoscilla* hemoglobin (VHb) gene was transformed into *S. bombicola* O-13–1 by homologous recombination to alleviate oxygen limitation. VHb expression improved the intracellular oxygen utilization efficiency under either oxygen-rich or oxygen-limited conditions. In shake flask culture, the production of SLs was higher in the recombinant (VHb^+) strain than in the wild-type (VHb^-) strain, while the oxygen uptake rate of the recombinant (VHb^+) strain was significantly lower than that of the wild-type (VHb^-) strain. In a 5 L bioreactor, the production of SLs did not increase significantly, but the DO level in the fermentation broth of the VHb^+ strain was 21.8% higher than that of VHb^- strain under oxygen-rich conditions. Compared to wide-type strains (VHb^-), VHb expression enhanced SLs production by 25.1% in the recombinants (VHb^+) under oxygen-limited conditions. In addition, VHb expression raised the transcription levels of key genes involved in the electron transfer chain (*NDH, SDH, COX*), TCA cycle (*CS*, *ICD*, *KDG1*) and SL synthesis (*CYP52M1* and *UGTA1*) in the recombinant (VHb^+) strains. VHb expression in *S. bombicola* could enhance SLs biosynthesis and intracellular oxygen utilization efficiency by increasing ATP production and cellular respiration. Our findings highlight the potential use of VHb to improve the oxygen utilization efficiency of *S. bombicola* in the industrial-scale production of SLs using industrial and agricultural by-products like molasses and waste oil as fermentation feedstock.

Keywords: sophorolipids, *Vitreoscilla* hemoglobin, fermentation, oxygen utilization efficiency, *Starmerella bombicola*

INTRODUCTION

Sophorolipid (SL) is a kind of glycolipid biosurfactant produced by the yeast *Starmerella bombicola* (Van Bogaert et al., 2011). Typically, SLs is composed of a hydrophilic sophorose and hydrophobic saturated or unsaturated long-chain ω- or ω-1 hydroxy fatty acids (Asmer et al., 1988; Ma et al., 2020). As one of the most important glycolipid biosurfactants, SLs have been widely used in cosmetics, petroleum exploitation, environmental remediation, pharmaceuticals and other industries due to its high productivity, high surface activities, low toxicity and good environmental compatibility (Van Bogaert et al., 2007; Oliveira et al., 2014).

The biosynthesis of SLs requires both hydrophilic and lipophilic carbon sources. The former is usually glucose, and the latter is vegetable or fat oil (Shah et al., 2010). The key step in the synthesis of SLs is hydroxylation of fatty acids, which is catalyzed by cytochrome P450 monooxygenase and consumes a large amount of oxygen (Van Bogaert et al., 2009; Li et al., 2016c). In fact, the low utilization level of oxygen in the fermentation process leads to the low utilization of oil-soluble substrates and a long fermentation cycle, which further increases the cost of SLs production (Asmer et al., 1988; Yang et al., 2012). Therefore, the dissolved oxygen (DO) level is often a limiting factor for yeast cell growth and SL synthesis during the high-density fermentation (Yang et al., 2012). A higher oxygen utilization rate is beneficial for sophorolipid production by *S. bombicola* (Guilmanov et al., 2002).

Vitreoscilla hemoglobin (VHb), an oxygen-binding protein, can facilitate the intracellular oxygen transport and improve the utilization efficiency of oxygen, which help alleviate the limitation of low DO on fermentation (Zhang et al., 2007; Stark et al., 2012; Zhang et al., 2014; Stark et al., 2015). The heterologous expression of VHb gene (*vgb*) in various hosts can improve cell growth, bioremediation, protein synthesis and metabolite synthesis (Setyawati et al., 2007; Wang et al., 2012; Stark et al., 2015). The expression of VHb raises cell density of *vgb*-bearing *Gordonia amarae* and improves the production of trehalose lipid biosurfactants (Dogan et al., 2006). The production of rhamnolipid biosurfactant is enhanced by 10-fold in the *vgb*-recombinant strain (PaJC) of *Pseudomonas aeruginosa* compared to its wild-type strain (Kahraman and Erenler, 2012). The heterologous expression of VHb is also particularly beneficial to polysaccharide-producing microorganisms grown in highly viscous broth (Li et al., 2016b; Liu et al., 2017). The bio-synthesis of SLs is an energy-requiring process that consumes a large amount of oxygen (Van Bogaert et al., 2009), so it is necessary to construct a recombinant VHb-expressing strain of *S. bombicola* to improve SLs production using fat and oil feedstock.

In the previous research, we had utilized the cheap and easily available raw materials like cane molasses and waste fried oil instead of expensive carbon sources (glucose and vegetable oil) as fermentation feedstock for biosynthesis of SLs in order to reduce the cost of SLs production (Li et al., 2018). In this study, the *vgb* gene encoding VHb was introduced into a sophorolipid-producing strain of *S. bombicola* O-13–1, and yeast cells were grown under either oxygen-deficient or oxygen-rich condition. The effects of VHb expression on several key parameters, such as biomass, glucose consumption, dissolved oxygen and sophorolipid production were investigated. The mechanism of VHb in sophorolipids synthesis was also addressed. This study will provide valuable evidence for resolving the problems caused by low levels of dissolved oxygen in submerged fermentation to improve the production of sophorolipid by *S. bombicola*.

MATERIALS AND METHODS

Strains, Plasmids and Media

The wild-type strain of *Starmerella bombicola* (O-13–1) was used as the parent strain (VHb^-), which was isolated from petroleum-contaminated soil in Shengli Oilfield, Dongying, Shangdong Province, China (Li et al., 2018). *Escherichia coli* DH5α was used as a host for the amplification of recombinant plasmids and was purchased from Tiangen Biotech (Beijing) Co., Ltd., China. Plasmid pFL4a containing hygromycin B resistance gene *hpt*II was kindly provided by Dr. Zhe Chi (Ocean University of China, Qingdao, Shangdong province, China). The plasmid pMD19-T (Simple) vector was purchased from TaKaRa Biotechnology (Dalian, China). *E. coli* transformants were selected in Luria-Bertani (LB) medium containing 100 μg/ml of ampicillin. Yeast transformants were grown in the YPD medium containing 500 μg/ml of hygromycin B. The primers and fragments were synthesized and sequenced by Tsingke Biological Technology (Beijing, China) (**Table 1**). LB medium contained 1% tryptone, 0.5% yeast extract, and 1% NaCl, with a pH 7.0–7.4. Seed medium (YPD) contained 1% yeast extract, 2% peptone, and 2% dextrose. Fermentation medium (w/v) consisted of 6% glucose, 6% vegetable oil, 1% yeast extract, 2% peptone, 0.5% sodium citrate, 0.4% $MgSO_4{\cdot}7H_2O$, 0.2% $(NH4)_2SO_4$, 0.2% KH_2PO_4, 0.01% NaCl, and 0.01% $CaCl_2$. Glucose and soybean oil were sterilized separately and added to the medium before fermentation.

Vector Construction

In order to express *Vitreoscilla* hemoglobin in *S. bombicola* O-13–1, the plasmid pSBEX-HPT-Vgb was constructed based on the vector pMD-19 (**Figure 1**), which contained 441 bp *vgb* fused downstream of the strong constitutive glyceraldehyde-3-phosphate dehydrogenase gene (GAPDH) promoter from strain O-13–1. Briefly, genomic DNA of *S. bombicola* was used as a template for PCR amplification using two pairs of primers 18S rDNA 1-F/18S rDNA 1-R and 18S rDNA 2-F/18S rDNA 2-R that were designed as homologous recombination sites according to the DNA sequence of *S. bombicola* (GenBank accession BCGO00000000). The PCR amplification products were purified and ligated to the pMD19-T vector, and the resulting construct was named pMD19-18S. The HPT expression cassette consisted of a strong constitutive *Starmerella* phosphoglycerate kinase (PGK) gene promoter (which was amplified with the primer *PGK*p-F/*PGK*p-R), the hygromycin B phosphotransferase gene (HPT) and poly A (which was amplified with the primer *HPT*-F/*HPT*-R from the vector pFl4a) (Chi et al., 2019); and it was inserted into pMD19T-18S

TABLE 1 | Primers used for plasmid construction and verification.

Genes	Primers (5′→3′)[a]	Restriction sites	Overlap
18s rDNA1-F	GAATTCACTCCTTGGTCCGTGTTTCAAGACGGG	EcoR I	
18s rDNA1-R	*GTGCCGAATATTAGGTCGACGGATCC*AGATTGTAACGGCGAGTGAACAGGC	Ssp I, Sal I, BamH I	i
18s rDNA2-F	*CCGTTACAATCTGGATCCGTCGAC*CTAATATTCGGCACCTTAACTCCGCGTTCGGTT	BamH I, Sal I, Ssp I	i
18s rDNA2-R	GCATGCTTGCCTGCGCGAGTATTTGGGTGGAAAACCCATA	Sph I	
HPT-F	GGATCCGGTGCTTAGGGTGCGTGTGCAAGG	BamH I	
HPT-R	*GCGGTGAGTTCAGGCTTTTTCAT*TTTTTCTGGTTTGGAGGACCTTG		ii
*PGK*p-F	*CCAAGGTCCTCCAAACCAGAAAAAA***ATG**AAAAAGCCTGAACTCACC		ii
*PGK*p-R	GTCGACGAGGGCAAAGAAATAGAGTAGATGCCGACCGGGATC	Sal I	
*GAPD*p-F	AATATTTCAGGTGCCACACGCGCATTAATCG	Ssp I	
*GAPD*p-R	GTCGAATGCATACGCGTCAATTGATTTCTCCTAATAGGCTGTCAGC	Sal I	
VGB-F	TTCGAA**ATG**CTCGACCAGCAGACCA	BstB I	
VGB-R	TGCGCA**AAT**GAGTTGACGGACTCGC	Mlu I	

[a]*The restriction sites are underlined; the start and stop codon are shown in bold; an overlapping sequence of two primers are marked with italic and the same Roman.*

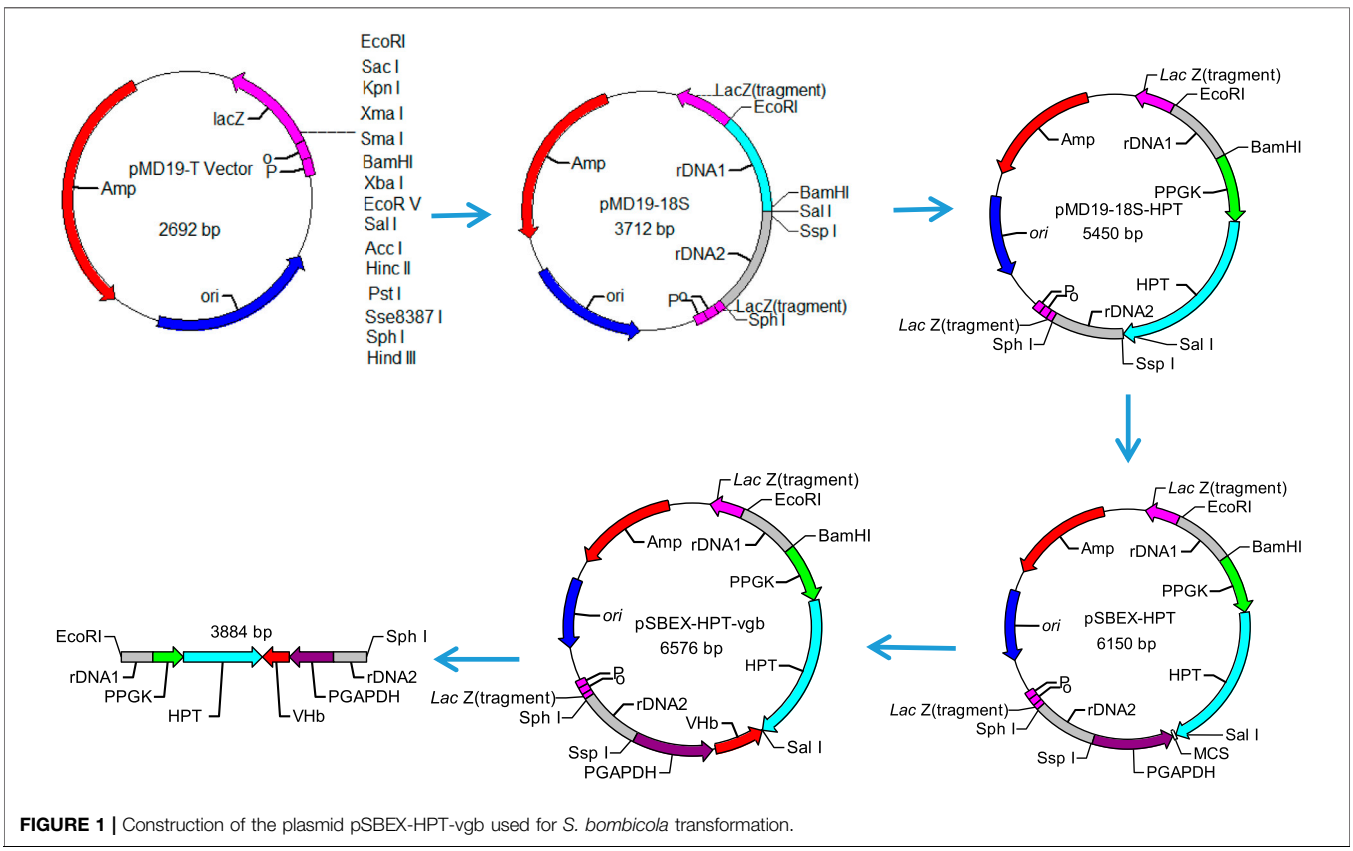

FIGURE 1 | Construction of the plasmid pSBEX-HPT-vgb used for *S. bombicola* transformation.

to yield the plasmid pMD19T-HPT-18S. In addition, the exogenous gene expression cassette consisted of the strong constitutive *Starmerella* glyceraldehyde-3-phosphate dehydrogenase (GAPDH) gene promoter (which was amplified with the primer *GAPD*p-F/*GAPD*p-R), multiple clone sites (MCS) and poly A; and it was inserted into pMD19T-HPT-18S to yield the expression vector pSBEX-HPT. After codon optimization, the nucleotide sequence of VHb gene (*VGB*, 441 bp fragment) was synthesized by Synbio Technologies (Jiangsu, China) and then amplified using PCR with the primer *VGB*-F/*VGB*-R carrying *BstB* I and *Mlu* I sites on each end. The PCR products were purified and ligated into the linearized vector pSBEX-HPT to form plasmid pSBEX-HPT-vgb, which was then transformed into *E. coli* DH5α to obtain the vgb-bearing *E. coli*, named DH5α-SBEX-HPT-vgb.

Transformation of Yeast by Electroporation

The transformation of yeast was carried out by electroporation (Manivasakam and Schiest, 1993). The recombinant plasmids pSBEX-HPT-vgb were linearized with restriction enzymes *Sph* I

and *EcoR* I (**Figure 1**). The linearized recombinant expression vectors were purified by agarose gel electrophoresis and transformed into wild-type *S. bombicola* strain (VHb^-) using the homologous transformation system. The preparation of competent cells of *S. bombicola*, electroporation of linearized recombinant expression fragments and screen of transformants were carried out according to the methods described elsewhere (Chi et al., 2012). The DNA of the transformants were extracted, and the successful transformation of the *vgb* gene was verified using PCR with *VGB*-F and *VGB*-R primers. Putative transformants were grown on YPD plates without hygromycin B for five rounds. After growth on nonselective YPD plates, those tested transformants can stably maintain hygromycin B resistance.

Identification of *Vitreoscilla* Hemoglobin (CO-Difference Spectrum Analysis)

The presence of the vgb gene was confirmed by PCR analysis (Ye et al., 2016). The activity of the expressed VHb protein was determined by CO-difference spectral analysis (Li et al., 2016b). Briefly, VHb^+ and VHb^- yeast cells were harvested from the fermentation medium by centrifugation at 5,000 rpm for 15 min. 5 g of the cells were washed twice with 0.85% saline solution. Around 1.5 g of the cells were resuspended with 30 ml phosphate buffer (pH 7.0) after centrifugation and then disrupted with an ultrasonifier (Liao et al., 2014). After centrifugation at 8,000 rpm for 5 min at 4°C to remove cell debris, the supernatant was reduced with excess sodium dithionite (2.5 mg/ml) and divided into two aliquots. One aliquot was bubbled with CO for 2 min and the other with air for the same period of time. The samples were then scanned in the range 400–460 nm on a spectrophotometer. The CO-difference spectrum for each sample was calculated by subtracting the absorbance of the air-bubbled sample from that of the CO-bubbled sample (Su et al., 2010)

Determination of Oxygen Uptake Rate

The oxygen uptake rate (OUR) was calculated according to the equation (Garcia-Ochoa et al., 2010): , where C_L is dissolved oxygen (DO) in the broth, t is cultured time. The concentrations of DO in the medium were determined using a dissolved oxygen sensor (InPro6860i/12/120/mA/HD, Mettler-Toledo) and was expressed as percent saturation (Ozbek and Gayik, 2001). The DO concentrations were recorded every 10 s, and the experiments were repeated two times.

Bioreactor-Scale Fermentation

To study the effect of VHb expression on *S. bombicola* O-13–1 under both the oxygen-enriched and oxygen-limited conditions, we compared the oxygen uptake rate, biomass, glucose consumption and sophorolipid production between the transformant VHb^+ and the wild type VHb^- in a 5 L bioreactor (BIOTECH-5BG, Shanghai Baoxing Bio-engineering, China) containing 2 L of fermentation broth. The fermentation broth was cultured under oxygen-enriched conditions (rotation speed 400 rpm, aeration 1.0 vvm) and oxygen-limited conditions (rotation speed 350 rpm, aeration 1.0 vvm). The sampling interval was 4 h.

Analytical Methods

Biomass was determined by measuring cell dry weight after removal of SLs and other hydrophobic substrates in the fermentation broth (Felse et al., 2007). SLs were extracted from the fermentation broth according to the method of Hu and Ju (2001). Briefly, 10 ml of fermentation broth was extracted two times with an equal volume of ethyl acetate as solvent. The solvent was then centrifuged at 8,000 rpm for 10 min at 4°C. The organic phase was vacuum-dried at 40°C to remove ethyl acetate. The residues were washed with 10 ml hexane to remove the remaining oil. The crude SLs were obtained after vaporizing the residual hexane at 40°C under vacuum. Glucose content was measured using the 3,5-dinitrosalicylic acid (DNS) method (Wang et al., 2010).

Expression of Several Selected Genes Using Quantitative Real-Time PCR

Total RNA was isolated using Fungal RNA Kit (OMEGA bio-tek, Norcross, GA, United States). The cDNA was synthesized by the Thermo Scientific Revert Aid First Strand cDNA Synthesis Kit. The gene primers are listed in **Table 2**. β-tubulin gene was used as an internal control. The PCR conditions were described as follows: 95 C for 10 min, 30 cycles of 95 C for 3 s, 56 C for 30 s, and 72 C for 60 s. The melting curve was analyzed to evaluate the specificity of primers used for RT-qPCR. All amplifications were performed in triplicates.

Relative expression levels of the selected genes were calculated using the $2^{-\Delta\Delta Ct}$ method (Zhang et al., 2011), in which C_T is threshold period, and Tubulin was used as the reference gene. In this study, the genes in wild-type strains VHb^- were used as control to normalize expression levels. Therefore, the comparative expression level of each gene in the strains VHb^- was set to be 1.

Statistical Analysis

Statistical analysis was performed with Student's *t*-test. Differences were considered statistically significant when *p*-values were <0.05 in a two-tailed analysis.

RESULTS AND DISCUSSION

Confirmation of the *vgb*-Bearing *S. bombicola*

To confirm the integration of the *vgb* gene into the genomes of *S. bombicola* O-13–1, genomic DNA of transformants was independently isolated and detected by PCR with the special primer pair listed in **Table 1**. Agarose gel electrophoresis of PCR products showed a clear band of the *vgb* fragment (441 bp) in the VHb^+ transformant, but not in the VHb^- strain (**Figure 2A**), indicating that exogenous *vgb* gene was successfully transformed into the host strain. The VHb^+ has a maximum absorption at 419 nm when CO is bound, so the biological activity of the VHb

TABLE 2 | Primers and relevant information of reference and target genes for quantitative real-time PCR.

Genes	Name	Primers (5′-3′)
NDH	NADH dehydrogenase	F: AACTCAATCCCTCGTCGTCAG
		R: AATAGCCTGTCCACTCTTTCCC
SDH	Succinate dehydrogenase	F: GCGTGAGTTTTCAACGGTGG
		R: ACCGACGGGAGGGGTTACTAT
COX	Cytochrome c oxidase	F: GGCATTTGGTCGGGTTCATA
		R: GCCCATCTTGACTCGCTACTGT
KDG1	Alpha-ketoglutarate dehydrogenase	F: TGGATTTCCGCCAATACCG
		R: GCTGAAAACACCAAACACGAG
ICD	Isocitrate dehydrogenase	F: TTCATGCGGAGGTTACGACA
		R: GCCTCGCCAATGTAAAGACG
CS	Citrate synthase	F: GTCTACTCACCAACTCAATCCCTC
		R: CCAATAGCCTGTCCACTCTTTC
CYP52M1	Cytochrome P450 monooxygenase	F: GGGTCCGTTTGAAAGCGTAAT
		R: TTGTAGCCCGTGATGGTTCG
UGTA	UDP-glucosyltransferase	F: TGGTTCATAGCGAGTTTCTTTGC
		R: CTGGCTGGATTTGTTTAGGGG
VGB	*Vireoscilla* hemoglobin	F: CGAGAACTGTCATAGCAAGAGCC
		R: ACATCATCAAGGCTACCGTTCC
Tubulin	Tubulin Z cytoskeleton	F: TGATGAGACGGGCTGGGAAT
		R: ACCGTTACTGAACCTTACAATGCC

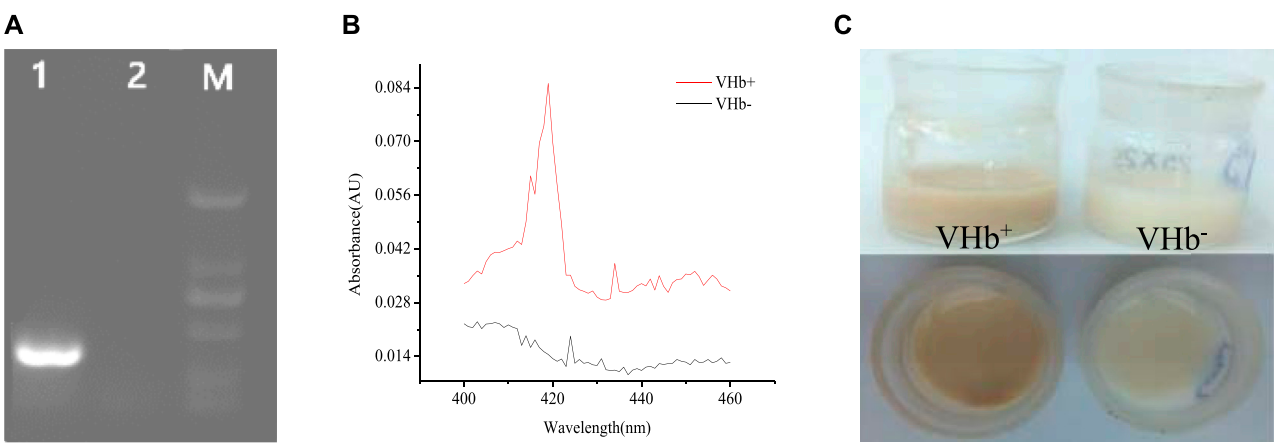

FIGURE 2 | Phenotypic analysis of the *S. bombicola vgb* strain. **(A)** Electrophoresis analysis of genomic DNA extracted from wild-type strains *Vitreoscilla* hemoglobin (VHb^-) and transformants (VHb^+) of *S. bombicola*. Lane 1: VHb^+ (441 bp); Lane 2: VHb^-(wild-type strain); Lane M: DL 2000 DNA marker (2000 bp, 1,000 bp, 750 bp, 500 bp, 250 bp, 100 bp); **(B)** CO-difference spectra of the *vgb*-bearing *S. bombicola* strain (VHb^+) and the wild-type strain (VHb^-); **(C)** The color of the VHb^+ and VHb^- strains.

was verified by CO-difference spectra (Geckil et al., 2001). The characteristic absorption peak at 419 nm was found in the CO-spectra of crude extracts of the *vgb*-bearing *S. bombicola*, but not in the wide type strain (**Figure 2B**), suggesting that biologically active VHb was successfully expressed in the VHb^+ strain. Similarly, the expression of VHb was also identified in *Pichia pastoris* (Wu and Fu, 2011) and *Aureobasidium melanogenum* P16 (Xue et al., 2019) by CO-difference spectral analysis. In addition, the VHb^+ cells appeared light brown (the color of the VHb), while the VHb^- cells remained milk white without change (**Figure 2C**). These results demonstrated that *vgb* was successfully expressed in *S. bombicola* O-13–1 transformants (VHb^+) and exhibited its biological activity.

Effects of *Vitreoscilla* hemoglobin Expression on Sophorolipids Fermentation of *S. bombicola* Cultivated in Shake Flasks

The sophorolipid production, biomass and oxygen uptake rate (OUR) of the recombinants and wild-type strains at 24 and 72 h were showed in **Figure 3**. At 24 h, there was no difference in the biomass and OUR between the recombinant strains (VHb^+) and

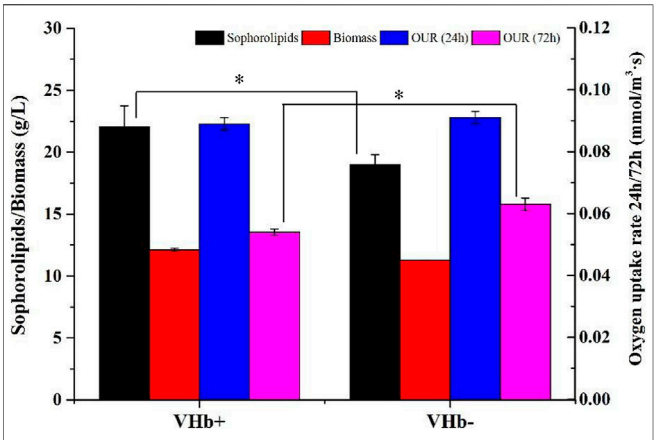

FIGURE 3 | Comparison of sophorolipid fermentation between the VHb$^+$ and VHb$^-$ strains cultivated in shake flasks (*p < 0.05).

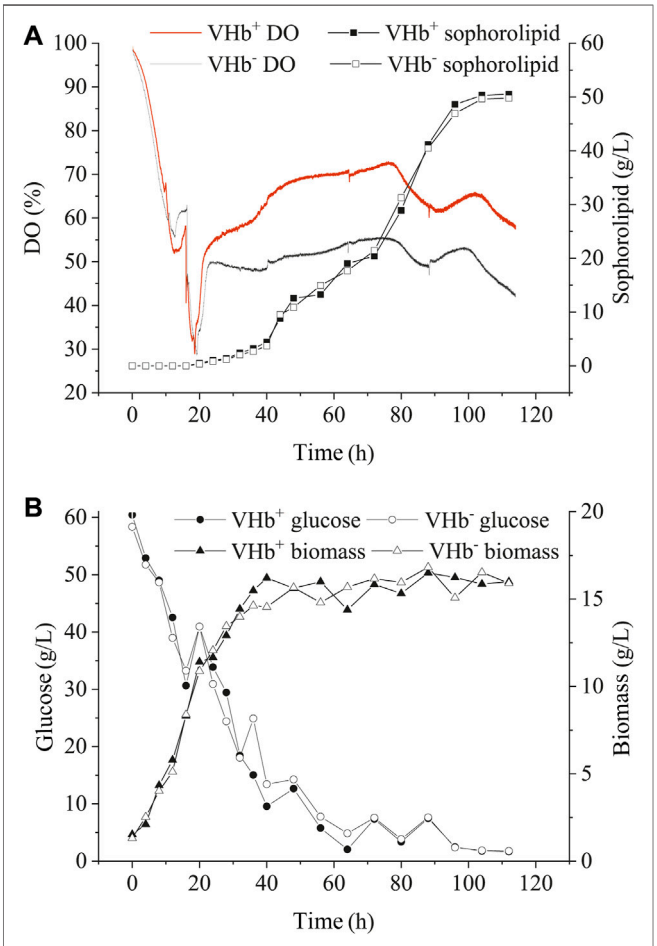

FIGURE 4 | Effects of VHb expression on DO content and SLs production **(A)**, residual sugar and biomass **(B)** under oxygen-rich conditions.

wild-type strains (VHb$^-$). At 72 h, the sophorolipids production of the recombinant strains (VHb$^+$) was higher than that of the wild-type strain (VHb$^-$), and the OUR of the VHb$^+$ was lower

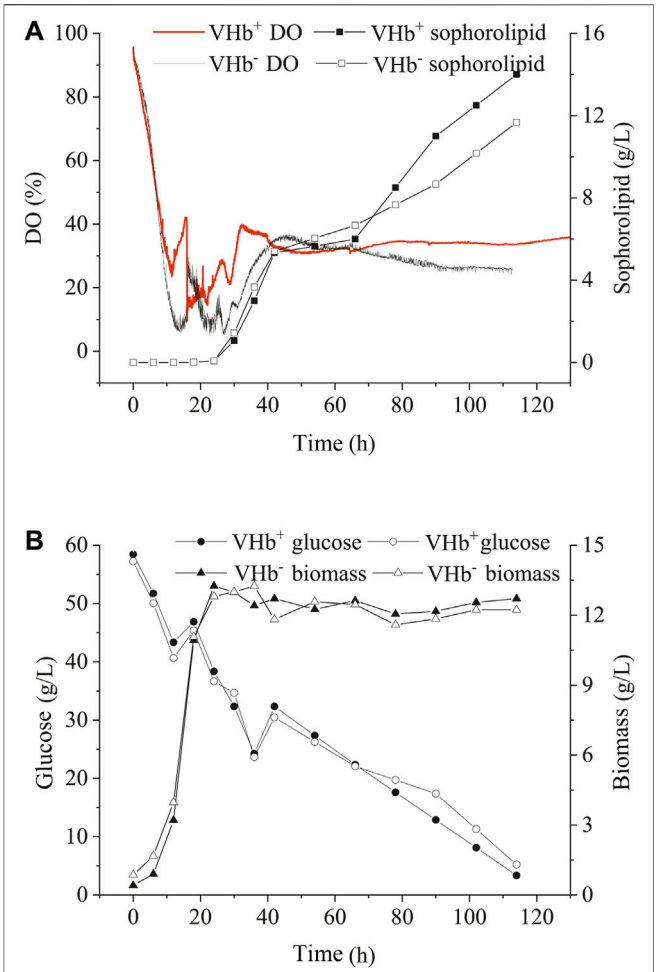

FIGURE 5 | Effects of VHb expression on DO content and sophorolipid production **(A)**, the residual sugar and biomass **(B)** under oxygen-limited conditions.

than that of the VHb$^-$. The results indicated that the expression of VHb could promote the utilization efficiency of intracellular oxygen, thereby reducing the OUR of the recombinant strains (VHb$^+$). The result is consistent with other studies (Huang et al., 2014; Wang Q. et al., 2018).

Effects of *Vitreoscilla* hemoglobin Expression on Sophorolipidss Production of *S. bombicola* Cultivated in a 5 L Bioreactor

The transformants (VHb$^+$) and wild-type strains (VHb$^-$) were incubated in a 5 L bioreactor under either oxygen-limited or oxygen-rich conditions. Under the oxygen-enrich condition, the recombinant strains (VHb$^+$) had similar biomass, sophorolipid production and glucose consumption with the wild-type strains (VHb$^-$) during the entire fermentation stage (**Figure 4B**). Interestingly, though there was no significant change in DO content of the fermentation broth between VHb$^+$ and VHb$^-$ strains at the early stage of fermentation (within 20 h, **Figure 4A**), the DO content of the fermentation broth for the VHb$^+$ strains

raised to be 21.8% higher than that for VHb^- strains at the late stage (40–112 h) of fermentation (**Figure 4A**). Previous researches have shown that VHb expression had no significant effects on the growth and metabolism of Ganoderma lucidum and *Pseudomonas aeruginosa* under oxygen-rich conditions (Li et al., 2016a, Li et al., 2016b; Geckil et al., 2001). However, other studies have also shown that VHb expression enhanced the biomass and yield of VHb recombinant strain under same conditions (Dogan et al., 2006; Gao et al., 2018).

Under oxygen-limited conditions, the changes in SLs production, glucose consumption and DO concentration of the fermentation broth were similar between the recombinants and wild-type strains during the early stage (within 40 h) of fermentation (**Figure 5**). After 72 h, SLs production, glucose consumption and biomass in the recombinants significantly increased compared with those in the wild-type strains, however, the consumption of DO in the recombinants decreased compared with that in the wild-type strains. In the end of fermentation, the production of SLs in the recombinants (VHb^+) boosted by 25.1% compared with that of the wild-type strains (VHb^-). Moreover, oxygen consumption in the recombinant strains (VHb^+) was obviously lower than that in the wild-type strains (VHb^-), especially in the late stages of fermentation (**Figure 5A**).

In the early stage of fermentation, the recombinant strains (VHb^+) and wild-type strains (VHb^-) showed no significant difference in OUR under the oxygen-rich or oxygen-limited conditions. However, in the later stage of fermentation, the DO content in the fermentation broth of the VHb^+ strains was higher than that of the VHb^- strains under oxygen-rich or oxygen-limited conditions, indicating that the expression of VHb could decrease oxygen consumption and promote the yield of SLs by the recombinants (VHb^+) (**Figures 4**, **5**). The results are consistent with previous reports concerning fungi and bacteria. For example, the concentration of pullulan and productivity were greatly enhanced by overexpression of VHb in *A. melanogenum* P16 under oxygen-limited conditions (Xue et al., 2019). The biomass and protein production increased in VHb-expressing Aspergillus sojae (Mora-Lugo et al., 2015) and Schwanniomyces occidentalis (Suthar and Chattoo, 2006). The bacterial cellulose production enhanced in *vgb*-bearing *Gluconacetobacter xylinus* under oxygen-limited conditions (Liu et al., 2018), and surfactin production improved by 24 and 51% in the VHb-expressing *Bacillus subtilis* THY-15/Pg3-srfA cultivated in the flasks and the fermentor, respectively (Wang Q. et al., 2018). These results indicated that the function of VHb might vary in different microorganisms under different growth conditions.

SLs production requires a certain amount of oxygen either in submerged fermentation (Guilmanov et al., 2002; Zhang et al., 2018) or solid-state fermentation (Jiménez-Peñalver et al., 2016; Jiménez-Peñalver et al., 2018). In this study, for the recombinants (VHb^+) cultivated in shake flasks, VHb expression did not raise the OUR during the first 24 h but reduced the absorption of oxygen by the recombinants (VHb^+) (**Figure 3**); in addition, the production of SLs was higher in the recombinant strains (VHb^+) than in the wild-type strains (VHb^-). The similar results were found in the strain cultivated in the 5 L fermentor (**Figures 4**, **5**). The reason that the OUR of the recombinant was lower and the intracellular oxygen utilization efficiency was higher than that of the reference strain on aerobic metabolism was not completely understood. Some researchers think that expression of VHb can improve the level of intracellular dissolved oxygen by enhancing oxygen delivery, thus improving the respiration and energy metabolism of the cell (Wei and Chen, 2008; Frey et al., 2011). The results above demonstrated that the VHb gene was successfully transformed in the yeast strain *S. bombicola* O-13–1, and VHb expression improved the oxygen utilization efficiency. Meanwhile, the expression of *vgb* in *S. bombicola* O-13–1 provided a new strategy to promote SLs production in highly viscous fermentation systems.

Effects of *Vitreoscilla* hemoglobin Expression on the Expression of Several Key Host Genes

The presence of VHb can regulate gene expression in its host (Stark et al., 2015). In this study, expression levels of several host genes, including two genes (CYP52*M1* and *UGTA1*) involved in SLs biosynthesis, three genes (*CS*, *ICD*, and *KDG1*) involved in tricarboxylic acid (TCA) cycle, and three genes (*NDH, SDH, COX*) involved in electron transport chain (ETC) and ATP production, were determined in the transformant strains and wild-type strains using qRT-PCR at 24 and 72 h (**Figure 6**). At 24 h, all genes above were expressed approximately at the same levels in the transformants and wild-type strains. At 72 h, however, the expression levels of these genes were higher in the transformants than in the wild-type strains. The results might partially explain the phenomenon that VHb expression did not improve the OUR of the yeast in the first 24 h but reduced oxygen uptake during SLs production. Similarly, VHb expression enhanced natamycin production in recombinant strains of *Streptomyces gilvosporeus* compared to wild-type strains (Wang H. et al., 2018), and ploy hydroxybutyrate (PHB) production was much higher in *vgb*-bearing strains Reh01 than in wild-type strains of *Cupriavidus necator* H16 (Tang et al., 2020). These results indicated that expression of *vgb* gene greatly raised the production of surfactants in the later stage of fermentation.

Cytochrome P450 monooxygenase is a key enzyme in SLs synthesis that hydroxylates the end of fatty acids and controls the chain length of the SLs hydroxy fatty acid tail (Van Bogaert et al., 2009). Uracil diphosphate (UDP)-glucosyltransferase is an enzyme responsible for the first glucosylation step in the SLs biosynthetic pathway (Saerens et al., 2011). In this study, the expression of two genes, including *cyp52m1* encoding cytochrome P450 monooxygenase and *ugta1* encoding uracil diphosphate glucosyltransferase, were determined to evaluate the effects of VHb expression on the biosynthesis of SLs (**Figure 6A**). VHb expression increased the transcriptional levels of *cyp52m1* and *ugta1* by 2.03 folds and 1.31 folds, respectively, compared to the wild-type strains.

A sufficient supply of oxygen is crucial for cellular respiration. In an electron transport chain (ETC), electrons can be transferred from electron donors (e.g., NADH or $FADH_2$) into oxygen as an electron acceptor to release protons for ATP synthesis, tricarboxylic acid (TCA) cycle is the main source of electron donors for the ETC. The biosynthesis of SLs is an energy-requiring process. The additional ATP for SLs production can be provided by enhancing the ETC and TCA cycle through

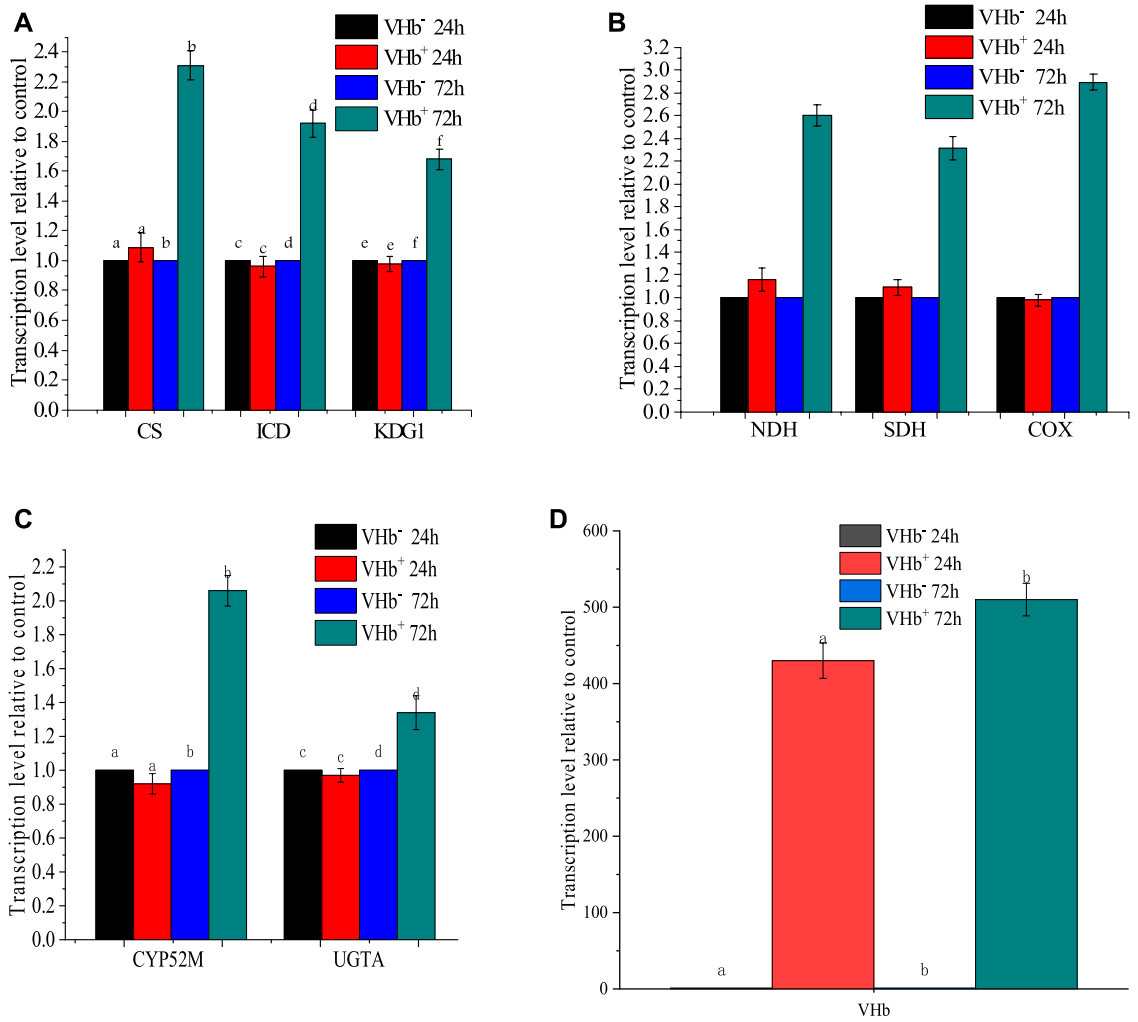

FIGURE 6 | Transcription levels of key genes involved in the TCA cycle, respiratory chain and sophorolipid biosynthesis at 24 and 72 h of fermentation. The transcription levels of genes in the recombinant strains were normalized to the transcription level of genes in the wild-type strains. **(A)** transcription levels of *CS*, *ICD*, and *KDG1*; **(B)** transcription levels of *NDH*, *SDH*, and *COX*; **(C)** transcription levels of *CYP52M* and *UGTA*; and **(D)** expression level of VHb.

heterologous expression of VHb. NADH dehydrogenase (NDH), succinate dehydrogenase (SDH) and cytochrome c oxidase (COX) are three main respiratory oxidases in *S. bombicola* (Freel et al., 2015). The transcription levels of *COX*, *NDH* and *SDH* in the recombinants promoted by 2.89, 2.55 and 2.28 folds compared to those in the wild-type strains, respectively (**Figure 6B**), indicating that the expression of VHb could boost cellular respiration and require more electron donors (NADH or FADH). Meanwhile, it suggested that VHb could provide oxygen directly to the terminal oxidases. This is consistent with the characteristics of VHb, which interacts with terminal respiratory oxidases to generate an efficient electron transfer for promoting energy generation (Stark et al., 2015). Given that citrate synthase (CS), isocitrate dehydrogenase (ICD), and alpha-ketoglutarate dehydrogenase (KGDH, coded by gene *KDG1*) are enzymes involved in the production of electron donors in the TCA cycle, the transcription levels of *CS*, *ICD* and *KDG1* were also measured (**Figure 6C**). The expression of these three genes in the recombinants improved by 2.27, 1.90 and 1.60 folds compared to those in the wild-type strains, respectively, indicating that the expression of VHb enhanced the transcription of genes involved in the ETC and TCA cycle.

As shown in **Figure 6D**, VHb had a higher expression level at 24 h of fermentation because the promoter used for expression was constitutive. However, there is no significant difference in the expression levels of these key genes involved in ETC, TCA cycle and SLs synthesis compared with the wild-type strain (VHb^-). At 72 h, though the expression level of VHb only raised by 1.18 folds, its expression significantly increased the expression of the key genes involved in the ETC, TCA cycle and SLs synthesis. However, it is still unknown about the mechanism underlying the effects of VHb expression on aerobic metabolism in *S. bombicola*, and more detailed studies at molecular levels should be conducted in the future.

The presence and function of VHb in promoting respiration and ATP formation has been considered to be responsible for the

improvements of cell growth, protein synthesis and metabolism (Stark et al., 2011). For instance, the transcription levels of *PGM*, *UGP* and *GLS* involved in polysaccharide biosynthesis were up-regulated by 1.51-, 1.55- and 3.83-fold, respectively, in vgb-bearing G. lucidum (Li et al., 2016b). Similarly, the transcription levels of key genes involved in the ETC, TCA cycle, and exopolysaccharides synthesis promoted in vgb-bearing strains (Liu et al., 2017; Xue et al., 2019).

CONCLUSION

A heterologous protein VHb was successfully expressed in S. bomcicola O-13–1 and was biochemically active. Compared with the wild-type strains, the expression of VHb in the recombinants significantly enhanced the intracellular oxygen utilization efficiency without improving the production of SLs. VHb expression could up-regulate the expression of key genes involved in the ETC, TCA cycle and SLs biosynthesis by improving cellular respiration and ATP supply. The findings highlight the potential use of VHb to improve the industrial-scale production of SLs utilizing agro-industrial waste as feedstock when the bioreactor is limited by the oxygen supply.

DATA AVAILABILITY STATEMENT

The original contributions presented in the study are included in the article/Supplementary Material, further inquiries can be directed to the corresponding author.

AUTHOR CONTRIBUTIONS

JL performed the experiment and drafted the article. HL and SY conducted analysis and interpretation of data. XX revised the article for important intellectual content. SL designed the experiment and published the article. All authors contributed to the article and approved the submitted version.

FUNDING

This work is supported by the National Key Research and Development Project of China (No. 2018YFC1407602), National Science Fund Projects of China (No. U1806212) and Major Scientific and Technological Innovation Project (MSTIP) of Shandong (No. 2019JZZY020705).

REFERENCES

Asmer, H.-J., Lang, S., Wagner, F., and Wray, V. (1988). Microbial Production, Structure Elucidation and Bioconversion of Sophorose Lipids. *J. Am. Oil Chem. Soc.* 65 (9), 1460–1466. doi:10.1007/BF02898308

Chi, Z., Wang, X.-X., Ma, Z.-C., Buzdar, M. A., and Chi, Z.-M. (2012). The Unique Role of Siderophore in Marine-Derived *Aureobasidium Pullulans* HN6.2. *BioMetals* 25 (1), 219–230. doi:10.1007/s10534-011-9499-1

Chi, Z., Liu, N.-N., Jiang, H., Wang, Q.-Q., Chen, J.-T., Liu, G.-L., et al. (2019). Relationship between β-d-Fructofuranosidase Activity, Fructooligosaccharides and Pullulan Biosynthesis in Aureobasidium Melanogenum P16. *Int. J. Biol. Macromolecules* 125, 1103–1111. doi:10.1016/j.ijbiomac.2018.12.141

Dogan, I., Pagilla, K. R., Webster, D. A., and Stark, B. C. (2006). Expression of *Vitreoscilla* Hemoglobin in *Gordonia Amarae* Enhances Biosurfactant Production. *J. Ind. Microbiol. Biotechnol.* 33 (8), 693–700. doi:10.1007/s10295-006-0097-0

Felse, P. A., Shah, V., Chan, J., Rao, K. J., and Gross, R. A. (2007). Sophorolipid Biosynthesis by *Candida Bombicola* from Industrial Fatty Acid Residues. *Enzyme Microb. Tech.* 40 (2), 316–323. doi:10.1016/j.enzmictec.2006.04.013

Freel, K. C., Friedrich, A., and Schacherer, J. (2015). Mitochondrial Genome Evolution in Yeasts: An All-Encompassing View. *FEMS yeast Res.* 15 (4), v23. doi:10.1093/femsyr/fov023

Frey, A. D., Shepherd, M., Jokipii-Lukkari, S., Häggman, H., and Kallio, P. T. (2011). The Single-Domain Globin of Vitreoscilla. *Adv. Microb. Physiol.* 58, 81–139. doi:10.1016/B978-0-12-381043-4.00003-9

Gao, R., Deng, H., Guan, Z., Liao, X., and Cai, Y. (2018). Enhanced Hypocrellin Production via Coexpression of Alpha-Amylase and Hemoglobin Genes in *Shiraia bambusicola*. *AMB Expr.* 8 (1), 71. doi:10.1186/s13568-018-0597-0

Garcia-Ochoa, F., Gomez, E., Santos, V. E., and Merchuk, J. C. (2010). Oxygen Uptake Rate in Microbial Processes: An Overview. *Biochem. Eng. J.* 49 (3), 289–307. doi:10.1016/j.bej.2010.01.011

Geckil, H., Stark, B. C., and Webster, D. A. (2001). Cell Growth and Oxygen Uptake of *Escherichia Coli* and *Pseudomonas Aeruginosa* Are Differently Effected by the Genetically Engineered *Vitreoscilla* Hemoglobin Gene. *J. Biotechnol.* 85 (1), 57–66. doi:10.1016/s0168-1656(00)00384-9

Guilmanov, V., Ballistreri, A., Impallomeni, G., and Gross, R. A. (2002). Oxygen Transfer Rate and Sophorose Lipid Production byCandida Bombicola. *Biotechnol. Bioeng.* 77 (5), 489–494. doi:10.1002/bit.10177

Hu, Y., and Ju, L.-K. (2001). Sophorolipid Production from Different Lipid Precursors Observed with LC-MS. *Enzyme Microb. Tech.* 29 (10), 593–601. doi:10.1016/S0141-0229(01)00439-2

Huang, X., Lu, X., and Li, J.-J. (2014). Cloning, Characterization and Application of a Glyceraldehyde-3-Phosphate Dehydrogenase Promoter from *Aspergillus Terreus*. *J. Ind. Microbiol. Biotechnol.* 41 (3), 585–592. doi:10.1007/s10295-013-1385-0

Jiménez-Peñalver, P., Gea, T., Sánchez, A., and Font, X. (2016). Production of Sophorolipids from Winterization Oil Cake by Solid-State Fermentation: Optimization, Monitoring and Effect of Mixing. *Biochem. Eng. J.* 115, 93–100. doi:10.1016/j.bej.2016.08.006

Jiménez-Peñalver, P., Castillejos, M., Koh, A., Gross, R., Sánchez, A., Font, X., et al. (2018). Production and Characterization of Sophorolipids from Stearic Acid by Solid-State Fermentation, a Cleaner Alternative to Chemical Surfactants. *J. Clean. Prod.* 172 (1), 2735–2747. doi:10.1016/j.jclepro.2017.11.138

Kahraman, H., and Erenler, S. O. (2012). Rhamnolipid Production by *Pseudomonas Aeruginosa* Engineered with the *Vitreoscilla* Hemoglobin Gene. *Appl. Biochem. Microbiol.* 48 (2), 188–193. doi:10.1134/s000368381202007x

Li, H.-J., He, Y.-L., Zhang, D.-H., Yue, T.-H., Jiang, L.-X., Li, N., et al. (2016a). Enhancement of Ganoderic Acid Production by Constitutively Expressing *Vitreoscilla* Hemoglobin Gene in *Ganoderma Lucidum*. *J. Biotechnol.* 227, 35–40. doi:10.1016/j.jbiotec.2016.04.017

Li, H.-J., Zhang, D.-H., Yue, T.-H., Jiang, L.-X., Yu, X., Zhao, P., et al. (2016b). Improved Polysaccharide Production in a Submerged Culture of *Ganoderma Lucidum* by the Heterologous Expression of *Vitreoscilla* Hemoglobin Gene. *J. Biotechnol.* 217, 132–137. doi:10.1016/j.jbiotec.2015.11.011

Li, W. W., Li, J. S., and Xin, S. (2016c). Alkane Utilization, the Expression and Function of Cytochrome P450in Sophorolipid Synthesis in *Starmerella Bombicola* CGMCC 1576. *J. Ind. Microbiol. Biotechnol.* 5, 58–63.

Li, J., Li, H., Liang, S., and Song, D. (2018). Characterization of Sophorolipids from the Yeast *Starmerella Bombicola* O-13-1 Using Waste Fried Oil and Cane Molasses as Substrates. *Desalination Water Treat.* 119, 267–275. doi:10.5004/dwt.2018.22062

Liao, B., Wang, Y., Su, J., Liu, F., and He, J. (2014). Expression of Vitreoscilla Hemoglobin in Bacillus Thuringiensis BMB171 Can Promote Manganese(II) Oxidation under Oxygen-Restricted Conditions. *Ann. Microbiol.* 64, 1865–1868. doi:10.1007/s13213-014-0825-z

Liu, X., Zhu, P., Jiang, R., Wu, L., Feng, X., Li, S., et al. (2017). Enhancement of Welan Gum Production in *Sphingomonas* Sp. HT-1 via Heterologous Expression of *Vitreoscilla* Hemoglobin Gene. *Carbohydr. Polym.* 156, 135–142. doi:10.1016/j.carbpol.2016.08.081

Liu, M., Li, S., Xie, Y., Jia, S., Hou, Y., Zou, Y., et al. (2018). Enhanced Bacterial Cellulose Production by *Gluconacetobacter Xylinus* via Expression of *Vitreoscilla* Hemoglobin and Oxygen Tension Regulation. *Appl. Microbiol. Biotechnol.* 102 (3), 1155–1165. doi:10.1007/s00253-017-8680-z

Ma, X., Meng, L., Zhang, H., Zhou, L., Yue, J., Zhu, H., et al. (2020). Sophorolipid Biosynthesis and Production from Diverse Hydrophilic and Hydrophobic Carbon Substrates. *Appl. Microbiol. Biotechnol.* 104 (1), 77–100. doi:10.1007/s00253-019-10247-w

Manivasakam, P., and Schiestl, R. H. (1993). High Efficiency Transformation ofSaccharomyces Cerevisiaeby Electroporation. *Nucl. Acids Res.* 21, 4414–4415. doi:10.1093/nar/21.18.4414

Mora-Lugo, R., Madrigal, M., Yelemane, V., and Fernandez-Lahore, M. (2015). Improved Biomass and Protein Production in Solid-State Cultures of an *Aspergillus Sojae* Strain Harboring the *Vitreoscilla* Hemoglobin. *Appl. Microbiol. Biotechnol.* 99 (22), 9699–9708. doi:10.1007/s00253-015-6851-3

Oliveira, M., Camilios-Neto, D., Baldo, C., Magri, A., and Celligoi, M. A. P. C. (2014). Biosynthesis and Production of Sophorolipids. *Int. J. Sci. Tech. Res.* 3 (11), 133–146.

Özbek, B., and Gayik, S. (2001). The Studies on the Oxygen Mass Transfer Coefficient in a Bioreactor. *J. Process. Biochem.* 36 (8), 729–741. doi:10.1016/S0032-9592(00)00272-7

Setyawati, M. I., Chien, L.-J., and Lee, C.-K. (2007). Expressing Vitreoscilla Hemoglobin in Statically Cultured Acetobacter Xylinum with Reduced O2 Tension Maximizes Bacterial Cellulose Pellicle Production. *J. Biotechnol.* 132 (1), 38–43. doi:10.1016/j.jbiotec.2007.08.012

Shah, V., Jurjevic, M., and Badia, D. (2010). Utilization of Restaurant Waste Oil as a Precursor for Sophorolipid Production. *Biotechnol. Prog.* 23 (2), 512–515. doi:10.1021/bp0602909

Stark, B. C., Dikshit, K. L., and Pagilla, K. R. (2011). Recent Advances in Understanding the Structure, Function, and Biotechnological Usefulness of the Hemoglobin from the Bacterium *Vitreoscilla*. *Biotechnol. Lett.* 33 (9), 1705–1714. doi:10.1007/s10529-011-0621-9

Stark, B. C., Dikshit, K. L., and Pagilla, K. R. (2012). The Biochemistry of *Vitreoscilla* Hemoglobin. *Comput. Struct. Biotechnol. J.* 3 (4), e201210002. doi:10.5936/csbj.201210002

Stark, B. C., Pagilla, K. R., and Dikshit, K. L. (2015). Recent Applications of *Vitreoscilla* Hemoglobin Technology in Bioproduct Synthesis and Bioremediation. *Appl. Microbiol. Biotechnol.* 99 (4), 1627–1636. doi:10.1007/s00253-014-6350-y

Su, Y., Li, X., Liu, Q., Hou, Z., Zhu, X., Guo, X., et al. (2010). Improved Poly-γ-Glutamic Acid Production by Chromosomal Integration of the Vitreoscilla Hemoglobin Gene (Vgb) in Bacillus Subtilis. *Bioresour. Tech.* 101 (12), 4733–4736. doi:10.1016/j.biortech.2010.01.128

Suthar, D. H., and Chattoo, B. B. (2006). Expression of Vitreoscilla Hemoglobin Enhances Growth and Levels of α-amylase in Schwanniomyces Occidentalis. *Appl. Microbiol. Biotechnol.* 72 (1), 94–102. doi:10.1007/s00253-005-0237-x

Tang, R., Weng, C., Peng, X., and Han, Y. (2020). Metabolic Engineering of *Cupriavidus Necator* H16 for Improved Chemoautotrophic Growth and PHB Production under Oxygen-Limiting Conditions. *Metab. Eng.* 61, 11–23. doi:10.1016/j.ymben.2020.04.009

Van Bogaert, I. N. A., Saerens, K., De Muynck, C., Develter, D., Soetaert, W., and Vandamme, E. J. (2007). Microbial Production and Application of Sophorolipids. *Appl. Microbiol. Biotechnol.* 76 (1), 23–34. doi:10.1007/s00253-007-0988-7

Van Bogaert, I. N. A., Demey, M., Develter, D., Soetaert, W., and Vandamme, E. J. (2009). Importance of the Cytochrome P450 Monooxygenase CYP52 Family for the Sophorolipid-Producing yeastCandida Bombicola. *FEMS Yeast Res.* 9 (1), 87–94. doi:10.1111/j.1567-1364.2008.00454.x

Van Bogaert, I. N. A., Zhang, J., and Soetaert, W. (2011). Microbial Synthesis of Sophorolipids. *Process Biochem.* 46 (4), 821–833. doi:10.1016/j.procbio.2011.01.010

Wang, J. L., Nie, G. X., Su-Zhen, L. I., Xie, Y. M., and Cao, X. L. (2010). Optimal Wavelength for Determining the Content of Reducing Sugar by DNS Method. *J. Henan Agric. Sci.* 04 (3), 115–118. doi:10.15933/j.cnki.1004-3268.2010.04.003

Wang, X., Sun, Y., Shen, X., Ke, F., Zhao, H., Liu, Y., et al. (2012). Intracellular Expression of *Vitreoscilla* Hemoglobin Improves Production of *Yarrowia Lipolytica* Lipase LIP2 in a Recombinant *Pichia pastoris*. *Enzyme Microb. Tech.* 50 (1), 22–28. doi:10.1016/j.enzmictec.2011.09.003

Wang, H., He, X., Sun, C., Gao, J., Liu, X., and Liu, H. (2018a). Enhanced Natamycin Production by Co-Expression of *Vitreoscilla* Hemoglobin and Antibiotic Positive Regulators in *Streptomyces Gilvosporeus*. *Biotechnol. Biotechnological Equipment* 32 (2), 470–476. doi:10.1080/13102818.2017.1419073

Wang, Q., Yu, H., Wang, M., Yang, H., and Shen, Z. (2018b). Enhanced Biosynthesis and Characterization of Surfactin Isoforms with Engineered *Bacillus Subtilis* through Promoter Replacement and *Vitreoscilla* Hemoglobin Co-expression. *Process Biochem.* 70 (7), 36–44. doi:10.1016/j.procbio.2018.04.003

Wei, X.-X., and Chen, G.-Q. (2008). Applications of the VHb Gene *Vgb* for Improved Microbial Fermentation Processes. *Methods Enzymol.* 436, 273–287. doi:10.1016/s0076-6879(08)36015-7

Wu, J. M., and Fu, W. C. (2011). Intracellular Co-Expression of Vitreoscilla Hemoglobin Enhances Cell Performance and β-Galactosidase Production in Pichia pastoris. *J. Biosci. Bioeng.* 113 (3), 332–337. doi:10.1016/j.jbiosc.2011.10.014

Xue, S.-J., Jiang, H., Chen, L., Ge, N., Liu, G.-L., Hu, Z., et al. (2019). Over-Expression of *Vitreoscilla* Hemoglobin (VHb) and Flavohemoglobin (FHb) Genes Greatly Enhances Pullulan Production. *Int. J. Biol. Macromolecules* 132, 701–709. doi:10.1016/j.ijbiomac.2019.04.007

Yang, X., Zhu, L., Xue, C., Chen, Y., Qu, L., and Lu, W. (2012). Recovery of Purified Lactonic Sophorolipids by Spontaneous Crystallization during the Fermentation of Sugarcane Molasses with *Candida Albicans* O-13-1. *Enzyme Microb. Tech.* 51 (6-7), 348–353. doi:10.1016/j.enzmictec.2012.08.002

Ye, W., Zhang, W., Chen, Y., Li, H., Li, S., Pan, Q., et al. (2016). A New Approach for Improving Epothilone B Yield in *Sorangium Cellulosum* by the Introduction of *Vgb epoF* Genes. *J. Ind. Microbiol. Biotechnol.* 43 (5), 641–650. doi:10.1007/s10295-016-1735-9

Zhang, L., Li, Y., Wang, Z., Xia, Y., Chen, W., and Tang, K. (2007). Recent Developments and Future Prospects of *Vitreoscilla* Hemoglobin Application in Metabolic Engineering. *Biotechnol. Adv.* 25, 123–136. doi:10.1016/j.biotechadv.2006.11.001

Zhang, H.-T., Zhan, X.-B., Zheng, Z.-Y., Wu, J.-R., Yu, X.-B., Jiang, Y., et al. (2011). Sequence and Transcriptional Analysis of the Genes Responsible for Curdlan Biosynthesis in *Agrobacterium* Sp. ATCC 31749 under Simulated Dissolved Oxygen Gradients Conditions. *Appl. Microbiol. Biotechnol.* 91 (1), 163–175. doi:10.1007/s00253-011-3243-1

Zhang, S., Wang, J., Wei, Y., Tang, Q., Ali, M. K., and He, J. (2014). Heterologous Expression of VHb Can Improve the Yield and Quality of Biocontrol Fungus *Paecilomyces Lilacinus*, during Submerged Fermentation. *J. Biotechnol.* 187, 147–153. doi:10.1016/j.jbiotec.2014.07.438

Zhang, Y., Jia, D., Sun, W., Yang, X., Zhang, C., Zhao, F., et al. (2018). Semicontinuous Sophorolipid Fermentation Using a Novel Bioreactor with Dual Ventilation Pipes and Dual Sieve-Plates Coupled with a Novel Separation System. *Microb. Biotechnol.* 11 (3), 455–464. doi:10.1111/1751-7915.13028

Conflict of Interest: The authors declare that the research was conducted in the absence of any commercial or financial relationships that could be construed as a potential conflict of interest.

Publisher's Note: All claims expressed in this article are solely those of the authors and do not necessarily represent those of their affiliated organizations, or those of the publisher, the editors, and the reviewers. Any product that may be evaluated in this article, or claim that may be made by its manufacturer, is not guaranteed or endorsed by the publisher.

frontiers in Bioengineering and Biotechnology

ORIGINAL RESEARCH
published: 04 November 2021
doi: 10.3389/fbioe.2021.784559

Engineering *Sphingobium* sp. to Accumulate Various Carotenoids Using Agro-Industrial Byproducts

Mengmeng Liu[1,2], Yang Yang[3], Li Li[4], Yan Ma[1], Junchao Huang[5] and Jingrun Ye[1]**

[1]School of Marine Science and Engineering, Qingdao Agricultural University, Qingdao, China, [2]Key Laboratory of Microbial Technology, Shandong University, Qingdao, China, [3]Qingdao Eighth People's Hospital, Qingdao, China, [4]Department of Laboratory Medicine, Qingdao Central Hospital, Qingdao, China, [5]Institute for Advanced Study, Shenzhen University, Shenzhen, China

Carotenoids represent the most abundant lipid-soluble phytochemicals that have been shown to exhibit benefits for nutrition and health. The production of natural carotenoids is not yet cost effective to compete with chemically synthetic ones. Therefore, the demand for natural carotenoids and improved efficiency of carotenoid biosynthesis has driven the investigation of metabolic engineering of native carotenoid producers. In this study, a new *Sphingobium* sp. was isolated, and it was found that it could use a variety of agro-industrial byproducts like soybean meal, okara, and corn steep liquor to accumulate large amounts of nostoxanthin. Then we tailored it into three mutated strains that instead specifically accumulated ~5 mg/g of CDW of phytoene, lycopene, and zeaxanthin due to the loss-of-function of the specific enzyme. A high-efficiency targeted engineering carotenoid synthesis platform was constructed in *Escherichia coli* for identifying the functional roles of candidate genes of carotenoid biosynthetic pathway in *Sphingobium* sp. To further prolong the metabolic pathway, we engineered the *Sphingobium* sp. to produce high-titer astaxanthin (10 mg/g of DCW) through balance in the key enzymes β-carotene ketolase (BKT) and β-carotene hydroxylase (CHY). Our study provided more biosynthesis components for bioengineering of carotenoids and highlights the potential of the industrially important bacterium for production of various natural carotenoids.

Keywords: *Sphingobium*, crop wastes, carotenoids, biosynthetic pathway, astaxanthin

OPEN ACCESS

Edited by:
Jun Xia,
Huaiyin Normal University, China

Reviewed by:
Yongteng Zhao,
Kunming University of Science and Technology, China
Jin Liu,
Peking University, China

****Correspondence:***
Junchao Huang
huangjc@mail.kib.ac.cn
Jingrun Ye
yejingrun@qau.edu.cn

Specialty section:
This article was submitted to Bioprocess Engineering, a section of the journal Frontiers in Bioengineering and Biotechnology

Received: *28 September 2021*
Accepted: *18 October 2021*
Published: *04 November 2021*

Citation:
Liu M, Yang Y, Li L, Ma Y, Huang J and Ye J (2021) Engineering Sphingobium *sp. to Accumulate Various Carotenoids Using Agro-Industrial Byproducts. Front. Bioeng. Biotechnol. 9:784559. doi: 10.3389/fbioe.2021.784559*

INTRODUCTION

Carotenoids play essential roles in light harvesting and photoprotection in photosynthetic organisms (Niyogi et al., 1997; Niyogi et al., 2001). With some exception, animals and humans cannot synthesize carotenoids *de novo* but take them from the diets, serving as precursors to vitamin A and macula pigments (Grumet et al., 2016). Carotenoids have been applied in food, feed, nutraceuticals, cosmetics, and pharmaceuticals (Cezare-Gomes et al., 2019; Ye et al., 2019). The pathway of carotenoid biosynthesis has been extensively studied in various organisms (Shumskaya and Wurtzel, 2013). The condensation of two geranylgeranyl diphosphate (GGPP) molecules was catalyzed by phytoene synthase (CrtB) to phytoene (C40), which is subsequently desaturated to produce lycopene by phytoene desaturase (CrtI). Next, lycopene was conferred diverse functional groups *via* various carotenoid-modifying enzymes, including lycopene cyclase (CrtY), carotene ketolase (CrtW), and carotene hydroxylase (CrtZ). The cyclic carotenoids derived from lycopene have diverse biological properties and functions (Kim et al., 2014).

Currently, commercial natural carotenoids (e.g., β-carotene, astaxanthin, and zeaxanthin) are extracted from a small number of specific plant tissues and a few microbes (Liu et al., 2019). Microbial production is the major source of natural-origin carotenoids, such as β-carotene and astaxanthin, because of higher growth rates and contents (Zhang et al., 2018). Most studies have mainly focused on the metabolic engineering of the noncarotenogenic *Escherichia coli* and yeast for carotenoid production (Park et al., 2018; Ma et al., 2019). However, the expression of a large number of heterologous genes commonly leads to the instability of the engineered strains because of the consumption of cellular metabolites and the influence on the metabolic flux distribution (Li and Huang, 2018). Engineering with few heterologous genes in the natural carotenogenic microorganism might overcome the above problems. In previous studies, a few attempts have been made to modify the biosynthetic pathway of carotenoids in microorganisms, which has the synthetic pathway of carotenoids, including *Synechocystis* sp., *Xanthophyllomyces dendrorhous*, and *Mucor circinelloides*. However, the yields of the target carotenoids are unsatisfactory (Lagarde et al., 2000; Papp et al., 2006; Breitenbach et al., 2019).

Now, the production capacity of carotenoids in wild-type microbes, by improving fermentation efficiency, is still unsatisfactory. The main challenge in carotenoid production using microbes is to develop new resources that could use cost-effective culture medium to produce high carotenoid content and microbial biomass (Rodrigues et al., 2019). A feasible strategy for meeting the challenge is to construct high-yield carotenoid microorganism by metabolic engineering that could use agro-industrial byproducts for reducing production cost and maintaining sustainable development. Glycerol, corn steep, and okara have attracted interest as raw materials for microbial to production of value-added chemicals and compounds (Liu et al., 2012a; Lee et al., 2019; Zhao et al., 2019; Kang et al., 2020). Crude glycerol is a byproduct generated from biodiesel production; okara and corn steep liquor are generated as byproducts during the manufacture of soymilk and corn starch. Although glycerol, okara, and corn steep liquor are considered as byproducts, they are nutrient rich. However, they are highly underused energy sources, as a large proportion is dumped into incinerators and landfills (Lee et al., 2019; Kang et al., 2020; Zhao et al., 2020).

Sphingobium is a representative genus of sphingomonads that are able to synthesize a number of carotenoids, including β-carotene and its derivatives zeaxanthin, astaxanthin, and nostoxanthin (Jenkins et al., 1979; Silva et al., 2004; Ma et al., 2016). Several studies have reported that the sphingomonad families could efficiently degrade environmental pollutants and biowaste (Liu et al., 2012b; Chen et al., 2014; Mishra et al., 2017). Furthermore, this family has been identified as safe (GRAS), and some members have been approved by the USA and the EU to synthesize gellan gum, an extracellular polysaccharide, which is a suspending agent, gelling, and stabilizing for a wide range of foods (Morris, 1990; Sutherland, 1998). Thus, the nonpathogenic and carotenogenic *Sphingobium* bacteria have potential as novel producers of various food-grade carotenoids.

The aim of this study is to target engineer a newly isolated nostoxanthin-accumulated strain *Sphingobium* sp. KIB that could use a variety of crop wastes to four novel strains, which accumulated large amounts of phytoene, lycopene, zeaxanthin, and astaxanthin, respectively. These results indicated that the *Sphingobium* strains have the potential of industrial production of carotenoids.

MATERIALS AND METHODS

Bacterial Strains and Culture Conditions

Sphingobium sp. KIB was stored in the China General Microbiological Culture Collection Center (CGMCC No.12394), which was isolated from Kunming Institute of Botany (Liu et al., 2019). *Sphingobium* sp. KIB and its mutants and engineered strains were cultured in basal salt medium (BSM) at 28°C with shaking (220 rpm). BSM medium contains 4 g of $(NH_4)_2HPO_4$, 10 g of glucose, 0.585 g of $MgSO_4$, 13.3 g of KH_2PO_4, 1.86 g of citric acid monohydrate, and 10 ml of trace element solution per liter. The trace element solution contains 15 mg of $CuCl_2{\cdot}2H_2O$, 25 mg of $CoCl_2{\cdot}6H_2O$, 25 mg of $NaMoO_4{\cdot}2H_2O$, 30 mg of H_3BO_3, 84 mg of disodium EDTA·H_2O, 80 mg of Zn $(CH_3COO)_2{\cdot}2H_2O$, 123 mg/L of $MnCl_2{\cdot}2H_2O$, and 600 mg of ferric citrate. The pH value was adjusted with KOH. For testing of the carbon sources or nitrogen source utilization, the glucose or $(NH_4)_2HPO_4$ was replaced by 10 g/L of other carbon sources or 4 g/L of other nitrogen sources. *E. coli* JM109 was cultured at 37°C in LB medium and was used to clone expressing constructs for various carotenoids. Ampicillin (100 μg/ml) and/or chloramphenicol (34 μg/ml) was used when required.

Mutagenesis and Mutant Selection

Sphingobium sp. KIB was cultivated to a cell density of 0.7–0.8 measured by OD600. The bacterial cells (20 ml) were pelleted by centrifugation at 4,000 × *g* for 3 min and washed twice with 20 ml of PBS buffer. The cells were resuspended in 20 ml of LB medium and then treated with N-methyl-N-nitro-nitrosoguanidine (MNNG) in a final concentration of 3.5 mM for 1 h in the dark. Following the mutagenesis treatment, cells were washed with the growth medium four times to dilute mutagen and then incubated 6 h on a shaker (28°C, 150 rpm). Subsequently, cells were plated on LB plates, and colonies were developed at 28°C for 3 days. Colonies were screened based on their pigmentation (Li et al., 2017). Carotenoids appear to be different in colors, e.g., the colorless phytoene, red lycopene, and yellow zeaxanthin. Thus, mutants could be isolated by visual color screening. Colonies with different colors from wild-type strain were selected for further analysis of pigment composition.

Molecular Characterization of Mutants

DNA isolation were carried out according to Ma et al. (2016). Based on the genome sequence (accession No. SRR8864026) of *Sphingobium* sp. KIB, primers (**Supplementary Table S1**) were designed to amplify the full length of CrtB, CrtI, CrtY, and CrtG genes. The PCR programs were list in **Supplementary Table S1**.

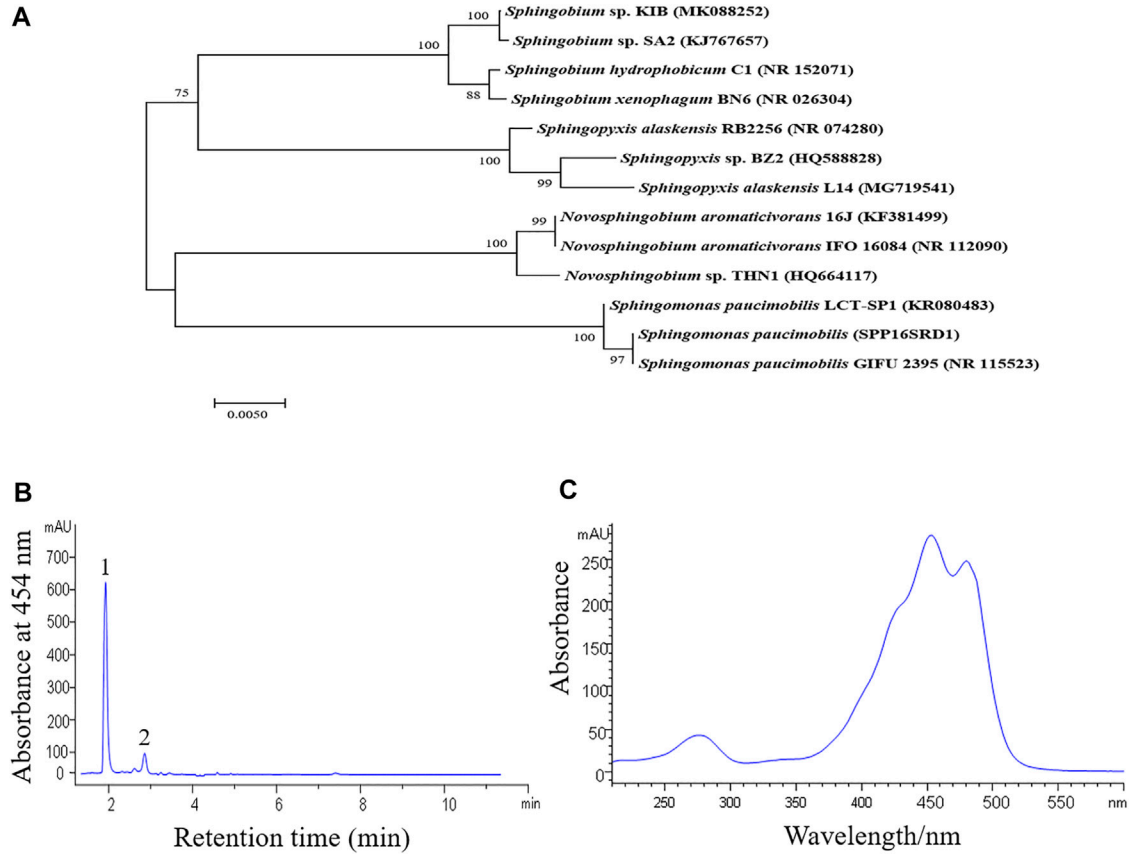

FIGURE 1 | Phylogenetic and carotenoid analysis of *Sphingobium* sp. KIB. **(A)** A phylogenetic tree based on the 16S rRNA gene sequences of *Sphingobium* sp. KIB and its related taxa. The tree was constructed by the neighbor-joining method. Numbers at nodes indicated bootstrap percentages (based on 1,000 resampled datasets). **(B)** Absorption profile of carotenoids extracted from the strain KIB. 1. Nostoxanthin, 2. Caloxanthin. **(C)** Absorption spectrum of peak 1.

PCR products were gel purified and sequenced. The Bio Edit software was used for sequence alignment.

Growth and Biomass Measurement

Exponential-phase cells were inoculated into 50 ml of culture medium in 250-ml Erlenmeyer flasks. Cultures were incubated at 28°C and 220 rpm in an orbital shaker. Samples were collected at an interval of 6 h for the determination of dry cell weight (DCW). For this, 2 ml of culture was washed twice with distilled water and then filtered through preweighted 0.22-μm membrane filters. Filtered cells were dried to a constant weight in an oven at 65°C.

Engineering Carotenoid Synthesis Platform in *Escherichia coli*

Recombinant DNA techniques were performed using standard methods. The plasmids and primers used in this study are listed in **Supplementary Table S1**. Relevant structures of the plasmids are listed in **Supplementary Figure S1**. The full length of CrtB, CrtI, CrtY, and CrtG genes were cloned, respectively, using *Sphingobium* sp. KIB genome DNA as a template and cloned into the plasmid pACYC184 to create plasmid pACCARcrtEB, pACCARcrtEBI, pACCARcrtEBIYZ, or pACCARcrtEBIYZG. *E. coli* JM109 carrying plasmid pACCARcrtEB, pACCARcrtEBI, pACCARcrtEBIYZ, or pACCARcrtEBIYZG displayed a white, red, yellow, or deep yellow phenotype due to the synthesis of phytoene, lycopene, zeaxanthin, or nostoxanthin.

Engineering *Sphingobium* sp. to Produce Astaxanthin

The plasmids pSPRGelb-DXS/IDI/CHY/CrtW, pSPRGelb-DXS/IDI/CHY/BKT, pSPRGelb-DXS/IDI/CrtZ/CrtW, and pSPRGelb-DXS/IDI/CrtZ/BKT were constructed according to Liu et al. The gene *CHY* was from *Haematococcus pluvialis*, and the gene *CrtZ* was from *Brevundimonas* sp. SD212. These two genes were cloned and then inserted into plasmid pSPRGelb-DXS/IDI at the SalI site, respectively, to construct the plasmids pSPRGelb-DXS/IDI/CHY and pSPRGelb-DXS/IDI/CrtZ. The gene *BKT* was from *Chlamydomonas reinhardtii*, and the gene *CrtW* was from *Brevundimonas* sp. SD212, and these two genes were cloned and then inserted into plasmids pSPRGelb-DXS/IDI/CHY and pSPRGelb-DXS/IDI/CrtZ at the SalI site, respectively, to construct the plasmids pSPRGelb-DXS/IDI/CHY/CrtW, pSPRGelb-DXS/IDI/CHY/BKT, pSPRGelb-DXS/IDI/CrtZ/CrtW, and pSPRGelb-DXS/IDI/CrtZ/BKT. Then these four

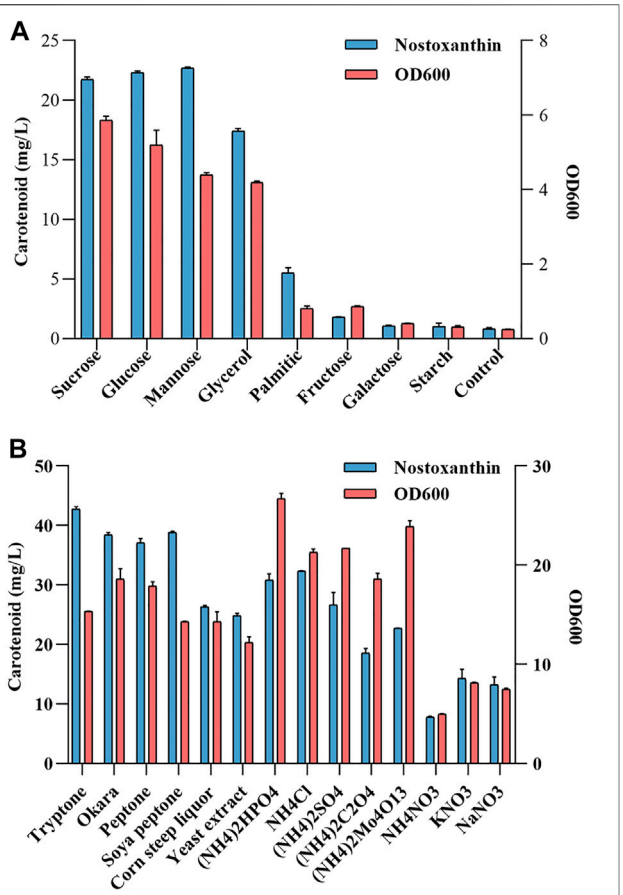

FIGURE 2 | Testing the carbon source **(A)** or nitrogen source **(B)** utilization of the *Sphingobium* sp. KIB.

plasmids were transformed using electrotransformation into *Sphingobium* sp. KIB-zea (Liu et al., 2019).

Extraction and Measurement of Carotenoids

Carotenoid analysis was performed according to Liu et al. (2019). Acetone was used to extract carotenoids. The acetone dissolved the carotenoids, which were blown to dryness with nitrogen gas and dissolved in 100 µl of acetone. Carotenoids were analyzed and quantitated using an Agilent Ultra-Performance Liquid Chromatography (UPLC) 1290 Infinity system equipped with an Agilent Eclipse Plus C18 RRHD 1.8-µm column (2.1 × 50 mm). The mobile phase consisted of solvent A (15% methanol, 60% acetonitrile, 5% isopropanol, and 20% water) and solvent B (15% methanol, 5% isopropanol, and 80% acetonitrile). The extracted carotenoids were eluted at a flow rate of 0.5 ml/min with the following process: 100% A for min; a liner gradient from 0 to 100% within 1 min; 100% B for 8 min. Compounds were detected at 454 and 280 nm, and the absorption spectra, retention times, and peak area of each carotenoid were compared with standards purchased from Sigma (China).

Phylogenetic Analysis

The standard chloroform/isopropanol method was used to extract genomic DNA from *Sphingobium* sp. KIB. Two primers, 27F (5′-AGAGTTTGATCCTGGCTCAG-3′) and 1429R (5′-GGTTACCTTGTTACGACTT-3′) were used for amplification of the 16S rRNA gene. The amplification product was purified and sequenced by Shenggong Bioscience Company (Shanghai, China). The 16S rRNA gene sequence of *Sphingobium* sp. KIB was submitted to GenBank (accession number MK088252). The phylogenetic tree was constructed using the neighbor-joining method *via* the MEGA 7.0 software.

RESULTS AND DISCUSSIONS

Isolation of a Nostoxanthin-Accumulating *Sphingobium* Strain

A yellow pigmented bacterial strain was isolated from tissue culture plates at Kunming Institute of Botany (KIB), which was revealed to be a rod-shaped and Gram-negative bacterium. Phylogenetic analysis based on the 16S rRNA gene sequences showed that the strain had the highest similarity to *Sphingobium* sp. SA2 (KJ767657.1) (**Figure 1A**). We, therefore, named the strain as *Sphingobium* sp. KIB. *Sphingobium* sp. KIB was found to produce nostoxanthin, a zeaxanthin derivative, up to 93% of total carotenoids (**Figures 1B,C**), which was much higher than the levels reported in its relatives (Jenkins et al., 1979; Zhu et al., 2012). We hypothesized that *Sphingobium* sp. KIB was a promising carotenoid-producing strain.

Utilization of Agro-Industrial Byproducts to Accumulate Carotenoids

Various carbon sources or nitrogen sources were tested as a potential nutrient for the fermentation of the *Sphingobium* sp. KIB. It was observed that most carbon sources and nitrogen sources were able to effectively support the growth of *Sphingobium* sp. KIB (**Figure 2**). Of the eight carbon sources tested, sucrose, glucose, mannose, and glycerol demonstrated the best carbon sources for carotenoid production and cell growth (**Figure 2A**). Of the 14 nitrogen sources investigated, tryptone, soya peptone, and okara were found to be the best one for carotenoid production, and $(NH_4)_2HPO_4$ was found to be the best one for cell growth (**Figure 2B**). These results demonstrated that the agro-industrial byproducts, such as glycerol, okara, and corn steep liquor, could be effectively used by *Sphingobium* sp. KIB to benefit cell growth and stimulate carotenoid accumulation. So, at the following studies, 10 g/L of glycerol was used as carbon source and 4 g/L okara was used as nitrogen source.

These byproducts were highly underused energy sources, as a large proportion is dumped into incinerators and landfills (Lee et al., 2019; Kang et al., 2020). It would be desirable to find that *Sphingobium* sp. KIB could use these agro-industrial byproducts to produce high-value carotenoids. Hence, *Sphingobium* sp. KIB could serve as a starting strain for the efficient production of zeaxanthin (Liu et al., 2019) and possibly other carotenoids using

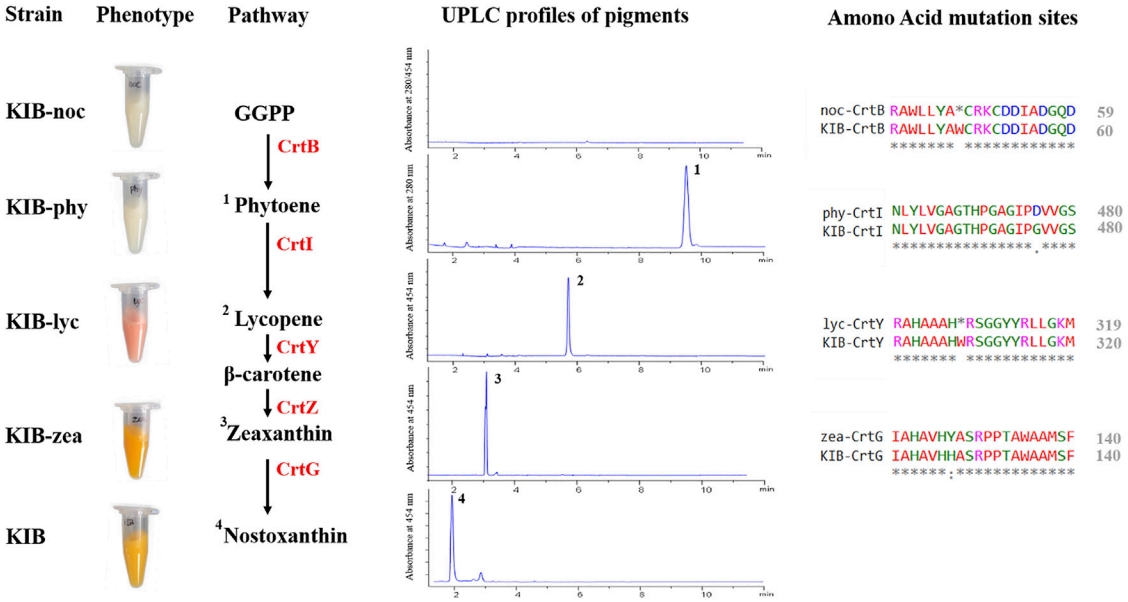

FIGURE 3 | Relevant information of the four mutants. The phenotypes, carotenoid biosynthetic pathway, carotenoid chromatograms, and amino acid substitutions of the mutated targets are shown. 1. Phytoene. 2. Lycopene. 3. Zeaxanthin. 4. Nostoxanthin. GGPP, geranylgeranyl-pyrophosphate; CrtB, phytoene synthase; CrtI, phytoene desaturase; CrtY, lycopene beta-cyclase; CrtZ, beta-carotene hydroxylase; CrtG, 2,2′-beta-ionone hydroxylase.

agro-industrial byproducts *via* knocking out or introducing the key enzymes involved in the carotenoid biosynthetic pathway.

Isolation of *Sphingobium* sp. KIB Mutants Accumulating Other Carotenoids

Sphingobium sp. KIB was treated with a chemical mutagen (MNNG) followed by a color-based screening process. About 100 colonies exhibiting different colors from wild-type strain were selected and subjected to pigment analysis. Four stable mutants, accumulating no carotenoid, phytoene, lycopene, or zeaxanthin, were successfully achieved based on their pigment profiles (**Figure 3**). *Sphingobium* sp. KIB-noc demonstrated a white color and accumulated no carotenoid due to a nonsense mutation in the *CrtB* gene that encodes phytoene synthase involved in catalyzing the first step of carotenoid formation (**Figure 3**). *Sphingobium* sp. KIB-phy also demonstrated a white color but predominantly accumulated the colorless carotenoid phytoene (up to 90% of total carotenoids) owing to one amino acid substitution (G476D) in the CrtI (**Figure 3**). *Sphingobium* sp. KIB-lyc exhibited a red color and mainly accumulated lycopene due to the nonsense mutation of CrtY, which is involved in converting lycopene to β-carotene (**Figure 3**). *Sphingobium* sp. KIB-zea was yellow and accumulated zeaxanthin up to 90% of total carotenoids, which consisted of an amino acid substitution (H127Y) in CrtG; the enzyme catalyzes zeaxanthin to nostoxanthin (**Figure 3**).

The four mutants showed similar growing status to their parent wild-type strain (**Figure 4A**). All strains reached their highest biomass at 36 h. Wild type and the mutants KIB-phy, KIB-lyc, and KIB-zea constitutively accumulated nostoxanthin, phytoene, lycopene, and zeaxanthin, respectively. The contents of the carotenoids in the strains increased over time, reaching the highest value of about 5.4 mg g^{-1} of dry cell weight at 48 h (**Figure 4B**). This result indicated that *Sphingobium* sp. KIB and its mutants maintained a homeostasis of carotenoids, irrespective of the kinds of carotenoids.

For further confirmation of the catalytic efficiency of carotenoid biosynthetic genes in *Sphingobium* sp. KIB, a high-efficiency targeted metabolic engineering carotenoid biosynthesis platform was constructed in *E. coli* (**Figure 5**). According to bioinformatic analysis (Liu et al., 2019) and mutant analysis, six enzymes, namely, CrtE (geranylgeranyl pyrophosphate synthase), CrtB (phytoene synthase), CrtI (phytoene desaturase), CrtY (lycopene beta-cyclase), CrtZ (beta-carotene hydroxylase), and CrtG (2,2′-beta-ionone hydroxylase) (GenBank: no. SRR8864026), involved in the successive condensation process from IPP and DMAPP to nostoxanthin, were identified. These engineered *E. coli* strains, named as E-phy, E-lyc, E-zea, and E-nos, were able to accumulate 6.01 ± 0.034 mg of phytoene, 5.96 ± 0.058 mg of lycopene, 5.99 ± 0.083 mg of zeaxanthin, and 6.03 ± 0.057 mg of nostoxanthin g^{-1} dry cell, respectively, when cultured in LB medium for 48 h (**Figure 5B**). From these analyses, we clarified the entire carotenoid biosynthesis pathway and found that the genes involved in carotenoid biosynthesis of *Sphingobium* sp. KIB, thus, provided more biosynthesis components for bioengineering of carotenoids.

Metabolic Engineering of *Sphingobium* to Produce High-Titer Astaxanthin

Some noncarotenogenic bacteria and yeast have been engineered to accumulate astaxanthin by heterologous

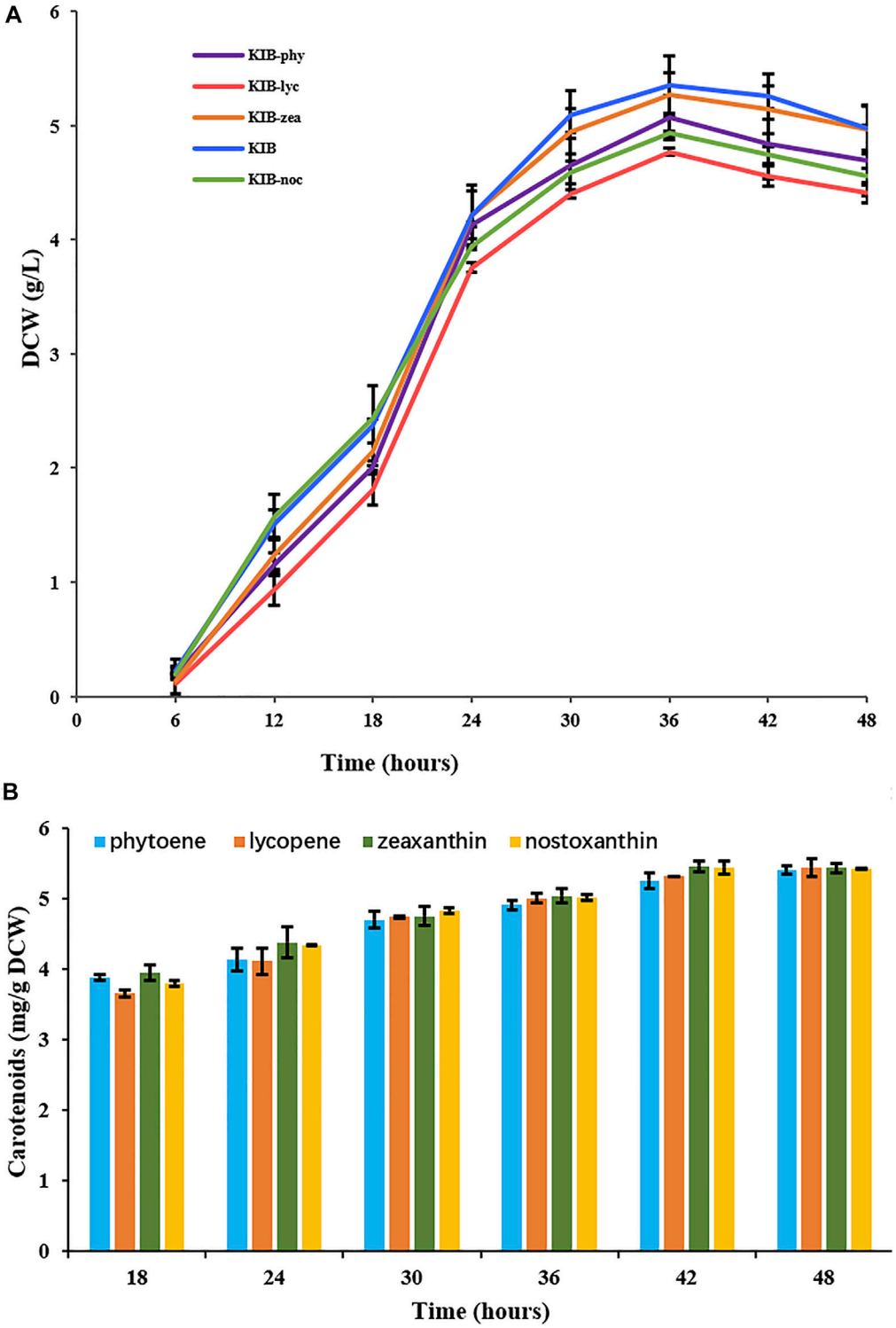

FIGURE 4 | Growth **(A)** and carotenoid contents **(B)** of *Sphingobium* sp. KIB and its mutants. KIB produced nostoxanthin, KIB-phy produced phytoene, KIB-lyc produced lycopene and KIB-zea produced zeaxanthin.

expression of a series of carotenogenic genes. However, the yield is less than unsatisfactory compared with other carotenoids (Jin et al., 2018). To further prolong the metabolic pathway, we engineered *Sphingobium* sp. KIB-zea to accumulate astaxanthin. A previous study suggested that the pathway from β-carotene to astaxanthin is the limited step of

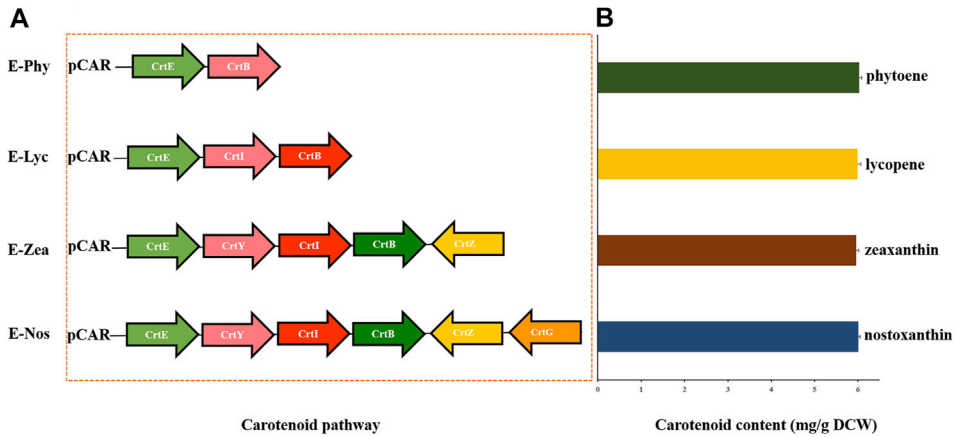

FIGURE 5 | Engineered *Escherichia coli* JM109 expressing the genes for the production of specific carotenoids. **(A)** Plasmids containing the carotenogenic genes from *Sphingobium* sp. KIB (*CrtE*, *CrtB*, *CrtI*, *CrtY*, *CrtZ*, and *CrtG*). **(B)** Contents of carotenoids in engineered strains of E-Phy, E-Lyc, E-Zea, and E-Nos detected by ultra-performance liquid chromatography (UPLC).

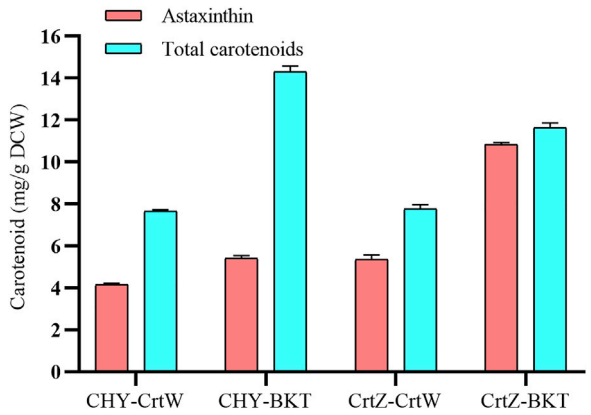

FIGURE 6 | Engineered *Sphingobium* sp. KIB-zea combination expressing two β-carotene ketolase and two β-carotene hydroxylase for the production of astaxanthin. BKT from *Chlamydomonas reinhardtii*; CrtW from *Brevundimonas* sp. SD212; CHY from *Haematococcus pluvialis*; CrtZ from *Brevundimonas* sp. SD212.

astaxanthin synthesis, which was catalyzed by β-carotene ketolase and β-carotene hydroxylase (Scaife et al., 2009). The combination of these two enzymes is critical to astaxanthin production. We combination express two β-carotene ketolase (*Chlamydomonas reinhardtii* BKT and *Brevundimonas* sp. SD212 CrtW) and two β-carotene hydroxylase (*Haematococcus pluvialis* CHY and *Brevundimonas* sp. SD212 CrtZ) to find a better combination for efficiently converting to astaxanthin in *Sphingobium* sp. KIB-zea. Among these four combinations, CrtZ and BKT was the best one with the highest titer of astaxanthin (10.75 mg/g DCW) and total carotenoids (11.6 mg/g DCW) (**Figure 6**). It should be pointed out that the high astaxanthin content in this strain represents 93% of total carotenoids, which will facilitate downstream processing to obtain a pure product.

Carotenoids are bioactive compounds with numerous biological functions. The increasing demand of various carotenoids has led to many methods to manufacture carotenoids. To date, commercial carotenoids are mainly produced through chemical synthesis. On an industrial scale, carotenoids can also be extracted from naturally producing organisms, e.g., astaxanthin from *Haematococcus pluvialis* (Lorenz and Cysewski, 2000), β-carotene from *Dunaliella* (Ben-Amotz, 1995), and *Blakeslea trispora* (Goksungur et al., 2002). In addition, heterologous biosynthesis of carotenoids in noncarotenogenic microorganisms, such as *E. coli* and *Saccharomyces cerevisiae*, has achieved great progress (Chen et al., 2013; Zhou et al., 2015; Shen et al., 2016). Bacterial cultivation is more convenient for large-scale production due to their unicellular nature and high growth rate (Silva et al., 2004; Shiloach and Fass, 2005). Hence, the noncarotenogenic bacterium *E. coli* has been engineered to produce significant amounts of carotenoids with different strategies. At least five heterologous genes were required to make *E. coli* produce zeaxanthin at a level of 1.1 mg g^{-1} dry cell weight (Misawa et al., 1990). Strategies, including coordinating the expression of two or more enzymes (Li et al., 2015), codon optimization (Wang et al., 2011), gene copy number adjustment (Misawa, 2011; Zelcbuch et al., 2013), and integrated multifactor (Li and Huang, 2018) were used to improve carotenoid production. Generally, two or more plasmids consisting of a number of genes had to be introduced into the host (Zelcbuch et al., 2013; Ma et al., 2016), or alternatively, the expression cassettes were integrated into the genomes of the targeted organisms (Zelcbuch et al., 2013; Lu et al., 2017). However, the introduction of too many foreign genes generally resulted in impediment of host growth and production instability (Shen et al., 2016). As a result, no engineered bacteria have been used for carotenoid production on a large scale.

Thus, carotenogenic microorganisms, in particular, those that are generally regarded as safe, e.g., sphingomonads species (Liu et al., 2012b; Kim et al., 2014; Ma et al., 2016), are promising hosts

for carotenoid production. Our strain *Sphingobium* sp. KIB produced nostoxanthin up to 93% of the total carotenoids, which was much higher than that from others (Silva et al., 2004; Asker et al., 2009; Zhu et al., 2012), and demonstrated that *Sphingobium* sp. KIB could effectively use agro-industrial byproducts, such as glycerol, okara, and corn steep liquor, to benefit cell growth and stimulate carotenoid accumulation. Furthermore, we demonstrated that this strain could be tailored to specifically produce various carotenoids at a level of over 5 mg g^{-1} dry cell weight through chemical mutagenesis and produce astaxanthin at a level of 10 mg g^{-1} dry cell weight through directed metabolic engineering. So far, *Sphingobium* species have not been reported to be animal pathogens. Moreover, *Sphingobium* was found to possibly play a role in preventing acute otitis media (AOM) (Chonmaitree et al., 2017). Hence, *Sphingobium* sp. KIB and its mutants could further serve as novel hosts for improved carotenoid productivity by metabolic engineering of the endogenous carotenoid pathways reported by us recently (Liu et al., 2019).

CONCLUSION

In conclusion, a new *Sphingobium* sp. was isolated and found that it could use agro-industrial byproducts, such as soybean meal, okara, and corn steep liquor, to accumulate large amounts of carotenoids. Then random mutagenesis or directed metabolic engineering was used to make the *Sphingobium* strain accumulate various high-value carotenoids, including phytoene, lycopene, zeaxanthin, and astaxanthin. Our study provided more biosynthesis components for bioengineering of carotenoids and highlights the potential of the industrially important bacterium for the production of various natural carotenoids.

DATA AVAILABILITY STATEMENT

The original contributions presented in the study are included in the article/**Supplementary Material**, further inquiries can be directed to the corresponding authors.

AUTHOR CONTRIBUTIONS

ML, YM, JH, and JY designed the research. ML and YM performed the research. ML analyzed the data. ML, YM, JH, and JY wrote the manuscript. ML, YY, and LL revised the manuscript.

FUNDING

This research was supported by the start-up funds from Qingdao Agriculture University (1120037, 1120036) and the National Natural Science Foundation of China (41806163).

SUPPLEMENTARY MATERIAL

The Supplementary Material for this article can be found online at: https://www.frontiersin.org/articles/10.3389/fbioe.2021.784559/full#supplementary-material

REFERENCES

Asker, D., Amano, S.-i., Morita, K., Tamura, K., Sakuda, S., Kikuchi, N., et al. (2009). Astaxanthin Dirhamnoside, a New Astaxanthin Derivative Produced by a Radio-Tolerant Bacterium, Sphingomonas Astaxanthinifaciens. *J. Antibiot.* 62, 397–399. doi:10.1038/ja.2009.50

Ben-Amotz, A. (1995). New Mode of Dunaliella Biotechnology: Two-phase Growth for β-carotene Production. *J. Appl. Phycol* 7, 65–68. doi:10.1007/bf00003552

Breitenbach, J., Pollmann, H., and Sandmann, G. (2019). Genetic Modification of the Carotenoid Pathway in the Red Yeast Xanthophyllomyces Dendrorhous: Engineering of a High-Yield Zeaxanthin Strain. *J. Biotechnol.* 289, 112–117. doi:10.1016/j.jbiotec.2018.11.019

Cezare-Gomes, E. A., Mejia-da-Silva, L. d. C., Pérez-Mora, L. S., Matsudo, M. C., Ferreira-Camargo, L. S., Singh, A. K., et al. (2019). Potential of Microalgae Carotenoids for Industrial Application. *Appl. Biochem. Biotechnol.* 188, 602–634. doi:10.1007/s12010-018-02945-4

Chen, Y.-F., Chao, H., and Zhou, N.-Y. (2014). The Catabolism of 2,4-xylenol and P-Cresol Share the Enzymes for the Oxidation of Para-Methyl Group in Pseudomonas Putida NCIMB 9866. *Appl. Microbiol. Biotechnol.* 98, 1349–1356. doi:10.1007/s00253-013-5001-z

Chen, Y. Y., Shen, H. J., Cui, Y. Y., Chen, S. G., Weng, Z. M., Zhao, M., et al. (2013). Chromosomal Evolution of *Escherichia coli* for the Efficient Production of Lycopene. *Bmc Biotechnol.* 13, 6. doi:10.1186/1472-6750-13-6

Chonmaitree, T., Jennings, K., Golovko, G., Khanipov, K., Pimenova, M., Patel, J. A., et al. (2017). Nasopharyngeal Microbiota in Infants and Changes during Viral Upper Respiratory Tract Infection and Acute Otitis media. *PLoS One* 12, e0180630. doi:10.1371/journal.pone.0180630

Goksungur, Y., Mantzouridou, F., and Roukas, T. (2002). Optimization of the Production of ?-carotene from Molasses byBlakeslea Trispora: a Statistical Approach. *J. Chem. Technol. Biotechnol.* 77, 933–943. doi:10.1002/jctb.662

Grumet, L., Taschler, U., and Lass, A. (2016). Hepatic Retinyl Ester Hydrolases and the Mobilization of Retinyl Ester Stores. *Nutrients* 9, 13. doi:10.3390/nu9010013

Jenkins, C. L., Andrewes, A. G., Mcquade, T. J., and Starr, M. P. (1979). The Pigment ofPseudomonas Paucimobilis Is a Carotenoid (Nostoxanthin), rather Than a Brominated Aryl-Polyene (Xanthomonadin). *Curr. Microbiol.* 3, 1–4. doi:10.1007/bf02603124

Jin, J., Wang, Y., Yao, M., Gu, X., Li, B., Liu, H., et al. (2018). Astaxanthin Overproduction in Yeast by Strain Engineering and New Gene Target Uncovering. *Biotechnol. Biofuels* 11, 230. doi:10.1186/s13068-018-1227-4

Kang, C. K., Jeong, S.-W., Yang, J. E., and Choi, Y. J. (2020). High-Yield Production of Lycopene from Corn Steep Liquor and Glycerol Using the Metabolically Engineered Deinococcus Radiodurans R1 Strain. *J. Agric. Food Chem.* 68, 5147–5153. doi:10.1021/acs.jafc.0c01024

Kim, S. H., Kim, J. H., Lee, B. Y., and Lee, P. C. (2014). The Astaxanthin Dideoxyglycoside Biosynthesis Pathway in Sphingomonas Sp. PB304. *Appl. Microbiol. Biotechnol.* 98, 9993–10003. doi:10.1007/s00253-014-6050-7

Lagarde, D., Beuf, L., and Vermaas, W. (2000). Increased Production of Zeaxanthin and Other Pigments by Application of Genetic Engineering Techniques to Synechocystis Sp. Strain PCC 6803. *Appl. Environ. Microbiol.* 66, 64–72. doi:10.1128/aem.66.1.64-72.2000

Lee, J. J., Cooray, S. T., Mark, R., and Chen, W. N. (2019). Effect of Sequential Twin Screw Extrusion and Fungal Pretreatment to Release Soluble Nutrients from Soybean Residue for Carotenoid Production. *J. Sci. Food Agric.* 99, 2646–2650. doi:10.1002/jsfa.9476

Li, J., Shen, J., Sun, Z., Li, J., Li, C., Li, X., et al. (2017). Discovery of Several Novel Targets that Enhance β-Carotene Production in *Saccharomyces cerevisiae*. *Front. Microbiol.* 8, 1116. doi:10.3389/fmicb.2017.01116

Li, S., and Huang, J. C. (2018). Assessment of Expression Cassettes and Culture Media for Different *Escherichia coli* Strains to Produce Astaxanthin. *Nat. Prod. Bioprospect* 8, 397. doi:10.1007/s13659-018-0172-z

Li, X.-R., Tian, G.-Q., Shen, H.-J., and Liu, J.-Z. (2015). Metabolic Engineering of *Escherichia coli* to Produce Zeaxanthin. *J. Ind. Microbiol. Biot* 42, 627–636. doi:10.1007/s10295-014-1565-6

Liu, M., Sandmann, G., Chen, F., and Huang, J. (2019). Enhanced Coproduction of Cell-Bound Zeaxanthin and Secreted Exopolysaccharides by Sphingobium Sp. *Via* Metabolic Engineering and Optimized Fermentation. *J. Agric. Food Chem.* 67, 12228–12236. doi:10.1021/acs.jafc.9b05342

Liu, X., Gai, Z., Tao, F., Tang, H., and Xu, P. (2012). Carotenoids Play a Positive Role in the Degradation of Heterocycles by Sphingobium Yanoikuyae. *Plos One* 7, e39522. doi:10.1371/journal.pone.0039522

Liu, X., Jensen, P. R., and Workman, M. (2012). Bioconversion of Crude Glycerol Feedstocks into Ethanol by Pachysolen Tannophilus. *Bioresour. Tech.* 104, 579–586. doi:10.1016/j.biortech.2011.10.065

Lorenz, R. T., and Cysewski, G. R. (2000). Commercial Potential for Haematococcus Microalgae as a Natural Source of Astaxanthin. *Trends Biotechnol.* 18, 160–167. doi:10.1016/s0167-7799(00)01433-5

Lu, Q., Bu, Y. F., and Liu, J. Z. (2017). Metabolic Engineering of *Escherichia coli* for Producing Astaxanthin as the Predominant Carotenoid. *Mar. Drugs* 15, 296. doi:10.3390/md15100296

Ma, T., Shi, B., Ye, Z., Li, X., Liu, M., Chen, Y., et al. (2019). Lipid Engineering Combined with Systematic Metabolic Engineering of *Saccharomyces cerevisiae* for High-Yield Production of Lycopene. *Metab. Eng.* 52, 134–142. doi:10.1016/j.ymben.2018.11.009

Ma, T., Zhou, Y., Li, X., Zhu, F., Cheng, Y., Liu, Y., et al. (2016). Genome Mining of Astaxanthin Biosynthetic Genes from Sphingomonas Sp. ATCC 55669 for Heterologous Overproduction in *Escherichia coli*. *Biotechnol. J.* 11, 228–237. doi:10.1002/biot.201400827

Misawa, N. (2011). Carotenoid β-Ring Hydroxylase and Ketolase from Marine Bacteria-Promiscuous Enzymes for Synthesizing Functional Xanthophylls. *Mar. Drugs* 9, 757–771. doi:10.3390/md9050757

Misawa, N., Nakagawa, M., Kobayashi, K., Yamano, S., Izawa, Y., Nakamura, K., et al. (1990). Elucidation of the Erwinia Uredovora Carotenoid Biosynthetic Pathway by Functional Analysis of Gene Products Expressed in Escherichia Coli. *J. Bacteriol.* 172, 6704–6712. doi:10.1128/jb.172.12.6704-6712.1990

Mishra, A., Kumar, J., and Melo, J. S. (2017). An Optical Microplate Biosensor for the Detection of Methyl Parathion Pesticide Using a Biohybrid of Sphingomonas Sp. Cells-Silica Nanoparticles. *Biosens. Bioelectron.* 87, 332–338. doi:10.1016/j.bios.2016.08.048

Morris, V. J. (1990). Biotechnically Produced Carbohydrates with Functional Properties for Use in Food Systems. *Food Biotechnol.* 4, 45–57. doi:10.1080/08905439009549721

Niyogi, K. K., Bjorkman, O., and Grossman, A. R. (1997). The Roles of Specific Xanthophylls in Photoprotection. *Proc. Natl. Acad. Sci.* 94, 14162–14167. doi:10.1073/pnas.94.25.14162

Niyogi, K. K., Shih, C., Soon Chow, W., Pogson, B. J., Dellapenna, D., and Björkman, O. (2001). Photoprotection in a Zeaxanthin- and Lutein-Deficient Double Mutant of Arabidopsis. *Photosynth Res.* 67, 139–145. doi:10.1023/a:1010661102365

Papp, T., Velayos, A., Bartók, T., Eslava, A. P., Vágvölgyi, C., and Iturriaga, E. A. (2006). Heterologous Expression of Astaxanthin Biosynthesis Genes in Mucor Circinelloides. *Appl. Microbiol. Biotechnol.* 69, 526–531. doi:10.1007/s00253-005-0026-6

Park, S. Y., Binkley, R. M., Kim, W. J., Lee, M. H., and Lee, S. Y. (2018). Metabolic Engineering of *Escherichia coli* for High-Level Astaxanthin Production with High Productivity. *Metab. Eng.* 49, 105–115. doi:10.1016/j.ymben.2018.08.002

Rodrigues, T. V. D., Amore, T. D., Teixeira, E. C., and Burkert, J. F. d. M. (2019). Carotenoid Production by Rhodotorula Mucilaginosa in Batch and Fed-Batch Fermentation Using Agroindustrial Byproducts. *Food Technol. Biotechnol. (Online)* 57, 388–398. doi:10.17113/ftb.57.03.19.6068

Scaife, M. A., Burja, A. M., and Wright, P. C. (2009). Characterization of Cyanobacterial β-carotene Ketolase and Hydroxylase Genes inEscherichia Coli, and Their Application for Astaxanthin Biosynthesis. *Biotechnol. Bioeng.* 103, 944–955. doi:10.1002/bit.22330

Shen, H.-J., Cheng, B.-Y., Zhang, Y.-M., Tang, L., Li, Z., Bu, Y.-F., et al. (2016). Dynamic Control of the Mevalonate Pathway Expression for Improved Zeaxanthin Production in *Escherichia coli* and Comparative Proteome Analysis. *Metab. Eng.* 38, 180–190. doi:10.1016/j.ymben.2016.07.012

Shiloach, J., and Fass, R. (2005). Growing *E. coli* to High Cell Density-A Historical Perspective on Method Development. *Biotechnol. Adv.* 23, 345–357. doi:10.1016/j.biotechadv.2005.04.004

Shumskaya, M., and Wurtzel, E. T. (2013). The Carotenoid Biosynthetic Pathway: Thinking in All Dimensions. *Plant Sci.* 208, 58–63. doi:10.1016/j.plantsci.2013.03.012

Silva, C., Cabral, J. M. S., and van Keulen, F. (2004). Isolation of a β-Carotene Over-producing Soil Bacterium, Sphingomonas Sp. *Biotechnol. Lett.* 26, 257–262. doi:10.1023/b:bile.0000013716.20116.dc

Sutherland, I. W. (1998). Novel and Established Applications of Microbial Polysaccharides. *Trends Biotechnol.* 16, 41–46. doi:10.1016/s0167-7799(97)01139-6

Wang, C., Yoon, S.-H., Jang, H.-J., Chung, Y.-R., Kim, J.-Y., Choi, E.-S., et al. (2011). Metabolic Engineering of *Escherichia coli* for α-farnesene Production. *Metab. Eng.* 13, 648–655. doi:10.1016/j.ymben.2011.08.001

Ye, J., Liu, M., He, M., Ye, Y., and Huang, J. (2019). Illustrating and Enhancing the Biosynthesis of Astaxanthin and Docosahexaenoic Acid in Aurantiochytrium Sp. SK4. *Mar. Drugs* 17, 45. doi:10.3390/md17010045

Zelcbuch, L., Antonovsky, N., Bar-Even, A., Levin-Karp, A., Barenholz, U., Dayagi, M., et al. (2013). Spanning High-Dimensional Expression Space Using Ribosome-Binding Site Combinatorics. *Nucleic Acids Res.* 41, e98. doi:10.1093/nar/gkt151

Zhang, Y., Liu, Z., Sun, J., Xue, C., and Mao, X. (2018). Biotechnological Production of Zeaxanthin by Microorganisms. *Trends Food Sci. Tech.* 71, 225–234. doi:10.1016/j.tifs.2017.11.006

Zhao, Y., Song, X., Zhong, D.-b., Yu, L., and Yu, X. (2020). γ-Aminobutyric Acid (GABA) Regulates Lipid Production and Cadmium Uptake by Monoraphidium Sp. QLY-1 under Cadmium Stress. *Bioresour. Tech.* 297, 122500. doi:10.1016/j.biortech.2019.122500

Zhao, Y., Wang, H.-P., Han, B., and Yu, X. (2019). Coupling of Abiotic Stresses and Phytohormones for the Production of Lipids and High-Value By-Products by Microalgae: A Review. *Bioresour. Tech.* 274, 549–556. doi:10.1016/j.biortech.2018.12.030

Zhou, P., Ye, L., Xie, W., Lv, X., and Yu, H. (2015). Highly Efficient Biosynthesis of Astaxanthin in *Saccharomyces cerevisiae* by Integration and Tuning of Algal crtZ and Bkt. *Appl. Microbiol. Biotechnol.* 99, 8419–8428. doi:10.1007/s00253-015-6791-y

Zhu, L., Wu, X., Li, O., Qian, C., and Gao, H. (2012). Cloning and Characterization of Genes Involved in Nostoxanthin Biosynthesis of Sphingomonas Elodea ATCC 31461. *PLoS One* 7, e35099. doi:10.1371/journal.pone.0035099

Conflict of Interest: The authors declare that the research was conducted in the absence of any commercial or financial relationships that could be construed as a potential conflict of interest.

Publisher's Note: All claims expressed in this article are solely those of the authors and do not necessarily represent those of their affiliated organizations, or those of the publisher, the editors and the reviewers. Any product that may be evaluated in this article, or claim that may be made by its manufacturer, is not guaranteed or endorsed by the publisher.

frontiers in Bioengineering and Biotechnology

ORIGINAL RESEARCH
published: 11 January 2022
doi: 10.3389/fbioe.2021.812316

Microbial Responses to the Reduction of Chemical Fertilizers in the Rhizosphere Soil of Flue-Cured Tobacco

Min-Chong Shen[1†], Yu-Zhen Zhang[2†], Guo-Dong Bo[1], Bin Yang[3], Peng Wang[3], Zhi-Yong Ding[3], Zhao-Bao Wang[2], Jian-Ming Yang[2], Peng Zhang[1]* and Xiao-Long Yuan[1]**

[1]Tobacco Research Institute of Chinese Academy of Agricultural Sciences, Qingdao, China, [2]College of Life Sciences, Qingdao Agricultural University, Qingdao, China, [3]Shandong Qingdao Tobacco Co., Ltd., Qingdao, China

OPEN ACCESS

Edited by:
Xiaoyan Liu,
Huaiyin Normal University, China

Reviewed by:
Guiqi Bi,
Agricultural Genomics Institute at Shenzhen (CAAS), China
Chen Shouwen,
Hubei University, China

***Correspondence:**
Zhao-Bao Wang
wangzhaobao123@126.com
Peng Zhang
zhangpeng@caas.cn
Xiao-Long Yuan
yuanxiaolong@caas.cn

[†]These authors have contributed equally to this work

Specialty section:
This article was submitted to Bioprocess Engineering, a section of the journal Frontiers in Bioengineering and Biotechnology

Received: 10 November 2021
Accepted: 22 December 2021
Published: 11 January 2022

Citation:
Shen M-C, Zhang Y-Z, Bo G-D, Yang B, Wang P, Ding Z-Y, Wang Z-B, Yang J-M, Zhang P and Yuan X-L (2022) Microbial Responses to the Reduction of Chemical Fertilizers in the Rhizosphere Soil of Flue-Cured Tobacco. Front. Bioeng. Biotechnol. 9:812316. doi: 10.3389/fbioe.2021.812316

The overuse of chemical fertilizers has resulted in the degradation of the physicochemical properties and negative changes in the microbial profiles of agricultural soil. These changes have disequilibrated the balance in agricultural ecology, which has resulted in overloaded land with low fertility and planting obstacles. To protect the agricultural soil from the effects of unsustainable fertilization strategies, experiments of the reduction of nitrogen fertilization at 10, 20, and 30% were implemented. In this study, the bacterial responses to the reduction of nitrogen fertilizer were investigated. The bacterial communities of the fertilizer-reducing treatments (D10F, D20F, and D30F) were different from those of the control group (CK). The alpha diversity was significantly increased in D20F compared to that of the CK. The analysis of beta diversity revealed variation of the bacterial communities between fertilizer-reducing treatments and CK, when the clusters of D10F, D20F, and D30F were separated. Chemical fertilizers played dominant roles in changing the bacterial community of D20F. Meanwhile, pH, soil organic matter, and six enzymes (soil sucrase, catalase, polyphenol oxidase, urease, acid phosphatase, and nitrite reductase) were responsible for the variation of the bacterial communities in fertilizer-reducing treatments. Moreover, four of the top 20 genera (unidentified JG30-KF-AS9, JG30-KF-CM45, *Streptomyces*, and *Elsterales*) were considered as key bacteria, which contributed to the variation of bacterial communities between fertilizer-reducing treatments and CK. These findings provide a theoretical basis for a fertilizer-reducing strategy in sustainable agriculture, and potentially contribute to the utilization of agricultural resources through screening plant beneficial bacteria from native low-fertility soil.

Keywords: reduction of chemical fertilizer, bacterial community, variation of bacterial community, sustainable agriculture, agricultural resource utilization

INTRODUCTION

Chemical fertilizers have resulted in the prosperity of agriculture worldwide (Jez et al., 2016). Unfortunately, because of the excessive use of chemical fertilizers, inappropriate fertilization strategies are responsible for the degradation of the physicochemical properties and microbial structure of agricultural soil (Sun et al., 2019). A healthy status of the agricultural soil, which is determined by a balanced microbiome, is vital to plants (Chen et al., 2021). The effects of the

physicochemical environment on the functions of the microbiome are linked to the comprehensive structures of the microbial communities. With the overuse of chemical fertilizers, especially nitrogen fertilizer, comes the recruitment of less beneficial bacteria and more pathogens in rhizosphere soil of plants (Achary et al., 2017; Saad et al., 2020), which leads to an ecological issue against sustainable agriculture.

In the People's Republic of China, the Ministry of Agriculture and Rural Affairs have proposed and started to request the reduction of the amounts of chemical fertilizers through its Policy I Document from 2015. Thus far, a series of experiments that evaluated the current methods for reducing the amounts of chemical fertilizers (Liu et al., 2021) and their effects on soils and plants were implemented on main food crops (rice, wheat, and maize) (Maltas et al., 2013; Geng et al., 2019). However, fewer aspects were researched in commercial crops than those in food crops. In China, tobacco is one of the most important commercial crops and has improved the income of farmers in tobacco-planting areas. To maintain the income, continuous planting and excessive chemical fertilizers are implemented in tobacco-planting soil (Anthony and Ferroni, 2012; Yang and Fang, 2015), which has deteriorated the biotic and abiotic properties of the soil. Regarding the requirements of tobacco for nitrogen, phosphorus, and potassium, phosphorus and potassium fertilizers are needed in larger amounts compared to those of other food crops (López-Arredondo et al., 2014; Heuer et al., 2017; Lisuma et al., 2020). Although the tobacco plant requires high levels of phosphorus- and potassium-containing fertilizers, its requirement for nitrogen is the highest. However, among the three major chemical fertilizers, the most serious damages to the soil environment are caused by nitrogen fertilizers. Therefore, reductions on nitrogen fertilization in the cultivation of tobacco can not only improve the economic benefits for tobacco farmers (Liu et al., 2020), but also help restore soil health and maintain the stability of the soil ecosystem.

In this study, a nitrogen-reducing strategy, which employs three different nitrogen-reducing levels (10, 20, and 30%), was implemented and the effects of these reduced levels on the composition and structure of the soil bacterial communities were investigated, based on diversity analyses. The correlation of the top 50 genera was demonstrated by heatmap analysis. The environmental factors that impacted the bacterial communities of the different treatments were studied. Furthermore, the biomarkers of the nitrogen-reducing strategies and the conventional fertilization (as the control group, CK) were analyzed. Subsequently, four of the top 20 genera were identified as key bacteria. These findings helped to understand the bacterial responses to the different gradient reductions of nitrogen fertilizer in tobacco-planted soil, which may provide a theoretical basis for screening beneficial bacteria from native habitats of soils with overuse of chemical fertilizers.

MATERIALS AND METHODS

Design of Field Experiments

This experiment was conducted in the Huangdao District, Qingdao, Shandong Province (32°01′40.61″ N, 120°10′53.60″ E), China, from March 19 to October 23, 2019. The local area has a subtropical monsoon climate, with an average annual rainfall of 1,062.3 mm, an annual average temperature of 15.3°C, an annual sunshine duration of 2,114.6 h, an annual frost-free period of about 218 days, and an average relative humidity of 80%. The previous crop in the experiment site was tobacco (Zhongyan 100 variety), which has been planted for three consecutive years. The flue-cured tobacco variety used in this experiment was the Zhongyan 100. The basic fertilizers of different treatments were implemented at April 22 according to the fertilization strategies (**Table 1**). The tobacco was transplanted at May 1, and potassium nitrate was applied as additional fertilizer at June 3.

Collection and Preprocessing of Soil Samples

Physicochemical experiments: The soil samples were collected 60 days after tobacco transplantation. A soil extractor was used to collect bulk soil (0–20 cm) (Fonseca et al., 2018) avoiding the fertilizer sites during the harvest period. The soil sample was brought to the laboratory, evenly spread, and located in an undisturbed place away from direct sunlight to dry naturally. The air-dried soil was ground, passed through 60-mesh and 100-mesh sieves, placed in a Ziploc bag, and sealed for storage until physicochemical properties were tested.

DNA extraction: The samples of tobacco rhizosphere soil, the one that adheres closely to tobacco roots, was collected using a sterilized brush and gentle shaking (Pétriacq et al., 2017). Three replicates were conducted for each treatment. The soil samples were immediately stored in a refrigerator at −20°C for extraction of soil DNA.

Determination of Soil Physicochemical Properties

The soil pH was measured using the potentiometric method, and the soil-liquid ratio was 1:2.5. The soil organic matter was determined through the oil bath heating potassium dichromate oxidation volumetric method (Chen et al., 2016). The soil moisture content was measured using the drying method (Su et al., 2014). The total nitrogen in the soil was determined through the Kjeldahl distillation method (Sáez-Plaza et al., 2013). The available phosphorus in the soil was leached with sodium bicarbonate-hydrochloric acid, and then determined using the molybdenum-antimony anti-colorimetric method (Han et al., 2020). The available potassium in the soil was first extracted with nitric acid, and then determined with the flame photometer method (Lu et al., 2017).

TABLE 1 | Fertilization strategies of field experiments.

Treatments	Fertilization strategies
CK	Fermented soybeans (N:P:K = 6:1:2), 300 kg ha^{-1}; Tobacco fomulated fertilizer (N:P:K = 10:10:20), 324 kg ha^{-1}; Diammonium Phosphate (N:P:K = 18:46:0), 30 kg ha^{-1}; Potassium sulfate (N:P:K = 0:0:50), 153 kg ha^{-1}
D10F	Fermented soybeans (N:P:K = 6:1:2), 270 kg ha^{-1}; Tobacco fomulated fertilizer (N:P:K = 10:10:20), 291.6 kg ha^{-1}; Diammonium Phosphate (N:P:K = 18:46:0), 27 kg ha^{-1}; Potassium sulfate (N:P:K = 0:0:50), 167.16 kg ha^{-1}; Calcium Superphosphate (N:P:K = 0:20:0), 24.6 kg ha^{-1}
D20F	Fermented soybeans (N:P:K = 6:1:2), 240 kg ha^{-1}; Tobacco fomulated fertilizer (N:P:K = 10:10:20), 259.2 kg ha^{-1}; Diammonium Phosphate (N:P:K = 18:46:0), 24 kg ha^{-1}; Potassium sulfate (N:P:K = 0:0:50), 181.32 kg ha^{-1}; Calcium Superphosphate (N:P:K = 0:20:0), 49.2 kg ha^{-1}
D30F	Fermented soybeans (N:P:K = 6:1:2), 210 kg ha^{-1}; Tobacco fomulated fertilizer (N:P:K = 10:10:20), 226.8 kg ha^{-1}; Diammonium Phosphate (N:P:K = 18:46:0), 21 kg ha^{-1}; Potassium sulfate (N:P:K = 0:0:50), 195.48 kg ha^{-1}; Calcium Superphosphate (N:P:K = 0:20:0), 73.8 kg ha^{-1}

Determination of Soil Enzymes

Soil invertase was determined using the 3,5-dinitrosalicylic acid colorimetric method (Dong et al., 2019). Catalase was measured through a volumetric method (Yang et al., 2015). The activity of polyphenol oxidase was determined through the pyrogallol colorimetric method (Goyeneche et al., 2013). Soil urease was determined with the indophenol colorimetric method (Jing et al., 2020). Soil phosphatase was determined with the disodium phenyl phosphate method (Shao et al., 2020). Soil nitrite reductase was first leached with sodium nitrite-aluminum potassium alum, and then measured through a colorimetric method (Safonov et al., 2018).

DNA Extraction and Amplicon Sequencing of 16S rRNA Genes

Each 0.5 g soil sample was obtained from well-mixed rhizosphere soil from one random replication. DNA was extracted from the soil using a DNA extraction kit (FastDNA^{TM} SPIN Kit for soil, MP Biomedicals, LLC, Solon, OH, United States) according to the manufacturer's instructions. Subsequently, the DNA was tested with 1% agarose gel and the successfully extracted DNA was stored at −20°C immediately.

The PCR of the V4-V5 variable region of the bacterial 16S rRNA genes was conducted using the specific primers 515F (5′-GTGCCAGCMGCCGCGGTAA-3′) and 907R (5′-CCGTCA ATTCCTTTGAGTTT-3′) (Fan et al., 2018). The amplification products were tested for specificity in 1% agarose gel. Then the library was constructed using the library construction kit TruSeq® DNA PCR-Free Sample Preparation kit (Illumina, San Diego, CA, United States). After the library was successfully constructed, the quantitative process was implemented using the Qubit® 2.0 Fluorometer (Life Technologies, Carlsbad, CA, United States) and qPCR. After the quantitative test, subsequent sequencing was performed on the Illumina MiSeq platform.

Processing and Analyses of Bioinformatic and Soil Data

The raw data after sequencing was spliced trough FLASH (V1.2.11, https://ccb.jhu.edu/software/FLASH/index.shtml) to obtain raw tags. Then QIIME software (V1.9.1, http://qiime.org/scripts/split_libraries_fastq.html) was used to filter raw tags. Subsequently, the Usearch (Version 7.0, http://www.drive5.com/usearch/) was used to detect and remove chimeras and get effective data (effective tags) (Callahan et al., 2016).

The valid data from all samples were clustered into the same operational taxonomic units (OTUs), the most frequently occurring sequence was screened as the representative sequence of OTUs, and the rRNA database SILVA (V138, https://www.arb-silva.de/) for species annotation analysis was used (Singleton et al., 2021). The phylogenetic relationship of all OTUs was constructed with the MUSCLE software (Version 3.8.31, http://www.drive5.com/muscle/) (Lu et al., 2019). Finally, all OTUs were uniformized based on the sequencing data of the sample with the smallest amount of data as the standard.

Follow-up analysis was performed based on the OTU information after the normalization process. Qiime software (Version 1.9.1, http://qiime.org/install/index.html) was used to calculate Shannon, Simpson, Ace, Chao1, PD whole tree indexes, and the R software (Version 3.6.0) was used to draw a dilution curve. Subsequently, Qiime software (Version 1.9.1) was used to calculate the Bray-Curtis distance, and the WGCNA, stats, and ggplot2 packages of the R software (Version 3.6.0) were used to draw PCoA diagrams. The Vegan package based on the R software (Version 3.6.0) was used to test the differences in the microbial community structure among different treatments through PERMANOVA. The Wilcoxon rank sum test was used to calculate the significance *p*-value in the LEfSe analysis, and the LDA was set to 3.0. Based on the analysis platform of Majorbio (Shanghai Majorbio Bio-pharm Technology Co., Ltd., Shanghai, China), the results of species annotations were used for further comparative analyses. All sequence data were submitted to the Sequence Read Archive (accession number: PRJNA780371) and are freely available at the NCBI (https://www.ncbi.nlm.nih.gov/sra/PRJNA780371).

The soil physicochemical properties data were analyzed using SPSS (Version 25.0) and the single factor ANOVA (Duncan's Multiple Range Test) in SPSS software was used to calculate the significance of the differences between different treatments. All pictures were drawn with Microsoft Excel (Version 2019), Origin (Version 2018) (OriginLab Corporation, Northampton, MA,

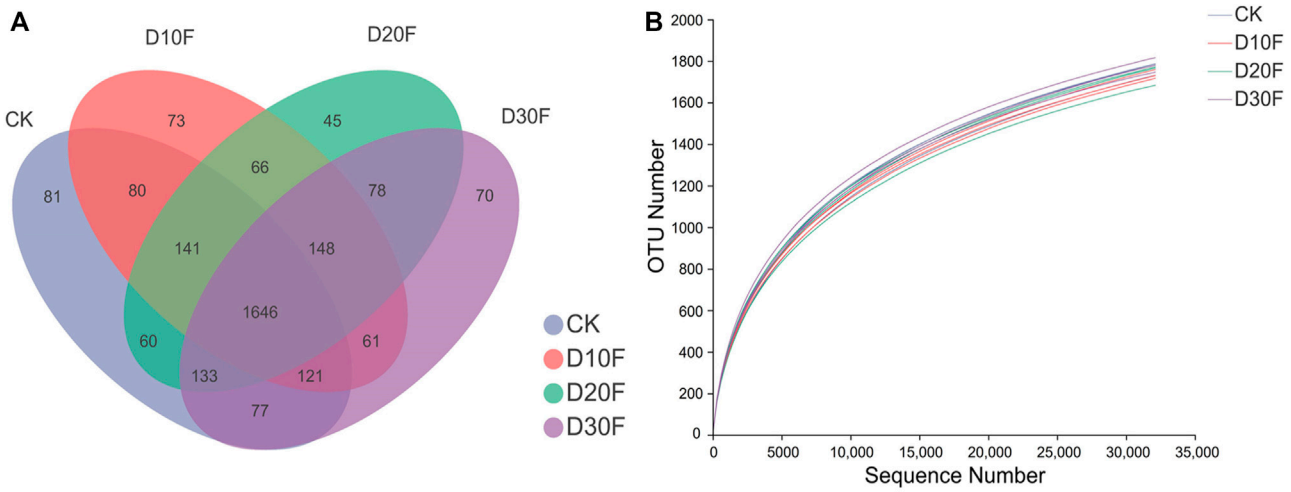

FIGURE 1 | Comparison of the bacterial communities in different treatments based on OTU numbers. **(A)** Venn diagram of OTU numbers for different treatments. Every circle indicates a treatment; the number of OTUs shared between different treatments was interpreted with the number in the overlapping circles, while the number in the non-overlapping area represented the number of unique OTUs for the specific treatment. **(B)** Rarefaction curves of bacterial communities for all treatments.

TABLE 2 | Statistic results of Alpha diversity indices of different treatments.

Sample name	Shannon	Simpson	Ace	Chao1	PD whole tree
CK	5.5763 ± 0.1364	0.0199 ± 0.0061a	2,261.33 ± 19.21	2,269.99 ± 44.07	130.38 ± 1.69
D10F	5.6680 ± 0.0668	0.0130 ± 0.0020ab	2,265.46 ± 25.63	2,260.42 ± 23.13	129.19 ± 0.68
D20F	5.6973 ± 0.1181	0.0116 ± 0.0022b	2,234.97 ± 64.75	2,217.07 ± 105.33	128.12 ± 3.98
D30F	5.7011 ± 0.1065	0.0147 ± 0.0029ab	2,233.57 ± 45.20	2,220.84 ± 69.04	131.81 ± 2.27

All data in the table are presented as means ± standard deviation (SD). Means followed by different lower-case letters are significantly different at the 5% level by DMRT (Duncan multiple range test).

United States) and the R software (Version 3.6.0). All results are presented as the mean ± standard deviation.

RESULTS

Reduction of Nitrogen Fertilizer Impacted the Composition of the Bacterial Communities

The Venn diagram illustrated the dissimilarity of the effects of different reductions in the amount of nitrogen fertilizer on bacterial communities based on OTU numbers. There were 1,646 shared common OTUs in all treatments, whereas CK, D10F, D20F, and D30F presented 81, 73, 45, and 70 unique OTUs, respectively (**Figure 1A**). The rarefaction curve showed that the abundance of bacterial communities in CK was higher than that of the fertilizer-reducing treatments, consistently with the results of the Venn diagram (**Figure 1B**). Additionally, the Simpson index of the alpha diversity decreased in the fertilizer-reducing treatments. D20F significantly ($p < 0.05$) decreased the Simpson index, when compared to CK, which indicated that the diversity of the bacterial community declined in D20F whereas, there were no significant differences in the other indices of alpha diversity (**Table 2**).

The taxonomic identification was implemented based on OTUs, and the top five dominant phyla were Actinobacteriota, Proteobacteria, Acidobacteriota, Chloroflexi, and Firmicutes (**Figure 2A**). Among them, the relative abundance of Actinobacteriota decreased in the D10F and D20F treatments, whereas it increased in D30F. The relative abundance of Proteobacteria decreased in the fertilizer-reducing treatments, whereas the relative abundance of Acidobacteriota and Chloroflexi increased in the treatments. In addition, D20F and D10F resulted in the largest relative abundance of Firmicutes and Patescibacteria, respectively, in all treatments. Meanwhile, D30F reduced the relative abundance of both Firmicutes and Patescibacteria, when compared to CK (**Figure 2B**). The top five dominant genera were identified as *Arthrobacter*, *Gaiellales*, unclassified *Intrasporangiaceae*, *Sphingomonas*, and *Nocardioides*, followed by *Bacillus*, unidentified JG30-KF-AS9, unclassified *Acidobacteriales*, and *Streptomyces*. Among them, *Arthrobacter* and unclassified *Intrasporangiaceae* were extremely close on the phylogenetic tree; while *Nocardioides*

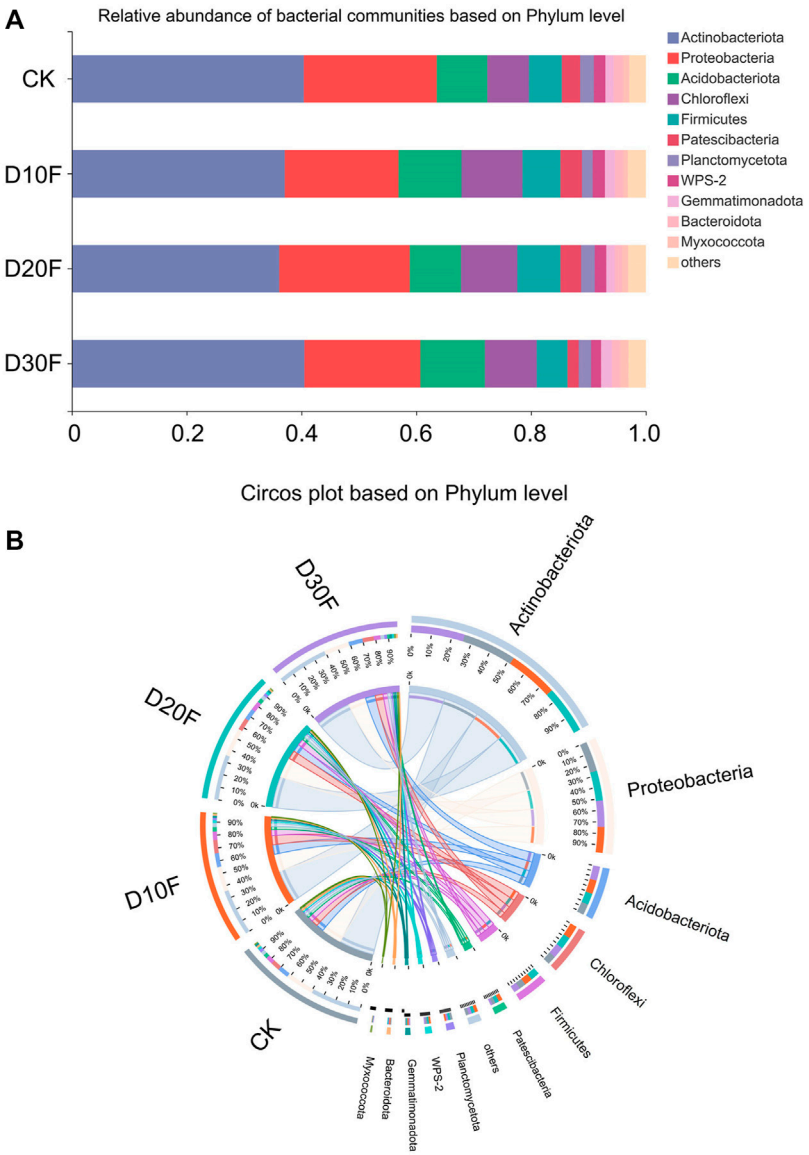

FIGURE 2 | Composition of the bacterial communities for different treatments, based on phylum. **(A)** Bar plot of relative abundance of bacterial communities based on phylum. **(B)** Circos plot of different treatments based on phylum.

and *Streptomyces* were secondarily close (**Supplementary Figure S1**).

Reduction of Nitrogen Fertilizer Impacted the Structure of Bacterial Communities

The beta diversity for all treatments based on analyses of dimensionality reduction demonstrated the variation of bacterial communities between different treatments (**Figure 3**). The PCA plot (R = 0.4722, p = 0.0020) showed that the bacterial communities of different treatments were separated. Gaps between the bacterial communities for the D10F and D20F treatments were larger than those for D30F and CK (**Figure 3A**). Evident separation between the bacterial communities of the fertilizer-reducing treatments (D10F, D20F, and D30F) and CK was shown in the PCoA plot (R^2 = 0.5646, p = 0.0010), whereas the clusters for the D10F and D20F treatments did not show obvious dissimilarity between each other (**Figure 3B**). The results of the NMDS analysis (R^2 = 0.5646, p = 0.0010) were consistent with the PCoA, except that the partition of D10F and D20F occurred along the NMDS1 arrow (**Figure 3C**). To emphasize the differences between groups, PLS-DA was implemented with a supervised algorithm. The results indicated obvious variation of the bacterial communities among all treatments. Additionally, both bacterial communities of the D10F and D20F treatments were

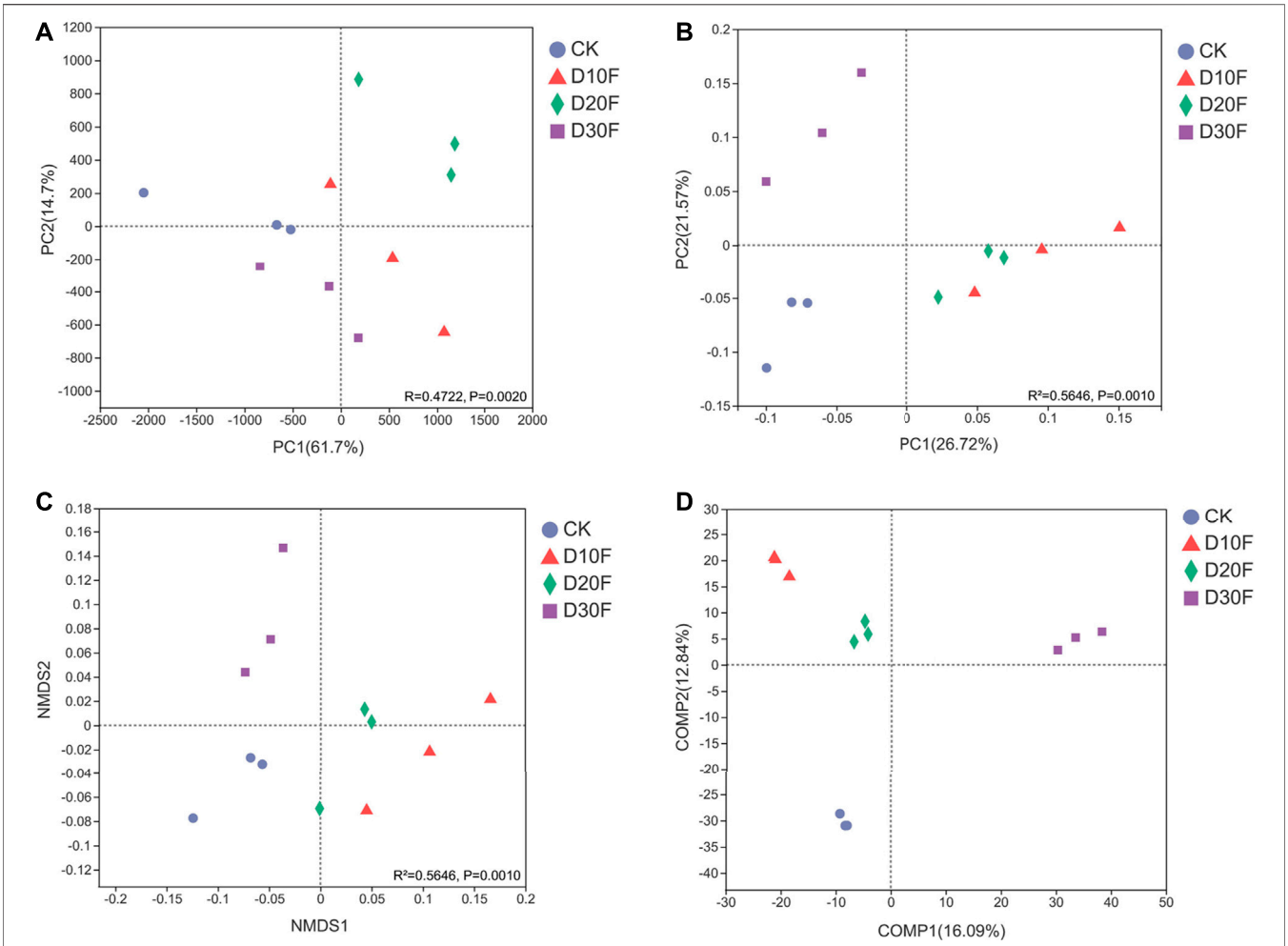

FIGURE 3 | Combined plot integrated with the PCA **(A)**, PCoA **(B)**, NMDS **(C)**, and PLS-DA **(D)** plots of the bacterial communities corresponding to beta diversity.

clustered in the same quadrant, while the clusters of the bacterial communities for D30F and CK were located in other two different quadrants (**Figure 3D**).

To further explore the structural differences of the bacterial communities among different treatments, investigations corresponding to differential genera were performed. The top 50 genera for all treatments were scanned and the heatmap was drawn based on their relative abundance. The result showed the differences in the bacterial composition between different treatments. The variation of the bacterial community composition between fertilizer-reducing treatments (D10F, D20F, and D30F) and CK was larger than that between D10F and D20F based on the genus, which was consistent with the results of PCoA, NMDS, and PLS-DA (**Figure 4A**). Furthermore, 76 taxa were analyzed as biomarkers of the corresponding treatments based on LEfSe analysis. Among them, 27 taxa were identified at the genus level, of which seven, eight, four, and eight were considered biomarkers for CK, D10F, D20F, and D30F, respectively (**Figure 4B**). Taking the relative abundance of each bacterial genus into consideration, the top 20 genera were investigated. The results indicated that four of the top 20 genera, unidentified JG30-KF-AS9, *Streptomyces*, unidentified JG30-KF-CM45, and *Elsterales*, were all significantly enriched in the fertilizer-reducing treatments, whose relative abundance increased in the D10F, D30F, D30F, and D20F, respectively. In addition, the relative abundance of *Arthrobacter* decreased in the fertilizer-reducing treatments (**Figure 4C**).

Correlation Between Bacterial Key Taxa and Dominant Environmental Factors

To better understand the bacterial interaction and response to the reduction in the amount of nitrogen fertilizer, the correlation among the top 50 genera was explored through heatmap analysis (**Figure 5**) and statistical analysis based on OTUs (**Supplementary Table S1**). The results illustrated that unidentified JG30-KF-AS9, *Streptomyces*, unidentified JG30-KF-CM45, and *Elsterales* had 28, 27, 32, and 29 positive interactions, respectively, while they had 21, 22, 17, and 20 negative interactions, respectively. Among them, unidentified JG30-KF-AS9 had four significantly positive correlations to *Geodermatophilus*, *Elsterales*, unidentified WWH38, and

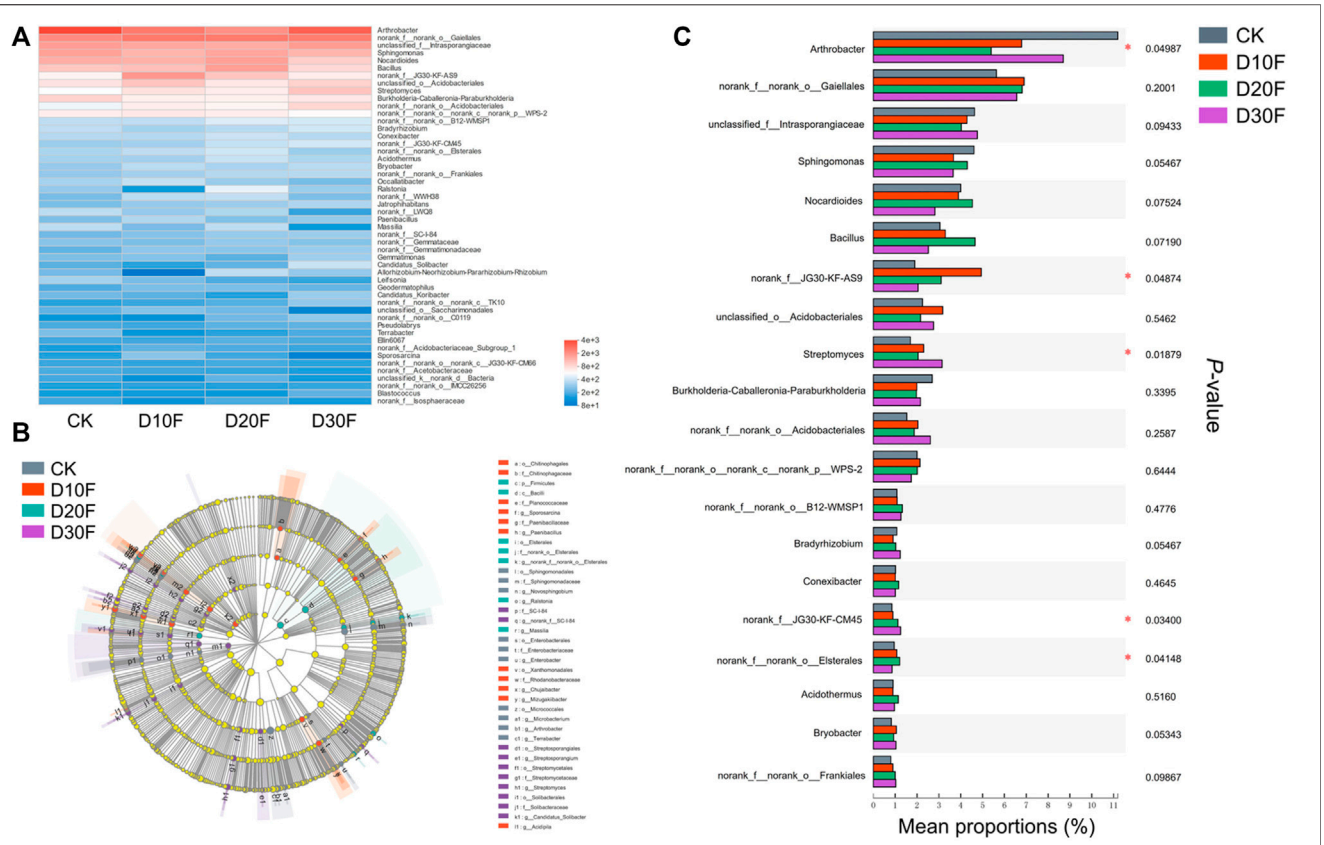

FIGURE 4 | Variation of the bacterial communities in different treatments based on genus. **(A)** Heatmap of the top 50 genera based on logarithmic statistics of identified OTUs among different treatments. **(B)** LDA Effect Size (LEfSe) analysis based on the genus among different treatments. **(C)** Bar plot of relative abundance of the top 20 genera among different treatments based on the Kruskal-Wallis H test.

Sporosarcina, and two significantly negative correlations to *Arthrobacter* and *Terrabacter*. *Streptomyces* had six significantly positive correlations to unidentified TK10, *Jatrophihabitans*, unidentified SC-I-84, *Bryobacter*, *Gemmatimonadaceae*, and *Paenibacillus*, and three significantly negative correlations to *Sphingomonas*, *Massilia*, and unidentified LWQ8. Unidentified JG30-KF-CM45 presented six significantly positive correlations to *Solibacter*, unidentified C0119, unidentified TK10, *Jatrophihabitans*, *Frankiales*, and unidentified SC-I-84, and one significantly negative correlation to *Leifsonia*. Additionally, *Elsterales* presented five significantly positive correlations to *Conexibacter*, unidentified WWH38, unidentified JG30-KF-AS9, *Bacillus*, and *Sporosarcina*, and three significantly negative correlations to *Gemmatimonas*, unclassified *Intrasporangiaceae*, and *Arthrobacter*.

To further clarify the effect of environmental factors on the bacterial communities of tobacco-planting soil, redundancy analyses (RDA) of different treatments were implemented (**Supplementary Tables S2, S3**, **Figure 6**). The results of RDA showed that soil organic matter and pH drove the bacterial community structure in D30F and D10F treatments, respectively. Total nitrogen (TN), available phosphorus (AP), and water content (WC) dominated the bacterial community variation in D20F together, while available potassium (AK) drove the bacterial community of CK. In addition, RDA1 and RDA2 explained 49.91 and 12.78% of the bacterial community variation, respectively (**Figure 6A**). Regarding the effect of enzymes on bacterial communities, RDA1 and RDA2 explained 48.66 and 9.57% of the bacterial community variation, respectively (**Figure 6B**). Six enzymes were investigated and all the enzymes dominated the bacterial community variation of the nitrogen-reducing treatments. Among them, acid phosphatase (ACP) and soil sucrase (S_SC) dominated the bacterial community structure in the D30F and D20F treatments, respectively, whereas catalase (CAT), polyphenol oxidase (PPO), nitrite reductase (NR), and urease (UE) collectively drove the bacterial community variation in the D10F treatment. Additionally, the arrows of nitrite reductase and urease were pointing in the directions between D30F and D10F, and between D20F and D10F, respectively.

Correlation Between Bacterial Key Taxa and Output Value of Tobacco Leaves

To verify the effects of nitrogen-reducing strategies on practical production of tobacco, the output value of tobacco leaves was evaluated based on the yield, ratio of first class, unit price and

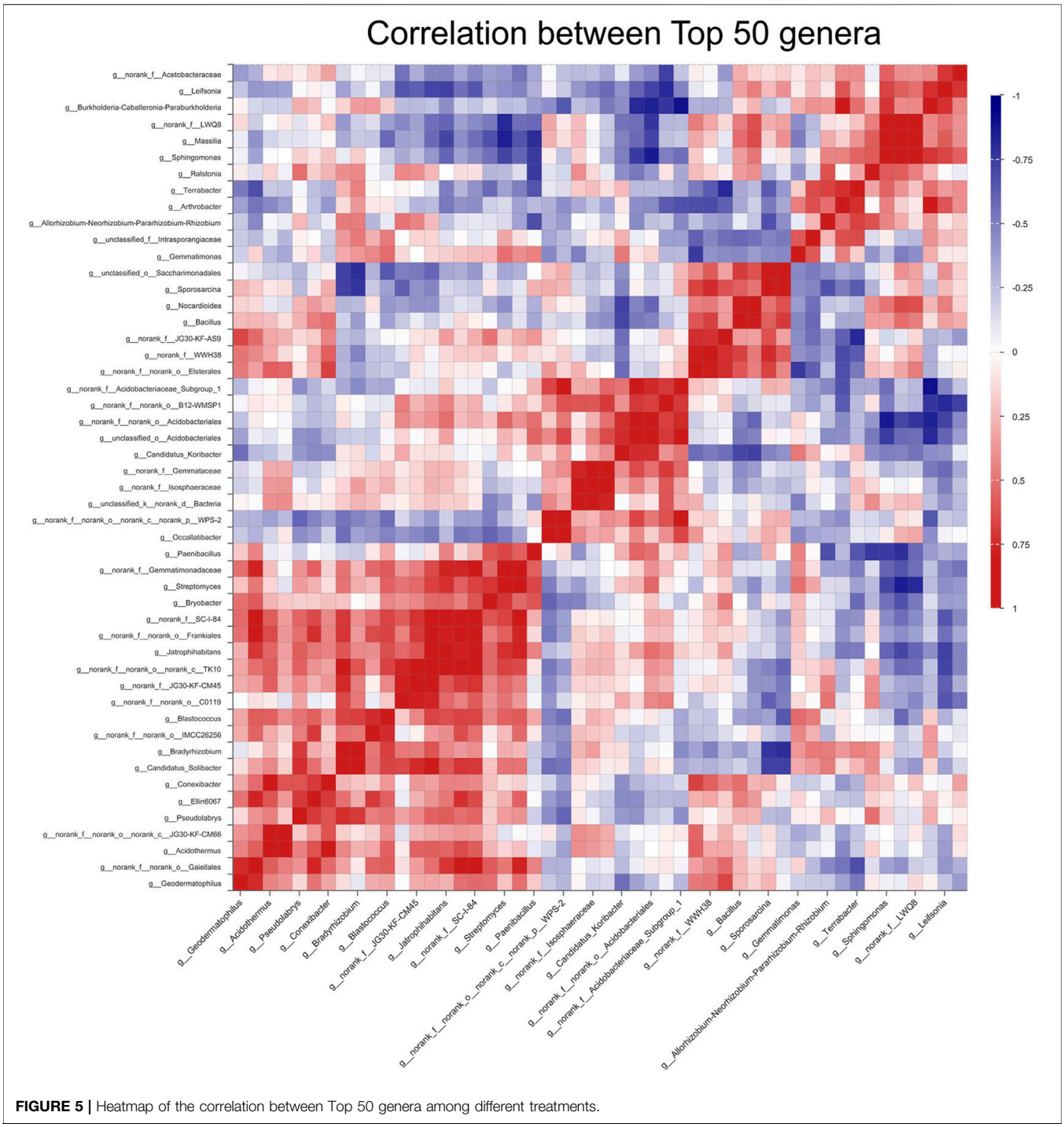

FIGURE 5 | Heatmap of the correlation between Top 50 genera among different treatments.

value indexes (**Table 3**). All nitrogen-reducing treatments could improve the ratio of first class and the unit price of tobacco leaves. Moreover, the yield of tobacco leaves was significantly ($p < 0.05$) increased by D10F and D20F, while the differences of yield between D10F and D20F, and CK and D30F were not significant. At the aspect of yield, D30F performed the worst in all treatments. Additionally, different unit prices, which were impacted by different treatments, brought significantly different output value of tobacco leaves. Among them, D10F made the highest output value, followed by D20F. Subsequently, D30F earned the lowest value, while there was no significant difference in output value between CK and D30F.

Furthermore, the correlation between differential genera, referring to those were significantly different from CK based on OTU statistics, and output value of tobacco leaves were analyzed by mantel test (**Table 4**). The results demonstrated

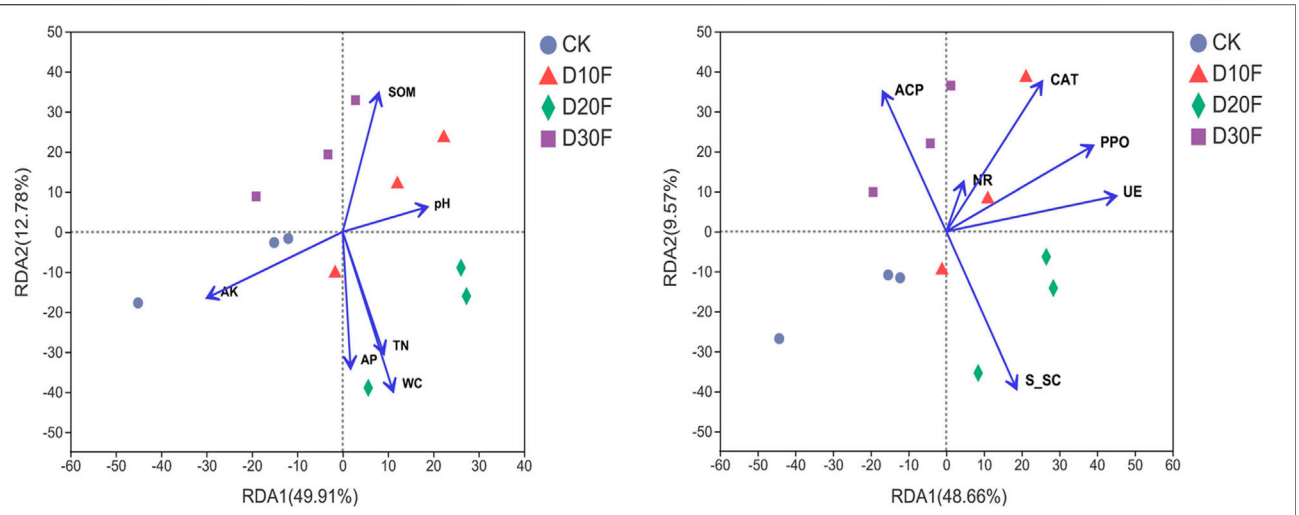

FIGURE 6 | Redundancy analysis (RDA) of different treatments fitting the physicochemical indicators **(A)** and enzyme indicators **(B)** to the bacterial community data. The direction and length of the blue arrow lines indicate the explanation of different indicators, which influence the bacterial communities.

TABLE 3 | Output value of tobacco leaves.

Treatments	Yield/kg ha^{-1}	Ratio of first class/%	Unit price/RMB kg^{-1}	Value/RMB ha^{-1}
CK	2,242.35 ± 104.25a	60.34	24.80	55,611.52 ± 2,584.07a
D10F	2,555.85 ± 50.40b	63.71	25.96	66,348.57 ± 1,309.14c
D20F	2,448.75 ± 52.35b	62.12	25.35	62,075.82 ± 1,325.58b
D30F	2,167.65 ± 70.95a	61.24	25.04	54,276.70 ± 1774.91a

All data in the table are presented as means ± standard deviation (SD). Means followed by different lower-case letters are significantly different at the 5% level by DMRT (Duncan multiple range test).

TABLE 4 | Mantel test analysis of correlations between key taxa and output value of tobacco leaves.

	Key taxa (D10F-CF-D20F)	
	R Value	*p* Value
Yield	0.3533	0.027
Output Value	0.4419	0.005

Key taxa refer to those are significantly different from CK based on OTU statistics.

that the differential genera shared by D10F and D20F had positive correlations with yield and output value of tobacco leaves. Significant R value represented the key taxa made great contributions to tobacco yield and its economic value.

DISCUSSION

The excessive use of chemical fertilizers was proved to be one of the most fatal issues in agricultural production (Smith and Siciliano, 2015). To cope with the increasing population worldwide, sufficient, even overloaded chemical fertilizers were added to the agricultural soil. With the rapid improvement of the crop yields came the potential risk of environmental pollution due to macronutrients (nitrogen, phosphorus, and potassium), which resulted in disturbing the physicochemical properties of the agricultural soil (Hui et al., 2021). Planting obstacles corresponding to improper physicochemical properties of the soil had brought much confusion to the determination of responsibilities for the declined plant yield (Gurdeep and Reddy, 2015). An integrated effect of biotic and abiotic processes determines the capacity of ecological systems of the agricultural field (Tkacz and Poole, 2015; Freschet et al., 2021).

Previous studies had shown when the reduction in nitrogen fertilizer ranged from 10 to 30%, the fundamental crops including rice, wheat, and maize, performed better than with conventional fertilization (Migliorati et al., 2014; Hofmeier et al., 2015; Ding et al., 2018). This article focused on the effects of reducing nitrogen fertilization on the tobacco-planting soil. The alpha diversity of the bacterial community declined with the decrease in the amount of nitrogen fertilizer. The beta diversity of the bacterial community demonstrated that the reduction in the amount of nitrogen fertilizer differentiated the bacterial community of the rhizosphere soil from that under conventional fertilization. Moreover, the bacterial community varied according to the different reduction in the amount of fertilizer. Interestingly, the variation of the bacterial community increased since the nitrogen application rate was

reduced by more than 30%, when compared to no more than 20% reduction of the fertilizer. Resulting from the decrease in the nutrient, more intense competition occurred within the bacterial community (Zhang et al., 2016). In the challenging process, the populations with poor competitiveness were outcompeted. Generally, the populations eliminated were located in limited and narrow ecological niches due to their low use efficiency of environmental resources and their imperfect competitive mechanism (Turnbull et al., 2013; Dini-Andreote et al., 2014). These weakly competitive bacteria were less potential to implement their functions. Hence, the surviving populations of the bacterial community after the strategy of reducing nitrogen fertilization were discussed.

With the changes in the diversity of the bacterial community, its functionality in soil ecological systems varied accordingly (Knelman et al., 2012; Eo and Park, 2016; Zhang et al., 2016). The bacterial genera whose relative abundance changed significantly were the key factors that leaded to the variation in the diversity of the bacterial community. Thorough analyses of the differential bacterial genera might help to clarify the direction and details of variation of the bacterial community, which reveals its subsequent potential changes of functions. Furthermore, the analyses can lead to the identification and screening of efficient functional strains based on the correlation analysis of the functional orientation of the bacterial community and key differential bacterial genera. Four genera, unidentified JG30-KF-AS9, JG30-KF-CM45, *Streptomyces*, and *Elsterales* were demonstrated as key species. In addition, all the environmental factors in our study were verified to dominate the variation of the bacterial community structures of the nitrogen-reducing treatments, except available potassium. The specific requirement of tobacco for potassium might have led to the changing direction of the bacterial community, which declined with the reduction in nitrogen fertilization.

Compared to conventional fertilization, the strategy of reducing nitrogen fertilization might change the relative abundance of JG30-KF-AS9 and JG30-KF-CM45 to improve the productive function of the bacterial community of the tobacco-planting soil (Chinta et al., 2021; Neupane et al., 2021; Zhang et al., 2021). Meanwhile, the reduction in nitrogen fertilizer might increase the relative abundance of *Streptomyces* (D30F) and *Elsterales* (D20F), which had the potential abilities to decrease the relative abundance of pathogens and their pathogenicity (Vurukonda et al., 2018; Wang et al., 2021; Momesso et al., 2022). The reduction in the amount of nitrogen fertilizer (10–30%) showed significant advantages for tobacco planting compared to CK, because of the soil microorganisms. Furthermore, this study found that JG30-KF-AS9, JG30-KF-CM45, *Streptomyces*, and *Elsterales* were beneficial genera that might potentially promote tobacco growth. Subsequent research on the isolation, enhancement, and application of these bacterial genera is of positive significance in the field of tobacco growth promotion and biological control.

Different from the strategies of adding exogenous microbial inoculants with plant-promoting or biological controlling functions, this research paid attention to the response of the native soil microbiome to the reduction of nitrogen fertilization without the addition of exogenous microorganisms. In this process, unidentified JG30-KF-AS9, JG30-KF-CM45, *Streptomyces*, and *Elsterales* demonstrated different functional vitalities from those when they were in the conventional habitat of CK. Native microorganisms have more potential to implement their functions due to stronger adaptability to the environment, when compared to exogenous microorganisms (Palozzi and Lindo, 2018). These findings have important guiding significance for screening indigenous highly functional microorganisms from poor soil environments, of which, the concept of turning waste into treasure is also conducive to the development of sustainable agriculture.

CONCLUSIONS

In this study, the reduction in the amount of nitrogen fertilizer resulted in diverse responses of the soil bacterial community at the rhizosphere of the flue-cured tobacco plant. The structure of bacterial communities of tobacco-planting soil varied from decreasing 10–30% nitrogen fertilizer, and the variation of bacterial communities was enlarged, when compared to conventional fertilization, respectively. Furthermore, seven, eight, four, and eight genera were identified as biomarkers of CK, D10F, D20F, and D30F, respectively. Considering the relative abundance of all the OTUs, unidentified JG30-KF-AS9, *Streptomyces*, unidentified JG30-KF-CM45, and *Elsterales* were the key bacterial genera that caused structural and functional variations of soil bacterial communities among different treatments. Additionally, all macronutrients, except available potassium, along with pH, soil organic matter, and six enzymes dominated the variation of the bacterial communities in nitrogen-reducing treatments. This study provides a feasible strategy of reducing the amount of nitrogen fertilizer in the tobacco growing industry. Additionally, these results provide a theoretical basis for isolating functional bacteria from native microbial resources of relatively poor soil environment.

DATA AVAILABILITY STATEMENT

The data presented in the study are deposited in the NCBI repository (https://www.ncbi.nlm.nih.gov/sra/PRJNA780371), accession number: PRJNA780371.

AUTHOR CONTRIBUTIONS

Conceptualization, X-LY, PZ and Z-BW; experiment implementation, G-DB, BY, PW, Z-YD, and J-MY; data processing, M-CS and Y-ZZ; writing-original draft preparation, M-CS; writing-review and editing, M-CS, X-LY, PZ, and Z-BW; funding acquisition, G-DB and PZ. All authors have read and approved the final manuscript.

FUNDING

This research was supported by the Key Projects of Shandong Qingdao Tobacco Co., Ltd. (No. YCSKY202007030-C1) and the Technology Project of Hubei Tobacco Co., Ltd. (No. 027Y2021-011). The authors declare that this study received funding from the Key Projects of Shandong Qingdao Tobacco Co., Ltd. (grant no. YCSKY202007030-C1) and the Technology Project of Hubei Tobacco Co. Ltd. (grant no. 027Y2021-011). The funders were not involved in the study design, collection, analysis, interpretation of data, the writing of this article or the decision to submit it for publication.

SUPPLEMENTARY MATERIAL

The Supplementary Material for this article can be found online at: https://www.frontiersin.org/articles/10.3389/fbioe.2021.812316/full#supplementary-material

REFERENCES

Achary, V. M. M., Ram, B., Manna, M., Datta, D., Bhatt, A., Reddy, M. K., et al. (2017). Phosphite: A Novel P Fertilizer for Weed Management and Pathogen Control. *Plant Biotechnol. J.* 15, 1493–1508. doi:10.1111/pbi.12803

Anthony, V. M., and Ferroni, M. (2012). Agricultural Biotechnology and Smallholder Farmers in Developing Countries. *Curr. Opin. Biotechnol.* 23, 278–285. doi:10.1016/j.copbio.2011.11.020

Callahan, B. J., Mcmurdie, P. J., Rosen, M. J., Han, A. W., Johnson, A. J. A., and Holmes, S. P. (2016). DADA2: High-Resolution Sample Inference from Illumina Amplicon Data. *Nat. Methods* 13, 581–583. doi:10.1038/nmeth.3869

Chen, D., Yu, X., Song, C., Pang, X., Huang, J., and Li, Y. (2016). Effect of Pyrolysis Temperature on the Chemical Oxidation Stability of Bamboo Biochar. *Bioresour. Technol.* 218, 1303–1306. doi:10.1016/j.biortech.2016.07.112

Chen, Q.-L., Hu, H.-W., He, Z.-Y., Cui, L., Zhu, Y.-G., and He, J.-Z. (2021). Potential of Indigenous Crop Microbiomes for Sustainable Agriculture. *Nat. Food* 2, 233–240. doi:10.1038/s43016-021-00253-5

Chinta, Y. D., Uchida, Y., and Araki, H. (2021). Roles of Soil Bacteria and Fungi in Controlling the Availability of Nitrogen from Cover Crop Residues during the Microbial Hot Moments. *Appl. Soil Ecol.* 168, 104135. doi:10.1016/j.apsoil.2021.104135

De Antoni Migliorati, M., Scheer, C., Grace, P. R., Rowlings, D. W., Bell, M., and Mcgree, J. (2014). Influence of Different Nitrogen Rates and DMPP Nitrification Inhibitor on Annual N2O Emissions from a Subtropical Wheat-Maize Cropping System. *Agric. Ecosyst. Environ.* 186, 33–43. doi:10.1016/j.agee.2014.01.016

Ding, W., Xu, X., He, P., Ullah, S., Zhang, J., Cui, Z., et al. (2018). Improving Yield and Nitrogen Use Efficiency through Alternative Fertilization Options for rice in China: A Meta-Analysis. *Field Crops Res.* 227, 11–18. doi:10.1016/j.fcr.2018.08.001

Dini-Andreote, F., de Cássia Pereira e Silva, M., Triadó-Margarit, X., Casamayor, E. O., Van Elsas, J. D., and Salles, J. F. (2014). Dynamics of Bacterial Community Succession in a Salt Marsh Chronosequence: Evidences for Temporal Niche Partitioning. *ISME J.* 8, 1989–2001. doi:10.1038/ismej.2014.54

Dong, Y., Zhao, J., Wang, L., Wang, H., Zou, X., and Zhang, J. (2019). Effect of Bisphenol A and Pentachlorophenol on Different Enzymes of Activated Sludge. *Sci. Total Environ.* 671, 1170–1178. doi:10.1016/j.scitotenv.2019.03.455

Eo, J., and Park, K.-C. (2016). Long-Term Effects of Imbalanced Fertilization on the Composition and Diversity of Soil Bacterial Community. *Agric. Ecosyst. Environ.* 231, 176–182. doi:10.1016/j.agee.2016.06.039

Fan, K., Weisenhorn, P., Gilbert, J. A., and Chu, H. (2018). Wheat Rhizosphere Harbors a Less Complex and More Stable Microbial Co-Occurrence Pattern Than Bulk Soil. *Soil Biol. Biochem.* 125, 251–260. doi:10.1016/j.soilbio.2018.07.022

Fonseca, J. P., Hoffmann, L., Cabral, B. C. A., Dias, V. H. G., Miranda, M. R., De Azevedo Martins, A. C., et al. (2018). Contrasting the Microbiomes from Forest Rhizosphere and Deeper Bulk Soil from an Amazon Rainforest Reserve. *Gene* 642, 389–397. doi:10.1016/j.gene.2017.11.039

Freschet, G. T., Pagès, L., Iversen, C. M., Comas, L. H., Rewald, B., Roumet, C., et al. (2021). A Starting Guide to Root Ecology: Strengthening Ecological Concepts and Standardising Root Classification, Sampling, Processing and Trait Measurements. *New Phytol.* 232, 973–1122. doi:10.1111/nph.17572

Geng, Y., Cao, G., Wang, L., and Wang, S. (2019). Effects of Equal Chemical Fertilizer Substitutions with Organic Manure on Yield, Dry Matter, and Nitrogen Uptake of Spring maize and Soil Nitrogen Distribution. *PloS one* 14, e0219512. doi:10.1371/journal.pone.0219512

Goyeneche, R., Di Scala, K., and Roura, S. (2013). Biochemical Characterization and Thermal Inactivation of Polyphenol Oxidase from Radish (Raphanus Sativus Var. Sativus). *LWT - Food Sci. Technol.* 54, 57–62. doi:10.1016/j.lwt.2013.04.014

Gurdeep, K., and Reddy, M. S. (2015). Effects of Phosphate-Solubilizing Bacteria, Rock Phosphate and Chemical Fertilizers on maize-wheat Cropping Cycle and Economics. *Pedosphere* 25, 428–437. doi:10.1016/S1002-0160(15)30010-2

Han, B., Song, L., Li, H., and Song, H. (2020). Immobilization of Cd and Phosphorus Utilization in Eutrophic River Sediments by Biochar-Supported Nanoscale Zero-Valent Iron. *Environ. Technol.* 42 (26), 4072–4078. doi:10.1080/09593330.2020.1745289

Heuer, S., Gaxiola, R., Schilling, R., Herrera-Estrella, L., López-Arredondo, D., Wissuwa, M., et al. (2017). Improving Phosphorus Use Efficiency: A Complex Trait with Emerging Opportunities. *Plant J.* 90, 868–885. doi:10.1111/tpj.13423

Hofmeier, M., Roelcke, M., Han, Y., Lan, T., Bergmann, H., Böhm, D., et al. (2015). Nitrogen Management in a Rice-Wheat System in the Taihu Region: Recommendations Based on Field Experiments and Surveys. *Agric. Ecosyst. Environ.* 209, 60–73. doi:10.1016/j.agee.2015.03.032

Hui, K., Tang, J., Cui, Y., Xi, B., and Tan, W. (2021). Accumulation of Phthalates under High Versus Low Nitrogen Addition in a Soil-Plant System with Sludge Organic Fertilizers Instead of Chemical Fertilizers. *Environ. Pollut.* 291, 118193. doi:10.1016/j.envpol.2021.118193

Jez, J. M., Lee, S. G., and Sherp, A. M. (2016). The Next green Movement: Plant Biology for the Environment and Sustainability. *Science* 353, 1241–1244. doi:10.1126/science.aag1698

Jing, Y., Zhang, Y., Han, I., Wang, P., Mei, Q., and Huang, Y. (2020). Effects of Different Straw Biochars on Soil Organic Carbon, Nitrogen, Available Phosphorus, and Enzyme Activity in Paddy Soil. *Sci. Rep.* 10, 1–12. doi:10.1038/s41598-020-65796-2

Knelman, J. E., Legg, T. M., O'Neill, S. P., Washenberger, C. L., González, A., Cleveland, C. C., et al. (2012). Bacterial Community Structure and Function Change in Association with Colonizer Plants during Early Primary Succession in a Glacier Forefield. *Soil Biol. Biochem.* 46, 172–180. doi:10.1016/j.soilbio.2011.12.001

Lisuma, J., Mbega, E., and Ndakidemi, P. (2020). Influence of Tobacco Plant on Macronutrient Levels in Sandy Soils. *Agronomy* 10, 418. doi:10.3390/agronomy10030418

Liu, G., Deng, L., Wu, R., Guo, S., Du, W., Yang, M., et al. (2020). Determination of Nitrogen and Phosphorus Fertilisation Rates for Tobacco Based on Economic Response and Nutrient Concentrations in Local Stream Water. *Agric. Ecosyst. Environ.* 304, 107136. doi:10.1016/j.agee.2020.107136

Liu, P., Qi, S., Li, D., and Ravenscroft, N. (2021). Promoting Agricultural Innovation as a Means of Improving China's Rural Environment. *J. Environ. Manage.* 280, 111675. doi:10.1016/j.jenvman.2020.111675

López-Arredondo, D. L., Leyva-González, M. A., González-Morales, S. I., López-Bucio, J., and Herrera-Estrella, L. (2014). Phosphate Nutrition: Improving Low-Phosphate Tolerance in Crops. *Annu. Rev. Plant Biol.* 65, 95–123. doi:10.1146/annurev-arplant-050213-035949

Lu, D., Li, C., Sokolwski, E., Magen, H., Chen, X., Wang, H., et al. (2017). Crop Yield and Soil Available Potassium Changes as Affected by Potassium Rate in rice-wheat Systems. *Field Crops Res.* 214, 38–44. doi:10.1016/j.fcr.2017.08.025

Lu, J., Zhang, X., Liu, Y., Cao, H., Han, Q., Xie, B., et al. (2019). Effect of Fermented Corn-Soybean Meal on Serum Immunity, the Expression of Genes Related to Gut Immunity, Gut Microbiota, and Bacterial Metabolites in Grower-Finisher Pigs. *Front. Microbiol.* 10, 2620. doi:10.3389/fmicb.2019.02620

Maltas, A., Charles, R., Jeangros, B., and Sinaj, S. (2013). Effect of Organic Fertilizers and Reduced-Tillage on Soil Properties, Crop Nitrogen Response and Crop Yield: Results of a 12-Year experiment in Changins, Switzerland. *Soil Tillage Res.* 126, 11–18. doi:10.1016/j.still.2012.07.012

Momesso, L., Crusciol, C. A. C., Leite, M. F. A., Bossolani, J. W., and Kuramae, E. E. (2022). Forage Grasses Steer Soil Nitrogen Processes, Microbial Populations, and Microbiome Composition in A Long-Term Tropical Agriculture System. *Agric. Ecosyst. Environ.* 323, 107688. doi:10.1016/j.agee.2021.107688

Neupane, A., Bulbul, I., Wang, Z., Lehman, R. M., Nafziger, E., and Marzano, S. L. (2021). Long Term Crop Rotation Effect on Subsequent Soybean Yield Explained by Soil and Root-Associated Microbiomes and Soil Health Indicators. *Sci. Rep.* 11, 9200–9213. doi:10.1038/s41598-021-88784-6

Palozzi, J. E., and Lindo, Z. (2018). Are Leaf Litter and Microbes Team Players? Interpreting Home-Field Advantage Decomposition Dynamics. *Soil Biol. Biochem.* 124, 189–198. doi:10.1016/j.soilbio.2018.06.018

Pétriacq, P., Williams, A., Cotton, A., Mcfarlane, A. E., Rolfe, S. A., and Ton, J. (2017). Metabolite Profiling of Non-Sterile Rhizosphere Soil. *Plant J.* 92, 147–162. doi:10.1111/tpj.13639

Saad, M. M., Eida, A. A., and Hirt, H. (2020). Tailoring Plant-Associated Microbial Inoculants in Agriculture: A Roadmap for Successful Application. *J. Exp. Bot.* 71, 3878–3901. doi:10.1093/jxb/eraa111

Sáez-Plaza, P., Navas, M. J., Wybraniec, S., Michałowski, T., and Asuero, A. G. (2013). An Overview of the Kjeldahl Method of Nitrogen Determination. Part II. Sample Preparation, Working Scale, Instrumental Finish, and Quality Control. *Crit. Rev. Anal. Chem.* 43, 224–272. doi:10.1080/10408347.2012.751787

Safonov, A. V., Babich, T. L., Sokolova, D. S., Grouzdev, D. S., Tourova, T. P., Poltaraus, A. B., et al. (2018). Microbial Community and *In Situ* Bioremediation of Groundwater by Nitrate Removal in the Zone of a Radioactive Waste Surface Repository. *Front. Microbiol.* 9, 1985. doi:10.3389/fmicb.2018.01985

Shao, T., Zhao, J., Liu, A., Long, X., and Rengel, Z. (2020). Effects of Soil Physicochemical Properties on Microbial Communities in Different Ecological Niches in Coastal Area. *Appl. Soil Ecol.* 150, 103486. doi:10.1016/j.apsoil.2019.103486

Singleton, C. M., Petriglieri, F., Kristensen, J. M., Kirkegaard, R. H., Michaelsen, T. Y., Andersen, M. H., et al. (2021). Connecting Structure to Function with the Recovery of over 1000 High-Quality Metagenome-Assembled Genomes from Activated Sludge Using Long-Read Sequencing. *Nat. Commun.* 12, 1–13. doi:10.1038/s41467-021-22203-2

Smith, L. E. D., and Siciliano, G. (2015). A Comprehensive Review of Constraints to Improved Management of Fertilizers in China and Mitigation of Diffuse Water Pollution from Agriculture. *Agric. Ecosyst. Environ.* 209, 15–25. doi:10.1016/j.agee.2015.02.016

Su, S. L., Singh, D. N., and Shojaei Baghini, M. (2014). A Critical Review of Soil Moisture Measurement. *Measurement* 54, 92–105. doi:10.1016/j.measurement.2014.04.007

Sun, Y., Hu, R., and Zhang, C. (2019). Does the Adoption of Complex Fertilizers Contribute to Fertilizer Overuse? Evidence from rice Production in China. *J. Clean. Prod.* 219, 677–685. doi:10.1016/j.jclepro.2019.02.118

Tkacz, A., and Poole, P. (2015). Role of Root Microbiota in Plant Productivity. *J. Exp. Bot.* 66, 2167–2175. doi:10.1093/jxb/erv157

Turnbull, L. A., Levine, J. M., Loreau, M., and Hector, A. (2013). Coexistence, Niches and Biodiversity Effects on Ecosystem Functioning. *Ecol. Lett.* 16, 116–127. doi:10.1111/ele.12056

Vurukonda, S. S. K. P., Giovanardi, D., and Stefani, E. (2018). Plant Growth Promoting and Biocontrol Activity of Streptomyces Spp. As Endophytes. *Int. J. Mol. Sci.* 19, 952. doi:10.3390/ijms19040952

Wang, J., Shi, X., Zheng, C., Suter, H., and Huang, Z. (2021). Different Responses of Soil Bacterial and Fungal Communities to Nitrogen Deposition in a Subtropical forest. *Sci. Total Environ.* 755, 142449. doi:10.1016/j.scitotenv.2020.142449

Yang, L., Zhao, F., Chang, Q., Li, T., and Li, F. (2015). Effects of Vermicomposts on Tomato Yield and Quality and Soil Fertility in Greenhouse under Different Soil Water Regimes. *Agric. Water Manage.* 160, 98–105. doi:10.1016/j.agwat.2015.07.002

Yang, X., and Fang, S. (2015). Practices, Perceptions, and Implications of Fertilizer Use in East-Central China. *Ambio* 44, 647–652. doi:10.1007/s13280-015-0639-7

Zhang, C., Liu, G., Xue, S., and Wang, G. (2016). Soil Bacterial Community Dynamics Reflect Changes in Plant Community and Soil Properties during the Secondary Succession of Abandoned Farmland in the Loess Plateau. *Soil Biol. Biochem.* 97, 40–49. doi:10.1016/j.soilbio.2016.02.013

Zhang, S., Fang, Y., Luo, Y., Li, Y., Ge, T., Wang, Y., et al. (2021). Linking Soil Carbon Availability, Microbial Community Composition and Enzyme Activities to Organic Carbon Mineralization of a Bamboo forest Soil Amended with Pyrogenic and Fresh Organic Matter. *Sci. Total Environ.* 801, 149717. doi:10.1016/j.scitotenv.2021.149717

Conflict of Interest: Authors BY, PW, Z-YD were employed by Shandong Qingdao Tobacco Co., Ltd.

The remaining authors declare that the research was conducted in the absence of any commercial or financial relationships that could be construed as a potential conflict of interest.

frontiers in Bioengineering and Biotechnology

ORIGINAL RESEARCH
published: 24 January 2022
doi: 10.3389/fbioe.2021.787764

Tailored Bioactive Compost from Agri-Waste Improves the Growth and Yield of Chili Pepper and Tomato

Asma Imran[1], Fozia Sardar[1†], Zabish Khaliq[1†], Muhammad Shoib Nawaz[1], Atif Shehzad[1], Muhammad Ahmad[1], Sumera Yasmin[1], Sughra Hakim[1], Babur S. Mirza[2], Fathia Mubeen[1] and Muhammad Sajjad Mirza[1]*

[1]Soil and Environmental Biotechnology Department, National Institute for Biotechnology and Genetic Engineering (NIBGE), Faisalabad, Pakistan, [2]Department of Biology, Missouri State University, Springfield, MO, United States

OPEN ACCESS

Edited by:
Xiaoyan Liu,
Huaiyin Normal University, China

Reviewed by:
Pankaj Srivastava,
Gandhi Institute of Technology and Management (GITAM), India
Abhishek Walia,
Chaudhary Sarwan Kumar Himachal Pradesh Krishi Vishvavidyalaya, India

***Correspondence:**
Asma Imran
asmaaslam2001@yahoo.com

[†]These authors have contributed equally to this work

Specialty section:
This article was submitted to Bioprocess Engineering, a section of the journal Frontiers in Bioengineering and Biotechnology

Received: 01 October 2021
Accepted: 07 December 2021
Published: 24 January 2022

Citation:
Imran A, Sardar F, Khaliq Z, Nawaz MS, Shehzad A, Ahmad M, Yasmin S, Hakim S, Mirza BS, Mubeen F and Mirza MS (2022) Tailored Bioactive Compost from Agri-Waste Improves the Growth and Yield of Chili Pepper and Tomato. Front. Bioeng. Biotechnol. 9:787764. doi: 10.3389/fbioe.2021.787764

An extensive use of chemical fertilizers has posed a serious impact on food and environmental quality and sustainability. As the organic and biofertilizers can satisfactorily fulfill the crop's nutritional requirement, the plants require less chemical fertilizer application; hence, the food is low in chemical residues and environment is less polluted. The agriculture crop residues, being a rich source of nutrients, can be used to feed the soil and crops after composting and is a practicable approach to sustainable waste management and organic agriculture instead of open-field burning of crop residues. This study demonstrates a feasible strategy to convert the wheat and rice plant residues into composted organic fertilizer and subsequent enrichment with plant-beneficial bacteria. The bioactive compost was then tested in a series of *in vitro* and *in vivo* experiments for validating its role in growing organic vegetables. The compost was enriched with a blend of micronutrients, such as zinc, magnesium, and iron, and a multi-trait bacterial consortium AAP (*Azospirillum*, *Arthrobacter*, and *Pseudomonas* spp.). The bacterial consortium AAP showed survival up to 180 days post-inoculation while maintaining their PGP traits. Field emission scanning electron microscopic analysis and fluorescence *in situ* hybridization (FISH) of bioactive compost further elaborated the morphology and confirmed the PGPR survival and distribution. Plant inoculation of this bioactive compost showed significant improvement in the growth and yield of chilies and tomato without any additional chemical fertilizer yielding a high value to cost ratio. An increase of ≈35% in chlorophyll contents, ≈25% in biomass, and ≈75% in yield was observed in chilies and tomatoes. The increase in N was 18.7 and 25%, while in P contents were 18.5 and 19% in chilies and tomatoes, respectively. The application of bioactive compost significantly stimulated the bacterial population as well as the phosphatase and dehydrogenase activities of soil. These results suggest that bioactive compost can serve as a source of bioorganic fertilizer to get maximum benefits regarding vegetable yield, soil quality, and fertilizer saving with the anticipated application for other food crops. It is a possible win-win situation for environmental sustainability and food security.

Keywords: multi-plant waste compost, bioactive compost, FESEM, fish, MPN-PCR, chili, tomato

1 INTRODUCTION

An exponential increase in the global population demands sustainability, safety, and security of food with minimum burden on the economy, Earth, and the environment. An input-intensive conventional farming, however, ensures food safety but leaves a long-term harmful impact on the production system, food quality, environmental sustainability, biodiversity, greenhouse gas emission, and human health. In the last 2 decades, concerted efforts have been made for exploring ways for the sustainable future food security with a lesser reliance on chemicals and to achieve the United Nations Sustainable Development Goals (SDGs) regarding sustainable life and environment (UNDP, 2021). Organic farming is a natural way of crop production that involves the use of ecologically safe crop-fertilization and pest-management strategies such as compost, green manure, biological fertilizers, or biopesticides. The incorporation of organic fertilizer, for example, compost developed from farm waste (crop residues, animal waste, *etc.*), into the soil replenishes the soil with plant nutrients that promise higher yields of subsequent crops (Gupta et al., 2007).

A huge amount of crop residues are wasted annually either by burning in the field (after harvest) or in the industry during the refining process (husk and bran) (Abbas et al., 2012). Around 40% of N, 35% P, 85% K, and 45% S taken up by the rice plants remain in vegetative parts (Dobermann and Fairhurst, 2002), which can be reused to nourish soil and plants (Tahir et al., 2006) or reutilized in the industry (Calabi–Floody et al., 2018). The burning causes a complete loss of N, 25% of P, 20% of K, and up to 60% of S (Dobermann and Fairhurst, 2002), and is a major contributor of air pollution and greenhouse gases (Udeigwe et al., 2015; Romasanta et al., 2017; Andini et al., 2018). Under the field condition, the degradation of straw is very slow, and crop impact is less positive because it is chemically stable yielding a high value to cost ratio and contains high lignocellulosic material with a high C: N ratio (Dobermann and Fairhurst, 2002; Chen, 2014). Composting is a microbial-driven process that accelerates the waste degradation and conversion of complex materials into usable, simpler organic and inorganic forms (Zhang et al., 2016; Bhattacharjya et al., 2021).

Composted organic fertilizers developed from farm waste significantly improve soil carbon status, nutrient balance, and overall growth and yield of plants (Das et al., 2003; Whitbread et al., 2003; Ye et al., 2020; Sharma et al., 2021). Having relatively lower ratios of nutrients than chemical fertilizers, the field application rate of compost is very high ($t\ ha^{-1}$) that makes it not only impracticable but also economically expensive to apply in large agricultural fields or organic agriculture. The problem can be solved by improving the quality and effectiveness of the compost either by enrichment with essential nutrients (bioactive compounds) or indirectly (microbes). Bioorganic fertilizer (BOF) combines the benefits of bacteria and the organic matter, and is more effective than the microorganisms alone or the organic matter (Li et al., 2021). Bioactive compounds or microbes stimulate various biological processes and exert direct positive impact on the plant. The addition of plant growth-promoting bacteria (PGPB) to the compost makes it biologically active and effective for seed germination and plant growth, soil rehabilitation, and disease suppression (Tahir et al., 2006; El-Akshar et al., 2016; Kaur et al., 2019). The phytohormone-producing PGPB mediate water and nutrient uptake due to increased root proliferation that ultimately improve plant growth and yield (Imran et al., 2021). The effectiveness of bioactive compost, however, depends upon the survival and physiological efficiency of microbes (Altaf et al., 2014) along with the organic contents and moisture-holding capacity of the compost (Mahdi et al., 2010; Calabi–Floody et al., 2019). However, the individual impacts of compost or PGPR on plant growth are well-documented, but the synergistic potential of BOF has only been reported in a few plants such as wheat (Akhtar et al., 2009; Kanwal et al., 2017), cotton (Zewail and Ahmed, 2015), sunflower (Arif et al., 2017), cucumber (Nadeem et al., 2017), and potato (Li et al., 2021) on a pot scale level.

Recent estimates show that global staple cereal production will increase 50% by 2050 (FAO and UNICEF, 2017), which will constantly require a huge amount of chemical fertilizer inputs on the one hand, and generate massive crops residues (e.g., straw, bran, and husk) on the other hand. Composting these crop residues and subsequent soil application will generate a sustainable organic agriculture system which will have minimum reliance on chemical inputs and crop waste burning (Liang et al., 2012). In this study, the focus was on the chilies and tomatoes as these are among the main vegetables grown around the globe and were not tested for enriched BOF earlier. Tomatoes are on the top with an estimated production of 180.77 million metric tons per year, and chili production is also on the boom, with an average of 38.03 million metric tons per year (Shahbandeh, 2021). It was hypothesized that enriched BOF will support the plant growth as well as improve soil health. The present study demonstrates the beneficial impact of biologically active compost for growing chilies and tomatoes without additional mineral fertilizer for sustainable management of crop waste, increased agriculture productivity, and safer environment.

2 MATERIALS AND METHODS

2.1 Development of Compost

Compost was developed in cemented plots (12 × 5 × 1.2 m) by using wheat and rice crop residues (<2 cm) from experimental fields. Wheat and rice straw were collected, completely dried, and co-composted with nitrogen-rich green plants *Sesbania bispinosa* and *Trifolium alexandrinum* (>2 cm), respectively, in the ratio of 2:1, and *Azolla pinnata* in the ratio of 1:4 for nitrogen enrichment/nitrogen urea (1.0 kg/40 kg compost) during composting to decrease the C: N ratio and speedup composting of raw materials (Rovshandeh et al., 2007). The aerobic composting technique was used to decompose heap (Liu et al., 2011), maintaining proper aeration and moisture level 50–55% by turning/mixing the raw material and the addition of required water after an interval of 15 days. Heap was covered with a plastic sheet to prevent loss of moisture and

heat produced. The temperature of the composting heap was taken using a thermometer at a regular interval of 15 days. The composted material was left for stabilization for 1 week, and then finally grounded (2.0 mm) and sieved to ensure homogeneity.

2.2 Analysis of Compost Metagenome

DNA was extracted from three replicates of both wheat and rice samples using a DNA Isolation Kit (MP Biomedicals, United States) according to the manufacturer's instructions. The eluted DNA was further processed for amplicon library construction for Illumina sequencing using a two PCR steps' approach with two different primer pairs for the V3–V4 region of the 16S rRNA gene as previously described (Hakim et al., 2020). Paired-end Illumina reads were assembled using the Mothur software (Schloss et al., 2009). The sequences where the forward and reverse sequence did not match were filtered out to minimize the effect of random sequencing error. Furthermore, the primer sequences were trimmed, and those of low-quality with read lengths <370 bp, homopolymers > 8 bases, and the sequences with >3 continuous ambiguous bases (i.e., N) were filtered out using Mothur. The high-quality sequences were screened for chimeras and clustered into operational taxonomic units (OTUs) at 97% of sequence similarity using the Ribosomal Database Project (RDP) platform. The sequences have been deposited in GenBank Sequence Read Archive under the Bio project.

2.3 Analysis of Compost Quality

The compost was characterized for quality parameters including pH, electrical conductivity, nitrogen and phosphorus content, and organic matter. Compost samples were mixed in water (1:5 ratio w/v) and placed at a shaker for 2 h. The pH and the electrical conductivity (EC) were taken using a pH meter (pH/ion analyzer 350, CORNING) and an EC meter (Multi-range Conductivity Meter Clarkson HI23151, Hanna Instruments, Italy), respectively (Roca–Pérez et al., 2009). The nitrogen content of the compost was determined by following the Kjeldahl method (Sparks et al., 2020), while phosphorus was determined by using the vanadium phosphomolybdate method (Yoshida et al., 1976), followed by taking absorbance through a spectrophotometer (double-beam UV-Vis, Camspec-M350, United Kingdom). Organic matter was quantified as described (Schollenberger, 1945).

2.4 Development of Bioactive Compost

2.4.1 Bacterial Consortium

The compost was enriched with a consortium of three PGPR strains, *Azospirillum brasilense* strain ER-20, *Arthrobacter oxydans* WP-2, and *Pseudomonas stutzeri* strain K1 abbreviated as AAP. The strains are well characterized and compatible with each other (Ref). Antibiotic-resistant derivatives of AAP strains were developed for successful and selective recovery from the compost by following the method of Hanif et al. (Hanif et al., 2015). The antibiotic-resistant derivatives of ER-20 and K-1 were developed against streptomycin 400 μg/ml, while WP-2 antibiotic-resistant derivatives were developed against streptomycin 200 μg/ml + rifampicin 20 μg/ml. The mean generation time, effectiveness, and efficiency of mutants were estimated before inoculating them to the compost.

Wild and antibiotic-resistant derivative strains were grown in the LB broth separately; after 24 h, a culture of each strain was centrifuged (4,000 rpm, 4°C for 15 min), and the cells were resuspended in saline to get an OD of 0.45 λ 600 nm.

2.4.2 Nutrients

The micronutrients were added to get a final concentration of Zn: 5 mg Kg^{-1}, Mg: 50 mg Kg^{-1}, and Fe: 50 mg Kg^{-1}. The nutrients were mixed thoroughly in the compost.

For the development of bioactive compost, fully grown bacterial strains (*Azospirillum brasilense* strain ER-20, *Arthrobacter oxydans* WP-2, and *Pseudomonas stutzeri* strain K1) were mixed in the ratio of 1:1:1 to get a consortium AAP. The cell pellet was obtained by centrifugation, resuspended in 500 ml normal saline, and mixed with the compost (100 ml 10^7 CFU per Kg compost). The nutrients were added during the mixing process. The compost was air-dried and then packed in the bags. The compost inoculated with saline was kept as a control.

2.5 Analysis of PGPR Efficacy in Bioactive Compost

2.5.1 Surface Morphology and Bacterial Distribution Using FESEM

Compost surface morphology, distribution, and population of inoculated bacteria were analyzed by FESEM at 30, 60, 90, 120, 150, and 180 dpi. For FESM analysis, 50–100 mg of samples were taken aseptically and dried at room temperature to avoid surface tension artifacts; then the samples were carefully mounted on an aluminum stub using a double stick carbon tape. The stub was washed with acetone and air-dried before sample mounting (Qu et al., 2017). The specimen was focused using coarse, and fine focus was used at 5,000X at 10kv to get the fine image of the sample.

2.5.2 Bacterial Detection Using Fluorescence *In Situ* Hybridization

The inoculated PGPR were detected using FISH at 90 dpi using fixation and hybridization protocol for soil samples (Amann et al., 1990; Stein et al., 2005; Bertaux et al., 2007) with slight modification. One gram of the bioactive compost sample was taken, diluted in 9.0 ml of extraction buffer (0.8 mM $MgSO_4{\cdot}7H_2O$, 1 mM $CaCl_2{\cdot}2H_2O$, 1.7 mM NaCl, and 5% Tween-20), and homogenized using a vortex mixer for 5–10 min. After sedimentation for 15 min, 3.0 ml from the supernatant was mixed with three volumes of 4% PFA (paraformaldehyde) and incubated overnight at 4°C. The fixed samples were centrifuged for 5 minutes at 5,000 rpm; the pellet was washed thrice with 1xPBS and resuspended in 1 ml 0.01% toluidine blue for 1 hour. Centrifugation and washing were repeated; the pellet was resuspended in 1:1 PBS ethanol and finally stored at −20°C. Fluorescently labeled oligonucleotide probes used in the FISH analysis are mentioned in **Supplementary Table S1**. These oligonucleotide probes were synthesized with indocarbocyanine (cy3) and fluorescein-5-isothiocyanate (FITC) at 5′ end (Interactiva Biotechnologie

GmbH, Ulm, Germany) (Majeed et al., 2018). Fixed samples were placed on slide wells, air-dried, and dehydrated by washings with 50, 80, and 100% ethanol, respectively (3 min each). A 2-µl oligonucleotide probe and 18 µl hybridization buffer were added to each well; compost samples were treated with hybridization buffer and 15 pmol of each FLUOS-labeled EUB 338 specific for bacteria and Cy3-labeled probe GAM42a specific for gamma Proteobacteria. After 3 h of hybridization at 46°C, samples were treated with a washing buffer for 20 min, and then washed with sterilized water, air-dried, shifted on a microscopic slide in Citifluor (mounting buffer), and observed on CLSM (Olympus FV 1000, Japan). Pure bacterial strains were also grown, and their cells were fixed, hybridized, washed, air-dried, and observed as described above (Amann et al., 1995).

2.5.3 Viability and Efficiency of PGPR

Survival of AAP consortium inoculated to the compost was analyzed at 7, 15, 30, 60, and 90 dpi using a standard serial dilution plating technique (Mislivec and Bruce, 1977; Somasegaran and Hoben, 1994). Wild strains were recovered on simple LB-agar plates, while antibiotic-resistant derivatives were recovered on LB-antibiotic selection media. The bacterial population from control (mock) bags was recovered on LB agar plates. Plates were incubated at 28°C for 24–48h until the appearance of colonies. The viable cells were calculated by counting CFU ml^{-1} at each interval on a colony counter and converted to log values.

Recovered colonies at each time were tested for their effectiveness as PGPR. P-solubilization was checked by spot inoculation on Pikovskaya's plate. The formation of the halo zone was confirmed each time and compared to pure culture (Pikovskaya, 1948). Similarly, IAA production was tested using the colorimetric method and compared to pure culture (Gordon and Weber, 1951). Nitrogen fixation was also detected by inoculation into the NFM (nitrogen-free malate) semisolid medium *via* the acetylene reduction assay (ARA) as described earlier (Mirza et al., 2001). Furthermore, 100 µL of the sample was taken from dilutions 1, 2, and 3 and added to the NFM semisolid medium at every time interval to calculate the most probable number (MPN) (Alexander, 1965).

2.5.4 PCR-Based Detection of Bacteria

Samples were collected in three replicates from both control (non-inoculated) as well as bioactive (inoculated) compost after three and 6 months. The DNA was extracted from 0.5 g compost samples using the Fast Prep soil DNA Spin Kit, and 10-fold serial dilutions of DNA were prepared for MPN–PCR. These dilutions along with original DNA from the pure culture of K-1 were used in MPN–PCR. Strain-specific primers (Mirza et al., 2006) were used for MPN–PCR-based detection of inoculated strain K-1 in the bioactive compost. PCR reaction and amplification conditions were the same as previously described (Mirza et al., 2006).

2.6 Plant Testing of Compost and Bioactive Compost

2.6.1 Experiment 1: Initial Testing of Wheat and Rice Compost and PGPR on Chili in Pots

This experiment was set up in a completely randomized design (CRD) with six treatments and three replicates each using rice-straw compost (RSC) and wheat-straw compost (WSC) separately. The bacterial inoculum used was AAP consortium. The treatments' details are as follows: T1 = Control soil + chemical fertilizer (CF), T2 = AAP-inoculated soil (B), T3 = RSC (CR), T4 = AAP-inoculated RSC (CRB), T5 = WSC (CW), and T6 = AAP-inoculated WSC (CWB). The soil and compost were thoroughly mixed by sieving three times in a ratio of 1:3 (v/v) and filled into the pots (8 inches dia and 9 inches depth). Three chilies' seedlings (Hybrid; Golden Hot) were transplanted in each pot. Pots were irrigated with tap water whenever required. Harvesting was done after maturity and plant growth parameters, that is, root length, shoot length, fresh weight, dry weight, number of chilies, fresh weight, and dry weight of chilies, were recorded at the time of harvesting.

2.6.2 Experiment 2: Testing of Wheat: Rice Compost Combination With PGPR for Chilies' Growth in Pots

After validation of the beneficial impact of wheat and rice straw composts and PGPR efficacy, a 1:1 combination rice-straw compost (RSC) and wheat-straw compost (WSC) was developed for enrichment with PGPR for further experiments. Bioactive compost and soil were thoroughly mixed in a 1:3 ratio (v/w) and passed through a 2-mm sieve, and then earthen pots (8-inch diameter and 9-inch depth) were filled with this mixture. Experimental set up includes three treatments: T1 = Control soil + chemical fertilizer (CF), T2 = Compost (C; RSC: WSC 1:1 v/v), and T3 = PGPR inoculated compost (CB; RSC: WSC 1:1 v/v + AAP). The experiment was laid out in the CRD using conditions similar to those of the abovementioned experiment.

2.6.3 Experiment 3: Testing of Bioactive Wheat: Rice Compost Combination for Chilies' Growth in Microplots

After validation of the results of pot experiment 2, the same treatments were validated in the microplots. The experimental set up includes same three treatments: T1 = Control soil + chemical fertilizer (CF), T2 = Compost (C; RSC: WSC 1:1 v/v), and T3 = PGPR inoculated compost (CB; RSC: WSC 1:1 v/v + AAP). The experiment was laid out in the RCBD using conditions similar to those the above-mentioned experiment in the chili growing season.

2.7 Experiment 4: Effect of Bioactive Compost on Chilies and Tomato plants in the Mini Tunnel

Plant experiments were conducted for 2 years to evaluate the effect of bioactive compost on chilies and tomatoes during the year 2018 and 2019. There treatments were classified as T1 = Control soil + chemical fertilizer (CF), T2 = simple compost (CS), T3 = nutrient-enriched compost (CN; RSC: WSC 1:1 v/v + FMZ), and T4 = Bioactive compost (BAC; RSC: WSC 1:1 v/v-AAP inoculated + FMZ). The experiment was carried out in the RCBD. Sowing of hybrid chili variety (Royal Hot) nursery was done on 15th October, while transplanting was done on 15th December on plot size = 3 m × 1 m (mini tunnel) with five replicates for each treatment. Tomato (variety Nadir) nursery sowing was done on

30th October, while transplantation was done on 20th December on a plot size of plot size: 3 × 1 m (mini tunnel) with five replicates for each treatment. The plant-to-plant distance was maintained at 25 cm. The compost was thoroughly mixed (1:3 v/v) in the 10–20 cm topsoil of the plot. Irrigation was done with tap water whenever required. Harvesting was done at 60, 90, 120, and 130 days post-transplantation (DPT). Data were recorded for morphological, physiological, and yield-related plant parameters. For morphological parameters, three plants from each replicate were uprooted, and mean shoot/root length and fresh/dry weights were recorded. For yield parameters, data were recorded from five plants from each replicate, and the mean was calculated.

2.7.1 Survival of Inoculated Bacteria in the Rhizosphere

For the detection and survival of bacteria inoculated to bioactive compost, PCR and FISH analyses were performed. The roots samples were carefully taken from different treatments, the total DNA was extracted from the rhizosphere 0.5 g soil using the Fast Prep soil DNA Spin Kit, and 10-fold serial dilutions of DNA were prepared for PCR. These dilutions along with original DNA from the pure culture of K-1 were used in PCR as described (Mirza et al., 2006). Similarly, the root samples were fixed and processed for FISH analysis as described (Majeed et al., 2018).

2.7.2 Analysis of Photosynthetic Efficiency

Different leaf photosynthetic parameters, that is, transpiration rate, stomatal diffusive resistance, leaf temperature, quantum, and relative humidity, were measured by using a leaf porometer (L1-1600 L1-COR USA). The porometer was attached to one side of broad leaves exposing the other surface to the ambient air to allow the energy emission by the leaf through radiation. Different parameters were calculated as the standard protocol. Chlorophyll a and b were determined using 500 mg fresh leaf extracted overnight with 80% acetone and centrifuged at 10,000 ×g for 5 min. The absorbance of the supernatant was estimated using a spectrophotometer at 480-, 645-, and 663-nm wavelengths against the solvent, and chlorophyll contents were calculated (Armon, 1949).

2.7.3 Analysis of Fruit Nutrient Contents

The data regarding total N contents in tomato and chili fruits were estimated using the Kjeldahl method (Keeney and Nelson, 1982), and total P contents were estimated using the vanadium phosphomolybdate method (Twine and Williams, 1971).

2.7.4 Soil Enzyme Activities

After plant harvesting, the rhizosphere soil was analyzed for alkaline phosphatase and dehydrogenase enzyme activity in response to different compost treatments. Alkaline phosphatase activity was analyzed as described by Kramer and Yerdei (1959). 1.0 g soil sample was mixed into 5.0 ml of 0.5% disodium phenyl phosphate followed by the addition of 0.2 ml toluene and incubated on a shaker at 37°C for 2 h. The soil suspension was filtered, 1 ml of filtrate in 4 ml water was mixed with 4 ml of borate buffer (0.05 ml, pH = 10 + 0.5 ml 2% 4-Amino antipyrine +0.5 ml 8% potassium ferrocyanide). Then incubation was performed at room temperature for 1 h, and the change from yellowish to red was observed. The optical density of the supernatant was measured at 510 nm on a spectrophotometer (UV-1201, Shimadzu Crop, Japan). The blank solution consists of water and reagent in a 1:1 ratio. 1,000 ppm standard stock of phenol was prepared by dissolving 1 g of phenol in up to 1,000 ml water. From the stock solution, various standards of 0.3, 0.5, 0.8, 1, 1.5, and 1.8 were prepared and a standard curve was plotted, and the equation was generated to calculate phosphatase activity of soil samples.

Soil dehydrogenase activity was measured using the method developed by Klein et al. (1971). 2.0 g soil was incubated with 2 ml of a 1% triphenyl tetrazolium chloride (TTC) solution in 0.1 M Tris HCl buffer (pH = 7.4) at 37°C for 24 h. Then 10 ml methanol was added and kept for 30 min at 37°C for the development of reddish-orange color (conversion of triphenyl tetrazolium chloride (TTC) to triphenyl formazan (TF)) followed by the measurement of optical density at 485 nm using a spectrophotometer (UV-1201, Shimadzu Crop, Japan). A blank solution was prepared using 2 ml of 1% TTC solution in 10 ml methanol as described above, while triphenyl formazan (TF) standards of 2, 10, 20, 30, 50, and 100 ppm were used to draw a standard curve for the quantification of soil dehydrogenase activity.

2.7.5 Total Soil Bacterial Count

The number of bacteria present in the rhizosphere of all the treatments was counted using standard colony-forming units (CFUs) by a serial dilution plating technique using the LB medium as described (Somasegaran and Hoben, 1994).

2.8 Statistical Analysis

The data were subjected to analysis of variance (ANOVA) using M state software, and significance was measured at LSD 0.05. Graphs were constructed using Microsoft Excel (2019) or Slide Write (7.0), and assembled using CorelDraw (R 12).

3 RESULTS

3.1 Analysis of Compost Metagenome

The relative distribution of bacterial phyla in the wheat compost and rice compost samples was evaluated using Illumina sequencing of the 16S rRNA gene (**Figure 1**). About 26,064 high-quality sequences were retrieved from wheat compost, while 12,888 sequences were recovered from rice compost. Sequence analyses revealed the presence of twenty kingdoms/phylum-level groups in wheat compost samples, of which *Proteobacteria* and *Bacteroidetes* were dominant phyla comprising 19.83 and 19.78% sequences, respectively, followed by *Firmicutes* (4.62%), *Chloroflexi* (2.92%), *Actinobacteria* (2.57%), and *Acidobacteria* (1.01%). Twenty phyla accounted for the sequences in the rice compost with eighteen phyla shared with wheat compost samples, while *Pacearchaeota*- and *Spirochetes*-related sequences were only detected in the rice compost. The *Proteobacteria* was the only dominant phylum accounting for 24.58% of the sequences in rice compost followed

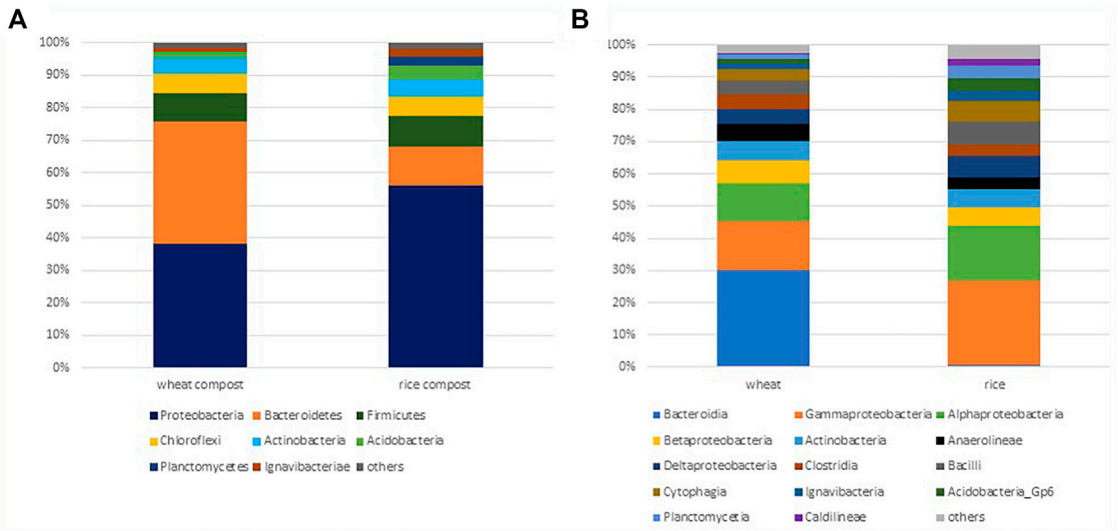

FIGURE 1 | (A) Phylum level. **(B)** Class level relative abundance of major bacteria (represented by >0.5% sequences) detected by 16S rRNA gene analysis in wheat and rice compost samples.

by *Bacteroidetes* (5.12%), *Firmicutes* (4.22%), *Chloroflexi* (2.57%), *Actinobacteria* (2.29%), and *Acidobacteria* (1.83%).

Taxonomic hit distribution at the class level shows that the class *Bacteroidia* was dominant in the wheat compost comprising 11.48% of sequences, followed by *Gammaproteobacteria* (5.88%) and *Alphaproteobacteria* (4.39%). In rice compost samples, the sequences representing the *Gammaproteobacteria* were by far the largest group accounting for 9.15% of sequences followed by *Alphaproteobacteria* (5.94%). The class *Bacteroidia* of phylum *Bacteroidetes* was underrepresented in the rice compost comprising only 0.19% of sequences, while the classes *Cytophagia* (2.23%) and *Sphingobacteriia* (0.33%) were relatively abundant. The classes *Actinobacteria*, *Anaerolineae*, *Betaproteobacteria*, *Deltaproteobacteria*, *Clostridia*, and *Bacilli* have a similar distribution in both wheat and rice composts comprising 1–3% of total sequences. Most bacterial classes observed were found in both composts, that is, wheat and rice compost, although the difference in the distribution of bacterial sequences was observed.

3.2 Appearance and Quality Analysis

The compost color was light brown to dark brown in appearance. Both simple as well as bioactive/enriched compost were ground down and passed through a 2.0-mm sieve to ensure the homogeneity of the product. Characteristic comparison between both types of compost for pH, electrical conductivity (ECe), percentage nitrogen (N) content, phosphorus (P) content, organic matter (OM), and moisture content is given in **Table 1**, which shows enriched compost has slightly higher pH, ECe but is according to the standard than that of the simple compost. Nitrogen, phosphorus organic matter, water holding capacity, and moisture levels are according to the standard values for the compost. Moreover, a non-significant amount of heavy metals Cu, Pb, Hg, Se, and Cd was detected in both types of composts.

3.3 Efficiency and Effectiveness of Bioactive Compost

The total viable bacteria cell count of wild strains in simple compost ranged from 3.88 to 5.73 at 7 and 180 dpi, respectively. Total viable cell counts in the compost inoculated with wild PGPR strains continuously increased from 7.0 dpi (6.99) to 90 = dpi (9.57) and decreased at later stages, that is, 180 dpi (7.61). Specific detection of antibiotic-resistant strains showed a similar trend, that is, a continuous increase from 7.0 dpi (6.18) to 90 dpi (9.55) and reduced at the final stage, that is, 180 dpi (7.92) (**Table 2**). This clearly shows that inoculated PGPR strains survived better in the compost up to 180 dpi.

The functional viability and efficiency of PGPR recovered from bioactive compost were repeatedly confirmed at each interval. No change in the P-solubilization ability of WP-2 was observed and remained comparable to that of the pure strain till 180 days. Indole-3-acetic acid production by ER-20, K-1, and WP-2 was also comparable to the pure strain, and no significant change was observed throughout (180 days). Similarly, the nitrogen-fixing ability of K-1 and ER-20 on the nitrogen-free malate (NFM) semisolid medium remained unchanged till 180 dpi.

3.3.1 Analysis of Bacterial Survival

FESM and FISH Analysis

FESEM analysis of simple and bioactive compost samples at 30, 60, 90, and 120 dpi showed variations in the morphology of compost in terms of particle size and structure. In bioactive compost, presence and distribution of inoculated PGPR can be seen in a scattered form on the surface as well as in the form of micro-colonies in the grooves of compost that provide micro-niche to the inoculated PGPR (**Figure 2**). It is clear from FESEM image analysis that the morphology of bioactive

TABLE 1 | Characteristic of the compost and bioactive compost.

Characteristic	Standard	Compost	Bioactive compost
Organic matter (%)	>20	50–60	50–60
pH	6–8.5	6.9–7.5	7.0–8.0
ECe	4.1	3.3–3.5	3.1–3.4
Total nitrogen (%)	≈2	2.3–3.0	2.7.0–3.1
Total phosphorus (%)	≈2	1.8–1.9	1.8–2.0
E. coli	<1,000 MPN/g	0	0
Salmonella	<3–4 MPN/g	0	0
Phytotoxicity (seed germination) assay	80–90%	85%	95%
Water holding capacity (g) water/g compost)	4	15.54	20.5
Cu (ppm)	13–20	16.65	17.41
Pb (ppm)		0.7–0.9	0.7–0.9
Hg (ppm)		0.4–0.5	0.4–0.5
Se, Cd (ppm)		0	0
Moisture contents (%)	<70	20	25

TABLE 2 | Total bacterial population analysis on compost and bioactive compost.

Days post-inoculation (dpi)	Log values of viable cells		
	Compost	Compost + wild PGPR strains	Compost + antibiotic-resistant PGPR strains
7	3.88 ± 0.65	6.99 ± 0.7	6.18 ± 0.6
15	4.60 ± 1.0	7.29 ± 0.6	7.24 ± 1.2
30	4.47 ± 1.4	8.63 ± 4.5	8.33 ± 2.4
60	4.65 ± 0.7	8.51 ± 5.2	8.53 ± 0.5
90	4.93 ± 4.0	9.57 ± 0.5	9.55 ± 0.6
180	5.73 ± 1.3	7.61 ± 0.5	7.92 ± 0.6

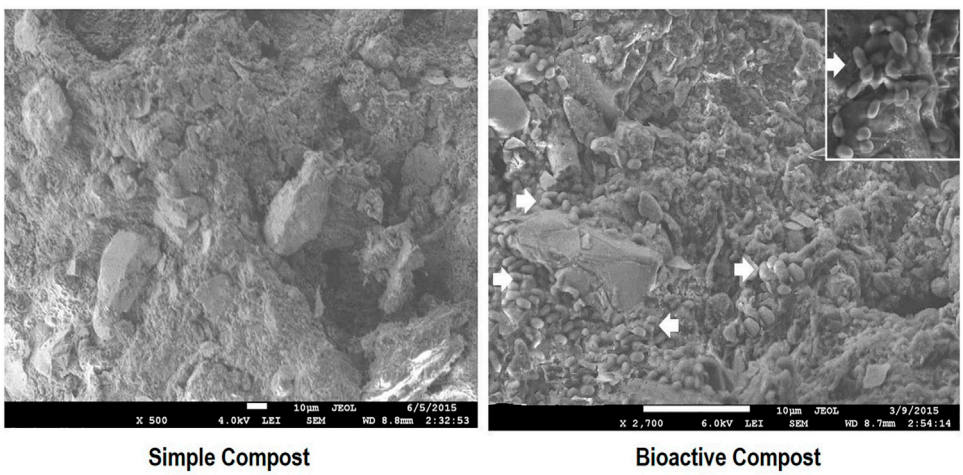

FIGURE 2 | Field emission scanning electron microscopic (FESEM) analysis of inoculated compost at 90 dpi to visualize PGPR composition and compost structure compared to non-inoculated.

compost is better than that of the simple compost. Most probably, high activity and competition of microbes for space and nutrients lead to the creation of grooves and fine-sized compost particles which can accommodate a large microbial population.

Confocal laser scanning microscopy (CLSM) images of hybridized antibiotic-resistant derivatives pure cultures: *A. brasilense* strain ER-20^{S}, *P. stutzeri* strain K-1^{S}, and *A. oxydans* WP-2^{S+R} labeled with FISH probes (EUB 338-green, GAM42-red) in **Figure 3A** show that all the fixation

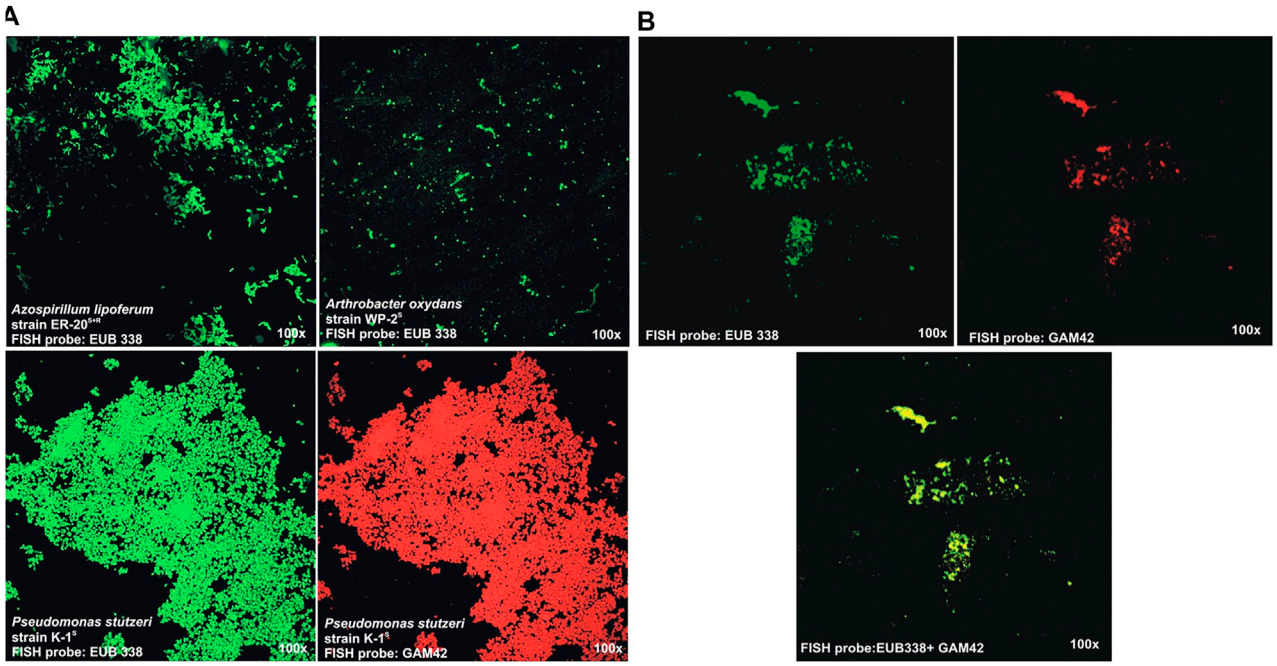

FIGURE 3 | Confocal laser scanning microscopy (CLSM) images of hybridized of *A. brasilense* strain ER-20^{S}, *P. stutzeri* strain K-1^{S}, and *A. oxydans* strain WP-2^{S+R} labeled with FISH probes (EUB 338-green, GAM42-red): **(A)** pure cultures and **(B)** bioactive compost at 180 dpi

and hybridization conditions were optimum, and the microscope setting was fine to give the fluorescent image of the inoculated bacteria. The CLSM analysis of compost samples processed for FISH captured a population of bacteria at 180 dpi (**Figure 3B**). However, this technique was able to identify the whole bacterial population at a particular time (using EUB338 probe), as well as Gamma Proteobacteria (using GAM42 probe) population captured on compost seems very low as compared to that which was calculated using viable cell counts after dilution plating. This might be due to the reason that the soil FISH protocol was modified for the fixation and hybridization of the compost samples which needs further optimization.

PCR-Based Detection

The DNA was extracted from compost samples in triplicates at 90 and 180 dpi for the detection of strain K-1. The result of PCR showed that *P. stutzeri* strain K-1 survived in the inoculated compost sample after 90 dpi as well as at 180 dpi (**Supplementary Figure S1**). The presence of 0.9 Kb DNA band in the inoculated compost DNA exactly corresponds to the amplified PCR product in pure culture of *P. stutzeri* strain K-1, which shows the specificity of primers for the detection of *P. stutzeri* strain K-1. Furthermore, the absence of any band in the non-inoculated compost samples showed the absence of any cross-reacting strain or bacterial species having a similar *rrs* sequence with bacterial *P. stutzeri* strain K-1. In compost samples, the PCR product of 0.9 Kb was detected in dilution from 10^{-4} to 10^{-6} at 90 dpi, while at 180 dpi the product was detected in dilution from 10^{-2} to 10^{-7}. The absence of any PCR product in lower dilutions and stock DNA may be due to the high humic acid contents of the compost which may hinder the PCR reaction.

3.4 Plant Evaluation of Bioactive Compost in Pots

The PGPR supplementation of compost exerted a significant positive effect on shoot length, shoot fresh weight, and dry weight of chilies in all the inoculated treatments as compared to non-inoculated compost or soil. The shoot growth, root growth, as well as leaf size were significantly better in the compost treatments and PGPR-supplemented treatments where the plants were healthy and strong visually (**Figures 4 A,B**). Similarly, PGPR stimulated root growth in inoculated treatments (**Figure 4A**) and shoot growth even when applied in soil (**Table 3**), which validates the *in vivo* efficacy of the PGPR inoculum. The initial analysis shows that both types of composts have a stimulatory effect on chilies' growth compared to soil (**Figures 4 A,B**; **Table 3**). The root length, shoot length, and plant fresh and dry weights were significantly higher in supplemented compost than in other treatments. On average, the response of the wheat and rice composts with PGPR supplementation was statistically similar. Initially, both wheat and rice composts were tested separately to see the individual impact, but later on, both of these composts were mixed in a 1:1 ratio for further analysis and testing in pots or the microplots.

The second experiment where the rice and wheat composts were mixed in a 1:1 ratio shows an increased growth of plant after the addition of compost and PGPR to the root zone (**Figure 5A**;

FIGURE 4 | (A) Inoculation response of rice and wheat compost and PGPR inoculum on the leaf and root growth of chilies compared with those grown in soil with chemical fertilizers. **(B)** Response of rice and wheat compost and PGPR inoculum on chilies' growth in pots compared with chili grown in soil with chemical fertilizers.

TABLE 3 | Individual impact of wheat and rice compost with/without PGPR consortium on the morphological growth of chili in pots.

Treatments	Root length (cm)	Shoot length (cm)	Plant fresh weight (g)	Plant dry weight (g)
Soil + Fertilizer (CF)	15.33 ± 0.21c	43.90 ± 0.66e	34.95 ± 0.43d	7.01 ± 0.29d
Soil + PGPR (B)	17.80 ± 0.36b	49.60 ± 0.10d	40.11 ± 0.39c	9.54 ± 0.29c
W-compost (CW)	17.83 ± 0.45b	50.90 ± 0.46c	44.41 ± 0.89b	11.02 ± 0.17b
W-compost + PGPR (CWB)	20.17 ± 0.35a	55.30 ± 0.36b	49.48 ± 0.68a	13.60 ± 0.35a
R-compost (CR)	17.83 ± 0.49b	50.17 ± 0.35cd	45.64 ± 0.87b	11.11 ± 0.29b
R-compost + PGPR (CRB)	20.47 ± 0.40a	56.13 ± 0.40a	50.64 ± 1.05a	13.58 ± 0.55a
LSD ($p < 0.05$)	0.32	0.34	0.62	0.28

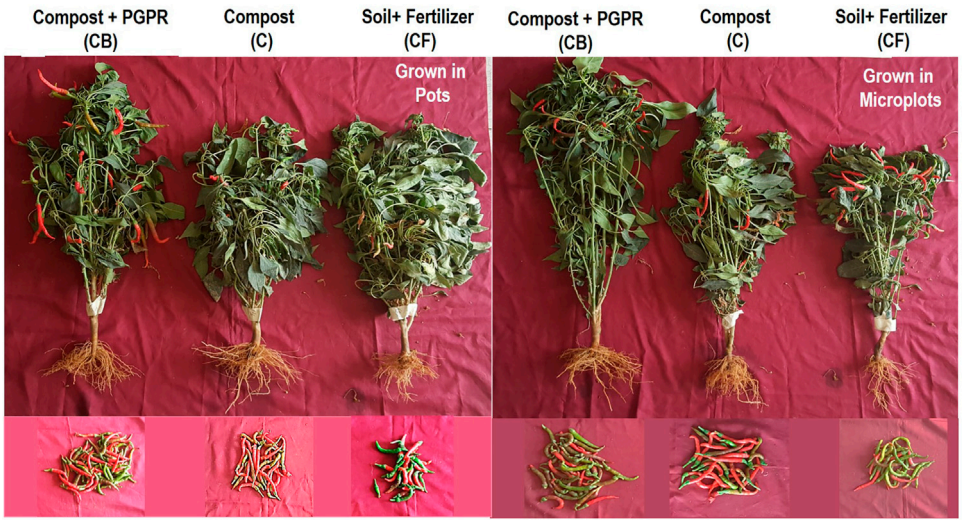

FIGURE 5 | Response of compost and PGPR inoculum on chilies growth and total yield per plant in pots and microplots compared with that grown in soil with chemical fertilizers.

TABLE 4 | The combined impact of wheat and rice composts (mixed as 1:1) with/without PGPR consortium on chili growth and yield in pots.

Treatments	Root length (cm)	Shoot length (cm)	Fresh weight/plant (g)	Dry weight/plant (g)
Soil + CF	13.13 ± 0.40c	44.70 ± 1.02c	37.32 ± 0.80c	7.93 ± 0.51c
Compost (C)	17.47 ± 0.31b	55.46 ± 0.83b	46.68 ± 0.76b	12.77 ± 0.54b
Compost + Bacteria (CB)	21.47 ± 0.21a	60.34 ± 0.53a	53.68 ± 0.88a	17.24 ± 0.41a
LSD ($p < 0.05$)	0.26	0.67	0.66	0.40
Treatments	**Chilies' fresh weight (g)**	**Chilies' dry weight (g)**	**No. of chilies/plant**	**Total yield/plant (g)**
Soil + CF	3.40 ± 0.13c	0.56 ± 0.03c	14.00 ± 1.00c	47.55 ± 3.81c
Compost (C)	4.49 ± 0.18b	0.82 ± 0.04b	22.00 ± 1.00b	98.66 ± 4.87b
Compost + Bacteria (CB)	5.70 ± 0.15a	1.19 ± 0.04a	31.67 ± 1.53a	154.02 ± 4.08a
LSD ($p < 0.05$)	0.13	0.03	0.98	3.49

TABLE 5 | Effect of PGPR-enriched compost on the growth of chilies grown in microplots.

Treatments	Root length (cm)	Shoot length (cm)	Fresh weight/plant (g)	Dry weight/plant (g)
Soil + CF	11.27 ± 0.35c	45.93 ± 0.42c	36.61 ± 0.72c	7.39 ± 0.24c
Compost (C)	15.30 ± 0.40b	52.60 ± 0.50b	46.39 ± 0.98b	11.01 ± 0.29b
Compost + Bacteria (CB)	18.93 ± 0.25a	57.63 ± 0.21a	55.67 ± 0.96a	13.92 ± 0.29a
LSD ($p < 0.05$)	0.28	0.32	0.73	0.22
Treatments	**Chilies' fresh weight (g)**	**Chilies' dry weight (g)**	**No of chilies/plant**	**Total yield/plant (g)**
Soil + CF	3.69 ± 0.20c	0.50 ± 0.04c	13.00 ± 1.00c	48.04 ± 5.91c
Compost (C)	4.16 ± 0.14b	0.73 ± 0.03b	19.00 ± 1.00b	78.95 ± 1.55b
Compost + Bacteria (CB)	4.84 ± 0.15a	1.04 ± 0.04a	30.00 ± 1.00a	145.18 ± 5.86a
LSD ($p < 0.05$)	0.14	0.03	0.82	3.99

Table 4). A significant increase in morphological, agronomic, physiological parameters and yield of chilies was observed by supplementation of compost with PGPR as compared to that without PGPR or soil (**Table 4**). The treatment response was maximum with CB followed by C and CF for all agronomic, physiological, and yield parameters. The addition of bacteria increased the no. of chili and total yield per plant (31.67, 154.02 g) compared to the compost without PGPR (22.00, 98.66 g) and soil (14, 47.55 g). These results validated our hypothesis that PGPR could survive in compost, and this

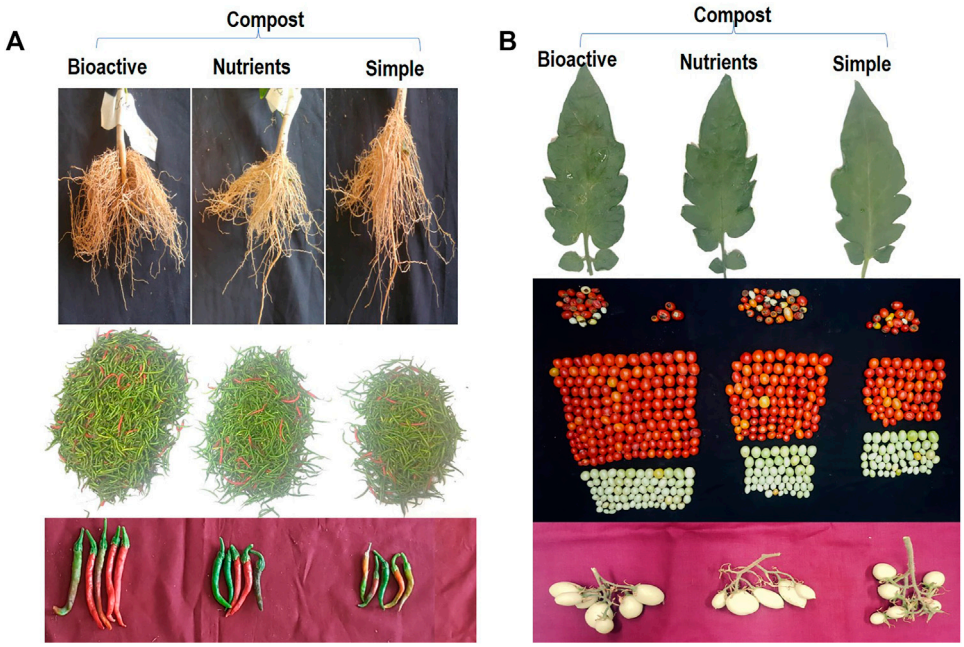

FIGURE 6 | Response of bioactive compost on chilies' root growth, total yield per plot, and size of the chili **(A)**, and tomato leaf growth, yield per plot (one picking), and the inflorescence **(B)** in microplots compared with other treatments.

TABLE 6 | Effect of bioactive compost on growth parameters of chilies grown in small tunnel for 2 years (2 years averaged data).

Parameters		Treatments			LSD ($p < 0.05$)
		Simple compost (C)	Nutrient-enriched compost (CN)	Bioactive compost (BAC)	
Plant growth parameters	Root length (cm)	10.83 ± 0.25c	13.87 ± 0.45b	16.80 ± 0.30a	0.28
	Shoot length (cm)	43.10 ± 1.51c	55.73 ± 1.60b	63.43 ± 1.65a	1.30
	Plant FW (g)	156.80 ± 2.55c	172.83 ± 6.94b	185.37 ± 6.38a	4.61
	Plant DW (g)	39.90 ± 1.21c	44.50 ± 0.96b	54.07 ± 1.56a	1.04
Plant yield parameters	No of chilies/plant	85.47 ± 4.52c	105.13 ± 2.07b	159.33 ± 3.42a	1.27
	Yield of chilies/plant (g)	266.66 ± 14.1c	363.76 ± 7.15b	1,058.6 ± 21.36a	5.60
	Total no of chilies	1,280.7 ± 14.15c	1,576.3 ± 13.80b	2,390.5 ± 44.6a	10.28
	Total yield of chilies (Kg)	3.999 ± 0.445c	5.4541 ± 0.477b	16.102 ± 6.54a	13.79
	Total N in fruit (mg/g)	0.184 ± 0.004c	0.206 ± 0.004b	0.226 ± 0.004a	0.004
	Total P in fruit (mg/g)	0.211 ± 0.004c	0.229 ± 0.004b	0.259 ± 0.003a	0.003
Photosynthetic activity	Diffusive resistance (s/cm)	2.20 ± 0.05a	1.50 ± 0.05b	1.13 ± 0.029c	0.04
	Quantum (μmol/sm^2)	753.5 ± 36.4c	895.9 ± 22.2b	1,096.5 ± 27.5a	23.9
	Transpiration rate (μg/Scm^2)	17.37 ± 1.4c	22.13 ± 1.5b	29.37 ± 1.43a	1.17
	Relative humidity (%)	28.00 ± 0.5a	27.67 ± 0.8a	27.50 ± 0.5a	0.49
	Leaf temp.(°C)	36.867 ± 0.4a	37.07 ± 0.3a	37.03 ± 0.42a	0.31
Photosynthetic pigments	Chlorophyll a (mg/gFW)	0.57 ± 0.030c	0.68 ± 0.023b	0.87 ± 0.056a	0.032
	Chlorophyll b (mg/gFW)	0.27 ± 0.027c	0.36 ± 0.03b	0.43 ± 0.026a	0.023
	Total Chl. (mg/gFW)	0.84 ± 0.052c	1.03 ± 0.05b	1.29 ± 0.072a	0.048
	Carotenoids (mg/gFW)	0.424 ± 0.015c	0.52 ± 0.01b	0.59 ± 0.010a	0.0097
	Chl. a/b ratio	2.11 ± 0.153a	1.90 ± 0.11a	2.04 ± 0.132a	0.1084
Soil enzyme	Phosphatase EU (10^2) μg/ml	6.05 ± 0.22c	8.45 ± 0.33b	9.45 ± 0.30a	0.1298
	Dehydrogenase EU (10^2) μg/ml	3.45 ± 0.11c	4.74 ± 0.19b	5.78 ± 0.17a	0.2325

TABLE 7 | Effect of bioactive compost on growth, yield, physiological and photosynthetic pigments of tomatoes grown in small tunnel, and post-harvest activity analysis of enzymes in soil (2 years averaged data).

Parameters		Treatments			LSD ($p < 0.05$)
		Simple compost (C)	Nutrient-enriched compost (CN)	Bioactive compost (BAC)	
Plant growth parameters	Plant height (cm)	132.390 ± 3.758b	140.767 ± 4.128b	151.597 ± 4.804a	3.4718
	Stem diameter (cm)	1.150 ± 0.050c	1.367 ± 0.029b	1.467 ± 0.029a	0.0304
	Leaf area	31.920 ± 1.502c	36.857 ± 1.925b	41.857 ± 2.804a	1.7527
	No. of lat. branches/plant	22.500 ± 0.901c	25.567 ± 0.957b	31.233 ± 1.776a	1.0418
	Lateral branch len. (cm)	95.35 ± 4.927c	110.033 ± 3.956b	120.250 ± 5.212a	3.8610
Plant yield parameters	Fruit fresh weight (g)	43.63 ± 2.38c	57.89 ± 1.99b	77.81 ± 2.49a	1.8756
	Fruit dry weight (g)	5.94 ± 0.079c	8.53 ± 0.45b	13.15 ± 0.26a	0.2468
	Fruit diameter (cm)	3.12 ± 0.1c	3.98 ± 0.15b	5.12 ± 0.17a	0.1161
	No. of marketable fruits/plant	49.67 ± 3.51c	82.33 ± 4.51b	112.58 ± 8.16a	4.6949
	Marketable yield/plant (g)	2,172.69 ± 270.62c	4,764.05 ± 245.05b	8,766.4 ± 795.2a	412.49
	Total no. marketable fruits	298 ± 21.071c	494 ± 27.06b	675.5 ± 48.94a	28.169
	Total marketable yield(g)	13.04 ± 1.62c	28.58 ± 1.47b	52.6 ± 4.77a	2.4750
	No. of non-marketable fruits/plant	28 ± 3.61a	29 ± 3a	15.33 ± 1.53b	2.3254
	Non-marketable yield/plant (g)	140 ± 18.03a	145 ± 15a	76.67 ± 7.64b	11.627
	Total non-marketable yield(g)	92 ± 9.17b	174 ± 18a	168 ± 21.63a	13.952
	Total non-marketable yield(g)	0.46 ± 0.05b	0.87 ± 0.09a	0.84 ± 0.11a	0.0698
	Total N in fruit (mg/g)	0.165 ± 0.003c	0.19 ± 0.002b	0.219 ± 0.002a	0.0021
	Total P in fruit (mg/g)	0.259 ± 0.003c	0.276 ± 0.004b	0.318 ± 0.005a	0.0032
Physiological parameters	Diff. resistance (s/cm)	3.040 ± 0.132a	3.003 ± 0.153a	1.830 ± 0.053b	0.0986
	Quantum (μmol/sm^2)	646.047 ± 17.252a	655.507 ± 10.410a	658.110 ± 15.985a	12.125
	Trans. rate (μg/Scm^2)	12.903 ± 0.202b	12.027 ± 0.175b	22.603 ± 0.734a	0.3680
	Relative humidity (%)	11.697 ± 0.230b	11.443 ± 0.454b	12.987 ± 0.414a	0.3090
	Leaf temp. (°C)	36.393 ± 0.614b	36.877 ± 0.866 ab	37.993 ± 0.340a	0.5254
Photosynthetic pigments	Chlorophyll a (mg/gFW)	0.687 ± 0.012c	0.794 ± 0.007b	0.994 ± 0.022a	0.0123
	Chlorophyll b (mg/gFW)	0.234 ± 0.007c	0.284 ± 0.005b	0.457 ± 0.027a	0.0131
	Total Chl. (mg/gFW)	0.921 ± 0.012c	1.077 ± 0.002b	1.450 ± 0.005a	0.0062
	Carotenoids (mg/gFW)	0.470 ± 0.010c	0.527 ± 0.006b	0.593 ± 0.006a	0.0061
	Chl. a/b ratio	2.940 ± 0.115a	2.799 ± 0.073a	2.182 ± 0.176b	0.1046
Soil enzyme activity	Phosphatase EU (10^2) μg/ml	6.970 ± 0.255c	9.107 ± 0.215b	10.953 ± 0.195a	0.1822
	Dehydrogenase EU (10^2) μg/ml	4.487 ± 0.180c	5.603 ± 0.130b	6.593 ± 0.185a	0.3335

PGPR-supplemented organic formulation exerts stimulatory effects on the growth of chilies.

Testing of the treatments in the microplots showed a similar growth-stimulatory response of compost + PGPR (**Figure 5B**; **Table 5**). Maximum plant growth was observed in CB with root length: 18.9 cm, shoot length: 57.6 cm, fresh wt.: 55.7 g, and dry weight: 13.92 g followed by the plants grown in simple compost where root length: 15 cm, shoot length: 52.6 cm, fresh wt.: 46.39 g, and dry weight: 11 g were observed (**Table 5**). Similarly, the maximum chilies per plant 30, fresh wt. 4.84 g, and dry wt. 1.04 g were observed in plants grown in the compost with PGPR (**Table 5**). Generally, PGPR-enriched compost showed a percent increase of 19, 40.5% in root length, 8.7, 20% in shoot length, 16.7, 34% in shoot fresh weight, 21, 47% in dry weight, 36.7–56.7% in the number of chilies per plant, 14–24% in average chili fresh weight, 30–52% in chili biomass, and 46–67% in total chili yield (g) over simple compost and soil, respectively.

3.4.1 Plant Evaluation of Bioactive Compost in Microplots

Bioactive compost displayed a positive effect on the growth and yield of chili pepper (**Figure 6A**; **Table 6**). The root growth, the number of chilies per plot, and the size of the chili were significantly better in the bioactive compost treatment than in other treatments (**Figure 6A**). Data show that bioactive compost improved chili pepper growth by a 12–22% increase in shoot length, 6–15% in plant fresh weight, and 18–26% in plant fresh dry weight as compared to that of the nutrient-enriched compost and simple compost, respectively, while nutrient-enriched compost showed a 21% increase in root length than that of the bioactive compost. But again, the augmented effect of bioactive compost was observed in different yield-related parameters like 34–46% increase in the number of chilies per plant and the total number of chilies and similarly 66–75% in the fresh weight of chilies per plant and overall fresh weight of total yield of chilies. Bioactive compost also increased 11–19% nitrogen content and 12–19% phosphorus content of chilies as compared to that of the nutrient-enriched compost and simple compost, respectively. Leaf photosynthetic parameters showed variable responses to different treatments; diffusive resistance was 94%, and relative humidity was higher in the simple compost than in the bioactive compost. Leaf temperature was more or less similar in all treatments, but 18–31% increase in quantum and 25–41% in the transpiration rate showed by bioactive compost compared to the other two treatments, respectively. Significant increase in chlorophyll pigments (a, 22–35% + b, 16–37%) 20–35%, and 12–28% in carotenoid contents were observed. Similarly, 11–36% increase in soil phosphatase and 18–46% in

TABLE 8 | Effect of bioactive compost on total viable bacterial population.

Days post-inoculation (dpi)	Log values of viable cells		
	Soil (CF)	Compost (C)	Bioactive compost (BAC)
7	8.18 ± 0.56	8.58 ± 0.65	9.75 ± 0.21
15	8.24 ± 1.27	9.10 ± 1.11	9.92 ± 0.39
30	8.33 ± 2.41	10.07 ± 1.43	10.79 ± 0.94
60	8.53 ± 0.54	11.15 ± 0.74	11.95 ± 2.14
90	8.55 ± 0.56	11.73 ± 1.25	12.20 ± 1.32

dehydrogenase with bioactive compost as compared to that of the nutrient-enriched compost and simple compost, respectively (**Table 6**), were observed.

Bioactive compost also displayed a positive effect on the visual growth and yield of tomatoes (**Figure 6B**). Leaf photosynthetic parameters and pigment contents were also improved by the treatment with bioactive compost and nutrient-enriched compost as compared to the application of compost. Bioactive compost displayed a 7–13% increase in plant height, 7–22% in stem diameter, 12–24% in leaf area, 18–28% in the number of lateral branches per plant, and 9–21% in their length. Similarly, in yield parameters, for example, 26–44% increase in fruit fresh weight, 35–55% in fruit dry weight, 22–39% in fruit diameter, 27–56% in the number of marketable fruits per plant and the total number of marketable fruits, 46–75% fresh weight of marketable fruits and total fresh weight of marketable fruits as compared to that of the nutrient-enriched compost and simple compost, respectively, were observed. But approximately 45% increase and 4% decrease in the number of non-marketable fruits per plant, total non-marketable fruits, fresh weight of non-marketable fruits, and total fresh weight of non-marketable fruits were also observed in bioactive compost–treated plants as compared to simple compost and nutrient-enriched compost, respectively. Fruits of bioactive treated plants were 13–25% richer with total nitrogen and 13–19% with phosphorus contents. Furthermore, leaf photosynthetic parameter response was mixed. All the treatments were non-significant for quantum and leaf temperature. Like chilies, diffusive resistance was also 66% higher in simple compost–treated plants than bioactive compost treatment, and non-significant with nutrient-enriched compost. Similarly, the transpiration rate and relative humidity treatment with simple compost and nutrient-enriched compost were non-significant, but bioactive compost showed 43–47% and 10–12% increase, respectively. Bioactive compost also showed a 20–31% increase in chlorophyll a, 38–49% in chlorophyll b, and a total of 26–37% in chlorophyll (a + b) and 11–21% in carotenoid contents as compared to that of nutrient-enriched and simple compost, respectively (**Table 7**).

Fruit Nutrient Analysis

Total N and P estimation in tomato and chili fruits showed a significantly higher amount of NP in the fruits. Chilies treated with the bioactive compost showed an 18.7 and 18.5% increase in NP, respectively, in comparison to the simple compost, while 9 and 11.7% increase in NP, respectively, in comparison to the nutrient-enriched compost. Similarly, bioactive compost–treated tomatoes showed a 24.7 and 18.5% increase in NP contents than the simple compost and approximately 13.2% than the nutrient-enriched compost (**Tables 6**, **7**).

Effect on Soil Enzymatic Activity

In the chilies' and tomatoes' microplot experiments, both alkaline phosphatase activity and dehydrogenase activity of soil treated with bioactive compost were significantly higher than those of the nutrient-enriched or simple compost. In chilies, post-harvest soil analysis showed an increase of 11–36% in alkaline phosphatase and 18–46% in dehydrogenase activity compared with nutrient-enriched compost and simple composts, respectively (**Table 6**). Similarly, in tomatoes, 17–36% increase in alkaline phosphatase and 15–32% in dehydrogenase activity with bioactive compost as compared to that of nutrient-enriched compost and simple compost, respectively (**Table 7**).

Total Bacterial Population

Analysis of the bacterial population in the rhizosphere from 7 dpi to 90 dpi shows that bacterial count remained the same in the soil, while it increased in the rhizosphere of compost and bioactive compost–treated plants. In soil, bacterial count remained 8.18–8.55, while it was increased from 8.58 to 11.73 and 9.75–12.20 in case of compost and bioactive compost, respectively (**Table 8**).

4 DISCUSSION

Extensive cultivation of staple cereals in response to rising global food demand has brought the consequences in the form of increased agricultural wastes, polluted environment, and nutrient-deprived soils. Moreover, the tunnel farming industry is developing at an exponential rate to fulfill the growing demand for off-season vegetables, fruits, and spices. Tunnel system uses plenty of chemical fertilizers and pesticides; as a result, vegetables/fruits are loaded with chemicals that subsequently cause serious health concerns in human beings. Reliance on chemical fertilizers not only reduces land productivity but also decreases the product quality. The plants grown in this way do not develop good plant characteristics such as good root system, shoot system, and nutritional characters and also will not get time to grow and mature properly. The use of organic fertilizers and biopesticides is highly recommended to improve the quality of soil, and the nutritional value of vegetables and fruits, and to make them suitable for human consumption. This study describes the re-

utilization of organic crop waste for the plant fertilization after composting and enrichment with plant-beneficial bacteria.

Wheat and rice straw were co-composted with nitrogen-rich green plants *Sesbania*, *Trifolium*, and *Azolla*. The purpose of co-composting with N-rich green plants was to decrease the C: N ratio and speed up the composting process. Both wheat and rice straw have high lignocellulosic content (high C: N ratio) which hinders the degradation and delays the composting process (Chen, 2014; Snelders et al., 2014). Nitrogen serves as a limiting factor during composting because it is an essential element for the microbe-driven composting process (Rovshandeh et al., 2007). Therefore, the C: N ratio is a good indicator of nitrogen availability as well as microbial activity. It has also been associated with temperature changes in the compost. In a recent study on wheat straw compost, temperature rise was observed with urea supplementation as compared to the non-supplemented compost. Both high microbial activity and temperature help to attain earlier maturity/stability of the compost (Zhang et al., 2016), but high temperature with high pH may lead to nitrogen loss through ammonia production as well (Diaz and Savage, 2007). Analysis of compost metagenome shows that *Proteobacteria* and *Bacteroidetes* were the most abundant phyla in wheat compost comprising 40% of the sequences, whereas in rice compost, *Proteobacteria*, particularly from class Gammaproteobacteria, were dominant. However, the phyla *Firmicutes*, *Chloroflexi*, *Actinobacteria*, and *Acidobacteria* showed a similar distribution in both compost samples accounting for 1–5% of total sequences. The bacteria from γ-*Proteobacteria*, *Firmicutes*, and *Actinobacteria* are reported to be highly involved in the maturation of composting during the final stage of the process, and their relative abundance is reported as an indicator of disease suppression during the process (Hadar and Papadopoulou, 2012). The *Bacteroidetes* are facultative anaerobic bacteria that are considered important during the initial and final stages of composting. Similarly, the higher abundance of *Bacteroidetes*, *Chloroflexi*, and *Planctomycetes* has been reported in mature compost (Kästner and Miltner, 2016).

Several quality factors are considered important while using compost for soil application (Milinković et al., 2019), which include maturity, nutrient content, electrical conductivity, pH, phytotoxic compounds, and contents of pollutants (Sæbø and Ferrini, 2006). The pH range of compost developed in this study was 6.9–7.5 without the addition of urea, while it was 7.3–7.9 with urea-added during composting, which is within the recommended pH range (6.9–8.3) for the compost (Ameen et al., 2016). Slightly higher pH in urea-supplemented compost indicates the production of ammonia (Haddadin et al., 2009) because high temperature and higher pH are associated to cause N-loss through ammonia volatilization (Diaz and Savage, 2007), but the temperature remained almost the same for both heaps (with or without urea) in this study, so there is a possibility that ammonia is condensed back to the compost due to sheet cover. A substantial increase in EC values (3.36–7.5) was observed in both types of composted materials which is in accordance with already reported results for the composting of wheat straw (Zhang et al., 2016). The moisture content of composting material was maintained at 50–55% which is the optimum level to facilitate the decomposition process by providing oxygen for the microbial activity because it is considered as one of the limiting factors for solid substrate (Pace et al., 1995; Jusoh et al., 2013). Both higher and lower moisture contents cause anaerobic conditions that lead to slower decomposition (Sherman, 1999; Diaz and Savage, 2007). In this study, rice and wheat straw of particle size of <2 cm with green plants of particle size >2 cm resulted in efficient degradation and composting of raw material. Studies have reported that particle size has a direct effect on the composting process and the quality of the final product as well. Calabi–Floody et al. (2018) have evaluated three particle sizes <1, 1–2, and >2 cm with 3 nitrogen doses and 3 fungal charges, and concluded that particle size <1 cm with 0.98 g/kg nitrogen dose and the 14-disc fungal charge is optimal for the good quality compost. Since microbes catalyze the transformation so, the higher surface area of the substrate means higher substrate availability for the microbial process (Agnew and Leonard, 2003). In this study, efficient composting was achieved with a relatively larger particle size possibly due to co-composting with the nitrogen-rich green plants and an additional dose of nitrogen (urea) fertilizer. It is a more convenient and practical approach to use a relatively larger particle size straw for large-scale production of compost rather than grinding to a fine size particle which is a labor-intensive and energy-consuming process. The final size of compost was maintained at 2 mm, which has been recently reported to be the best particle size for the final compost product by Tang et al. (2020).

To enhance the organic benefits, the compost was enriched with the plant-beneficial bacteria and micronutrients. Making the compost biologically active multiplies its agricultural and environmental benefits as the organic and biofertilizers work in synergy (Neugart et al., 2018). The plant-beneficial bacteria are highly active in converting the unavailable forms of nutrients (N, P, Zn, *etc*.) and stimulate the root and shoot growth by producing phytohormones. Organic matter helps in the survival of bacteria in the product as well as in the rhizosphere. The better the survival of bacteria in compost, the higher will be the efficacy of the final product (Siddiq et al., 2018). The present study demonstrates the survival and activity of bacteria up to 180 dpi that is due to high organic matter, wide surface area, and optimal water holding capacity. Moreover, it is easily available and inexpensive for mass production. Siddiq et al. (2018) reported compost as good carrier material for PGPR inoculum with higher physiological activity and long shelf life of inoculated PGPR. Sohaib et al. (2020) further supported this hypothesis that an ideal carrier material should have higher organic matter, surface area, moisture content, and neutral pH, and be favorable for the growth of bacteria along with the fact that it should be easily available and inexpensive. Such carrier material provides a selective advantage to PGPR to survive under stressful conditions. Moisture levels 30–50% have been reported as optimal for a carrier material (Sangeetha and Stella, 2012). Wheat straw compost has been already reported as a carrier material for nitrogen-fixing cyanobacteria (Dhar et al., 2007). SEM analysis of compost showed the survival of microbes as

dispersed cells on the surface and micro-colonies in the grooves. It further showed efficient degradation of lignocellulose and the development of micro-niche for the microbes. It has been reported that grooves on the surface of carrier material provide a microenvironment to the PGPR for the colonization and better performance of a differential physiological activity (Roy et al., 2010). Scanning electron microscopy (SEM) can effectively monitor the microstructures and grooves (Dresbøll and Magid, 2006), and has been used to study the homogeneity, particle size, pore size, maturity, and stability of rice and wheat straw (Arora and Kaur, 2019; Bhattacharyya et al., 2020) for downstream application as a carrier material. The bacterial presence and survival were further validated using FISH, but the detection limit remained low in this study contrary to that reported previously for compost samples (Franke–Whittle et al., 2005). This might be due to the sensitivity of the probe or the fixation and hybridization conditions used for the compost sample in this study which might affect the detection of the selected population. A specific primer set developed against inoculated *P. stutzeri* strain K-1 (Mirza et al., 2006) was used for the PCR-based detection of K-1 at 90 and 180 dpi which shows that the bacterium in the consortium can survive in the compost. The primer specificity has already been reported on other *Pseudomonas* including non-nitrogen fixing strains and other related species (Mirza et al., 2006).

Application of PGPR with rice and wheat straw compost in this study has significantly improved chili and tomato plants' fresh and dry weight, leaf photosynthetic efficiency, and overall yield. Several studies have reported that compost (with or without PGPR) improve the growth, yield, and disease tolerance of chili (Ahmad et al., 2011; Kausar et al., 2014; Nur et al., 2019), and increased soil fertility (Rahman et al., 2012). Similarly, the beneficial impact of compost has been documented on tomatoes (Rasool et al., 2021). Compost or vermiculate compost enriched with a multi-strain consortium or potassium humate have shown salt stress mitigation in wheat (Sohaib et al., 2020), seed germination in barley (El-Akshar et al., 2016), and improved sorghum production (Hameeda et al., 2007). PGPR fortified rice straw compost protected rice from blast disease (Ng et al., 2016), and nitrogen-enriched wheat straw compost carrying PGPR improved nutrient use efficiency and seed quality of sunflower (Arif et al., 2017).

Moreover, total N and P contents of fruits were also increased with the application of different nutrient-enriched compost and bioactive compost. It has been well established that to some extent, PGPR and the compost can be used as alternatives to NPK fertilizers because they can enrich the soil with these nutrients (Sarwar et al., 2018; Laslo and Mara, 2019). PGPR colonize the roots and assist the plant in the uptake of NPK (García et al., 2004); that is why a prominent increase in the growth, yield, and nutrient content in tomatoes and chilies was observed with bioactive compost. But the bacterial population and their affinity with the plant roots are itself dependent on several factors including properties of soil, nature of root exudates, and quorum-sensing signaling molecules (Brimecombe et al., 2000; Nawaz et al., 2020). Compost has been also reported to increase the population of beneficial microbes in the soil and rhizosphere (Arancon et al., 2006). Similarly, in this study, total bacterial population in the rhizosphere was increased with the compost compared to that of the soil. This clearly shows that the organic product has supported the bacterial activity in the rhizosphere which was then resulted in the form of better plant growth and yield.

Post-harvest soil enzymatic analysis of tomato and chili rhizosphere soil showed a significant increase in soil alkane phosphatase and dehydrogenase activities. Compost dehydrogenase and alkaline phosphate activity is a measure of microbial activity and maturity (Gaind and Nain, 2010). Soil dehydrogenase activity indicates microbial activity (Salazar et al., 2011), while soil alkaline phosphate activity, on the other hand, is used as a measure of soil richness along with the microbial activity (Versaw and Harrison, 2002). It has been reported previously that the rice straw compost showed a significant increase in soil alkaline phosphatase and dehydrogenase activities with rice yield comparable to the inorganic fertilizer (Goyal et al., 2009). A significant increase in the activity of both enzymes with reduced plant uptake for heavy metals Cd and Zn by rice straw compost has been reported (Tang et al., 2020) mainly due to EC and available potassium content. Long-term application of wheat straw compost enhances soil enzyme activity, reduces the availability of heavy metals Cu and Cd (Xie et al., 2009), and improves the growth of maize, wheat, soybean, pearl millet, and sorghum (Liu et al., 2010).

4.1 Cost Benefit Analysis and Policy Recommendations

The cost of tomatoes grown in the tunnel is 56% higher than that of those grown without the tunnel (Khan and Khan, 2020); due to higher inputs (costs of seeds, fertilizers, pesticides, irrigation, and labor), the benefit–cost (B/C) ratio is, however, high, that is, 2.29 for tomatoes grown with tunnel compared to tomatoes grown without tunnel, where the B/C ratio is 1.48. Fertilizers are the major input cost to any crop grown, and changing their prices changes the overall economics of any crop. This study recommends the use of bioactive compost (BAC) without any additional chemical fertilizer, thus further reducing the input cost with a simultaneous increase in yield which further guarantees an even higher B/C ratio for the tunnel system as well as the simple field. In tomato and chili, it is recommended to use 100 Kg BAC per acer of the tunnel and mix before forming beds. It is further recommended that in cereals or other crops which require higher fertilizer inputs, BAC at 100 Kg per acer should be mixed during the field preparation with concomitant decrease in the chemical fertilizers applied during field preparation or seed sowing. This may be followed by the 50% use of the recommended second or third chemical fertilizer dose application as well. The overall outcome will be a lesser chemical input and higher yield returns with low chemical residues in the fruits and seeds.

5 CONCLUSION

Application of enriched organic fertilizers and bioactive compost to infertile agricultural lands could have enormous benefits both environmentally and economically. The present study

demonstrates the plant-beneficial impact of bioactive compost and suggests using this bioactive compost in the organic farming of tomatoes and chilies, both in the tunnel and in the field yielding high VCR for both crops. The conversion of farm waste into compost is an effective approach to manage rapidly increasing farms waste. Enrichment of compost with beneficial bacteria will further improve its efficacy and enhance the impact as demonstrated in the present study.

DATA AVAILABILITY STATEMENT

The datasets presented in this study can be found in online repositories. Compost metagenome data can be retrieved from NCBI database through Bio-Project PRJNA773634 while the 16SrRNA data is available under accession nos. HE662867, HE661626, AJ278107.

AUTHOR CONTRIBUTIONS

AI conceived, planned and executed the study, analyzed the data, and finalized the manuscript; FS and ZK did lab and plant experiments as part of their MPhil research work; MSN wrote the first draft and carried out statistical analysis; AS did the pot experiments; MA helped in pot experiment; SY helped in the FISH analysis; SH and BSM helped in metagenomic analysis; FM helped in compost development; and MSM supervised the studies. All authors approved the final version of the manuscript.

FUNDING

The research was carried out by the support funds provided by Higher Education Commission under HEC-NRPU Project 3814 (Year 2016–2019).

ACKNOWLEDGMENTS

The authors are thankful to AARI, Faislabad, for helping in providing the chili and tomato nurseries for compost testing and Dr. Ayesha Ehsan for SEM analysis.

SUPPLEMENTARY MATERIAL

The Supplementary Material for this article can be found online at: https://www.frontiersin.org/articles/10.3389/fbioe.2021.787764/full#supplementary-material

REFERENCES

Abbas, M., Atiq-Ur-Rahman, M., Manzoor, F., and Farooq, A. (2012). A Quantitative Analysis and Comparison of Nitrogen, Potassium and Phosphorus in rice Husk and Wheat Bran Samples. *Pab* 1, 14–15. doi:10.19045/bspab.2012.11003

Agnew, J. M., and Leonard, J. J. (2003). The Physical Properties of Compost. *Compost. Sci. Utilization* 11, 238–264. doi:10.1080/1065657x.2003.10702132

Ahmad, I., Hussain, Z., Raza, S., Memon, N., and Naqvi, S. A. (2011). Response of Vegetative and Reproductive Components of Chili to Inorganic and Organic Mulches. *Pakistan J. Agric. Sci.* 48, 19–24.

Akhtar, M. J., Asghar, H. N., Shahzad, K., and Arshad, M. (2009). Role of Plant Growth Promoting Rhizobacteria Applied in Combination with Compost and mineral Fertilizers to Improve Growth and Yield of Wheat (*Triticum aestivum* L.). *Pakistan J. Bot.* 41, 381–390.

Alexander, M. (1965). Most-probable-number Method for Microbial Populations. *Methods Soil Anal. Part 2 Chem. Microbiol. Properties* 9, 1467–1472.

Altaf, M. A., Hussain, M., Ali, M., Ahmad, S. S., Hussain, A., Ali, A., et al. (2014). Significance of Carrier Material for the Inoculation of Microbes in Legumes. *Int. J. Econ. Plants* 1, 56–64.

Amann, R. I., Krumholz, L., and Stahl, D. A. (1990). Fluorescent-oligonucleotide Probing of Whole Cells for Determinative, Phylogenetic, and Environmental Studies in Microbiology. *J. Bacteriol.* 172, 762–770. doi:10.1128/jb.172.2.762-770.1990

Amann, R. I., Ludwig, W., and Schleifer, K. H. (1995). Phylogenetic Identification and *In Situ* Detection of Individual Microbial Cells without Cultivation. *Microbiol. Rev.* 59, 143–169. doi:10.1128/mr.59.1.143-169.1995

Ameen, A., Ahmad, J., Munir, N., and Raza, S. (2016). Physical and Chemical Analysis of Compost to Check its Maturity and Stability. *Eur. J. Pharm. Med. Res.* 1, 84–87.

Andini, A., Bonnet, S., Rousset, P., and Hasanudin, U. (2018). Impact of Open Burning of Crop Residues on Air Pollution and Climate Change in Indonesia.

Arancon, N. Q., Edwards, C. A., and Bierman, P. (2006). Influences of Vermicomposts on Field Strawberries: Part 2. Effects on Soil Microbiological and Chemical Properties. *Bioresour. Tech.* 97, 831–840. doi:10.1016/j.biortech.2005.04.016

Arif, M. S., Shahzad, S. M., Riaz, M., Yasmeen, T., Shahzad, T., Akhtar, M. J., et al. (2017). Nitrogen-enriched Compost Application Combined with Plant Growth-promoting Rhizobacteria (PGPR) Improves Seed Quality and Nutrient Use Efficiency of sunflower. *J. Plant Nutr. Soil Sci.* 180, 464–473. doi:10.1002/jpln.201600615

Armon, D. (1949). Copper Enzymes in Isolated Chloroplast. *Plant Physiol.* 24, 1–15.

Arora, M., and Kaur, A. (2019). Scanning Electron Microscopy for Analysing Maturity of Compost/vermicompost from Crop Residue Spiked with Cattle Dung, Azolla Pinnata and Aspergillus terreus. *Environ. Sci. Pollut. Res.* 26, 1761–1769. doi:10.1007/s11356-018-3673-8

Bertaux, J., Gloger, U., Schmid, M., Hartmann, A., and Scheu, S. (2007). Routine Fluorescence *In Situ* Hybridization in Soil. *J. Microbiol. Methods* 69, 451–460. doi:10.1016/j.mimet.2007.02.012

Bhattacharjya, S., Sahu, A., Phalke, D. H., Manna, M. C., Thakur, J. K., Mandal, A., et al. (2021). *In Situ* decomposition of Crop Residues Using Lignocellulolytic Microbial Consortia: a Viable Alternative to Residue Burning. *Environ. Sci. Pollut. Res. Int.*, 1–18. doi:10.1007/s11356-021-12611-8

Bhattacharyya, P., Bhaduri, D., Adak, T., Munda, S., Satapathy, B. S., Dash, P. K., et al. (2020). Characterization of rice Straw from Major Cultivars for Best Alternative Industrial Uses to Cutoff the Menace of Straw Burning. *Ind. Crops Prod.* 143, 111919. doi:10.1016/j.indcrop.2019.111919

Brimecombe, M. J., De Leij, F. A., and Lynch, J. M. (2000). "The Effect of Root Exudates on Rhizosphere Microbial Populations," in *The Rhizosphere* (Florida, United States: CRC Press), 111–156.

Calabi-Floody, M., Medina, J., Rumpel, C., Condron, L. M., Hernandez, M., Dumont, M., et al. (2018). "Smart Fertilizers as a Strategy for Sustainable Agriculture," in *Advances in Agronomy* (Elsevier), 119–157. doi:10.1016/bs.agron.2017.10.003

Calabi-Floody, M., Medina, J., Suazo, J., Ordiqueo, M., Aponte, H., Mora, M. d. L. L., et al. (2019). Optimization of Wheat Straw Co-composting for Carrier Material Development. *Waste Manag.* 98, 37–49. doi:10.1016/j.wasman.2019.07.041

Chen, H. (2014). "Chemical Composition and Structure of Natural Lignocellulose," in *Biotechnology of Lignocellulose* (Springer), 25–71. doi:10.1007/978-94-007-6898-7_2

Das, K., Medhi, D., and Guha, B. (2003). Application of Crop Residues in Combination with Chemical Fertilizers for Sustainable Productivity in rice (Oryza Sativa)-Wheat (*Triticum aestivum*) System. *Indian J. Agron.* 48, 8–11.

Dhar, D. W., Prasanna, R., and Singh, B. V. (2007). Comparative Performance of Three Carrier Based Blue green Algal Biofertilizers for Sustainable rice Cultivation. *J. Sustain. Agric.* 30, 41–50. doi:10.1300/j064v30n02_06

Diaz, L., and Savage, G. (2007). Factors that Affect the Process. *Compost. Science Technology* 1.

Dobermann, A., and Fairhurst, T. (2002). Rice Straw Management. *Better Crops Int.* 16, 7–11.

Dresbøll, D. B., and Magid, J. (2006). Structural Changes of Plant Residues during Decomposition in a Compost Environment. *Bioresour. Tech.* 97, 973–981.

El-Akshar, Y., Hasanin, M. S., Mahmoud, Y., Mohamed, A., Afifi, M., and Ismail, F. S. (2016). Determine Improve Nutrient Digestibility by *In-Vitro* Rumen Method of Germination Barley Seeds on rice Straw as Agriculture media after Additive Different Levels of Potassium Humate, Compost tea and Plant Growth Promoting (PGPR). *Afr. J. Agric. Sci. Tech.* 4, 549–562.

Fao, I., and Unicef, W. (2017). *The State of Food Security and Nutrition in the World 2017. Building Resilience for Peace and Food Security*. Rome: FAO.

Franke-Whittle, I. H., Klammer, S. H., and Insam, H. (2005). Design and Application of an Oligonucleotide Microarray for the Investigation of Compost Microbial Communities. *J. Microbiol. Methods* 62, 37–56. doi:10.1016/j.mimet.2005.01.008

Gaind, S., and Nain, L. (2010). Exploration of Composted Cereal Waste and Poultry Manure for Soil Restoration. *Bioresour. Technol.* 101, 2996–3003. doi:10.1016/j.biortech.2009.12.016

García, J. a. L., Probanza, A., Ramos, B., Palomino, M., and Mañero, F. J. G. (2004). Effect of Inoculation of Bacillus Licheniformis on Tomato and Pepper. *Agronomie* 24, 169–176.

Gordon, S. A., and Weber, R. P. (1951). Colorimetric Estimation of Indoleacetic Acid. *Plant Physiol.* 26, 192–195. doi:10.1104/pp.26.1.192

Goyal, S., Singh, D., Suneja, S., and Kapoor, K. (2009). Effect of rice Straw Compost on Soil Microbiological Properties and Yield of rice. *Indian J. Agric. Res.* 43, 263–268.

Gupta, R. K., Yadvinder-Singh, J., Ladha, J. K., Bijay-Singh, G., Singh, J., Singh, G., et al. (2007). Yield and Phosphorus Transformations in a Rice-Wheat System with Crop Residue and Phosphorus Management. *Soil Sci. Soc. Am. J.* 71, 1500–1507. doi:10.2136/sssaj2006.0325

Hadar, Y., and Papadopoulou, K. K. (2012). Suppressive Composts: Microbial Ecology Links between Abiotic Environments and Healthy Plants. *Annu. Rev. Phytopathol.* 50, 133–153. doi:10.1146/annurev-phyto-081211-172914

Haddadin, M. S. Y., Haddadin, J., Arabiyat, O. I., and Hattar, B. (2009). Biological Conversion of Olive Pomace into Compost by Using *Trichoderma harzianum* and *Phanerochaete Chrysosporium*. *Bioresour. Technol.* 100, 4773–4782. doi:10.1016/j.biortech.2009.04.047

Hakim, S., Mirza, B. S., Imran, A., Zaheer, A., Yasmin, S., Mubeen, F., et al. (2020). Illumina Sequencing of 16S *rRNA* Tag Shows Disparity in Rhizobial and Non-rhizobial Diversity Associated with Root Nodules of Mung Bean (*Vigna Radiata* L.) Growing in Different Habitats in Pakistan. *Microbiol. Res.* 231, 126356. doi:10.1016/j.micres.2019.126356

Hameeda, B., Harini, G., Rupela, O. P., and Reddy, G. (2007). Effect of Composts or Vermicomposts on Sorghum Growth and Mycorrhizal Colonization. *Afr. J. Biotechnol.* 6 (1), 9–12.

Hanif, M. K., Hameed, S., Imran, A., Naqqash, T., Shahid, M., and Van Elsas, J. D. (2015). Isolation and Characterization of a Î²-Propeller Gene Containing Phosphobacterium Bacillus Subtilis Strain KPS-11 for Growth Promotion of Potato (Solanum tuberosum L.). *Front. Microbiol.* 06, 583. doi:10.3389/fmicb.2015.00583

Imran, A., Hakim, S., Tariq, M., Nawaz, M. S., Laraib, I., Gulzar, U., et al. (2021). Diazotrophs for Lowering Nitrogen Pollution Crises: Looking Deep Into the Roots. *Front. Microbiol.* 12, 637815. doi:10.3389/fmicb.2021.637815

Jusoh, M. L. C., Manaf, L. A., and Latiff, P. A. (2013). Composting of rice Straw with Effective Microorganisms (EM) and its Influence on Compost Quality. *J. Environ. Health Sci. Engineer* 10, 17. doi:10.1186/1735-2746-10-17

Kanwal, S., Ilyas, N., Batool, N., and Arshad, M. (2017). Amelioration of Drought Stress in Wheat by Combined Application of PGPR, Compost, and mineral Fertilizer. *J. Plant Nutr.* 40, 1250–1260. doi:10.1080/01904167.2016.1263322

Kästner, M., and Miltner, A. (2016). Application of Compost for Effective Bioremediation of Organic Contaminants and Pollutants in Soil. *Appl. Microbiol. Biotechnol.* 100, 3433–3449.

Kaur, M., Kaur, S., Devi, R., and Kapoor, S. (2019). Wheat Straw and maize Stalks Based Compost for Cultivation of Agaricus Bisporus.

Kausar, H., Razi Ismail, M., Saud, H. M., Othman, R., Habib, S. H., and Siddiqui, Y. (2014). Bio-efficacy of Microbial Infused rice Straw Compost on Plant Growth Promotion and Induction of Disease Resistance in Chili. *Compost. Sci. Utilization* 22, 1–10. doi:10.1080/1065657x.2013.870942

Keeney, D., and Nelson, D. (1982). "Nitrogen-inorganic Forms in Methods of Soil Analysis, Part 2. Chemical and Microbiological Properties," in *SSSA Book Series No 9* (Madison, WI: Soil Science Society of America and American Society of Agronomy), 643–693.

Khan, M. B., and Khan, J. (2020). An Economic Analysis of Tunnel Farming in Enhancing Productivity of Off-Season Vegetables in District Peshawar. *Sarhad J. Agric.* 36 (1), 153–160.

Klein, D. A., Loh, T. C., and Goulding, R. L. (1971). A Rapid Procedure to Evaluate the Dehydrogenase Activity of Soils Low in Organic Matter. *Soil Biol. Biochem.* 3, 385–387. doi:10.1016/0038-0717(71)90049-6

Kramer, M., and Yerdei, G. (1959). Application of the Method of Phosphatase Activity Determination in Agricultural Chemistry. *Soviet Soil Sci.* 9, 1100–1103.

Laslo, É., and Mara, G. (2019). Is PGPR an Alternative for NPK Fertilizers in Sustainable Agriculture? *Microbial Interventions in Agriculture and Environment* (Springer), 51–62. doi:10.1007/978-981-13-8391-5_3

Li, W., Zhang, F., Cui, G., Wang, Y., Yang, J., Cheng, H., et al. (2021). Effects of Bio-Organic Fertilizer on Soil Fertility, Microbial Community Composition, and Potato Growth. *ScienceAsia* 47, 347–356. doi:10.2306/scienceasia1513-1874.2021.039

Liang, S., Li, X., and Wang, J. (2012). "Land Cover and Land Use Changes," in *Advanced Remote Sensing: Terrestrial Information Extraction and Applications*.

Liu, E., Yan, C., Mei, X., He, W., Bing, S. H., Ding, L., et al. (2010). Long-term Effect of Chemical Fertilizer, Straw, and Manure on Soil Chemical and Biological Properties in Northwest China. *Geoderma* 158, 173–180. doi:10.1016/j.geoderma.2010.04.029

Liu, J., Xu, X.-H., Li, H.-T., and Xu, Y. (2011). Effect of Microbiological Inocula on Chemical and Physical Properties and Microbial Community of Cow Manure Compost. *Biomass and bioenergy* 35, 3433–3439. doi:10.1016/j.biombioe.2011.03.042

Mahdi, S. S., Hassan, G., Samoon, S., Rather, H., Dar, S. A., and Zehra, B. (2010). Bio-fertilizers in Organic Agriculture. *J. Phytology*.

Majeed, A., Kaleem Abbasi, M., Hameed, S., Yasmin, S., Hanif, M. K., Naqqash, T., et al. (2018). Pseudomonas Sp. AF-54 Containing Multiple Plant Beneficial Traits Acts as Growth Enhancer of Helianthus Annuus L. Under Reduced Fertilizer Input. *Microbiol. Res.* 216, 56–69. doi:10.1016/j.micres.2018.08.006

Milinković, M., Lalević, B., Jovičić-Petrović, J., Golubović-Ćurguz, V., Kljujev, I., and Raičević, V. (2019). Biopotential of Compost and Compost Products Derived from Horticultural Waste—Effect on Plant Growth and Plant Pathogens' Suppression. *Process Saf. Environ. Prot.* 121, 299–306.

Mirza, M. S., Mehnaz, S., Normand, P., Prigent-Combaret, C., Moënne-Loccoz, Y., Bally, R., et al. (2006). Molecular Characterization and PCR Detection of a Nitrogen-Fixing Pseudomonas Strain Promoting rice Growth. *Biol. Fertil. Soils* 43, 163–170. doi:10.1007/s00374-006-0074-9

Mislivec, P. B., and Bruce, V. R. (1977). Direct Plating versus Dilution Plating in Qualitatively Determining the Mold flora of Dried Beans and Soybeans. *Journal-Association Official Anal. Chemists* 60, 741–743. doi:10.1093/jaoac/60.3.741

Nadeem, S. M., Imran, M., Naveed, M., Khan, M. Y., Ahmad, M., Zahir, Z. A., et al. (2017). Synergistic Use of Biochar, Compost and Plant Growth-Promoting Rhizobacteria for Enhancing Cucumber Growth under Water Deficit Conditions. *J. Sci. Food Agric.* 97, 5139–5145. doi:10.1002/jsfa.8393

Nawaz, M. S., Arshad, A., Rajput, L., Fatima, K., Ullah, S., Ahmad, M., et al. (2020). Growth-stimulatory Effect of Quorum Sensing Signal Molecule N-Acyl-Homoserine Lactone-Producing Multi-Trait Aeromonas Spp. On Wheat Genotypes under Salt Stress. *Front. Microbiol.* 11, 553621. doi:10.3389/fmicb.2020.553621

Neugart, S., Wiesner-Reinhold, M., Frede, K., Jander, E., Homann, T., Rawel, H. M., et al. (2018). Effect of Solid Biological Waste Compost on the Metabolite Profile of *Brassica rapa* ssp. chinensis. *Front. Plant Sci.* 9, 305. doi:10.3389/fpls.2018.00305

Ng, L. C., Sariah, M., Radziah, O., Zainal Abidin, M. A., and Sariam, O. (2016). Development of Microbial-Fortified rice Straw Compost to Improve Plant Growth, Productivity, Soil Health, and rice Blast Disease Management of Aerobic rice. *Compost. Sci. Utilization* 24, 86–97. doi:10.1080/1065657x.2015.1076750

Nur, H., Sugeng, P., and Nurul, A. (2019). The Effect of Compost Combined with Phosphate Solubilizing Bacteria and Nitrogen-Fixing Bacteria for Increasing the Growth and Yield of Chili Plants. *Russ. J. Agric. Socio-Economic Sci.* 92.

Pace, M. G., Miller, B. E., and Farrell-Poe, K. L. (1995). The Composting Process.

Pikovskaya, R. (1948). Mobilization of Phosphorus in Soil in Connection with the Vital Activity of Some Microbial Species.

Qu, P., Huang, H., Zhao, Y., and Wu, G. (2017). Physicochemical Changes in rice Straw after Composting and its Effect on rice-straw-based Composites. *J. Appl. Polym. Sci.* 134. doi:10.1002/app.44878

Rahman, M. A., Rahman, M. M., Begum, M., and Alam, M. F. (2012). Effect of Bio Compost, Cow Dung Compost and NPK Fertilizers on Growth, Yield and Yield Components of Chilli. *Int. J. Biosci.* 2, 51–55.

Rasool, M., Akhter, A., Soja, G., and Haider, M. S. (2021). Role of Biochar, Compost and Plant Growth Promoting Rhizobacteria in the Management of Tomato Early Blight Disease. *Sci. Rep.* 11, 6092. doi:10.1038/s41598-021-85633-4

Roca-Pérez, L., Martínez, C., Marcilla, P., and Boluda, R. (2009). Composting rice Straw with Sewage Sludge and Compost Effects on the Soil–Plant System. *Chemosphere* 75, 781–787.

Romasanta, R. R., Sander, B. O., Gaihre, Y. K., Alberto, M. C., Gummert, M., Quilty, J., et al. (2017). How Does Burning of rice Straw Affect CH 4 and N 2 O Emissions? A Comparative experiment of Different On-Field Straw Management Practices. *Agric. Ecosyst. Environ.* 239, 143–153. doi:10.1016/j.agee.2016.12.042

Rovshandeh, J., Esmaieli, M., Charani, P., and Ardeh, S. (2007). Effect of mineral Components and of white Rot Fungus on the Composting Process of Mixed Hardwood Barks. *Cellulose Chem. Tech.* 41, 451.

Roy, D., Deb, B., and Sharma, G. (2010). Evaluation of Carrier Based Inoculants of Azotobacter Chroococcum Strain SDSA-12/2 in Improving Growth and Yield Summer (Ahu) rice Cv. *Ir-36. Biofrontiers* 1, 36–40.

Sæbø, A., and Ferrini, F. (2006). The Use of Compost in Urban green Areas–A Review for Practical Application. *Urban For. Urban Green.* 4, 159–169.

Sajjad Mirza, M., Ahmad, W., Latif, F., Haurat, J., Bally, R., Normand, P., et al. (2001). Isolation, Partial Characterization, and the Effect of Plant Growth-Promoting Bacteria (PGPB) on Micro-propagated Sugarcane *In Vitro*. *Plant and Soil* 237, 47–54. doi:10.1023/a:1013388619231

Salazar, S., Sánchez, L. E., Alvarez, J., Valverde, A., Galindo, P., Igual, J. M., et al. (2011). Correlation Among Soil Enzyme Activities under Different forest System Management Practices. *Ecol. Eng.* 37, 1123–1131. doi:10.1016/j.ecoleng.2011.02.007

Sangeetha, D., and Stella, D. (2012). Survival of Plant Growth Promoting Bacterial Inoculants in Different Carrier Materials. *Int. J. Pharm. Biol. Arch.* 3, 170–178.

Sarwar, M., Patra, J. K., and Jihui, B. (2018). Comparative Effects of Compost and NPK Fertilizer on Vegetative Growth, Protein, and Carbohydrate of *Moringa Oleifera* Lam Hybrid PKM-1. *J. Plant Nutr.* 41, 1587–1596. doi:10.1080/01904167.2018.1462385

Schloss, P. D., Westcott, S. L., Ryabin, T., Hall, J. R., Hartmann, M., Hollister, E. B., et al. (2009). Introducing Mothur: Open-Source, Platform-independent, Community-Supported Software for Describing and Comparing Microbial Communities. *Appl. Environ. Microbiol.* 75, 7537–7541. doi:10.1128/aem.01541-09

Schollenberger, C. J. (1945). Determination of Soil Organic Matter. *Soil Sci.* 59, 53–56. doi:10.1097/00010694-194501000-00008

Shahbandeh, M. (2021). Vegetables Production Worldwide by Type 2019. [Online]. Statista. Available: https://www.statista.com/statistics/264065/global-production-of-vegetables-by-type/(Accessed September 22, 2021).

Sharma, S., Singh, P., Choudhary, O. P., and Neemisha, fnm. (2021). Nitrogen and rice Straw Incorporation Impact Nitrogen Use Efficiency, Soil Nitrogen Pools and Enzyme Activity in rice-wheat System in north-western India. *Field Crops Res.* 266, 108131. doi:10.1016/j.fcr.2021.108131

Sherman, R. (1999). *Large-scale Organic Materials Composting*. NC Cooperative Extension Service.

Siddiq, S., Usman Saleem, K. A., Anayat, A., Affan, Q. M., Anwar, M. F., Nazir, H., et al. (2018). Comparison of Conventional and Non-conventional Carriers for Bacterial Survival and Plant Growth. *Int. J. Agric. Innov. Res.* 6, 4.

Snelders, J., Dornez, E., Benjelloun-Mlayah, B., Huijgen, W. J. J., De Wild, P. J., Gosselink, R. J. A., et al. (2014). Biorefining of Wheat Straw Using an Acetic and Formic Acid Based Organosolv Fractionation Process. *Bioresour. Technol.* 156, 275–282. doi:10.1016/j.biortech.2014.01.069

Sohaib, M., Zahir, Z. A., Khan, M. Y., Ans, M., Asghar, H. N., Yasin, S., et al. (2020). Comparative Evaluation of Different Carrier-Based Multi-Strain Bacterial Formulations to Mitigate the Salt Stress in Wheat. *Saudi J. Biol. Sci.* 27, 777–787. doi:10.1016/j.sjbs.2019.12.034

Somasegaran, P., and Hoben, H. J. (1994). "Counting Rhizobia by a Plant Infection Method," in *Handbook for Rhizobia* (Springer), 58–64. doi:10.1007/978-1-4613-8375-8_6

Sparks, D. L., Page, A., Helmke, P., and Loeppert, R. H. (2020). *Methods of Soil Analysis, Part 3: Chemical Methods*. John Wiley & Sons.

Stein, S., Selesi, D., Schilling, R., Pattis, I., Schmid, M., and Hartmann, A. (2005). Microbial Activity and Bacterial Composition of H2-Treated Soils with Net CO2 Fixation. *Soil Biol. Biochem.* 37, 1938–1945. doi:10.1016/j.soilbio.2005.02.035

Tahir, M., Arshad, M., Naveed, M., Zahir, Z., Shaharoona, B., and Ahmad, R. (2006). Enrichment of Recycled Organic Waste with N Fertilizer and PGPR Containing ACC-Deaminase for Improving Growth and Yield of Tomato. *Soil Environ.* 25, 105–112.

Tang, J., Zhang, L., Zhang, J., Ren, L., Zhou, Y., Zheng, Y., et al. (2020). Physicochemical Features, Metal Availability and Enzyme Activity in Heavy Metal-Polluted Soil Remediated by Biochar and Compost. *Sci. Total Environ.* 701, 134751. doi:10.1016/j.scitotenv.2019.134751

Twine, J. R., and Williams, C. H. (1971). The Determination of Phosphorus in Kjeldahl Digests of Plant Material by Automatic Analysis. *Commun. Soil Sci. Plant Anal.* 2, 485–489. doi:10.1080/00103627109366341

Udeigwe, T. K., Teboh, J. M., Eze, P. N., Hashem Stietiya, M., Kumar, V., Hendrix, J., et al. (2015). Implications of Leading Crop Production Practices on Environmental Quality and Human Health. *J. Environ. Manag.* 151, 267–279. doi:10.1016/j.jenvman.2014.11.024

UNDP, 2021; The Sdgs In Action. Available at: https://www.undp.org/sustainable-development-goals?utm_source=EN&utm_medium =GSR&utm_content=US_UNDP_PaidSearch_Brand_English&utm_campaign=CENTRAL&c_src=CENTRAL&c_src2=GSR&gclid=CjwKCAjwiY6MBhBqEiwARFSCPnnwFIlLSdqrSYX2Ls312A8-VEXwh_HZwxS9VMjim7hu4H5Q1b8ymRoCntkQAvD_BwE

Versaw, W. K., and Harrison, M. J. (2002). A Chloroplast Phosphate Transporter, PHT2;1, Influences Allocation of Phosphate within the Plant and Phosphate-Starvation Responses. *Plant Cell* 14, 1751–1766. doi:10.1105/tpc.002220

Whitbread, A., Blair, G., Konboon, Y., Lefroy, R., and Naklang, K. (2003). Managing Crop Residues, Fertilizers and Leaf Litters to Improve Soil C, Nutrient Balances, and the Grain Yield of rice and Wheat Cropping Systems in Thailand and Australia. *Agric. Ecosyst. Environ.* 100, 251–263. doi:10.1016/s0167-8809(03)00189-0

Xie, W., Zhou, J., Wang, H., Chen, X., Lu, Z., Yu, J., et al. (2009). Short-term Effects of Copper, Cadmium and Cypermethrin on Dehydrogenase Activity and Microbial Functional Diversity in Soils after Long-Term mineral or Organic Fertilization. *Agric. Ecosyst. Environ.* 129, 450–456. doi:10.1016/j.agee.2008.10.021

Ye, L., Zhao, X., Bao, E., Li, J., Zou, Z., and Cao, K. (2020). Bio-organic Fertilizer with Reduced Rates of Chemical Fertilization Improves Soil Fertility and Enhances Tomato Yield and Quality. *Sci. Rep.* 10 (1), 177. doi:10.1038/s41598-019-56954-2

Yoshida, S., Forno, D. A., and Cock, J. H. (1976). *Laboratory Manual for Physiological Studies of rice*. 3rd Ed. Manila, Philippines: Laboratory manual for physiological studies of rice.

Zewail, R., and Ahmed, H. (2015). Effect of Some Biofertilizers (PGPR, Biosoal and Compost tea) on Growth, Yield, Fiber Quality and Yarn Properties of Egyptian cotton.(Promising Hybrid 10229xg86). *Agric. Res. Cent. Giza, Egypt. Annal Agric. Sci., Moshtohor* 53, 199–210.

Zhang, L., Jia, Y., Zhang, X., Feng, X., Wu, J., Wang, L., and Chen, G. (2016). Wheat straw: an inefficient substrate for rapid natural lignocellulosic composting. *Bioresource technology* 209, 402–406. doi:10.1016/j.biortech.2016.03.004

Conflict of Interest: The authors declare that the research was conducted in the absence of any commercial or financial relationships that could be construed as a potential conflict of interest.

Publisher's Note: All claims expressed in this article are solely those of the authors and do not necessarily represent those of their affiliated organizations, or those of the publisher, the editors, and the reviewers. Any product that may be evaluated in this article, or claim that may be made by its manufacturer, is not guaranteed or endorsed by the publisher.

frontiers in Bioengineering and Biotechnology

REVIEW
published: 27 January 2022
doi: 10.3389/fbioe.2021.802543

Biological Approaches for Extraction of Bioactive Compounds From Agro-industrial By-products: A Review

Ailton Cesar Lemes[1], Mariana Buranelo Egea[2], Josemar Gonçalves de Oliveira Filho[3], Gabrielle Victoria Gautério[1], Bernardo Dias Ribeiro[1] and Maria Alice Zarur Coelho[1]**

[1]Department of Biochemical Engineering, School of Chemistry, Federal University of Rio de Janeiro (UFRJ), Rio de Janeiro, Brazil, [2]Goiano Federal Institute, Rio Verde, Brazil, [3]School of Pharmaceutical Sciences, São Paulo State University (UNESP), Araraquara, Brazil

Bioactive compounds can provide health benefits beyond the nutritional value and are originally present or added to food matrices. However, because they are part of the food matrices, most bioactive compounds remain in agroindustrial by-products. Agro-industrial by-products are generated in large quantities throughout the food production chain and can—when not properly treated—affect the environment, the profit, and the proper and nutritional distribution of food to people. Thus, it is important to adopt processes that increase the use of these agroindustrial by-products, including biological approaches, which can enhance the extraction and obtention of bioactive compounds, which enables their application in food and pharmaceutical industries. Biological processes have several advantages compared to nonbiological processes, including the provision of extracts with high quality and bioactivity, as well as extracts that present low toxicity and environmental impact. Among biological approaches, extraction from enzymes and fermentation stand out as tools for obtaining bioactive compounds from various agro-industrial wastes. In this sense, this article provides an overview of the main bioactive components found in agroindustrial by-products and the biological strategies for their extraction. We also provide information to enhance the use of these bioactive compounds, especially for the food and pharmaceutical industries.

Keywords: enzyme extraction, fermentation, health benefits, bioactivities, agroindustrial

OPEN ACCESS

Edited by:
Jun Xia,
Huaiyin Normal University, China

Reviewed by:
Haixia Chen,
Tianjin University, China
Amir Mahboubi Soufiani,
University of Boras, Sweden

****Correspondence:***
Ailton Cesar Lemes
ailtonlemes@eq.ufrj.br
Maria Alice Zarur Coelho
alice@eq.ufrj.br

Specialty section:
This article was submitted to Bioprocess Engineering, a section of the journal Frontiers in Bioengineering and Biotechnology

Received: *26 October 2021*
Accepted: *14 December 2021*
Published: *27 January 2022*

Citation:
Lemes AC, Egea MB, Oliveira Filho JGd, Gautério GV, Ribeiro BD and Coelho MAZ (2022) Biological Approaches for Extraction of Bioactive Compounds From Agro-industrial By-products: A Review. Front. Bioeng. Biotechnol. 9:802543. doi: 10.3389/fbioe.2021.802543

1 INTRODUCTION

The world produces large amounts of agroindustrial raw materials, mainly used for human and animal consumption and energy production (FAO, 2017; Sadh et al., 2018a). However, losses of up to 50% of the raw materials are estimated and occur mainly during harvest, post-harvest, slaughter, transport, processing, storage, and consumption (Arah et al., 2016; Lemes et al., 2020a). The losses can represent about 680 billion dollars per year (Dora et al., 2020) and correspond to about 25%–35% of the food produced in the world. These losses of raw material can be equivalent to 1.3 billion tons a year of material that is no longer consumed or transformed from appropriate processes (Ishangulyyev et al., 2019).

Due to its composition, residues can show slow degradability, resulting in accumulation and negative environmental impact (Sadh et al., 2018a). Thus, it is relevant to identify new applications to convert these residues into high-value-added products (Irmak, 2017). In general, agro-industrial

residues present considerable concentrations of compounds such as fibers, lipids, carbohydrates, peptides, carotenoids, phenolic compounds, and other compounds, which have multiple functionalities and bioactivities and can be applied as ingredients in other products (Varzakas et al., 2016; Coman et al., 2020; Lopes and Ligabue-Braun, 2021).

The bioactive compounds present in the residue matrices can be potentially used in the prevention and treatment of several diseases, such as hypertension (Oliveira Filho et al., 2020), diabetes (Valencia-Mejía et al., 2019), cardiovascular disease (Rangel-Huerta et al., 2015), and neurological disease (Mohd Sairazi and Sirajudeen, 2020). In addition, bioactive compounds can be incorporated into foods, increasing their nutritional, sensorial, and technological properties (e.g., water and oil holding capacities, foaming, emulsion, and gelatinization) (Egea et al., 2018; Guimarães et al., 2019).

The proper use of agro-industrial matrices requires the production/extraction of bioactive compounds through ecofriendly strategies instead of conventional processes, followed by optimizing process conditions (Lemes et al., 2016a; Heemann et al., 2019). In this context, biological processes stand out, as they can enhance the production, extraction, and application of components from agro-industrial matrices in a more attractive way (Jegatheesan et al., 2020). Due to their selectivity, biological strategies present some advantages, including the production of extracts with high quality and bioactivity, as well as low toxicity (Chen, 2015; Habeebullah et al., 2020; Wang and Lü, 2021). Among the biological approaches, one consists of (1) extraction using enzymes that release compounds from the matrix under optimized conditions, making the process efficient (Marathe et al., 2019), and another is the (2) fermentation using different microorganisms that transform waste into products of interest, such as ethanol, proteins, peptides, enzymes, and pigments (Sadh et al., 2018b; Martínez-Espinosa, 2020).

In this sense, this article provides an overview of the main bioactive components found in agro-industrial by-products and the biological strategies for their extraction. We also provide information to enhance the use of these bioactive compounds, especially for the food and pharmaceutical industries.

2 GENERATION OF AGRO-INDUSTRIAL WASTE

The agroindustry generates large amounts of waste regardless of the production chain step (Palhares et al., 2020; Chauhan et al., 2021). This waste generation can impact the environment according to factors that include the degree of development of the countries, education, population awareness, public policies, overexploitation, and waste of natural resources (Bedoić et al., 2019; Palhares et al., 2020). For example, in the steps involving food processing, losses reaching up to 40% of production are verified, mainly due to inefficiency in the production processing and management system, deformed or damaged products, and packaging disposable, among others, which generate refusal on the part of consumers (Dora et al., 2020).

Waste can be from plant or animal sources (**Figure 1**). The vegetable by-products include leaves, stems, seeds, bark, straw, fibers, bagasse, and fruit skins, among others (Ezejiofor et al., 2014). For fruits and vegetables, for example, the production of industrial solid waste is verified, which includes items removed from fruits and vegetables during cleaning, processing, cooking, and packaging (EPA, 2012). For cereals, the waste generation corresponding to 35% of the total production is verified, including liquid residues (rice milling wastewater, parboiled rice effluent, corn steep liquor, and bakery wastewater) and solid wastes (corn pericarp, corn grits, and brewer's spent grain), which are highly polluting due to large amounts of organic load, solid waste, and nutrients (Hassan et al., 2021). In general, vegetable residues present high carbohydrates (starch, cellulose, and hemicellulose), lignin, organic acids, minerals, and vitamins (Kumar et al., 2020).

On the other hand, animal by-products comprise large amounts of carcasses, skins, hooves, heads, feathers, viscera, bones, fat, meat trimmings, blood, and other animal fluids (Ockerman and Hansen, 2000; Waldron, 2007), as well as meat out of specification and significant amounts of milk processing residues such as whey and other fractions from the separation process (Ben-Othman et al., 2020). The meat sector, for example, records losses of up to 23% of everything produced, including consumption losses, industrial processing, distribution, inadequate storage conditions, and failures in the freezing process (Karwowska et al., 2021). The dairy industry generates around 4 to 11 million tons of waste per year, including whey, dairy sludge, and wastewater (processing, cleaning, and sanitary), with great pollutant potential (Ahmad et al., 2019; Lemes et al., 2020a). In general, animal residues present high levels of proteins, lipids, and minerals (Jayathilakan et al., 2012; Jain and Anal, 2016; Maysonnave et al., 2020).

Due to the complex chemical composition, animal and vegetable residues can be used as a low-cost raw material to obtain bioactive compounds using suitable processes (Lemes et al., 2016a; Prado et al., 2020).

3 BIOACTIVE COMPOUNDS

Bioactive compounds can be used with functions like to (1) improve quality in conventional food (nutritional, sensory, and technological properties), (2) produce functional foods that provide physiological benefits in terms of essential nutritional aspects, (3) produce nutraceuticals, isolated components of food or agroindustrial wastes that provide proven physiological benefits (Birch and Bonwick, 2018; Daliu et al., 2018; Aguiar et al., 2019; Reque and Brandelli, 2021), (4) and compose films for application as smart, active, and/or bioactive food packaging (Nogueira et al., 2020; Oliveira Filho et al., 2021). This wide application of bioactive compounds occurs due to several effects attributed to bioactive compounds, including protection of the immune system, anti-inflammatory action, reduction of damage from cell oxidation, and the occurrence of chronic noncommunicable diseases (Silva et al., 2019; Alongi and Anese, 2021).

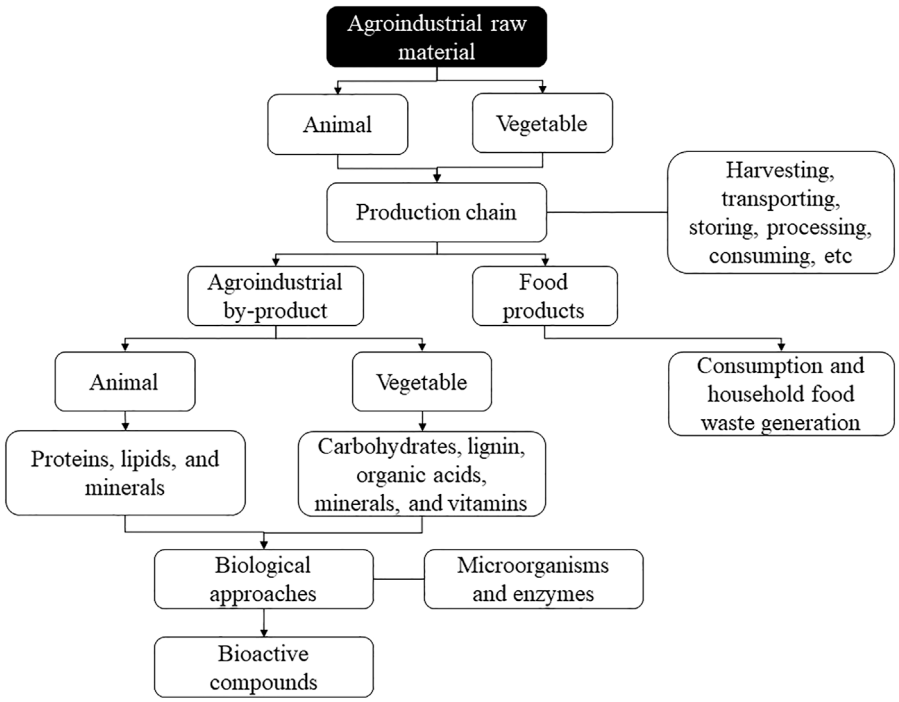

FIGURE 1 | General steps that involve the generation of agroindustrial wastes and their use to produce bioactive components.

Several wastes can be used to obtain bioactive compounds, including cereal bran, which is rich in phenolic compounds, flavonoids, glucans, and pigments (Pauline et al., 2020); fruit and vegetable wastes, which are sources of phenolic compounds (Trombino et al., 2021); and complex carbohydrates (Pérez et al., 2002), as well as animal wastes, e.g., fish wastes rich in omega 3 (Bonilla-Méndez and Hoyos-Concha, 2018) and milk processing wastes as sources of peptides (Pires et al., 2021).

Among the main bioactive compounds found in agro-industrial wastes with more interest for application in the food and pharmaceutical industries are (1) bioactive peptides, (2) phenolic compounds, (3) carbohydrates, and (4) other molecules with distinct biological and technological properties. Below we describe these bioactive compounds of interest.

1) Bioactive peptides are protein fragments with up to 20 amino acid residues and that have an impact on body functions, which depend on their composition and amino acid sequence in the structure (Lemes et al., 2016b). Due to their high protein value, cakes and meals can serve as a source of peptides or amino acids that, once released, demonstrate higher biological activity such as antioxidant, antihypertensive, anti-inflammatory, and immune-modulating activities (Lemes et al., 2016b; Lemes et al., 2020b; Velliquette et al., 2020).

Peptides with antioxidant activity exert biological effects on the human body and have attracted great interest for their safety and wide distribution (Brandelli et al., 2015). When applied directly to food, peptides can decrease the occurrence and speed of oxidation reactions, which is especially interesting in replacing synthetic antioxidants related to toxic effects on human health. Currently, studies report the antioxidant activities of plant-derived hydrolysates, such as soybean (Yang et al., 2019), sunflower (Prado et al., 2020), corn (Zhang et al., 2019), beans (Paula et al., 2020), and peanut flour (Yu et al., 2021), as well as hydrolysates from animal by-products such as fish (Hemker et al., 2020) and poultry (Bouhamed et al., 2020).

The antihypertensive property has been mentioned for several peptide molecules with the potential to inhibit the activity of renin, angiotensin-converting enzyme, and angiotensin II receptors *in vitro* and *in vivo*, increasing the levels of nitric oxide in the blood (Lemes et al., 2020b). As a result, peptides show potential for application in antihypertensive prevention and treatment, reducing cardiovascular complications, mainly when associated with physical activity and a healthy diet.

2) Phenolic compounds are one of the main groups of secondary metabolites produced by plants and are of particular interest due to their bioactive properties such as antioxidant, antihypertensive, and antimicrobial activities and inhibition of carcinogenesis (Tanase et al., 2014; Tanase et al., 2019). In addition, phenolic compounds have been suggested for applications in food as active agents to control lipid oxidation and microbial growth in foods (Huang et al., 2020; Zhang et al., 2020) and in the pharmaceutical and cosmetic industries such as mouthwashes, eye creams, and different herbal cosmetics (Petti and Scully, 2009; Saraf and Kaur, 2010; Gaur and Agnihotri, 2014).

3) Carbohydrates are an important energy source and play numerous key roles in all living organisms (Jiang et al., 2021). They are at high levels in residues of vegetable origin, especially starch, lignocellulose (cellulose, hemicellulose, and lignin), and β-glucans, among others (Kumar et al., 2020). Starch is the main

storage carbohydrate in plants and is a mixture of two glucose polymers: amylose and amylopectin (Lovegrove et al., 2017). Starches are used in various sectors of the industry in a wide range of products besides food applications (Di-Medeiros-Leal et al., 2021). Lignocellulose is the main polymeric compound formed by plant metabolism as structural material and is widely present in agro-industrial waste. This carbohydrate type has variable amounts of cellulose, hemicellulose, and lignin and can be converted into different high-value products, contributing to waste reduction (Fortunati et al., 2016). β-Glucan is a polysaccharide with several biological activities with scientifically proven beneficial health effects. Cereal wastes from barley, oats, and residual yeast biomass can also be used as a source of β-glucan (Tosh et al., 2010; Du et al., 2014; Vieira et al., 2017; Guedes et al., 2019; Liu et al., 2021).

4) Other molecules can be obtained, including lipid molecules such as lycopene-type carotenoids that can act as natural pigments in their application in foods and fatty acids.

Lycopene is a carotenoid, not a vitamin A precursor, mainly found in tomatoes and by-products of tomato processing (Anarjan and Jouyban, 2017). In addition to acting as a natural pigment giving a red-orange color, lycopene can react to free radicals, preventing cellular compounds' degradation, including DNA (Moritz and Tramonte, 2006; Caseiro et al., 2020; Adetunji et al., 2021). All fractions of tomato can be used, including the skin, which contains about 510–734 mg of lycopene/kg of dry matter (DM), in addition to significant amounts of lutein, β-carotene, and *cis*-β-carotene (Knoblich et al., 2005; Nour et al., 2018), and the seed, which has a lycopene content of ~130 μg lycopene/kg DM (Knoblich et al., 2005). Solid fractions can also be used for lycopene extraction (Trombino et al., 2021) from the use of solvents, supercritical extraction (Machmudah et al., 2012; Urbonaviciene and Viskelis, 2017; Hatami et al., 2019), pulsed electric field-assisted extraction (Pataro et al., 2020), and ohmic technology (Coelho et al., 2019), among others. In addition to lycopene, tomato by-products contain tocopherols, sterols and terpenes, fatty acids, phenolic compounds, and flavonoids, showing great versatility in obtaining several bioactive compounds (Kalogeropoulos et al., 2012).

Polyunsaturated fatty acids (PUFAs) of the omega-3 and omega-6 types are in vegetable oils, fish, and nuts. As with marine products, vegetable and nut by-products can be a source of PUFA that is underutilized. Fish by-products that are sources of marine oils can be used in the production of enzymatic PUFA synthesis of acylglycerols directly from glycerol and omega-3 fatty acid concentrates. The main acids present in omega-3 are docosahexaenoic acid (DHA), eicosapentaenoic acid (EPA), and α-linolenic acid, while acids present in omega-6 are arachidonic and linolenic acids (Dave and Routray, 2018).

4 BIOLOGICAL VS. NON-BIOLOGICAL APPROACHES

The recovery of compounds of interest from agricultural wastes and by-products involves conventional and novel solid–liquid and liquid–liquid extractions. Conventional methods are based on the extraction capacity of different solvents and applying thermal factors and/or homogenization, such as maceration, infusion, Soxhlet extraction, and hydro-distillation. However, these methods have presented some disadvantages such as long duration in the case of solid–liquid extraction, e.g., low extraction selectivity and specificity, decomposition of thermolabile compounds, and low purity of the product after the purification process, as well as high operation pressure, energy need, and amount of solvent with high purity (Gligor et al., 2019; Becerra et al., 2021).

On the other hand, novel extraction methods had been proposed, such as substituting molecular solvents with ionic liquids, eutectic solvents, and supercritical fluids or using different nonthermal energies (ultrasound, microwave, and pulsed electric field). However, the cell wall of plant matrices (and their components, cellulose, hemicellulose, starch, pectin, lignin, and proteins) can make the extraction of compounds a challenge.

In biological conversion processes (enzymatic or fermentation), cell wall recalcitrance is a resistance of plant cell walls to biological deconstruction for enzymes and microorganisms (Zeng et al., 2017) that varies among plant species and phenotypes (Silveira et al., 2013). However, extensive research has been carried out to establish effective protocols for pretreatment of cell wall material, such as lignocellulose, before using the waste for biological conversion (Baruah et al., 2018; Mankar et al., 2021). Available pretreatments include physical (milling, microwave, extrusion, and ultrasonication), chemical (alkali, acid, ionic liquids, organosolv, and deep eutectic solvents), physicochemical (steam, ammonia and CO_2 explosion, and liquid hot water), and biological (whole-cell and enzymatic pretreatment) methods (Baruah et al., 2018).

Biological processes using microorganisms or enzymes can hydrolyze molecules, disrupt cell walls, increase permeability, and allow intracellular materials to be accessible for extraction. The microorganisms can utilize agricultural wastes as substrates under specific pH, temperature, moisture, and water activity conditions for their growth and production of the compounds of interest. The use of enzymes from microorganisms, plants, and mammalian cells and tissues—which catalyze reactions with high specificity, regioselectivity, and mild conditions—could improve the extraction efficiency of different compounds (polyphenols, carotenoids, terpenoids, and others) or even convert this compounds into valuable compounds as biofuels, surfactants, and pharmaceuticals (Gligor et al., 2019; Marathe et al., 2019; Becerra et al., 2021; Sharma et al., 2021).

4.1 Extraction of Bioactive Components With Enzymes From Agro-industrial Wastes

The enzyme-assisted extraction (EAE) method can be employed in pretreatments of raw materials, improving extraction time, solvent use, and the quality and purity of a product while lowering production costs compared with classical extraction processes. Different enzymes could be applied including cellulases,

TABLE 1 | Examples of enzyme-assisted extraction of bioactive compounds from agroindustrial by-products.

Enzymes	Matrix/Metabolite	Extraction conditions	References
Pectinase, alpha-amylase, hemicellulase, cellulase, and glucoamylase	Guarana (*Paullinia cupana*) seeds/ Caffeine and tannins	Solvent-biomass ratio: 5 ml/g, solvent: water, 50–70°C, enzyme loading: 0.1–1% v/v biomass, 5.5 h, 200 rpm	Ribeiro et al. (2012)
Proteases, pectinase, cellulase, and hemicellulase	Flaxseed meal/polyphenols and proteins	Solvent-biomass ratio: 6.58 ml/g, solvent: water or 10% ethanol v/v, 50°C, enzyme loading: 0.3–2.0%, v/v, 1.5 h, 200 rpm	Ribeiro et al. (2013)
Cellulase, glucosidase, and pectinase	Grape skins/Anthocyanins and flavanols	Solvent-biomass ratio: 20 ml/g, solvent:12.5% ethanol solution with 4 g/L tartaric acid, pH 3.6, 20–30°C, enzyme loading: 15 mg/L, 72 h	Nogales-Bueno et al. (2020)
Pectinase, and α- and β-Glycosidase	Grape pomace/aroma compounds (alcohols, esters, terpenes, and others)	Particle diameter: < 500 μm, Solvent-biomass ratio: 0.6 ml/g, solvent: 70% ethanol/Milli-Q water solution, pH 5.0, 35°C enzyme loading: 0.9 g/10 ml, 48 h, 120 rpm	Liang et al. (2020)
Protease	Blue crab (*Portunus segnis*) shells/ carotenoproteins	Solvent-biomass ratio: 5 ml/g, solvent: water (pH 8.0), 50°C, enzyme loading: 20 U/g biomass, 60 min	Hamdi et al. (2020)
Proteases and cellulase	*Salvia officinalis* leaves/Rosmarinic acid	Solvent-biomass ratio: 25.76 ml/g, solvent: water (pH 6.9), 54.3°C, enzyme loading: 4.49%, w/w, 2 h with stirring	Su et al. (2020)
Pectinase	Spent coffee ground/flavonoids	Solvent-biomass ratio: 15 ml/g, solvent: sodium acetate buffer (200 mM, pH 5.5), 37°C, enzyme loading: 0.67% v/v, 60 min	Khairil Anuar et al. (2020)
Cellulase and hemicellulase	Japanese Peppermint (*Mentha arvensis*) leaves/essential oil	Solvent-biomass ratio: 10 ml/g, solvent: water, 40°C enzyme loading: 2%w/v, 3 h, 120 strokes/min	Shimotori et al. (2020)
Polygalacturonase, pectin lyase, celulase, and xylanase	Unsold ripened tomatoes/ carotenoids	solvent: acetate buffer (100 mM, pH 5.5), 50°C, enzyme loading: 25 U/g, 180 min	Lombardelli et al. (2020)
Lysozyme	Spirulin (*Arthrospira platensis*)/ C-phycocyanin	Solvent-biomass ratio: 8 ml/g, solvent: phosphate buffer (100 mM, pH 6.8), 37°C, enzyme loading: 0.6% w/v, 16 h + US: 20kHz, 50% amplitude, 2.5 min	Tavanandi and Raghavarao, (2020)
Proteases, hemicellulase, pectinase, and cellulase	Tiger nut (*Cyperus esculentus*)/oil	Particle diameter: < 600 μm, Solvent-biomass ratio: 10 ml/g, solvent: water, pH 4.9, 45°C enzyme loading: 2% w/v, 180 min, 120 rpm; MW: 2.45GHz, 300 W, US: 25 KHz, 460 W, 30 min, 40°C	Hu et al. (2020)
Polygalacturonase, celulase, and hemicellulases	*Opuntia ficus-indica* cladodes/ isorhamnetin conjugates	Solvent-biomass ratio: 5 ml/g, solvent: ethanol/ water 90/10, pH 4.0, 40°C enzyme loading: 1.5% w/ v, 30 min, $scCO_2$: pressure 100 bar, flow rate: 18 g/ min, 10–40 min, 60°C, co-solvent: 20% ethanol	Antunes-Ricardo et al. (2020)
β-glucosidase, tannase, and cellulase	Citrus pectin by-product/aglycone flavanones	Solvent-biomass ratio: 12.5 ml/g, solvent: acetate buffer (20 mM, pH 5.0), 40°C, enzyme loading: 20 U/g biomass, 24 h, 120 rpm	Barbosa et al. (2021)
Cellulase, xylanase, and pectinase	Red beets/betalains	Solvent-biomass ratio: 15 ml/g, solvent: acetate buffer (pH 5.5), 25°C, enzyme loading: 24 U/g, 4 h	Lombardelli et al. (2021)
Cellulase, hemicellulase, and pectinase	Licorice roots/glycyrrhizic acid	Particle diameter: < 2 μm, Solvent-biomass ratio: 5 ml/g, solvent: acetate buffer, pH 5.0, 45°C enzyme loading: 2% w/v, 1 h with stirring	Giahi et al. (2021)
Beta-glucanase, pectinase, protease, and ferulic acid esterase	Sweet cherry (*Prunus avium*) pomace/polyphenols	Solvent-biomass ratio: 2.63 ml/g, solvent: sodium phosphate buffer (100 mM), pH 10.0, 70°C enzyme loading: 2–140 μl/g, 18.4–40 min, 750 rpm	Domínguez-Rodríguez et al. (2021)
Cellulase	Passion fruit/polyphenols	Particle diameter: < 180 μm, Solvent-biomass ratio: 50 ml/g, solvent: water, pH 5.0, 30°C enzyme loading: 6% w/v, 47 min, US: 50 kHz, 300 W	Wang et al. (2021)
α-Amylase, β-glucanase, protease, hemicellulases, lipase, phytase, cellulases, and pectinase	Mango peel/phenolic acids	Solvent: sodium phosphate buffer, pH 4.5–7.5, 37–63°C enzyme loading: 2.3–4.1% w/v, 60–120 min, US: 40 kHz, 45–120 W	Sharif et al. (2021)

(Continued on following page)

TABLE 1 | (*Continued*) Examples of enzyme-assisted extraction of bioactive compounds from agroindustrial by-products.

Enzymes	Matrix/Metabolite	Extraction conditions	References
Pectinases	Pomelo (*Citrus maxima*) peel by-products/flavonoids	Particle diameter: < 149 μm, Solvent-biomass ratio: 142.99 ml/g, solvent: water, enzyme loading: 3.45% w/v, 65.23 min + US: 40 kHz, 69.26 min, 30°C	Anh et al. (2021)
Cellulase, pectinase, and tannase	Olive pomace/polyphenols	Solvent-biomass ratio: 15 ml/g, solvent: water, pH 5.0, 60°C enzyme loading: 2% w/v, 17 min, 120 rpm, MW: 2.45 GHz, 600 W	Macedo et al. (2021)

hemicellulases, pectinases, amylases, proteases, and lipases, as free or immobilized forms. The enzyme behavior depends on operational conditions such as pH, temperature, enzyme and substrate concentration, solid/liquid ratio, the particle size of the substrate, and reaction time (Becerra et al., 2021).

Among the advantages related to enzyme's use at the industrial scale is the cost reduction since enzymes acting as catalysts provide process savings compared to conventional strategies (Singh et al., 2016). To further reduce the cost of applying processes using enzymes, agro-industrial waste available in large quantities can be used in the production of enzymes (Lemes et al., 2016a) using simpler purification protocols or coupling techniques to purify the target product (Lemes et al., 2014; Lemes et al., 2019). Another factor that supports the application of enzymes and cost reduction in the process is the possibility of their immobilization, resulting in their recyclable use, allowing their application in defined cycles, and maintaining their selectivity, catalytic activity, and the generation of products in large quantities (Braga et al., 2014; Basso and Serban, 2019).

Greener processes have also been proposed by combining enzymes with ultrasound, microwave, and alternative solvent-based extraction methods, which can result in higher product quality, decreased production costs and solvents, or increased enzymatic treatment efficiency and extraction yields. These complementary treatments may be employed before or after EAE and simultaneously with the process, and their features consist of shortened extraction periods, nontoxicity, non-flammability, use of recyclable solvents, overall simplified steps, and customizable process parameters (Gligor et al., 2019; Wen et al., 2020; Picot-Allain et al., 2021). **Table 1** shows examples of the use of enzymes in the extraction and recovery of these bioactive compounds from agro-industrial wastes.

4.2 Fermentation Processes as a Tool to Obtain Bioactive Compounds From Agro-industrial Wastes

The fermentation process as a tool for obtaining bioactive compounds from agroindustrial wastes can be seen under different perspectives (**Figure 2**) as follows: (1) the target compound is the main product of microbial fermentation of agro-wastes, (2) the target compound is one of the products resulting from microbial fermentation of agro-wastes, and (3) microbial fermentation of agro-wastes produces enzymes, which will be applied to recover the target compound from a particular substrate.

4.2.1 Production of Bioactive Compounds Using Fermentation of Agro-industrial Wastes

The production of bioactive compounds through fermentation can be carried out with various microorganisms and their respective species (bacteria, yeasts, filamentous fungi, and others) (Moreira et al., 2018; Shin et al., 2019; Gulsunoglu et al., 2020; Jiang et al., 2020; Silva et al., 2020; Sinha et al.,

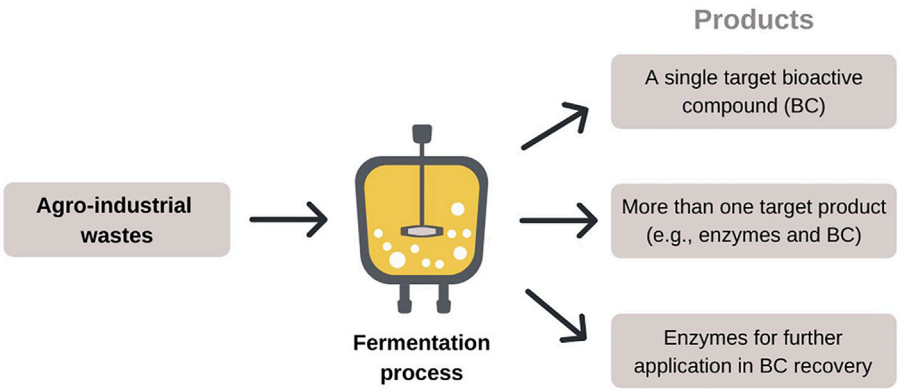

FIGURE 2 | Perspectives about the fermentation process to obtain bioactive compounds (BC).

2021). In addition, wild or genetically modified microorganisms (Cipolatti et al., 2019; Yang et al., 2020) can be applied in fermentative processes to obtain high-added-value compounds. The fermentation product can be part of the cell metabolism of microbial species or be extracted from the substrate by the microorganism's action. The target compound can also be produced by the microorganism intracellularly (Rodrigues et al., 2019)—which needs cell rupture steps after fermentation for the compound recovery (Gomes et al., 2020)—or extracellularly (Acosta et al., 2020).

Fermentative strategies differ between solid (SSF) and submerged (SmF) states. The choice of the fermentation process will depend on the used microorganism and the process recovery of target compounds. In the SmF approach, microorganisms are grown in a liquid medium containing the nutrients (Dey et al., 2016). The target compounds are secreted into the fermentation medium and then recovered in a separation step, such as centrifugation. SmF offers better control of cultivation conditions and is most suitable for bacteria and yeasts requiring high moisture content. SmF also allows the proper mixing of nutrients due to the high amount of free water and is a method of easy handling and scaling up. Nevertheless, the target products tend to be diluted at the end of fermentation (Bagewadi et al., 2018; Sánchez et al., 2021).

In contrast, SSF utilizes solid substrates in the absence or near absence of free water, which is a more appropriate condition for the growth of filamentous fungi (Soccol et al., 2017). Microbial growth and product formation occur on the surface of a solid substrate that works as support or on an inert material impregnated with nutrient solution (Thomas et al., 2013). After the SSF process, the target compounds are recovered through extraction and separation steps. SSF presents minimal problems with microbial contamination due to the low water contents in the medium and offers high volumetric productivity, concentrated target compounds, tolerance of high substrate concentration, and less wastewater generation (Manan and Webb, 2017; Krishania et al., 2018).

In both fermentation strategies, agro-industrial wastes can be utilized as a nutritional source for microorganism species to obtain bioactive compounds (Kaur et al., 2019; Reque et al., 2019; Abdeshahian et al., 2020; Jiang et al., 2020; Sharma and Ghoshal, 2020; Sinha et al., 2021). Regarding the complex matrices of some wastes, pretreatments are applied before the fermentation to facilitate the microorganism's access to nutrients (Acosta et al., 2020).

The choice of substrate will depend on the nutritional needs of the microbial species to produce the target compounds. A combination of wastes from different sources can also be an alternative to supply the nutritional requirements for microbial growth (Otero et al., 2019). In addition, the fermentation of wastes to produce bioactive compounds can be optimized through some approaches including response surface methodology (Moayedi et al., 2018; Rodrigues et al., 2019; Abdeshahian et al., 2020; Yang et al., 2020) and one factor at a time (Amorim et al., 2019; Kaur et al., 2019). The main bioactive compounds that can be produced using the biological approach were highlighted, as well as the particularities of each process.

Protein hydrolysates with biological actives can be obtained using one-step fermentation from wastes (Mechmeche et al., 2017; Fontoura et al., 2019). Moayedi et al. (2016) established a fermentative process with the *Bacillus subtilis* strain to convert tomato waste proteins into antioxidant and antibacterial hydrolysates. Mechmeche et al. (2017) investigated the bioconversion of tomato seed meal extract into antioxidant peptides through a fermentative process with *Lactobacillus planetarium*, which showed a promising ability to degrade and convert tomato seed proteins into peptides, also contributing to the antioxidant activity of the hydrolysates. Maciel et al. (2017) explored the keratinolytic potential of *Chryseobacterium* sp. and *Bacillus* sp. to convert feathers into protein hydrolysates with better *in vitro* nutritional features, suggesting a good prospect for their use in animal feed. Similarly, Fontoura et al. (2019) obtained protein hydrolysates with antioxidant properties through SmF of feathers with *Chryseobacterium* sp. Jiang et al. (2020) proposed an optimized production of bioactive peptides with antioxidant activity by *B. subtilis* from corn gluten meals.

Some studies have investigated the production of phenolic compounds through bioconversion of wastes. Shin et al. (2019) evaluated the fermentation of black rice by *Aspergillus* species under SSF to produce antioxidant phenolic compounds. After 3 days of fermentation, a maximum production of 1,660 μg protocatechuic acid/g of substrate was achieved. The authors also pointed the requirement to pretreat the waste for the extraction of phenolic compounds. Reque et al. (2017) addressed the bioprocessing of wheat middlings by *Bacillus* sp. to increase its antioxidant phenolic compound content. Besides changes in the phenolic profiles, the bioprocessed wheat middlings exhibited higher antioxidant capacity and total phenolic amounts than the unfermented waste. In the same way, Gulsunoglu et al. (2020) evaluated the effect of SSF with four *Aspergillus* spp. as a strategy to enhance the contents of phenolic compounds of apple peels. As a result, the 7-day fermentation enhanced apple peels' phenolic contents and antioxidant activity by between threefold and fivefold. The enhancement of antioxidant phenolic compounds through bioprocessing of by-products from fig (Buenrostro-Figueroa et al., 2017) and apricot (Dulf et al., 2017) is also reported. The bioprocessing of brewer's spent grain can favor both its phenolic compound and bioactive peptides contents, thus contributing to its antioxidant activity (Verni et al., 2020).

Potential prebiotic oligomers can be produced under microbial fermentation of wastes (Amorim et al., 2019; Reque et al., 2019). Wheat middlings, a by-product from wheat flour production, showed good aspects to be utilized as a substrate for xylooligosaccharide (XOS) production by *B. subtilis,* demonstrating prebiotic activity through *in vitro* tests with *Lactobacillus acidophilus*, a commercial probiotic strain (Reque et al., 2019). Likewise, brewers' spent grain was fermented by a genetically modified *B. subtilis* to produce arabino-xylooligosaccharides (AXOS), and after optimizing the fermentation process, AXOS with a degree of polymerization (DP) of 2–6 were obtained. Furthermore, AXOS yield using a genetically modified strain increased 33% in comparison to the

wild type (Amorim et al., 2018). In both cases, the bioconversion of wastes into xylooligomers occurred due to the ability of strains to secrete xylanases, the main enzymes involved in XOS production. Yang et al. (2020) proposed an efficient preparation of oligogalacturonides (OGS) using fermentation of citrus peel wastes with an engineered *Pichia pastoris* strain. The one-step fermentation of mandarin and orange peel wastes resulted in OGS with a DP of 2–7 and 2–6, respectively, and a maximal OGS yield of 26.1% after process optimization.

β-Glucan, a polysaccharide with several biological activities, is commonly extracted from cereal by-products (Karimi et al., 2019) and brewing/winery spent yeasts (Pinto et al., 2015; Varelas, 2016). However, β-glucan can also be produced by fermentation processes from wastes. Abdeshahian et al. (2020) investigated the production of extracellular β-glucan from sugarcane straw by *Lasiodiplodia theobromae*. The highest β-glucan yield and productivity were 0.047 g/g glucose and 0.014 g/L·h, respectively, at 72 h of fermentation. Acosta et al. (2020) evaluated the use of soybean molasses (unhydrolyzed and hydrolyzed forms) as a raw material for the fermentative production of β-glucan by *L. theobromae*. Maximum β-glucan production (1.06 g/L) and yield (0.13 g/g) were obtained in fermentations using unhydrolyzed molasses. Bzducha-Wróbel et al. (2020) proposed the valorization of waste potato juice water for β-glucan preparation with the *Candida utilis* strain, resulting in a β-glucan yield of 63 g/100 g yeast dry weight after 72 h of fermentation.

Natural pigments as carotenoids can be produced through biotechnological processes from wastes (Cipolatti et al., 2019; Otero et al., 2019). Corn steep liquor and sugarcane molasses were used as substrates to produce carotenoids by the *Rhodotorula mucilaginosa* strain through batch and fed-batch fermentation. Among the two fermentation approaches evaluated, the fed-batch process increased the carotenoid production by 400% compared to the batch process (Rodrigues et al., 2019). Onion peels, potato skin, mung bean husk, and pea pods were also evaluated as substrates to produce carotenoids under SmF with *R. mucilaginosa*. These wastes were chosen based on the high concentrations of sugars (onion peels and potato skin) and nitrogen (mung bean and pea pods). As a result, it was found that onion peels and mung bean husk are potential substrates for the production of microbial carotenoids as β-carotene, phytoene, torulene, and torularhodin (Sharma and Ghoshal, 2020). Olive mill wastes (Ghilardi et al., 2020), coffee pulp and husk (Moreira et al., 2018), and wastes from the vegetable and fruit markets (Sinha et al., 2021) were explored in carotenoid production by *Rhodotorula* species, showing good prospects as cheap substrates. Orange, carrot, and papaya peels were used as substrates to produce β-carotene under SSF with *Blakeslea trispora*, resulting in good yields in synthetic media (Kaur et al., 2019).

4.2.2 Low-Cost Microbial Enzymes for Further Recovery of Bioactive Compounds

Microbial enzymes produced by the fermentation of wastes are extensively applied to recover bioactive compounds (Zanutto-Elgui et al., 2019; Gautério et al., 2021a). Several studies have already demonstrated the effective use of wastes to obtain microbial hydrolases such as proteases, lipases, and carbohydrases (Pereira et al., 2019; Ahmad et al., 2020; Gautério et al., 2020).

The use of agro-industrial wastes reduces the production costs of microbial enzymes, being an alternative to replace synthetic and commercial substrates. The expenses related to the recovery of target compounds are also positively affected, as enzymatic extracts have a lower cost than pure commercial enzymes. Nevertheless, it is necessary to verify if the application requires purified enzymatic extracts since the inclusion of purification steps would result in a more costly process (Lemes et al., 2014; Lemes et al., 2019).

Zanutto-Elgui et al. (2019) produced bioactive peptides from bovine and goat milk subjected to the proteolytic activity of *Aspergillus oryzae* and *Aspergillus flavipes* proteases. Proteolytic enzymes from fungal species were effectively produced under SSF in wheat bran and then applied in the hydrolysis of milk proteins. The milk peptides showed broad antimicrobial and antioxidant activities *in vitro*, thus demonstrating a good prospect for biotechnological applications of these bioactive compounds. Oliveira et al. (2015) evaluated the production of soy protein hydrolysates with a microbial protease preparation. First, the protease production occurred using SmF from feather meal broth with the *Chryseobacterium* sp. strain. Then the enzymatic hydrolysis of soy protein isolate (SPI) occurred using the microbial protease extract, thus evaluating soluble peptides, antioxidant activity, and emulsifying capabilities of the hydrolysates. The authors pointed out that enzymatic hydrolysis increased soluble peptide content and positively affected SPI's antioxidant and emulsifying properties. Moreover, the enzymatic treatment was demonstrated as a promising approach to obtain antioxidant compounds for food application, besides providing functional properties.

Gautério et al. (2020) utilized rice bran as a xylan source to produce xylanases by the *Aureobasidium pullulans* strain. In a subsequent study, crude and partially purified xylanases from *A. pullulans* CCT 1261 were applied in beechwood xylan hydrolysis, resulting in XOS, and the pretreatment did not influence the total concentration of XOS (Gautério et al., 2021a). The optimization of the hydrolytic process also demonstrated the successful use of crude xylanase to obtain XOS with low xylose release (Gautério et al., 2021b).

Kupski et al. (2018) applied a fungal cellulolytic complex to provide functional compounds—mainly proteins and phenolic compounds—from soybean meal (SBM) and corn husk (CH). The cellulolytic enzymes were obtained using SSF of rice husk and bran with *Rhizopus oryzae* CCT 7560 and then used to hydrolyze SBM and CH. Enzymatic hydrolysis resulted in 34% cellulose reduction in SBM, whereas, in CH, it was 55%. This reduction increased the protein (74%) and starch (95%) digestibility in SBM. In CH, in turn, the reduction allowed the release of phenolic compounds (21%). As mentioned by the authors, available protein in SBM can be used as a food supplement, whereas the phenolic contents from CH can be applied as a food additive.

4.2.3 Simultaneous Production of Bioactive Compounds Using Fermentation of Agro-industrial Wastes

The use of agro-industrial wastes to produce bioactive compounds via fermentation strategies has undergone several advances. One of them refers to co-production, which is cost-efficient and meets the sustainable context of the circular economy. Some examples include the simultaneous production of antioxidant compounds and proteolytic enzymes (Lemes et al., 2016a); lignocellulolytic enzymes and phenolic compounds (Leite et al., 2019); xylanases and xylooligomers (Menezes et al., 2017; Pereira et al., 2018); proteolytic enzymes and protein hydrolysates (Bernardo et al., 2019); lipids and carotenoids (Kot et al., 2019; Costa et al., 2020; Silva et al., 2020); and antioxidant peptides and pigments (Bertolini et al., 2021), among others.

The co-production has some challenges to be overcome such as (1) optimization of the fermentation process, which becomes more complicated when the aim is to obtain the maximum yield of all the target compounds; (2) application of treatments to wastes, which can sometimes favor the production of only the target compound; and (3) separation of compounds produced, where questions related to the application and purity of the target compounds—use of a mixture or use of each compound separately—must be analyzed.

5 DOWNSTREAM PROCESSING OF BIOACTIVE COMPOUNDS FROM AGRO-INDUSTRIAL WASTES

The recovery and purification of bioactive compounds are strongly related to the particularities of the target biomolecule and its future application. Some bioactive compounds' characteristics, such as the nature of the compound, cell location (intracellular or extracellular), size, structure, charge, and solubility, among others, will determine the steps to be applied for its recovery and purification. Furthermore, the purity required of the target compound as well as the preservation of their bioactivity must also be considered when establishing the purification steps.

Using agro-industrial wastes to obtain bioactive compounds using biotechnological approaches also influences the subsequent recovery and purification steps. Waste features such as particle size, solubility, viscosity, and recalcitrance can interfere with the extraction, cell disruption, and purification of the target compound, in addition to determining the number of downstream steps. Another critical point is related to the separation of bioactive compounds produced simultaneously in the same medium. All these aspects determine the complexity and costs of purification designs (Lemes et al., 2014; Lemes et al., 2020a).

Bioactive compounds produced by enzymatic hydrolysis or SmF procedures can be separated from the medium using solid–liquid techniques (e.g., filtration and centrifugation). Target compounds produced by SSF need to be recovered by extraction. The extraction approaches applied to bioactive compounds include solvent extraction (e.g., organic, eutectic, and ionic liquid solvents), ultrasound-assisted extraction, microwave-assisted extraction, enzymatic-assisted extraction, pulsed electric field, subcritical and supercritical fluid extraction, aqueous two-phase system, and three-phase partitioning (Zainal-Abidin et al., 2017; Sagar et al., 2018; Yan et al., 2018). Some examples include the extraction of β-carotene (Kaur et al., 2019) and phenolic compounds (Gulsunoglu et al., 2020) using organic solvents after SSF of fruit and vegetable peels; the extraction of lycopene using organic solvent (ethanol) after enzymatic-assisted treatment of tomato by-products (Azabou et al., 2016); the extraction of phenolic compounds using ionic liquids (Magro and Castro, 2020) and ultrasound-assisted procedure (Ajila et al., 2011) after SSF of lentil grains and apple pomace, respectively; and the extraction of phenolic compounds from fermented orange pomace using supercritical CO_2 and cosolvents (Espinosa-Pardo et al., 2017).

Regarding intracellular target compounds, a step of cell disruption or cell permeabilization and subsequent extraction procedure is required, and both can occur separately or simultaneously (Kalil et al., 2017). The cell disruption/destabilization techniques applied to releasing compounds include bead milling, ultrasonication, high-pressure homogenization, osmotic shock, freeze–thawing, and lysis procedures with enzymes, chemicals, and heating (Gomes et al., 2020).

Purification processes applied to bioactive compounds are diverse and range from low- to high-resolution techniques. Some of the mentioned procedures in the literature are aqueous-phase separation (Wang et al., 2019), membrane technology (Pezeshk et al., 2019; Singh et al., 2020), and chromatography (Moayedi et al., 2018; Fontoura et al., 2019). Each technique can be applied alone or combined in purification designs, considering the aspects of the target compounds mentioned above. The challenge is to establish a purification process that results in desirable compound purity in the highest yield possible (Lemes et al., 2014).

6 POTENTIAL APPLICATIONS OF BIOACTIVE COMPOUNDS RECOVERED FROM WASTE AND BY-PRODUCTS

The growing demand for foods with beneficial effects on health, while contributing to the sustainable use of natural resources, stimulates the use of by-products to obtain bioactive compounds (Vilas-Boas et al., 2021), which have multiple applications in food, acting as antimicrobials, antioxidants, natural dyes, fortifying ingredients, texture modifiers, and others (Veneziani et al., 2017).

Figure 3 shows an overview of the potential application of bioactive compounds recovered from food by-products in meat, dairy, bakery, chocolate, and juice products, where the compounds are used as food ingredients with a defined role in the protection and technological properties of food.

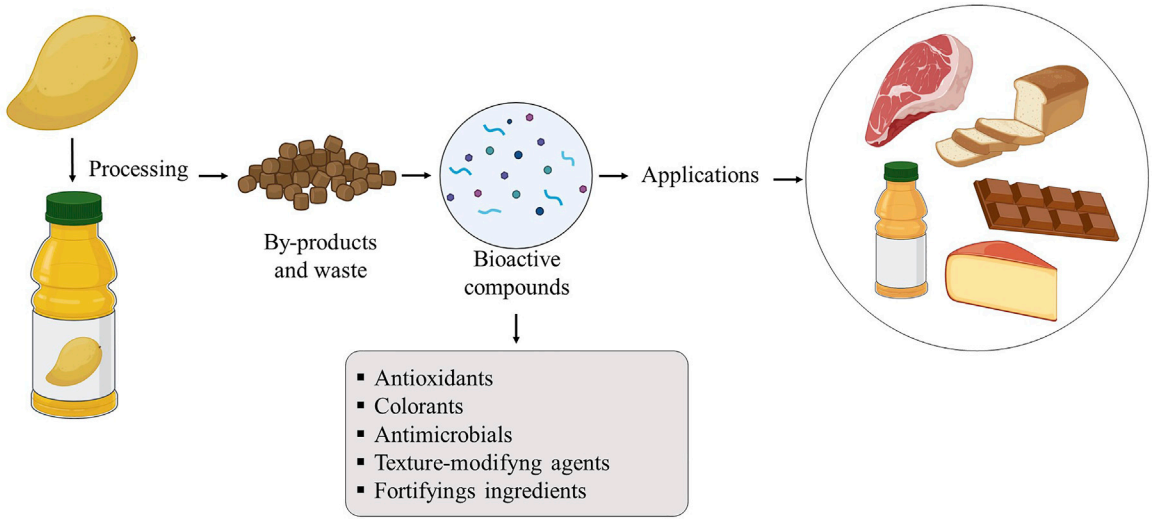

FIGURE 3 | Potential applications of bioactive compounds recovered from by-products.

TABLE 2 | Application of bioactive compounds in food products.

Bioactive compound	Addition levels	Food product	Formulation properties	References
Amaranthus spp. Seeds extract rich in antifungal peptides	7.04 and 22.96%	Bread	↑ nutritional value (protein and free amino acids) Delay in the appearance of fungal mycelium in storage No changes in taste and flavor	Rizzello et al. (2009)
Phenolics and carbohydrate fractions of okra seed and seedless pod	300 mg, 600 mg, and 1 g/500 g	Bread	↑ bread antioxidant activity ↓ antioxidant activity (30–40%) with thermal processing; ↓formation of harmful compound N^{ε}-(carboxymethyl)lysine Acceptable color change acceptable with little effect on quality	Peng et al. (2010)
Grape seed extract powder	20 g CE/kg	Frozen fish	Inhibition of the formation of lipid hydroperoxides and thiobarbituric acid reactive substances (TBARS)	Özen et al. (2011)
Grape seed extracts	1 g/kg	Dry cured sausage "chorizo"	↓ oxidation determined using TBARS method and the total volatile compounds of lipid oxidation ↑ sensory acceptance compared to those formulated with BHT, chestnut extract and control	Lorenzo et al. (2013)
Hull, bur, and leaf chestnut extracts	250–1,000 mg/kg	Beef patties	↓ lipid oxidation in hamburgers ↑ reduction of metmyoglobin at higher doses It did not affect sensory acceptance	Zamuz et al. (2018)
Grape seed extract	0.5 g/100 g	Petit Suisse cheese	↑ total phenolics and antioxidant activity (up to 28 days) 73% sensory acceptance 77% inhibition of angiotensin-converting enzyme (ACE) activity	Deolindo et al. (2019)
Camu-camu (*Myrciaria dubia*) seed extract	1.0 g/100 g	Yogurt	↑ antioxidant and chemical reducing capacity (FRAP, DPPH, and FCRC methods) The camu-camu yogurt containing 0.25 g/100 g of lyophilized camu-camu (*Myrciaria dubia*) seed extract had an acceptance rate of 84%	Fidelis et al. (2020)

A large number of studies report the addition of bioactive compounds from by-products in various food systems (**Table 2**), being applied as antioxidant and antimicrobial agents and also as agents to improve the nutritional and functional value of food products such as frozen fish (Özen et al., 2011), yogurt (Fidelis et al., 2020), dry cured sausage "chorizo" (Lorenzo et al., 2013), beef patties (Zamuz et al., 2018), bread (Rizzello et al., 2009; Peng et al., 2010), and petit Suisse cheese (Deolindo et al., 2019).

The antioxidant potential of extracts from by-products is frequently used in foods and has been mainly associated with their content of total phenolic compounds determined through different methods (Lorenzo et al., 2013; Zamuz et al., 2018; Fidelis et al., 2020) since the compounds have chemical properties and

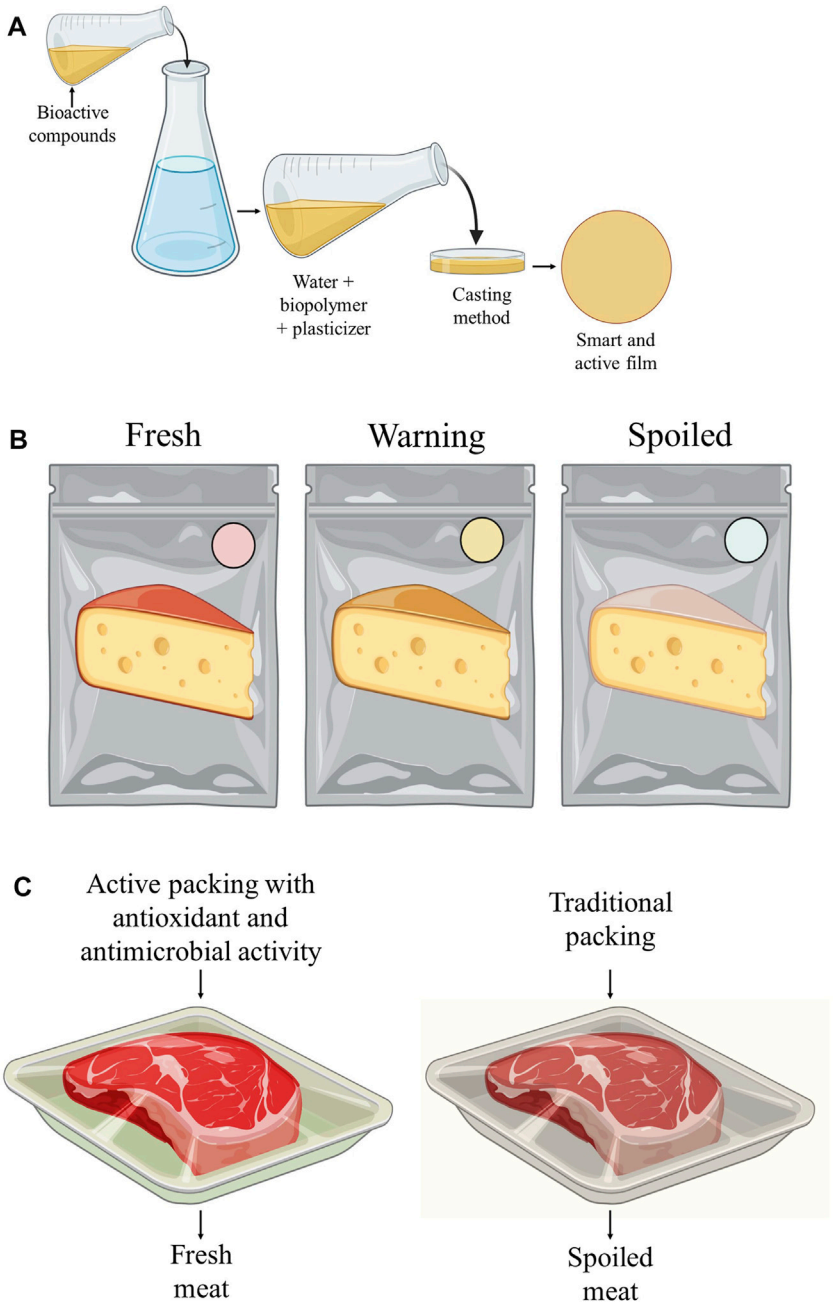

FIGURE 4 | (A) production of films by casting. **(B)** application as smart packaging, and **(C)** application as active food packaging.

structural diversity that influences the mechanism of action associated with this bioactivity (Vuolo et al., 2019).

Phenolic compounds such as aliphatic alcohols, terpenes, acids, aldehydes, ketones, anthocyanins, and isoflavonoids are the main bioactive compounds in by-products with antimicrobial properties (Arshad and Batool, 2017) and, therefore, with potential for incorporation into food matrices. In addition to these compounds, water-soluble extracts rich in antimicrobial peptides can be obtained from agro-industrial by-products such as amaranth seed extract to inhibit fungal species isolated from bakery products, in which when applied to the bread matrix (gluten free and with bread flour wheat), the inhibitory activity is verified during the entire shelf life of the products (Rizzello et al., 2009).

In addition to the antioxidant and antimicrobial potentials, bioactive compounds may have other biological properties such as antiproliferative, antidiabetic, and antihypertensive activities (Ben-Othman et al., 2020). For example, Fidelis et al. (2020) observed that camu-camu seed extract has a high content of total phenolics (46.3% w/w), contain mainly vescalagin, castalagin,

gallic acid, procyanidin A2, and (−)-epicatechin. This extract demonstrated high antioxidant and antiproliferative activities against HepG2 cells and Caco-2 cells, inhibiting α-amylase (40.7%), α-glucosidase (16.6%), and angiotensin-converting enzymes (34.4%). The application of the extract in yogurts increased the antioxidant capacity without affecting sensory acceptance (84%), an important factor for the application of any new ingredient in formulations.

Other components, such as betalain anthocyanins, curcumins, tannins, and carotenoids, commonly applied in foods as natural colorings (Luzardo-Ocampo et al., 2021), have also been used for the development of active and smart biodegradable food packaging (**Figure 4**) (Alizadeh-Sani et al., 2020). Anthocyanins extracted from the residue of processing blueberry juice, for example, have already been used in the production of smart films using cassava starch capable of monitoring the quality of orange juice, corn oil, and chicken pieces. Anthocyanin acts as an indicator of pH change during storage, as its color is altered due to structural changes when there is pH variation (Luchese et al., 2018).

Anthocyanin extracted from black plum bark is also efficiently applied in films based on chitosan and TiO_2, where incorporation results in high barrier properties against water vapor and UV-vis light and better mechanical strength (Zhang et al., 2019). In addition, it results in a higher free radical scavenging capacity and antimicrobial activity (*Escherichia coli*, *Staphylococcus aureus, Salmonella*, and *Listeria monocytogenes*), besides promoting the production of films capable of eliminating ethylene with potential application in pH-sensitive foods by detecting their changes and causing a color change.

Betacyanins extracted from the shell of dragon fruits can also be used to monitor the quality of fish freshness through their incorporation into intelligent packaging based on glucomannan–polyvinyl alcohol (Ardiyansyah et al., 2018). The presence of betacyanins also promotes a noticeable change from purple to yellow coloration due to the deterioration process of the product, which is, consequently, accompanied by increased levels of total volatile basic nitrogen (TVBN).

Protein hydrolysates, obtained through the enzymatic hydrolysis of proteins from agro-industrial by-products, have also been used as active agents in food films. Active food films based on alginate and protein hydrolysates obtained from the by-product of cottonseed oil extraction promote the formation of films with excellent visible light barrier properties, antioxidant activity, and antimicrobial potential against *S. aureus*, *Colletotrichum gloeosporioides,* and *Rhizopus oligosporus* (Oliveira-Filho et al., 2019).

Another prominent use of by-products is in the production of nutraceuticals, which are bioactive compounds used to meet the body's needs and usually consumed in pharmaceutical preparations, such as pills, tablets, capsules, powders, and bottles (Kumar et al., 2017). Among the most commonly marketed and used nutraceuticals are amino acids, carotenoids (β-carotene, lutein, zeaxanthin, and lycopene), fatty acids (omega-3 and omega-6), minerals (copper, selenium, and zinc), polyphenols, vitamins (C and E), and several others (Souyoul et al., 2018), which can be extracted from agro-industrial by-products.

The possibility of applying bioactive components in food products and in new technologies to promote food quality and safety is huge. Due to the diversity of compounds and their possible interactions and diverse activities, each component must be properly evaluated to produce food, beverages, and active and smart packaging applied to food to guarantee maximum potential in the applications.

7 CONCLUSION AND FUTURE DIRECTIONS

Large amounts of agro-industrial residues are generated during the processing of animal and vegetable materials, making it extremely necessary to adopt strategies for the integral use of residues or, even, for conversion into higher-value-added products. Biological approaches have several advantages compared to nonbiological processes, including the provision of extracts with high quality and high bioactivity, as well as with low toxicity.

Bioactive compounds obtained from by-products using the biological approach can be applied to develop foods and active or smart agents for biodegradable materials and packaging while contributing to consumer health, food safety, and sustainable use of natural resources.

That is why the biological approach is an important tool that must be continually improved and encouraged, especially due to the diversity of components that can be produced and the possible interactions and varied activities; each component must be properly evaluated to guarantee maximum potential in the applications.

AUTHOR CONTRIBUTIONS

All authors listed have made a substantial, direct, and intellectual contribution to the work and approved it for publication.

ACKNOWLEDGMENTS

The authors acknowledge the Coordenação de Aperfeiçoamento de Pessoal de Nível Superior—Brasil (CAPES—Finance Code 001), Conselho Nacional de Desenvolvimento Científico (CNPq), Fundação Carlos Chagas Filho de Amparo à Pesquisa do Estado do Rio de Janeiro (FAPERJ), and Instituto Federal Goiano (IF Goiano).

REFERENCES

Abdeshahian, P., Ascencio, J. J., Philippini, R. R., Antunes, F. A. F., dos Santos, J. C., and da Silva, S. S. (2020). Utilization of Sugarcane Straw for Production of β-glucan Biopolymer by Lasiodiplodia Theobromae CCT 3966 in Batch Fermentation Process. *Bioresour. Techn.* 314, 123716. doi:10.1016/j.biortech.2020.123716

Acosta, S. B. P., Marchioro, M. L. K., Santos, V. A. Q., Calegari, G. C., Lafay, C. B. B., Barbosa-Dekker, A. M., et al. (2020). Valorization of Soybean Molasses as Fermentation Substrate for the Production of Microbial Exocellular β-Glucan. *J. Polym. Environ.* 28 (8), 2149–2160. doi:10.1007/s10924-020-01758-z

Adetunji, C. O., Akram, M., Mtewa, A. G., Jeevanandam, J., Egbuna, C., Ogodo, A. C., et al. (2021). "Biochemical and Pharmacotherapeutic Potentials of Lycopene in Drug Discovery," in *Preparation of Phytopharmaceuticals for the Management of Disorders* (Elsevier), 307–360. doi:10.1016/b978-0-12-820284-5.00015-0

Aguiar, L. M., Geraldi, M. V., Betim Cazarin, C. B., and Maróstica Junior, M. R. (2019). "Chapter 11 - Functional Food Consumption and its Physiological Effects," in *Bioactive Compounds*. Editor M.R.S. Campos (Woodhead Publishing), 205–225. doi:10.1016/b978-0-12-814774-0.00011-6

Ahmad, T., Aadil, R. M., Ahmed, H., Rahman, U. u., Soares, B. C. V., Souza, S. L. Q., et al. (2019). Treatment and Utilization of Dairy Industrial Waste: A Review. *Trends Food Sci. Techn.* 88, 361–372. doi:10.1016/j.tifs.2019.04.003

Ahmad, W., Tayyab, M., Aftab, M. N., Hashmi, A. S., Ahmad, M. D., Firyal, S., et al. (2020). Optimization of Conditions for the Higher Level Production of Protease: Characterization of Protease from Geobacillus SBS-4S. *Waste Biomass Valor.* 11 (12), 6613–6623. doi:10.1007/s12649-020-00935-4

Ajila, C. M., Brar, S. K., Verma, M., Tyagi, R. D., and Valéro, J. R. (2011). Solid-state Fermentation of Apple Pomace Using Phanerocheate Chrysosporium - Liberation and Extraction of Phenolic Antioxidants. *Food Chem.* 126 (3), 1071–1080. doi:10.1016/j.foodchem.2010.11.129

Alizadeh-Sani, M., Mohammadian, E., Rhim, J.-W., and Jafari, S. M. (2020). pH-Sensitive (Halochromic) Smart Packaging Films Based on Natural Food Colorants for the Monitoring of Food Quality and Safety. *Trends Food Sci. Technol.* 105, 93–144. doi:10.1016/j.tifs.2020.08.014

Alongi, M., and Anese, M. (2021). Re-thinking Functional Food Development through a Holistic Approach. *J. Funct. Foods* 81, 104466. doi:10.1016/j.jff.2021.104466

Alves Magro, A. E., and de Castro, R. J. S. (2020). Effects of Solid-State Fermentation and Extraction Solvents on the Antioxidant Properties of Lentils. *Biocatal. Agric. Biotechnol.* 28, 101753. doi:10.1016/j.bcab.2020.101753

Amorim, C., Silvério, S. C., and Rodrigues, L. R. (2019). One-step Process for Producing Prebiotic Arabino-Xylooligosaccharides from brewer's Spent Grain Employing Trichoderma Species. *Food Chem.* 270, 86–94. doi:10.1016/j.foodchem.2018.07.080

Amorim, C., Silvério, S. C., Silva, S. P., Coelho, E., Coimbra, M. A., Prather, K. L. J., et al. (2018). Single-step Production of Arabino-Xylooligosaccharides by Recombinant Bacillus Subtilis 3610 Cultivated in Brewers' Spent Grain. *Carbohydr. Polym.* 199, 546–554. doi:10.1016/j.carbpol.2018.07.017

Anarjan, N., and Jouyban, A. (2017). Preparation of Lycopene Nanodispersions from Tomato Processing Waste: Effects of Organic Phase Composition. *Food Bioproducts Process.* 103, 104–113. doi:10.1016/j.fbp.2017.03.003

Antunes-Ricardo, M., Mendiola, J. A., García-Cayuela, T., Ibañez, E., Gutiérrez-Uribe, J. A., Pilar Cano, M., et al. (2020). Enzyme-assisted Supercritical Fluid Extraction of Antioxidant Isorhamnetin Conjugates from Opuntia Ficus-Indica (L.) Mill. *J. Supercrit. Fluids* 158, 104713. doi:10.1016/j.supflu.2019.104713

Arah, I. K., Ahorbo, G. K., Anku, E. K., Kumah, E. K., and Amaglo, H. (2016). Postharvest Handling Practices and Treatment Methods for Tomato Handlers in Developing Countries: A Mini Review. *Adv. Agric.* 2016, 1–8. doi:10.1155/2016/6436945

Ardiyansyah, M. W., Apriliyanti, M. W., Wahyono, A., Fatoni, M., Poerwanto, B., and Suryaningsih, W. (2018). The Potency of Betacyanins Extract from a Peel of Dragon Fruits as a Source of Colourimetric Indicator to Develop Intelligent Packaging for Fish Freshness Monitoring. *IOP Conf. Ser. Earth Environ. Sci.* 207, 012038. doi:10.1088/1755-1315/207/1/012038

Arshad, M. S., and Batool, S. (2017). "Natural Antimicrobials, Their Sources and Food Safety," in *Food Additives*. Editors D. N. Karunaratne and G. Pamunuwa (London, UK: IntechOpen), 87–102.

Azabou, S., Abid, Y., Sebii, H., Felfoul, I., Gargouri, A., and Attia, H. (2016). Potential of the Solid-State Fermentation of Tomato by Products by Fusarium Solani Pisi for Enzymatic Extraction of Lycopene. *LWT - Food Sci. Techn.* 68, 280–287. doi:10.1016/j.lwt.2015.11.064

Bagewadi, Z. K., Mulla, S. I., and Ninnekar, H. Z. (2018). Optimization of Endoglucanase Production from Trichoderma harzianum Strain HZN11 by central Composite Design under Response Surface Methodology. *Biomass Conv. Bioref.* 8 (2), 305–316. doi:10.1007/s13399-017-0285-3

Barbosa, P. d. P. M., Ruviaro, A. R., and Macedo, G. A. (2021). Conditions of Enzyme-Assisted Extraction to Increase the Recovery of Flavanone Aglycones from Pectin Waste. *J. Food Sci. Technol.* 58 (11), 4303–4312. doi:10.1007/s13197-020-04906-4

Baruah, J., Nath, B. K., Sharma, R., Kumar, S., Deka, R. C., Baruah, D. C., et al. (2018). Recent Trends in the Pretreatment of Lignocellulosic Biomass for Value-Added Products. *Front. Energ. Res.* 6, 141. doi:10.3389/fenrg.2018.00141

Basso, A., and Serban, S. (2019). Industrial Applications of Immobilized Enzymes-A Review. *Mol. Catal.* 479, 110607. doi:10.1016/j.mcat.2019.110607

Bedoić, R., Ćosić, B., and Duić, N. (2019). Technical Potential and Geographic Distribution of Agricultural Residues, Co-products and By-Products in the European Union. *Sci. Total Environ.* 686, 568–579. doi:10.1016/j.scitotenv.2019.05.219

Ben Hamad Bouhamed, S., Krichen, F., and Kechaou, N. (2020). Feather Protein Hydrolysates: a Study of Physicochemical, Functional Properties and Antioxidant Activity. *Waste Biomass Valor.* 11 (1), 51–62. doi:10.1007/s12649-018-0451-2

Ben-Othman, S., Jõudu, I., and Bhat, R. (2020). Bioactives from Agri-Food Wastes: Present Insights and Future Challenges. *Molecules* 25 (3), 510. doi:10.3390/molecules25030510

Bernardo, B. d. S., Ramos, R. F., Callegaro, K., and Daroit, D. J. (2019). Co-production of Proteases and Bioactive Protein Hydrolysates from Bioprocessing of Feather Meal. *Braz. Arch. Biol. Technol.* 62, 1–9. doi:10.1590/1678-4324-2019180621

Bertolini, D., Jiménez, M. E. P., Dos Santos, C., Corrêa, A. P. F., and Brandelli, A. (2021). Microbial Bioconversion of Feathers into Antioxidant Peptides and Pigments and Their Liposome Encapsulation. *Biotechnol. Lett.* 43 (4), 835–844. doi:10.1007/s10529-020-03067-w

Dey, T. B., Chakraborty, S., Jain, K. K., Sharma, A., and Kuhad, R. C. (2016). Antioxidant Phenolics and Their Microbial Production by Submerged and Solid State Fermentation Process: A Review. *Trends Food Sci. Techn.* 53, 60–74. doi:10.1016/j.tifs.2016.04.007

Birch, C. S., and Bonwick, G. A. (2018). Ensuring the Future of Functional Foods. *Int. J. Food Sci. Technol.* 54 (5), 1467–1485. doi:10.1111/ijfs.14060

Bonilla-Méndez, J. R., and Hoyos-Concha, J. L. (2018). Methods of Extraction Refining and Concentration of Fish Oil as a Source of omega-3 Fatty Acids. *Ciencia y Tecnología Agropecuaria* 19, 645–668. doi:10.21930/rcta.vol19_num2_art:684

Braga, A. R. C., Silva, M. F., Oliveira, J. V., Treichel, H., and Kalil, S. J. (2014). a New Approach to Evaluate Immobilization of β-Galactosidase on Eupergitc: Structural, Kinetic, and Thermal Characterization. *Química Nova* 37 (5), 796–803. doi:10.5935/0100-4042.20140128

Brandelli, A., Daroit, D. J., and Corrêa, A. P. F. (2015). Whey as a Source of Peptides with Remarkable Biological Activities. *Food Res. Int.* 73, 149–161. doi:10.1016/j.foodres.2015.01.016

Buenrostro-Figueroa, J. J., Velázquez, M., Flores-Ortega, O., Ascacio-Valdés, J. A., Huerta-Ochoa, S., Aguilar, C. N., et al. (2017). Solid State Fermentation of Fig (Ficus Carica L.) By-Products Using Fungi to Obtain Phenolic Compounds with Antioxidant Activity and Qualitative Evaluation of Phenolics Obtained. *Process Biochem.* 62, 16–23. doi:10.1016/j.procbio.2017.07.016

Bzducha-Wróbel, A., Koczoń, P., Błażejak, S., Kozera, J., and Kieliszek, M. (2020). Valorization of Deproteinated Potato Juice Water into β-Glucan Preparation of C. Utilis Origin: Comparative Study of Preparations Obtained by Two Isolation Methods. *Waste Biomass Valor.* 11 (7), 3257–3271. doi:10.1007/s12649-019-00641-w

Caseiro, M., Ascenso, A., Costa, A., Creagh-Flynn, J., Johnson, M., and Simões, S. (2020). Lycopene in Human Health. *LWT* 127, 109323. doi:10.1016/j.lwt.2020.109323

Chauhan, C., Dhir, A., Akram, M. U., and Salo, J. (2021). Food Loss and Waste in Food Supply Chains. A Systematic Literature Review and Framework Development Approach. *J. Clean. Prod.* 295, 126438. doi:10.1016/j.jclepro.2021.126438

Chen, H. (2015). "Lignocellulose Biorefinery Feedstock Engineering," in *Lignocellulose Biorefinery Engineering*. Editor H. Chen (Woodhead Publishing), 37–86. doi:10.1016/b978-0-08-100135-6.00003-x

Cipolatti, E. P., Remedi, R. D., Sá, C. d. S., Rodrigues, A. B., Gonçalves Ramos, J. M., Veiga Burkert, C. A., et al. (2019). Use of Agroindustrial Byproducts as Substrate for Production of Carotenoids with Antioxidant Potential by Wild Yeasts. *Biocatal. Agric. Biotechnol.* 20, 101208. doi:10.1016/j.bcab.2019.101208

Coelho, M., Pereira, R., Rodrigues, A. S., Teixeira, J. A., and Pintado, M. E. (2019). Extraction of Tomato By-Products' Bioactive Compounds Using Ohmic Technology. *Food Bioproducts Process.* 117, 329–339. doi:10.1016/j.fbp.2019.08.005

Coman, V., Teleky, B.-E., Mitrea, L., Martău, G. A., Szabo, K., Călinoiu, L.-F., et al. (2020). "Bioactive Potential of Fruit and Vegetable Wastes," in *Advances in Food and Nutrition Research*. Editor F. Toldrá (Academic Press), 157–225. doi:10.1016/bs.afnr.2019.07.001

Costa, W. A. d., Padilha, C. E. d. A., Oliveira Júnior, S. D. d., Silva, F. L. H. d., Silva, J., Ancântara, M. A., et al. (2020). Oil-lipids, Carotenoids and Fatty Acids Simultaneous Production by Rhodotorula Mucilaginosa CCT3892 Using Sugarcane Molasses as Carbon Source. *Braz. J. Food Technol.* 23, 1–11. doi:10.1590/1981-6723.06419

Pereira, A. S., Fontes-Sant'Ana, G. C., and Amaral, P. F. F. (2019). Mango Agro-Industrial Wastes for Lipase Production from Yarrowia Lipolytica and the Potential of the Fermented Solid as a Biocatalyst. *Food Bioproducts Process.* 115, 68–77. doi:10.1016/j.fbp.2019.02.002

Daliu, P., Santini, A., and Novellino, E. (2018). A Decade of Nutraceutical Patents: where Are We Now in 2018. *Expert Opin. Ther. Patents* 28 (12), 875–882. doi:10.1080/13543776.2018.1552260

Dave, D., and Routray, W. (2018). Current Scenario of Canadian Fishery and Corresponding Underutilized Species and Fishery Byproducts: A Potential Source of omega-3 Fatty Acids. *J. Clean. Prod.* 180, 617–641. doi:10.1016/j.jclepro.2018.01.091

Di-Medeiros-Leal, M. C. B., Ribeiro, G. O., Ribeiro, M. L. R., Ferreira, A. G., Braga, A. R. C., Egea, M. B., et al. (2021). "Analysis and Characterization of Starches from Alternative Sources," in *Biodegradable Polymers, Blends and Composites*. Editors Sanjay Mavinkere. Rangappa, Jyotishkumar. Parameswaranpillai, Suchart. Siengchin, and M. Ramesh (United Kingdom: Elsevier), 465–488.

Domínguez-Rodríguez, G., Marina, M. L., and Plaza, M. (2021). Enzyme-assisted Extraction of Bioactive Non-extractable Polyphenols from Sweet Cherry (Prunus Avium L.) Pomace. *Food Chem.* 339, 128086. doi:10.1016/j.foodchem.2020.128086

Dora, M., Wesana, J., Gellynck, X., Seth, N., Dey, B., and De Steur, H. (2020). Importance of Sustainable Operations in Food Loss: Evidence from the Belgian Food Processing Industry. *Ann. Oper. Res.* 290 (1), 47–72. doi:10.1007/s10479-019-03134-0

Du, B., Zhu, F., and Xu, B. (2014). β-Glucan Extraction from Bran of hull-less Barley by Accelerated Solvent Extraction Combined with Response Surface Methodology. *J. Cereal Sci.* 59 (1), 95–100. doi:10.1016/j.jcs.2013.11.004

Dulf, F. V., Vodnar, D. C., Dulf, E.-H., and Pintea, A. (2017). Phenolic Compounds, Flavonoids, Lipids and Antioxidant Potential of Apricot (Prunus Armeniaca L.) Pomace Fermented by Two Filamentous Fungal Strains in Solid State System. *Chem. Cent. J.* 11 (1), 92. doi:10.1186/s13065-017-0323-z

Egea, M. B., Bolanho, B. C., Lemes, A. C., Bragatto, M. M., Silva, M. R., Carvalho, J. C. M., et al. (2018). Low Cost Cassava, Peach palm and Soy By-Products for the Nutritional Enrichment of Cookies: Physical, Chemical and Sensorial Characteristics. *Int. Food Res. J.* 25 (3), 1204–1212.

EPA (2012). "Industrial Food Processing Waste Analyses," in *Office of Resource Conservation and Recovery* (U.S. Environmental Protection Agency). https://www.epa.gov.

Espinosa-Pardo, F. A., Nakajima, V. M., Macedo, G. A., Macedo, J. A., and Martínez, J. (2017). Extraction of Phenolic Compounds from Dry and Fermented orange Pomace Using Supercritical CO2 and Cosolvents. *Food Bioproducts Process.* 101, 1–10. doi:10.1016/j.fbp.2016.10.002

Ezejiofor, T., Enebaku, U. E., and Ogueke, C. (2014). Waste to Wealth- Value Recovery from Agro-Food Processing Wastes Using Biotechnology: A Review. *Bbj* 4, 418–481. doi:10.9734/bbj/2014/7017

FAO; Food and Agriculture Organization of the United Nations (2017). *The Future of Food Andagriculture - Trends and Challenges*. Roma: FAO.

Fidelis, M., de Oliveira, S. M., Sousa Santos, J., Bragueto Escher, G., Silva Rocha, R., Gomes Cruz, A., et al. (2020). From Byproduct to a Functional Ingredient: Camu-Camu (Myrciaria Dubia) Seed Extract as an Antioxidant Agent in a Yogurt Model. *J. Dairy Sci.* 103 (2), 1131–1140. doi:10.3168/jds.2019-17173

Fontoura, R., Daroit, D. J., Corrêa, A. P. F., Moresco, K. S., Santi, L., Beys-da-Silva, W. O., et al. (2019). Characterization of a Novel Antioxidant Peptide from Feather Keratin Hydrolysates. *New Biotechnol.* 49, 71–76. doi:10.1016/j.nbt.2018.09.003

Fortunati, E., Luzi, F., Puglia, D., and Torre, L. (2016). "Extraction of Lignocellulosic Materials from Waste Products," in *Multifunctional Polymeric Nanocomposites Based on Cellulosic Reinforcements*. Editors D. Puglia, E. Fortunati, and J. M. Kenny (William Andrew Publishing), 1–38. doi:10.1016/b978-0-323-44248-0.00001-8

Gaur, S., and Agnihotri, R. (2014). Green tea: A Novel Functional Food for the Oral Health of Older Adults. *Geriatr. Gerontol. Int.* 14 (2), 238–250. doi:10.1111/ggi.12194

Gautério, G. V., da Silva, L. G. G., Hübner, T., da Rosa Ribeiro, T., and Kalil, S. J. (2020). Maximization of Xylanase Production by Aureobasidium Pullulans Using a By-Product of rice Grain Milling as Xylan Source. *Biocatal. Agric. Biotechnol.* 23, 101511. doi:10.1016/j.bcab.2020.101511

Gautério, G. V., da Silva, L. G. G., Hübner, T., Ribeiro, T. d. R., and Kalil, S. J. (2021a). Xylooligosaccharides Production by Crude and Partially Purified Xylanase from Aureobasidium Pullulans: Biochemical and Thermodynamic Properties of the Enzymes and Their Application in Xylan Hydrolysis. *Process Biochem.* 104, 161–170. doi:10.1016/j.procbio.2021.03.009

Gautério, G. V., Hübner, T., Ribeiro, T. d. R., Ziotti, A. P. M., and Kalil, S. J. (2021b). Xylooligosaccharide Production with Low Xylose Release Using Crude Xylanase from Aureobasidium Pullulans: Effect of the Enzymatic Hydrolysis Parameters. *Appl. Biochem. Biotechnol.*, 1–20. doi:10.1007/s12010-021-03658-x

Ghilardi, C., Sanmartin Negrete, P., Carelli, A. A., and Borroni, V. (2020). Evaluation of Olive Mill Waste as Substrate for Carotenoid Production by Rhodotorula Mucilaginosa. *Bioresour. Bioproc.* 7 (1), 52. doi:10.1186/s40643-020-00341-7

Giahi, E., Jahadi, M., and Khosravi-Darani, K. (2021). Enzyme-assisted Extraction of Glycyrrhizic Acid from Licorice Roots Using Heat Reflux and Ultrasound Methods. *Biocatal. Agric. Biotechnol.* 33, 101953. doi:10.1016/j.bcab.2021.101953

Giuseppe Rizzello, C., Coda, R., De Angelis, M., Di Cagno, R., Carnevali, P., and Gobbetti, M. (2009). Long-term Fungal Inhibitory Activity of Water-Soluble Extract from Amaranthus Spp. Seeds during Storage of Gluten-free and Wheat Flour Breads. *Int. J. Food Microbiol.* 131 (2-3), 189–196. doi:10.1016/j.ijfoodmicro.2009.02.025

Gligor, O., Mocan, A., Moldovan, C., Locatelli, M., Crişan, G., and Ferreira, I. C. F. R. (2019). Enzyme-assisted Extractions of Polyphenols - A Comprehensive Review. *Trends Food Sci. Techn.* 88, 302–315. doi:10.1016/j.tifs.2019.03.029

Gomes, T. A., Zanette, C. M., and Spier, M. R. (2020). An Overview of Cell Disruption Methods for Intracellular Biomolecules Recovery. *Prep. Biochem. Biotechnol.* 50 (7), 635–654. doi:10.1080/10826068.2020.1728696

Guimarães, R. M., Pimentel, T. C., de Rezende, T. A. M., Silva, J. d. S., Falcão, H. G., Ida, E. I., et al. (2019). Gluten-free Bread: Effect of Soy and Corn Co-products on the Quality Parameters. *Eur. Food Res. Technol.* 245 (7), 1365–1376. doi:10.1007/s00217-019-03261-9

Gulsunoglu, Z., Purves, R., Karbancioglu-Guler, F., and Kilic-Akyilmaz, M. (2020). Enhancement of Phenolic Antioxidants in Industrial Apple Waste by Fermentation with Aspergillus Spp. *Biocatal. Agric. Biotechnol.* 25, 101562. doi:10.1016/j.bcab.2020.101562

Guedes, J. S., Pimentel, T. C., Diniz-Silva, H. T., Tayse da Cruz Almeida, E., Tavares, J. F., Leite de Souza, E., et al. (2019). Protective Effects of β-glucan Extracted from Spent brewer Yeast during Freeze-Drying, Storage and Exposure to Simulated Gastrointestinal Conditions of Probiotic Lactobacilli.

Lebensmittel-Wissenschaft und-Technologie 116, 108496. doi:10.1016/j.lwt.2019.108496

Hamdi, M., Nasri, R., Dridi, N., Li, S., and Nasri, M. (2020). Development of Novel High-Selective Extraction Approach of Carotenoproteins from Blue Crab (Portunus Segnis) Shells, Contribution to the Qualitative Analysis of Bioactive Compounds by HR-ESI-MS. *Food Chem.* 302, 125334. doi:10.1016/j.foodchem.2019.125334

Hassan, G., Shabbir, M. A., Ahmad, F., Pasha, I., Aslam, N., Ahmad, T., et al. (2021). Cereal Processing Waste, an Environmental Impact and Value Addition Perspectives: A Comprehensive Treatise. *Food Chem.* 363, 130352. doi:10.1016/j.foodchem.2021.130352

Hatami, T., Meireles, M. A. A., and Ciftci, O. N. (2019). Supercritical Carbon Dioxide Extraction of Lycopene from Tomato Processing By-Products: Mathematical Modeling and Optimization. *J. Food Eng.* 241, 18–25. doi:10.1016/j.jfoodeng.2018.07.036

Heemann, A. C. W., Heemann, R., Spier, M. R., and Santin, E. (2019). Enzyme-assisted Extraction of Polyphenols from green Yerba Mate. *Braz. J. Food Techn.* 22, 1–10. doi:10.1590/1981-6723.22217

Hemker, A. K., Nguyen, L. T., Karwe, M., and Salvi, D. (2020). Effects of Pressure-Assisted Enzymatic Hydrolysis on Functional and Bioactive Properties of tilapia (Oreochromis niloticus) By-Product Protein Hydrolysates. *Lebensmittel-Wissenschaft und-Technologie* 122, 109003. doi:10.1016/j.lwt.2019.109003

Hernández Becerra, E., De Jesús Pérez López, E., and Zartha Sossa, J. W. (2021). Recovery of Biomolecules from Agroindustry by Solid-Liquid Enzyme-Assisted Extraction: a Review. *Food Anal. Methods* 14 (8), 1744–1777. doi:10.1007/s12161-021-01974-w

Hu, B., Li, Y., Song, J., Li, H., Zhou, Q., Li, C., et al. (2020). Oil Extraction from Tiger Nut (Cyperus Esculentus L.) Using the Combination of Microwave-Ultrasonic Assisted Aqueous Enzymatic Method - Design, Optimization and Quality Evaluation. *J. Chromatogr. A* 1627, 461380. doi:10.1016/j.chroma.2020.461380

Huang, M., Wang, H., Xu, X., Lu, X., Song, X., and Zhou, G. (2020). Effects of Nanoemulsion-Based Edible Coatings with Composite Mixture of Rosemary Extract and ε-poly-l-lysine on the Shelf Life of Ready-To-Eat carbonado Chicken. *Food Hydrocolloids* 102, 105576. doi:10.1016/j.foodhyd.2019.105576

Irmak, S. (2017). "Biomass as Raw Material for Production of High-Value Products," in *Biomass Volume Estimation and Valorization for Energy*. Editor J. S. Tumuluru (London, UK: IntechOpen). doi:10.5772/65507

Ishangulyyev, R., Kim, S., and Lee, S. (2019). Understanding Food Loss and Waste-Why Are We Losing and Wasting Food. *Foods* 8 (8), 297. doi:10.3390/foods8080297

Jain, S., and Anal, A. K. (2016). Optimization of Extraction of Functional Protein Hydrolysates from Chicken Egg Shell Membrane (ESM) by Ultrasonic Assisted Extraction (UAE) and Enzymatic Hydrolysis. *Food Sci. Techn. (Campinas)* 69, 295–302. doi:10.1016/j.lwt.2016.01.057

Jayathilakan, K., Sultana, K., Radhakrishna, K., and Bawa, A. S. (2012). Utilization of Byproducts and Waste Materials from Meat, Poultry and Fish Processing Industries: a Review. *J. Food Sci. Technol.* 49 (3), 278–293. doi:10.1007/s13197-011-0290-7

Jegatheesan, V., Shu, L., Lens, P., and Chiemchaisri, C. (2020). *Valorisation of Agro-Industrial Residues – Volume I: Biological Approaches*. Springer.

Jiang, H., Qin, X., Wang, Q., Xu, Q., Wang, J., Wu, Y., et al. (2021). Application of Carbohydrates in Approved Small Molecule Drugs: A Review. *Eur. J. Med. Chem.* 223, 113633. doi:10.1016/j.ejmech.2021.113633

Jiang, X., Cui, Z., Wang, L., Xu, H., and Zhang, Y. (2020). Production of Bioactive Peptides from Corn Gluten Meal by Solid-State Fermentation with Bacillus Subtilis MTCC5480 and Evaluation of its Antioxidant Capacity *In Vivo*. *Lebensmittel-Wissenschaft und-Technologie* 131, 109767. doi:10.1016/j.lwt.2020.109767

Kalil, S. J., Moraes, C. C., Sala, L., and Burkert, C. A. V. (2017). "Bioproduct Extraction from Microbial Cells by Conventional and Nonconventional Techniques," in *Food Bioconversion* (Elsevier), 179–206. doi:10.1016/b978-0-12-811413-1.00005-x

Kalogeropoulos, N., Chiou, A., Pyriochou, V., Peristeraki, A., and Karathanos, V. T. (2012). Bioactive Phytochemicals in Industrial Tomatoes and Their Processing Byproducts. *LWT - Food Sci. Techn.* 49 (2), 213–216. doi:10.1016/j.lwt.2011.12.036

Karimi, R., Azizi, M. H., and Xu, Q. (2019). Effect of Different Enzymatic Extractions on Molecular Weight Distribution, Rheological and Microstructural Properties of Barley Bran β-glucan. *Int. J. Biol. Macromolecules* 126, 298–309. doi:10.1016/j.ijbiomac.2018.12.165

Karwowska, M., Łaba, S., and Szczepański, K. (2021). Food Loss and Waste in Meat Sector-Why the Consumption Stage Generates the Most Losses. *Sustainability* 13 (11), 6227. doi:10.3390/su13116227

Kaur, P., Ghoshal, G., and Jain, A. (2019). Bio-utilization of Fruits and Vegetables Waste to Produce β-carotene in Solid-State Fermentation: Characterization and Antioxidant Activity. *Process Biochem.* 76, 155–164. doi:10.1016/j.procbio.2018.10.007

K. Habeebullah, S. F., Sattari, Z., Al-Haddad, S., Fakhraldeen, S., Al-Ghunaim, A., Al-Yamani, F., et al. (2020). Enzyme-assisted Extraction of Bioactive Compounds from Brown Seaweeds and Characterization. *J. Appl. Phycol* 32 (1), 615–629. doi:10.1007/s10811-019-01906-6

Khairil Anuar, M., Mohd Zin, Z., Juhari, N. H., Hasmadi, M., Smedley, K. L., and Zainol, M. K. (2020). Influence of Pectinase–Assisted Extraction Time on the Antioxidant Capacity of Spent Coffee Ground (SCG). *Food Res.* 4, 2054–2061.

Knoblich, M., Anderson, B., and Latshaw, D. (2005). Analyses of Tomato Peel and Seed Byproducts and Their Use as a Source of Carotenoids. *J. Sci. Food Agric.* 85 (7), 1166–1170. doi:10.1002/jsfa.2091

Kot, A. M., Błażejak, S., Kieliszek, M., Gientka, I., Bryś, J., Reczek, L., et al. (2019). Effect of Exogenous Stress Factors on the Biosynthesis of Carotenoids and Lipids by Rhodotorula Yeast Strains in media Containing Agro-Industrial Waste. *World J. Microbiol. Biotechnol.* 35 (10), 157. doi:10.1007/s11274-019-2732-8

Krishania, M., Sindhu, R., Binod, P., Ahluwalia, V., Kumar, V., Sangwan, R. S., et al. (2018). "Design of Bioreactors in Solid-State Fermentation," in *Current Developments in Biotechnology and Bioengineering*. Editors A. Pandey, C. Larroche, and C. R. Soccol (Elsevier), 83–96. doi:10.1016/b978-0-444-63990-5.00005-0

Kumar, K., Yadav, A. N., Kumar, V., Vyas, P., and Dhaliwal, H. S. (2017). Food Waste: a Potential Bioresource for Extraction of Nutraceuticals and Bioactive Compounds. *Bioresour. Bioproc.* 4 (1), 1–14. doi:10.1186/s40643-017-0148-6

Kumar, S., Kushwaha, R., and Verma, M. L. (2020). "Recovery and Utilization of Bioactives from Food Processing Waste," in *Biotechnological Production of Bioactive Compounds*. Editors M. L. Verma and A. K. Chandel (Elsevier), 37–68. doi:10.1016/b978-0-444-64323-0.00002-3

Kupski, L., Telles, A. C., Gonçalves, L. M., Nora, N. S., and Furlong, E. B. (2018). Recovery of Functional Compounds from Lignocellulosic Material: An Innovative Enzymatic Approach. *Food Biosci.* 22, 26–31. doi:10.1016/j.fbio.2018.01.001

Leite, P., Silva, C., Salgado, J. M., and Belo, I. (2019). Simultaneous Production of Lignocellulolytic Enzymes and Extraction of Antioxidant Compounds by Solid-State Fermentation of Agro-Industrial Wastes. *Ind. Crops Prod.* 137, 315–322. doi:10.1016/j.indcrop.2019.04.044

Lemes, A. C., Álvares, G. T., Egea, M. B., Brandelli, A., and Kalil, S. J. (2016a). Simultaneous Production of Proteases and Antioxidant Compounds from Agro-Industrial By-Products. *Bioresour. Techn.* 222, 210–216. doi:10.1016/j.biortech.2016.10.001

Lemes, A. C., Gautério, G. V., Folador, G. O., Sora, G. T. S., and Pala, L. C. (2020a). "Reintrodução de resíduos agroindustriais na produção de alimentos," in *Realidades e perspectivas em Ciência dos Alimentos*. Editor W. V. Nogueira (Nova Xavantina: MT: Editora Pantanal).

Lemes, A. C., Machado, J. R., Brites, M. L., Luccio, M. D., and Kalil, S. J. (2014). Design Strategies for Integratedβ-Galactosidase Purification Processes. *Chem. Eng. Technol.* 37 (10), 1805–1812. doi:10.1002/ceat.201300433

Lemes, A. C., Paula, L. C., Oliveira Filho, J. G., Prado, D. M. F., Medronha, G. A., and Egea, M. B. (2020b). Bioactive Peptides with Antihypertensive Property Obtained from Agro-Industrial Byproducts - Mini Review. *Austin J. Nutr. Metab.* 7 (3), 1–5.

Lemes, A. C., Silvério, S. C., Rodrigues, S., and Rodrigues, L. R. (2019). Integrated Strategy for Purification of Esterase from Aureobasidium Pullulans. *Sep. Purif. Techn.* 209, 409–418. doi:10.1016/j.seppur.2018.07.062

Lemes, A., Sala, L., Ores, J., Braga, A., Egea, M., and Fernandes, K. (2016b). A Review of the Latest Advances in Encrypted Bioactive Peptides from Protein-Rich Waste. *International Journal of Molecular Sciences* 17 (6), 1–24. doi:10.3390/ijms17060950

Liang, Z., Pai, A., Liu, D., Luo, J., Wu, J., Fang, Z., et al. (2020). Optimizing Extraction Method of Aroma Compounds from Grape Pomace. *J. Food Sci.* 85 (12), 4225–4240. doi:10.1111/1750-3841.15533

Liu, Y., Wu, Q., Wu, X., Algharib, S. A., Gong, F., Hu, J., et al. (2021). Structure, Preparation, Modification, and Bioactivities of β-glucan and Mannan from Yeast Cell wall: A Review. *Int. J. Biol. Macromolecules* 173, 445–456. doi:10.1016/j.ijbiomac.2021.01.125

Lombardelli, C., Benucci, I., Mazzocchi, C., and Esti, M. (2021). A Novel Process for the Recovery of Betalains from Unsold Red Beets by Low-Temperature Enzyme-Assisted Extraction. *Foods* 10 (2), 236. doi:10.3390/foods10020236

Lombardelli, C., Liburdi, K., Benucci, I., and Esti, M. (2020). Tailored and Synergistic Enzyme-Assisted Extraction of Carotenoid-Containing Chromoplasts from Tomatoes. *Food Bioproducts Process.* 121, 43–53. doi:10.1016/j.fbp.2020.01.014

Lopes, F. C., and Ligabue-Braun, R. (2021). Agro-Industrial Residues: Eco-Friendly and Inexpensive Substrates for Microbial Pigments Production. *Front. Sustain. Food Syst.* 5, 65. doi:10.3389/fsufs.2021.589414

Lorenzo, J. M., González-Rodríguez, R. M., Sánchez, M., Amado, I. R., and Franco, D. (2013). Effects of Natural (Grape Seed and Chestnut Extract) and Synthetic Antioxidants (Buthylatedhydroxytoluene, BHT) on the Physical, Chemical, Microbiological and Sensory Characteristics of Dry Cured Sausage "chorizo". *Food Res. Int.* 54 (1), 611–620. doi:10.1016/j.foodres.2013.07.064

Lovegrove, A., Edwards, C. H., De Noni, I., Patel, H., El, S. N., Grassby, T., et al. (2017). Role of Polysaccharides in Food, Digestion, and Health. *Crit. Rev. Food Sci. Nutr.* 57 (2), 237–253. doi:10.1080/10408398.2014.939263

Luchese, C. L., Abdalla, V. F., Spada, J. C., and Tessaro, I. C. (2018). Evaluation of Blueberry Residue Incorporated Cassava Starch Film as pH Indicator in Different Simulants and Foodstuffs. *Food Hydrocolloids* 82, 209–218. doi:10.1016/j.foodhyd.2018.04.010

Luzardo-Ocampo, I., Ramírez-Jiménez, A. K., Yañez, J., Mojica, L., and Luna-Vital, D. A. (2021). Technological Applications of Natural Colorants in Food Systems: A Review. *Foods* 10 (3), 634. doi:10.3390/foods10030634

Macedo, G. A., Santana, Á. L., Crawford, L. M., Wang, S. C., Dias, F. F. G., and de Moura Bell, J. M. L. N. (2021). Integrated Microwave- and Enzyme-Assisted Extraction of Phenolic Compounds from Olive Pomace. *Lebensmittel-wissenschaft + [i.e. Technologie* 138, 110621. doi:10.1016/j.lwt.2020.110621

Machmudah, S., Zakaria, S., Winardi, S., Sasaki, M., Goto, M., Kusumoto, N., et al. (2012). Lycopene Extraction from Tomato Peel By-Product Containing Tomato Seed Using Supercritical Carbon Dioxide. *J. Food Eng.* 108 (2), 290–296. doi:10.1016/j.jfoodeng.2011.08.012

Maciel, J. L., Werlang, P. O., Daroit, D. J., and Brandelli, A. (2017). Characterization of Protein-Rich Hydrolysates Produced through Microbial Conversion of Waste Feathers. *Waste Biomass Valor.* 8 (4), 1177–1186. doi:10.1007/s12649-016-9694-y

Mankar, A. R., Pandey, A., Modak, A., and Pant, K. K. (2021). Pretreatment of Lignocellulosic Biomass: A Review on Recent Advances. *Bioresour. Techn.* 334, 125235. doi:10.1016/j.biortech.2021.125235

Marathe, S. J., Jadhav, S. B., Bankar, S. B., Kumari Dubey, K., and Singhal, R. S. (2019). Improvements in the Extraction of Bioactive Compounds by Enzymes. *Curr. Opin. Food Sci.* 25, 62–72. doi:10.1016/j.cofs.2019.02.009

Martínez-Espinosa, R. (2020). "Introductory Chapter: A Brief Overview on Fermentation and Challenges for the Next Future," in *New Advances on Fermentation Processes*. Editor R. M. Martínez-Espinosa (London, UK: IntechOpen).

Maysonnave, G. S., Mello, R. d. O., Vaz, F. N., Ávila, M. M. d., Pascoal, L. L., and Rodrigues, A. C. T. (2020). Physicochemical Characterization of By-Products from Beef Cattle slaughter and Economic Feasibility of Commercialization. *Acta Sci. Anim. Sci.* 42, e46545–7. doi:10.4025/actascianimsci.v42i1.46545

Mechmeche, M., Kachouri, F., Ksontini, H., and Hamdi, M. (2017). Production of Bioactive Peptides from Tomato Seed Isolate by Lactobacillus Plantarum Fermentation and Enhancement of Antioxidant Activity. *Food Biotechnol.* 31 (2), 94–113. doi:10.1080/08905436.2017.1302888

Menezes, B. S., Rossi, D. M., and Ayub, M. A. Z. (2017). Screening of Filamentous Fungi to Produce Xylanase and Xylooligosaccharides in Submerged and Solid-State Cultivations on rice Husk, Soybean hull, and Spent Malt as Substrates. *World J. Microbiol. Biotechnol.* 33 (3), 58. doi:10.1007/s11274-017-2226-5

Moayedi, A., Hashemi, M., and Safari, M. (2016). Valorization of Tomato Waste Proteins through Production of Antioxidant and Antibacterial Hydrolysates by Proteolytic Bacillus Subtilis: Optimization of Fermentation Conditions. *J. Food Sci. Technol.* 53 (1), 391–400. doi:10.1007/s13197-015-1965-2

Moayedi, A., Mora, L., Aristoy, M. C., Safari, M., Hashemi, M., and Toldrá, F. (2018). Peptidomic Analysis of Antioxidant and ACE-Inhibitory Peptides Obtained from Tomato Waste Proteins Fermented Using Bacillus Subtilis. *Food Chem.* 250, 180–187. doi:10.1016/j.foodchem.2018.01.033

Mohd Sairazi, N. S., and Sirajudeen, K. N. S. (2020). Natural Products and Their Bioactive Compounds: Neuroprotective Potentials against Neurodegenerative Diseases. *Evidence-Based Complement. Altern. Med.* 2020, 1–30. doi:10.1155/2020/6565396

Moreira, M. D., Melo, M. M., Coimbra, J. M., Reis, K. C. d., Schwan, R. F., and Silva, C. F. (2018). Solid Coffee Waste as Alternative to Produce Carotenoids with Antioxidant and Antimicrobial Activities. *Waste Manag.* 82, 93–99. doi:10.1016/j.wasman.2018.10.017

Moritz, B., and Tramonte, V. L. C. (2006). Biodisponibilidade Do Licopeno. *Rev. Nutr.* 19, 265–273. doi:10.1590/s1415-52732006000200013

Nguyen Tram Anh, M., Van Hung, P., and Thi Lan Phi, N. (2021). Optimized Conditions for Flavonoid Extraction from Pomelo Peel Byproducts under Enzyme- and Ultrasound-Assisted Extraction Using Response Surface Methodology. *J. Food Qual.* 2021, 1–10. doi:10.1155/2021/6666381

Nogales-Bueno, J., Baca-Bocanegra, B., Heredia, F. J., and Hernández-Hierro, J. M. (2020). Phenolic Compounds Extraction in Enzymatic Macerations of Grape Skins Identified as Low-level Extractable Total Anthocyanin Content. *J. Food Sci.* 85 (2), 324–331. doi:10.1111/1750-3841.15006

Nogueira, G. F., Oliveira, R. A. d., Velasco, J. I., and Fakhouri, F. M. (2020). Methods of Incorporating Plant-Derived Bioactive Compounds into Films Made with Agro-Based Polymers for Application as Food Packaging: A Brief Review. *Polymers* 12 (11), 2518. doi:10.3390/polym12112518

Nour, V., Panaite, T., Ropota, M., Turcu, R., Trandafir, I., and Corbu, A. (2018). Nutritional and Bioactive Compounds in Dried Tomato Processing Waste. *CyTA - J. Food* 16 (1), 222–229. doi:10.1080/19476337.2017.1383514

Ockerman, H. W., and Hansen, C. L. (2000). "Poultry By-Products," in *Animal by Product Processing and Utilization*. Editors H. W. Ockerman and C. L. Hansen (New York: CRC Press), 439–455.

Oliveira Filho, J. G. d., Braga, A. R. C., Oliveira, B. R. d., Gomes, F. P., Moreira, V. L., Pereira, V. A. C., et al. (2021). The Potential of Anthocyanins in Smart, Active, and Bioactive Eco-Friendly Polymer-Based Films: A Review. *Food Res. Int.* 142, 110202. doi:10.1016/j.foodres.2021.110202

Oliveira, C. F., Corrêa, A. P. F., Coletto, D., Daroit, D. J., Cladera-Olivera, F., and Brandelli, A. (2015). Soy Protein Hydrolysis with Microbial Protease to Improve Antioxidant and Functional Properties. *J. Food Sci. Technol.* 52 (5), 2668–2678. doi:10.1007/s13197-014-1317-7

Oliveira Filho, J. G. d., Rodrigues, J. M., Valadares, A. C. F., Almeida, A. B. d., Lima, T. M. d., Takeuchi, K. P., et al. (2019). Active Food Packaging: Alginate Films with Cottonseed Protein Hydrolysates. *Food Hydrocolloids* 92, 267–275. doi:10.1016/j.foodhyd.2019.01.052

Oliveira Filho, J. G., Rodrigues, J. M., Valadares, A. C. F., de Almeida, A. B., Valencia-Mejia, E., Fernandes, K. F., et al. (2020). Bioactive Properties of Protein Hydrolysate of Cottonseed Byproduct: Antioxidant, Antimicrobial, and Angiotensin-Converting Enzyme (ACE) Inhibitory Activities. *Waste Biomass Valor.* 12, 1395–1404. doi:10.1007/s12649-020-01066-6

Otero, D. M., Bulsing, B. A., Huerta, K. d. M., Rosa, C. A., Zambiazi, R. C., Burkert, C. A. V., et al. (2019). Carotenoid-producing Yeasts in the Brazilian Biodiversity: Isolation, Identification and Cultivation in Agroindustrial Waste. *Braz. J. Chem. Eng.* 36, 117–129. doi:10.1590/0104-6632.20190361s20170433

Özalp Özen, B., Eren, M., Pala, A., Özmen, İ., and Soyer, A. (2011). Effect of Plant Extracts on Lipid Oxidation during Frozen Storage of Minced Fish Muscle. *Int. J. Food Sci. Techn.* 46 (4), 724–731. doi:10.1111/j.1365-2621.2010.02541.x

Palhares, J. C. P., Oliveira, V. B. V., Freire-Junior, M., Cerdeira, A. L., and Prado, H. A. (2020). *Responsible Consumption and Production: Contributions of Embrapa*. Brasília, DF: Embrapa.

Pasini Deolindo, C. T., Monteiro, P. I., Santos, J. S., Cruz, A. G., Cristina da Silva, M., and Granato, D. (2019). Phenolic-rich Petit Suisse Cheese Manufactured with Organic Bordeaux Grape Juice, Skin, and Seed Extract: Technological,

Sensory, and Functional Properties. *LWT - Food Sci. Techn.* 115, 108493. doi:10.1016/j.lwt.2019.108493

Pataro, G., Carullo, D., Falcone, M., and Ferrari, G. (2020). Recovery of Lycopene from Industrially Derived Tomato Processing By-Products by Pulsed Electric fields-assisted Extraction. *Innovative Food Sci. Emerging Tech.* 63, 102369. doi:10.1016/j.ifset.2020.102369

Paula, L. C. d., Lemes, A. C., Silva Neri, H. F. d., Ghedini, P. C., Batista, K. d. A., and Fernandes, K. F. (2020). Antioxidant and Anitoperoxidative Effect of Polypeptides from Common Beans (Phaseolus vulgaris, Cv BRS Pontal). *Braz. J. Develop.* 6 (7), 50569–50580. doi:10.34117/bjdv6n7-635

Pauline, M., Roger, P., Sophie Natacha Nina, N. E., Arielle, T., Eugene, E. E., and Robert, N. (2020). Physico-chemical and Nutritional Characterization of Cereals Brans Enriched Breads. *Scientific Afr.* 7, e00251. doi:10.1016/j.sciaf.2019.e00251

Peng, X., Ma, J., Cheng, K.-W., Jiang, Y., Chen, F., and Wang, M. (2010). The Effects of Grape Seed Extract Fortification on the Antioxidant Activity and Quality Attributes of Bread. *Food Chem.* 119 (1), 49–53. doi:10.1016/j.foodchem.2009.05.083

Pereira, G. F., de Bastiani, D., Gabardo, S., Squina, F., and Ayub, M. A. Z. (2018). Solid-state Cultivation of Recombinant Aspergillus nidulans to Co-produce Xylanase, Arabinofuranosidase, and Xylooligosaccharides from Soybean Fibre. *Biocatal. Agric. Biotechnol.* 15, 78–85. doi:10.1016/j.bcab.2018.05.012

Pérez, J., Muñoz-Dorado, J., De la Rubia, T., and Martínez, J. (2002). Biodegradation and Biological Treatments of Cellulose, Hemicellulose and Lignin: an Overview. *Int. Microbiol.* 5 (2), 53–63. doi:10.1007/s10123-002-0062-3

Petti, S., and Scully, C. (2009). Polyphenols, Oral Health and Disease: A Review. *J. dentistry* 37 (6), 413–423. doi:10.1016/j.jdent.2009.02.003

Pezeshk, S., Ojagh, S. M., Rezaei, M., and Shabanpour, B. (2019). Fractionation of Protein Hydrolysates of Fish Waste Using Membrane Ultrafiltration: Investigation of Antibacterial and Antioxidant Activities. *Probiotics Antimicro. Prot.* 11 (3), 1015–1022. doi:10.1007/s12602-018-9483-y

Picot-Allain, C., Mahomoodally, M. F., Ak, G., and Zengin, G. (2021). Conventional versus green Extraction Techniques - a Comparative Perspective. *Curr. Opin. Food Sci.* 40, 144–156. doi:10.1016/j.cofs.2021.02.009

Pinto, M., Coelho, E., Nunes, A., Brandão, T., and Coimbra, M. A. (2015). Valuation of Brewers Spent Yeast Polysaccharides: A Structural Characterization Approach. *Carbohydr. Polym.* 116, 215–222. doi:10.1016/j.carbpol.2014.03.010

Pires, A. F., Marnotes, N. G., Rubio, O. D., Garcia, A. C., and Pereira, C. D. (2021). Dairy By-Products: A Review on the Valorization of Whey and Second Cheese Whey. *Foods* 10 (5), 1067. doi:10.3390/foods10051067

Prado, D. M. F., Almeida, A. B., Oliveira-Filho, J. G., Alves, C. C. F., Egea, M. B., and Lemes, A. C. (2020). Extraction of Bioactive Proteins from Seeds (Corn, Sorghum, and sunflower) and sunflower Byproduct: Enzymatic Hydrolysis and Antioxidant Properties. *Curr. Nutr. Food Sci.* 17 (3), 310–320. doi:10.2174/1573401316999200731005803

Rangel-Huerta, O., Pastor-Villaescusa, B., Aguilera, C., and Gil, A. (2015). A Systematic Review of the Efficacy of Bioactive Compounds in Cardiovascular Disease: Phenolic Compounds. *Nutrients* 7 (7), 5177–5216. doi:10.3390/nu7075177

Reque, P., and Brandelli, A. (2021). Encapsulation of Probiotics and Nutraceuticals: Applications in Functional Food Industry. *Trends Food Sci. Techn.* 114, 1–10. doi:10.1016/j.tifs.2021.05.022

Reque, P. M., Orlandini Werner, J. A., Barreto Pinilla, C. M., Folmer Corrêa, A. P., Rodrigues, E., and Brandelli, A. (2017). Biological Activities of Wheat Middlings Bioprocessed with Bacillus Spp. *LWT* 77, 525–531. doi:10.1016/j.lwt.2016.12.010

Reque, P. M., Pinilla, C. M. B., Gautério, G. V., Kalil, S. J., and Brandelli, A. (2019). Xylooligosaccharides Production from Wheat Middlings Bioprocessed with Bacillus Subtilis. *Food Res. Int.* 126, 108673. doi:10.1016/j.foodres.2019.108673

Ribeiro, B. D., Barreto, D. W., and Coelho, M. A. Z. (2013). Enzyme-Enhanced Extraction of Phenolic Compounds and Proteins from Flaxseed Meal. *ISRN Biotechnol.* 2013, 1–6. doi:10.5402/2013/521067

Ribeiro, B. D., Coelho, M. A. Z., and Barreto, D. W. (2012). Obtenção de extratos de guaraná ricos em cafeína por processo enzimático e adsorção de taninos. *Braz. J. Food Technol.* 15, 261–270. doi:10.1590/s1981-67232012005000020

Rodrigues, T. V. D., Amore, T. D., Teixeira, E. C., and Burkert, J. F. d. M. (2019). Carotenoid Production by Rhodotorula Mucilaginosa in Batch and Fed-Batch Fermentation Using Agroindustrial Byproducts. *Food Technol. Biotechnol. (Online)* 57 (3), 388–398. doi:10.17113/ftb.57.03.19.6068

Sadh, P. K., Duhan, S., and Duhan, J. S. (2018a). Agro-industrial Wastes and Their Utilization Using Solid State Fermentation: a Review. *Bioresour. Bioproc.* 5 (1), 1. doi:10.1186/s40643-017-0187-z

Sadh, P., Kumar, S., Chawla, P., and Duhan, J. (2018b). Fermentation: A Boon for Production of Bioactive Compounds by Processing of Food Industries Wastes (By-Products). *Molecules* 23 (10), 2560. doi:10.3390/molecules23102560

Sagar, N. A., Pareek, S., Sharma, S., Yahia, E. M., and Lobo, M. G. (2018). Fruit and Vegetable Waste: Bioactive Compounds, Their Extraction, and Possible Utilization. *Compr. Rev. Food Sci. Food Saf.* 17 (3), 512–531. doi:10.1111/1541-4337.12330

Sánchez, Ó. J., Montoya, S., and Vargas, L. M. (2021). "Polysaccharide Production by Submerged Fermentation," in *Polysaccharides: Bioactivity and Biotechnology*. Editors K. G. Ramawat and J. -M. Mérillon (Cham: Springer International Publishing), 1–19.

Saraf, S., and Kaur, C. (2010). Phytoconstituents as Photoprotective Novel Cosmetic Formulations. *Phcog Rev.* 4 (7), 1. doi:10.4103/0973-7847.65319

Sharif, T., Bhatti, H. N., Bull, I. D., and Bilal, M. (2021). Recovery of High-Value Bioactive Phytochemicals from Agro-Waste of Mango (Mangifera Indica L.) Using Enzyme-Assisted Ultrasound Pretreated Extraction. *Biomass Conv. Bioref.* doi:10.1007/s13399-021-01589-5

Sharma, P., Gaur, V. K., Sirohi, R., Varjani, S., Hyoun Kim, S., and Wong, J. W. C. (2021). Sustainable Processing of Food Waste for Production of Bio-Based Products for Circular Bioeconomy. *Bioresour. Techn.* 325, 124684. doi:10.1016/j.biortech.2021.124684

Sharma, R., and Ghoshal, G. (2020). Optimization of Carotenoids Production by Rhodotorula Mucilaginosa (MTCC-1403) Using Agro-Industrial Waste in Bioreactor: A Statistical Approach. *Biotechnol. Rep.* 25, e00407. doi:10.1016/j.btre.2019.e00407

Shimotori, Y., Watanabe, T., Kohari, Y., Chiou, T.-Y., Ohtsu, N., Nagata, Y., et al. (2020). Enzyme-assisted Extraction of Bioactive Phytochemicals from Japanese Peppermint (Mentha Arvensis L. Cv. 'Hokuto'). *J. Oleo Sci.* 69 (6), 635–642. doi:10.5650/jos.ess19181

Shin, H.-Y., Kim, S.-M., Lee, J. H., and Lim, S.-T. (2019). Solid-state Fermentation of Black rice Bran with Aspergillus Awamori and Aspergillus Oryzae: Effects on Phenolic Acid Composition and Antioxidant Activity of Bran Extracts. *Food Chem.* 272, 235–241. doi:10.1016/j.foodchem.2018.07.174

Silva, J., Honorato da Silva, F. L., Santos Ribeiro, J. E., Nóbrega de Melo, D. J., Santos, F. A., and Lucena de Medeiros, L. (2020). Effect of Supplementation, Temperature and pH on Carotenoids and Lipids Production by Rhodotorula Mucilaginosa on Sisal Bagasse Hydrolyzate. *Biocatal. Agric. Biotechnol.* 30, 101847. doi:10.1016/j.bcab.2020.101847

Silva, L. B. A. R., Pinheiro-Castro, N., Novaes, G. M., Pascoal, G. d. F. L., and Ong, T. P. (2019). Bioactive Food Compounds, Epigenetics and Chronic Disease Prevention: Focus on Early-Life Interventions with Polyphenols. *Food Res. Int.* 125, 108646. doi:10.1016/j.foodres.2019.108646

Silveira, R. L., Stoyanov, S. R., Gusarov, S., Skaf, M. S., and Kovalenko, A. (2013). Plant Biomass Recalcitrance: Effect of Hemicellulose Composition on Nanoscale Forces that Control Cell Wall Strength. *J. Am. Chem. Soc.* 135 (51), 19048–19051. doi:10.1021/ja405634k

Singh, R. D., Muir, J., and Arora, A. (2020). Concentration of Xylooligosaccharides with a Low Degree of Polymerization Using Membranes and Their Effect on Bacterial Fermentation. *Biofuels, Bioproducts and Biorefining* 15, 61–73. doi:10.1002/bbb.2145

Singh, R., Kumar, M., Mittal, A., and Mehta, P. K. (2016). Microbial Enzymes: Industrial Progress in 21st century. *3 Biotech.* 6 (2), 174. doi:10.1007/s13205-016-0485-8

Sinha, S., Singh, G., Arora, A., and Paul, D. (2021). Carotenoid Production by Red Yeast Isolates Grown in Agricultural and "Mandi" Waste. *Waste Biomass Valor.* 12 (7), 3939–3949. doi:10.1007/s12649-020-01288-8

Soccol, C. R., Costa, E. S. F. d., Letti, L. A. J., Karp, S. G., Woiciechowski, A. L., and Vandenberghe, L. P. d. S. (2017). Recent Developments and Innovations in Solid State Fermentation. *Biotechnol. Res. Innovation* 1 (1), 52–71. doi:10.1016/j.biori.2017.01.002

Souyoul, S. A., Saussy, K. P., and Lupo, M. P. (2018). Nutraceuticals: A Review. *Dermatol. Ther. (Heidelb)* 8 (1), 5–16. doi:10.1007/s13555-018-0221-x

Su, C. H., Pham, T. T. T., and Cheng, H. H. (2020). Aqueous Enzymatic Extraction of Rosmarinic Acid from Salvia Officinalis : Optimisation Using Response Surface Methodology. *Phytochem. Anal.* 31 (5), 575–582. doi:10.1002/pca.2922

Tanase, C., Boz, I., Stingu, A., Volf, I., and Popa, V. I. (2014). Physiological and Biochemical Responses Induced by spruce Bark Aqueous Extract and Deuterium Depleted Water with Synergistic Action in sunflower (Helianthus Annuus L.) Plants. *Ind. Crops Prod.* 60, 160–167. doi:10.1016/j.indcrop.2014.05.039

Tanase, C., Coşarcă, S., and Muntean, D.-L. (2019). A Critical Review of Phenolic Compounds Extracted from the Bark of Woody Vascular Plants and Their Potential Biological Activity. *Molecules* 24 (6), 1182. doi:10.3390/molecules24061182

Tavanandi, H. A., and Raghavarao, K. S. M. S. (2020). Ultrasound-assisted Enzymatic Extraction of Natural Food Colorant C-Phycocyanin from Dry Biomass of Arthrospira Platensis. *Lebensmittel-Wissenschaft und-Technologie* 118, 108802. doi:10.1016/j.lwt.2019.108802

Thomas, L., Larroche, C., and Pandey, A. (2013). Current Developments in Solid-State Fermentation. *Biochem. Eng. J.* 81, 146–161. doi:10.1016/j.bej.2013.10.013

Tosh, S. M., Brummer, Y., Miller, S. S., Regand, A., Defelice, C., Duss, R., et al. (2010). Processing Affects the Physicochemical Properties of β-Glucan in Oat Bran Cereal. *J. Agric. Food Chem.* 58 (13), 7723–7730. doi:10.1021/jf904553u

Trombino, S., Cassano, R., Procopio, D., Di Gioia, M. L., and Barone, E. (2021). Valorization of Tomato Waste as a Source of Carotenoids. *Molecules* 26 (16), 5062. doi:10.3390/molecules26165062

Urbonaviciene, D., and Viskelis, P. (2017). The Cis-Lycopene Isomers Composition in Supercritical CO2 Extracted Tomato By-Products. *LWT - Food Sci. Techn.* 85, 517–523. doi:10.1016/j.lwt.2017.03.034

Valencia-Mejía, E., Batista, K. A., Fernández, J. J. A., and Fernandes, K. F. (2019). Antihyperglycemic and Hypoglycemic Activity of Naturally Occurring Peptides and Protein Hydrolysates from Easy-To-cook and Hard-To-cook Beans (Phaseolus vulgaris L.). *Food Res. Int.* 121, 238–246. doi:10.1016/j.foodres.2019.03.043

Varelas, V., Tataridis, P., Liouni, M., and Nerantzis, E. T. (2016). Valorization of Winery Spent Yeast Waste Biomass as a New Source for the Production of β-Glucan. *Waste Biomass Valor.* 7, 807–817. doi:10.1007/s12649-016-9530-4

Varzakas, T., Zakynthinos, G., and Verpoort, F. (2016). Plant Food Residues as a Source of Nutraceuticals and Functional Foods. *Foods* 5 (4), 88. doi:10.3390/foods5040088

Velliquette, R. A., Fast, D. J., Maly, E. R., Alashi, A. M., and Aluko, R. E. (2020). Enzymatically Derived sunflower Protein Hydrolysate and Peptides Inhibit NFκB and Promote Monocyte Differentiation to a Dendritic Cell Phenotype. *Food Chem.* 319, 126563. doi:10.1016/j.foodchem.2020.126563

Veneziani, G., Novelli, E., Esposto, S., Taticchi, A., and Servili, M. (2017). "Chapter 11 - Applications of Recovered Bioactive Compounds in Food Products," in *Olive Mill Waste*. Editor C. M. Galanakis (Academic Press), 231–253. doi:10.1016/b978-0-12-805314-0.00011-x

Verni, M., Pontonio, E., Krona, A., Jacob, S., Pinto, D., Rinaldi, F., et al. (2020). Bioprocessing of Brewers' Spent Grain Enhances its Antioxidant Activity: Characterization of Phenolic Compounds and Bioactive Peptides. *Front. Microbiol.* 11, 1831. doi:10.3389/fmicb.2020.01831

Vieira, E. F., Melo, A., and Ferreira, I. M. P. L. V. O. (2017). Autolysis of Intracellular Content of Brewer's Spent Yeast to Maximize ACE-Inhibitory and Antioxidant Activities. *LWT - Food Sci. Techn.* 82, 255–259. doi:10.1016/j.lwt.2017.04.046

Vilas-Boas, A. A., Pintado, M., and Oliveira, A. L. S. (2021). Natural Bioactive Compounds from Food Waste: Toxicity and Safety Concerns. *Foods* 10 (7), 1564. doi:10.3390/foods10071564

Vuolo, M. M., Lima, V. S., and Maróstica Junior, M. R. (2019). "Chapter 2 - Phenolic Compounds: Structure, Classification, and Antioxidant Power," in *Bioactive Compounds*. Editor M. R. S. Campos (Woodhead Publishing), 33–50. doi:10.1016/b978-0-12-814774-0.00002-5

Waldron, K. (2007). "Waste Minimization, Management and Co-product Recovery in Food Processing: an Introduction," in *Handbook of Waste Management and Co-product Recovery in Food Processing*. Editor K. Waldron (Cambridge, England: Woodhead Publishing), 3–20. doi:10.1533/9781845692520.1.3

Wang, T., and Lü, X. (2021). "Overcome Saccharification Barrier," in *Advances in 2nd Generation of Bioethanol Production*. Editor X. Lü (Woodhead Publishing), 137–159. doi:10.1016/b978-0-12-818862-0.00005-4

Wang, W., Gao, Y.-T., Wei, J.-W., Chen, Y.-F., Liu, Q.-L., and Liu, H.-M. (2021). Optimization of Ultrasonic Cellulase-Assisted Extraction and Antioxidant Activity of Natural Polyphenols from Passion Fruit. *Molecules* 26 (9), 2494. doi:10.3390/molecules26092494

Wang, Y.-Y., Ma, H., Ding, Z.-C., Yang, Y., Wang, W.-H., Zhang, H.-N., et al. (2019). Three-phase Partitioning for the Direct Extraction and Separation of Bioactive Exopolysaccharides from the Cultured Broth of Phellinus Baumii. *Int. J. Biol. Macromolecules* 123, 201–209. doi:10.1016/j.ijbiomac.2018.11.065

Webb, C., and Webb, C. (2017). Design Aspects of Solid State Fermentation as Applied to Microbial Bioprocessing. *Jabb* 4, 1–25. doi:10.15406/jabb.2017.04.00094

Wen, L., Zhang, Z., Sun, D.-W., Sivagnanam, S. P., and Tiwari, B. K. (2020). Combination of Emerging Technologies for the Extraction of Bioactive Compounds. *Crit. Rev. Food Sci. Nutr.* 60 (11), 1826–1841. doi:10.1080/10408398.2019.1602823

Yan, J.-K., Wang, Y.-Y., Qiu, W.-Y., Ma, H., Wang, Z.-B., and Wu, J.-Y. (2018). Three-phase Partitioning as an Elegant and Versatile Platform Applied to Nonchromatographic Bioseparation Processes. *Crit. Rev. Food Sci. Nutr.* 58 (14), 2416–2431. doi:10.1080/10408398.2017.1327418

Yang, G., Tan, H., Li, S., Zhang, M., Che, J., Li, K., et al. (2020). Application of Engineered Yeast Strain Fermentation for Oligogalacturonides Production from Pectin-Rich Waste Biomass. *Bioresour. Techn.* 300, 122645. doi:10.1016/j.biortech.2019.122645

Yang, J., Wu, X.-B., Chen, H.-L., Sun-Waterhouse, D., Zhong, H.-B., and Cui, C. (2019). A Value-Added Approach to Improve the Nutritional Quality of Soybean Meal Byproduct: Enhancing its Antioxidant Activity through Fermentation by Bacillus Amyloliquefaciens SWJS22. *Food Chem.* 272, 396–403. doi:10.1016/j.foodchem.2018.08.037

Yu, J., Mikiashvili, N., Bonku, R., and Smith, I. N. (2021). Allergenicity, Antioxidant Activity and ACE-Inhibitory Activity of Protease Hydrolyzed Peanut Flour. *Food Chem.* 360, 129992. doi:10.1016/j.foodchem.2021.129992

Zainal-Abidin, M. H., Hayyan, M., Hayyan, A., and Jayakumar, N. S. (2017). New Horizons in the Extraction of Bioactive Compounds Using Deep Eutectic Solvents: A Review. *Analytica Chim. Acta* 979, 1–23. doi:10.1016/j.aca.2017.05.012

Zamuz, S., López-Pedrouso, M., Barba, F. J., Lorenzo, J. M., Domínguez, H., and Franco, D. (2018). Application of hull, Bur and Leaf Chestnut Extracts on the Shelf-Life of Beef Patties Stored under MAP: Evaluation of Their Impact on Physicochemical Properties, Lipid Oxidation, Antioxidant, and Antimicrobial Potential. *Food Res. Int.* 112, 263–273. doi:10.1016/j.foodres.2018.06.053

Zanutto-Elgui, M. R., Vieira, J. C. S., Prado, D. Z. d., Buzalaf, M. A. R., Padilha, P. d. M., Elgui de Oliveira, D., et al. (2019). Production of Milk Peptides with Antimicrobial and Antioxidant Properties through Fungal Proteases. *Food Chem.* 278, 823–831. doi:10.1016/j.foodchem.2018.11.119

Zeng, Y., Himmel, M. E., and Ding, S.-Y. (2017). Visualizing Chemical Functionality in Plant Cell walls. *Biotechnol. Biofuels* 10 (1), 263. doi:10.1186/s13068-017-0953-3

Zhang, D., Bi, W., Kai, K., Ye, Y., and Liu, J. (2020). Effect of Chlorogenic Acid on Controlling Kiwifruit Postharvest Decay Caused by Diaporthe Sp. *Lebensmittel-wissenschaft + [i.e. Technologie* 132, 109805. doi:10.1016/j.lwt.2020.109805

Zhang, S., Zhang, M., Yang, R., Zhang, S., and Lin, S. (2019a). Preparation, Identification, and Activity Evaluation of Antioxidant Peptides from Protein Hydrolysate of Corn Germ Meal. *J. Food Process. Preservation* 43 (10), e14160. doi:10.1111/jfpp.14160

Zhang, X., Liu, Y., Yong, H., Qin, Y., Liu, J., and Liu, J. (2019b). Development of Multifunctional Food Packaging Films Based on Chitosan, TiO2 Nanoparticles and Anthocyanin-Rich Black Plum Peel Extract. *Food Hydrocolloids* 94, 80–92. doi:10.1016/j.foodhyd.2019.03.009

Conflict of Interest: The authors declare that the research was conducted in the absence of any commercial or financial relationships that could be construed as a potential conflict of interest.

Publisher's Note: All claims expressed in this article are solely those of the authors and do not necessarily represent those of their affiliated organizations, or those of the publisher, the editors, and the reviewers. Any product that may be evaluated in this article, or claim that may be made by its manufacturer, is not guaranteed or endorsed by the publisher.

frontiers in Bioengineering and Biotechnology

ORIGINAL RESEARCH
published: 08 February 2022
doi: 10.3389/fbioe.2021.769816

Characterization and Secretory Expression of a Thermostable Tannase from *Aureobasidium melanogenum* T9: Potential Candidate for Food and Agricultural Industries

Lu Liu[1,2], *Jing Guo*[1], *Xue-Feng Zhou*[3], *Ze Li*[4], *Hai-Xiang Zhou*[1]* and *Wei-Qing Song*[1]*

[1]Department of Clinical Laboratory, Qingdao Municipal Hospital, Qingdao, China, [2]School of Medicine and Pharmacy, Ocean University of China, Qingdao, China, [3]Clinical Trial Research Center, The Affiliated Central Hospital of Qingdao University, Qingdao, China, [4]College of Advanced Agricultural Sciences, Linyi Vocational University of Science and Technology, Linyi, China

Being a key industrial enzyme, tannase is extensively applied in various fields. Despite the characterizations of a large number of tannases, there are hardly a few tannases with exceptional thermostability. In this detailed study, a tannase-encoding gene named *tanA* was identified from *Aureobasidium melanogenum* T9 and heterologously expressed in *Yarrowia lipolytica* host of food grade. The purified tannase TanA with a molecular weight of above 63.0 kDa displayed a specific activity of 941.4 U/mg. Moreover, TanA showed optimum activity at 60°C and pH 6.0. Interestingly, TanA exhibited up to 61.3% activity after incubation for 12 h at 55°C, signifying its thermophilic property and distinguished thermostability. Additionally, TanA was a multifunctional tannase with high specific activities to catalyze the degradation of various gallic acid esters. Therefore, this study presents a novel tannase, TanA, with remarkable properties, posing as a potential candidate for food and agricultural processing.

Keywords: tannin, tannase, thermostability, *Aureobasidium melanogenum*, *Yarrowia lipolytica*

OPEN ACCESS

Edited by:
Shangyong Li,
Qingdao University, China

Reviewed by:
Yasser Gaber,
Beni-Suef University, Egypt
Satya P. Singh,
Saurashtra University, India

***Correspondence:**
Wei-Qing Song
songweiqing68@163.com
Hai-Xiang Zhou
pro.zhouhaixiang@163.com

Specialty section:
This article was submitted to Bioprocess Engineering, a section of the journal Frontiers in Bioengineering and Biotechnology

Received: *02 September 2021*
Accepted: *30 December 2021*
Published: *08 February 2022*

Citation:
Liu L, Guo J, Zhou X-F, Li Z, Zhou H-X and Song W-Q (2022) Characterization and Secretory Expression of a Thermostable Tannase from Aureobasidium melanogenum T9: Potential Candidate for Food and Agricultural Industries. Front. Bioeng. Biotechnol. 9:769816. doi: 10.3389/fbioe.2021.769816

INTRODUCTION

As a type of polyphenol compound generated to resist a bad growth environment, tannins are extensively present in higher plants (Chung et al., 1998). The formation of stable complexes with various biological macromolecules, such as polysaccharides and proteins, provides lower nutritive value to food, thus making them nutritionally undesirable (Pan et al., 2020). According to some reports, tannins are one of the primary causes of low food intake, slow growth, low level of fodder utilization rate, and low protein breakdown in laboratory animals (Becker and Makkar, 1999; Min et al., 2005; Sengil and Oezacar, 2009). Therefore, the removal of tannins becomes an integral process during food and feed processing. Fortunately, there still exist some special microorganisms which can grow and reproduce stably in an environment containing tannins, making the full utmost of the secreted enzymes to decompose tannins into small-molecule phenolic compounds (Chhokar et al., 2013).

Tannase (EC 3.1.1.20), also known as tannin acylhydrolase, is a hydrolase that can effectively hydrolyze ester bonds and carboxyphenol bonds in hydrolyzable tannins, including ellagitannins (ETs), gallotannins (GTs), and other gallic acid esters to produce polyphenol compounds such as gallic acid (Aguilar and Gutierrez-Sanchez, 2001; Zhang et al., 2015; Govindarajan et al., 2016). The

enzymatic degradation of tannins is considered a safe and environmentally friendly method that can effectively overcome the shortcomings of traditional hydrolysis methods and significantly improve the yield and purity of products (Raghuwanshi et al., 2011; Jana et al., 2013; Ghosh and Mandal, 2015; Ebrahimzade et al., 2018). Therefore, tannases have played a significant role in industrial production, especially in the fields of feed, food, brewing, and pharmaceuticals (Chhokar et al., 2013; Wang et al., 2022). Rapeseed meal is considered to be one of the sources of high-quality plant protein feed due to its high protein content and balanced amino acid composition. However, rapeseed meal contains a variety of anti-nutritional factors, like tannins, that seriously affect its palatability as well as nutritive value, severely limiting the application of rapeseed meal in animal feeding (Shim et al., 2003). Interestingly, Lorusso *et al.* (1996) reported that the tannase produced by *Trametes versicolor* could degrade more than 80% of tannins in rapeseed meal within 30 min, strengthening the application of tannase in the processing of rapeseed meal feed. Furthermore, the transformation of ester catechins (also belonging to tannins) in green tea to non-ester catechins for improving the taste of tea drinks is another important use for tannases (Ozturk et al., 2016). Therefore, these properties of tannases are of great interest among researchers.

Currently, owing to the characteristics of biochemical diversity and liable genetic manipulations, microbial fermentation is the major approach for the continuous production of tannases (Beniwal et al., 2013). Numerous studies have been conducted for screening tannase-producing microorganisms, of which bacteria and fungi have shown enhanced enzyme production ability (Banerjee et al., 2012; Kanpiengjai et al., 2019). However, tannases produced by bacteria demonstrated limitations in low activity and poor thermostability, imposing major concerns of large-scale application (Rivas et al., 2019). Thus, there are relatively scarce studies of bacterial tannases. On the other hand, the complex heredity of fungi makes genetic manipulations difficult (Beniwal et al., 2010). These collectively present challenges in identifying tannases with better properties for industrial application—for example, tannases play a pivotal role in green tea deep processing to improve the appearance, aroma, and flavor of tea and the extraction efficiency of polyphenols (Cao et al., 2019). During the extraction of green tea, the extraction yield increased with increasing temperature within a certain range (Shao et al., 2020). However, since the enzyme catalysis reaction is usually temperature-limited, tea processing and extraction consume a prolonged time (over 2 h) at a lower range of temperature from 30 to 40°C, thereby reducing product quality and production efficiency (Hong et al., 2013). Therefore, it becomes necessary to screen genetically stable microorganisms with the capability to produce tannases of high vigor and thermal stability. Jana *et al.* (2013) reported that the high-temperature and solvent-resistant tannase produced from *Bacillus subtilis* PAB2 had a half-life of up to 4.5 h in an environment of 60°C. Shao *et al.* (2020) screened *Aspergillus niger* FJ0118 that could generate tannase rAntan1 with strong temperature tolerance, and its half-life at 60°C was persisting for about 5.4 h. Nevertheless, the majority of the reported thermostable tannases cannot reach food grade due to safety concerns.

Aureobasidium melanogenum T9, with the capability to degrade tannins, has been successfully isolated from the starter of red wine (Zhang et al., 2019). In this study, the gene of encoding tannin-degrading enzyme, *tanA*, was identified and heterologously expressed in the *Yarrowia lipolytica* yeast of food grade. The detailed characterization of tannase TanA displayed superior thermal stability and unique robustness, thus laying a solid foundation for its application in the industry.

MATERIALS AND METHODS

Bioinformatics Analysis of TanA

In the previous research, the genome of *A. melanogenum* T9 strain was sequenced and annotated by Novogene (Zhang et al., 2019); *in silico* studies were performed to determine the encoding gene sequence of TanA. By using HMMER3, the protein sequence was compared with carbohydrate-active enzyme database to acquire the message. The filter condition was set to *E* value $<1\ E^{-5}$. The theoretical molecular weight (Mw) and isoelectric point (pI) value were obtained through online prediction (http://web.expasy.org/compute_pi/). SignalP 4.1 server was applied for signal peptide analysis (http://www.cbs.dtu.dk/services/SignalP-4.1/). NetNGlyc 1.0 server was applied to predict N-glycosylation sites (http://www.cbs.dtu.dk/services/NetNGlyc/). The conserved domain database of the National Center for Biotechnology Information (NCBI, Bethesda, MD, United States) was used for domain analysis (https://www.ncbi.nlm.nih.gov/cdd).

To study the evolutionary relationship among TanA and other tannases derived from microorganisms, a bootstrapped phylogenetic tree was constructed by neighbor-joining method with MEGA 6.0 software (Tamura et al., 2013) on the basis of the amino acid sequences of related tannases obtained from NCBI (https://www.ncbi.nlm.nih.gov/). Multiple sequence alignment was carried out using DNAMAN 6.0 software (Lynnon Biosoft, Foster City, CA, United States). The 3D model of tannase TanA (accession no.: QEP28943.1) of *A. melanogenum* T9 was built on the basis of the crystal structure of feruloyl esterase AoFaeB from *Aspergillus oryzae* RIB40 (PDB: 3WMT) (Suzuki et al., 2014), using basic modeling module in modeller 9. 20. Fifty homologous models were firstly constructed, and one model with the highest score was obtained.

Secretory Expression of TanA

The *tanA* gene without signal sequence was synthesized by Synbio Technologies (Suzhou, China) following codon optimization. The linearized DNA fragment was successfully transformed into the *Y. lipolytica* URA^- strain (Zhang et al., 2018). The *Y. lipolytica* cultivation and the purification steps of TanA generally followed those of Zhou *et al.* (2020). After culturing in GPPB liquid media [30.0 g/L glucose, 2.0 g/L yeast extract, 1.0 g/L $(NH_4)_2SO_4$, 3.0 g/L K_2HPO_4, 2.0 g/L KH_2PO_4, 0.1 g/L $MgSO_4{\cdot}7H_2O$, pH 6.8] for 72 h at 30°C, the tannase activities of the positive transformants were discovered (Pan et al., 2020). In comparison, the recombinant strain 72 displayed optimal

extracellular activity. Afterwards, 100 ml of the supernatant was concentrated firstly by ultrafiltration with a centrifugal filter 3 K device (Millipore, Burlington, MA, United States), and then it was injected into the His60 Ni Superflow affinity chromatography column purchased from Clontech Laboratories, Inc. (TaKaRa, Dalian, China), which was already equilibrated with 50 mM phosphate buffer (pH 7.4) containing 300 mM NaCl and 20 mM imidazole. After successive washing using the same buffer containing 40 mM imidazole and elution using the same buffer containing a linear gradient of imidazole (50–400 mM), the 6×His-tagged TanA was obtained (Zhang et al., 2021). The fractions with tannase activity were pooled and concentrated *via* Millipore centrifugal filter 3 K device. Meanwhile, the enzyme solution was desalted, and the buffer was replaced with 50 mM Tris-HCl (pH 7.4) for further characterization of TanA. During the purification of TanA, a BCA protein assay kit (TaKaRa, Dalian, China) was used to determine the total protein concentration. Moreover, 12% sodium dodecyl sulfate–polyacrylamide gel electrophoresis (SDS-PAGE) was used to verify the Mw and purity of TanA.

Determination of Tannase Activity

TanA activity was determined by measuring the amount of gallic acid produced in the reaction, generally according to the description in Sharma *et al.* (2000). Briefly, 0.5 ml of properly diluted enzyme solution was mixed with 4.5 ml of 0.5% (w/v) propyl gallate in 100 mM Na_2HPO_4–citric acid buffer (pH 5.0) at 40°C for 10 min. The gallic acid content was measured by the formation of chromogen violet staining between 0.667% (w/v) rhodanine in ethanol and gallic acid, followed by recording the absorbance at 520 nm by a spectrophotometer. One unit of enzyme activity was defined as the amount of tannase that generates 1 μmol gallic acid per minute.

Temperature and pH Properties for TanA Activity

The optimum temperature was determined by carrying out a TanA-mediated hydrolysis reaction at different temperatures ranging from 20 to 70°C. For the purpose of assessing thermostability, the residual activity of purified TanA was investigated after incubating at 20–70°C for 12 h. Additionally, propyl gallate solutions were prepared with 100 mM disparate pH buffers (glycine–NaOH, pH 8.5–11.0; Na_2HPO_4–citric acid, pH 2.0–8.0) to conduct as substrates of enzymatic reaction for the confirmation of optimum pH. The pH stability of TanA was surveyed through measuring the rest of enzyme activity after incubation at 40°C for 12 h in buffers of different pH.

Effects of Chemicals and Metal Ions on TanA Activity

The catalytic reactions were performed using propyl gallate liquors with 1 and 5 mM of different compounds or metal ions as substrates. The reaction that took place in a propyl gallate solution without any compound/metal ion was considered the control.

Degradation of Gallic Acid Esters by TanA

The substrate specificity of tannase TanA was analyzed according to its specific activities assayed under the standard method described above using 0.5% (w/v) of different gallic acid esters as substrates, including methyl gallate (MG), propyl gallate (PG), tannic acid (TA), gallocatechin gallate (GCG), epicatechin gallate (ECG), and epigallocatechin gallate (EGCG). The chemical structures of the substrates are displayed in **Supplementary Figure S1**. Meanwhile, the Michaelis constants (K_m) were calculated against these substrates based on the double-reciprocal plot of Lineweaver–Burk (Lineweaver and Burk, 1934).

In order to further investigate the capability of TanA to degrade these substrates, excess tannase TanA (0.5 U per milligram of each substrate, namely, 2.5 U/ml of each reaction solution) was incubated with 0.5% (w/v) of each gallic acid ester (pH 6.0); the catalytic reaction mixtures were stirred continuously at 55°C for 2 h. After incubation, the solution of each degraded product was immediately loaded onto the Millipore centrifugal filter 3 K device to remove the protein and unsolved materials. High-performance liquid chromatography (HPLC) was employed to confirm the transformation of these substrates, and the analysis method was described briefly as follows: Diamonsil C_{18} column (3.0 × 250 mm, 5 μm), wavelength of 278 nm, mobile phase A (acetonitrile) and B (0.5% acetic acid–water), and flow velocity of 1.0 ml/min by gradient elution as reported (Ni et al., 2015).

RESULTS

Bioinformatics Analysis of TanA

The genomic DNA of *A. melanogenum* T9 strain sequencing illustrated a putative tannase-encoding gene *tanA*. The deduced amino acid sequence was deposited into the Genebank database, and the accession number QEP28943.1 was provided (Zhang et al., 2019). The open reading frame of *tanA* was composed of 1,587 bp encoding a protein of 528 amino acids, of which the first 19 amino acids (highlighted by the blue box in **Figure 1**) were anticipated as the signal peptide, which was consistent with the secretion feature. The theoretical pI and Mw were predicted to be 5.50 and 57.2 kDa, respectively. Interestingly, the BLAST tool of NCBI revealed that TanA possessed the conserved domain closely related to the tannase and ferulic acid esterase family (data not shown).

Then, a phylogenetic tree was built to determine the ascription of TanA. As illustrated in **Figure 2**, the present enzyme TanA, which was on the same branch as the tannase from *Pyrenophora tritici-repentis* (accession no.: PWO06677.1), distinctly pertained to the tannase and feruloyl esterase family. Moreover, sequence comparative analysis was performed among TanA and other members of the tannase and feruloyl esterase family (**Figure 1**), including the tannase from *Trichoderma harzianum* (accession no.: KKP04619.1), the tannase from *Cadophora* sp. DSE1049 (accession no.: PVH72277.1), the tannase from *Fusarium langsethiae* (accession no.: KPA35627.1), the tannase from *P. tritici-repentis* (accession no.: PWO06677.1), the tannase from *Aspergillus ruber* CBS 135680 (accession no.: EYE96818.1), the tannase from *Rutstroemia* sp. NJR-2017a BVV2 (accession no.: PQE10574.1), the tannase from *Penicillium camemberti* (accession no.:

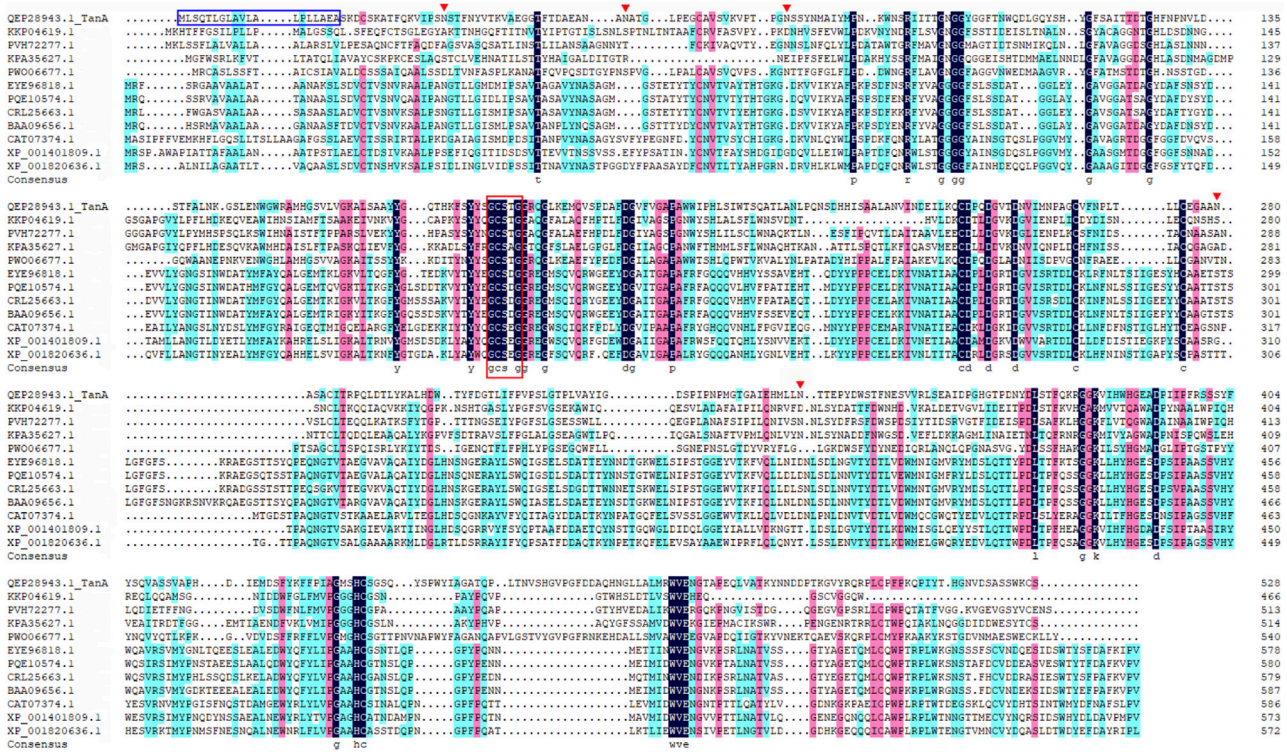

FIGURE 1 | Multiple sequence alignment among TanA and other reported tannases. The signal peptide is boxed in blue, the Gly-X-Ser-X-Gly conserved domain is highlighted by a red box, and the predicted N-glycosylation sites are marked with red inverted triangles.

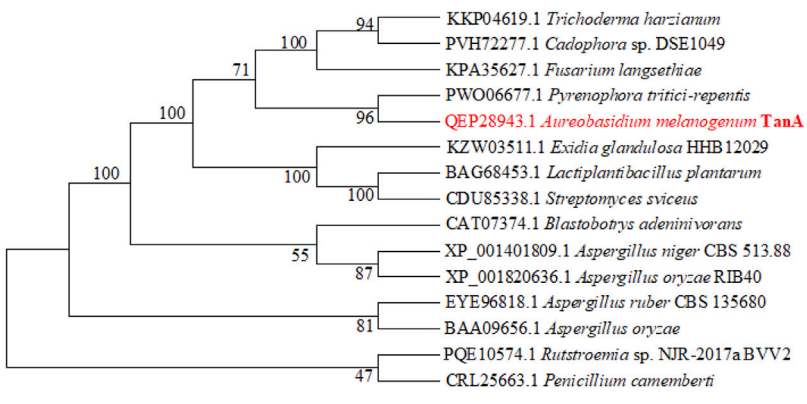

FIGURE 2 | The phylogenetic tree constructed according to the sequences of TanA and other tannases. TanA researched in this study is in red.

CRL25663.1), the tannase from *A. oryzae* (accession no.: BAA09656.1), the tannase from *Blastobotrys adeninivorans* (accession no.: CAT07374.1), the tannase from *A. niger* CBS 513.88 (accession no.: XP_001401809.1), and the tannase from *A. oryzae* RIB40 (accession no.: XP_001820636.1). The multiple sequence alignment showed that TanA retained a typical Gly-X-Ser-X-Gly conserved domain (represented by the red box in **Figure 1**). The 3D structure of TanA in this study has been constructed through homology modeling, and the molecular graphic image was prepared using PyMOL 2.0.3 (Schrödinger, LLC, Portland, OR, United States) and displayed in **Supplementary Figure S2**.

Secretory Expression of TanA in *Y. lipolytica*

The secretory expression of TanA was further studied in the heterogenous host of food grade with significant cellular exocrine ability, *Y. lipolytica* (Madzak, 2015). The tannase activity was measured as 89.4 U/ml following 72 h of incubation in GPPB

TABLE1 | Purification of tannase TanA.

Purification step	Total protein (mg)	Total activity (U)	Specific activity (U/mg)	Purification fold	Yield (%)
Crude enzyme	57.5	8,940.0	155.5	1	100
Ni-IDA agarose	5.81	5,469.5	941.4	6.05	61.2

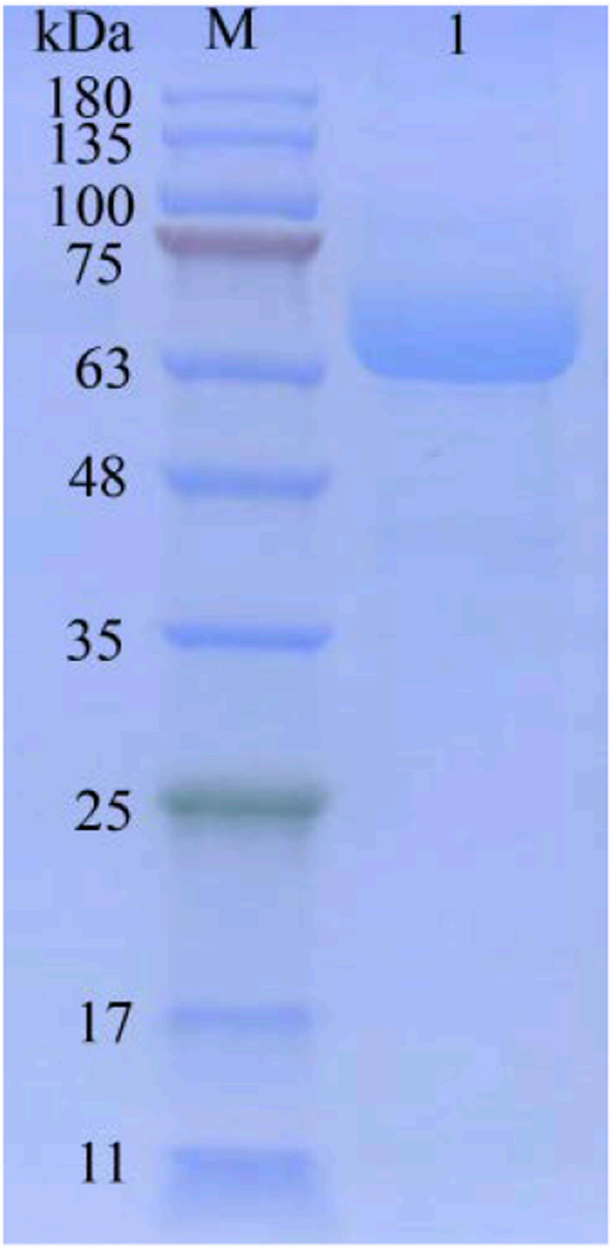

FIGURE 3 | SDS-PAGE of purified TanA. Lane 1: purified TanA; lane M: prestained protein ladder.

medium. The summary of TanA purification is listed in **Table 1**. After Ni-IDA affinity chromatography, the purified TanA was obtained, with a specific activity of 941.4 U/mg. The SDS-PAGE analysis of the purified TanA protein depicted a predominant band observed at approximately 63.0 kDa (**Figure 3**), a bit larger than the theoretical calculation, which could be possibly due to the glycosylation of the protein. To this end, NetNGlyc 1.0 server was employed to forecast five N-glycosylation recognition sites of TanA (marked with red and inverted triangles in **Figure 1**). In addition, the fusion of 6×His-tag introduced several extra amino acids into the recombinant TanA.

Effects of Temperature on TanA Activity

As demonstrated in **Figure 4A**, the activity of TanA was linearly correlated to temperature rise, with optimal response at 60°C and over 80% activity retention from 40 to 70°C. Interestingly, TanA still showed 85.2 and 81.5% of optimum activity even under the conditions of 65 and 70°C (**Figure 4A**). It was further observed that TanA exhibited impressive stability below 55°C. It could maintain up to 61.3% activity even after 12 h of incubation at 55°C (**Figure 4B**). Therefore, TanA demonstrated thermophilic property with superior thermostability.

Effects of pH on TanA Activity

As TanA displayed the optimal catalytic activity at pH 6.0 (**Figure 5A**), the effects of pH was elucidated. TanA maintained exceeding 70% of its activity after incubation for 12 h at 40°C within the wide pH range from 3.5 to 7.5 (**Figure 5B**), indicating that it possessed favorable stability under acidic to weakly alkaline conditions.

Effects of Chemicals or Metal Ions on TanA Activity

The effects of various metal ions and chemicals on the activity of TanA are shown in **Figure 6**. Cu^{2+}, Ba^{2+}, Al^{3+}, and Mg^{2+} strongly inhibited the activity of TanA. However, a slightly activated effect was observed in the presence of Fe^{2+}; the relative activity reached 118.2% with 5 mM Fe^{2+}. Contrastingly, the enzymatic activity was obviously enhanced by Zn^{2+}, Mn^{2+}, and Co^{2+} at both 1 and 5 mM, which was increased to 131.5, 145.8, and 127.5%, respectively, with 5 mM of these cation ions. Other chemical compounds, especially mercaptoethanol (ME), manifested dramatic inactivation effects on TanA, whose activity was reduced to 21.6% compared to the control when subjected to 1 mM of ME and even was thoroughly lost after 5 mM of ME was added into the reaction solution, which perhaps is attributed to the significant ability of ME to damage disulfide bonds.

Substrate Specificity of TanA and Degradation Product Analysis

In order to study the substrate specificity of TanA, various gallic acid esters were employed as substrates. The specific activities and

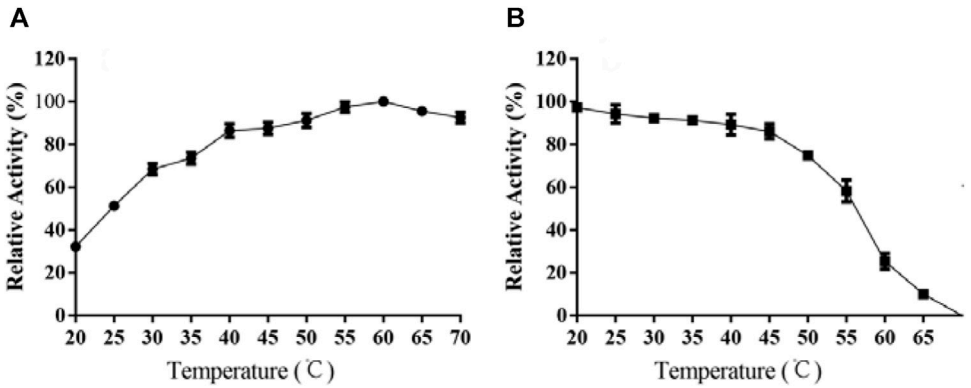

FIGURE 4 | Effects of temperature on the activity **(A)** and stability **(B)** of TanA. **(A)** The optimal temperature of TanA was assessed in the range of 20–70°C, regarding the activity at optimum temperature as 100%. **(B)** The temperature stability of TanA was determined by measuring the residual activity after incubation under 20–70°C for 12 h; the initial activity was taken as 100%.

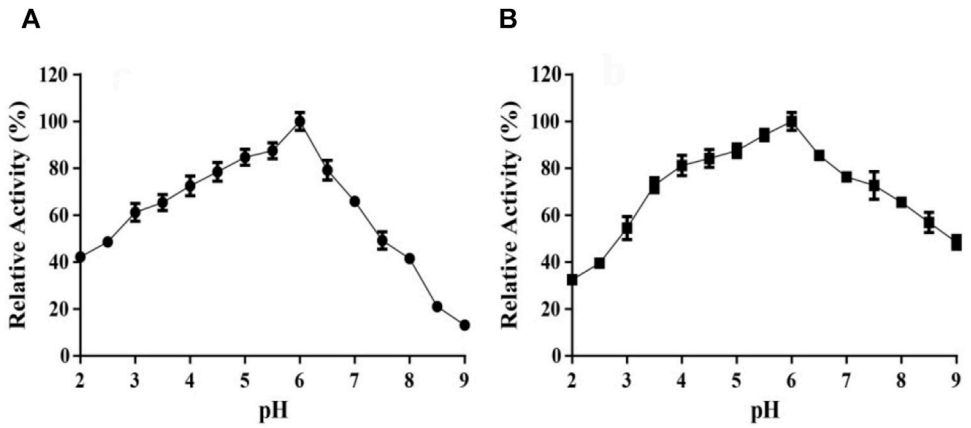

FIGURE 5 | Effects of pH on the activity **(A)** and stability **(B)** of TanA. **(A)** The optimal pH of TanA was investigated in the pH range of 2–11 with 100 mM buffers (glycine–NaOH, pH 8.5–11.0; Na_2HPO_4–citric acid, pH 2.0–8.0) by taking the activity at the optimum pH as 100%. **(B)** The pH stability of TanA was surveyed after incubation for 12 h at 40°C in the pH range of 2–11 with the buffers described above; the highest residual activity was set as 100%. The indifferent data ranging from pH 9 to 11 were neglected and not shown in both figures **(A)** and **(B)**.

K_m values of TanA against these substrates are listed in **Table 2**. TanA showed multifunctional property with high specific activities and affinities toward all the gallic acid esters utilized. Although the synthetic substrate PG demonstrated the highest specific activity of TanA at 941.4 U/mg, it still exhibited considerable catalysis ability against other substrates, especially toward some natural substrates, such as GCG, ECG, and EGCG (**Table 2**). For further testing of the abilities of TanA to degrade diverse gallic acid esters, the HPLC analysis of degradation products is displayed in **Supplementary Figure S3** . After catalytic decomposition by TanA at 55°C for 2 h, no gallic acid ester could be detected in the reaction solutions, and all kinds of substrates were almost thoroughly transformed (**Supplementary Figure S3**). In the chromatograms of the transformation products after tannase TanA treatment against MG (**Supplementary Figure S3A**), PG (**Supplementary Figure S3B**), and TA (**Supplementary Figure S3C**), only the peaks of gallic acid could be revealed due to other degraded products (methanol for MG, propanol for PG, and glucose for TA) with no ultraviolet absorption. Significantly, the ester catechins that are ubiquitous in green tea, including GCG (**Supplementary Figure S3D**), ECG (**Supplementary Figure S3E**), and EGCG (**Supplementary Figure S3F**), were converted successfully to gallocatechin (GC), epicatechin (EC), and epigallocatechin (EGC), respectively, which belong to the non-eater catechins.

DISCUSSION

The previous study of the genes related to tannin degradation in *A. melanogenum* T9 has suggested that there existed several tannases (including TanA, TanB, and TanC) with different molecular masses, amino acid sequences, gene expression patterns, and diverse properties, which are together

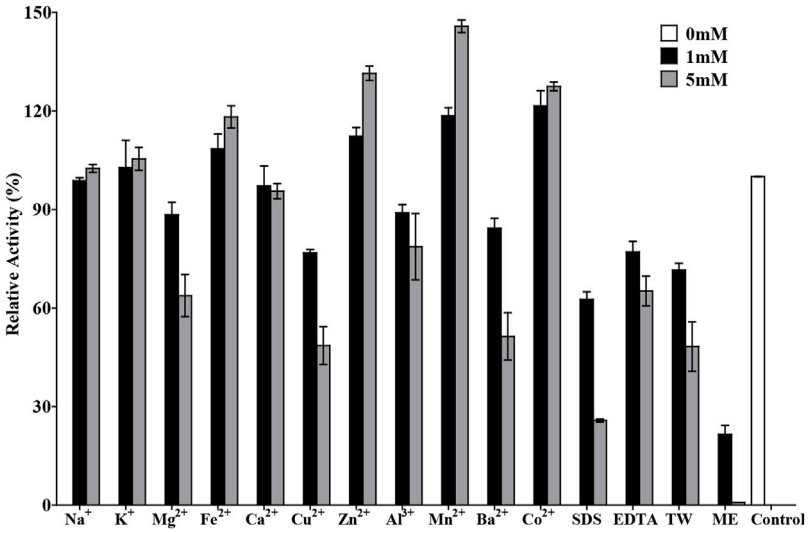

FIGURE 6 | Effects of chemicals and metal ions on the activity of TanA. The activity assayed without any chemical compound or metal ion was taken as control. SDS, sodium dodecyl sulfate; EDTA, ethylene diamine tetraacetic acid; TW, Tween 80; ME, mercaptoethanol.

TABLE 2 | Comparison of substrate specificities for TanA.

Substrate	Specific activity (U/mg)	K_m (mM)
TA	723.8	2.15
GCG	703.1	1.86
ECG	756.2	2.13
PG	941.4	1.71
MG	506.8	2.81
EGCG	623.2	2.52

TA, tannic acid; GCG, gallocatechin gallate; ECG, epicatechin gallate; PG, propyl gallate; MG, methyl gallate; EGCG, epigallocatechin gallate.

responsible for the catalyzed hydrolysis of tannins in the strain T9 (Zhang et al., 2019). The tannases from different categories are often produced in the same fungal species due to species-specific accumulative effects and the impacts of exterior circumstances. Tannase subtypes are distinguished depending on their physical and chemical properties, such as molecular size, family, presence or absence of a signal peptide, and more, which guarantee that microorganisms are able to degrade both intra- and extracellular tannins under various physiological conditions, namely, temperature, pH, ion strength, *etc*. Therefore, it is of great significance to figure out the metabolic mechanism of tannins in *A. melanogenum* in future work.

TanA exhibited a typical conserved domain, Gly-X-Ser-X-Gly, almost present in all tannase sequences of fungi and bacteria (boxed in red in **Figure 1**). This unique sequence of serine hydrolase effectively binds to the tannic substrates, thereby promoting catalytic activity (Zhang et al., 2019). Moreover, a mutation analysis explained that the disulfide bond between Cys202 and Cys458 played a vital part in regulating the activity of AoFaeB (Suzuki et al., 2014). Interestingly, TanA also showed several cysteine residues probably involved in disulfide bond formation at similar sites as that of AoFaeB. For the sake of surveying this, the homology model of TanA was built. Meanwhile, four disulfide bonds with a 3D structure have been predicted (**Supplementary Figure S2**), including Cys161–Cys415, Cys230–Cys247, Cys256–Cys265, and Cys487–Cys508, among which the first disulfide bond was similar to the one in AoFaeB as described above, indicating that the disruption of disulfide bonds when subjected to ME affected TanA activity and stability to a great extent (**Figure 6**).

It is shown in **Figure 4A** that TanA displayed an optimal response at 60°C, with over 80% relative activity from 40 to 70°C, illustrating its thermophilic property and making it suitable for most of the hydrolysis processes assisted by tannases which were carried out at increased temperatures (Abdulhameed et al., 2005). However, a lot of studies demonstrated that many tannases from bacteria (Jana et al., 2014), mold (Iibuchi et al., 1968; Lekha and Lonsane, 1997; Madzak, 2015; Sivashanmugam and Jayaraman, 2011), and even yeast (Wang et al., 2020) showed optimal activity at approximately 40°C. Considering thermal stability, as exhibited in the diagram of **Figure 4B**, TanA depicted superior heat resistance property at a temperature below 55°C, maintaining up to 61.3% activity even after 12 h of incubation. Studies showed thermostability in the range of 30–50°C for most fungal tannases (**Table 3**). TanA possessed better temperature stability compared to other tannases from fungi. Although the tannase from *P. notatum* NCIM923 (Gayen and Ghosh, 2013) and the tannase from *K. marxianus* NRRL Y-8281 (Mahmoud et al., 2018) could maintain their stability up to 60 and 70°C, respectively, according to their researches (**Table 3**), their thermostability at high temperatures was, in fact, worse than TanA. The purified tannase from *P. notatum* retained 60% of its thermostability at 60°C within only 1 h (Gayen and Ghosh, 2013). Meanwhile, the tannase from *K. marxianus* could also remain stable at 70°C for only 60 min (Mahmoud et al., 2018). Also belonging to thermophilic tannases, the extracellular tannase derived from

TABLE 3 | Biochemical properties of TanA and other reported tannases.

Source	Specific activity (U/mg)	Optimal pH/temperature (°C)	Temperature-stable range (°C)	pH-stable range	References
Penicillium notatum	22.48	5.0/40	30–60	3.0–8.0	Gayen and Ghosh (2013)
Emericella nidulans	1.91	5.0/45	22–50	4.0–5.0	Goncalves *et al*. (2011)
Aspergillus phoenicis	10.0	6.0/60	40–50	2.5–7.0	Riul *et al*. (2013)
A. niger	N.D.	6.0/80	30–60	3.0–8.0	Shao *et al*. (2020)
Sporidiobolus ruineniae	16.232	7.0/40	20–50	5.0–9.0	Kanpiengjai *et al*. (2020)
Kluyveromyces marxianus	1,026.12	4.5, 8.5/35	30–70	4.0–6.0	Mahmoud *et al*. (2018)
Streptomyces sviceus	114.0	8.0/50	63–69	6.5–8.0	Wu *et al*. (2015)
Lactobacillus plantarum	84.34	8.0/40	N.D.	N.D.	Iwamoto *et al*. (2008)
A. melanogenum	941.4	6.0/60	20–55	3.5–7.5	This study

A. phoenicis, whose optimal temperature was the same as TanA, was stable for 1 h at 40–50°C, with a half-life of only 20 min at 60°C (Riul et al., 2013). In industrial production such as green tea deep processing, the degradation of tannins often takes a longer time at a relatively high temperature, and the tannase TanA retained most of its activity within at least 12 h under 55°C. This concludes that TanA is a thermophilic tannase with sturdy thermostability, which quite better satisfy the industrial application. Contrastingly, the optimal temperature for the tannase rAntan1, with strong thermal stability from *A. niger* FJ0118, was 80°C. It could persist to be stable at 60°C for about 5.4 h (Shao et al., 2020). Although owning favorable activity and stability at high temperature, rAntan1 expressed by *Pichia pastoris* cannot reach food grade because of the use of methanol when inducing tannase expression. The thermophilic and thermostable properties of TanA and rAntan1 may be partially attributed to glycosylated formation during expression in yeast (Zhou et al., 2020), corresponding to the predicted N-glycosylation recognition sites (**Figure 1**). Yang *et al.* (2007) indicated that the tea steeped in water at 70°C contained the highest contents of active components. Thus, the thermophilic and thermostable tannases, such as TanA and rAntan1, are rare in nature but necessary in industrial production. Some pieces of literature have reviewed the wide application of thermostable tannases in tea extracts to decrease the formation of tea cream (on account of the presence of tannins), thereby improving the taste of tea beverages (Chávez-González et al., 2012). In addition, thermo-tolerant tannases were also applied in the production of instant green tea powder to enhance the color and taste (Ozturk et al., 2016; Cao et al., 2019). In the process of catalytic degradation of tannins, thermostable tannases can enhance high-temperature extraction efficiency, simplify the production process, reduce the costs, and improve the product quality, which are reasons for the application of TanA in industrial production, such as in green tea deep processing.

TanA maintained over 60% activity within the broad pH scope of 3.0–7.0, with maximum activity at pH 6.0 (**Figure 5A**). For pH stability, TanA still retained over 70% of its activity after incubation for 12 h within the wide pH from 3.5 to 7.5, indicating advisable stability under acidic to weakly alkaline conditions (**Figure 5B**). It was consistent with the reported fungal tannases—for instance, the tannase derived from *A. niger* possessed an optimal pH of 6.0 and excellent stability at pH 3.0–8.0 (Shao et al., 2020). The tannase from *A. oryzae* had an optimum pH of 5.5 along with stability between pH 4.5 and 7.5 and over 80% activity retention (Abdel-Naby et al., 2016). On the other hand, the tannase from *E. nidulans* (pH 4.0–5.0) and the tannase from *Aspergillus thorny* (pH 5.0–6.0) displayed limited pH stability (Goncalves et al., 2011; Tanash et al., 2011). Therefore, remarkable stability at high temperatures and a wide pH range become integral properties of TanA, which reduce the risk of pollution during the fermentation process and thereby establish the foundation for its industrial application in tannin biodegradation and gallic acid preparation.

TanA has been incubated with several gallic acid esters to study the substrate specificity. As shown in **Table 2**, TanA revealed outstanding specific activities to decompose various substrates, illustrating its multifunctional property. The activity of TanA on synthetic substrate PG was significantly superior, whereas the specific activities on some natural substrates (*e.g.*, 703.1 U/mg against GCG, 756.2 U/mg against ECG, and 623.2 U/mg against EGCG) were also quite considerable (**Table 2**). Many reported tannases exhibited quite lower activities toward some ester catechins that naturally exist in green tea, such as ECG and EGCG (Bhoite et al., 2013; Ramírez-Coronel et al., 2003; Sharma et al., 2008). Although Mahmoud *et al.* (2018) stated a high activity toward TA (1,026.12 U/mg), the tannase from *K. marxianus* NRRL Y-8281 was most active on TA (100%), followed by MG (74.3%) and PG (64.5%) and expressing minimum enzymatic activity against EGCG (only 10.5%). Obviously, these enzymes cannot satisfy the application in industrial processing when against natural ester catechins. In addition, the HPLC analysis results of transformation products by TanA further confirmed the almost complete degradation of varying kinds of tannins (especially the natural ester catechins in many plants) at a high temperature within 2 h (**Supplementary Figure S3**). Previous research reported that immobilized tannase could carry out 98% conversion of TA within 6 h (Mahendran et al., 2006). However, tannase from *Bacillus sphaericus* converted 90.8% TA after as long as 24 h (Raghuwanshi et al., 2011). By contrast, the higher efficiency of TanA, along with high bioconversion, undoubtedly benefited from its favorable activities toward different gallic acid esters. Moreover, plants

in nature, such as oilseed rape and many fruits, usually contain various hydrolyzable tannins (GTs and ETs) (Lorusso et al., 1996). Thus, the multifunction property gives the tannase TanA the capability to decompose diverse gallic acid esters, which is fully conducive when against different kinds of tannins in the plants. The prime cause of the bitter taste of tea is the presence of ester catechins (mainly EGCG and ECG) (Shao et al., 2020). The reported tannase rAntan1 displayed similar substrate specificity as TanA. Enzymatic extraction reduced the proportion of easter catechins in tea polyphenols, weakened the bitter taste, and improved the overall taste of the tea beverage (Shao et al., 2020). Similarly, the TanA-mediated extraction processing can also effectively transform the ester catechins to the non-ester ones (such as EGC and EC) in green tea, thereby improving the taste of tea drinks. Besides this, the green tea catechins possess many biological activities, such as antiviral, antibacterial, antitumor, and antioxidant properties, which are closely related to the presence of multiple hydroxyl groups and galloyl groups in their structures (Xu et al., 2021).

Tannins are ubiquitously present in higher plants, and biodegradation by tannases is essential in industrial processing, such as in feed additives (Lorusso et al., 1996), myrobalan juice (Srivastava and Kar, 2009), and green tea (Cao et al., 2019; Shao et al., 2020). In addition, many active substances, such as catechins and gallic acid, employ tannases for their respective extraction (Chhokar et al., 2013). Rapeseed meal processing is a worthy example illustrating the application of tannases. The agro-industrial chain of canola oil production generates a large mass of rapeseed meals but faces challenges during recycling owing to the high content of tannins, resulting in huge wastes (Lorusso et al., 1996; Shim et al., 2003). Fortunately, the efficient decomposition of tannins through enzymatic catalysis aids in the production of rapeseed meal feed with added value (Lorusso et al., 1996). In other words, tannases play significant roles in various fields, such as food, brewing, pharmacy, and feed. However, tannases of food grade with advisable properties are still rather rare but necessary. In this research, a novel thermophilic tannase, TanA, with favorable thermostability was demonstrated, with detailed characterizations suggesting a potent candidate for the food and agricultural industries.

DATA AVAILABILITY STATEMENT

The datasets presented in this study can be found in online repositories. The names of the repository/repositories and accession number(s) can be found below: https://www.ncbi.nlm.nih.gov/genbank/, QEP28943.1.

AUTHOR CONTRIBUTIONS

LL contributed to methodology, formal analysis, validation, writing of the original draft, and in review and editing. JG contributed to conceptualization, investigation, and manuscript review and revision. X-FZ contributed to data curation, and manuscript review and revision. ZL contributed to software. W-QS contributed to methodology, resources, supervision, and project administration. H-XZ contributed to methodology, resources, review and editing, supervision, and project administration.

FUNDING

This research was funded by the Shandong Provincial Natural Science Foundation, China (ZR2016BQ42, ZR2020MC003, and ZR2017BC029) and the National Key R and D Program of China (2019YFD0901902).

ACKNOWLEDGMENTS

The authors would like to thank all the reviewers and editors who participated in the review and MJEditor (www.mjeditor.com) for its linguistic assistance during the preparation of this manuscript.

SUPPLEMENTARY MATERIAL

The supplementary material for this article can be found online at: https://www.frontiersin.org/articles/10.3389/fbioe.2021.769816/full#supplementary-material

REFERENCES

Abdel-Naby, M. A., El-Tanash, A. B., Sherief, A. D. A., and Sherief, A. (2016). Structural Characterization, Catalytic, Kinetic and Thermodynamic Properties of *Aspergillus Oryzae* Tannase. *Int. J. Biol. Macromolecules* 92, 803–811. doi:10.1016/j.ijbiomac.2016.06.098

Abdulhameed, S., Kiran, G., and Pandey, A. (2005). Purification and Characterization of Tannin Acyl Hydrolase from *Aspergillus Niger* ATCC 16620. *Food Technol. Biotech.* 43, 133–138. doi:10.1016/j.fm.2004.02.005

Aguilar, C. N., and Gutierrez-Sanchez, G. (2001). Review: Sources, Properties, Applications and Potential Uses of Tannin Acyl Hydrolase. *Food Sci. Technol. Int.* 7, 373–382. doi:10.1106/69m3-b30k-cf7q-rj5g

Banerjee, A., Jana, A., Pati, B. R., Mondal, K. C., and Das Mohapatra, P. K. (2012). Characterization of Tannase Protein Sequences of Bacteria and Fungi: An In Silico Study. *Protein J.* 31, 306–327. doi:10.1007/s10930-012-9405-x

Becker, K., and Makkar, H. P. S. (1999). Effects of Dietary Tannic Acid and Quebracho Tannin on Growth Performance and Metabolic Rates of Common Carp (*Cyprinus carpio* L.). *Aquaculture* 175, 327–335. doi:10.1016/S0044-8486(99)00106-4

Beniwal, V., Chhokar, V., Singh, N., and Sharma, J. (2010). Optimization of Process Parameters for the Production of Tannase and Gallic Acid by *Enterobacter Cloacae* MTTC 9125. *Biocatal. Agric. Biotechnol.* 6, 389–397. doi:10.1007/s13297-017-2490-2

Beniwal, V., Kumar, A., Goel, G., and Chhokar, V. (2013). A Novel Low Molecular Weight Acido-Thermophilic Tannase from *Enterobacter Cloacae* MTCC 9125. *Biocatal. Agric. Biotechnol.* 2, 132–137. doi:10.1016/j.bcab.2013.03.002

Bhoite, R. N., Navya, P., and Murthy, P. S. (2013). Purification and Characterisation of a Coffee Pulp Tannase Produced by *Penicillium Verrucosum*. *J. Food Sci. Eng.* 3, 323–331. doi:10.1016/j.fbp.2013.10.007

Cao, Q.-Q., Zou, C., Zhang, Y.-H., Du, Q.-Z., Yin, J.-F., Shi, J., et al. (2019). Improving the Taste of Autumn Green tea with Tannase. *Food Chem.* 277, 432–437. doi:10.1016/j.foodchem.2018.10.146

Chávez-González, M., Rodríguez-Durán, L. V., Balagurusamy, N., Prado-Barragán, A., Rodríguez, R., Contreras, J. C., et al. (2012). Biotechnological Advances and Challenges of Tannase: An Overview. *Food Bioproc. Technol* 5, 445–459. doi:10.1007/s11947-011-0608-5

Chhokar, V., Sharma, J., Kumar, A., and Beniwal, V. (2013). Recent Advances in Industrial Application of Tannases: A Review. *Recent Pat. Biotechnol.* 7, 228–233. doi:10.2174/18722083113076660013

Chung, K.-T., Wong, T. Y., Wei, C.-I., Huang, Y.-W., and Lin, Y. (1998). Tannins and Human Health: A Review. *Crit. Rev. Food Sci. Nutr.* 38, 421–464. doi:10.1080/10408699891274273

Ebrahimzadeh, S. K., Navidshad, B., Farhoomand, P., and Mirzaei Aghjehgheshlagh, F. (2018). Effects of Exogenous Tannase Enzyme on Growth Performance, Antioxidant Status, Immune Response, Gut Morphology and Intestinal Microflora of Chicks Fed Grape Pomace. *S. Afr. J. Anim. Sci.* 48, 2–9. doi:10.4314/sajas.v48i1.2

Gayen, S., and Ghosh, U. (2013). Purification and Characterization of Tannin Acyl Hydrolase Produced by Mixed Solid State Fermentation of Wheat Bran and Marigold Flower byPenicillium notatumNCIM 923. *Biomed. Res. Int.* 2013, 1–6. doi:10.1155/2013/596380

Ghosh, K., and Mandal, S. (2015). Nutritional Evaluation of Groundnut Oil Cake in Formulated Diets for Rohu, Labeo Rohita (Hamilton) Fingerlings after Solid State Fermentation with a Tannase Producing Yeast, *Pichia Kudriavzevii* (GU939629) Isolated from Fish Gut. *Aquacult. Rep.* 2, 82–90. doi:10.1016/j.aqrep.2015.08.006

Gonçalves, H. B., Riul, A. J., Terenzi, H. F., Jorge, J. A., and Guimarães, L. H. S. (2011). Extracellular Tannase from *Emericella Nidulans* Showing Hypertolerance to Temperature and Organic Solvents. *J. Mol. Catal. B: Enzymatic* 71, 29–35. doi:10.1016/j.molcatb.2011.03.005

Govindarajan, R. K., Revathi, S., Rameshkumar, N., Krishnan, M., and Kayalvizhi, N. (2016). Microbial Tannase: Current Perspectives and Biotechnological Advances. *Biocatal. Agric. Biotechnol.* 6, 168–175. doi:10.1016/j.bcab.2016.03.011

Hong, Y.-H., Jung, E. Y., Park, Y., Shin, K.-S., Kim, T. Y., Yu, K.-W., et al. (2013). Enzymatic Improvement in the Polyphenol Extractability and Antioxidant Activity of Green Tea Extracts. *Biosci. Biotechnol. Biochem.* 77, 22–29. doi:10.1271/bbb.120373

Iibuchi, S., Minoda, Y., and Yamada, K. (1968). Studies on Tannin Acyl Hydrolase of Microorganisms. *Agric. Biol. Chem.* 32, 803–809. doi:10.1271/bbb1961.32.803

Iwamoto, K., Tsuruta, H., Nishitaini, Y., and Osawa, R. (2008). Identification and Cloning of a Gene Encoding Tannase (Tannin Acylhydrolase) from Lactobacillus Plantarum ATCC 14917T. *Syst. Appl. Microbiol.* 31, 269–277. doi:10.1016/j.syapm.2008.05.004

Jana, A., Maity, C., Halder, S. K., Das, A., Pati, B. R., Mondal, K. C., et al. (2013). Structural Characterization of Thermostable, Solvent Tolerant, Cytosafe Tannase from *Bacillus Subtilis* PAB2. *Biochem. Eng. J.* 77, 161–170. doi:10.1016/j.bej.2013.06.002

Jana, A., Halder, S. K., Banerjee, A., Paul, T., Pati, B. R., Mondal, K. C., et al. (2014). Biosynthesis, Structural Architecture and Biotechnological Potential of Bacterial Tannase: A Molecular Advancement. *Bioresour. Technol.* 157, 327–340. doi:10.1016/j.biortech.2014.02.017

Kanpiengjai, A., Unban, K., Nguyen, T.-H., Haltrich, D., and Khanongnuch, C. (2019). Expression and Biochemical Characterization of a New Alkaline Tannase from *Lactobacillus Pentosus*. *Protein Expr. Purif.* 157, 36–41. doi:10.1016/j.pep.2019.01.005

Kanpiengjai, A., Khanongnuch, C., Lumyong, S., Haltrich, D., Nguyen, T.-H., and Kittibunchakul, S. (2020). Co-Production of Gallic Acid and a Novel Cell-Associated Tannase by a Pigment-Producing Yeast, *Sporidiobolus Ruineniae* A45.2. *Microb. Cel Fact.* 19, 95–99. doi:10.1186/s12934-020-01353-w

Lekha, P. K., and Lonsane, B. K. (1997). Production and Application of Tannin Acyl Hydrolase: State of the Art. *Adv. Appl. Microbiol.* 44, 215–260. doi:10.1016/S0065-2164(08)70463-5

Lineweaver, H., and Burk, D. (1934). The Determination of Enzyme Dissociation Constants. *J. Am. Chem. Soc.* 56, 658–666. doi:10.1021/ja01318a036

Lorusso, L., Lacki, K., and Duvnjak, Z. (1996). Decrease of Tannin Content in Canola Meal by an Enzyme Preparation from *Trametes Versicolor*. *Biotechnol. Lett.* 18, 309–314. doi:10.1007/BF00142950

Madzak, C. (2015). *Yarrowia Lipolytica*: Recent Achievements in Heterologous Protein Expression and Pathway Engineering. *Appl. Microbiol. Biotechnol.* 99, 4559–4577. doi:10.1007/s00253-015-6624-z

Mahendran, B., Raman, N., and Kim, D.-J. (2006). Purification and Characterization of Tannase from *Paecilomyces Variotii*: Hydrolysis of Tannic Acid Using Immobilized Tannase. *Appl. Microbiol. Biotechnol.* 70, 444–450. doi:10.1007/s00253-005-0082-y

Mahmoud, A. E., Fathy, S. A., Rashad, M. M., Ezz, M. K., and Mohammed, A. T. (2018). Purification and Characterization of a Novel Tannase Produced by *Kluyveromyces Marxianus* Using Olive Pomace as Solid Support, and its Promising Role in Gallic Acid Production. *Int. J. Biol. Macromolecules* 107, 2342–2350. doi:10.1016/j.ijbiomac.2017.10.117

Min, B. R., Attwood, G. T., Mcnabb, W. C., Molan, A. L., and Barry, T. N. (2005). The Effect of Condensed Tannins from *Lotus Corniculatus* on the Proteolytic Activities and Growth of Rumen Bacteria. *Anim. Feed Sci. Technol.* 121, 45–58. doi:10.1016/j.anifeedsci.2005.02.007

Ni, H., Chen, F., Jiang, Z. D., Cai, M. Y., Yang, Y. F., Xiao, A. F., et al. (2015). Biotransformation of tea Catechins Using *Aspergillus Niger* Tannase Prepared by Solid State Fermentation on tea Byproduct. *LWT - Food Sci. Technol.* 60, 1206–1213. doi:10.1016/j.lwt.2014.09.010

Ozturk, B., Seyhan, F., Ozdemir, I. S., Karadeniz, B., Bahar, B., Ertas, E., et al. (2016). Change of Enzyme Activity and Quality during the Processing of Turkish Green tea. *LWT - Food Sci. Technol.* 65, 318–324. doi:10.1016/j.lwt.2015.07.068

Pan, J., Wang, N.-N., Yin, X.-J., Liang, X.-L., and Wang, Z.-P. (2020). Characterization of a Robust and pH-Stable Tannase from Mangrove-Derived Yeast *Rhodosporidium Diobovatum* Q95. *Mar. Drugs* 18, 546–552. doi:10.3390/md18110546

Raghuwanshi, S., Dutt, K., Gupta, P., Misra, S., and Saxena, R. K. (2011). *Bacillus Sphaericus*: The Highest Bacterial Tannase Producer with Potential for Gallic Acid Synthesis. *J. Biosci. Bioeng.* 111, 635–640. doi:10.1016/j.jbiosc.2011.02.008

Ramírez-Coronel, M. A., Viniegra-González, G., Darvill, A., and Augur, C. (2003). A Novel Tannase from Aspergillus niger with β-Glucosidase Activity. *Microbiology* 149, 2941–2946. doi:10.1099/mic.0.26346-0

Riul, A. J., Gonçalves, H. B., Jorge, J. A., and Guimarães, L. H. S. (2013). Characterization of a Glucose- and Solvent-Tolerant Extracellular Tannase from *Aspergillus Phoenicis*. *J. Mol. Catal. B: Enzymatic* 85-86, 126–133. doi:10.1016/j.molcatb.2012.09.001

Rivas, B. D. L., Rodríguez, H., Anguita, J., and Muñoz, R. (2019). Bacterial Tannases: Classification and Biochemical Properties. *Appl. Microbiol. Biotechnol.* 103, 603–623. doi:10.1007/s00253-018-9519-y

Şengil, İ. A., and Özacar, M. (2009). Competitive Biosorption of Pb2+, Cu2+ and Zn2+ Ions from Aqueous Solutions onto Valonia Tannin Resin. *J. Hazard. Mater.* 166, 1488–1494. doi:10.1016/j.jhazmat.2008.12.071

Shao, Y., Zhang, Y.-H., Zhang, F., Yang, Q.-M., Weng, H.-F., Xiao, Q., et al. (2020). Thermostable Tannase from *Aspergillus Niger* and its Application in the Enzymatic Extraction of Green tea. *Molecules* 25, 952–969. doi:10.3390/molecules25040952

Sharma, S., Bhat, T. K., and Dawra, R. K. (2000). A Spectrophotometric Method for Assay of Tannase Using Rhodanine. *Anal. Biochem.* 279, 85–89. doi:10.1006/abio.1999.4405

Sharma, S., Agarwal, L., and Saxena, R. K. (2008). Purification, Immobilization and Characterization of Tannase from *Penicillium Variable*. *Bioresour. Technol.* 99, 2544–2551. doi:10.1016/j.biortech.2007.04.035

Shim, Y. H., Chae, B. J., and Lee, J. H. (2003). Effects of Phytase and Carbohydrases Supplementation to Diet with a Partial Replacement of Soybean Meal with Rapeseed Meal and Cottonseed Meal on Growth Performance and Nutrient Digestibility of Growing Pigs. *Asian Australas. J. Anim. Sci.* 16, 1339–1347. doi:10.5713/ajas.2003.1339

Sivashanmugam, K., and Jayaraman, G. (2011). Production and Partial Purification of Extracellular Tannase by *Klebsiella Pneumoniae* MTCC 7162 Isolated from Tannery Effluent. *Afr. J. Biotechnol.* 10, 1364–1374. doi:10.1186/1471-2180-11-37

Srivastava, A., and Kar, R. (2009). Characterization and Application of Tannase Produced by *Aspergillus Niger* ITCC 6514.07 on Pomegranate Rind. *Braz. J. Microbiol.* 40, 782–789. doi:10.1590/S1517-83822009000400008

Suzuki, K., Hori, A., Kawamoto, K., Thangudu, R. R., Ishida, T., Igarashi, K., et al. (2014). Crystal Structure of a Feruloyl Esterase Belonging to the Tannase Family: A Disulfide Bond Near a Catalytic Triad. *Proteins* 82, 2857–2867. doi:10.1002/prot.24649

Tamura, K., Stecher, G., Peterson, D., Filipski, A., and Kumar, S. (2013). MEGA6: Molecular Evolutionary Genetics Analysis Version 6.0. *Mol. Biol. Evol.* 30, 2725–2729. doi:10.1093/molbev/mst197

Tanash, D. A., Sherief, A., and Nour, A. (2011). Catalytic Properties of Immobilized Tannase Produced from *Aspergillus Aculeatus* Compared with the Free Enzyme. *Braz. J. Chem. Eng.* 28, 381–391. doi:10.1590/S0104-66322011000300004

Wang, Z.-P., Cao, M., Li, B., Ji, X.-F., Zhang, X.-Y., Zhang, Y.-Q., et al. (2020). Cloning, Secretory Expression and Characterization of a Unique pH-Stable and Cold-Adapted Alginate Lyase. *Mar. Drugs* 18, 189. doi:10.3390/md18040189

Wang, Z.-P., Wang, P.-K., Ma, Y., Lin, J.-X., Wang, C.-L., Zhao, Y.-X., et al. (2022). Laminaria Japonica Hydrolysate Promotes Fucoxanthin Accumulation in Phaeodactylum Tricornutum. *Bioresour. Technol.* 344, 126117. doi:10.1016/j.biortech.2021.126117

Wu, M., Wang, Q., Mckinstry, W. J., and Ren, B. (2015). Characterization of a Tannin Acyl Hydrolase from *Streptomyces Sviceus* with Substrate Preference for Digalloyl Ester Bonds. *Appl. Microbiol. Biotechnol.* 99, 2663–2672. doi:10.1007/s00253-014-6085-9

Xu, Y.-Q., Gao, Y., and Granato, D. (2021). Effects of Epigallocatechin Gallate, Epigallocatechin and Epicatechin Gallate on the Chemical and Cell-Based Antioxidant Activity, Sensory Properties, and Cytotoxicity of a Catechin-Free Model Beverage. *Food Chem.* 339, 128060. doi:10.1016/j.foodchem.2020.128060

Yang, D.-J., Hwang, L. S., and Lin, J.-T. (2007). Effects of Different Steeping Methods and Storage on Caffeine, Catechins and Gallic Acid in Bag tea Infusions. *J. Chromatogr. A* 1156, 312–320. doi:10.1016/j.chroma.2006.11.088

Zhang, S., Gao, X., He, L., Qiu, Y., Zhu, H., and Cao, Y. (2015). Novel Trends for Use of Microbial Tannases. *Prep. Biochem. Biotechnol.* 45, 221–232. doi:10.1080/10826068.2014.907182

Zhang, P., Wang, Z.-P., Sheng, J., Zheng, Y., Ji, X.-F., Zhou, H.-X., et al. (2018). High and Efficient Isomaltulose Production Using an Engineered *Yarrowia Lipolytica* Strain. *Bioresour. Technol.* 265, 577–580. doi:10.1016/j.biortech.2018.06.081

Zhang, L.-L., Li, J., Wang, Y.-L., Liu, S., Wang, Z.-P., and Yu, X.-J. (2019). Integrated Approaches to Reveal Genes Crucial for Tannin Degradation in *Aureobasidium Melanogenum* T9. *Biomolecules* 9, 439–445. doi:10.3390/biom9090439

Zhang, L.-L., Jiang, X.-H., Xiao, X.-F., Zhang, W.-X., Shi, Y.-Q., Wang, Z.-P., et al. (2021). Expression and Characterization of a Novel Cold-Adapted Chitosanase from marine *Renibacterium* Sp. Suitable for Chitooligosaccharides Preparation. *Mar. Drugs* 19, 596. doi:10.3390/md19110596

Zhou, H.-X., Xu, S.-S., Yin, X.-J., Wang, F.-L., and Li, Y. (2020). Characterization of a New Bifunctional and Cold-Adapted Polysaccharide Lyase (PL) Family 7 Alginate Lyase from *Flavobacterium* Sp. *Mar. Drugs* 18, 388. doi:10.3390/md18080388

Conflict of Interest: The authors declare that the research was conducted in the absence of any commercial or financial relationships that could be construed as a potential conflict of interest.

Publisher's Note: All claims expressed in this article are solely those of the authors and do not necessarily represent those of their affiliated organizations or those of the publisher, the editors, and the reviewers. Any product that may be evaluated in this article or claim that may be made by its manufacturer is not guaranteed or endorsed by the publisher.

frontiers in Bioengineering and Biotechnology

ORIGINAL RESEARCH
published: 10 February 2022
doi: 10.3389/fbioe.2021.813079

Purification, Characterization, and Hydrolysate Analysis of Dextranase From *Arthrobacter oxydans* G6-4B

Nannan Liu[1,2], Peiting Li[3], Xiujin Dong[4], Yusi Lan[3], Linxiang Xu[1,2], Zhen Wei[1,2] and Shujun Wang[3]*

[1]*Jiangsu Key Laboratory of Marine Bioresources and Environment, Jiangsu Ocean University, Lianyungang, China,* [2]*Co-Innovation Center of Jiangsu Marine Bio-industry Technology, Jiangsu Ocean University, Lianyungang, China,* [3]*College of Food Science and Engineering, Jiangsu Ocean University, Lianyungang, China,* [4]*School of Marine Science and Fisheries, Jiangsu Ocean University, Lianyungang, China*

Dextran has aroused increasingly more attention as the primary pollutant in sucrose production and storage. Although enzymatic hydrolysis is more efficient and environmentally friendly than physical methods, the utilization of dextranase in the sugar industry is restricted by the mismatch of reaction conditions and heterogeneity of hydrolysis products. In this research, a dextranase from *Arthrobacter oxydans* G6-4B was purified and characterized. Through anion exchange chromatography, dextranase was successfully purified up to 32.25-fold with a specific activity of 288.62 U/mg protein and a Mw of 71.12 kDa. The optimum reaction conditions were 55°C and pH 7.5, and it remained relatively stable in the range of pH 7.0–9.0 and below 60°C, while significantly inhibited by metal ions, such as Ni^{+}, Cu^{2+}, Zn^{2+}, Fe^{3+}, and Co^{2+}. Noteworthily, a distinction of previous studies was that the hydrolysates of dextran were basically isomalto-triose (more than 73%) without glucose, and the type of hydrolysates tended to be relatively stable in 30 min; dextranase activity showed a great influence on hydrolysate. In conclusion, given the superior thermal stability and simplicity of hydrolysates, the dextranase in this study presented great potential in the sugar industry to remove dextran and obtain isomalto-triose.

Keywords: isomalto-oligosaccharides, dextran, *Arthrobacter oxydans*, hydrolysis, purification

OPEN ACCESS

Edited by:
Zhipeng Wang,
Qingdao Agricultural University, China

Reviewed by:
Pau Loke Show,
University of Nottingham Malaysia Campus, Malaysia
Hailong Wang,
Shandong University, China

****Correspondence:***
Nannan Liu
lnn1903@163.com

Specialty section:
This article was submitted to Bioprocess Engineering, a section of the journal Frontiers in Bioengineering and Biotechnology

Received: *11 November 2021*
Accepted: *08 December 2021*
Published: *10 February 2022*

Citation:
Liu N, Li P, Dong X, Lan Y, Xu L, Wei Z and Wang S (2022) Purification, Characterization, and Hydrolysate Analysis of Dextranase From Arthrobacter oxydans *G6-4B. Front. Bioeng. Biotechnol. 9:813079. doi: 10.3389/fbioe.2021.813079*

1 INTRODUCTION

On the condition that internal tissue of sugar cane was damaged by mechanical cutting or burning, it was vulnerable to be infected by contaminant microorganisms, such as *Leuconostoc mesenteroides* (Jiménez, 2009). Under suitable conditions, the dextransucrase from microorganisms hydrolyzed sucrose and formed dextran. In the sugarcane industry, dextran is regarded as the most widespread contaminant indicator used for quality control purposes (Oliveira et al., 2002), which could contribute to the increasing viscosity of cane juice, affecting the settling velocity and reducing raw sugar quality (Eggleston et al., 2011). The blockage of filters caused by increasing viscosity of juice and the presence of high molecular weight (Mw) dextran cause juice spills and economic losses. It was conservatively estimated that 8.8 lb will be lost, while 0.1% increase of dextran in the juice (1,000 ppm) of sugar per ton (Jiménez, 2009). Given the economic losses of dextran to the sugar industry, much attention has been drawn to hydrolyze and remove dextran in various approaches. A wide range of previous studies suggested that the depolymerization of dextran by dextranase was

evaluated as the most appropriate method compared with other physical methods with poor economic feasibility (Purushe et al., 2012; Sufiate et al., 2018a; Tanoue Batista et al., 2021). Consequently, with the rapid development of protein spatial structure analysis (Chew et al., 2019; Sankaran et al., 2019; Krishna Koyande et al., 2020; Wang et al., 2022), it is a burning problem to explore the enzymatic properties and application suitable for sugar processing of dextranase.

Dextran is a macromolecular polymer (10^5–10^7 Da) composed of glucosaccharides linked mainly by α-1,6-glycoside bonds, frequently synthesized from sucrose by contaminant microorganisms (Martínez et al., 2021; Tanoue Batista et al., 2021). Dextranase (EC 3.2.1.11) catalyzes the hydrolysis of α-1,6-glycoside bond in dextran and cleave dextran into lower Mw fractions, isomalto-oligosaccharides (IMOs), or glucose (Khalikova et al., 2005; Zohra et al., 2015; Ren et al., 2018). In the same enzymatic hydrolysis system, a massive number of hydrolysates are present simultaneously, for instance, different Mw IMOs and dextran (Park et al., 2012; Zohra et al., 2015; Münkel and Wefers, 2019). Intriguingly, the degree of polymerization of effective oligosaccharides from 2 to 10 monosaccharide units imply multiple applications and highly commercial interest in the food and health market (Seo et al., 2007). As a non-digestible food, IMOs are beneficial to reduce the risk of cancer, obesity, and type II diabetes (Huang et al., 2020). Based primarily on extensive literature, the sources of dextranase are diverse, including bacteria [*Streptococcus mutans* (Suzuki et al., 2012) and *Bacteroides thetaiotaomicron* (Pittrof et al., 2021)], yeast [*Lipomyces starkeyi* (Chen et al., 2008)], and fungi [*Chaetomium gracile* (Zhao et al., 2021), *Penicillium funiculosum* (Volkov et al., 2019), and *Aspergillus allahabadii* (Netsopa et al., 2019)]. Depending on the spatial structure and catalytic characteristics, dextranase can be basically categorized into GH49 and GH66 families (Ren et al., 2019). Currently, isolation and purification of dextranase from extracellular products of microorganisms, such as *Catenovulum* (Ren et al., 2018), *Streptococcus* (Suzuki et al., 2012), and *Arthrobacter* (Ren et al., 2019), have made considerable progress in unraveling enzymology properties. Despite these advances, it has continued to be a significant challenge to address the limitation of low thermal stability and hydrolysates with irregular percentages for application. Most dextranase have been reported to maintain relatively high thermal stability below 50°C (Cai et al., 2014; Jiao et al., 2014; Wang et al., 2014; Sufiate et al., 2018b; Lai et al., 2019), even lower. Furthermore, it brings complicated steps for subsequent purification of hydrolysis products, involving glucose to IMOs even low Mw dextran with different percentages (Goulas et al., 2004; Ren et al., 2018; Abraham et al., 2019; Lai et al., 2019).

However, previous research suggested that it was challenging to control the Mw of hydrolysates synthesized by dextranase (Huang et al., 2020). In addition, industrial utilization of dextranase has been constrained by the adaptation of reaction conditions to sugar processing. Therefore, it is an efficient idea to exploit suitable dextranase in decreasing the viscosity of sugar cane juice and obtain IMOs with prebiotic functions in this study.

In order to overcome the dextran in sugarcane juice and harvest prebiotic functional products, the exploitation of dextranase with high thermal stability and hydrolysates of relatively concentrated Mw remained the objectives of the present work. In this research, a marine bacterium producing dextranase was screened, and the enzymatic characterization and protein structure were analyzed. Different hydrolyzing strategies were implemented to observe the types and proportions of hydrolytic products. The results provided new insights into the application of dextranase in the sugar industry.

2 MATERIALS AND METHODS

2.1 Materials and Chemicals

The dextran (T20, T40, and T70) and agarose (sepharose) used in this study were of analytical pure grade and purchased from GE Healthcare. Oligosaccharide standard and Coomassie brilliant blue R250 and G250 were available from Sigma-Aldrich. All other reagents were of analytical grade and obtained from Sinopharm Chemical Reagent Corporation (Shanghai, China).

2.2 Isolation and Identification of Strains

In the course of this experiment, samples played a significant role. Samples collected from Gaogong Island were diluted with appropriate concentration and then spread on 2216E medium (Solarbio, China) containing Dextran blue 2000, cultured at 30°C for 48–72 h. The main focus of this step was to select strains with large transparent zone for further purification and enzyme activity determination. Afterward, the best dextranase-producing strain G6-4B was characterized by researching the biochemical and morphological characters. Genomic DNA was extracted, and 16S rDNA was amplified by PCR using universal primers (27F 5′-AGAGTTTGATCCTGGCTCAG-3′/1492R 5′-GGTTACCTT GTTACGCTT-3′). The amplified product was purified by PCR purification kit (Bioneer, USA), and nucleotide sequencing was blasted in NCBI (https://www.ncbi.nlm.nih.gov/). MEGA 6.0 software was used to make multiple comparisons with other strains of similar genetic relationships, and neighbor-joining method was taken to build a phylogenetic tree.

2.3 Analysis of Protein Sequence and Structure

The composition and spatial structure of amino acids dominate most of the properties of enzymes, so the comparative analysis with other dextranase previously reported was executed. Dextranase sequence was searched from the whole-genome sequence annotations, then blasted in NCBI. Signal peptides, isoelectric points, and protein molecules were projected by SignalP-5.0 Server (http://www.cbs.dtu.dk/services/SignalP/) and ExPASy (https://prosite.expasy.org/). The 3D structure of protein was predicted by the Swiss model (https://swissmodel.expasy.org/).

2.4 Dextranase Production

The strain G6-4B was inoculated into the medium containing 5 g/L of peptone, 1 g/L of yeast extract, 10 g/L of dextran T20, and

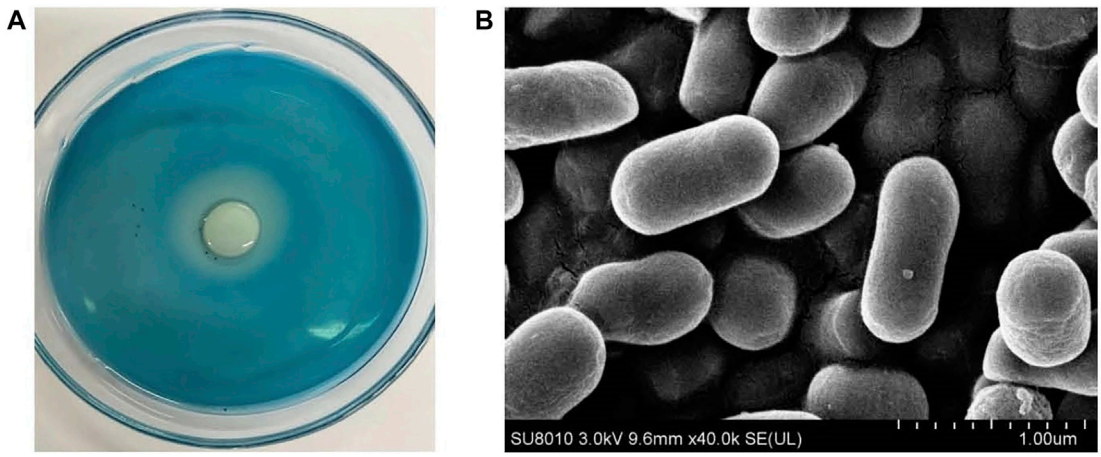

FIGURE 1 | Transparent zone formed by G6-4B on the plate containing blue dextran **(A)** and scanning electron micrograph **(B)**.

10 g/L of NaCl with pH 7.5. The fermentation supernatant was collected by centrifugation (Multifuge X3R, Thermo Fisher) as crude enzyme liquid after 30 h cultivation at 30°C, 180 rpm.

2.5 Purification of Dextranase

Ammonium sulfate was gradually (increasing by 10%) added to the crude enzyme solution, kept at 4°C, and placed on a magnetic stirrer to ensure complete dissolution. The dextranase activity and total protein content in both precipitation and supernatant with different concentrations of ammonium sulfate were measured to confirm the most suitable concentration. Then the activity of dextranase in the precipitate was maximized for 8 h, 4°C at the most suitable concentration. Precipitated protein was obtained by centrifugation at 12,000 × *g*, 4°C for 10 min, then dissolved and dialyzed in 10 mM Tris-HCl buffer (pH 7.5). Subsequently, Millipore Centrifugal Filter Units (4 ml, 10 kD) were used for ultrafiltration of dextranase and centrifuged at 3,500 × *g*, 4°C until to a required volume. Then 200 µl of dextranase ultrafiltrated was loaded on Q Sepharose Fast Flow (1.6 cm × 10 cm, GE Healthcare, Sweden), and purification analysis was performed in AKTA pure L1 system (GE Healthcare, Sweden). The chromatography column was equilibrated by 50 mM Tris-HCl (pH 7.5) before loading. Gradient elution was carried out with 1 M NaCl at a flow rate of 1 ml/min for 10 min and collected by an automatic fraction collector. The dextranase activity and protein content in each collecting tube were determined, then the separation enzyme was ultrafiltrated by Millipore Centrifugal Filter Units (4 ml, 10 kD). All of the above were designed to acquire approximately purified dextranase.

2.6 Dextranase Characterization

2.6.1 Effects of Temperature and pH on Dextranase Activity and Stability

In this experiment, various temperatures and pH were set to investigate the essential character of dextranase. The activity of dextranase was determined at different reaction temperatures (40°C–70°C) and diverse pH (4.0–9.0), respectively. Incubated at 40, 50, and 60°C for 0–5 h, the thermal stability was evaluated by measuring the dextranase activity at each interval. Analogously, the pH values of the enzyme solution were adjusted to 4.0–9.0 by various buffer solutions, then the residual activities were determined under the optimum condition after 1 h cultivation. Buffer systems were based on previous experiments (Ren et al., 2018; Lai et al., 2019), including 50 mM acetic acid-sodium acetate buffer (pH 4.0–5.5), 50 mM sodium phosphate buffer (pH 5.5–7.5), and 50 mM Tris-HCl (pH 7.5–9.0).

2.6.2 Effects of Metal Ions on Dextranase Activity

The enzyme solution was mixed with a series of metal ions at 55°C, and the final concentration of metal ions reached 1, 5, and 10 mM by appropriate dilution. Relative enzyme activity was determined by percentage conversion with the enzyme activity without metal ions as the control after 30 min.

2.7 Hydrolysate Analysis

In preliminary experiments, estimated different enzymatic hydrolysis systems were estimated: hydrolysis of 3% T20, T40, and T70 for 1 h (3 U/ml), hydrolysis of 3% T20 for 30 min, 1 and 3 h (3 U/ml), and 0.5% T20 hydrolyzed by different concentrations of dextranase (0.5, 1, and 5 U/ml) for half an hour. All the above reactions were implemented at 55°C and pH 7.5. Finally, hydrolysates were filtered by a 0.22-µm membrane and subjected to HPLC and LC-MS. The products were detected and analyzed by Waters Sugar-Pak1 (300 mm × 7.8 mm; Milford, United States) HPLC with a differential refraction detector. Methods of HPLC were based on previous experiments (Ren et al., 2018). In order to further identify the hydrolysates, LC-MS was performed. The liquid chromatography was Agilent 1100 Series LC Chem Station and analyzed by Zorbax SB-C_{18} (5 µm, 0.5 mm × 250 mm, Agilent Technologies, United States). The mobile phase was 15 mM PTA acetonitrile solution (70%, pH 7.0) at 10 µl/min, the column temperature was adjusted to 35°C, and the injection volume was 2 µl. ESI-IT-TOF (SHIMADZU, JAPAN) high-resolution tandem resolution mass spectrometry was used for detection under the following conditions: in positive ion mode, the spray voltage and current were 3.6 kV, and 0.5 L/

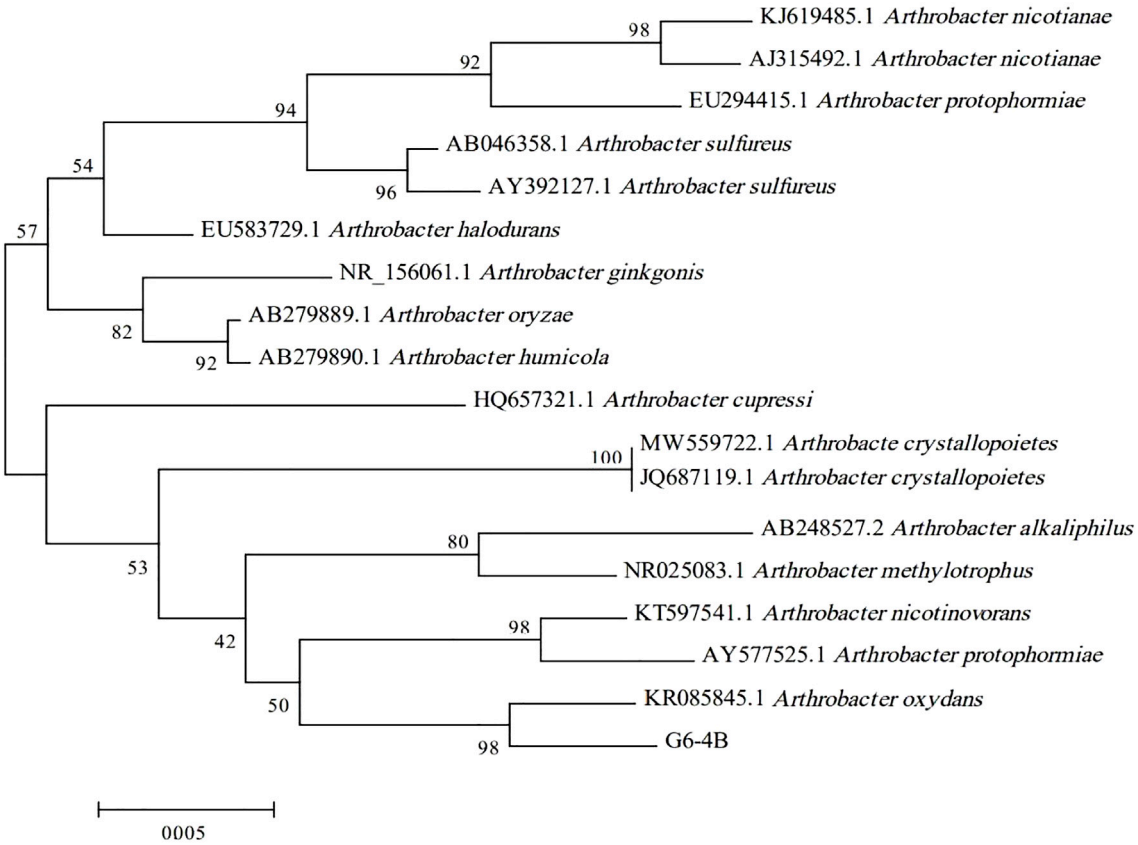

FIGURE 2 | Phylogenetic tree based on 16S rDNA gene sequences.

min, respectively; the ion source temperature was 200°C, the detection voltage was 1.8 kV.

3 RESULT

3.1 Isolation and Identification of Dextranase-Producing Strain

The strain G6-4B (**Figure 1**) illustrated the highest dextranase-producing ability according to the size of clear zone. Based on the sequence alignment of 16S rDNA and the construction of a phylogenetic tree (**Figure 2**), strain G6-4B was characterized as *Arthrobacter oxydans* (accession number OL377850). The 16S rDNA sequence was compared with other related species sequences by BLAST, and the greatest similarity with *Arthrobacter oxydans* was revealed.

3.2 Structural Characteristics of Dextranase

The amino acid sequence-encoded dextranase potentially was searched in annotation information for complete genome sequencing of G6-4B and identified as dextranase of the GH49 family by comparison in the NCBI (accession number OL439772). A total of 640 amino acids with a predicted Mw of 71.12 kDa were consistent with the result of SDS-PAGE gel, which followed. As expected, the isoelectric point was forecast to be 4.8, and there were four glycosylation sites in the total sequence. The SignalP-5.0 indicated that a 32-amino acid signal peptide at the N-terminal belongs to SPI. Swiss model prediction results showed that the sequence identity with dextranase (6nzs.1. A) from *Arthrobacter oxydans* KQ11 was 88.74%. In correspondence with dextranase of GH49, the dextranase in this study was partitioned into two main domains: the N-terminal domain was identified as a β sandwich composed of 190 amino acids, and the other domain was a right-handed parallel β-helix consisting of three parallel sheets at C-terminal (Larsson et al., 2003). β-helix is one type of β-solenoids and provides a large elongated surface to accommodate multiple binding sites when combining with flexible molecules, such as carbohydrates (Kajava and Steven, 2006). All structural characteristics above were favorable for combination with dextran and hydrolysis reaction.

3.3 Purification and Characterization of Dextranase

3.3.1 Ammonium Sulfate Precipitation

Ammonium sulfate gradients increasing experiment displayed that 70% ammonium sulfate could precipitate the maximum dextranase proteins from fermentation supernatant. Compared with the crude enzyme solution, dextranase was purified 7.40-fold

TABLE 1 | Purification of dextranase from G6-4B

Purification Step	Total activity (U) (mg)	Table protein (mg)	Specific activity (U/mg)	Purification (Fold)	Yield (%)
Culture	3103.73	346.40	8.96	1	100
Ammonium sulfate precipitatio	1446.96	21.84	66.26	7.40	46.62
Ultrafiltration	1215.11	7.94	153.04	17.08	39.15
Anion exchange chromatograph	337.69	1.17	288.62	32.25	10.88

with a specific activity of 66.26 U/mg protein and a yield of 46.62% **Table 1**. The optimal concentration of ammonium sulfate and enzyme activity precipitated are discrepants closely linked to the source of dextranase.

3.3.2 Ultrafiltration

The ultrafiltration of dextranase was treated with Millipore Centrifugal Filter Units (10 kD) to remove other low-Mw interfering proteins. Through a filter, about 7.47% of dextranase activity was lost, and specific enzyme activity was enhanced to 153.04 U/mg of protein.

3.3.3 Anion Exchange Chromatography

In line with the isoelectric point of dextranase, anion exchange chromatography was adopted in order to optimize the purification. Dextranase was successfully purified up to 32.25-fold with a specific activity of 288.62 U/mg of protein and retained 10.88%. Finally, it was issued as a single band of an estimated Mw of 70 kDa in SDS-PAGE gel, which was supported by the results of the predicted SignalP-5.0 (**Figure 3**).

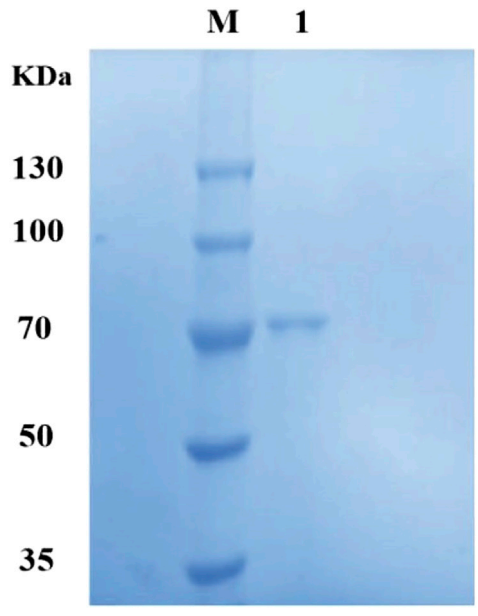

FIGURE 3 | Sodium dodecyl sulfate-polyacrylamide gel electrophoresis (SDS-PAGE) of dextranase from G6-4B. M, protein marker; Lane 1, purified dextranase.

3.3.4 Effects of Temperature and pH on Dextranase Activity and Stability

Dextranase from G6-4B performed a comparatively higher activity in 40°C–60°C (**Figure 4A**); 55°C was the optimum temperature upon further experimentation. Above 70°C, nearly 66% of the enzyme activity (190.49 U/mg) was significantly lost compared with the optimal temperature. The thermal stability diagram suggested that the dextranase activity remained at least 93% (268.42 U/mg) for 3 h at 50°C, and nearly 60% (173.17 U/mg) was maintained following storage at 60°C for 5 h (**Figure 4C**). **Figures 4B**,D showed the effects of pH on dextranase activity and stability. It appeared that the highest activity was at pH 7.5, and the relatively high level remained in the range of pH 7.0–9.0, which was consistent with the pH of sugarcane juice increasing above 7.0 during the sugar manufacturing process (Jiménez, 2009). However, under acidic conditions (at pH 3.0–6.0), more than 50% of the enzyme activity was lost. In general, dextranases from strain G6-4B could maintain a relatively high level in neutral to alkalescent environment.

3.3.5 Effects of Metal Ions on Dextranase Activity

Certain metal ions like Ca^{2+}, Mn^{2+}, and Mg^{2+}, which were reported to exist in sugarcane juice, were required for alkaline protease highest activity (Ma et al., 2007). **Table 2** indicated the efforts of various metal ions with three concentrations (1, 5, and 10 mM) of dextranase activity. Ba^{2+}, Ca^{2+}, and Mg^{2+} showed less than 40% inhibiting effects to dextranase activity while the dextranase activity was completely inhibited when Ni^{+}, Cu^{2+}, Zn^{2+}, Fe^{3+}, and Co^{2+}presented in the buffer, even at low concentrations (1 mM). Several metal ions, such as Mn^{2+}, Na^{+}, K^{+}, and NH_4^{+} showed higher inhibition with the increase of ions concentration (10 mM). No metal ions were discovered to increase the dextranase activity, which was opposite to the report of dextranase from *Hypocrea lixii* F1002 (Wu et al., 2011). Future studies could fruitfully explore this issue further by genetic modification or other means to match the requirements of the sugar industry.

3.4 Analysis of End Products of Different Hydrolysis Systems

More generally, dextranase could degrade high-Mw dextran to oligosaccharides with different degrees of polymerization or low Mw dextran by hydrolysis of α-1,6 glycoside bond (Gan et al., 2014). Especially, the Mw of dextran, dextranase activity, and hydrolysis time are very sensitive to the degree of hydrolysate polymerization. **Figure 5** and **Table 3** display the HPLC and LC-MS results of the principal products released by dextranase from G6-4B in different hydrolysis systems. What is noteworthy in this study was that the types of end products of hydrolyzing different

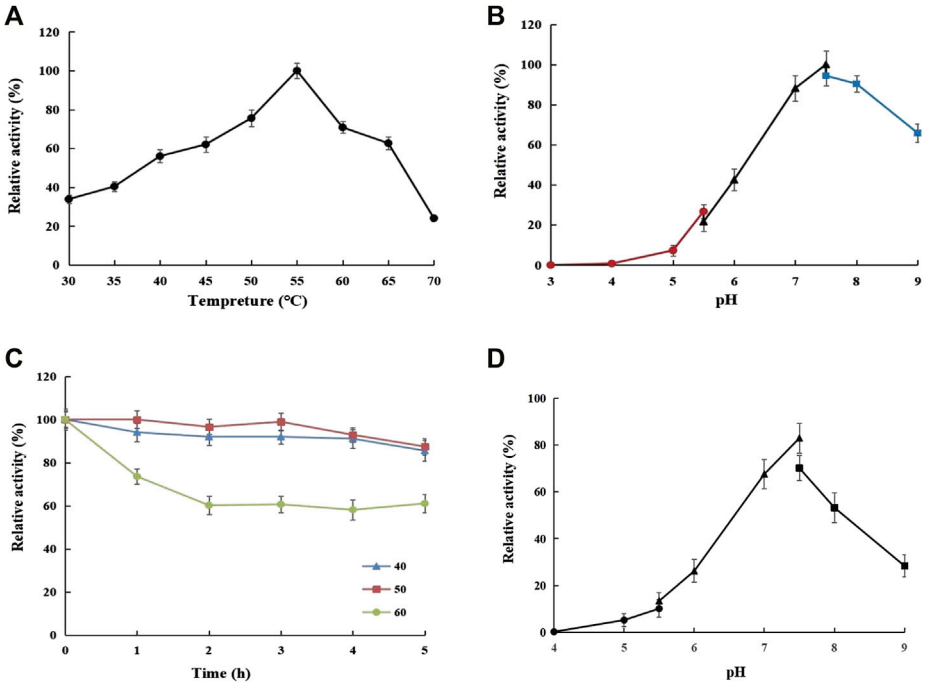

FIGURE 4 | Effects of temperature **(A)** and pH **(B)** on dextranase activity and stability **(C)** and **(D)**.

Mw dextrans (T20, T40, and T70) were mainly isomalto-triose; the polymerization of hydrolysates did not affiliate with the reaction time markedly after 30 min. On the other hand, dextranase activity had a great influence on the type of hydrolysates.

3.4.1 Influence of the Degree of Dextran Polymerization on Final Products

Investigations on the hydrolysis of dextran with varying Mw were a sign of the progress of decomposition changes when starting from the disparate initial Mw, especially in lower enzyme levels (Abraham et al., 2019). Consequently, the effects of dextran polymerization on the type of hydrolytic products by dextranase from G6-4B were first investigated in this study. More than 70% of the hydrolysates in 30 min were G3 and G4, with a small amount of dextran substrate (3% T20, 3% T40, and 3% T70), which were not completely hydrolyzed, as evidenced by HPLC results (**Figure 5B**). However, hydrolysis of dextran from T20 to T70 did not yield glucose or medium Mw dextran. This characteristic of dextranase creates significant superiority in the production of oligosaccharides with a certain degree of polymerization.

TABLE 2 | Inhibition of metal ions to dextranase

Compound	Relative activity(%)	Relative activity(%)	Relative activity(%)
	1 mM	5 mM	10 mM
Control	101.13 ± 3.79	103.53±5.28	104.27 ± 4.03
Si^{2+}	64.23 ± 3.08	62.29±2.84	59.17 ± 2.73
Mn^{2+}	61.51 ± 5.32	40.99±3.18	23.30 ± 1.85
Mg^{2+}	76.57 ± 4.03	72.49±3.71	61.61 ± 2.83
Co^{2+}	5.22 ± 0.64	0	0
Na^{+}	65.30 ± 5.19	55.77±4.80	41.29 ± 3.55
Ni^{+}	0	0	0
Cu^{2+}	0	0	0
Ba^{2+}	75.02 ± 4.28	68.80 ± 5.02	69.09 ± 2.76
Ca^{2+}	72.10 ± 4.16	64.91 ± 3.64	61.22 ± 1.81
Li^{+}	59.08 ± 3.08	54.21 ± 4.11	54.60 ± 1.64
Zn^{2+}	0	0	0
K^{+}	65.20 ± 2.86	60.73 ± 3.74	38.47 ± 0.59
Fe^{3+}	0	0	0
NH_4^{+}	55.67 ± 4.73	44.10 ± 2.52	34.19 ± 2.07

3.4.2 Effect of Reaction Time on the Final Products

Generally, the Mw of decomposition products decreased with the increase in incubation time following a gradual pattern (Abraham et al., 2019). Moreover, the proportion of hydrolysates varied with the extension of incubation time. **Figure 5C** shows the hydrolysates at different incubation times. After 30 min of hydrolysis, more than 70% of dextran was completely hydrolyzed to oligosaccharides (G3 accounted for more than 70%, and the rest was mainly G4). When the incubation time was extended from 30 min to 3 h, the types of hydrolysates did not change significantly.

3.4.3 Effect of Enzyme Activity on End Products

The results were summarized in **Figure 5D**, reflecting that the increases in dextranase activity resulted in hydrolysates of different components gradually becoming simple (incubation for 30 min), indicating that the concentration of dextranase was the key factor determining hydrolysates. Residual dextran and oligosaccharides (G7, G4, and G3) remained coexisting at an activity of 0.5 U/ml.

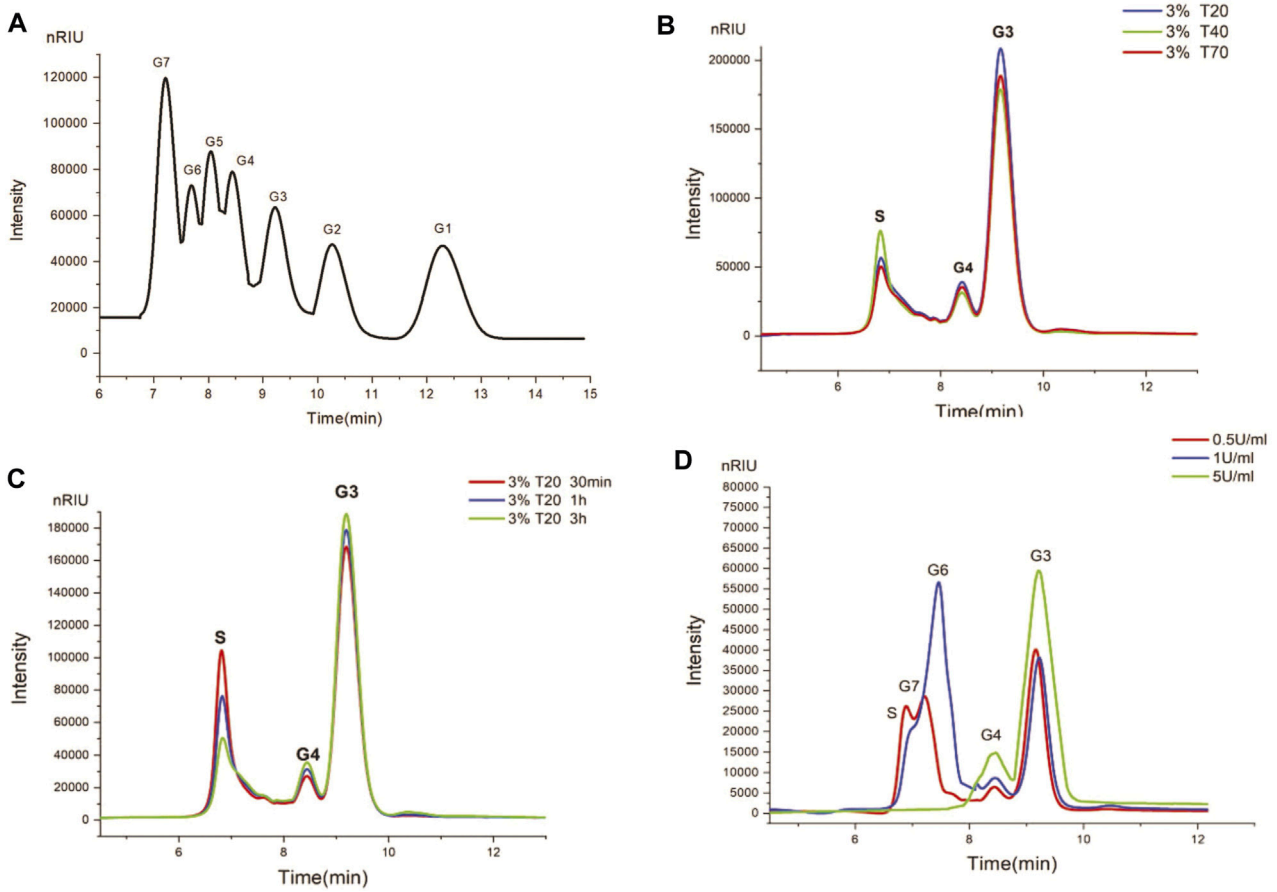

FIGURE 5 | Hydrolysates of different hydrolysis systems by HPLC. **(A)** standards from G1 to G7 were glucose, maltose, isomalto-triose, isomalto-tetraose, isomalto-pentaose, isomalto-hexaose, and isomalto-heptaose, respectively. **(B)** Hydrolysates of 3% T20, 3%T40, and 3%T70 after 1 h. **(C)** Hydrolysates of 3% T20 after 30 min, 1 h, and 3 h. **(D)** Hydrolysates of 0.5%T20 by different dextranase activity (0.5, 1, and 5 U/ml).

When enzyme activity increased to 1 U/ml, the content of residual dextran decreased gradually, while the content of oligosaccharides (G6, G4, and G3) accumulated. Finally, species of hydrolysates (principally G3 and G4) remained stable at 5 U/ml; increasing more activity did not affect hydrolysates.

3.4.4 LC-MS Analysis of End Products

Considering that the Mw of dextran synthesized by contaminant microorganisms kept a general concentration of 0.1%–0.5% (Abraham et al., 2019), the hydrolysates of 0.5% T20 for 30 min were selected for LC-MS. **Table 3** reveals that the major hydrolysates were isomalto-triose, accounting for 73.19%, and the rest were isomalto-tetraose (11.58%), isomalto-hexaose (8.03%), and isomalto-heptaose (7.19%). Depending on the above data, the possibility of controlling the types of hydrolysates could be realized by regulating the activity level of dextranase, especially to obtain isomalto-triose.

TABLE 3 | LC-MS results of hydrolysates by dextranase

Compound	Mass	Abund	Relative amount
$C_{18}H_{32}O_{16}$	504.17	4802	73.19%
$C_{24}H_{42}O_{21}$	666.22	760	11.58%
$C_{36}H_{62}O_{31}$	990.33	527	8.03%
$C_{42}H_{72}O_{36}$	1152.38	472	7.19%

4 DISCUSSION

According to previous reports, the sources of dextranase were extensive, ranging from ocean, soil, and the tissues of diverse plants. Consistent with G6-4B in this research, dextranase production strains, such as *A. oxydans* KQ11 (Wang et al., 2014) and *Catenovulum* sp. DP03 (Cai et al., 2014) reported, were both derived from the marine environment. Dextranase from various microbial sources showed discrepant structures, and the Mw tended to be concentrated at 40–140 kDa, although there were exceptions. The Mw of dextranase from *Penicillium lilacinum* (Das and Dutta, 1996) was only 26 kDa, while the Mw of dextranase from *Bacillus licheniformis* KIBGE-IB25 (Zohra et al., 2015) was large up to 158 kDa. The Mw of dextranase from G6-4B

was analogous to the dextranase from *C. gracile* (71 and 77 kDa), which were commercially used for dextran removal in the sugar industry (Khalikova et al., 2005). Additionally, in the light of the crystal structure of dextranase protein published in Protein Date Bank (PDB), the Mw of dextranase in GH66 (3VMN, 5AXG) was generally higher than that of GH49 (6NZS, 1OGO). It was conjectured that the differences were attributed to various domain compositions of the two families.

High thermal stability is one of the preconditions for dextranase application in the sugar industry. Previous results (Cai et al., 2014; Jiao et al., 2014; Wang et al., 2014; Sufiate et al., 2018b; Lai et al., 2019) had shown that the optimum reaction temperature of dextranase mostly ranged from 25°C to 60°C, which was possibly related to the physiological characteristics and survival environment of various strains. In general, the rate of chemical reaction increases with high temperature. However, as a protein, when the temperature is exorbitant, the enzyme protein will be irreversibly deformed, resulting in the enzyme losing catalytic activity. Similarly, within a certain pH range, the enzyme shows catalytic activity, but beyond the pH range, the enzyme activity will fade or even lose. Deng et al. (2020) reported that the expression of dextranase from marine bacteria in *Escherichia coli* showed no activity at 50°C for 1 h. On the contrary, a thermostable dextranase isolated from the Great Artesian Basin of Australia exhibited optimum activity at 70°C (Wynter et al., 1996). In order to neutralize more acid pH values produced by juice derived from the deteriorated sugar cane, large amounts of lime were consumed. So, the pH values of juice varied from acidic (pH 5.5–6.0) to neutral or slightly alkaline (pH 7.0–8.0), with a relatively wide range. At the stage of juice clarification, the temperature was generally up to 65°C or higher (Jiménez, 2009). Compared with dextranase from the majority strains, dextranase in this study has greatly improved the tolerance to high temperature; such characteristics were more adaptable for the application of high-temperature sugar milling processes in the sugarcane industry. Nevertheless, the performance of pH and metal ion stability was not satisfactory (Lee et al., 2017; Phong et al., 2018). Relatively high enzyme activity could be maintained only in neutral to slightly alkaline environment, distinguished from the dextranase from *Streptomyces* sp. NK458 (Purushe et al., 2012) and *Chaetomium gracile* (Zhao et al., 2021), which displayed high enzyme activity ranging from pH 5.0 to 10.0 (>50% activity). Certain metal ions exhibited to promote dextranase activity, for example, Fe^{2+} and Li^{+} (Huang et al., 2019). Moreover, contrary to the results of our study, the existence of Co^{2+}, Mn^{2+}, Ca^{2+} accelerated the activity of dextranase from *A. allahabadii* X26 (Netsopa et al., 2019). Therefore, the stability still needs to be further improved to better adapt to industrial applications.

The main hydrolysates of different Mw dextran were all isomalto-triose, accompanied by a small amount of isomalto-tetraose, isomalto-hexaose, and isomalto-heptaose. The species of hydrolysates were greatly affected by dextranase activity, did not change with time extension after 30 min of reaction. Compared with the dextranase from *H. lixii* F1002 (Gan et al., 2014), which obtained a series of dextran with decreasing Mw within 90 min, the dextranase in this study reflected a distinct hydrolysis process. The species of hydrolysates were significantly different from most reported dextranase, which hydrolysates was relatively dispersed, including glucose (Lai et al., 2019), maltose (Lai et al., 2019), isomalto-triose (Ren et al., 2018), to dextran of medium Mw (Abraham et al., 2019). In addition, this reaction pattern was significantly different from the previously reported hydrolysis trend of dextranase (Deng et al., 2020), in which, the proportion of hydrolysates varied from 0.5 to 6 h. These phenomena indicated that the dextranase in this study was suitable for the application in the sugar industry, which was largely realized within the first 30 min of incubation time. Based on the catalytic properties of dextranase, the production of IMOs with specific Mw by dextranase has been developed by immobilization technology or the construction of multiple enzymatic reaction systems. For example, the formation ratio of IMOs with specific Mw was controlled by establishing a double enzyme reaction system of dextranase and dextransucrose maltose acceptor reaction (Huang et al., 2020). IMOs with polymerization degree of 8–10 could be quantitatively produced by immobilizing dextranase on epoxy-activated global convective interaction medium (CIM®) disk and adjusting the amount of immobilized enzyme, substrate concentration, and flow rate (Bertrand et al., 2014). Future studies could conduct an inquiry into the association between hydrolysates with dextranase and pay attention to more efficient development and utilization of dextranase.

5 CONCLUSION

The dextranase-producing strain *Arthrobacter oxydans* G6-4B was isolated and identified from Gaogong island. The dextranase was successfully purified up to 32.25-fold with a specific activity of 288.62 U/mg protein. A total of 640 amino acids encoded dextranase with a Mw of 71.12 kDa and belonging to the GH49 family. The pH and temperature optima were around 7.5 and 55°C, respectively. The types of products obtained by hydrolysis of dextran with different Mw (T20, T40, and T70) were relatively consistent; isomalto-triose accounted for more than 73%, without glucose and maltose. Given its superior thermal stability and relative simplicity of hydrolysates, the dextranase in this study presented great potential in the sugar industry to remove dextran and obtain iso-maltose with prebiotic effects. Even if many unknown factors determine the hydrolysates of dextranase, our research has bridged the gap between theory and application.

DATA AVAILABILITY STATEMENT

The original contributions presented in the study are included in the article/Supplementary Material, further inquiries can be directed to the corresponding author.

AUTHOR CONTRIBUTIONS

NL and PL designed the experiments. NL, PL, and YL performed the experiments. NL, LX, and ZW analyzed the data. NL and XD wrote the manuscript. SW reviewed the manuscript. All authors approved the final manuscript.

FUNDING

This research was funded by the Natural Science Foundation of Jiangsu Province (BK20201028) and National Natural Science Foundation of China (Grant No: 32172154). This work was supported by the Research Start-up Fund of Jiangsu Ocean University and the Priority Academic Program Development of Jiangsu Higher Education Institutions.

REFERENCES

Abraham, K., Weigelt, J., Rudolph, S., and Flöter, E. (2019). Systematic Study on the Enzymatic Decomposition of Various Dextran Fractions. *Process Biochem.* 80, 129–137. doi:10.1016/j.procbio.2019.01.024

Bertrand, E., Pierre, G., Delattre, C., Gardarin, C., Bridiau, N., Maugard, T., et al. (2014). Dextranase Immobilization on Epoxy CIM Disk for the Production of Isomaltooligosaccharides From Dextran. *Carbohydr. Polym.* 111, 707–713. doi:10.1016/j.carbpol.2014.04.100

Cai, R., Lu, M., Fang, Y., Jiao, Y., Zhu, Q., Liu, Z., et al. (2014). Screening, Production, and Characterization of Dextranase From *Catenovulum* Sp. *Ann. Microbiol.* 64, 147–155. doi:10.1007/s13213-013-0644-7

Chen, L., Zhou, X., Fan, W., and Zhang, Y. (2008). Expression, Purification and Characterization of a Recombinant Lipomyces Starkey Dextranase in *Pichia pastoris*. *Protein Expr. Purif.* 58, 87–93. doi:10.1016/j.pep.2007.10.021

Chew, K. W., Chia, S. R., Lee, S. Y., Zhu, L., and Show, P. L. (2019). Enhanced Microalgal Protein Extraction and Purification Using Sustainable Microwave-Assisted Multiphase Partitioning Technique. *Chem. Eng. J.* 367, 1–8. doi:10.1016/j.cej.2019.02.131

Das, D. K., and Dutta, S. K. (1996). Purification, Biochemical Characterization and Mode of Action of an Extracellular Endo-Dextranase From the Culture Filtrate of *Penicillium Lilacinum*. *Int. J. Biochem. Cell Biol.* 28, 107–113. doi:10.1016/1357-2725(95)00105-0

Deng, T., Feng, Y., Xu, L., Tian, X., Lai, X., Lyu, M., et al. (2020). Expression, Purification and Characterization of a Cold-Adapted Dextranase From Marine Bacteria and its Ability to Remove Dental Plaque. *Protein Expr. Purif.* 174, 105678. doi:10.1016/j.pep.2020.105678

Eggleston, G., Côté, G., and Santee, C. (2011). New Insights on the Hard-To-Boil Massecuite Phenomenon in Raw Sugar Manufacture. *Food Chem.* 126, 21–30. doi:10.1016/j.foodchem.2010.10.038

Gan, W., Zhang, H., Zhang, Y., and Hu, X. (2014). Biosynthesis of Oligodextrans With Different Mw by Synergistic Catalysis of Dextransucrase and Dextranase. *Carbohydr. Polym.* 112, 387–395. doi:10.1016/j.carbpol.2014.06.018

Goulas, A. K., Cooper, J. M., Grandison, A. S., and Rastall, R. A. (2004). Synthesis of Isomaltooligosaccharides and Oligodextrans in a Recycle Membrane Bioreactor by the Combined Use of Dextransucrase and Dextranase. *Biotechnol. Bioeng.* 88, 778–787. doi:10.1002/bit.20257

Huang, R., Zhong, L., Xie, F., Wei, L., Gan, L., Wang, X., et al. (2019). Purification, Characterization and Degradation Performance of a Novel Dextranase From *Penicillium cyclopium* CICC-4022. *Int. J.Mol. Sci.* 20, 1360. doi:10.3390/ijms20061360

Huang, S.-X., Hou, D.-Z., Qi, P.-X., Wang, Q., Chen, H.-L., Ci, L.-Y., et al. (2020). Enzymatic Synthesis of Non-Digestible Oligosaccharide Catalyzed by Dextransucrase and Dextranase from Maltose Acceptor Reaction. *Biochem. Biophysical Res. Commun.* 523, 651–657. doi:10.1016/j.bbrc.2019.12.010

Jiao, Y.-L., Wang, S.-J., Lv, M.-S., Jiao, B.-H., Li, W.-J., Fang, Y.-W., et al. (2014). Characterization of a Marine-Derived Dextranase and its Application to the Prevention of Dental Caries. *J. Ind. Microbiol. Biotechnol.* 41, 17–26. doi:10.1007/s10295-013-1369-0

Jiménez, E. R. (2009). Dextranase in Sugar Industry: A Review. *Sugar Tech.* 11, 124–134. doi:10.1007/s12355-009-0019-3

Kajava, A. V., and Steven, A. C. (2006). β-Rolls, β-Helices, and Other β-Solenoid Proteins. *Adv. Protein Chem.* 73, 55–96. doi:10.1016/s0065-3233(06)73003-0

Khalikova, E., Susi, P., and Korpela, T. (2005). Microbial Dextran-Hydrolyzing Enzymes: Fundamentals and Applications. *Microbiol. Mol. Biol. Rev.* 69, 306–325. doi:10.1128/mmbr.69.2.306-325.2005

Krishna Koyande, A., Tanzil, V., Murraly Dharan, H., Subramaniam, M., Robert, R. N., Lau, P.-L., et al. (2020). Integration of Osmotic Shock Assisted Liquid Biphasic System for Protein Extraction from Microalgae Chlorella Vulgaris. *Biochem. Eng. J.* 157, 107532. doi:10.1016/j.bej.2020.107532

Lai, X., Liu, X., Liu, X., Deng, T., Feng, Y., Tian, X., et al.(2019). The Marine *Catenovulum Agarivorans* MNH15 and Dextranase: Removing Dental Plaque. *Mar. Drugs.* 17, 592. doi:10.3390/md17100592

Larsson, A. M., Andersson, R., Ståhlberg, J., Kenne, L., and Jones, T. A. (2003). Dextranase from Penicillium Minioluteum. *Structure.* 11, 1111–1121. doi:10.1016/s0969-2126(03)00147-3

Lee, S. Y., Khoiroh, I., Ooi, C. W., Ling, T. C., and Show, P. L. (2017). Recent Advances in Protein Extraction Using Ionic Liquid-Based Aqueous Two-Phase Systems. *Separation Purif. Rev.* 46, 291–304. doi:10.1080/15422119.2017.1279628

Ma, C., Ni, X., Chi, Z., Ma, L., and Gao, L. (2007). Purification and Characterization of an Alkaline Protease from the marine Yeast *Aureobasidium Pullulans* for Bioactive Peptide Production from Different Sources. *Mar. Biotechnol.* 9, 343–351. doi:10.1007/s10126-006-6105-6

Martínez, D., Menéndez, C., Chacón, O., Fuentes, A. D., Borges, D., Sobrino, A., et al. (2021). Removal of Bacterial Dextran in Sugarcane Juice by *Talaromyces minioluteus* Dextranase Expressed Constitutively in Pichia Pastoris. *J. Biotechnol.* 333, 10–20. doi:10.1016/j.jbiotec.2021.04.006

Münkel, F., and Wefers, D. (2019). Fine Structures of Different Dextrans Assessed by Isolation and Characterization of Endo-Dextranase Liberated Isomalto-Oligosaccharides. *Carbohydr. Polym.* 215, 296–306. doi:10.1016/j.carbpol.2019.03.027

Netsopa, S., Niamsanit, S., Araki, T., Kongkeitkajorn, M. B., and Milintawisamai, N. (2019). Purification and Characterization Including Dextran Hydrolysis of Dextranase from *Aspergillus allahabadii* X26. *Sugar Tech.* 21, 329–340. doi:10.1007/s12355-018-0652-9

Oliveira, A. S. d., Rinaldi, D. A., Tamanini, C., Voll, C. E., and Hauly, M. C. O. (2002). Fatores que Interferem na Produção de Dextrana por Microrganismos Contaminantes da Cana-de-Açúcar. *Semina: Tech. Ex.* 23, 93. doi:10.5433/1679-0375.2002v23n1p93

Park, T.-S., Jeong, H. J., Ko, J.-A., Ryu, Y. B., Park, S.-J., Kim, D., et al. (2012). Biochemical Characterization of Thermophilic Dextranase from a Thermophilic Bacterium, *Thermoanaerobacter Pseudethanolicus*. *J. Microbiol. Biotechnol.* 22, 637–641. doi:10.4014/jmb.1112.12024

Phong, W. N., Show, P. L., Le, C. F., Tao, Y., Chang, J.-S., and Ling, T. C. (2018). Improving Cell Disruption Efficiency to Facilitate Protein Release from Microalgae Using Chemical and Mechanical Integrated Method. *Biochem. Eng. J.* 135, 83–90. doi:10.1016/j.bej.2018.04.002

Pittrof, S. L., Kaufhold, L., Fischer, A., and Wefers, D. (2021). Products Released from Structurally Different Dextrans by Bacterial and Fungal Dextranases. *Foods.* 10, 244. doi:10.3390/foods10020244

Purushe, S., Prakash, D., Nawani, N. N., Dhakephalkar, P., and Kapadnis, B. (2012). Biocatalytic Potential of an Alkalophilic and Thermophilic Dextranase as a Remedial Measure for Dextran Removal During Sugar Manufacture. *Bioresour. Technology.* 115, 2–7. doi:10.1016/j.biortech.2012.01.002

Ren, W., Cai, R., Yan, W., Lyu, M., Fang, Y., and Wang, S. (2018). Purification and Characterization of a Biofilm-Degradable Dextranase from a Marine Bacterium. *Mar. Drugs.* 16, 51. doi:10.3390/md16020051

Ren, W., Liu, L., Gu, L., Yan, W., Feng, Y. L., Dong, D., et al. (2019). Crystal Structure of GH49 Dextranase from *Arthrobacter Oxidans* KQ11: Identification of Catalytic Base and Improvement of Thermostability Using Semirational Design Based on B-Factors. *J. Agric. Food Chem.* 67, 4355–4366. doi:10.1021/acs.jafc.9b01290

Sankaran, R., Bong, J. H., Chow, Y. H., Wong, F. W. F., Ling, T. C., and Show, P. L. (2019). Reverse Micellar System in Protein Recovery - A Review of the Latest Developments. *Curr. Protein Pept. Sci.* 20, 1012–1026. doi:10.2174/1389203720666190628142203

Seo, E.-S., Nam, S.-H., Kang, H.-K., Cho, J.-Y., Lee, H.-S., Ryu, H.-W., et al. (2007). Synthesis of Thermo- and Acid-Stable Novel Oligosaccharides by Using

Dextransucrase with High Concentration of Sucrose. *Enzyme Microb. Technology.* 40, 1117–1123. doi:10.1016/j.enzmictec.2006.08.017

Sufiate, B. L., Soares, F. E. F., Gouveia, A. S., Moreira, S. S., Cardoso, E. F., Tavares, G. P., et al. (2018a). Statistical Tools Application on Dextranase Production from Pochonia Chlamydosporia (VC4) and its Application on Dextran Removal from Sugarcane Juice. *Acad. Bras. Ciênc.* 90, 461–470. doi:10.1590/0001-3765201820160333

Sufiate, B. L., Soares, F. E. d. F., Moreira, S. S., Gouveia, A. d. S., Cardoso, E. F., Braga, F. R., et al. (2018b). *In Vitro* and In Silico Characterization of a Novel Dextranase from *Pochonia Chlamydosporia*. *3 Biotech.* 8, 167. doi:10.1007/s13205-018-1192-4

Suzuki, N., Kim, Y. M., Fujimoto, Z., Momma, M., Okuyama, M., Mori, H., et al. (2012). Structural Elucidation of Dextran Degradation Mechanism by Streptococcus Mutans Dextranase Belonging to Glycoside Hydrolase Family 66. *J. Biol. Chem.* 287, 19916. doi:10.1074/jbc.M112.342444

Tanoue Batista, M. C., Soccol, C. R., Spier, M. R., Libardi Junior, N., and Porto de Souza Vandenberghe, L. (2021). Potential Application of Dextranase Produced by Penicillium aculeatum in Solid-State Fermentation from Brewer's Spent Grain in Sugarcane Process Factories. *Biocatal. Agric. Biotechnol.* 35, 102086. doi:10.1016/j.bcab.2021.102086

Volkov, P. V., Gusakov, A. V., Rubtsova, E. A., Rozhkova, A. M., Matys, V. Y., Nemashkalov, V. A., et al. (2019). Properties of a Recombinant GH49 Family Dextranase Heterologously Expressed in Two Recipient Strains of *Penicillium* Species. *Biochimie.* 157, 123–130. doi:10.1016/j.biochi.2018.11.010

Wang, D., Lu, M., Wang, X., Jiao, Y., Fang, Y., Liu, Z., et al. (2014). Improving Stability of a Novel Dextran-Degrading Enzyme from marine *Arthrobacter Oxydans* KQ11. *Carbohydr. Polym.* 103, 294–299. doi:10.1016/j.carbpol.2013.12.025

Wang, Z.-P., Wang, P.-K., Ma, Y., Lin, J.-X., Wang, C.-L., Zhao, Y.-X, et al. (2022). Laminaria japonica Hydrolysate Promotes Fucoxanthin Accumulation in *Phaeodactylum tricornutum*. *Bioresour. Technol.* 344, 126117. doi:10.1016/j.biortech.2021.126117

Wu, D.-T., Zhang, H.-B., Huang, L.-J., and Hu, X.-Q. (2011). Purification and Characterization of Extracellular Dextranase from a Novel Producer, *Hypocrea Lixii* F1002, and its Use in Oligodextran Production. *Process Biochem.* 46, 1942–1950. doi:10.1016/j.procbio.2011.06.025

Wynter, C., Patel, B. K. C., Bain, P., Jersey, J., Hamilton, S., and Inkerman, P. A. (1996). A Novel Thermostable Dextranase from a *Thermoanaerobacter* Species Cultured from the Geothermal Waters of the Great Artesian Basin of Australia. *FEMS Microbiol. Lett.* 140, 271–276. doi:10.1111/j.1574-6968.1996.tb08348.x

Zhao, J., Wang, L., Wei, X., Li, K., and Liu, J. (2021). Food-Grade Expression and Characterization of a Dextranase from *Chaetomium Gracile* Suitable for Sugarcane Juice Clarification. *Chem. Biodivers.* 18, e2000797. doi:10.1002/cbdv.202000797

Zohra, R. R., Aman, A., Ansari, A., Haider, M. S., and Qader, S. A. U. (2015). Purification, Characterization and End Product Analysis of Dextran Degrading Endodextranase from *Bacillus Licheniformis* KIBGE-IB25. *Int. J. Biol. Macromolecules.* 78, 243–248. doi:10.1016/j.ijbiomac.2015.04.007

Conflict of Interest: The authors declare that the research was conducted in the absence of any commercial or financial relationships that could be construed as a potential conflict of interest.

Publisher's Note: All claims expressed in this article are solely those of the authors and do not necessarily represent those of their affiliated organizations, or those of the publisher, the editors, and the reviewers. Any product that may be evaluated in this article, or claim that may be made by its manufacturer, is not guaranteed or endorsed by the publisher.

frontiers | Frontiers in Bioengineering and Biotechnology

ORIGINAL RESEARCH
published: 12 April 2022
doi: 10.3389/fbioe.2022.866419

Fungal Inhibition of Agricultural Soil Pathogen Stimulated by Nitrogen-Reducing Fertilization

Min-Chong Shen[1], *You-Zhi Shi*[2], *Guo-Dong Bo*[1] *and Xin-Min Liu*[1]*

[1]Tobacco Research Institute of Chinese Academy of Agricultural Sciences, Qingdao, China, [2]Cigar Institute of China Tobacco Hubei Industrial Co., Ltd., Yichang, China

Plant health is the fundamental of agricultural production, which is threatened by plant pathogens severely. The previous studies exhibited the effects of different pathogen control strategies (physical, chemical, and microbial methods), which resulted from bringing in exogenous additives, on microbial community structures and functions. Nevertheless, few studies focused on the potential inhibitory abilities of native microbial community in the soil, which could be activated or enhanced by different fertilization strategies. In this study, three plant diseases (TMV, TBS, and TBW) of tobacco, fungal community of tobacco rhizosphere soil, and the correlation between them were researched. The results showed that nitrogen-reducing fertilization strategies could significantly decrease the occurrence rate and the disease index of three tobacco diseases. The results of bioinformatics analyses revealed that the fungal communities of different treatments could differentiate the nitrogen-reducing fertilization group and the control group (CK). Furthermore, key genera which were responsible for the variation of fungal community were explored by LEfSe analysis. For instance, *Tausonia* and *Trichocladium* increased, while *Naganishia* and *Fusicolla* decreased under nitrogen-reducing fertilization conditions. Additionally, the correlation between tobacco diseases and key genera was verified using the Mantel test. Moreover, the causal relationship between key genera and tobacco diseases was deeply explored by PLS–PM analysis. These findings provide a theoretical basis for a nitrogen-reducing fertilization strategy against tobacco diseases without exogenous additives and make contributions to revealing the microbial mechanism of native-valued fungal key taxa against tobacco diseases, which could be stimulated by agricultural fertilization management.

Keywords: nitrogen-reducing fertilization, variation of fungal community, fungal inhibition, cash crop, sustainable agriculture

OPEN ACCESS

Edited by:
Zhipeng Wang,
Qingdao Agricultural University, China

Reviewed by:
Guodong Liu,
Shandong University, China
Weiyi Wang,
Third Institute of Oceanography, China

***Correspondence:**
Xin-Min Liu
liuxinmin@caas.cn

Specialty section:
This article was submitted to Bioprocess Engineering, a section of the journal Frontiers in Bioengineering and Biotechnology

Received: *31 January 2022*
Accepted: *11 March 2022*
Published: *12 April 2022*

Citation:
Shen M-C, Shi Y-Z, Bo G-D and Liu X-M (2022) Fungal Inhibition of Agricultural Soil Pathogen Stimulated by Nitrogen-Reducing Fertilization. Front. Bioeng. Biotechnol. 10:866419. doi: 10.3389/fbioe.2022.866419

INTRODUCTION

Plant diseases can devastate agriculture by reducing crop yields and causing severe economic losses (Strange and Scott, 2005). Plant diseases caused by soilborne pathogens can diminish the yields of vegetables, fruits, and other economically important crops by up to 20% (Jaiswal et al., 2018). The perniciousness of plant diseases has risen significantly due to current agricultural practices including intensive cultivation, overuse of fertilizers, utilization of high-yield but pathogen-susceptible cultivars, and consecutive years of continuous cropping (Chakraborty and Newton, 2011; Ghorbanpour et al.,

2018). Thus, disease management strategies targeting plant pathogens are of vital importance (Peng et al., 2017).

Much effort has been expended in exploring disease management strategies under various circumstances. Physical methods such as heating and solarizing the soil are laborious, and they can hardly eradicate pathogens (De Carvalho Pontes et al., 2019). Chemical methods such as pesticides are expensive, they can poison the environment, and they can result in pesticide-resistant bacterial populations (Morais et al., 2019) that may become ineffective in the face of the bacterial genetic variability (Kim et al., 2016). Crop rotation is a slow method for reducing pathogen density in soil, making it unsuitable when severe disease breakout (Chellemi et al., 2016). Biocontrol bacteria are receiving increasing attention as a potential alternative to traditional methods for controlling plant diseases (Choi et al., 2020; Ogunnaike et al., 2021; Ahmed et al., 2022), based on being harmless, effective, and sustainable (Xie et al., 2020). Previous studies have identified various biocontrol agents including *Bacillus* spp. (Cao et al., 2011), *Paenibacillus polymyxa* (Chunyu et al., 2017), *Streptomyces* spp. (Abo-Zaid et al., 2020), and *Pseudomonas fluorescens* (Huang et al., 2020). Additionally, a non-native arbuscular mycorrhizal fungal inoculant has been reported to improve the growth and enhance the resistance system of multiple plants (Pellegrino et al., 2012; Aliyu et al., 2019; Yang L et al., 2021).

Previous research corresponding to physical, chemical, and microbial strategies against plant diseases discovered that most of the strategies could convert the microbial community of the rhizosphere soil of plants into an enhanced status of pathogen resistance (Hu et al., 2020; Liu et al., 2020). According to the principle of low cost and environmental friendliness, strategies without exogenous additives received more and more attention. Evidence had demonstrated that nitrogen-reducing fertilization could change the microbial community of planting soils (Zhou et al., 2020; Yang T et al., 2021). As a no-additive strategy, the inhibitory effect of nitrogen-reducing fertilization against tobacco diseases was little researched.

In this study, a nitrogen-reducing fertilization strategy was used in the process of tobacco planting. The occurrence rate and disease index of tobacco diseases, including tobacco mosaic virus (TMV), tobacco black shank (TBS), and tobacco bacterial wilt (TBW), were investigated. The fungal community of tobacco rhizosphere soil differentiated the nitrogen-reducing treatments from the control group (CK). The key taxa which contributed to the variation of fungal community due to nitrogen-reducing fertilization were analyzed and identified. Moreover, the dominant role played by the key taxa to help inhibit tobacco diseases was verified using the Mantel test. This study contributed to reveal the conversion of the fungal community against tobacco pathogens, which provided a feasible, economic, and eco-friendly fertilization strategy in the tobacco-planting industry.

MATERIALS AND METHODS

Design of Field Experiments

This experiment was conducted in Huangdao district, Qingdao, Shandong Province (36°00′44.86″ N, 119°51′35.30″ E), China, from April 10 to 15 October 2020. The average annual rainfall of the experimental field was 696.6 mm, the annual sunshine duration was 2,110.1 h, and the annual average temperature was 12.5 C. The previous crop in the experiment site was tobacco (Zhongyan 100 variety), which had been planted for four consecutive years. The flue-cured tobacco variety used in this experiment was Zhongyan 100. The fertilization procedure in this experiment was carried out according to the fertilization strategies (**Supplementary Table S1**). The tobacco was transplanted at May 5, and tobacco diseases were investigated on July 23, according to the grade and investigation method of tobacco diseases and insect pests (Tobacco Research Institute, 2008).

Collection and Preprocessing of Soil Samples

Rhizosphere soil is the soil that lies much closer to the plant roots. The samples of tobacco rhizosphere soil were collected using a sterilized brush and by gentle shaking (Pétriacq et al., 2017). Three replicates were prepared for each treatment. The soil samples were immediately stored in a −20°C refrigerator for subsequent extraction of soil DNA.

DNA Extraction and Amplicon Sequencing of ITS Genes

About 500 mg soil sample was collected from well-mixed rhizosphere soil from each replication. DNA was extracted from the soil using a DNA extraction kit (FastDNA™ SPIN Kit for soil, MP Biomedicals, LLC, Solon, OH, United States) according to the manufacturer's instructions. Subsequently, DNA was tested with 1% agarose gel, and the successfully extracted DNA was stored at −20°C immediately.

The PCR of the ITS1 region of the fungal ITS gene sequencing was conducted using the specific primers CTT GGTCATTTAGAGGAAGTAA and GCTGCGTTCTTCATC GATGC. The amplification products were tested for specificity in 1% agarose gel (Yuan et al., 2020). Then, the library was constructed using the library construction kit TruSeq® DNA PCR-Free Sample Preparation kit (Illumina, San Diego, CA, United States). After the library was successfully constructed, the quantitative process was implemented using the Qubit® 2.0 Fluorometer (Life Technologies, Carlsbad, CA, United States) and qPCR. After the quantitative test, subsequent sequencing was performed on the Illumina MiSeq platform.

Processing and Analyses of Bioinformatics and Tobacco Disease Data

The raw data after sequencing were assembled and attached by FLASH (V1.2.11, https://ccb.jhu.edu/software/FLASH/index.shtml) to obtain raw tags. Subsequently, QIIME software (V1.9.1, http://qiime.org/scripts/split_libraries_fastq.html) was used to filter raw tags. Then, the UCHIME algorithm (http://www.drive5.com/usearch/manual/uchime_algo.html) (Haas et al., 2011) was used to detect and remove chimeras against the

Unite database (https://unite.ut.ee/) (Edgar et al., 2011) and get effective data (effective tags) (Callahan et al., 2016).

The valid data from all samples were clustered into the same operational taxonomic units (OTUs), and the OTUs with the highest frequency were selected as the representative of OTU sequences. The ITS database Unite (https://unite.ut.ee/) for species annotation analysis was used subsequently (Kõljalg et al., 2013). Finally, all OTUs were uniformized based on the smallest amount of sequencing data as the standard.

Afterward, the normalization process was followed by analyses performed based on the OTU statistics. Qiime software (version 1.9.1, http://qiime.org/install/index.html) was used to calculate Shannon, Simpson, Ace, Chao1, and PD whole tree indexes, and R software (version 3.6.0) was used to draw a rarefaction curve. Then, the Bray–Curtis distance was calculated by Qiime software (version 1.9.1), and the WGCNA, stats, and ggplot2 packages of R software (version 3.6.0) were used to draw PCA, PCoA, NMDS, and PLS-DA plots. The vegan package based on R software (version 3.6.0) was used to test the differences in the microbial community structure among different treatments through PERMANOVA. Subsequently, the significance *P*-value in the LEfSe analysis was conducted using the Wilcoxon rank-sum test. The LDA was set to 3.0. The correlation between fungal data and tobacco disease data was calculated, according to the Mantel test (Li Y. et al., 2021). Based on the analysis platform of Majorbio (Shanghai Majorbio Bio-pharm Technology Co., Ltd., Shanghai, China), the results of species annotations were used for further comparative analyses. The raw sequence data were uploaded to the Sequence Read Archive (accession number: PRJNA808161), which could be freely available on the NCBI (https://www.ncbi.nlm.nih.gov/bioproject/PRJNA808161).

The tobacco diseases data were analyzed by SPSS (version 25.0), and the single-factor ANOVA (Duncan's multiple range test) in SPSS software was used to calculate the significance of the differences among nitrogen-reducing fertilization and CK. All figures were drawn through Origin (version 2018) (OriginLab Corporation, Northampton, MA, United States) and R software (version 3.6.0). All results were presented as mean ± standard deviation.

RESULTS

Nitrogen-Reducing Fertilization Impacted the Occurrence and Severity of Tobacco Diseases

Regarded as the main plant diseases of tobacco, tobacco mosaic virus (TMV), tobacco black shank (TBS), and tobacco bacterial wilt (TBW) were investigated. The disease occurrence rates and disease indexes of the three diseases were calculated among all treatments (**Table 1**). The results demonstrated that nitrogen-reducing fertilization could decrease the occurrence rate and the disease index of tobacco diseases. In particular, all three nitrogen-reducing fertilization strategies (RNTe, RNTw, and RNTh) reduced the occurrence rate of TMV and TBS significantly ($p < 0.05$), compared to CK. Although the inhibitory effects of nitrogen-reducing fertilization strategies were weakened when they were faced by TBW, the difference of the disease occurrence rate between RNTe and CK reached the significant level ($p < 0.05$). Furthermore, the tendency of the disease index of these three tobacco diseases was consistent with the principle of their occurrence rates, except that there were no significant differences between RNTh and CK in the disease index of TBS.

Nitrogen-Reducing Fertilization Impacted the Structure of Fungal Communities

To explore the microbial mechanism of the inhibitory effect of nitrogen-reducing fertilization strategies on tobacco diseases, the fungal community of different treatments was further researched. The composition of the fungal community was influenced by nitrogen-reducing fertilization (**Figure 1** and **Supplementary Figure S1**). The lowest rarefaction curve occurred in RNTe, which represented that the richness of fungal community was smallest in RNTe, compared to other treatments (**Figure 1A**). The Venn diagram indicated that 754, 655, 752, and 737 OTUs were observed in CK, RNTe, RNTw, and RNTh, respectively. Among them, all treatments shared 414 common OTUs, whereas CK, RNTe, RNTw, and RNTh owned 90, 31, 63, and 50 unique OTUs, respectively (**Figure 1B**). According to the results of annotation, Ascomycota, Basidiomycota, and Mortierellomycota were the dominant fungi based on the phylum level. Due to nitrogen-reducing fertilization, the relative abundance of Ascomycota was decreased, whereas the relative abundance of Basidiomycota was improved. Additionally, the relative abundance of Mortierellomycota was up and down among different treatments, without an apparent discipline (**Figure 1C**). Corresponding to the genus level, the relative abundance of *Tausonia* was increased by nitrogen-reducing fertilization, while that of more genera (such as *Fusarium* and *Aspergillus*) was declined (**Figure 1D**).

Based on the heat map analysis, compared with the control, nitrogen reduction treatment increased the abundance of some genera and decreased the abundance of other genera (**Figure 2A**). In particular, nitrogen reduction treatment showed a strong trend of decreasing the relative abundance of genera for an increase in the relative abundance of certain bacterial genera. Based on the ternary analysis, the distribution of the main dominant bacterial genera (based on relative abundance) was relatively uniform among different nitrogen reduction treatments (**Figure 2B**). It demonstrated the common effect of different nitrogen reduction treatments on soil fungal communities. In addition, compared with RNTh, more species of the genera were enriched in RNTe and RNTw treatment, especially RNTw.

In different analyses, the fungal communities of the CK treatment were clustered into a unique area, revealing that the fungal community structure of the nitrogen-reducing treatment was significantly different from that of CK (**Figure 3**). In addition, the fungal communities of RNTw and RNTh clustered into a much closer location, which indicated that the community structure of the two was more similar.

TABLE 1 | Occurrence rate and index of tobacco diseases in different treatments.

Treatment	Disease occurrence rate/%			Disease index		
	TMV	TBS	TBW	TMV	TBS	TBW
CK	32.74 ± 0.91d	20.93 ± 1.09d	33.02 ± 1.30b	6.91 ± 0.13d	5.41 ± 0.08c	9.57 ± 0.18b
RNTe	16.38 ± 0.80a	11.29 ± 1.16a	28.11 ± 1.36a	5.05 ± 0.20a	4.07 ± 0.13a	9.14 ± 0.15a
RNTw	24.15 ± 0.96b	16.13 ± 0.32b	29.80 ± 1.59ab	5.67 ± 0.09b	4.88 ± 0.08b	9.27 ± 0.10ab
RNTh	28.06 ± 1.21c	18.62 ± 1.26c	31.47 ± 1.61ab	6.32 ± 0.22c	5.27 ± 0.09c	9.41 ± 0.12ab

TMV: tobacco mosaic virus; TBS: tobacco black shank; TBW: tobacco bacterial wilt. All data in the table are presented as means ± standard deviation (SD). Means followed by different lowercase letters are significantly different at the 5% level by DMRT (Duncan's multiple range test).

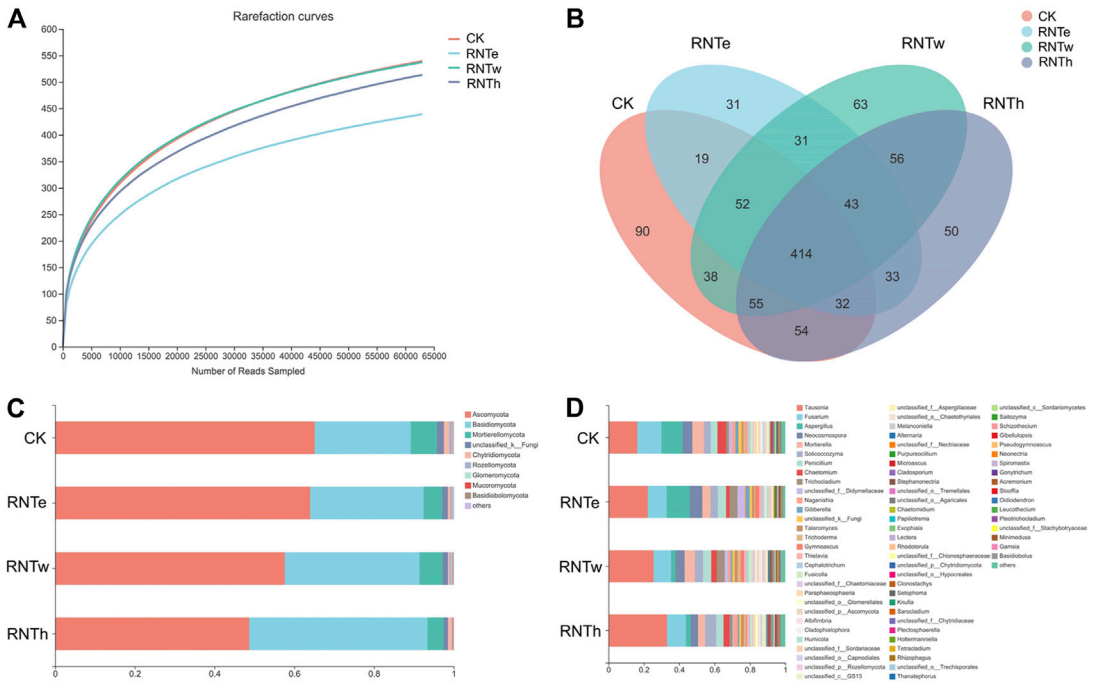

FIGURE 1 | Composition of fungal communities in different treatments, based on OTU level. **(A)** Rarefaction curves of different treatments. **(B)** Venn diagram of different treatments, based on the number of OTUs. **(C)** Main taxa of fungi in different treatments at the phylum level. **(D)** Main taxa of fungi in different treatments at the genus level.

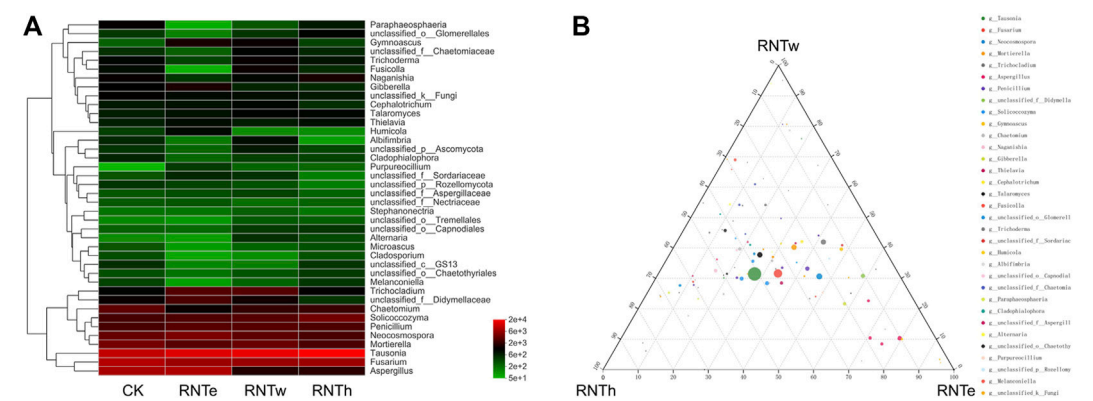

FIGURE 2 | Composition of fungal communities in different treatments, based on the genus level. **(A)** Heat map of top 40 genera of different treatments. **(B)** Ternary analysis of different treatments, based on the genus level.

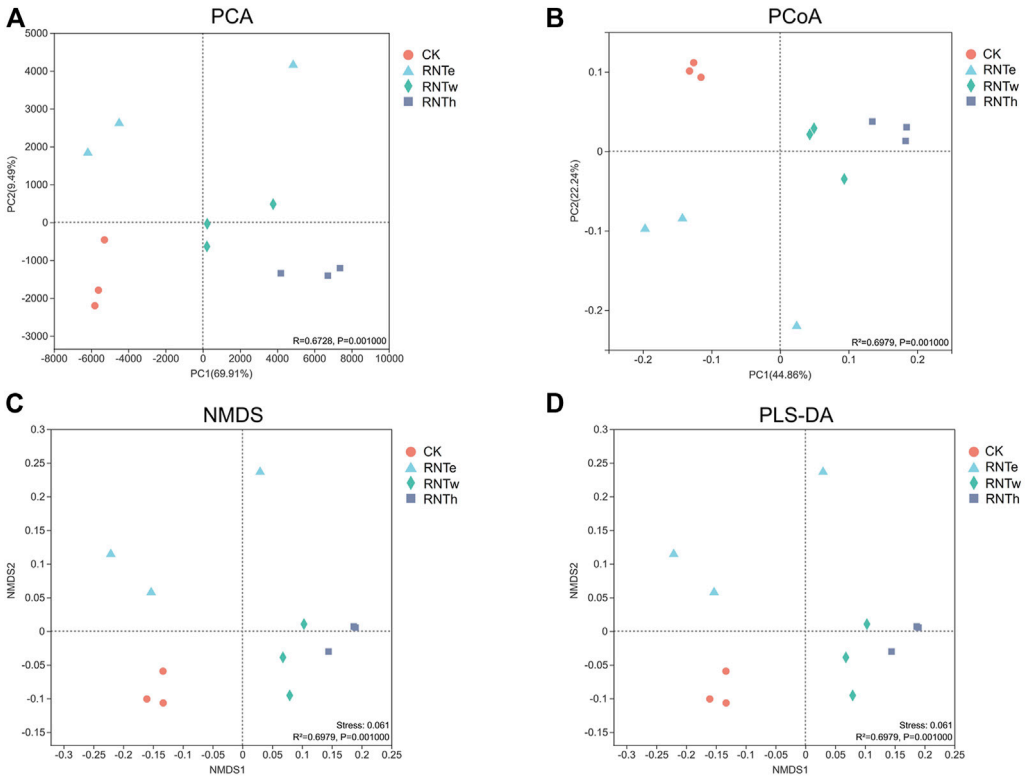

FIGURE 3 | Combined plots of PCA **(A)**, PCoA **(B)**, NMDS **(C)**, and PLS-DA **(D)** of fungal communities in different treatments.

Nitrogen-Reducing Fertilization Drove the Differentiation of Key Taxa Among Different Treatments

Furthermore, the LEfSe analysis of different treatments revealed that biomarkers of different treatments were identified as 4 phyla and 64 genera, among which CK, RNTe, RNTw, and RNTh had 17, 8, 16, and 23 genera, respectively (**Figures 4A,B**). Based on the relative abundance, the top 20 genera with significant differences among different treatments were further analyzed, revealing the key genera that caused the changes in the fungal community structure in the nitrogen reduction treatment, compared to CK (**Figure 4C**). Specifically, the relative abundance of *Tausonia*, *Trichocladium*, unclassified *Didymellaceae*, *Gymnoascus*, *Humicola*, and unclassified *Sordariaceae* was significantly ($p < 0.05$) enhanced by nitrogen-reducing fertilization, whereas the relative abundance of *Chaetomium*, *Naganishia*, *Trichoderma*, *Fusicolla*, *Paraphaeosphaeria*, *Albifimbria*, *Cladophialophora*, and unclassified *GS13* was significantly declined by nitrogen-reducing fertilization ($p < 0.05$).

Furthermore, the fungal community functions of different treatments were predicted (**Figure 5**). In this study, different types of saprophytic functions are the dominant functions of fungal communities in different treatments. Compared with the control, nitrogen reduction treatment reduced the pathological nutritional functions of animals and plants and enhanced their saprophytic nutritional functions. In addition, nitrogen reduction treatments significantly enhanced unknown functions of the fungal community. The dominant effect of nitrogen reduction treatment in the process of tobacco growing is not only derived from its changes in common functions but also related to its activation of new and unknown functions.

Correlation Between Fungal Key Taxa and Tobacco Diseases

To verify the microbial mechanism of the inhibitory effect against tobacco diseases caused by nitrogen-reducing fertilization, the Mantel test was implemented between key taxa and the results of tobacco diseases (**Table 2**). The results of the Mantel test indicated that the key taxa, whose relative abundances were significantly ($p < 0.05$) different from CK, had strong correlations to the occurrence rates and disease indexes of tobacco diseases among different treatments. Interestingly, the correlations between fungal key taxa were much stronger in inhibition against TMV and TBS with the R values (occurrence rate) of 0.7733 and 0.6927, and the R values (disease index) of 0.7194 and 0.7197, rather than in the inhibition against TBW.

To deeply pursue the causal relationship between key genera and those three tobacco diseases, partial least squares path modeling (PLS-PM) was employed to analyze the paths among all the modules (**Figure 6**). Five modules, the key genera whose relative abundances were significantly increased

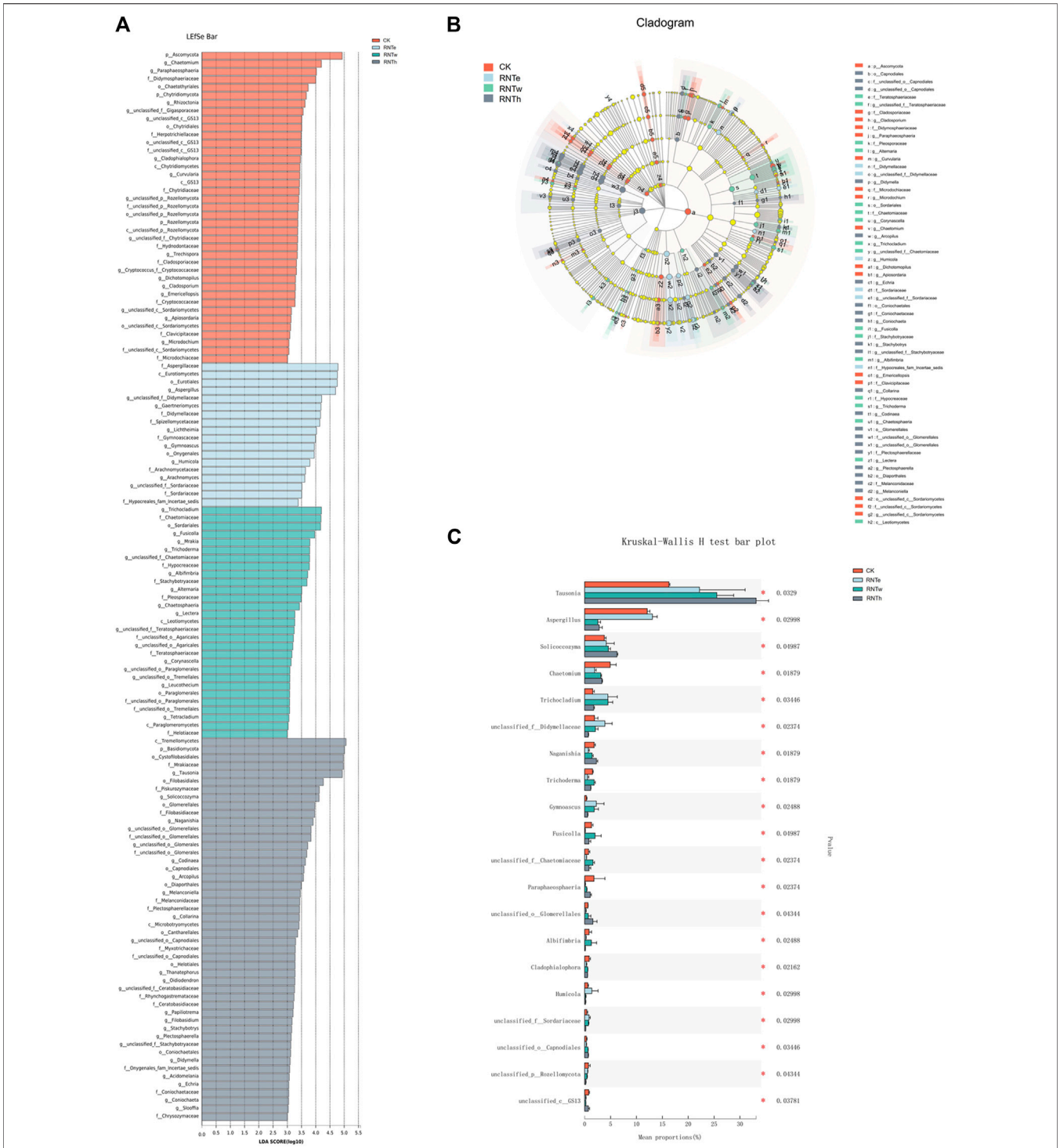

FIGURE 4 | Combined plots of exploring key taxa among different treatments. **(A)** LDA effect size (LEfSe) analysis based on the genus among different treatments. **(B)** Cladogram of biomarkers among different treatments. **(C)** Bar plot of top 20 significant differential taxa based on the Kruskal–Wallis H test.

by nitrogen-reducing fertilization (InKG), the key genera whose relative abundances were significantly decreased by nitrogen-reducing fertilization (DeKG), TMV, TBS, and TBW, were set to establish an analysis model. The goodness of fit (Gof) was 0.7481, which meant the prediction power of the model was of 74.81%. The results of path coefficients showed that InKG had a negative causal relationship with TMV and TBS and had a positive causal relationship with TBW, whereas DeKG had a positive causal

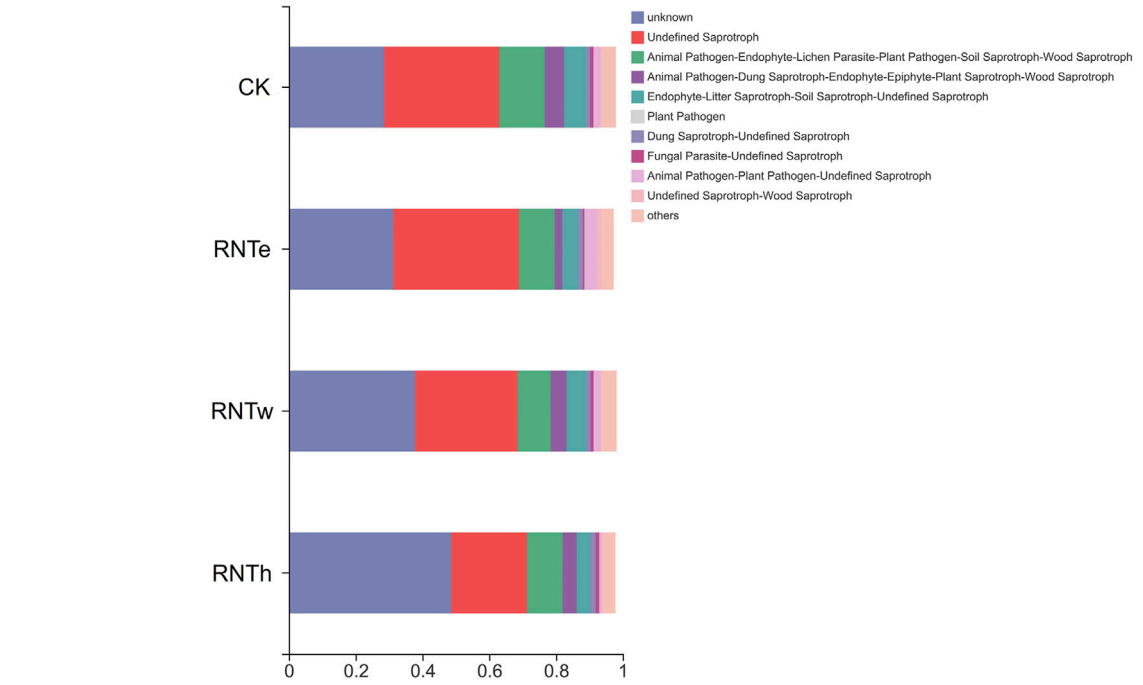

FIGURE 5 | Predictive functions of fungal communities of different treatments.

TABLE 2 | Mantel test of correlations between key taxa and the results of tobacco diseases.

		Key taxa (CK-RNTe)	
		R value	**P value**
Occurrence rate	TMV	0.7733	0.001
	TBS	0.6927	0.001
	TBW	0.3658	0.021
Disease index	TMV	0.7194	0.001
	TBS	0.7197	0.001
	TBW	0.3281	0.048

Key taxa refer to those that are significantly different from CK, based on OTU statistics.

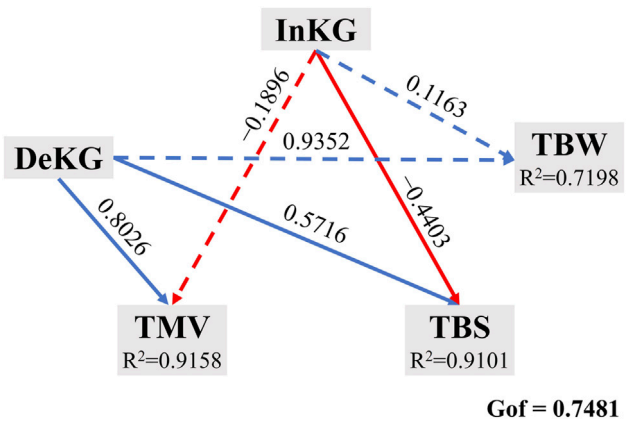

FIGURE 6 | PLS-PM diagram based on the path coefficients between different modules. Blue and red arrow lines represent the positive and negative causal relationship between each two modules, respectively. The lines composed of dash lines means the calculated result of the relationship between the two modules did not reach the significant ($p < 0.05$) level. InKG: the key genera whose relative abundances were significantly increased by nitrogen-reducing fertilization. DeKG: the key genera whose relative abundances were significantly decreased by nitrogen-reducing fertilization. Gof: goodness of fit. R^2 indicated the amount of variance in the endogenous latent variable explained by its independent latent variables.

relationship with those three tobacco diseases. However, among these path coefficients, the causal relationships between InKG, TMV, and TBW were not significant ($p < 0.05$). Additionally, the causal relationship between DeKG and TBW did not reach a significant ($p < 0.05$) level neither. Furthermore, the R^2 values of TMV, TBS, and TBW, which represented the amount of variance of the three diseases explained by this model, were 0.9158, 0.9101, and 0.7198, respectively.

DISCUSSION

Plant health is the fundamental of agricultural production, which is threatened by plant pathogens severely. Regarded as one of the most popular commodities, merchandise corresponding to tobacco plays an important role in undertaking the national economic task. However, the tobacco-planting industry is hindered by plant diseases such as tobacco mosaic virus, tobacco black shrank, and tobacco bacterial wilt (Hu Q. et al., 2021; Hu Y. et al., 2021). Chemicals, chemical pesticide, soil

fumigation, and microbial inoculants consist of the mainstream pathogen control strategies that have earned great achievements fighting against plant diseases (Alori and Babalola, 2018; Ren et al., 2018; Raymaekers et al., 2020; Long et al., 2021). The previous studies exhibited the effects of different pathogen control strategies, which resulted from exogenous additives, on microbial community structures and functions (Preininger et al., 2018; Li et al., 2020; Vassilev et al., 2020). Nevertheless, without additives, the soil microbial structure could be changed according to different amounts of fertilizers (Li B.-B. et al., 2021). It would be of great help to the agricultural management which could prevent cash crops from plant diseases using a fertilization strategy.

In this study, nitrogen-reducing fertilization strategies showed an obvious inhibitory effect against tobacco diseases, especially against TMV and TBS. Through the composition and structure of fungal communities between nitrogen-reducing fertilization and CK, the variation of fungal communities was explored to exhibit the effects of nitrogen-reducing fertilization on converting the microbial community into an inhibition-enhanced status. Previous studies had indicated that the appropriate reduction of chemical fertilizers, especially nitrogen fertilizer, could improve the yield of crops and impact the microbial community in rhizosphere soil of plants. Some research studies paid attention to the effects of the nitrogen-reducing strategy on fungal community of food crops such as wheat, rice, and maize (Wen et al., 2020; Liu et al., 2021; Wang et al., 2021). Wang et al. found that *Humicola*, *Tausonia*, and *Codinaea* could improve the chemical quality of tobacco (Wang et al., 2022). Nevertheless, few had focused on the fungal inhibitory effect of nitrogen-reducing fertilization on tobacco diseases.

Interestingly, the bioinformatics of the fungal community of all treatments were found to be closely correlated to the results of tobacco diseases. Based on LEfSe analysis and Kruskal–Wallis H test, the key taxa that dominated the variation of fungal communities between nitrogen-reducing fertilization and CK were excavated and summarized. Previous evidence verified that those abundance-improved genera, which were enhanced by nitrogen-reducing fertilization, were more likely to benefit the plants and their soil environment. For instance, *Tausonia* could help plants to tolerate low temperature and improve the fermentation process (Kim et al., 2020). *Trichocladium* was verified to be used as biofertilizers and biofungicides, which played an important role in declining the tobacco disease occurrence rate and index. Furthermore, some species of *Trichocladium* could produce cellulolytic enzymes, which provided microorganisms with carbon sources and provided tobacco with nutrients (Kubicek et al., 2019). Meanwhile, nitrogen-reducing fertilization not only enhanced the beneficial fungi in tobacco rhizosphere soil but also decreased the negative. For instance, *Naganishia* (Horváth et al., 2020), *Trichoderma* (Poveda et al., 2020), *Fusicolla* (Clocchiatti et al., 2021), *Paraphaeosphaeria* (Ding et al., 2020), and *Albifimbria* (Matić et al., 2019) were reported to be plant pathogens that destroyed the growth and yield of many crops (Masachis et al., 2016).

Afterward, the correlation between key taxa and tobacco diseases was analyzed, based on the Mantel test (Crabot et al., 2019). The results indicated that the key taxa, whose relative abundances were significantly ($p < 0.05$) different from CK, made great contributions to the present variation of occurrence rates and disease indexes of tobacco diseases among different treatments. It proved that the key taxa excavated in this study were the dominant reason why nitrogen-reducing fertilization could decrease the occurrence rate and disease index of tobacco diseases. Although the results of correlation between key taxa and tobacco diseases emphasized the importance of the key genera, the causal relationships between these genera and tobacco diseases were beyond understanding. Hence, the PLS-PM analysis was implemented to address this issue (Sanchez, 2013). Through the results, the operating mechanisms of key genera, which were integrated into two modules (InKG and DeKG), in the performance of inhibiting tobacco diseases were revealed. From the aspect of TMV, the inhibitory effect of nitrogen-reducing fertilization against TMV primarily owed to the decreased key genera which caused by this strategy. When it came to TBS, the increased key genera and decreased key genera both made contributions to the inhibitory effect of this strategy, whereas InKG and DeKG did not have significant path coefficients with TBW, which indicated that there was no obvious causal relationship between key genera and TBW. The reason why RNTe could decline the TBW should be further explored beyond the fungal community of rhizosphere soil. The endogenous fungus of tobacco was suggested to be researched.

Moreover, the inhibitory effect of nitrogen-reducing fertilization was highest in RNTe, while the efficiency declined from RNTe to RNTh. It demonstrated that the reducing amount of nitrogen fertilizer was limited according to the performance of this strategy. In the present research, ten percentage of nitrogen-reducing fertilization was appropriate for tobacco planting against diseases. Additionally, the inhibitory effect of nitrogen-reducing fertilization against TBW was much lower than that against TMV and TBS. Other methods should be cooperated with this fertilization strategy to better protect tobacco from TBW.

CONCLUSION

In this study, the inhibitory effect of nitrogen-reducing fertilization strategy against tobacco diseases was investigated to be significantly effective in tobacco-planting agriculture. The best performance of disease control occurred in 10% reduction of nitrogen fertilizer. The variation of the fungal community between nitrogen-reducing fertilization and CK was highly consistent with the circumstances of tobacco diseases. Furthermore, the positive genera such as *Tausonia* and *Trichocladium* and the negative genera such as *Naganishia* and *Fusicolla* were identified to be the key genera which dominated the fungal inhibition against tobacco diseases, due to the economic and eco-friendly fertilization strategy. This study provides a constructive strategy to inhibit tobacco diseases in continuous cropping areas of tobacco. It also provides a theoretical basis for developing the potential fungal inhibitory

effects of native microorganisms stimulated by nitrogen-reducing fertilization.

DATA AVAILABILITY STATEMENT

The data presented in the study are deposited in the NCBI repository (https://www.ncbi.nlm.nih.gov/bioproject/PRJNA808161), accession number: PRJNA808161.

AUTHOR CONTRIBUTIONS

Conceptualization: X-ML and M-CS; experiment implementation: G-DB, Y-ZS, and M-CS; data processing: M-CS and G-DB; writing—original draft preparation: M-CS; writing—review and editing: M-CS, Y-ZS, and X-ML; and funding acquisition: X-ML. All authors have read and approved the final manuscript.

FUNDING

This research was supported by the Key Projects of Shandong Qingdao Tobacco Co., Ltd. (No. YCSKY202007030-C1) and the Technology Project of Hubei Tobacco Co., Ltd. (No. 027Y2021-011).

SUPPLEMENTARY MATERIAL

The Supplementary Material for this article can be found online at: https://www.frontiersin.org/articles/10.3389/fbioe.2022.866419/full#supplementary-material

REFERENCES

Abo-Zaid, G. A., Matar, S. M., and Abdelkhalek, A. (2020). Induction of Plant Resistance against Tobacco Mosaic Virus Using the Biocontrol Agent Streptomyces Cellulosae Isolate Actino 48. *Agronomy* 10, 1620. doi:10.3390/agronomy10111620

Ahmed, W., Yang, J., Tan, Y., Munir, S., Liu, Q., Zhang, J., et al. (2022). Ralstonia Solanacearum, a Deadly Pathogen: Revisiting the Bacterial Wilt Biocontrol Practices in Tobacco and Other Solanaceae. *Rhizosphere* 21, 100479. doi:10.1016/j.rhisph.2022.100479

Aliyu, I. A., Yusuf, A. A., Uyovbisere, E. O., Masso, C., and Sanders, I. R. (2019). Effect of Co-application of Phosphorus Fertilizer and In Vitro-produced Mycorrhizal Fungal Inoculants on Yield and Leaf Nutrient Concentration of Cassava. *PLoS One* 14, e0218969. doi:10.1371/journal.pone.0218969

Alori, E. T., and Babalola, O. O. (2018). Microbial Inoculants for Improving Crop Quality and Human Health in Africa. *Front. Microbiol.* 9, 2213. doi:10.3389/fmicb.2018.02213

Callahan, B. J., Mcmurdie, P. J., Rosen, M. J., Han, A. W., Johnson, A. J. A., and Holmes, S. P. (2016). DADA2: High-Resolution Sample Inference from Illumina Amplicon Data. *Nat. Methods* 13, 581–583. doi:10.1038/nmeth.3869

Cao, Y., Zhang, Z., Ling, N., Yuan, Y., Zheng, X., Shen, B., et al. (2011). Bacillus Subtilis SQR 9 Can Control Fusarium Wilt in Cucumber by Colonizing Plant Roots. *Biol. Fertil. Soils* 47, 495–506. doi:10.1007/s00374-011-0556-2

Chakraborty, S., and Newton, A. C. (2011). Climate Change, Plant Diseases and Food Security: an Overview. *Plant Pathol.* 60, 2–14. doi:10.1111/j.1365-3059.2010.02411.x

Chellemi, D. O., Gamliel, A., Katan, J., and Subbarao, K. V. (2016). Development and Deployment of Systems-Based Approaches for the Management of Soilborne Plant Pathogens. *Phytopathology* 106, 216–225. doi:10.1094/phyto-09-15-0204-rvw

Choi, K., Choi, J., Lee, P. A., Roy, N., Khan, R., Lee, H. J., et al. (2020). Alteration of Bacterial Wilt Resistance in Tomato Plant by Microbiota Transplant. *Front. Plant Sci.* 11, 1186. doi:10.3389/fpls.2020.01186

Chunyu, L., Weicong, H., Bin, P., Yan, L., Saifei, Y., Yuanyuan, D., et al. (2017). Rhizobacterium Bacillus Amyloliquefaciens Strain SQRT3-Mediated Induced Systemic Resistance Controls Bacterial Wilt of Tomato. *Pedosphere* 27, 1135–1146.

Clocchiatti, A., Hannula, S. E., Van Den Berg, M., Hundscheid, M. P. J., and De Boer, W. (2021). Evaluation of Phenolic Root Exudates as Stimulants of Saptrophic Fungi in the Rhizosphere. *Front. Microbiol.* 12, 644046. doi:10.3389/fmicb.2021.644046

Crabot, J., Clappe, S., Dray, S., and Datry, T. (2019). Testing the Mantel Statistic with a Spatially-constrained Permutation Procedure. *Methods Ecol. Evol.* 10, 532–540. doi:10.1111/2041-210x.13141

De Carvalho Pontes, N., Yamada, J. K., Fujinawa, M. F., Dhingra, O. D., and De Oliveira, J. R. (2019). Soil Fumigation with Mustard Essential Oil to Control Bacterial Wilt in Tomato. *Eur. J. Plant Pathol.* 155, 435–444. doi:10.1007/s10658-019-01777-0

Ding, T., Li, Z., Guo, L., and Li, J. (2020). First Report of Leaf Spots and Necrosis Caused by Paraphaeosphaeria Recurvifoliae on Yucca Gloriosa in China. *Plant Dis.* 104, 986. doi:10.1094/pdis-07-19-1383-pdn

Edgar, R. C., Haas, B. J., Clemente, J. C., Quince, C., and Knight, R. (2011). UCHIME Improves Sensitivity and Speed of Chimera Detection. *Bioinformatics* 27, 2194–2200. doi:10.1093/bioinformatics/btr381

Ghorbanpour, M., Omidvari, M., Abbaszadeh-Dahaji, P., Omidvar, R., and Kariman, K. (2018). Mechanisms Underlying the Protective Effects of Beneficial Fungi against Plant Diseases. *Biol. Control.* 117, 147–157. doi:10.1016/j.biocontrol.2017.11.006

Haas, B. J., Gevers, D., Earl, A. M., Feldgarden, M., Ward, D. V., Giannoukos, G., et al. (2011). Chimeric 16S rRNA Sequence Formation and Detection in Sanger and 454-pyrosequenced PCR Amplicons. *Genome Res.* 21, 494–504. doi:10.1101/gr.112730.110

Horváth, E., Sipiczki, M., Csoma, H., and Miklós, I. (2020). Assaying the Effect of Yeasts on Growth of Fungi Associated with Disease. *BMC Microbiol.* 20, 320. doi:10.1186/s12866-020-01942-0

Hu, D., Li, S., Li, Y., Peng, J., Wei, X., Ma, J., et al. (2020). Streptomyces Sp. Strain TOR3209: a Rhizosphere Bacterium Promoting Growth of Tomato by Affecting the Rhizosphere Microbial Community. *Sci. Rep.* 10, 20132–20215. doi:10.1038/s41598-020-76887-5

Hu, Q., Zhang, H., Zhang, L., Liu, Y., Huang, C., Yuan, C., et al. (2021a). Two Tobamovirus Multiplication 2A Homologs in Tobacco Control Asymptomatic Response to Tobacco Mosaic Virus. *Plant Physiol.* 187, 2674–2690. doi:10.1093/plphys/kiab448

Hu, Y., Zhao, W., Li, X., Feng, J., Li, C., Yang, X., et al. (2021b). Integrated Biocontrol of Tobacco Bacterial Wilt by Antagonistic Bacteria and Marigold. *Sci. Rep.* 11, 1–12. doi:10.1038/s41598-021-95741-w

Huang, K., Jiang, Q., Liu, L., Zhang, S., Liu, C., Chen, H., et al. (2020). Exploring the Key Microbial Changes in the Rhizosphere that Affect the Occurrence of Tobacco Root-Knot Nematodes. *Amb Express* 10, 72–11. doi:10.1186/s13568-020-01006-6

Jaiswal, A. K., Frenkel, O., Tsechansky, L., Elad, Y., and Graber, E. R. (2018). Immobilization and Deactivation of Pathogenic Enzymes and Toxic Metabolites by Biochar: a Possible Mechanism Involved in Soilborne Disease Suppression. *Soil Biol. Biochem.* 121, 59–66. doi:10.1016/j.soilbio.2018.03.001

Kim, M.-J., Lee, H.-W., Kim, J. Y., Kang, S. E., Roh, S. W., Hong, S. W., et al. (2020). Impact of Fermentation Conditions on the Diversity of white colony-forming Yeast and Analysis of Metabolite Changes by white colony-forming Yeast in Kimchi. *Food Res. Int.* 136, 109315. doi:10.1016/j.foodres.2020.109315

Kim, S. G., Hur, O.-S., Ro, N.-Y., Ko, H.-C., Rhee, J.-H., Sung, J. S., et al. (2016). Evaluation of Resistance to Ralstonia Solanacearum in Tomato Genetic Resources at Seedling Stage. *Plant Pathol. J.* 32, 58–64. doi:10.5423/ppj.nt.06.2015.0121

Kõljalg, U., Nilsson, R. H., Abarenkov, K., Tedersoo, L., Taylor, A. F., Bahram, M., et al. (2013). *Towards a Unified Paradigm for Sequence-based Identification of Fungi*. Wiley Online Library.

Kubicek, C. P., Steindorff, A. S., Chenthamara, K., Manganiello, G., Henrissat, B., Zhang, J., et al. (2019). Evolution and Comparative Genomics of the Most Common Trichoderma Species. *BMC Genomics* 20, 485. doi:10.1186/s12864-019-5680-7

Li, B.-B., Roley, S. S., Duncan, D. S., Guo, J., Quensen, J. F., Yu, H.-Q., et al. (2021a). Long-term Excess Nitrogen Fertilizer Increases Sensitivity of Soil Microbial Community to Seasonal Change Revealed by Ecological Network and Metagenome Analyses. *Soil Biol. Biochem.* 160, 108349. doi:10.1016/j.soilbio.2021.108349

Li, H., Qiu, Y., Yao, T., Ma, Y., Zhang, H., and Yang, X. (2020). Effects of PGPR Microbial Inoculants on the Growth and Soil Properties of Avena Sativa, Medicago Sativa, and Cucumis Sativus Seedlings. *Soil Tillage Res.* 199, 104577. doi:10.1016/j.still.2020.104577

Li, Y., Chen, H., Song, L., Wu, J., Sun, W., and Teng, Y. (2021b). Effects on Microbiomes and Resistomes and the Source-specific Ecological Risks of Heavy Metals in the Sediments of an Urban River. *J. Hazard. Mater.* 409, 124472. doi:10.1016/j.jhazmat.2020.124472

Liu, H., Brettell, L. E., Qiu, Z., and Singh, B. K. (2020). Microbiome-mediated Stress Resistance in Plants. *Trends Plant Sci.* 25, 733–743. doi:10.1016/j.tplants.2020.03.014

Liu, J., Li, S., Yue, S., Tian, J., Chen, H., Jiang, H., et al. (2021). Soil Microbial Community and Network Changes after Long-Term Use of Plastic Mulch and Nitrogen Fertilization on Semiarid farmland. *Geoderma* 396, 115086. doi:10.1016/j.geoderma.2021.115086

Long, Z.-Q., Yang, L.-L., Zhang, J.-R., Liu, S.-T., Jiao Xie, J., Wang, P.-Y., et al. (2021). Fabrication of Versatile Pyrazole Hydrazide Derivatives Bearing a 1,3,4-Oxadiazole Core as Multipurpose Agricultural Chemicals against Plant Fungal, Oomycete, and Bacterial Diseases. *J. Agric. Food Chem.* 69, 8380–8393. doi:10.1021/acs.jafc.1c02460

Masachis, S., Segorbe, D., Turrà, D., Leon-Ruiz, M., Fürst, U., El Ghalid, M., et al. (2016). A Fungal Pathogen Secretes Plant Alkalinizing Peptides to Increase Infection. *Nat. Microbiol.* 1, 16043–16049. doi:10.1038/nmicrobiol.2016.43

Matić, S., Gilardi, G., Gullino, M. L., and Garibaldi, A. (2019). Emergence of Leaf Spot Disease on Leafy Vegetable and Ornamental Crops Caused by Paramyrothecium and Albifimbria Species. *Phytopathology* 109, 1053–1061. doi:10.1094/PHYTO-10-18-0396-R

Morais, T. P., Zaini, P. A., Chakraborty, S., Gouran, H., Carvalho, C. P., Almeida-Souza, H. O., et al. (2019). The Plant-Based Chimeric Antimicrobial Protein SlP14a-PPC20 Protects Tomato against Bacterial Wilt Disease Caused by Ralstonia Solanacearum. *Plant Sci.* 280, 197–205. doi:10.1016/j.plantsci.2018.11.017

Ogunnaike, B., Bogle, D., Banga, J. R., and Parker, R. (2021). Biological Control Systems and Disease Modeling. *Front. Bioeng. Biotechnol.* 9, 262. doi:10.3389/fbioe.2021.677976

Pellegrino, E., Turrini, A., Gamper, H. A., Cafà, G., Bonari, E., Young, J. P. W., et al. (2012). Establishment, Persistence and Effectiveness of Arbuscular Mycorrhizal Fungal Inoculants in the Field Revealed Using Molecular Genetic Tracing and Measurement of Yield Components. *New Phytol.* 194, 810–822. doi:10.1111/j.1469-8137.2012.04090.x

Peng, D., Luo, K., Jiang, H., Deng, Y., Bai, L., and Zhou, X. (2017). Combined Use ofBacillus Subtilisstrain B-001 and Bactericide for the Control of Tomato Bacterial Wilt. *Pest Manag. Sci.* 73, 1253–1257. doi:10.1002/ps.4453

Pétriacq, P., Williams, A., Cotton, A., Mcfarlane, A. E., Rolfe, S. A., and Ton, J. (2017). Metabolite Profiling of Non-sterile Rhizosphere Soil. *Plant J.* 92, 147–162. doi:10.1111/tpj.13639

Poveda, J., Eugui, D., and Abril-Urias, P. (2020). "Could Trichoderma Be a Plant Pathogen? Successful Root Colonization," in *Trichoderma* (Springer), 35–59. doi:10.1007/978-981-15-3321-1_3

Preininger, C., Sauer, U., Bejarano, A., and Berninger, T. (2018). Concepts and Applications of Foliar spray for Microbial Inoculants. *Appl. Microbiol. Biotechnol.* 102, 7265–7282. doi:10.1007/s00253-018-9173-4

Raymaekers, K., Ponet, L., Holtappels, D., Berckmans, B., and Cammue, B. P. A. (2020). Screening for Novel Biocontrol Agents Applicable in Plant Disease Management - A Review. *Biol. Control.* 144, 104240. doi:10.1016/j.biocontrol.2020.104240

Ren, Z., Li, Y., Fang, W., Yan, D., Huang, B., Zhu, J., et al. (2018). Evaluation of Allyl Isothiocyanate as a Soil Fumigant against Soil-Borne Diseases in Commercial Tomato (Lycopersicon esculentumMill.) Production in China. *Pest Manag. Sci.* 74, 2146–2155. doi:10.1002/ps.4911

Sanchez, G. (2013). *PLS Path Modeling with R*. Berkeley: Udemy, 551. 383.

Strange, R. N., and Scott, P. R. (2005). Plant Disease: a Threat to Global Food Security. *Annu. Rev. Phytopathol.* 43, 83–116. doi:10.1146/annurev.phyto.43.113004.133839

Tobacco Research Institute (2008). *Grade and Investigation Method of Tobacco Diseases and Insect Pests*. Qingdao: General Administration of Quality Supervision, Inspection and Quarantine of the People's Republic of China; Standardization Administration of China.

Vassilev, N., Vassileva, M., Martos, V., Garcia Del Moral, L. F., Kowalska, J., Tylkowski, B., et al. (2020). Formulation of Microbial Inoculants by Encapsulation in Natural Polysaccharides: Focus on Beneficial Properties of Carrier Additives and Derivatives. *Front. Plant Sci.* 11, 270. doi:10.3389/fpls.2020.00270

Wang, J. L., Liu, K. L., Zhao, X. Q., Zhang, H. Q., Li, D., Li, J. J., et al. (2021). Balanced Fertilization over Four Decades Has Sustained Soil Microbial Communities and Improved Soil Fertility and rice Productivity in Red Paddy Soil. *Sci. Total Environ.* 793, 148664. doi:10.1016/j.scitotenv.2021.148664

Wang, M., Zhang, L., He, Y., Huang, L., Liu, L., Chen, D., et al. (2022). Soil Fungal Communities Affect the Chemical Quality of Flue-Cured Tobacco Leaves in Bijie, Southwest China. *Sci. Rep.* 12, 2815. doi:10.1038/s41598-022-06593-x

Wen, Y.-C., Li, H.-Y., Lin, Z.-A., Zhao, B.-Q., Sun, Z.-B., Yuan, L., et al. (2020). Long-term Fertilization Alters Soil Properties and Fungal Community Composition in Fluvo-Aquic Soil of the North China Plain. *Sci. Rep.* 10, 7198. doi:10.1038/s41598-020-64227-6

Xie, S., Vallet, M., Sun, C., Kunert, M., David, A., Zhang, X., et al. (2020). Biocontrol Potential of a Novel Endophytic Bacterium from mulberry (Morus) Tree. *Front. Bioeng. Biotechnol.* 7, 488. doi:10.3389/fbioe.2019.00488

Yang, L., Zou, Y.-N., Tian, Z.-H., Wu, Q.-S., and Kuča, K. (2021). Effects of Beneficial Endophytic Fungal Inoculants on Plant Growth and Nutrient Absorption of Trifoliate orange Seedlings. *Scientia Horticulturae* 277, 109815. doi:10.1016/j.scienta.2020.109815

Yang, T., Lupwayi, N., Marc, S.-A., Siddique, K. H. M., and Bainard, L. D. (2021). Anthropogenic Drivers of Soil Microbial Communities and Impacts on Soil Biological Functions in Agroecosystems. *Glob. Ecol. Conservation* 27, e01521. doi:10.1016/j.gecco.2021.e01521

Yuan, X.-L., Cao, M., Shen, G.-M., Zhang, H.-B., Du, Y.-M., Zhang, Z.-F., et al. (2020). Characterization of Nuclear and Mitochondrial Genomes of Two Tobacco Endophytic Fungi Leptosphaerulina Chartarum and Curvularia Trifolii and Their Contributions to Phylogenetic Implications in the Pleosporales. *Ijms* 21, 2461. doi:10.3390/ijms21072461

Zhou, S.-M., Zhang, M., Zhang, K.-K., Yang, X.-W., He, D.-X., Yin, J., et al. (2020). Effects of Reduced Nitrogen and Suitable Soil Moisture on Wheat (*Triticum aestivum* L.) Rhizosphere Soil Microbiological, Biochemical Properties and Yield in the Huanghuai Plain, China. *J. Integr. Agric.* 19, 234–250. doi:10.1016/s2095-3119(19)62697-3

Conflict of Interest: Author Y-ZS was employed by Cigar Institute of China Tobacco Hubei Industrial Co., Ltd.

The remaining authors declare that the research was conducted in the absence of any commercial or financial relationships that could be construed as a potential conflict of interest.

frontiers | Frontiers in Bioengineering and Biotechnology

ORIGINAL RESEARCH
published: 03 May 2022
doi: 10.3389/fbioe.2022.732948

Valorization of Brewer's Spent Grain Using Biological Treatments and its Application in Feeds for European Seabass (*Dicentrarchus labrax*)

Helena Fernandes[1,2], *José Manuel Salgado*[2,3], *Marta Ferreira*[3], *Martina Vršanská*[4], *Nélson Fernandes*[1], *Carolina Castro*[1,2], *Aires Oliva-Teles*[1], *Helena Peres*[1,2] *and Isabel Belo*[3]*

[1]Departamento de Biologia, Faculdade de Ciências, Universidade Do Porto, Rua Do Campo Alegre Ed. FC4, Porto, Portugal, [2]Interdisciplinary Centre of Marine and Environmental Research (CIIMAR), Terminal de Cruzeiros Do Porto de Leixões, Av. General Norton de Matos, Matosinhos, Portugal, [3]Centre of Biological Engineering, University of Minho, Campus de Gualtar, Braga, Portugal, [4]Department of Chemistry and Biochemistry, Mendel University in Brno, Brno, Czech Republic

OPEN ACCESS

Edited by:
Tajalli Keshavarz,
University of Westminster,
United Kingdom

Reviewed by:
Giovani Leone Zabot,
Federal University of Santa Maria,
Brazil
Patrícia Melchionna Albuquerque,
University of the State of Amazonas,
Brazil

***Correspondence:**
Isabel Belo
ibelo@deb.uminho.pt

Specialty section:
This article was submitted to Bioprocess Engineering, a section of the journal Frontiers in Bioengineering and Biotechnology

Received: 29 June 2021
Accepted: 28 February 2022
Published: 03 May 2022

Citation:
Fernandes H, Salgado JM, Ferreira M, Vršanská M, Fernandes N, Castro C, Oliva-Teles A, Peres H and Belo I (2022) Valorization of Brewer's Spent Grain Using Biological Treatments and its Application in Feeds for European Seabass (Dicentrarchus labrax). Front. Bioeng. Biotechnol. 10:732948. doi: 10.3389/fbioe.2022.732948

Brewer's spent grain (BSG) is the main brewery industry by-product, with potential applications in the feed and food industries due to its carbohydrate composition. In addition, the lignocellulosic nature of BSG makes it an adequate substrate for carbohydrases production. In this work, solid-state fermentation (SSF) of BSG was performed with *Aspergillus ibericus,* a non-mycotoxin producer fungus with a high capacity to hydrolyze the lignocellulosic matrix of the agro-industrial by-products. SSF was performed at different scales to produce a crude extract rich in cellulase and xylanase. The potential of the crude extract was tested in two different applications: -(1) - the enzymatic hydrolysis of the fermented BSG and (2) - as a supplement in aquafeeds. SSF of BSG increased the protein content from 25% to 29% (w/w), while the fiber content was reduced to 43%, and cellulose and hemicellulose contents were markedly reduced to around 15%. The scale-up of SSF from 10 g of dry BSG in flasks to 50 g or 400 g in tray-type bioreactors increased 55% and 25% production of cellulase and xylanase, up to 323 and 1073 U g^{-1} BSG, respectively. The optimum temperature and pH of maximal activities were found to be 55°C and pH 4.4 for xylanase and 50°C and pH 3.9 for cellulase, cellulase being more thermostable than xylanase when exposed at temperatures from 45°C to 60°C. A Box–Behnken factorial design was applied to optimize the hydrolysis of the fermented BSG by crude extract. The crude extract load was a significant factor in sugars release, highlighting the role of hydrolytic enzymes, while the load of fermented BSG, and addition of a commercial β-glucosidase were responsible for the highest phenolic compounds and antioxidant activity release. The lyophilized crude extract (12,400 and 1050 U g^{-1} lyophilized extract of xylanase and cellulase, respectively) was also tested as an enzyme supplement in aquafeed for European seabass (*Dicentrarchus labrax*) juveniles. The dietary supplementation with the crude extract significantly improved feed and protein utilization. The processing of BSG using biological treatments, such as SSF with *A. ibericus,* led to the production of a nutritionally enriched BSG and a crude extract with highly efficient carbohydrases capable of hydrolyzing lignocellulosic substrates, such as BSG, and with the potential to be used as feed enzymes with remarkable results in improving feed utilization of an important aquaculture fish species.

Keywords: solid-state fermentation, brewer's spent grain, enzymatic hydrolysis, carbohydrases, aquaculture

INTRODUCTION

The brewery industry produces millions of tons of residues, arising environmental and ecological concerns (Farcas et al., 2017). Brewer's spent grain (BSG) is an insoluble material comprising barley grain husks, small parts of the pericarp, and seed coat layers of the grains (Mussatto, 2014), representing 85% of the total residues originated from the brewing industry (Nocente et al., 2019). BSG is a lignocellulosic material mainly constituted by arabinoxylan, cellulose, and lignin, which can be degraded by hydrothermal, enzymatic, or acidic hydrolysis (Farcas et al., 2017). The protein content of BSG varies depending on the type of barley or other cereal mixture and the conditions applied during wort production (Mussatto, 2014; Farcas et al., 2017). BSG also presents phenolic compounds, such as ferulic and *p*-coumaric acids, with antioxidant properties (Aliyu & Bala, 2013), mainly associated with sugars, organic acids, lipids, and amines, limiting their bioavailability and antioxidant capacity (Dulf et al., 2016). BSG can be utilized for the production of a wide range of enzymes, such as carbohydrases, proteases, and laccases (Mussatto, 2014). Moreover, BSG can be used to obtain other value-added products, such as phenolic compounds (Birsan et al., 2019; Alonso-Riaño et al., 2020), lactic acid (Mussatto, 2014), and fermentable sugars (Paz et al., 2019). Concomitantly, BSG has numerous applications in the food industry (Canedo et al., 2016; Nocente et al., 2019), animal nutrition (Getu et al., 2020; San Martin et al., 2020), and in the production of biofuels (Dudek et al., 2019; Hakobyan et al., 2020). However, to enhance the BSG nutritional value and obtain high-valued compounds, such as protein, enzymes, and phenolic compounds, BSG may undergo biotechnological processes, such as solid-state fermentation (SSF).

SSF is a biotechnological procedure that adds value to the economically uninteresting agro-industrial by-products by promoting the growth of selected microorganisms, using these by-products as physical and nutritional support. During the SSF of lignocellulosic substrates, filamentous fungi partially degrade the vegetable matrix by producing carbohydrate-degrading enzymes (carbohydrases), increasing the release of matrix-linked phenolic compounds. SSF can be used as a pretreatment to enhance the fermentable sugar yield by promoting the lignocellulosic cell-wall disruption (Fernandes et al., 2019) or obtain a nutritionally enhanced biomass or a bioactive extract with, for example, antioxidant and enzymatic properties, without resorting to hazardous chemicals for the extraction (Martins et al., 2011). Ascomycetes fungi are suitable for the SSF of a wide range of lignocellulosic-rich substrates due to their ability to produce enzymes that degrade the complex lignocellulosic matrix (Ferreira et al., 2016). Among the Ascomycetes fungi, *Aspergillus* spp. has been extensively used to produce different value-added compounds, such as organic acids, chitosan, and a wide range of enzymes, including high levels of carbohydrases (Ferreira et al., 2016).

For the monogastric animal feed industry, including aquafeeds, the utilization of carbohydrases is utterly important, given their potential to enhance the digestibility of non-starch polysaccharides (NSPs) present in plant feedstuffs, such as cellulose and hemicellulose, which are indigestible for monogastric animals. In aquafeeds, the utilization of extracts rich in enzymes and/or phenolic compounds with antioxidant properties derived from the SSF of the agro-industrial by-products has been applied with promising results. For instance, Novelli et al. (2017) observed that incorporating fungal phytase and protease produced by SSF of the agro-industrial by-products with *A. oryzae* and *A. niger*, respectively, improved the dry matter, protein, lipid, and energy digestibility in Nile tilapia (*Oreochromis niloticus*). A commercial enzymatic mixture obtained from the SSF with *A. niger* (Synergen™, Alltech, United States) significantly improved feed utilization and growth of Nile tilapia (Bowyer et al., 2020). Including 0.1% Synergen™ in diets with white lupin meal enhanced the growth and feed efficiency of common carp (*Cyprinus carpio*) (Anwar et al., 2020). These enzymatic supplements have shown to be highly efficient in improving fish feed utilization with high environmental and economic relevance for the long-term sustainability of aquaculture and marine ecosystems.

It was previously observed that *A. ibericus* produced xylanase (313.8 U g^{-1}), cellulase (51.3 U g^{-1}), and β-glucosidase (4.06 U g^{-1}) during SSF of BSG (Leite et al., 2019). The present study aimed to scale up the production of these enzymes and tested them as a novel functional additive to aquafeeds. In the first step, BSG was fermented by *A. ibericus* for hydrolytic enzyme production. This crude enzymatic extract was characterized by its thermostability, optimum pH, and temperature. In a second step, this crude extract was used to hydrolyze the remaining fermented BSG, and the optimum conditions, within the range of values defined for each variable, to maximize sugars and phenolic compounds release were determined. To validate the application of this extract as an aquafeed enzyme supplement, a feeding trial was carried out to assess its effect on growth performance and feed utilization efficiency of European seabass (*Dicentrarchus labrax*) juveniles. A schematic diagram of the process is presented in **Figure 1**.

MATERIALS AND METHODS

Ethical Approval

This study was approved by the ORBEA Animal Welfare Committee of CIIMAR and the Portuguese National Authority for Animal Health (DGAV). Experiments were directed by trained scientists (Functions A, B, C, and D defined in article 23 of the European Union Directive 2010/63) and conducted following the Federation of Laboratory Animal Science Association (FELASA) recommendations and the EU Directive (2010/63/EU) on the protection of animals for scientific purposes.

BSG and Selected Microorganism

BSG, provided by *Unicer*, Porto, Portugal, a soft-drink company, was constituted by Pilsner malt, barley, and corn gritz. The fungus species used in the SSF was *Aspergillus ibericus* (MUM 03.49), isolated from wine grapes (Serra et al., 2006). The fungus was maintained in potato dextrose agar at 4°C until utilization.

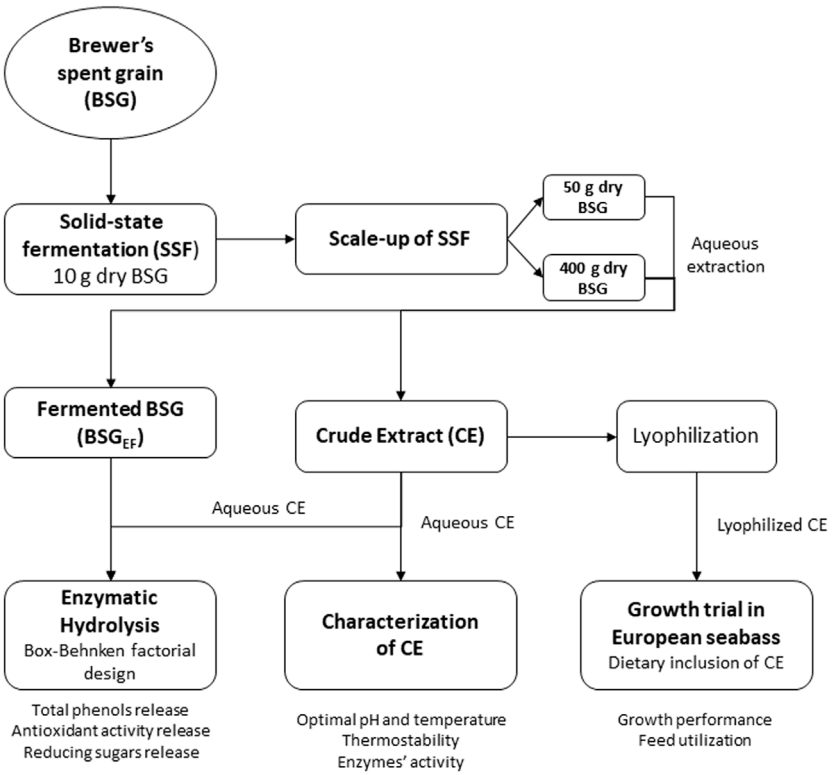

FIGURE 1 | Schematic diagram of the production of a crude extract from solid-state fermentation of brewer's spent grain with *A. ibericus* and its application to further hydrolyze the fermented BSG and as an aquafeed enzyme supplement.

Solid-State Fermentation of BSG and Production of the Crude Extract

The SSF was performed in duplicate in 500 ml cotton-plugged Erlenmeyer flasks with 10 g of dry BSG without nutritional supplements. BSG was sterilized at 121°C for 15 min and then inoculated with a spore's suspension of *A. ibericus* (2×10^6 spores/g dry BSG) following the optimized SSF of BSG described by Leite et al. (2019). Initial moisture of BSG was around 70% but was adjusted to 75% (w/w, wet basis) with the inoculum suspension and distilled water if needed. The height of the SSF bed in flasks was 1.5 cm. Each Erlenmeyer flask was then incubated at 25°C for 7 days. The approximate composition of BSG was determined before and after SSF, as present in **Table 1**.

The scale-up of SSF was performed in trays (16 x 11 x 6 cm or 43 x 33 x 7 cm), with 50 g or 400 g of BSG, in duplicate and triplicate, respectively, without additional nutrients. In each tray, the bed height was adjusted to 2.5 cm and the moisture level was adjusted to 75% with distilled water, followed by sterilization at 121°C for 15 min. Each tray was inoculated with a spore's suspension with 2×10^6 spores/g dry BSG, covered with perforated plastic wrap, and was incubated at 25°C for 7 days.

After the SSF, the fermented BSG was subjected to aqueous extraction with distilled water (1:5, g BSG: ml of water) for 30 min, with continuous agitation, at room temperature, followed by filtration through a nylon net (particle size <0.1 mm). The crude extract was obtained after the centrifugation (4,000 *g*, 15 min) of the liquid phase, separating the crude extract from the fungal biomass in suspension. A part of the crude extract was stored at −20°C for cellulase and xylanase activity analysis and the Box–Behnken factorial design experiments, and the other part was lyophilized to allow its incorporation in the fish diets. The extracted and fermented solid remaining after filtration (BSG_{EF}) and the fungal biomass remaining after centrifugation were dried at 50°C, weighed, and stored at room temperature to be characterized.

Optimum Temperature and pH for Xylanase and Cellulase Activities of the Crude Extract

To study the effect of temperature on xylanase and cellulase activities of the crude extract, the enzymatic activities were measured at temperatures ranging from 30°C to 70°C, with 5°C intervals, at a constant pH of 4.8. To assess the effect of the pH on these enzymes, the activities were measured at a constant temperature of 50°C and pH ranging from 2.6 to 5.8, and using sodium citrate 0.05 N as a buffer.

Thermostability of Cellulase and Xylanase of the Crude Extract

The thermostability of cellulase and xylanase of the crude extract was determined by measuring the enzymatic activities after

TABLE 1 | Proximal composition of BSG before and after the SSF by *A. ibericus* in 500-ml cotton-plugged Erlenmeyer flasks followed by aqueous extraction (mean ± standard deviation)* and percentage of mass variation of each component.

Compound (% w/w dry basis)	Unfermented BSG	BSG_{EF}	Mass variation (%)
Protein	25.30 ± 0.02[a]	29.31 ± 0.31[b]	25
Fiber	59.94 ± 2.01[b]	43.30 ± 0.30[a]	53
Cellulose	21.16 ± 0.99[b]	14.73 ± 0.39[a]	55
Hemicellulose	23.77 ± 1.4[b]	15.29 ± 0.2[a]	58
Lignin	15.01 ± 0.41[a]	13.28 ± 0.72[a]	42

$\%\ Mass\ variation = \frac{((\%w/w)_{unfermented} \times 10\ g - (\%w/w)_{fermented} \times 6.45g)}{(\%w/w)_{unfermented} \times 10\ g}$.

*Means in the same row and different superscript letters are significantly different (Tukey's test, $p<0.05$).

incubation at 45°C, 50°C, and 60°C for 120 min. The enzymatic activity assay was then performed at standard conditions (temperature of 50°C, pH 4.8) and expressed as a percentage of relative activity respectively to the initial value.

Enzymatic Hydrolysis of BSG_{EF}

An incomplete Box–Behnken design was performed to determine the optimal conditions for the hydrolysis of BSG_{EF} within the experimental levels used in each variable, aiming to maximize antioxidant activity potential and saccharification. The Box–Behnken design was performed with three factors at three levels (-1, 0, and +1), namely, the BSG_{EF} load (% w/v), crude extract amount (expressed as U cellulase g^{-1} of dry BSG_{EF}), and commercial β-glucosidase amount (expressed as U g^{-1} of dry BSG_{EF}). The design was performed in a set of 15 experiments, and three central point replicates were used to estimate the experimental error. For statistical calculations, the independent variables were coded, and the correspondence between the coded and uncoded variables is shown in **Table 2**. The dependent variables were the maximum values of total phenols, antioxidant activity, and reducing sugars released after enzymatic hydrolysis.

The Box–Behnken design experiments were performed as follows: BSG_{EF} was submitted to enzymatic hydrolysis with the crude extract and/or a commercial β-glucosidase (from *Aspergillus niger*, Megazyme; E-AMGDF). For that purpose, BSG_{EF} was mixed with sodium citrate buffer (0.05 N, pH 3.9), autoclaved for 15 min at 121°C, and mixed with the crude extract and/or commercial β-glucosidase. Thymol (0.07 g/l) was added to avoid contamination during hydrolysis. The mixtures were then incubated for 72 h at 45 °C with constant shaking (150 rpm). At the end of the enzymatic hydrolysis (72 h), the liquid was separated from the solid fraction by vacuum filtration, and the liquid fraction was stored at −20 °C for analysis of phenolic compounds, antioxidant activity, and free reducing sugars.

Based on the Box–Behnken design results, the best conditions predicted by the model within the levels studied for each variable to maximize the sugars and phenolic compounds released during the hydrolysis of BSG_{EF} with crude extract were tested in duplicate.

Effect of Dietary Supplementation With the Crude Extract in European Seabass Growth and Feed Efficiency

To test the potential of the crude extract as an exogenous enzyme supplement for aquafeeds, a growth trial with a carnivorous aquaculture species, European seabass (*Dicentrarchus labrax*), was performed. For that purpose, three isoproteic (48% crude protein) and isolipidic (16% crude lipids) diets were formulated, containing 10% of fish meal and 60% of plant feedstuffs (% diet) as main protein sources, and fish oil as the main lipid source. The lyophilized crude extract (12,400 and 1050 U g^{-1} of xylanase and cellulase, respectively) was incorporated in the diets (w/w) at increasing levels of 0 (control diet), 0.1% (CE0.1 diet), and 0.4% (CE0.4 diet), corresponding to around 0 U, 1000 U, and 4000 U of cellulase g^{-1} diet (dry matter basis).

The growth trial was conducted in a thermoregulated recirculating water system, equipped with nine fiberglass tanks of 60 l capacity. The fish were obtained from a commercial aquaculture facility and acclimatized to the experimental system conditions for 15 days. Then, nine groups of 15 fish with an initial body weight of 22 g were established and randomly assigned to each tank. Triplicate groups were fed each experimental diet, by hand, until apparent satiety, twice a day, 6 days per week, for 64 days. Feed consumption was recorded weekly. During the trial, the water temperature was maintained at 23.8 ± 0.1°C, salinity at 32.0 ± 0.9‰, and nitrites and ammonia levels were kept below 0.05 mg ml^{-1}. The water flow in each tank was kept at 5 L min^{-1}. At the beginning and end of the experiment, fish were bulk-weighed after 1 day of feed deprivation to determine the growth and feed utilization parameters, namely, final body weight, weight gain, daily growth index, feed intake, feed efficiency, and protein efficiency ratio. Five fish from the initial stock and from each tank at the end of the trial were sampled and pooled for the whole-body composition analysis to measure the nitrogen and energy retention.

Analytical Methods

Protein and Lignocellulosic Composition of Unfermented BSG and BSG_{EF}

The protein content of the unfermented BSG and BSG_{EF} was assessed by the *Kjeldahl* method after the digestion with sulfuric acid (>95%) using a *Kjetelc* system (Foss 8400) and applying the factor 6.25 to convert N to protein. The lignocellulosic characterization of the unfermented BSG and BSG_{EF} was carried out following the method described by Leite et al. (2016).

Enzyme Activity Determination

Cellulase, xylanase, and β-glucosidase activities were measured in the crude extract. Cellulase activity was measured using

carboxymethyl cellulose (2% w/v) as the substrate in sodium citrate buffer 0.05 N (pH 4.8), incubated at 50°C for 30 min, and the reducing sugars measured by the DNS method. Xylanase activity was determined using xylan (1% w/v) as substrate in sodium citrate buffer 0.05 N (pH 4.8), incubated at 50°C for 15 min, and the liberated reducing sugars measured by the DNS method (Miller, 1959). β-glucosidase activity was determined in accordance with the method by Leite et al. (2016) using β-D-glucopyranoside (pNPG) as substrate in acetate buffer (50 mM, pH 5).

One unit (U) of enzyme activity was defined as the enzyme quantity necessary to release 1 μmol of xylose/min or 1 μmol glucose/min from each substrate for xylanase or cellulase activities, respectively, and to release 1 μmol/min of *p*-nitrophenol for β-glucosidase activity. The enzymatic activities were expressed as U per gram of dry BSG or per gram of lyophilized crude extract (U g^{-1}).

Total Phenols, Antioxidant Activity, and Reducing Sugar Analysis

After the enzymatic hydrolysis of BSG_{EF}, total phenol (TP) content was determined by the Folin–Ciocalteau method, using gallic acid as standard, and the results were expressed in mg gallic acid equivalents (GAE)/g BSG_{EF}. The antioxidant activity (AA) was analyzed by the DPPH method, as described by Fernandes et al. (2019), and the results were expressed in μmol Trolox equivalents (TE)/g BSG_{EF}. The released reducing sugars (glucose, xylose, and arabinose) were analyzed by high-performance liquid chromatography using a Jasco830-IR intelligent refractive-index detector with a Varian MetaCarb 87H column. The column was eluted with 0.005 M H_2SO_4, and the flux was settled at 0.7 ml min^{-1} at 60°C. The results for each sugar and total released reducing sugars (sum of glucose, xylose, and arabinose) were expressed as mg g^{-1} BSG_{EF}.

Statistical Analysis

The Box–Behnken experimental design data were evaluated using the response surface methodology by *Statistica 10* software (Informer Technologies Inc., LA, United States), and the dependent variables were optimized using the *Solver* tool (Microsoft Excel 2019; Redmon, WA, United States). The statistical analysis of data was performed by one-way analysis of variance (ANOVA), and Tukey's multiple range test was used to detect significant differences among means ($p < 0.05$).

StatgraphicPlus Centurion XVI (Statgraphics Technologies Inc., Virginia, United States) was used to evaluate the data of the Box–Behnken experimental design, and *IBM SPSS Statistics 26* (IBM, NY, United States) was used for the data of the growth trial with the European seabass.

RESULTS

BSG Fermentation

The fungi *A. ibericus* grew well in wet BSG at the used operational conditions, and fungal dry biomass of 1.8% (w/w, per dry mass of unfermented BSG) was produced.

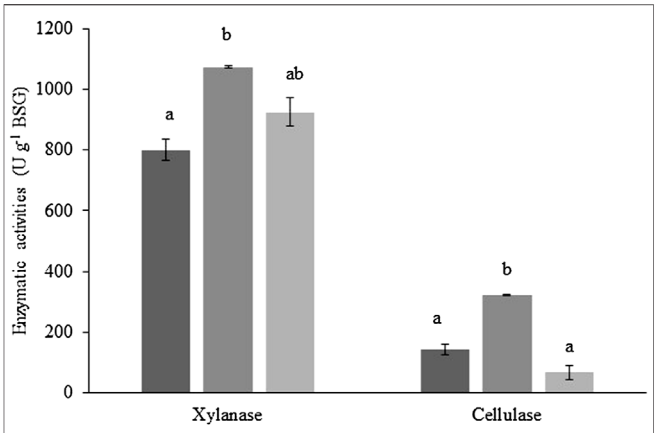

FIGURE 2 | Xylanase and cellulase activities obtained by the SSF at different scales (black—10 g, dark gray—50 g, and light gray—400 g of dry BSG). Treatments without a common letter are statistically different (Tukey's test; $p < 0.05$). Values are presented as the mean ± standard deviation of two (10 g and 50 g of dry BSG) and three (400 g of dry BSG) independent replicates.

At the end of the small-scale SSF using 10 g BSG in flasks, it was possible to recover 6.45 g of dry fermented BSG after aqueous extraction, corresponding to a total mass decrease of 35.5%. This BSG mass loss was due to the solubilization of BSG components that occurred through the SSF, resulting in a total protein mass decrease of 25%. Nevertheless, BSG_{EF} has a higher content of protein (29.3%, w/w) and a lower content of lignocellulosic fiber than the unfermented BSG (**Table 1**). The fiber content of BSG_{EF} was reduced by 53% relative to the unfermented BSG, corresponding to 58% hemicellulose, 55% cellulose, and 42% lignin degradation.

SSF Scale-Up and Crude Extract Production

Xylanase and cellulase production throughout the scale-up process of SSF of BSG, without nutrient supplementation, is presented in **Figure 2**. Values for β-glucosidase activity are not shown, given its low activity; however, the highest β-glucosidase activity (5.3 ± 0.3 U g^{-1} BSG) was achieved using 50 g of BSG in SSF. Maximum xylanase (1,072.9 ± 4.2 U g^{-1} BSG) and cellulase (323.2 ± 0.9 U g^{-1} BSG) activities were, in both cases, obtained by the SSF of 50 g of BSG, corresponding to an activity increase of 25% and 55%, respectively, relative to the SSF of 10 g of BSG. Further increase in the quantity of BSG subjected to SSF, up to 400 g, slightly (14%) decreased xylanase activity without statistical significance, but cellulase activity was significantly reduced by 79%. However, the enzyme activities obtained with 10 g and 400 g of BSG (40-fold scale-up) were not statistically different.

Optimum Temperature and pH for the Crude Extract Xylanase and Cellulase Activity

The effect of temperature on xylanase and cellulase activities is presented in **Figure 3**. Xylanase activity significantly increased

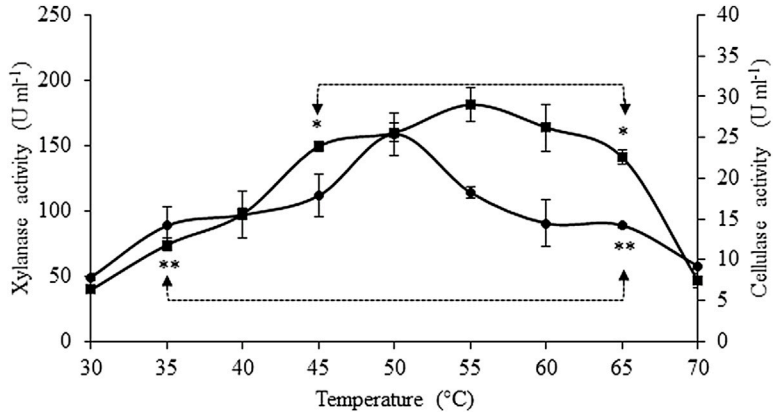

FIGURE 3 | Effect of temperature on xylanase (■) and cellulase (●) activities. Asterisks represent the interval of temperatures and pH in which no statistical differences were detected (Tukey's test, $p < 0.05$) for xylanase (*) and cellulase activities (**). Values are presented as the mean ± standard deviation of two independent replicates.

($p < 0.05$) from 30°C to 45°C (3.8-fold), with its optimal range of temperature observed between 45°C and 65° C and a maximum activity at 55° C (181.5 ± 13.1 U ml^{-1} crude extract), without significant statistical differences among those values. Above 65° C, a significant drop of 67% in xylanase activity was observed when the reactional temperature was 70° C. Maximum cellulase activity was attained at 50° C (25.4 ± 2.6 U mL^{-1} crude extract), but no statistically significant differences ($p < 0.05$) were found for cellulase activities in the temperatures ranging between 35°C and 65° C. The lowest values of cellulase activity were found at 30°C and 70° C, being 69% and 64% lower, respectively, than the those observed at 50°C.

The effects of pH on the crude extract xylanase and cellulase activity are presented in **Figure 4**. Xylanase activity was the highest at pH ranging between 3.9 and 4.8, with maximum activity (182.2 ± 3.4 U ml^{-1} crude extract) at pH 4.4, without significant statistical differences ($p < 0.05$) among the activities within this pH range. High levels of xylanase activity were still observed at pH ranging from 3.6 to 5.4, with activity values above 78% of the maximum value. At the lowest pH studied, xylanase activity decreased 74%, while the activity only decreased 41% at the highest pH. Optimum cellulase activity was observed at pH 3.9 (33.5 ± 0.8 U ml^{-1} crude extract), and this value was statistically different from the values obtained at all the other pH conditions tested. The cellulase activity in the crude extract was above 61% of its maximum value at pH ranging between 3.6 and 4.8 (66% in this case), but was totally inactive at pH 5.8.

Thermostability of Crude Extract Xylanase and Cellulase Activity

Figure 5 shows the variation of xylanase and cellulase activities with the storage time at 45°C, 50°C, and 60°C. Cellulase was more thermostable than xylanase at all temperatures tested. For example, at 45°C, cellulase and xylanase maintained 91% and 64% of their activity, respectively, after 120 min of storage. Moreover, cellulase retained 69% and 61% of its initial activity after 2 h of storage at 50°C and 60°C, respectively. On the other hand, xylanase remained practically stable at 45°C, but at 50°C and 60°C, the activity decreased to 58% and 96% from its initial value, respectively, after 30 min.

Enzymatic Hydrolysis of BSG_{EF}

Response surface methodology was used to predict the crude extract quantity, BSG_{EF} load, and commercial β-glucosidase supplementation level that maximizes total phenol (TP) release, reducing sugars, and antioxidant activity (AA) during the enzymatic hydrolysis of BSG_{EF}, within the range of values defined for each variable. The quantity of crude extract was determined based on the cellulase units due to its lower content and higher stability than xylanase in the crude extract at the enzymatic hydrolysis pH used. Commercial β-glucosidase addition was considered since its activity in the crude extract is low.

The matrix design, number of experiments performed, and increase of AA, TP, and sugar content released by enzymatic hydrolysis are presented in **Table 2**. In comparison with the control (without enzymatic treatment), the TP increase ranged from 8.2 to 49.3 mg GAE g^{-1} (run 4 and 6, respectively), the variation of AA ranged from −4.5 to 83.5 μmol TE g^{-1} (run 14 and 9, respectively), and the total sugars ranged from 9.76 to 65.5 mg g^{-1} (run 12 and 6, respectively).

The models for the three variables studied showed a good fit, with an adjusted R^2 above 0.95, which indicates that more than 95% of the variability of TP, AA, and reducing sugars is explained by the models (**Table 3**). The three models were statistically significant ($p < 0.05$), and the high F-value obtained (higher than F_{tab}) also demonstrated the excellent fit of the three models.

Figure 6 shows each dependent variable in function of the two independent variables with a higher effect in the enzymatic hydrolysis, and the third independent variable fixed at the center level. The higher amount of AA and TP was released at the highest levels of the β-glucosidase addition and the lowest level of the BSG_{EF} load (**Figures 6A,B**). The quantity of crude

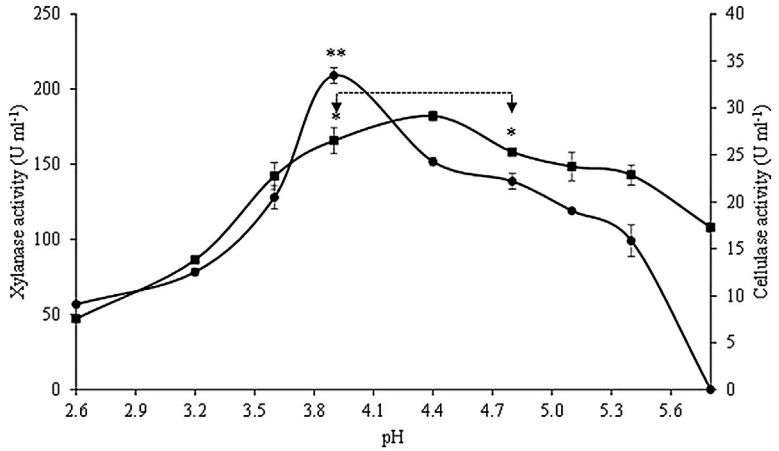

FIGURE 4 | Effect of pH on xylanase (■) and cellulase (●) activities. Asterisks represent the interval of temperatures and pH in which no statistical differences were detected (Tukey's test, $p < 0.05$) for xylanase (*) and cellulase activities (**). Values are presented as the mean ± standard deviation of two independent replicates.

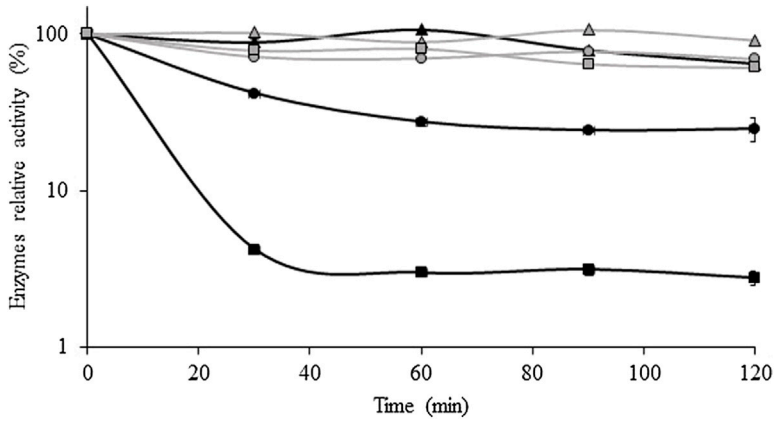

FIGURE 5 | Thermal stability of xylanase and cellulase obtained after the solid-state fermentation of BSG at 45 °C (▲), 50 °C (●), and 60 °C (■). Xylanase and cellulase activities are represented by black and gray symbols, respectively. Values are presented as the mean ± standard deviation of two independent replicates.

extract did not affect the TP and AA release but had a high effect on reducing sugar release than the addition of β-glucosidase (**Figure 6C**).

The model predicted that the ideal conditions to maximize AA release (93.5 μmol TE g^{-1}) during BSG_{EF} enzymatic hydrolysis, among the levels tested for each variable, are 150 U g^{-1} of cellulase from the crude extract, 1% (w/v) BSG_{EF}, and 20 U g^{-1} β-glucosidase. To maximize TP release (40.9 mg g^{-1}), the optimal conditions predicted by the model within the studied levels are 100 U g^{-1} of cellulase from the crude extract, 1% (w/v) BSG_{EF}, and 20 U g^{-1} β-glucosidase. To maximize sugars yield (65.5 mg g^{-1}), the optimal conditions within the levels tested in the present study predicted by the model are 50 U g^{1} of cellulase from crude extract, 2.5% (w/v) BSG_{EF}, and no addition of β-glucosidase.

According to these results, the optimal conditions for enzymatic hydrolysis of BSG_{EF} were tested. Under these conditions, AA (89.5 ± 2.5 μmol TE g^{-1}), TP (39.2 ± 1.3 mg g^{-1}), and reducing sugars (65.5 mg g^{-1}) release were similar to those predicted by the model, revealing that the model used was reasonably accurate. The sugar yield with these optimal conditions was 2.4 times higher than that achieved by the enzymatic hydrolysis of the unfermented BSG.

Effect of Dietary Supplementation With Crude Extract in European Seabass Growth and Feed Efficiency

The crude extract dietary supplementation effect on growth and feed utilization of the European seabass is presented in **Table 4**. Growth performance, measured as final body weight, weight gain, and daily growth index, was not affected by the dietary treatments. However, feed efficiency and protein efficiency ratio of fish fed with the CE0.4 diet were higher than those of

TABLE 2 | Matrix of the experimental design and identification of the different conditions applied in each experiment. Each variable and coded levels used in the Box–Behnken experimental design matrix are identified. Values are present as the mean [X_1–crude extract; X_2–load of BSG_{EF}; X_3–commercial β-glucosidase; TPV–total phenols variation; AAV–antioxidant activity variations; RS–released sugars; pentoses (xylose + arabinose)].

Independent variables				*Experimental values*				
Runs	**X_1**	**X_2**	**X_3**	**TPV (mg GAE g^{-1})**	**AAV (μmol TE g^{-1})**	**RS (mg g^{-1})**	**Glucose (mg g^{-1})**	**Pentoses (mg g^{-1})**
1	1	0	−1	10.42 ± 0.50	16.06 ± 0.86	32.11 ± 1.61	17.03	15.08
2	0	0	0	8.61 ± 0.48	42.52 ± 8.84	35.26 ± 1.76	18.17	17.09
3	0	0	0	10.67 ± 0.72	42.36 ± 1.32	38.25 ± 1.91	19.54	18.7
4	−1	0	−1	8.18 ± 0.41	30.46 ± 2.20	16.82 ± 0.84	11.66	5.17
5	1	−1	0	18.92 ± 0.66	59.22 ± 13.77	30.82 ± 1.54	17.14	13.68
6	0	−1	−1	49.30 ± 0.25	28.79 ± 0.82	65.5 ± 3.06	27.43	33.83
7	1	0	1	12.19 ± 0.50	59.25 ± 3.45	18.99 ± 0.82	8.91	7.42
8	−1	0	1	15.11 ± 2.02	41.06 ± 12.83	18.64 ± 0.93	9.60	9.04
9	0	−1	1	42.87 ± 0.26	83.48 ± 5.61	34.13 ± 1.71	18.0	16.13
10	−1	−1	0	29.47 ± 2.96	56.83 ± 12.29	27.42 ± 1.37	13.72	13.71
11	0	0	0	11.04 ± 2.48	32.08 ± 3.29	36.8 ± 0.66	13.72	3.58
12	−1	1	0	8.89 ± 0.92	3.98 ± 1.61	9.76 ± 0.49	9.6	3.46
13	0	1	1	9.11 ± 0.32	0.81 ± 3.29	14.72 ± 0.74	7.5	4.86
14	1	1	0	8.76 ± 0.45	−4.54 ± 0.82	18.07 ± 0.9	12.0	6.07
15	0	1	−1	8.29 ± 0.63	−0.66 ± 1.41	21.2 ± 1.06	13.72	7.49

Independent variables	**Identification**	**Coded levels**		
		-1	**0**	**1**
Crude extract (U cellulase g^{-1} of dry BSG_{EF})*	X_1	50	100	150
BSG_{EF} (% w/v)	X_2	1	2.5	4
Commercial β-glucosidase (U g^{-1} dry BSG_{EF})	X_3	0	10	20

**50 U g^{-1} of cellulase activity corresponds to 165.1 U g^{-1} xylanase activity and 1.06 U g^{-1} of β-glucosidase.*

TABLE 3 | Quantitative model assessment tools (TPV—total phenol variation; AAV—antioxidant activity variations; RS—released sugars).

Tools	*Dependent variables*		
	TPV	**AAV**	**RS**
R^2	0.9981	0.9924	0.9981
R^2 adjusted	0.9924	0.9471	0.978
F-value	85.91	21.88	89.76
Significance level	98.84	95.55	98.89

the control diet. Nitrogen (% nitrogen intake) and energy (kJ kg^{-1} ABW day^{-1}) retention tend to be higher with the CE0.4 diet, but no significant differences were detected.

DISCUSSION

BSG_{EF} Production

The SSF of BSG resulted in solid matrix deconstruction leading to total mass solubilization of around 35%, mainly due to the remarkable reduction of hemicellulose and cellulose of 58% and 55%, respectively. Lignin was also reduced but to a smaller extent (42%), probably due to the inability of *A. ibericus* to produce lignin peroxidases. Opazo et al. (2012) carried out the SSF of soybean meal with cellulolytic bacteria and achieved 24% reduction in the NSP content, which compares well with the 28% reduction observed in the present study. The SSF of rice straw using *A. terreus* showed a reduction of 16% and 33% of cellulose and hemicellulose contents, respectively (Jahromi et al., 2011).

The SSF resulted in an absolute protein reduction of 25% in BSG, which may be due to the protein consumed by *A. ibericus* during the SSF (Gowthaman et al., 2001). Moreover, the protein decrease of BSG_{EF} can also be due to the extraction of soluble protein when aqueous extraction was carried out to obtain the crude extract at the end of the SSF. However, besides the absolute high protein decrease observed after SSF, the fermented BSG has a remarkably reduced lignocellulosic matrix and a considerable absolute protein content, which shows the nutritional and digestibility upgrade that the SSF exerted on BSG. Therefore, the fermented BSG could be a viable alternative to traditional feedstuffs commonly used in formulated feeds, such as in diets for aquatic animals (Dawood & Koshio, 2019).

SSF Scale-Up

Successful upscaling processes of the SSF need the utilization of bioreactors with optimized designs that assure the maintenance and monitoring of ideal growing conditions of the fungi (Webb, 2017). This study has successfully scaled-up the SSF by 5-fold or 40-fold of BSG mass. Moreover, maximum enzymatic activities were observed using 50 g of BSG, showing that the solid bed-height increase from the flask to tray system did not affect the enzyme production. This better performance of the SSF in the tray-type system than that of the Erlenmeyer flask may be explained by the lower ratio of headspace to a total volume

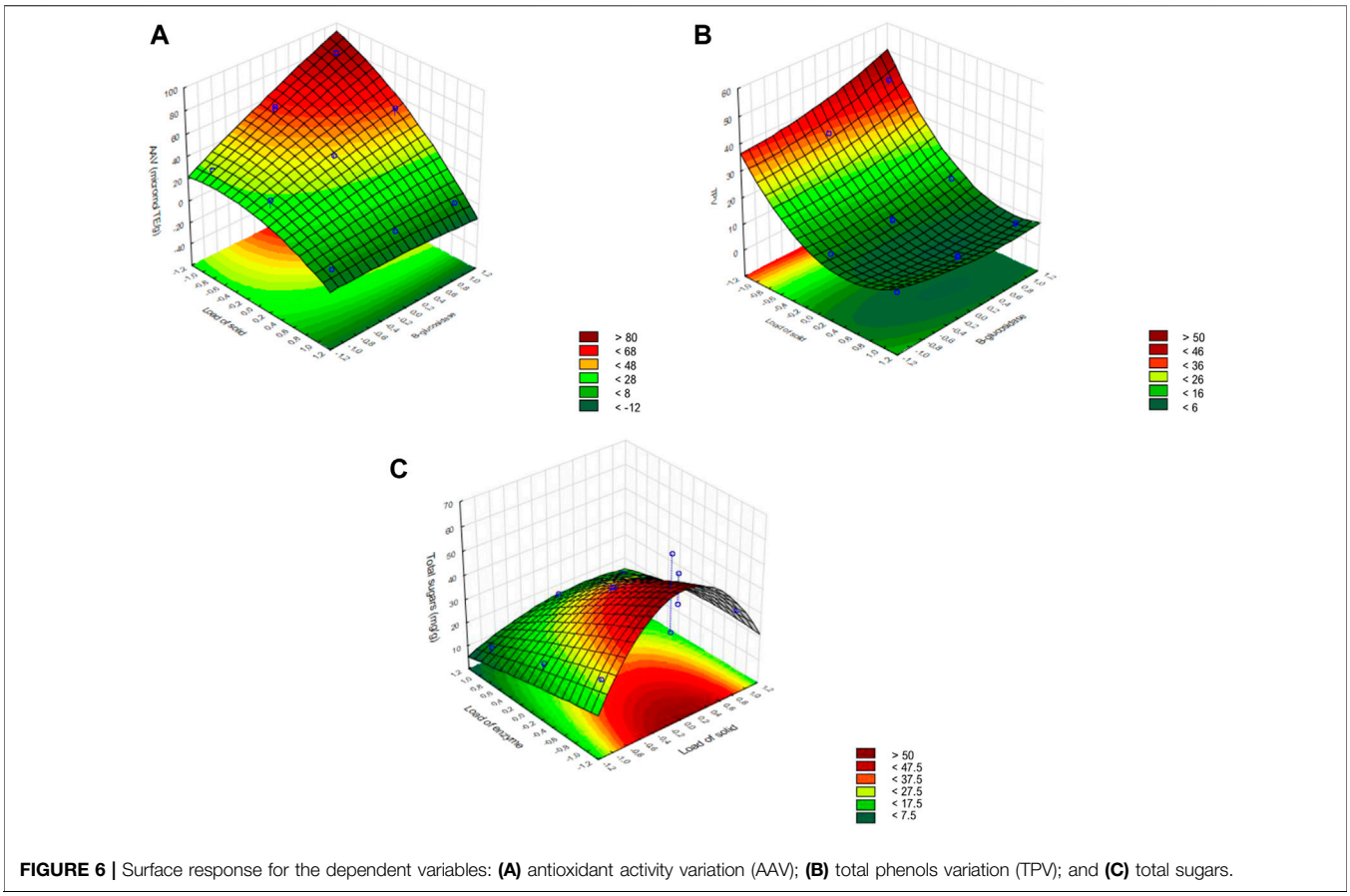

FIGURE 6 | Surface response for the dependent variables: **(A)** antioxidant activity variation (AAV); **(B)** total phenols variation (TPV); and **(C)** total sugars.

TABLE 4 | Growth performance and feed utilization of the European seabass juveniles fed with the experimental diets for 64 days*.

Diets	Control	CE0.1	CE0.4	SEM
Initial body weight (g)	22.00	22.01	22.02	0.01
Final body weight (g)	35.08	35.67	36.78	0.51
Weight gain (g kg^{-1} ABW day^{-1})	8.95	9.29	9.84	0.27
Daily growth index	0.92	0.96	1.02	0.03
Feed intake (g kg^{-1} ABW day^{-1})	13.73	12.59	11.36	0.56
Feed efficiency	0.65^{a}	$0.74^{a,b}$	0.88^{b}	0.04
Protein efficiency ratio	1.36^{a}	$1.54^{a,b}$	1.80^{b}	0.08
Nitrogen retention (g kg^{-1} ABW day^{-1})	0.24	0.25	0.24	0.01
Nitrogen retention (% NI)	22.64	25.71	26.84	0.99
Energy retention (kJ kg^{-1} ABW day^{-1})	72.48	64.45	80.86	5.89
Energy retention (% EI)	22.02	21.24	29.14	1.87

*Values are presented as the mean (n = 3) and standard error of the mean (SEM). Values in the same row and different superscript letters are significantly different (Tukey' test; $p < 0.05$).

Average body weight (ABW) = ((initial body weight, IBW + final body weight, FBW)/2).

Weight gain = (FBW-IBW ×1,000)/(ABW × time in days).

Daily growth index = ($FBW^{1/3}$ - $IBW^{1/3}$)/time in days) ×100.

Feed efficiency = wet weight gain/dry feed intake.

Protein efficiency ratio = wet weight gain/dry protein intake.

Nitrogen retention (g/kg ABW/day) = ((FBW×FBN – IBW×IBN) ×1,000)/(ABW × time in days); IBN and FBN: initial and final nitrogen content.

Energy retention (g/kg ABW/day) = ((FBW×FBE – IBW×IBE) ×1,000)/(ABW × time in days); IBE and FBN: initial and final energy content.

Energy retention (% energy intake) = whole-body energy retention/energy intake; EI) ×100.

that reduces moisture loss. The further increase of BSG mass up to 400 g in trays resulted in a decrease of cellulase activity compared to the 50 g of BSG, despite the same bed-height. The production of this enzyme may be conditioned by inefficient substrate mixing, performed manually every day during the SSF, resulting in temperature increase and, concomitantly, compromising the production of the enzymes by the fungi (Webb, 2017). In the previous work, Sousa et al. (2018) observed that the SSF of BSG with *A. ibericus* resulted in the highest enzymatic activities among other agro-industrial substrates and fungi utilized, obtaining an extract with about 55 and 50 U g^{-1} of xylanase and cellulase activities, respectively. The SSF of 400 g of BSG with *A. brasiliensis* resulted in xylanase, cellulase, and β-glucosidase activities of 3,152, 7.3, and 19 U g^{-1} dry BSG, respectively (Outeiriño et al., 2019). The successful scale-up of the SSF of different agricultural by-products from flasks to tray-type bioreactors was also previously achieved for glucoamylase production by *A. niger* (Nahid et al., 2012). Furthermore, up-scaling from 24-g flasks to the 5.5-kg bioreactor of the SSF of a mixture of agro-industrial by-products with *Trichoderma asperellum* also increased the lipase, cellulase, and amylase production (Rayhane et al., 2019). Contrarily, scaling-up the SSF of wheat bran combined with sugarcane bagasse from 10 g up to 15 kg in a pilot packed-bed bioreactor led to a decrease of lipase activity by 57% (Pitol et al., 2017).

Optimal Temperature and pH for Enzymes Activity

Cellulase and xylanase produced by *A. ibericus* during the SSF of BSG and present in the crude enzymatic extract were characterized regarding their activity with temperature and pH conditions and their thermostability. This characterization is fundamental to assess the optimal conditions for further utilization in diverse industrial processes.

In the present study, the optimum temperature that maximizes xylanase activity was determined to range between 45°C and 65°C, with maximum activity at 55°C. Similarly, maximum activity of xylanase produced by *Aspergillus flavus* was attained at 55°C (Chen et al., 2019), that of xylanase produced by *Simplicilium obclavatum* during the wheat bran SSF was attained at 50°C (Roy et al., 2013), that of xylanase produced by *Rhyzopus oryzae* during the SSF of raw oil palm frond leaves was attained at 60°C (Ezeilo et al., 2020), and that of xylanase produced by *A. niger* after 10 days of the SSF of BSG was attained at 50°C (Liguori et al., 2021). However, other authors reported lower optimal temperatures for xylanase activity, such as that produced from *Pediococcus acidilactici*, showing maximum activity at 40°C (Adiguzel et al., 2019). Cellulase activity was maximum at 50°C, but good activity levels were observed between 35°C and 65°C. Similarly, optimum cellulase activity was also observed at 50°C when fermenting raw oil palm leaves with *Rhizopus oryzae* (Ezeilo et al., 2020), at 55°C for the cellulase produced by *Trichoderma reesei* (Astolfi et al., 2019), and at 60°C for the cellulase produced by *A. niger* during the SSF of BSG (Liguori et al., 2021).

Regarding optimum pH, maximum xylanase activity was achieved at pH 4.4, while maximum cellulase activity was achieved at pH 3.9. Similarly, higher activities of cellulase and xylanase produced by *A. fumigatus* during the SSF of untreated oil palm trunk were observed at acid pH (4), while above the pH of 5, the enzymatic activities were dramatically reduced (Ang et al., 2013). In addition, *A. terreus* showed optimum cellulase activity in the pH range of 4–5 (Narra et al., 2014). Contrarily, the highest xylanase and cellulase activities obtained by the SSF of BSG with *A. niger* were found at neutral pH (Liguori et al., 2021).

The characterization of optimal temperature and pH of xylanase and cellulase in the crude enzymatic extract anticipates that these enzymes are suitable for converting different agro-industrial materials with different industrial applications. For example, these enzymes can be used in pulp, paper, food, and beverage industries as well to produce second-generation biofuels (Manisha & Yadav, 2017; Astolfi et al., 2019; Liguori et al., 2021), given their suitability to work at increasing temperatures and challenging pH levels.

Thermostability of Crude Extract Xylanase and Cellulase

The thermostable enzymes have many advantages in the industrial and biorefinery processes of lignocellulosic materials. Generally, the enzymatic hydrolysis of lignocellulosic materials is carried out at temperatures ranging between 40°C and 50°C (Patel et al., 2019).

The present results showed that cellulase activity is more stable than xylanase, remaining practicably stable (less than 20% loss) for the first 60 min at all temperatures tested. On the other hand, xylanase activity had an identical profile to cellulase only at 45°C, showing significant activity loss as the temperature increased, being residual (around 4% of relative activity) after 30 min at 60°C. Delabona et al. (2013) also observed a decrease of xylanase and cellulase activities produced by *A. fumigatus* after 30 and 40 min at 60°C, respectively, although cellulase still maintained 60% of its activity after 1 h. Xylanase activity also showed less thermostability than cellulase in the enzymatic cocktail produced by *A. niger* during the SSF of sugarcane bagasse (Vasconcellos et al., 2015). In this study, the thermostability of endo-cellulases depended on the type of fermentation as enzymes produced by the SSF have shown higher stability than enzymes produced by the submerged fermentation (Vasconcellos et al., 2015).

Enzymatic Hydrolysis of BSG_{EF} With Crude Extract

One of the aims of the present study was to develop a SSF-based biorefining strategy to maximize the release of reducing sugars and phenolic compounds from the hydrolysis of BSG_{EF}. Pretreatment of lignocellulosic substrates for biorefineries, involving chemical and physical treatment, is a common procedure to increase the yield of different cell compounds (Socaci et al., 2018; Birsan et al., 2019; Alonso-Riaño et al., 2020). Biological pretreatment, such as SSF, is a new alternative strategy followed in this study. To maximize the release of AA, TP, and reducing sugars, the BSG_{EF} was subjected to the enzymatic hydrolysis with the crude extract.

The optimum enzymatic hydrolysis conditions were determined based on the Box–Behnken experimental design. The response surface methodology was highly accurate to identify each variable's importance among the levels tested in the release of AA, TP, and reducing sugars from BSG_{EF}, as the predicted values estimated by the model and the experimentally obtained values of TP, AA, and reducing sugars release were very similar, and the data showed a good fit to the model with high significance levels.

During the BSG_{EF} hydrolysis, among the tested levels for each variable, a low level of BSG_{EF} (1%) and β-glucosidase supplementation is required to increase the TP and AA release, while the crude extract quantity had no effect on TP and AA release. Thus, further increase of the enzymatic level (from crude enzymatic extract and β-glucosidase) may lead to higher TP and AA release from BSG_{EF} than the one obtained herein. The required supplementation with β-glucosidase may be attributed to the BSG_{EF} lignocellulosic structure that was previously modified during the SSF by the action of *A. ibericus*. Cellulose degradation by the integrated action of endo-glucanases, exo-glucanases, and β-glucosidase, and β-glucosidase acts in cellobiose hydrolysis (Lakhundi et al., 2015). The action of β-glucosidase results in the release of glucose (Lakhundi et al., 2015) and phenolic compounds

TABLE 5 | Phenolics yield obtained after different pretreatments of BSG reported in the present work and other studies.

Treatment	Conditions	Phenolic yield	References
SSF	2 g BSG, 7 days, 25°C, *A. niger*	2 mg GAE g^{-1}	Leite et al. (2019)
Alkaline	2 g BSG, NaOH 2 M, 4 h, 65°C	16.2 mg GAE g^{-1}	Alonso-Riaño et al. (2020)
Acidic	0.2 g BSG, methanol and Sulphur acid, 20 h, 85°C	30 mg GAE g^{-1}	Alonso-Riaño et al. (2020)
Ultra-sounds	20 kHz, 1 h, 47°C	3.3 mg GAE g^{-1}	Alonso-Riaño et al. (2020)
Organic solvents	2 g BSG, methanol, ethanol, or acetone, 30 min	1.2 mg GAE g^{-1}	Socaci et al. (2018)
Enzymatic hydrolysis	10–100 µl carbohydrases g^{-1} dry BSG, 4 h or 9 h, 50°C	0.56 mg GAE g^{-1}	Crowley et al. (2017)
Enzymatic hydrolysis	50 U cellulase g^{-1} dry BSG_{EF}, 72 h, 45°C	49.2 mg GAE g^{-1}	Present work

linked to glycosides into their respective aglycones (Martins et al., 2011). Since the crude extract had low β-glucosidase activity (5.3 U g^{-1} BSG) compared to that of xylanase and cellulase (1,072.9 U g^{-1} BSG and 323.2 U g^{-1}, respectively), the addition of a commercial β-glucosidase aimed to potentiate the release of phenolic compounds with antioxidant activity. Previously, Ajila et al. (2011) observed that phenolic compounds released from apple pomace were positively correlated with β-glucosidase, resulting in increased antioxidant activity. With other substrates, such as citrus by-products, β-glucosidase increased the release of TP and AA (Ruviaro et al., 2019). However, the enzymatic hydrolysis of BSG with β-glucosidase to extract phenolic compounds was not yet studied.

In the present work, the enzymatic hydrolysis of BSG_{EF}, for 72 h, extracted 49.2 mg GAE g^{-1} BSG of TP, which was much higher than that obtained with other treatments, such as the SSF, alkaline and acid hydrolysis, ultrasounds, or organic solvents (**Table 5**). Enzymatic treatments allow releasing phenolic compounds linked to hemicellulose and lignin, which are not hydrolyzed by organic solvents (Alonso-Riaño et al., 2020) or which can be destroyed when in contact with strong acidic or alkaline conditions (Crowley et al., 2017).

Alonso-Riaño et al. (2020) evaluated TP extraction from BSG with three xylanase levels, achieving maximum extraction of 42 mg GAE g^{-1} with the highest enzyme load. Using the commercial carbohydrases (10–100 µl carbohydrases g^{-1} dry BSG), 0.56 mg GAE g^{-1} of TP was obtained from BSG by Crowley et al. (2017), whereas in the present work, TP release from BSG reached 49.2 mg GAE g^{-1}, highlighting the advantages of enzymatic hydrolysis of BSG after a biological pretreatment with the SSF.

By the enzymatic hydrolysis of BSG_{EF}, the release of reducing sugars was highest when a low quantity of crude extract and an intermediate level of BSG_{EF} were used without the addition of commercial β-glucosidase. The low level of crude extract required to release reducing sugars from BSG_{EF} may be due to the previous partial disruption of BSG cell wall during the SSF before the enzymatic hydrolysis, which may have improved the enzymatic hydrolysis efficiency. Therefore, SSF worked as a pretreatment that potentiated the reducing sugars yield following the enzymatic hydrolysis. The importance of pretreatments to enhance the enzymatic hydrolysis efficiency of lignocellulosic materials has been pointed out (Paz et al., 2019). Llimós et al. (2020) observed that lignocellulosic enzymes produced during the SSF of BSG with *A. niger* released 0.56 g sugars per gram of dry BSG.

Other pretreatment procedures are often applied before the enzymatic hydrolysis, such as chemical pretreatments using diluted acids (Rojas-Chamorro et al., 2020). A combination of alkaline and ionic liquid pretreatments enhanced the sugar yield of sunflower stalk with hydrolyzed fungal carbohydrases (Nargotra et al., 2018). In addition, alkaline and ionic pretreatments combined with the fungal enzyme hydrolysis of BSG increased xylose release (Paz et al., 2019). Other novel pretreatments, as those using deep eutectic solvents, such as choline chloride–glycerol at 115°C, resulted in a yield of 160 mg glucose g^{-1} of pretreated BSG (Procentese et al., 2018). Biological pretreatments, such as SSF, have also been used. For example, Méndez-Hernández et al. (2019) subjected the corn stover to a biological pretreatment using a thermotolerant fungus, *Fomes* sp., and observed a 60% improvement of sugars released after 7 days in comparison to the untreated corn stover. The SSF followed by the enzymatic hydrolysis of a green macroalgae (*Ulva rigida*) with enzymes produced during the SSF increased the glucose yield by 53% (Fernandes et al., 2019). Outeiriño et al. (2019) reported that an enzymatic cocktail produced during the SSF of *A. brasiliensis* resulted in 44.8% and 21.5% saccharification of glucan and xylan, respectively. Given the promising yields following the application of biological treatments, the fungal pretreatment is an environmental-friendly procedure with great potential and efficiency in recovering reducing sugars by modifying the lignocellulosic structure of diverse agro-industrial by-products.

Growth Performance

Diets for aquaculture fish, particularly those for the carnivorous species, rely on fish meal and agricultural ingredients such as soybean, corn gluten, and wheat. However, to ensure the long-term sustainability and profitability of aquaculture, the use of locally produced ingredients and agro-industrial by-products is of utmost importance (Oliva-Teles et al., 2015). The nutritional value of these alternative ingredients for aquaculture fish is generally low due to the reduced nutrient digestibility and the presence of anti-nutritional factors, such as NSPs (Daniel, 2018), which can impair growth, feed utilization, and fish welfare and health (Gatlin et al., 2007; Xavier et al., 2012).

To counteract the adverse effects of plant-feedstuff NSP, technological strategies have been developed, such as pretreatment of plant feedstuffs and diet supplementation with carbohydrases (Castillo & Gatlin, 2015). The use of carbohydrases to increase the digestibility of plant-based

diets is a promising strategy for aquaculture since fish have limited capacity to utilize dietary carbohydrates (Sinha et al., 2011). In the present study, the crude extract was lyophilized to allow its incorporation in the diets, but other methods of concentration can be considered in a scaled-up process, such as alternative lower power-consuming methods that are already in use at the industrial level. The inclusion of the crude extract linearly increased the feed efficiency and protein efficiency ratio ($R = 0.81$, $p < 0.01$; $R = 0.79$, $p < 0.01$, respectively). These results may be attributed to an increase in dietary carbohydrate availability due to the NSP hydrolysis by the action of the crude extract carbohydrases. Other authors also observed the beneficial effects of dietary supplementation with exogenous carbohydrases on feed utilization in different fish species (Magalhães et al., 2016; Diógenes et al., 2018; Maas et al., 2019). Maas et al. (2019) observed that a plant-based diet supplemented with an enzymatic cocktail of xylanase and phytase improved the growth and feed utilization of Nile tilapia (*Oreochromis niloticus*) after 6 weeks of feeding. Magalhães et al. (2016) observed an increase in feed utilization in white seabream (*Diplodus sargus*) fed with a diet supplemented with commercial nonstarch carbohydrases. Other studies also included enzymes obtained by the SSF in plant feedstuff-rich diets with positive results regarding nutrient utilization and growth performance in Nile tilapia (Novelli et al., 2017; Bowyer et al., 2020) and common carp (Anwar et al., 2020). In addition to the direct action upon the NSPs, dietary carbohydrase supplementation may also reduce digestive viscosity and, concomitantly, favor the access and time of action of the endogenous fish enzymes, increasing feed and protein utilization (revised by Castillo & Gatlin, 2015). For example, in turbot (*Scophthalmus maximus*), dietary supplementation with carbohydrases increased the amylase and lipase activity, whereas the total protease activity was not affected. In hybrid tilapia, dietary carbohydrases supplementation increased amylase but not protease or lipase activities (Li et al., 2009), while in white seabream only amylase activity was increased (Magalhães et al., 2018). Further studies are required to study the effect of dietary supplementation with the crude extract on the endogenous digestive enzymes activity.

The dietary supplementation with the crude extract increased feed efficiency, that is, decreased the amount of feed required per unit of fish produced. In aquaculture production, increasing feed efficiency is the most important feature to increase the production efficiency and economic profit and reduce environmental impacts (Besson et al., 2017) as more than 60% of the total aquaculture costs are associated with feed costs (Troell et al., 2014; Daniel, 2018). In addition, production of feed enzymes from the SSF of agro-industrial materials, such as BSG, also represent a probability towards the reduction of production costs and sustainability of enzyme industry (Lizardi-Jiménez & Hernández-Martínez, 2017) and contributes to the reduction of lignocellulosic biomass disposal in the environment (Sakhuja et al., 2021).

CONCLUSION

A SSF-based biorefining strategy was applied to convert BSG into two distinct products: a protein-enriched fermented BSG with a modified lignocellulosic structure and a functional crude extract with highly active carbohydrases. BSG was fermented with *Aspergillus ibericus* to produce a crude extract to be used to further hydrolyze the fermented BSG or applied as a feed enzyme supplement in aquafeeds.

According to the Box–Behnken response surface methodology, the load of crude extract is a fundamental parameter to maximize the release of reducing sugars from BSG_{EF}, while both the load of BSG_{EF} and β-glucosidase addition are key variables to maximize the release of total phenolics and antioxidant activity.

Potential application of this crude extract in aquafeeds was demonstrated in the European seabass fed with high plant-based diets, where a positive effect was confirmed in terms of feed and protein utilization.

Future work must be carried out to assess the feasibility of including the nutritionally enhanced fermented BSG in diets and test if higher inclusion levels of the crude extract can further improve feed utilization and growth of the European seabass.

DATA AVAILABILITY STATEMENT

The raw data supporting the conclusions of this article will be made available by the authors, without undue reservation.

ETHICS STATEMENT

The animal study was reviewed and approved by the ORBEA Animal Welfare Committee of CIIMAR and Portuguese National Authority for Animal Health (DGAV).

AUTHOR CONTRIBUTIONS

HF carried out the enzymatic hydrolysis of Box–Behnken experimental design, data analysis, and writing of the manuscript. JMS and IB participated in research conceptualization, optimization of solid-state fermentation, obtention of the enzymatic extract, data analysis, and writing. MF and MV carried out chemical analysis. NF and CC performed the growth experiment in European seabass and chemical analysis. AO-T participated in research conceptualization and writing. HP participated in the funding acquisition, research conceptualization, supervision, and writing. All authors discussed the results and contributed to the final manuscript.

FUNDING

This study was supported by the project "SPO3-Development of innovative sustainable protein and omega-3 rich feedstuffs for aquafeeds, from local agro-industrial by-products", reference

POCI-01-0145-FEDER-030377, funded by the European Regional Development Fund (ERDF) and Portuguese Foundation for Science and Technology (FCT) and by the strategic funding of the UIDB/04469/2020 unit. HF and CC were supported by grants SFRH/BD/131219/2017 and SFRH/BPD/114942/2016, respectively, from FCT, MCTES, FSE, and UE under the North Portugal Regional Operational Program (NORTE 2020). José Manuel Salgado was supported by the grant CEB/N2020—INV/01/2016 from Project "BIOTECNORTE—Underpinning Biotechnology to foster the north of Portugal bioeconomy" (NORTE-01-0145-FEDER-000004).

ACKNOWLEDGMENTS

The authors thank *Unicer*, a soft-drink company (Porto, Portugal), for providing the brewer's spent grain used in this study.

REFERENCES

Adiguzel, G., Faiz, O., Sisecioglu, M., Sari, B., Baltaci, O., Akbulut, S., et al. (2019). A Novel Endo-β-1,4-Xylanase from Pediococcus Acidilactici GC25; Purification, Characterization and Application in Clarification of Fruit Juices. *Int. J. Biol. Macromolecules* 129, 571–578. doi:10.1016/j.ijbiomac.2019.02.054

Ajila, C. M., Gassara, F., Brar, S. K., Verma, M., Tyagi, R. D., and Valéro, J. R. (2011). Polyphenolic Antioxidant Mobilization in Apple Pomace by Different Methods of Solid-State Fermentation and Evaluation of its Antioxidant Activity. *Food Bioproc. Technol.* 5 (7), 2697–2707. doi:10.1007/s11947-011-0582-y

Aliyu, S., and Bala, M. (2013). Brewer's Spent Grain: A Review of its Potentials and Applications. *Afr. J. Biotechnol.* 10 (3), 324–331. doi:10.4314/ajb.v10i3

Alonso-Riaño, P., Sanz Diez, M. T., Blanco, B., Beltrán, S., Trigueros, E., and Benito-Román, O. (2020). Water Ultrasound-Assisted Extraction of Polyphenol Compounds from Brewer's Spent Grain: Kinetic Study, Extract Characterization, and Concentration. *Antioxidants* 9 (3), 265–318. doi:10.3390/antiox9030265

Ang, S. K., E.M., S., Y., A., A.A, S., and M.S, M. (2013). Production of Cellulases and Xylanase by Aspergillus Fumigatus SK1 Using Untreated Oil Palm Trunk Through Solid State Fermentation. *Process Biochem.* 48 (9), 1293–1302. doi:10.1016/j.procbio.2013.06.019

Anwar, A., Wan, A. H., Omar, S., El-Haroun, E., and Davies, S. J. (20202019). The Potential of a Solid-State Fermentation Supplement to Augment White Lupin (Lupinus Albus) Meal Incorporation in Diets for Farmed Common Carp (*Cyprinus carpio*). *Aquacult. Rep.* 17, 100348. doi:10.1016/j.aqrep.2020.100348

Astolfi, V., Astolfi, A. L., Mazutti, M. A., Rigo, E., Di Luccio, M., Camargo, A. F., et al. (2019). Cellulolytic Enzyme Production from Agricultural Residues for Biofuel Purpose on Circular Economy Approach. *Bioproc. Biosyst. Eng.* 42 (5), 677–685. doi:10.1007/s00449-019-02072-2

Besson, M., De Boer, I. J. M., Vandeputte, M., Van Arendonk, J. A. M., Quillet, E., Komen, H., et al. (2017). Effect of Production Quotas on Economic and Environmental Values of Growth Rate and Feed Efficiency in Sea Cage Fish Farming. *PLoS ONE* 12 (3), e0173131–15. doi:10.1371/journal.pone.0173131

Birsan, R. I., Wilde, P., Waldron, K. W., and Rai, D. K. (2019). Recovery of Polyphenols from Brewer's Spent Grains. *Antioxidants* 8 (9), 380–392. doi:10.3390/antiox8090380

Bowyer, P. H., El-Haroun, E. R., Salim, H. S., and Davies, S. J. (2020). Benefits of a Commercial Solid-State Fermentation (SSF) Product on Growth Performance, Feed Efficiency and Gut Morphology of Juvenile Nile tilapia (*Oreochromis niloticus*) Fed Different UK Lupin Meal Cultivars. *Aquaculture* 523 (March), 735192. doi:10.1016/j.aquaculture.2020.735192

Canedo, M. S., de Paula, F. G., da Silva, F. A., and Vendruscolo, F. (2016). Protein Enrichment of Brewery Spent Grain from Rhizopus Oligosporus by Solid-State Fermentation. *Bioproc. Biosyst. Eng.* 39 (7), 1105–1113. doi:10.1007/s00449-016-1587-8

Castillo, S., and Gatlin, D. M. (2015). Dietary Supplementation of Exogenous Carbohydrase Enzymes in Fish Nutrition: A Review. *Aquaculture* 435 (January 2015), 286–292. doi:10.1016/j.aquaculture.2014.10.011

Chen, Z., Liu, Y., Zaky, A. A., Liu, L., Chen, Y., Li, S., et al. (2019). Characterization of a Novel Xylanase from Aspergillus flavus with the Unique Properties in Production of Xylooligosaccharides. *J. Basic Microbiol.* 59 (4), 351–358. doi:10.1002/jobm.201800545

Crowley, D., O'Callaghan, Y., McCarthy, A. L., Connolly, A., Fitzgerald, R. J., and O'Brien, N. M. (2017). Aqueous and Enzyme-Extracted Phenolic Compounds from Brewers' Spent Grain (BSG): Assessment of Their Antioxidant Potential. *J. Food Biochem.* 41 (3), e12370–11. doi:10.1111/jfbc.12370

Daniel, N. (2018). A Review on Replacing Fish Meal in Aqua Feeds Using Plant Protein Sources. *Int. J. Fish. Aquat. Stud.* 6 (2), 164–179.

Dawood, M. A. O., and Koshio, S. (2019). Application of Fermentation Strategy in Aquafeed for Sustainable Aquaculture. *Rev. Aquacult.* 12, 987–1002. doi:10.1111/raq.12368

Delabona, P. d. S., Pirota, R. D. P. B., Codima, C. A., Tremacoldi, C. R., Rodrigues, A., and Farinas, C. S. (2013). Effect of Initial Moisture Content on Two Amazon Rainforest Aspergillus Strains Cultivated on Agro-Industrial Residues: Biomass-Degrading Enzymes Production and Characterization. *Ind. Crops Prod.* 42 (1), 236–242. doi:10.1016/j.indcrop.2012.05.035

Diógenes, A. F., Castro, C., Carvalho, M., Magalhães, R., Estevão-Rodrigues, T. T., Serra, C. R., et al. (2018). Exogenous Enzymes Supplementation Enhances Diet Digestibility and Digestive Function and Affects Intestinal Microbiota of Turbot (*Scophthalmus maximus*) Juveniles Fed Distillers' Dried Grains with Solubles (DDGS) Based Diets. *Aquaculture* 486 (December 2017), 42–50. doi:10.1016/j.aquaculture.2017.12.013

Dudek, M., Świechowski, K., Manczarski, P., Koziel, J. A., and Białowiec, A. (2019). The Effect of Biochar Addition on the Biogas Production Kinetics from the Anaerobic Digestion of Brewers' Spent Grain. *Energies* 12 (8), 1518–1522. doi:10.3390/en12081518

Dulf, F. V., Vodnar, D. C., and Socaciu, C. (2016). Effects of Solid-State Fermentation with Two Filamentous Fungi on the Total Phenolic Contents, Flavonoids, Antioxidant Activities and Lipid Fractions of Plum Fruit (Prunus Domestica L.) By-Products. *Food Chem.* 209, 27–36. doi:10.1016/j.foodchem.2016.04.016

Ezeilo, U. R., Wahab, R. A., and Mahat, N. A. (2020). Optimization Studies on Cellulase and Xylanase Production by Rhizopus Oryzae UC2 Using Raw Oil Palm Frond Leaves as Substrate Under Solid State Fermentation. *Renew. Energ.* 156, 1301–1312. doi:10.1016/j.renene.2019.11.149

Farcas, A. C., Socaci, S. A., Mudura, E., Dulf, F. V., Vodnar, D. C., Tofana, M., et al. (2017). Exploitation of Brewing Industry Wastes to Produce Functional Ingredients. *Brewing Technol.* 2, 64. doi:10.5772/32009

Fernandes, H., Salgado, J. M., Martins, N., Peres, H., Oliva-Teles, A., and Belo, I. (2019). Sequential Bioprocessing of Ulva Rigida to Produce Lignocellulolytic Enzymes and to Improve its Nutritional Value as Aquaculture Feed. *Bioresour. Technol.* 281, 277–285. doi:10.1016/j.biortech.2019.02.068

Ferreira, J. A., Mahboubi, A., Lennartsson, P. R., and Taherzadeh, M. J. (2016). Waste Biorefineries Using Filamentous Ascomycetes Fungi: Present Status and Future Prospects. *Bioresour. Technol.* 215, 334–345. doi:10.1016/j.biortech.2016.03.018

Gatlin, D. M., Barrows, F. T., Brown, P., Dabrowski, K., Gaylord, T. G., Hardy, R. W., et al. (2007). Expanding the Utilization of Sustainable Plant Products in Aquafeeds: A Review. *Aquaculture Res.* 38 (6), 551–579. doi:10.1111/j.1365-2109.2007.01704.x

Getu, K., Getachew, A., Berhan, T., and Getnet, A. (2020). Supplementary Value of Ensiled Brewers Spent Grain Used as Replacement to Cotton Seed Cake in the Concentrate Diet of Lactating Crossbred Dairy Cows. *Trop. Anim. Health Prod.* 52, 3675–3683. doi:10.1007/s11250-020-02404-5

Gowthaman, M. K., Krishna, C., and Moo-Young, M. (2001). Fungal Solid State Fermentation - An Overview. *Appl. Mycol. Biotechnol.* 1 (C), 305–352. doi:10.1016/S1874-5334(01)80014-9

Hakobyan, L., Gabrielyan, L., Blbulyan, S., and Trchounian, A. (2021). The Prospects of Brewery Waste Application in Biohydrogen Production by Photofermentation of Rhodobacter Sphaeroides. *Int. J. Hydrogen. Energ.* 46, 289–296. doi:10.1016/j.ijhydene.2020.09.184

Jahromi, M. F., Liang, J. B., Rosfarizan, M., Goh, Y. M., Shokryazdan, P., and Ho, Y. W. (2011). Efficiency of Rice Straw Lignocelluloses Degradability by Aspergillus Terreus ATCC 74135 in Solid State Fermentation. *Afr. J. Biotechnol.* 10 (21), 4428–4435. doi:10.5897/AJB10.2246

Lakhundi, S., Siddiqui, R., and Khan, N. A. (2015). Cellulose Degradation: A Therapeutic Strategy in the Improved Treatment of Acanthamoeba Infections. *Parasites Vectors* 8 (1), 1–16. doi:10.1186/s13071-015-0642-7

Leite, P., Salgado, J. M., Venâncio, A., Domínguez, J. M., and Belo, I. (2016). Ultrasounds Pretreatment of Olive Pomace to Improve Xylanase and Cellulase Production by Solid-State Fermentation. *Bioresour. Technol.* 214, 737–746. doi:10.1016/j.biortech.2016.05.028

Leite, P., Silva, C., Salgado, J. M., and Belo, I. (2019). Simultaneous Production of Lignocellulolytic Enzymes and Extraction of Antioxidant Compounds by Solid-State Fermentation of Agro-Industrial Wastes. *Ind. Crops Prod.* 137 (May), 315–322. doi:10.1016/j.indcrop.2019.04.044

Li, J. S., Li, J. L., and Wu, T. T. (2009). Effects of Non-Starch Polysaccharides Enzyme, Phytase and Citric Acid on Activities of Endogenous Digestive Enzymes of tilapia (*Oreochromis niloticus* × *Oreochromis aureus*). *Aquacult. Nutr.* 15 (4), 415–420. doi:10.1111/j.1365-2095.2008.00606.x

Liguori, R., Pennacchio, A., Vandenberghe, L. P. d. S., De Chiaro, A., Birolo, L., Soccol, C. R., et al. (2021). Screening of Fungal Strains for Cellulolytic and Xylanolytic Activities Production and Evaluation of Brewers' Spent Grain as Substrate for Enzyme Production by Selected Fungi. *Energies* 14 (15), 4443. doi:10.3390/en14154443

Lizardi-Jiménez, M. A., and Hernández-Martínez, R. (2017). Solid State Fermentation (SSF): Diversity of Applications to Valorize Waste and Biomass. *3 Biotech.* 7 (1). doi:10.1007/s13205-017-0692-y

Llimós, J., Martínez-Avila, O., Marti, E., Corchado-Lopo, C., Llenas, L., and Gea, T. (2020). Brewer's Spent Grain Biotransformation to Produce Lignocellulolytic Enzymes and Polyhydroxyalkanoates in a Two-Stage Valorization Scheme. *Biomass Convers. Biorefinery.* doi:10.1007/s13399-020-00918-4

Maas, R. M., Verdegem, M. C. J., and Schrama, J. W. (2019). Effect of Non-Starch Polysaccharide Composition and Enzyme Supplementation on Growth Performance and Nutrient Digestibility in Nile tilapia (*Oreochromis niloticus*). *Aquacult Nutr.* 25 (3), 622–632. doi:10.1111/anu.12884

Magalhães, R., Díaz-Rosales, P., Diógenes, A. F., Enes, P., Oliva-Teles, A., and Peres, H. (2018). Improved Digestibility of Plant Ingredient-Based Diets for European Seabass (*Dicentrarchus labrax*) with Exogenous Enzyme Supplementation. *Aquacult Nutr.* 24 (4), 1287–1295. doi:10.1111/anu.12666

Magalhães, R., Lopes, T., Martins, N., Díaz-Rosales, P., Couto, A., Pousão-Ferreira, P., et al. (2016). Carbohydrases Supplementation Increased Nutrient Utilization in White Seabream (*Diplodus sargus*) Juveniles Fed High Soybean Meal Diets. *Aquaculture* 463 (May 2016), 43–50. doi:10.1016/j.aquaculture.2016.05.019

Manishaand Yadav, S. K. (2017). Technological Advances and Applications of Hydrolytic Enzymes for Valorization of Lignocellulosic Biomass. *Bioresour. Technol.* 245, 1727–1739. doi:10.1016/j.biortech.2017.05.066

Martins, S., Mussatto, S. I., Martínez-Avila, G., Montañez-Saenz, J., Aguilar, C. N., and Teixeira, J. A. (2011). Bioactive Phenolic Compounds: Production and Extraction by Solid-State Fermentation. A Review. *Biotechnol. Adv.* 29 (3), 365–373. doi:10.1016/j.biotechadv.2011.01.008

Méndez-Hernández, J. E., Loera, O., Méndez-Hernández, E. M., Herrera, E., Arce-Cervantes, O., and Soto-Cruz, N. Ó. (2019). Fungal Pretreatment of Corn Stover by Fomes Sp. EUM1: Simultaneous Production of Readily Hydrolysable Biomass and Useful Biocatalysts. *Waste Biomass Valor.* 10 (9), 2637–2650. doi:10.1007/s12649-018-0290-1

Miller, G. L. (1959). Use of Dinitrosalicylic Acid Reagent for Determination of Reducing Sugar. *Anal. Chem.* 31, 426–428. doi:10.1021/ac60147a030

Mussatto, S. I. (2014). Brewer's Spent Grain: A Valuable Feedstock for Industrial Applications. *J. Sci. Food Agric.* 94 (7), 1264–1275. doi:10.1002/jsfa.6486

Nahid, P., Vossoughi, M., Roostaazad, R., Ahmadi, M., Zarrabi, A., and Hosseini, S. M. (2012). Production of Glucoamylase by Aspergillus niger Under Solid State Fermentation. *Ije* 25 (1), 1–7. doi:10.5829/idosi.ije.2012.25.01b.01

Nargotra, P., Sharma, V., Gupta, M., Kour, S., and Bajaj, B. K. (2018). Application of Ionic Liquid and Alkali Pretreatment for Enhancing Saccharification of Sunflower Stalk Biomass for Potential Biofuel-Ethanol Production. *Bioresour. Technol.* 267 (May), 560–568. doi:10.1016/j.biortech.2018.07.070

Narra, M., Dixit, G., Divecha, J., Kumar, K., Madamwar, D., and Shah, A. R. (2014). Production, Purification and Characterization of a Novel GH 12 Family Endoglucanase from Aspergillus Terreus and its Application in Enzymatic Degradation of Delignified Rice Straw. *Int. Biodeterioration Biodegradation* 88, 150–161. doi:10.1016/j.ibiod.2013.12.016

Nocente, F., Taddei, F., Galassi, E., and Gazza, L. (2019). Upcycling of Brewers' Spent Grain by Production of Dry Pasta with Higher Nutritional Potential. *Lwt* 114 (April), 108421. doi:10.1016/j.lwt.2019.108421

Novelli, P. K., Barros, M. M., Pezzato, L. E., de Araujo, E. P., de Mattos Botelho, R., and Fleuri, L. F. (2017). Enzymes Produced by Agro-Industrial Co-Products Enhance Digestible Values for Nile tilapia (*Oreochromis niloticus*): A Significant Animal Feeding Alternative. *Aquaculture* 481 (August), 1–7. doi:10.1016/j.aquaculture.2017.08.010

Oliva-Teles, A., Enes, P., and Peres, H. (2015). Replacing Fishmeal and Fish Oil in Industrial Aquafeeds for Carnivorous Fish. *Feed Feeding Practices Aquacult.*, 203–233. doi:10.1016/b978-0-08-100506-4.00008-8

Opazo, R., Ortúzar, F., Navarrete, P., Espejo, R., and Romero, J. (2012). Reduction of Soybean Meal Non-Starch Polysaccharides and α-Galactosides by Solid-State Fermentation Using Cellulolytic Bacteria Obtained from Different Environments. *PLoS ONE* 7 (9), e44783. doi:10.1371/journal.pone.0044783

Outeiriño, D., Costa-Trigo, I., Pinheiro de Souza Oliveira, R., Pérez Guerra, N., and Domínguez, J. M. (2019). A Novel Approach to the Biorefinery of Brewery Spent Grain. *Process Biochem.* 85 (June), 135–142. doi:10.1016/j.procbio.2019.06.007

Patel, A. K., Singhania, R. R., Sim, S. J., and Pandey, A. (2019). Thermostable Cellulases: Current Status and Perspectives. *Bioresour. Technol.* 279, 385–392. doi:10.1016/j.biortech.2019.01.049

Paz, A., Outeiriño, D., Pérez Guerra, N., and Domínguez, J. M. (2019). Enzymatic Hydrolysis of Brewer's Spent Grain to Obtain Fermentable Sugars. *Bioresour. Technol.* 275 (December 2018), 402–409. doi:10.1016/j.biortech.2018.12.082

Pitol, L. O., Finkler, A. T. J., Dias, G. S., Machado, A. S., Zanin, G. M., Mitchell, D. A., et al. (2017). Optimization Studies to Develop a Low-Cost Medium for Production of the Lipases of Rhizopus Microsporus by Solid-State Fermentation and Scale-Up of the Process to a Pilot Packed-Bed Bioreactor. *Process Biochem.* 62 (July), 37–47. doi:10.1016/j.procbio.2017.07.019

Procentese, A., Raganati, F., Olivieri, G., Russo, M. E., Rehmann, L., and Marzocchella, A. (2018). Deep Eutectic Solvents Pretreatment of Agro-Industrial Food Waste. *Biotechnol. Biofuels* 11 (1), 1–12. doi:10.1186/s13068-018-1034-y

Rayhane, H., Josiane, M., Gregoria, M., Yiannis, K., Nathalie, D., Ahmed, M., et al. (2019). From Flasks to Single Used Bioreactor: Scale-Up of Solid State Fermentation Process for Metabolites and Conidia Production by Trichoderma Asperellum. *J. Environ. Manage.* 252 (October 2019), 109496. doi:10.1016/j.jenvman.2019.109496

Rojas-Chamorro, J. A., Romero, I., López-Linares, J. C., and Castro, E. (2020). Brewer's Spent Grain as a Source of Renewable Fuel Through Optimized Dilute Acid Pretreatment. *Renew. Energ.* 148, 81–90. doi:10.1016/j.renene.2019.12.030

Roy, S., Dutta, T., Sarkar, T. S., and Ghosh, S. (2013). Novel Xylanases from Simplicillium Obclavatum MTCC 9604: Comparative Analysis of Production, Purification and Characterization of Enzyme from Submerged and Solid State Fermentation. *SpringerPlus* 2 (1), 1–10. doi:10.1186/2193-1801-2-382

Ruviaro, A. R., Barbosa, P. d. P. M., and Macedo, G. A. (2019). Enzyme-Assisted Biotransformation Increases Hesperetin Content in Citrus Juice By-Products. *Food Res. Int.* 124 (December 2017), 213–221. doi:10.1016/j.foodres.2018.05.004

Sakhuja, D., Ghai, H., Rathour, R. K., Kumar, P., Bhatt, A. K., and Bhatia, R. K. (2021). Cost-Effective Production of Biocatalysts Using Inexpensive Plant Biomass: A Review. *3 Biotech.* 11 (6). doi:10.1007/s13205-021-02847-z

San Martin, D., Orive, M., Iñarra, B., Castelo, J., Estévez, A., Nazzaro, J., et al. (2020). Brewers' Spent Yeast and Grain Protein Hydrolysates as Second-Generation

Feedstuff for Aquaculture Feed. *Waste Biomass Valor.* 11 (10), 5307–5320. doi:10.1007/s12649-020-01145-8

Serra, R., Cabanes, F. J., Perrone, G., Castella, G., Venancio, A., Mule, G., et al. (2006). Aspergillus ibericus: A New Species of Section Nigri Isolated from Grapes. *Mycologia* 98 (2), 295–306. doi:10.3852/mycologia.98.2.295

Sinha, A. K., Kumar, V., Makkar, H. P. S., De Boeck, G., and Becker, K. (2011). Non-Atarch Polysaccharides and Their Role in Fish Nutrition - A Review. *Food Chem.* 127 (4), 1409–1426. doi:10.1016/j.foodchem.2011.02.042

Socaci, S. A., Fărcaş, A. C., Diaconeasa, Z. M., Vodnar, D. C., Rusu, B., and Tofană, M. (2018). Influence of the Extraction Solvent on Phenolic Content, Antioxidant, Antimicrobial and Antimutagenic Activities of Brewers' Spent Grain. *J. Cereal Sci.* 80, 180–187. doi:10.1016/j.jcs.2018.03.006

Sousa, D., Venâncio, A., Belo, I., and Salgado, J. M. (2018). Mediterranean Agro-Industrial Wastes as Valuable Substrates for Lignocellulolytic Enzymes and Protein Production by Solid-State Fermentation. *J. Sci. Food Agric.* 98 (14), 5248–5256. doi:10.1002/jsfa.9063

Troell, M., Naylor, R. L., Metian, M., Beveridge, M., Tyedmers, P. H., Folke, C., et al. (2014). Does Aquaculture Add Resilience to the Global Food System? *Proc. Natl. Acad. Sci. U.S.A.* 111 (37), 13257–13263. doi:10.1073/pnas.1404067111

Vasconcellos, V. M., Tardioli, P. W., Giordano, R. L. C., and Farinas, C. S. (2015). Production Efficiency versus Thermostability of (Hemi)cellulolytic Enzymatic Cocktails from Different Cultivation Systems. *Process Biochem.* 50 (11), 1701–1709. doi:10.1016/j.procbio.2015.07.011

Webb, C. (2017). Design Aspects of Solid State Fermentation as Applied to Microbial Bioprocessing. *Jabb* 4 (1). doi:10.15406/jabb.2017.04.00094

Xavier, B., Sahu, N. P., Pal, A. K., Jain, K. K., Misra, S., Dalvi, R. S., et al. (2012). Water Soaking and Exogenous Enzyme Treatment of Plant-Based Diets: Effect on Growth Performance, Whole-Body Composition, and Digestive Enzyme Activities of Rohu, Labeo Rohita (Hamilton), Fingerlings. *Fish. Physiol. Biochem.* 38 (2), 341–353. doi:10.1007/s10695-011-9511-2

Conflict of Interest: The authors declare that the research was conducted in the absence of any commercial or financial relationships that could be construed as a potential conflict of interest.

Publisher's Note: All claims expressed in this article are solely those of the authors and do not necessarily represent those of their affiliated organizations, or those of the publisher, the editors, and the reviewers. Any product that may be evaluated in this article, or claim that may be made by its manufacturer, is not guaranteed or endorsed by the publisher.

frontiers | Frontiers in Bioengineering and Biotechnology

REVIEW
published: 16 May 2022
doi: 10.3389/fbioe.2022.864787

Production of Gluconic Acid and Its Derivatives by Microbial Fermentation: Process Improvement Based on Integrated Routes

Yan Ma[1†], *Bing Li*[1†], *Xinyue Zhang*[1], *Chao Wang*[2*] *and Wei Chen*[1*]

[1]School of Marine Science and Engineering, Qingdao Agricultural University, Qingdao, China, [2]Dongcheng District Center for Disease Control and Prevention, Beijing, China

Gluconic acid (GA) and its derivatives, as multifunctional biological chassis compounds, have been widely used in the food, medicine, textile, beverage and construction industries. For the past few decades, the favored production means of GA and its derivatives are microbial fermentation using various carbon sources containing glucose hydrolysates due to high-yield GA production and mature fermentation processes. Advancements in improving fermentation process are thriving which enable more efficient and economical industrial fermentation to produce GA and its derivatives, such as the replacement of carbon sources with agro-industrial byproducts and integrated routes involving genetically modified strains, cascade hydrolysis or micro- and nanofiltration in a membrane unit. These efforts pave the way for cheaper industrial fermentation process of GA and its derivatives, which would expand the application and widen the market of them. This review summarizes the recent advances, points out the existing challenges and provides an outlook on future development regarding the production of GA and its derivatives by microbial fermentation, aiming to promote the combination of innovative production of GA and its derivatives with industrial fermentation in practice.

Keywords: gluconic acid, microbial fermentation, synthetic pathway, regulatory mechanisms, agro-industrial byproducts, integrated routes

OPEN ACCESS

Edited by:
Shangyong Li,
Qingdao University, China

Reviewed by:
Yinjun Zhang,
Zhejiang University of Technology, China
Wenjun Han,
Shandong University, China

***Correspondence:**
Chao Wang
ccwcceo@163.com
Wei Chen
chenwei@qau.edu.cn

[†]These authors have contributed equally to this work

Specialty section:
This article was submitted to Bioprocess Engineering, a section of the journal Frontiers in Bioengineering and Biotechnology

Received: *28 January 2022*
Accepted: *14 April 2022*
Published: *16 May 2022*

Citation:
Ma Y, Li B, Zhang X, Wang C and Chen W (2022) Production of Gluconic Acid and Its Derivatives by Microbial Fermentation: Process Improvement Based on Integrated Routes. Front. Bioeng. Biotechnol. 10:864787. doi: 10.3389/fbioe.2022.864787

1 INTRODUCTION

Gluconic acid (GA, $C_6H_{12}O_7$, 2,3,4,5,6-pentahydroxyhexanoic acid), a bio-based additive, has been widely used in the food, medicine, textile and construction industries. GA is an aldonic acid derived from ß-D-glucose via a site-specific oxidation, in which the aldehyde group (-CHO) at C-1 is oxidized electrochemically or catalytically into a carboxyl group (-COOH). It is readily soluble in water with pK_a of 3.70 at 25°C. GA can convert into the forms of its gluconolactones (D-1,5-gluconolactone and D-1,4-gluconolactone) and gluconates in an aqueous solution where they are in equilibrium with each other (**Figure 1**). For example, the commercial GA aqueous solution (50%) contains about 5% of its lactones at room temperature (Lim and Dolzhenko, 2021). Under certain conditions, GA is prone to be oxidized to keto-D-gluconic acid (Hustede et al., 2012). Currently, the annual worldwide market of GA is between US$ 50 million and US$ 80 million, and its industrial consumption will probably exceed 1.2×10^5 tonnes by 2024 (Ahuja and Singh, 2018). In addition, GA and its derivatives are designated as "generally recognized as safe" (GRAS) by the U.S. Food and Drug

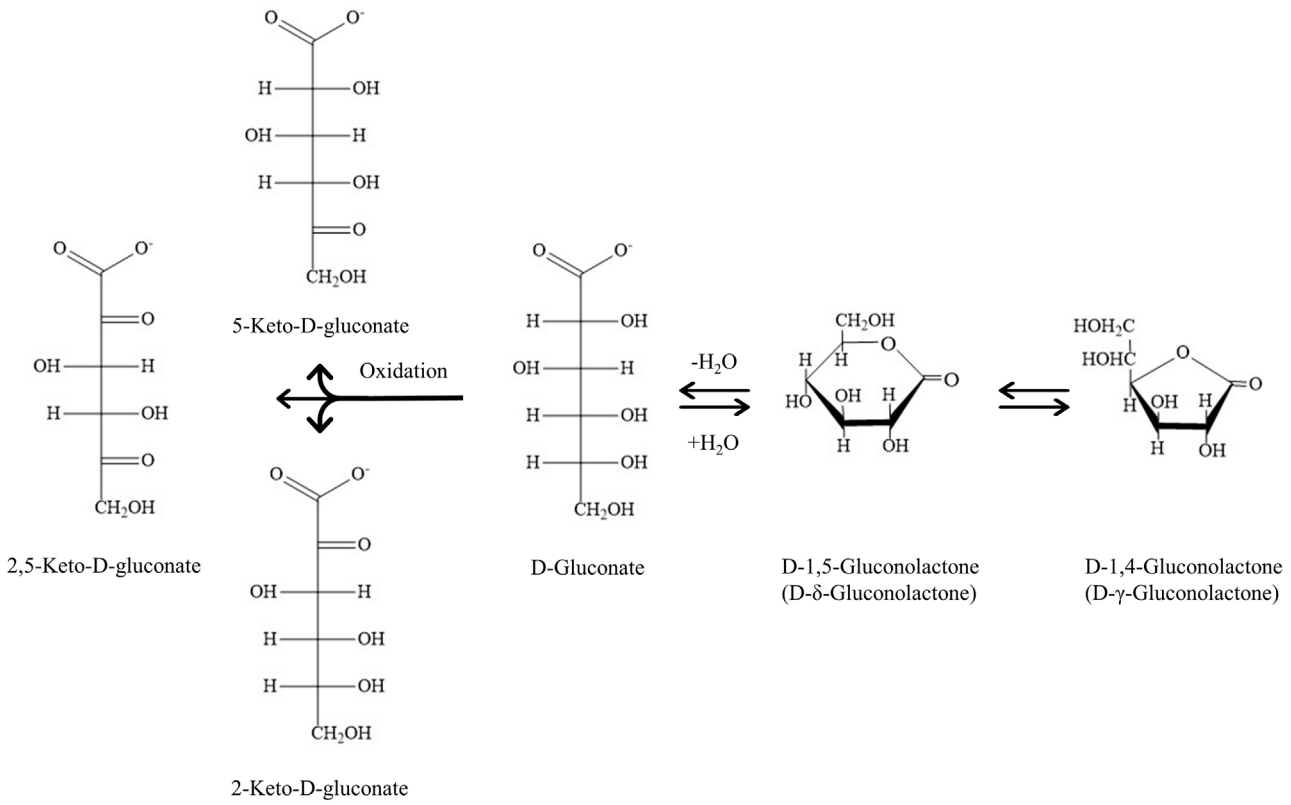

FIGURE 1 | Gluconic acid (GA) and its derivatives. Chemical equilibrium of GA and its lactones and GA transformation to keto-gluconates by a strong oxidant in aqueous solution.

Administration (US FDA), the European Parliament and the Council Directive No. 95/2/EC and World Health Organization (WHO) (Pal et al., 2016).

Over the past 50 years, GA and its derivatives have been applied globally with different shares in the construction (45%), food (35%), medicine (10%) and other (10%) industries (Kohtaro and Isato, 2019). Several features of GA and its derivatives made them very attractive in commercial applications. GA is a versatile organic acid, which is noncorrosive, mildly acidic, less irritating, odorless, nontoxic, and easily degradable. Thus, as a food additive under the laws of some countries, GA and its derivatives are commonly added to dairy products, beverages and bakery to maintain flavor and prevent precipitation. For instance, taking advantage of the chelating ability of GA, Choi and Zhong added it to skim milk powder to reduce the turbidity of dispersions (Choi and Zhong, 2020).

This chelating ptoperty of GA also enable its numerous applications in the chemical fields. On one hand, GA can serve as a green solvent for metal extraction/coordination and organic synthesis. For example, GA is capable of recovering lithium and cobalt from related wasted materials (Roshanfar et al., 2018). On the other hand, it is a mild and eco-friendly metal cleaning agent for dishwashing, laundry, and water conditioning.

In the medicine industry, some divalent metal salts (Ca^{2+}, Mg^{2+}, Fe^{2+} and Zn^{2+}) of GA can act as mineral nutrients to treat elemental deficiencies (such as osteoporosis and anemia) of humans and animals. Recent studies have shown that 1.25 mmol/L calcium gluconate (equivalent to the concentration of free calcium ions in mammalian blood) can disrupt the drug-resistant *Staphylococcus aureus* biofilm by hindering the formation of extracellular polymeric substance (EPS) matrix (Liu et al., 2021). Mycielska et al. proposed that gluconate can inhibit tumor growth and alter metabolic characteristics of tumor tissue via blocking citrate uptake (Mycielska et al., 2019). Moreover, GA and its derivatives can be overoxidized to synthesize keto-GA, glucuronic acid and glucaric acid, which are raw materials to produce some short-chain organic acids, such as formic acid, ascorbic acid, tartaric acid and xylonic (Stottmeister et al., 2005; De Muynck et al., 2007; Jin et al., 2016).

Chemical approaches and biological fermentation are mainly selected to produce GA in modern times. Although the one-step conversion to synthesize GA by chemical and electrolytic oxidation is efficient, the expensive electrolysis cost, environmental toxicity and biological hazards limit the industrial application of chemical approaches (Pal et al., 2016). With biological fermentation dominating industrial-scale production, industrial fermentation advances rapidly,

TABLE 1 | Gluconate-producing fungi and bacteria with application value in the last decades.

Gluconate-producing fungi	References	Gluconate-producing bacteria	References
Aspergillus niger	Ajala et al., 2017 Chuppa-Tostain et al., 2018 Ahmed et al. (2015)	*Acetobacter diazotrophicus*	Pal et al. (2016)
Aspergillus carneus	Lim and Dolzhenko, (2021)	*Acetobacter methanolicus*	Pal et al. (2016)
Aspergillus terreus	Ahmad Anas et al. (2012)	*Gluconobacter oxydans*	Pal et al., 2017 Hou et al., 2018 Yao et al., 2017 Zhou and Xu, 2019 Jiang et al. (2016)
Aureobasidium pullulans	Anastassiadis and Rehm, 2006a Anastassiadis and Rehm, 2006b Anastassiadis et al., 2003 Ma et al. (2018)	*Gluconobacter japonicus*	Cañete-Rodríguez et al. (2016)
Penicillium variabile	Crognale et al. (2008)	*Pseudomonas taetrolens*	Alonso et al. (2015)
Penicillium puberulum	Ahmed et al. (2015)	*Zymomonas mobilis*	Ferraz et al. (2001)
Penicillium frequentans	Ahmed et al. (2015)	*Azospirillum brasiliensis*	Rodriguez et al. (2004)
Penicillium chrysogenum	Ramachandran et al. (2006)	*Klebsiella pneumoniae*	Wang et al. (2016)
Penicillium glaucum	Ramachandran et al. (2006)	*Pseudomonas plecoglossicida*	Wang et al., 2018
Penicillium notatum	Ramachandran et al. (2006)	*Pseudomonas ovalis*	Pal et al. (2016)
Penicillium oxalicum	Han et al. (2018)	*Pseudomonas acidovorans*	Ramachandran et al. (2017)
Saccharomyces cerevisiae	Kapat et al. (2001)	*Pseudomonas fluorescens*	Sun et al. (2015)
		Rhodotorula rubra	Ramachandran et al. (2017)

making previous *Penicillium* spp. fermentation (Herrick and May 1928) replaced by the filamentous fungi fermentation and *Acetobacter* spp. submerged fermentation with a higher efficiency and specificity (Anastassiadis and Morgunov, 2007). **Table 1** lists the reported microorganisms with application value for GA production in the last decades. The significant advantages of producing GA by fermentation stem from the use of various biomass materials as substrates and mature fermentation processes. In addition, GA can also be produced using immobilized enzymes (Singh et al., 2003; Singh, 2008) and immobilized cells (Blandino et al., 2001; Zhao et al., 2014) in fermentation. Nowadays, the cutting-edge research in the fermentation of GA focuses on the integrated routes, which mixes the use of agro-industrial byproducts, genetically engineered enzymes and more efficient bioreactor with purification systems.

For the past few decades, microbial fermentation routes have covered almost all production of GA and its derivatives with considerable progress. The properties, applications and sources of GA, as well as the typical microorganisms, fermentation methods and downstream processing during the fermentation are well summed up in a series of reviews (Anastassiadis and Morgunov, 2007; Singh and Kumar, 2007; Cañete-Rodríguez et al., 2016; Pal et al., 2016; Ramachandran et al., 2017). In this review, we first introduced the latest advancements in the fermentation of GA and its derivatives and focused on their regulatory mechanisms in fungi and bacteria. Then, the defects of these processes were discussed as well. Finally, we summarized the recent developments of cheap agro-industrial byproducts as carbon sources and the innovative integrated routes in the fermentation of GA and its derivatives.

2 PRODUCTION OF GLUCONIC ACID AND ITS DERIVATIVES BY FERMENTATION

In the global industrial fermentation market, organic acids fall into the third largest category of products, only next to antibiotics and amino acids. GA and its derivatives account for a large share in the organic acid market owing to their wide application (Anastassiadis and Morgunov, 2007). At present, the most commonly used strains in microbial fermentation to produce GA are *Aspergillus* spp. and *Gluconobacter* spp. Within these microbial factories, the industrial fermentation processes for GA production have been developed specifically for *Aspergillus niger and Gluconobacter oxydans*. Therefore, the GA synthesis mechanism and fermentation process of *A. niger* and *G. oxydans* are the most thoroughly studied.

2.1 Production Status and Recent Progress of Gluconic Acid and Its Derivatives

2.1.1 Fungal Fermentation: *A. niger* as an Example

A. niger is an ideal candidate for fermentation due to its robust growth, high yield and easy separation of GA products (Bankar et al., 2009). Currently, producing GA by industrial fermentation is mostly based on the specific fermentation process of *A. niger* which was patented by Blom in 1952 (Blom et al., 1952) and improved by Ziffer et al., in 1971 (Ziffer et al., 1971). In *A. niger,* glucose oxidase (GOD, EC 1.1.3.4) is the responsible enzyme for the catalytic oxidation of glucose to GA. GOD is a flavoprotein mainly present in cell walls and extracellular fluid, whose activity accounts for approximately 80% of the total enzymatic activity, as proved in both *Aspergillus* sp. and *Penicillium* sp. (Johnstone-Robertson et al., 2008; Bankar et al., 2009). The GOD-catalyzed oxidation reaction is an aerobic fermentation process with

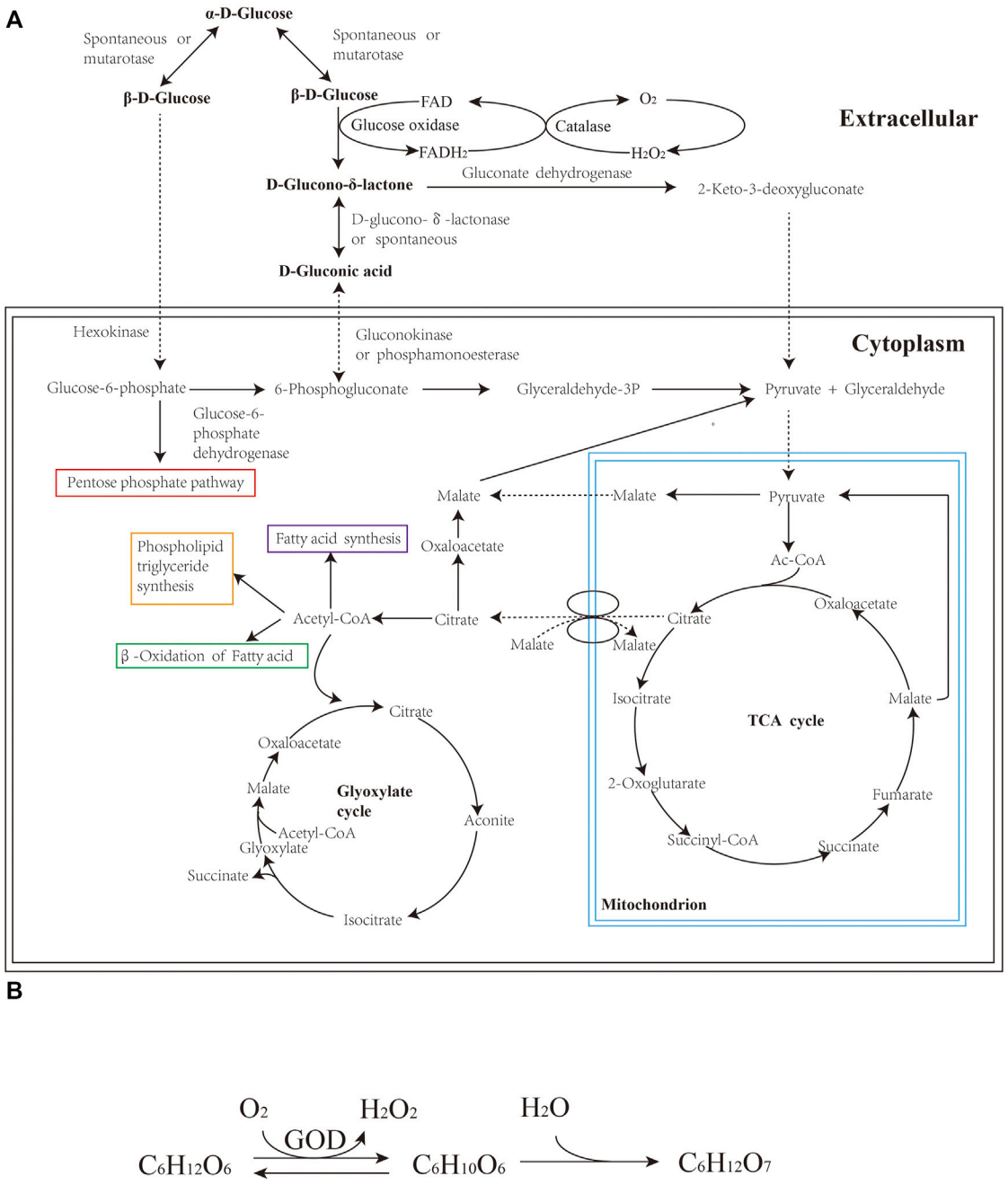

FIGURE 2 | (A) Pathway of GA from glucose in fungi; **(B)** Overall reaction mechanism of GA in fungi.

extremely high oxygen consumption. **Figure 2A** depicts the biochemical metabolism of GA production derived from *A. niger* involving the overall oxidation process. D-Glucose is converted into D-glucono-δ-lactone by a dehydrogenation reaction, during which H_2O_2 is generated as a byproduct. H_2O_2 is then decomposed into O_2 and H_2O in the presence of catalase. **Figure 2B** shows the overall reaction process from D-glucose to GA in fungi. D-glucono-δ-lactone undergoes spontaneous hydrolysis under neutral or alkaline conditions. As the reaction proceeds, the accumulation of GA makes the medium acidic, after which lactones are hydrolyzed by lactonase. Subsequently, GA penetrates cell walls and is then metabolized through the pentose phosphate pathway.

Submerged fermentation is commonly adopted in *A. niger* fermentation on an industrial scale. Sodium gluconate production accounts for more than 80% of the total production of GA derivatives in the globe (Roehr et al., 2001). Thus, sodium gluconate production by submerged fermentation

of *A. niger* with glucose syrups (70 °Brix strength) is taken as an example here. Noteworthily, the seed medium for *A. niger* inoculation requires a low C/N ratio, while the fermentation medium needs a high C/N ratio in practice. For inoculum development, 10^6 conidia cm^{-3} are inoculated into vegetative seed media to obtain pellet-like mycelia after incubation at 30°C for 15–24 h. Then the seed density of 20–50 pellets cm^{-3} of is selected for subsequent fermentation (Moresi and Parente., 2014). However, Lu et al. reported that the optimum seed morphology for GA biosynthesis was a dispersed pattern rather than pellets. The highest overall yield of 1.051 ± 0.012 g/g was achieved and the average GA production rate (21.0 ± 0.9 g/L/h) in the dispersed pattern was 39.1% higher than that in the case of small pellets (Lu et al., 2015).

During the fermentation process, a large amount of glucose (120–350 g/L) and nitrogen and phosphorus source at a low concentration (20 mM) should be contained in the fermentation medium, of which pH is kept at 4.5–6.5 by a neutralizer NaOH and the air flow should be maintained high (Cañete-Rodríguez et al., 2016). All fermentation factors are monitored under continuous automatic control, including ventilatory capacity, dissolved oxygen (DO), pressure, temperature, pH and foam level. The mycelia can be reused up to 5 times with the intermittent addition of glucose throughout the fed-batch cultivation. The conversion rate of glucose is quite high (about 9–15 g/L/h) with a yield of 0.97–1 g/g at pH of 6.0–6.5 around 34°C (Ramachandran et al., 2017). At present, batch fermentation is equipped with sensors to online monitor and control physicochemical parameters. On this basis, a calculated automatic feedback strategy was applied successfully in cell-recycle continuous fermentation with *A. niger*, which significantly increased the conversion rate of glucose (31.05 ± 0.29 g/L/h) with a yield of 0.984 ± 0.067 mol/mol (Lu et al., 2016a; Lu et al., 2016b).

The downstream purification of sodium gluconate from the fermentation medium relies on electrodialysis, anion/cation exchange and membrane separation. The mycelia are separated by using aseptic centrifugation or vacuum filtration from the cultivation fluid. Then the clarified cultivation fluid undergoes a series of steps such as filtration, precipitation, decolorization, neutralization, evaporation and crystallization to obtain sodium gluconate (98%) in the technical grade. Free GA, like 50% (w/w) GA aqueous solution, can be recovered by passing the concentrated sodium gluconate through a cation exchanger column to remove Na^+ ions. Purified D-1,5-gluconolactone and D-1,4-gluconolactone can be obtained from supersaturated solutions of GA at 30–70°C and higher than 70°C respectively (Moresi and Parente., 2014). The conventional purification processes generate a huge amount of wastewater and demand relatively high manpower, leading to environmental pollution and expensive production cost. Thus, in the continuous batch-fermentation with a high cell density and GA concentration, the major technological bottleneck lies in product separation and purification from fermentation media. Several membrane integrated systems are combined with fermenters to improve the downstream process. Generally, microfiltration and ultrafiltration membranes are used to recycle the mycelia and proteins back to fermenters, Moreover, nanofiltration, reverse osmosis and electrodialysis membrane are adopted in separating GA product instead of the filtration of ion exchange in conventional downstream processes. Vikramachakravarthi et al. have used a neutral or charged nanofiltration membrane for the purification of GA and achieved a good result (Vikramachakravarthi et al., 2014).

2.1.2 Bacterial Fermentation: *G. Oxydans* as an Example

Different from GA production in fungi, the oxidation of glucose in bacteria is catalyzed by glucose dehydrogenase (GDH, EC 1.1.99.17). *G. oxydans* is preferred over *A. niger* in continuous fermentation because the chemostat cultivation cannot be performed on the latter. During the metabolism of *G. oxydans*, organics undergo incomplete oxidation (namely overflow metabolism) due to the lack of a glycolysis pathway and enzymes for tricarboxylic acid cycle (TCA). Therefore, *G. oxydans* oxidizes glucose to produce intermediate products like GA instead of CO_2 and H_2O. GA can be synthesized via two alternative pathways in *G. oxydans* (**Figure 3**). The first is the direct glucose oxidation pathway located in the periplasmic space and catalyzed by a membrane-bound PQQ-dependent GDH (EC 1.1.99.17). D-glucose is oxidized to D-δ-gluconolactone and then to D-GA which can be further oxidized to 2-keto-gluconate and 2,5-diketo-gluconate by flavin-dependent gluconate dehydrogenase and 2-keto-gluconate dehydrogenase, respectively. These two membranes-bound dehydrogenases can transfer electrons to the respiratory chain and produce the energy, while heme serves as the prosthetic group. Moreover, D-GA can also be oxidized to 5-keto-gluconate by a membrane-bound PQQ-dependent 5-keto-gluconate dehydrogenase. The second pathway is in the cytoplasm and the oxidation products flows to the pentose phosphate pathway at pH 7.5. In this pathway, D-glucose is transferred into cells and converted to D-GA by a $NADP^+$-dependent glucose dehydrogenase (EC 1.1.1.47), then further oxidized to 2-keto-gluconate (at neutral pH) or 5-keto-gluconate (at acidic pH) by 2-keto-gluconate reductase and 5-keto-gluconate reductase, respectively. In either case, D-GA is mainly produced in the periplasm of *G. oxydans* where the activity of PQQ-dependent GDH is approximately 27-fold higher than that of $NADP^+$-dependent GDH in cytoplasm (Pronk et al., 1989). The incomplete oxidation of glucose results in the accumulation of nearly quantitative amounts of the GA product outside the cells. GA is released into the medium via porins present in the outer membrane. Its genomic sequencing (Prust et al., 2005) reveal multiple metabolic pathways and confirms the synthetic pathways mentioned above.

G. oxydans is a strictly aerobic bacterium which can carry out highly effective continuous fermentation. It is also well known that the rapid growth of *G. oxydans* is difficult even in a complete medium due to its low ingestion of carbon sources. Maximum biomass of *G. oxydans* is achieved in the media containing D-mannitol or D-sorbitol as a carbon source. However, the oxidation reaction catalyzed by membrane-bound GDH is a nongrowth associated process (Macauley et al., 2001; Zhou et al., 2018). The key factor influencing the continuous

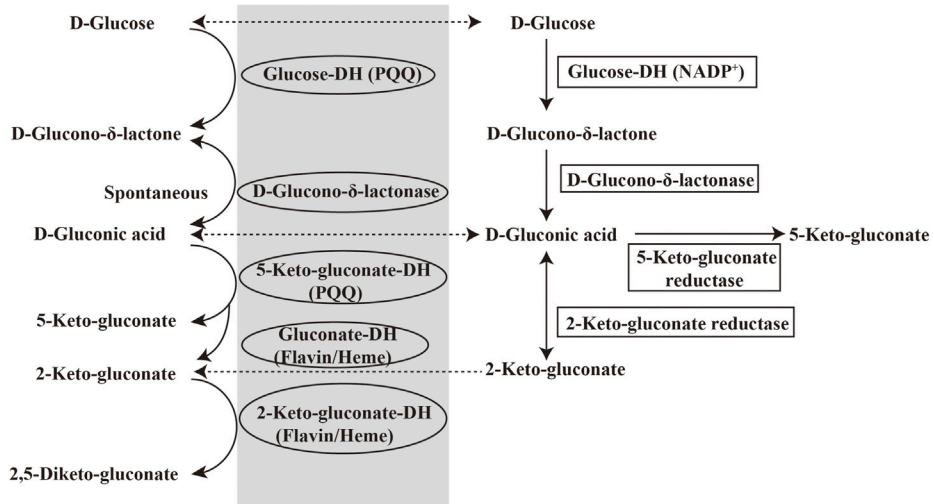

FIGURE 3 | Pathway of GA from glucose in bacteria.

fermentation of *G. oxydans* is improving glucose conversion rate while ensuring certain biomass. For this reason, the seed medium on which *G. oxydans* is inoculated usually contains D-mannitol (25 g/L) or D-sorbitol (50 g/L) and yeast extract (5 g/L) to obtain enough biomass, while the fermentation medium needs D-sorbitol (50 g/L) and quite high concentration of glucose for the balance of enough biomass and the higher yield of GA and derivatives (Banerjee et al., 2018; Zhou and Xu, 2019). In continuous culture, *G. oxydans* responds slowly to pH decrease, and lower pH (<4.5) is advantageous to the formation of the incomplete oxidation product because the pentose phosphate pathway is inhibited. Generally, the glucose oxidation catalyzed by membrane-bound GDH is dominant when the glucose concentrations is above 15 mM and pH below 3.5 (Ramachandran et al., 2017). Meanwhile, *G. oxydans* is highly sensitive to DO concentration, and the rate of oxygen transfer determines the production rate of GA from glucose during fermentations. Yuan et al. conducted a batch fermentation using *G. oxydans* for 5-keto-D-gluconate production, and obtained a maximum 5-keto-D-gluconate concentration of 117.75 g/L with a productivity of 2.10 g/L/h under the condition that DO was continuously maintained above 20% (Yuan et al., 2015).

Similar to fungal fermentation, downstream processing steps such as centrifugation, evaporation, product precipitation, liquid–liquid extraction and adsorption (with anion-exchange resin or activated carbon) are involved in removing the residual microbial cells, water and volatile compounds (Varnicic et al., 2015). Especially, the batch processes requiring frequent shut-down and start-up of a system lead to low productivity and high labor cost (Banerjee et al., 2018). Such limitations can be overcome via combining membrane systems with continuous fermentation to maintain a high cell density and the continuous removal of products (Pal et al., 2016).

2.2 Regulation of Synthesizing Gluconic Acid and Its Derivatives

2.2.1 Fungal Regulation

GA production via fungal fermentation is directly related to GOD activity. Extensive experimental evidence shows that the activity of GOD can be markedly increased by the following factors: 1) the media containing glucose or the substrates whose hydrolysates are glucose; 2) increasing pH by adding an appropriate neutralizer (NaOH and $CaCO_3$); 3) maintaining a high DO level in the fermentation broth; 4) keeping high cell membrane permeability and suitable osmotic potential by approaches such as adding surfactant-like matter to release periplasmic GOD. Mu et al. enhanced the thermostability and pH tolerance of GOD from *A. niger* by using in *silico* design which significantly improved the GA yield by more than twice, accompanied with almost complete conversion of 324 g/L D-glucose to GA within 18 h (Mu et al., 2019). Furthermore, with the increase in the fungal concentration, pH becomes an important parameter for GA production. It can produce many kinds of weak organic acids (such as citric acid, GA, and oxalic acid) whose accumulation depends on the medium pH during GA fermentation (Vassilev and Vassileva, 1992). pH lower than 3.5 can trigger the tricarboxylic acid cycle (TCA) and promote the formation of citric acid. The optimal pH for GA production by fungal fermentation is 4.5–6.0. For example, the optimum pH for *A. niger* fermentation is 5.5 (Znad et al., 2004).

Besides, GA synthesis is a strictly aerobic process sensitive to the DO content in the medium. It has been reported that the

oxygen concentration gradient and the volumetric oxygen transfer coefficient are important monitoring indicators for fermentation, which can largely influence the transfer rate of oxygen from the gas phase to the liquid phase (Ramachandran et al., 2017). Tian et al. demonstrated that sufficient oxygen supply for improving sodium gluconate synthesis can not only directly affect the substrate but also regulates glucose metabolism to form sodium gluconate (Tian et al., 2018). Therefore, the air flow rate and the agitation rate are crucial to controlling the DO content in the medium. In most cases, the oxygen in fermenters is exactly the oxygen in the air, whereas some scholars introduce high-pressure pure oxygen into the medium for boosting the conversion efficiency. Shen et al. observed that the highest yield of sodium gluconate rose to 0.903 mol/mol in *A. niger* fermentation within 15.5 h when the inlet oxygen concentration was raised to 32% by regulating the appropriate proportions of air and pure oxygen to appropriate values, and the yield of main by-product (citric acid) also dramatically decreased from 1.36 to 0.34 g/L (Shen et al., 2017). Fernandes et al. reported that an increased oxygen transfer rate by enhancing air pressure up to 4 bar favored the GA production of by *Aureobasidium. pullulans* (Fernandes et al., 2021).

H_2O_2, a byproduct of GA synthesis, plays an inhibitory role in GA production. Only the activity of reduced GOD is reported sensitive to H_2O_2 (Witteveen et al., 1992). Although there exists gluconolactonase in *A. niger* which can accelerate the conversion from glucono-δ-lactone to GA, some scholars recommend removing lactones from media because their accumulation is disadvantageous to both the rate of glucose oxidation and the production of gluconates (Roukas, 2000).

Mutagenizing strains is also needed by GA fermentation to improve the conversion efficiency of the substrate and reduce the cost of industrial production. So far, the maximal GA production of 76.3 g/L has been obtained from solid-state fermentation by *A. niger* ARNU-4, a mutant improved by genetic manipulation, which has a remarkable ability to utilize the untreated sugarcane molasses and tea waste as substrates (Sharma et al., 2007). A recombinant strain z19, which was constructed by simultaneously expressing the GOD and catalase from *A. niger* in the wild-type *Penicillium oxalicum* strain with cellulolytic ability and has been utilized for sodium gluconate production from cellulose (Han et al., 2018). Overexpressing the GOD gene made the transformant GOEX8 to produce considerably more calcium gluconate (160.5 ± 5.6 g/L) and higher GOD activity (1,438.6 ± 73.2 U/mg of protein) than its parent strain (Ma et al., 2018). The UV-induced mutant UV-112 of an acid-producing *A. niger* strain isolated from onions has a much higher glucose conversion rate than the original strain (0.66 g/g vs 0.25 g/g) (Prabu et al., 2012).

2.2.2 Bacterial Regulation

The secondary oxidation of GA to keto-GA limits bacterial fermentation for the industrial production of GA. The formation of keto-GA can be inhibited when the glucose concentration is higher than 15 mM and the pH is lower than 3.5 (Sarkar et al., 2010). Under optimal industrial conditions, the GA production efficiency of *G. oxydans* is 75–80%, which is however significantly dependent on pH, glucose concentration, and air flow. For example, during the batch fermentation of *G. oxydans* for producing 5-keto-D-gluconate, DO needs to be continuously maintained above 20% to ensure the product concentration of 5-keto-D-gluconate to reach 117.75 g/L with a productivity of 2.10 g/L/h (Yuan et al., 2015). *G. oxydans* 621H (DSM 2343) is reported suitable for GA production via biological fermentation due to its high oxidizability even in the case of poor cell growth (Sievers and Swings, 2005). Different types of bacteria oxidize glucose in different pathways. *Acetobacter* spp. metabolize D-glucose through the pentose phosphate pathway and the TCA cycle, while *G. oxydans* can only metabolize glucose through the pentose phosphate pathway and the Entner-Doudoroff pathway due to its lack of a complete TCA cycle. In other bacteria with the ability to produce a high yield of GA (e.g., *Acidomonas methanolica* and *Gluconacetobacter diazotrophicus*), the oxidation of glucose to GA is assisted by PQQ-dependent GDH on the cytoplasmic membrane, along with synthesizing ATP in the electron transport chain (Krajewski et al., 2010).

Usually, bacteria can usually achieve the goal of increasing the production of GA and its derivatives after genetic modification. Wang et al. knocked out the gluconic acid dehydrogenase encoding gene of *Klebsiella pneumoniae*, which blocked the keto-GA pathway and increased GA production to 422 g/L (Wang et al., 2016). However, the pathogenicity of *K. pneumoniae* limits its industrial fermentation and commercial applications. The recombinant strain *G. oxydans* ZJU2 was constructed by knocking out a gluconate-2-dehydrogenase encoding gene and a pyruvate decarboxylase encoding gene and then expressing a exogenous GDH from *Xanthomonas campestris*. The recombinant strain was applied to batch fermentation to yield 5- keto-D-gluconate with quite high productivity of 2.10 g/L/h (Yuan et al., 2015). Zeng et al. knocked out the gluconate-5-dehydrogenase encoding gene in a competitive pathway and overexpressed the gluconate-2-dehydrogenase in the synthetic pathway of 2- keto-D-gluconate in *Gluconobacter japonicus*, which increased the titre of 2- keto-D-gluconate by 63.81% in shake flasks (Zeng et al., 2019). **Table 2** summarizes the GA production by fermentation of high-yielding strains in recent years.

2.3 Bottlenecks Existing in Industrial Fermentation to Produce Gluconic Acid and Its Derivatives

Bacteria such as *G. oxydans* are more sensitive to high-concentration glucose during fermentation to produce GA and its derivatives. The secondary oxidation of GA is a double-edged sword for industrial production by fermentation. For one thing, it provides more possibilities for the fermentation of different keto-GA products. For another thing, a large amount of keto-GA is generated in this process which leads to difficult product separation of target products. Both the effective inhibition of various by-products in fermentation process and the separation and purification of the target products in downstream processes are the problems that need to be solved in the industrial bacterial fermentation routes to produce GA and its derivatives.

TABLE 2 | Reported high-yield GA production in recent years.

Strains	Fermentation Type	GA (g/L)	Volumetric Productivity (g/L/h)	References
A. niger	batch culture in air-lift bioreactor	150	2.3	Klein et al. (2002)
A. niger AN151	submerged fermentation	330	21.0 ± 0.9	Lu et al. (2015)
A. niger JCM 5549	immobilization/batch	272	6.1	Matsui et al. (2013)
A. niger SIIM M276	batch	76.67	0.86	Zhang et al. (2016)
A. niger NCIM 548	immobilization/batch	92	2.04	Mukhopadhyay et al. (2004)
A. niger IAM 2094	batch	80–100	1.13	Ikeda et al. (2006)
A. niger ORS-4410	batch	80.60	0.131	Singh et al. (2003)
A. niger ORS-4410	semi-continuous batch	110.94	0.9375	Singh, (2008)
A. pullulans (De Bary) DSM 7085	continuous batch in a cascading operation of two bioreactors	350–370	12.7–13.9	Anastassiadis and Rehm, (2006b)
P. variabile P16	double feeding fed-batch	240	2.02	Crognale et al. (2008)
G. oxydans NBIMCC 1043	batch	148.5	9.03	Velizarov and Beschkov, (1994)
G. oxydans DSM2003	cascade hydrolysis/batch fermentation	118.9	1.65	Hou et al. (2018)
Klebsiella pneumoniae Δgad	fed-batch	422	4.22	Wang et al. (2016)

Fungal fermentation, such as *A. niger*, features a high yield and less byproduct produced, which is thus widely used to produce GA on an industrial scale. However, there are still many problems to be addressed in the process: 1) Filamentous fungi and $CaCO_3$ cannot be reused in industrial fermentation. Biomass recycling is a common means in the fermentation industry for rational resource utilization and cost savings. However, filamentous fungi (e.g., *A. niger*) exhibit diverse forms during liquid fermentation, such as dispersed mycelia, clusters and balls (Tang et al., 2015). During industrial fermentation, mycelia are entangled with $CaCO_3$, protein flocculants, and activated carbon, which hinders the secondary utilization of strains and $CaCO_3$ due to difficult separation (Novalic et al., 1997). 2) The inoculated spores of *A. niger*-like mold for fermentation require to be cultured for a long time under complex culture conditions, and spore contamination is prone to occur (Anastassiadis S. and Rehm H. J., 2006). They can produce spore powder polluting the environment. Thus, workers are protected from spore powder-induced inhalation allergy through equipment and facilities in modern industrial fermentation. Mycotoxins can be produced from the metabolism of some *A. niger* species, and 3–10% of *A. niger* is positive in the detection of ochratoxin A and aflatoxin. This necessitates the toxin detection of new strains and those modified by molecular biological approaches or UV mutation under controllable fermentation conditions, especially for the food and medicine industries (Schuster et al., 2002). 3) *A. niger* also suffers from the failure to continuous fed-batch fermentation, a single carbon source type, and the curb of product synthesis by high-concentration carbon sources. Since the GOD in *A. niger* is highly active only in glucose-containing media, glucose or carbon sources with glucose as hydrolysates are used in the industrial fermentation of *A. niger*. Although *A. niger* shows a high conversion rate (>90%) in the case of proper glucose content, it can form excess mycelia during fermentation with high-concentration carbon sources, which diminishes the yield because of increasing the viscosity of media and reducing air flow and assimilation in medium (Ramachandran et al., 2017). Continuous fed-batch fermentation is a widely used method in the fermentation industry. However, it is infeasible to use glucose at a rather high concentration (>300 g/L) in *A. niger* fermentation (Roehr et al., 2001). The GOD in *A. pullulans* is less dependent on glucose, and economical carbon sources such as inulin can be utilized directly (Jiang et al., 2016). Anastassiadis and Rehm reported several methods to produce GA by continuous fermentation of *A. pullulans*, with the GA yield reaching 375 g/L and the product recovery 78% (Anastassiadis S. and Rehm H.-J., 2006). Thus, it has always been meaningful to develop new strains for industrial production of GA and its derivatives and combine the strains with suitable industrial production processes.

3 AGRO-INDUSTRIAL BYPRODUCTS AS SUBSTRATES FOR THE PRODUCTIONS OF GLUCONIC ACID AND ITS DERIVATIVES

Currently, many researchers are searching for new raw materials in hope of achieving high-added-value products with more economical and environmental-friendly methods (Wang et al., 2022). Hence, raw materials such as glucose and sucrose are gradually replaced by agro-industrial byproducts (e.g., hydrolysates of sugarcane, corn stover feedstock, corn cob, tea waste, starch, inulin, whey, figs, bananas, grapes, strawberry surpluses, wastepaper and lignocellulose) in the production of the fermentation for GA and its derivatives by fermentation. On one hand, these agro-industrial byproducts are rich in carbohydrates, the microbial fermentation of which enables the sustainable utilization of resources. Among numerous industrial and agricultural waste fermentation media, starch and polysaccharide media are superior to lignocellulose medium which requires pretreatment at high temperature, high pressure and low pH. Singh et al. obtained the mutant *A. niger* strain ORS-4.410 after continuous UV irradiation with excellent fermentability for saccharides derived from agricultural wastes (grapes and bananas) in batch fermentation and semi-continuous fermentation (Singh, 2008). Jordan et al. reported that the hydrolysis of lignocellulose can yield many compounds (e.g., carboxylic acids, furan aldehydes, and aromatic compounds) toxic to or suppressing microorganisms (Jordan et al., 2011). Zhang et al. also conducted tolerance tests on cell

growth, GA production and GOD activity of *A. niger* SIIM M276 to corn stover hydrolysates (several furan derivatives, organic acids and phenolic compounds). They found that furfural influenced GA fermentation most, which can almost totally inhibit fungal metabolism at a concentration higher than 1.0 g/L (Zhang et al., 2014). Then researchers optimized the parameters of *A. niger* fermentation to produce GA and obtained 76.67 g/L GA in fermenters by using corn stover hydrolysates subjected to dry dilute acid pretreated (Zhang et al., 2016). However, the latest evidence showed that the acetic acid can act as an inhibitor for the oxidation from glucose to GA in *G. oxydans* fermentation to facilitate 2-keto-GA accumulation and improve gluconate dehydrogenase activity (Dai et al., 2022). Inspired by this, Zhou et al. co-produced xylooligosaccharides and GA from sugarcane bagasse with an economical approach involving the pre-hydrolysis treatment by acetic acid and obtained a GA yield of 96.3% by maintaining low pH stress (Zhou and Xu, 2019).

On the other hand, these diverse forms and different properties of agro-industrial byproducts as substrates also contribute to more changes in fermentation processes. Taking raw materials as substrates/supports has greatly promoted the development of the solid-state fermentation (SSF). Media, fermentation parameters and other factors including oxygen transfer, temperature, humidity, and aeration have been thoroughly studied. Sharma et al., evaluated the ability of SSF with tea waste as solid support to produce GA by *A. niger* (ARNU-4) strain, and optimized some parameters such as moisture content (70%), temperature (30 °C), aeration rate (2.5 L/min), and inoculum size (3%) for maximum GA production (76.3 g/L). Additives (e.g., jaggary, yeast extract, cheese whey, and mustard oil) with different concentrations were supplemented for further enhancing the production ability of *A. niger*. However, only yeast extract (0.5%) was proved an effective additive to enhance the GA production (82.2 g/L) (Sharma et al., 2007). Roukas et al. investigated the production of GA and citric acid with dry fig by SSF of *A. niger* ATCC 10577 and obtained the maximum transformation rate (685 g/kg) for GA from dry fig after adding 6% (w/w) methanol into the substrate (Roukas, 2000). To pursue a more efficient and economical fermentation process, Hou et al. carried out cascade hydrolysis and fermentation (CHF) without solid/liquid separation for GA and xylonic acids in a highly viscous hydrolysate slurry. The CHF process overcomes the inhibitiory effect of the intermediate glucono-1,4-lactone on cellulase activity and produced 118.9 g/L of GA and 59.3 g/L of xylonic acid (Hou et al., 2018).

4 INNOVATIVE INTEGRATED ROUTES FOR THE PRODUCTION OF GLUCONIC ACID AND ITS DERIVATIVES

In moving toward a sustainable efficient technology regime nowadays, integrated production strategies are gradually adopted for the production of GA and its derivatives rather than conventional fermentation methods. Multiple biotechnologies have been combined in their production, such as immobilized cells, immobilized enzymes, enzymatic modification, polymer material, bimetallic catalysts, surface modification and novel reactors. Researchers have developed many alternative processes to minimize the production costs associated with raw materials and product separation. Ruales-Salcedo et al. proposed a hybrid process consisting of a multi-enzyme production system and *in situ* GA recovery by a liquid membrane in Taylor flow, which increased the GA productivity and yield to 1.6- and 1.7-fold higher than those in the multi-enzyme system containing sodium acetate buffer, respectively (Ruales-Salcedo et al., 2020). Yu et al. immobilized three types of enzymes (cellulase, GOD and catalase) on a reversible soluble Eudragit L-100 and then applied the system to the catalytic synthesis of GA from corn straw, with the conversion rate of cellulose to GA reaching 61.41% (Yu et al., 2021). Huang et al. also reported that ε-Poly-L-lysine was an ideal donor of amino to GOD and catalase. The immobilized GOD and catalase with surface amine modification were demonstrated 1.56 times higher activity recovery than that of before (Huang et al., 2018). DNA-guided enzyme assembly was reported that can enhance the production of GA directly from cellulose (Chen et al., 2017). Multiple studies have indicated that the integration of multi-stage micro- and nanofiltration in appropriate membrane units with various fermentation processes can significantly enhance the production efficiency of GA and its derivatives (Dekonda et al., 2014; Pal et al., 2016; Kuznetsov et al., 2017). Pal et al. obtained 93 g/L GA with a yield of 0.94 g/g by using the membrane-integrated hybrid fermentation system. The performance parameters of this system established the superiority of the novel technology over the traditional ones (Banerjee et al., 2018). Nevertheless, with the development of high-yielding strains for GA and the gradual maturity of industrial fermentation, integrated routes with more complicated operations and higher costs are more difficult to apply in industrial production. More concise and economical integrated production strategies are expected in the future.

5 SUMMARY AND OUTLOOK

GA and its derivatives have broad application prospects in the food, medicine, construction and biotechnology industries. Microbial fermentation to produce GA has become a viable mode for commercial production. GA production is a simple one-step oxidative fermentation process. To reduce the cost of traditional fermentation, researchers have focused on the evaluation of cheaper agro-industrial byproducts for fermentation. This plays a significant role in promoting the development of GA fermentation in industrial practice. Meanwhile, they have also improved the fermentation process. Technological innovations have been merged recently with fermentation using agro-industrial byproducts to form the integrated routes. However, these integrated routes are rarely achieved in industrial fermentation applications.

Some problems need to be tackled for greater benefits, including complicated reaction steps, fermentation waste discharge and a decrease in enzyme activity. Since the market demand is expanded increasingly as evident from foregoing reviews, current strains for industrial fermentation to yield GA face more and more challenges in production. Researchers are expected to keep screening and transforming strains with a strong ability for industrial production of GA, combining the advantages of fungal and bacterial fermentation while improving the fermentation process. Ultimately, all these efforts will pave the way for cheaper GA production by industrial fermentation, which would promote the combination of innovative GA production processes and industrial fermentation in practice.

AUTHOR CONTRIBUTIONS

YM and WC outlined this manuscript. YM drafted the manuscript. BL, CW and XZ revised the manuscript. All authors contributed to the article and approved the submitted version.

FUNDING

The work was supported by the National Natural Science Foundation of China (Grant No. 41806163) and Talent Research Foundation of Qingdao Agricultural University (663/1117023, 663/1120036, 663/1120058).

REFERENCES

Ahmed, A. S., Farag, S. S., Hassan, I. A., and Botros, H. W. (2015). Production of Gluconic Acid by Using Some Irradiated Microorganisms. *J. Radiat. Res. Appl. Sci.* 8 (3), 374–380. doi:10.1016/j.jrras.2015.02.006

Ahuja, K., and Singh, S. (2018). *Gluconic Acid Market by Application, by Downstream Potential, Regional Outlook, Application Potential, Price Trend, Competitive Market Share & Forecast, 2018–2024*. Selbyville, DE: Global Market Insights Inc, 240.

Ajala, E. O., Ajala, M. A., Ogunniyi, D. S., and Sunmonu, M. O. (2017). Kinetics of Gluconic Acid Production and Cell Growth in a Batch Bioreactor by Aspergillus niger Using Breadfruit Hydrolysate. *J. Food Process Eng.* 40 (3), e12461. doi:10.1111/jfpe.12461

Alonso, S., Rendueles, M., and Díaz, M. (2015). Simultaneous Production of Lactobionic and Gluconic Acid in Cheese Whey/glucose Co-fermentation by Pseudomonas Taetrolens. *Bioresour. Technol.* 196, 314–323. doi:10.1016/j.biortech.2015.07.092

Anastassiadis, S., Aivasidis, A., and Wandrey, C. (2003). Continuous Gluconic Acid Production by Isolated Yeast-Like Mould Strains of Aureobasidium Pullulans. *Appl. Microbiol. Biotechnol.* 61 (2), 110–117. doi:10.1007/s00253-002-1180-8

Anastassiadis, S., and Morgunov, I. (2007). Gluconic Acid Production. *Biot* 1 (2), 167–180. doi:10.2174/187220807780809472

Anastassiadis, S., and Rehm, H.-J. (2006b). Continuous Gluconic Acid Production by the Yeast-like *Aureobasidium Pullulans* in a Cascading Operation of Two Bioreactors. *Appl. Microbiol. Biotechnol.* 73 (3), 541–548. doi:10.1007/s00253-006-0499-y

Anastassiadis, S., and Rehm, H. J. (2006a). Continuous Gluconic Acid Production by *Aureobasidium Pullulans* with and without Biomass Retention. *Electron. J. Biotechnol.* 9 (5), 1. doi:10.2225/vol9-issue5-fulltext-18

Banerjee, S., Kumar, R., and Pal, P. (2018). Fermentative Production of Gluconic Acid: A Membrane-Integrated Green Process. *J. Taiwan Inst. Chem. Eng.* 84, 76–84. doi:10.1016/j.jtice.2018.01.030

Bankar, S. B., Bule, M. V., Singhal, R. S., and Ananthanarayan, L. (2009). Glucose Oxidase - an Overview. *Biotechnol. Adv.* 27 (4), 489–501. doi:10.1016/j.biotechadv.2009.04.003

Blandino, A., Macı´as, M., and Cantero, D. (2001). Immobilization of Glucose Oxidase within Calcium Alginate Gel Capsules. *Process Biochem.* 36 (7), 601–606. doi:10.1016/s0032-9592(00)00240-5

Blom, R. H., Pfeifer, V. F., Moyer, A. J., TraufRer, D. H., Conway, H. F., Crocker, C. K., et al. (1952). Sodium Gluconate Production. Fermentation with *Aspergillus niger*. *Ind. Eng. Chem.* 44 (2), 435–440. doi:10.1021/ie50506a061

Cañete-Rodríguez, A. M., Santos-Dueñas, I. M., Jiménez-Hornero, J. E., Ehrenreich, A., Liebl, W., and García-García, I. (2016). Gluconic Acid: Properties, Production Methods and Applications-An Excellent Opportunity for Agro-Industrial By-Products and Waste Bio-Valorization. *Process Biochem.* 51 (12), 1891–1903. doi:10.1016/j.procbio.2016.08.028

Chen, Q., Yu, S., Myung, N., and Chen, W. (2017). DNA-guided Assembly of a Five-Component Enzyme Cascade for Enhanced Conversion of Cellulose to Gluconic Acid and H 2 O 2. *J. Biotechnol.* 263, 30–35. doi:10.1016/j.jbiotec.2017.10.006

Choi, I., and Zhong, Q. (2021). Gluconic Acid as a Chelator to Improve Clarity of Skim Milk Powder Dispersions at pH 3.0. *Food Chem.* 344, 128639. doi:10.1016/j.foodchem.2020.128639

Crognale, S., Petruccioli, M., Fenice, M., and Federici, F. (2008). Fed-batch Gluconic Acid Production from *Penicillium variabile* P16 under Different Feeding Strategies. *Enzyme Microb. Technol.* 42 (5), 445–449. doi:10.1016/j.enzmictec.2008.01.002

Chuppa-Tostain, G., Hoarau, J., Watson, M., Adelard, L., Shum, C. S. A., Caro, Y., et al. (2018). Production of Aspergillus niger Biomass on Sugarcane Distillery Wastewater: Physiological Aspects and Potential for Biodiesel Production. *Fungal Biol Biotechnol.* 1 (1). doi:10.1186/s40694-018-0045-6

Dai, L., Jiang, W., Jia, R., Zhou, X., and Xu, Y. (2022). Directional Enhancement of 2-Keto-Gluconic Acid Production from Enzymatic Hydrolysate by Acetic Acid-Mediated Bio-Oxidation with *Gluconobacter Oxydans*. *Bioresour. Technol.* 348, 126811. doi:10.1016/j.biortech.2022.126811

De Muynck, C., Pereira, C. S. S., Naessens, M., Parmentier, S., Soetaert, W., and Vandamme, E. J. (2007). The GenusGluconobacter Oxydans: Comprehensive Overview of Biochemistry and Biotechnological Applications. *Crit. Rev. Biotechnol.* 27 (3), 147–171. doi:10.1080/07388550701503584

Dekonda, V. C., Kumar, R., and Pal, P. (2014). Production of L (+) Glutamic Acid in a Fully Membrane-Integrated Hybrid Reactor System: Direct and Continuous Production under Non-neutralizing Conditions. *Industrial Eng. Chem. Res.* 53, 19019–19027. doi:10.1021/ie503499w

Fernandes, S., Belo, I., and Lopes, M. (2021). Highly Aerated Cultures Boost Gluconic Acid Production by the Yeast-like Fungus *Aureobasidium Pullulans*. *Biochem. Eng. J.* 175, 108133. doi:10.1016/j.bej.2021.108133

Ferraz, H., Alves, T., and Borges, C. (2001). Coupling of an Electrodialysis Unit to a Hollow Fiber Bioreactor for Separation of Gluconic Acid from Sorbitol Produced by *Zymomonas Mobilis* Permeabilized Cells. *J. Membr. Sci.* 191 (1-2), 43–51. doi:10.1016/s0376-7388(01)00447-1

Han, X., Liu, G., Pan, Y., Song, W., and Qu, Y. (2018). Consolidated Bioprocessing for Sodium Gluconate Production from Cellulose Using *Penicillium oxalicum*. *Bioresour. Technol.* 251, 407–410. doi:10.1016/j.biortech.2017.12.028

Herrick, H. T., and May, O. E. (1928). The Production of Gluconic Acid by the *Penicillium Luteum-purpurogenum* Group. II. Some Optimal Conditions for Acid Formation. *J. Frankl. Inst.* 206 (1), 103–104. doi:10.1016/s0016-0032(28)90752-8

Hou, W., Zhang, M., and Bao, J. (2018). Cascade Hydrolysis and Fermentation of Corn Stover for Production of High Titer Gluconic and Xylonic Acids. *Bioresour. Technol.* 264, 395–399. doi:10.1016/j.biortech.2018.06.025

Huang, J., Zhuang, W., Ge, L., Wang, K., Wang, Z., Niu, H., et al. (2019). Improving Biocatalytic Microenvironment with Biocompatible ε-poly-l-lysine for One Step Gluconic Acid Production in Low pH Enzymatic Systems. *Process Biochem.* 76, 118–127. doi:10.1016/j.procbio.2018.10.018

Hustede, H., Haberstroh, H.-J., and Schinzig, E. (2012). Gluconic Acid. *Ullmann's Encycl. Industrial Chem.* 17, 37–44. doi:10.1002/14356007.a12_449

Ikeda, Y., Park, E., and Okuda, N. (2006). Bioconversion of Waste Office Paper to Gluconic Acid in a Turbine Blade Reactor by the Filamentous Fungus

Aspergillus niger. *Bioresour. Technol.* 97 (8), 1030–1035. doi:10.1016/j.biortech.2005.04.040

Jiang, H., Ma, Y., Chi, Z., Liu, G.-L., and Chi, Z.-M. (2016). Production, Purification, and Gene Cloning of a β-Fructofuranosidase with a High Inulin-Hydrolyzing Activity Produced by a Novel Yeast Aureobasidium Sp. P6 Isolated from a Mangrove Ecosystem. *Mar. Biotechnol.* 18 (4), 500–510. doi:10.1007/s10126-016-9712-x

Jin, X., Zhao, M., Vora, M., Shen, J., Zeng, C., Yan, W., et al. (2016). Synergistic Effects of Bimetallic PtPd/TiO2 Nanocatalysts in Oxidation of Glucose to Glucaric Acid: Structure Dependent Activity and Selectivity. *Ind. Eng. Chem. Res.* 55 (11), 2932–2945. doi:10.1021/acs.iecr.5b04841

Johnstone-Robertson, M., Clarke, K. G., and Harrison, S. T. L. (2008). Characterization of the Distribution of Glucose Oxidase inPenicillium Sp. CBS 120262 andAspergillus niger NRRL-3 Cultures and its Effect on Integrated Product Recovery. *Biotechnol. Bioeng.* 99 (4), 910–918. doi:10.1002/bit.21642

Jordan, D. B., Braker, J. D., Bowman, M. J., Vermillion, K. E., Moon, J., and Liu, Z. L. (2011). Kinetic Mechanism of an Aldehyde Reductase of *Saccharomyces cerevisiae* that Relieves Toxicity of Furfural and 5-Hydroxymethylfurfural. *Biochimica Biophysica Acta (BBA) - Proteins Proteomics* 1814 (12), 1686–1694. doi:10.1016/j.bbapap.2011.08.011

Kapat, A., Jung, J.-K., and Park, Y.-H. (2001). Enhancement of Glucose Oxidase Production in Batch Cultivation of Recombinant *Saccharomyces cerevisiae*: Optimization of Oxygen Transfer Condition. *J. Appl. Microbiol.* 90 (2), 216–222. doi:10.1046/j.1365-2672.2001.01233.x

Katsuya Tooyama, T. M., Tooyama, K., and Sato, S. (2013). Simultaneous Saccharification of Corn Starch in Gluconic Acid Production by *Aspergillus niger* Immobilized on Nonwoven Fabric in a Pressurized Reactor. *Microb. Biochem. Technol.* 05, 088–091. doi:10.4172/1948-5948.1000106

Kirimura, K., and Yoshioka, I. (2019). Gluconic and Itaconic Acids. *Compr. Biotechnol.* 3 (3), 166–171. (Third Edition). doi:10.1016/B978-0-444-64046-8.00158-0

Klein, J., Rosenberg, M., Markoš, J., Dolgoš, O., Krošlák, M., and Krištofı´ková, L. u. (2002). Biotransformation of Glucose to Gluconic Acid by Aspergillus niger-study of Mass Transfer in an Airlift Bioreactor. *Biochem. Eng. J.* 10 (3), 197–205. doi:10.1016/S1369-703X(01)00181-4

Krajewski, V., Simic´, P., Mouncey, N. J., Bringer, S., Sahm, H., and Bott, M. (2010). Metabolic Engineering of *Gluconobacter Oxydans* for Improved Growth Rate and Growth Yield on Glucose by Elimination of Gluconate Formation. *Appl. Environ. Microbiol.* 76 (13), 4369–4376. doi:10.1128/aem.03022-09

Kuznetsov, A., Beloded, A., Derunets, A., Grosheva, V., Vakar, L., Kozlovskiy, R., et al. (2017). Biosynthesis of Lactic Acid in a Membrane Bioreactor for Cleaner Technology of Polylactide Production. *Clean. Techn Environ. Policy* 19 (3), 869–882. doi:10.1007/s10098-016-1275-z

Lim, H. Y., and Dolzhenko, A. V. (2021). Gluconic Acid Aqueous Solution: A Bio-Based Catalytic Medium for Organic Synthesis. *Sustain. Chem. Pharm.* 21, 100443. doi:10.1016/j.scp.2021.100443

Liu, J., Madec, J.-Y., Bousquet-Mélou, A., Haenni, M., and Ferran, A. A. (2021). Destruction of *Staphylococcus aureus* Biofilms by Combining an Antibiotic with Subtilisin A or Calcium Gluconate. *Sci. Rep.* 11 (1), 6225. doi:10.1038/s41598-021-85722-4

Lu, F., Li, C., Wang, Z., Zhao, W., Chu, J., Zhuang, Y., et al. (2016b). High Efficiency Cell-Recycle Continuous Sodium Gluconate Production by *Aspergillus niger* Using On-Line Physiological Parameters Association Analysis to Regulate Feed Rate Rationally. *Bioresour. Technol.* 220, 433–441. doi:10.1016/j.biortech.2016.08.062

Lu, F., Ping, K., Wen, L., Zhao, W., Wang, Z., Chu, J., et al. (2015). Enhancing Gluconic Acid Production by Controlling the Morphology of *Aspergillus niger* in Submerged Fermentation. *Process Biochem.* 50 (9), 1342–1348. doi:10.1016/j.procbio.2015.04.010

Lu, F., Wang, Z., Zhao, W., Chu, J., and Zhuang, Y. (2016a). A Simple Novel Approach for Real-Time Monitoring of Sodium Gluconate Production by On-Line Physiological Parameters in Batch Fermentation by *Aspergillus niger*. *Bioresour. Technol.* 202, 133–141. doi:10.1016/j.biortech.2015.11.077

Ma, Y., Chi, Z., Li, Y.-F., Jiang, H., Liu, G.-L., Hu, Z., et al. (2018). Cloning, Deletion, and Overexpression of a Glucose Oxidase Gene in Aureobasidium Sp. P6 for Ca2+-Gluconic Acid Overproduction. *Ann. Microbiol.* 68 (12), 871–879. doi:10.1007/s13213-018-1393-4

Macauley, S., McNeil, B., and Harvey, L. M. (2001). The GenusGluconobacterand its Applications in Biotechnology. *Crit. Rev. Biotechnol.* 21 (1), 1–25. doi:10.1080/20013891081665

Moresi, M., and Parente, E. (2014). "Fermentation (Industrial) | Production of Some Organic Acids (Citric, Gluconic, Lactic, and Propionic)," in *Encyclopedia of Food Microbiology*. Editors C. A. Batt and M. L. Tortorello. Second Edition (Academic Press), 804–815. doi:10.1016/B978-0-12-384730-0.00111-7,

Mu, Q., Cui, Y., Tian, Y. e., Hu, M., Tao, Y., and Wu, B. (2019). Thermostability Improvement of the Glucose Oxidase from *Aspergillus niger* for Efficient Gluconic Acid Production via Computational Design. *Int. J. Biol. Macromol.* 136, 1060–1068. doi:10.1016/j.ijbiomac.2019.06.094

Mukhopadhyay, R., Chatterjee, S., Chatterjee, B. P., Banerjee, P. C., and Guha, A. K. (2005). Production of Gluconic Acid from Whey by Free and Immobilized *Aspergillus niger*. *Int. Dairy J.* 15 (3), 299–303. doi:10.1016/j.idairyj.2004.07.010

Mycielska, M. E., Mohr, M. T. J., Schmidt, K., Drexler, K., Rümmele, P., Haferkamp, S., et al. (2019). Potential Use of Gluconate in Cancer Therapy. *Front. Oncol.* 9, 522. doi:10.3389/fonc.2019.00522

N.G., A. A., Arbain, D., and Ahmad, M. S. (2012). Effects of Selected Medium Components for Production of Glucose Oxidase by a Local Isolate *Aspergillus terreus* UniMAP AA-1. *APCBEE Procedia* 2, 125–128. doi:10.1016/j.apcbee.2012.06.023

Novalic, S., Kongbangkerd, T., and Kulbe, K. D. (1997). Separation of Gluconate with Conventional and Bipolar Electrodialysis. *Desalination* 114 (1), 45–50. doi:10.1016/s0011-9164(97)00153-7

Pal, P., Kumar, R., and Banerjee, S. (2016). Manufacture of Gluconic Acid: A Review towards Process Intensification for Green Production. *Chem. Eng. Process. Process Intensif.* 104, 160–171. doi:10.1016/j.cep.2016.03.009

Pal, P., Kumar, R., Nayak, J., and Banerjee, S. (2017). Fermentative Production of Gluconic Acid in Membrane-Integrated Hybrid Reactor System: Analysis of Process Intensification. *Chem. Eng. Process. Process Intensif.* 122, 258–268. doi:10.1016/j.cep.2017.10.016

Prabu, R., Chand, T., and Raksha, S. (2012). Improvement ofAspergillus Nigerfor Sodium Gluconate Synthesis by UV Mutation Method. *E-Journal Chem.* 9 (4), 2052–2057. doi:10.1155/2012/768901

Pronk, J. T., Levering, P. R., Olijve, W., and van Dijken, J. P. (1989). Role of NADP-dependent and Quinoprotein Glucose Dehydrogenases in Gluconic Acid Production by *Gluconobacter Oxydans*. *Enzyme Microb. Technol.* 11 (3), 160–164. doi:10.1016/0141-0229(89)90075-6

Prust, C., Hoffmeister, M., Liesegang, H., Wiezer, A., Fricke, W. F., Ehrenreich, A., et al. (2005). Complete Genome Sequence of the Acetic Acid Bacterium *Gluconobacter Oxydans*. *Nat. Biotechnol.* 23 (2), 195–200. doi:10.1038/nbt1062

Ramachandran, S., Fontanille, P., Pandey, A., and Larroche, C. (2006). Gluconic Acid: Properties, Applications and Microbial Production[J]. *Food Technol. Biotechnol.* 44 (2), 185–195.

Ramachandran, S., Nair, S., Larroche, C., and Pandey, A. (2017). *Gluconic Acid [M]//Current Developments in Biotechnology and Bioengineering*. Elsevier, 577–599. doi:10.1016/B978-0-444-63662-1.00026-9

Rodriguez, H., Gonzalez, T., Goire, I., and Bashan, Y. (2004). Gluconic Acid Production and Phosphate Solubilization by the Plant Growth-Promoting Bacterium *Azospirillum* Spp. *Naturwissenschaften* 91 (11), 552–555. doi:10.1007/s00114-004-0566-0

Roehr, M., Kubicek, C. P., and Komínek, J. (2001). "Gluconic Acid," in *Biotechnology Set*. Editors H. J. Rehm and G. Reed. second ed. (Weinheim, Germany: Wiley-VCH Verlag GmbH), 347–362. doi:10.1002/9783527620999.ch10f

Roshanfar, M., Golmohammadzadeh, R., and Rashchi, F. (2019). An Environmentally Friendly Method for Recovery of Lithium and Cobalt from Spent Lithium-Ion Batteries Using Gluconic and Lactic Acids. *J. Environ. Chem. Eng.* 7, 102794. doi:10.1016/j.jece.2018.11.039

Roukas, T. (2000). Citric and Gluconic Acid Production from Fig by *Aspergillus niger* Using Solid-State Fermentation. *J. Industrial Microbiol. Biotechnol.* 25 (6), 298–304. doi:10.1038/sj.jim.7000101

Ruales-Salcedo, A. V., Higuita, J. C., and Fontalvo, J. (2020). Integration of a Multi-Enzyme System with a Liquid Membrane in Taylor Flow Regime for the Production and *In Situ* Recovery of Gluconic Acid from Cellulose. *Chem. Eng. Process. - Process Intensif.* 157, 108140. doi:10.1016/j.cep.2020.108140

Sarkar, D., Yabusaki, M., Hasebe, Y., Ho, P. Y., Kohmoto, S., Kaga, T., et al. (2010). Fermentation and Metabolic Characteristics of *Gluconacetobacter Oboediens*

for Different Carbon Sources. *Appl. Microbiol. Biotechnol.* 87 (1), 127–136. doi:10.1007/s00253-010-2474-x

Schuster, E., Dunn-Coleman, N., Frisvad, J. C., and Van Dijck, P. W. (2002). On the Safety of *Aspergillus niger*--A Review. *Appl. Microbiol. Biotechnol.* 59 (4–5), 426–435. doi:10.1007/s00253-002-1032-6

Sharma, A., Vivekanand, V., and Singh, R. P. (2007). Solid-state Fermentation for Gluconic Acid Production from Sugarcane Molasses by *Aspergillus niger* ARNU-4 Employing Tea Waste as the Novel Solid Support. *Bioresour. Technol.* 99 (9), 3444–3450. doi:10.1016/j.biortech.2007.08.006

Shen, Y., Tian, X., Zhao, W., Hang, H., and Chu, J. (2017). Oxygen-enriched Fermentation of Sodium Gluconate by *Aspergillus niger* and its Impact on Intracellular Metabolic Flux Distributions. *Bioprocess Biosyst. Eng.* 41 (1), 77–86. doi:10.1007/s00449-017-1845-4

Sievers, M., and Swings, J. (2005). *Acetobacteraceae Bergey's Manual of Systematics of Archaea and Bacteria*. Hoboken, NJ: John Wiley & Sons, Inc. doi:10.1002/9781118960608

Singh, O. V., Jain, R. K., and Singh, R. P. (2003). Gluconic Acid Production under Varying Fermentation Conditions byAspergillus niger. *J. Chem. Technol. Biotechnol.* 78, 208–212. doi:10.1002/jctb.748

Singh, O. V., and Kumar, R. (2007). Biotechnological Production of Gluconic Acid: Future Implications. *Appl. Microbiol. Biotechnol.* 75 (4), 713–722. doi:10.1007/s00253-007-0851-x

Singh, O. V. (2008). Modulated Gluconic Acid Production from Immobilized Cells ofAspergillus niger ORS-4.410 Utilizing Grape Must. *J. Chem. Technol. Biotechnol.* 83 (6), 780–787. doi:10.1002/jctb.1866

Stottmeister, U., Aurich, A., Wilde, H., Andersch, J., Schmidt, S., and Sicker, D. (2005). White Biotechnology for Green Chemistry: Fermentative 2-Oxocarboxylic Acids as Novel Building Blocks for Subsequent Chemical Syntheses. *J. Ind. Microbiol. Biotechnol.* 32 (11–12), 651–664. doi:10.1007/s10295-005-0254-x

Sun, W., Xiao, F., Wei, Z., Cui, F., Yu, L., Yu, S., et al. (2015). Non-sterile and Buffer-free Bioconversion of Glucose to 2-Keto-Gluconic Acid by Using *Pseudomonas Fluorescens* AR4 Free Resting Cells. *Process Biochem.* 50 (4), 493–499. doi:10.1016/j.procbio.2015.01.011

Tang, W., Xia, J., Chu, J., Zhuang, Y., and Zhang, S. (2015). Development and Application of Morphological Analysis Method in Aspergillus niger Fermentation. *Sheng Wu Gong Cheng Xue Bao* 31 (2), 291–299. PMID: 26062350.

Tian, X., Shen, Y., Zhuang, Y., Zhao, W., Hang, H., and Chu, J. (2018). Kinetic Analysis of Sodium Gluconate Production by *Aspergillus niger* with Different Inlet Oxygen Concentrations. *Bioprocess Biosyst. Eng.* 41, 1697–1706. doi:10.1007/s00449-018-1993-1

Varničić, M., Vidaković-Koch, T., and Sundmacher, K. (2015). Gluconic Acid Synthesis in an Electroenzymatic Reactor. *Electrochimica Acta* 174, 480–487. doi:10.1016/j.electacta.2015.05.151

Vassilev, N., and Vassileva, M. (1992). Production of Organic Acids by Immobilized Filamentous Fungi. *Mycol. Res.* 96 (7), 563–570. doi:10.1016/s0953-7562(09)80981-7

Velizarov, S., and Beschkov, V. (1994). Production of Free Gluconic Acid by Cells ofGluconobacter Oxydans. *Biotechnol. Lett.* 16 (7), 715–720. doi:10.1007/BF00136477

Vikramachakravarthi, D., Kumar, R., and Pal, P. (2014). Production of L (+) Glutamic Acid in a Fully Membrane-Integrated Hybrid Reactor System: Direct and Continuous Production under Non-neutralizing Conditions. *Ind. Eng. Chem. Res.* 53 (49), 19019–19027. doi:10.1021/ie503499w

Wang, D., Sun, L., Sun, W. J., Cui, F. J., Gong, J. S., and Zhang, X. M. (2018). Purification, Characterization and Gene Identification of a Membrane-bound Glucose Dehydrogenase From 2-keto-d-Gluconic Acid Industrial Producing Strain Pseudomonas plecoglossicida JUIM01. *Int. J. Biol. Macromol.* 118, 534–541. doi:10.1016/j.ijbiomac.2018.06.097

Wang, D., Wang, C., Wei, D., Shi, J., Kim, C. H., Jiang, B., et al. (2016). Gluconic Acid Production by Gad Mutant of *Klebsiella pneumoniae*. *World J. Microbiol. Biotechnol.* 32 (8), 132. doi:10.1007/s11274-016-2080-x

Wang, Z.-P., Wang, P.-K., Ma, Y., Lin, J.-X., Wang, C.-L., Zhao, Y.-X., et al. (2022). *Laminaria Japonica* Hydrolysate Promotes Fucoxanthin Accumulation in *Phaeodactylum Tricornutum*. *Bioresour. Technol.* 344 (PtA), 126117. doi:10.1016/j.biortech.2021.126117

Witteveen, C. F. B., Veenhuis, M., and Visser, J. (1992). Localization of Glucose Oxidase and Catalase Activities in *Aspergillus niger*. *Appl. Environ. Microbiol.* 58 (4), 1190–1194. doi:10.1128/aem.58.4.1190-1194.1992

Yao, R., Hou, W., and Bao, J. (2017). Complete Oxidative Conversion of Lignocellulose Derived Non-glucose Sugars to Sugar Acids by Gluconobacter Oxydans. *Bioresour. Technol.* 244, 1188–1192. doi:10.1016/j.biortech.2017.08.078

Yu, X., Zhang, Z., Li, J., Su, Y., Gao, M., Jin, T., et al. (2021). Co-immobilization of Multi-Enzyme on Reversibly Soluble Polymers in Cascade Catalysis for the One-Pot Conversion of Gluconic Acid from Corn Straw. *Bioresour. Technol.* 321, 124509. doi:10.1016/j.biortech.2020.124509

Yuan, J., Wu, M., Lin, J., and Yang, L. (2016). Enhancement of 5-Keto-D-Gluconate Production by a Recombinant *Gluconobacter Oxydans* Using a Dissolved Oxygen Control Strategy. *J. Biosci. Bioeng.* 122 (1), 10–16. doi:10.1016/j.jbiosc.2015.12.006

Zeng, W., Cai, W., Liu, L., Du, G., Chen, J., and Zhou, J. (2019). Efficient Biosynthesis of 2-Keto-D-Gluconic Acid by Fed-Batch Culture of Metabolically Engineered *Gluconobacter Japonicus*. *Synthetic Syst. Biotechnol.* 4 (3), 134–141. doi:10.1016/j.synbio.2019.07.001

Zhang, H., Zhang, J., and Bao, J. (2016). High Titer Gluconic Acid Fermentation by *Aspergillus niger* from Dry Dilute Acid Pretreated Corn Stover without Detoxification. *Bioresour. Technol.* 203, 211–219. doi:10.1016/j.biortech.2015.12.042

Zhang, S., Winestrand, S., Chen, L., Li, D., Jönsson, L. J., and Hong, F. (2014). Tolerance of the Nanocellulose-Producing Bacterium *Gluconacetobacter Xylinus* to Lignocellulose-Derived Acids and Aldehydes. *J. Agric. Food Chem.* 62 (40), 9792–9799. doi:10.1021/jf502623s

Zhao, F., Li, H., Jiang, Y., Wang, X., and Mu, X. (2014). Co-immobilization of Multi-Enzyme on Control-Reduced Graphene Oxide by Non-covalent Bonds: An Artificial Biocatalytic System for the One-Pot Production of Gluconic Acid from Starch. *Green Chem.* 16 (5), 2558–2565. doi:10.1039/C3GC42545B

Zhou, X., and Xu, Y. (2019). Integrative Process for Sugarcane Bagasse Biorefinery to Co-produce Xylooligosaccharides and Gluconic Acid. *Bioresour. Technol.* 282, 81–87. doi:10.1016/j.biortech.2019.02.129

Zhou, X., Zhou, X., Liu, G., Xu, Y., and Balan, V. (2018). Integrated Production of Gluconic Acid and Xylonic Acid Using Dilute Acid Pretreated Corn Stover by Two-Stage Fermentation. *Biochem. Eng. J.* 137, 18–22. doi:10.1016/j.bej.2018.05.005

Ziffer, J. A., Gaffney, S., and Rothenberg, S. (1971). Aldonic Acid and Aldonate Compositions and Production Thereof. *Br. Pat.* 79, 113.

Znad, H., Markoš, J., and Baleš, V. (2004). Production of Gluconic Acid from Glucose by *Aspergillus niger*: Growth and Non-growth Conditions. *Process Biochem.* 39 (11), 1341–1345. doi:10.1016/S0032-9592(03)00270-X

Conflict of Interest: The authors declare that the research was conducted in the absence of any commercial or financial relationships that could be construed as a potential conflict of interest.

Publisher's Note: All claims expressed in this article are solely those of the authors and do not necessarily represent those of their affiliated organizations, or those of the publisher, the editors and the reviewers. Any product that may be evaluated in this article, or claim that may be made by its manufacturer, is not guaranteed or endorsed by the publisher.

Advantages of publishing in Frontiers

OPEN ACCESS
Articles are free to read for greatest visibility and readership

FAST PUBLICATION
Around 90 days from submission to decision

HIGH QUALITY PEER-REVIEW
Rigorous, collaborative, and constructive peer-review

TRANSPARENT PEER-REVIEW
Editors and reviewers acknowledged by name on published articles

Frontiers
Avenue du Tribunal-Fédéral 34
1005 Lausanne | Switzerland

Visit us: www.frontiersin.org
Contact us: frontiersin.org/about/contact

REPRODUCIBILITY OF RESEARCH
Support open data and methods to enhance research reproducibility

DIGITAL PUBLISHING
Articles designed for optimal readership across devices

FOLLOW US
@frontiersin

IMPACT METRICS
Advanced article metrics track visibility across digital media

EXTENSIVE PROMOTION
Marketing and promotion of impactful research

LOOP RESEARCH NETWORK
Our network increases your article's readership